USING PSEUDOTYPES TO STUDY HETEROSUBTYPIC ANTIBODY RESPONSES ELICITED BY SEASONAL INFLUENZA VACCINATION

FRANCESCA FERRARA

A thesis submitted in partial fulfilment of the requirements of the University of Kent and the University of Greenwich for the Degree of Doctor of Philosophy

January 2015

pages 232

DECLARATION

I certify that this work has not been accepted in substance for any degree, and is not concurrently being submitted for any degree other than that of Doctor of Philosophy being studied at University of Greenwich and Kent. I also declare that this work is the result of my own investigations except where otherwise identified by references and that I have not plagiarised the work of others.

Signature: Francesca Ferrara

ACKNOWLEDGEMENTS

I would like to express my gratitude to my supervisors, Dr. Nigel Temperton and Dr. Simon Scott, for supporting me during these years. Their expertise, experience, patience, and understanding allowed me to work with enthusiasm. Their encouragements have been essential, especially when they gave me the opportunity to present my work at numerous conferences.

Special thanks to all present and past colleagues and friends of Viral Pseudotype Unit: Dr. Edward Wright, Dr. Helen Leech, Dr. Eleonora Molesti (thanks for your help and friendship), Stuart Mather, Rebecca Kinsley, Keith Grehan (thanks for the bioinformatic discussions), Emma Bentley, Sonia Marruganti, and George Carnell.

A special thank to Dr. Craig Thompson for the invaluable suggestions and discussions in these last months of my PhD.

I express my thanks and gratitude to all the collaborators for providing reagents essential for this work.

I would like to thank also all the Academic Staff and the PhD colleagues that I have met at the School of Pharmacy. A special thank to Carmen, Diana, Evelina, and Stefania: thank you for your friendship, your encouragements, and the nice discussions.

Finally, I would like to thank all my family.

Grazie mille a tutti!

ABSTRACT

Influenza viruses represent an important public health burden since they cause annual epidemics associated with severe illness and mortality in high-risk populations. Additionally, zoonotic influenza virus infections have potential to produce intermittent pandemics, which have led to millions of deaths globally. However, strategies to prevent influenza severity and spread can be implemented. It is known that antibodies against the haemagglutinin play a key role in protection from influenza virus infection, thus both seasonal and pandemic influenza vaccines aim to elicit such antibodies. Generally, they are directed against haemagglutinin globular head epitopes and are able to neutralize closely related influenza strains, but recently antibodies able to neutralize multiple influenza strains and subtypes have also been described. The discovery of these antibodies, primarily directed against the haemagglutinin stalk, has generated interest in understanding how they are generated and how widespread they are in the human population. Furthermore, eliciting such antibodies has become the aim of many 'universal' vaccine approaches. However, the study of these cross-reactive antibodies using classical serological assays is problematic since the current assays have been shown to be relatively insensitive in detecting them.

The main objective of this thesis was to study the presence and breadth of cross-reactive neutralizing responses in human populations. To overcome the limitations of current serological tests in detecting these responses, lentiviral pseudotype particles bearing the haemagglutinins of different influenza A subtypes and influenza B strains were used as surrogate antigens in neutralization assays. After the generation of these novel tools and the establishment of appropriate controls, pseudotype particle neutralization assays were employed to investigate cross-reactive antibody responses in pre- and post-vaccination sera. Next, the use of chimeric haemagglutinins, in which the globular head was substituted with the head of a different subtype, was incorporated into the pseudotype system. This allowed the differentiation between haemagglutinin head-directed and stalk-directed antibody responses. The ability to efficiently detect broadly neutralizing antibody responses, including those directed against the haemagglutinin stalk, shows that pseudotype particles are tools that should be further characterised and implemented to be used in sero-epidemiological studies and for 'universal' vaccine immunogenicity studies.

CONTENTS

TABLES

FIGURES

ABBREVIATIONS

Amp Pr	Ampicillin promoter
ANOVA	Analysis of Variance
APHA	Animal and Plant Health Agency
ATP	adenosine triphosphate
BEAST	Bayesian evolutionary analysis by sampling trees
BSA	bovine serum albumin
cat.no.	catalogue number
$CD4^+$	cluster of differentiation 4 positive T lymphocyte
$CD8^+$	cluster of differentiation 8 positive T lymphocyte
CDC	Centers for Disease Control and Prevention
cDNA	complementary deoxyribonucleic acid
CPE	cytopathic effect
cPPT	central polypurine tract cis-active sequence
cRNA	complementary ribonucleic acid
csv	comma-separated value
DC	dendritic cell
df	degree of freedom
DMEM	Dulbecco's Modified Eagle Medium
DMSO	dimethyl sulfoxide
DNA	deoxyribonucleic acid
dNTPs	deoxyribonucleotides
ECD	extracellular domain
EDTA	Ethylenediaminetetraacetic acid
eGFP	enhanced green fluorescence protein
ELISA	Enzyme-Linked Immunosorbent Assay
emGFP	emerald Green Fluorescent Protein
ER	endoplasmic reticulum

FAO	Food and Agricultural Organization of the United Nations
FBS	Fetal Bovine Serum
Fc	Fragment crystallizable
FITC	Fluorescein isothiocyanate
Fw	forward (primer)
g	gravity
GC-rich	guanosine citosine rich
GFP	Green Fluorescent Protein
GISAID	Global Initiative on Sharing Avian Influenza Data
HA	haemagglutinin
HAT	human airway trypsin-like protease
hCMV	human cytomegalovirus
hCMV IE Pr	human cytomegalovirus immediate-early promoter
HEF	haemagglutinin–esterase-fusion
HEK	Human Embryonic Kidney
HI	haemagglutination inhibition
HIV-1	human immunodeficiency virus type-1
HKY	Hasegawa, Kishino and Yano
HPAI	Highly Pathogenic Avian influenza
HSV	Herpes Simplex Virus
IC_{50}	half maximal inhibitory concentration
IC_{90}	90% inhibitory concentration
ICH	International Conference on Harmonisation of Technical Requirements for Registration of Pharmaceuticals for Human Use
IE	immediate-early
IFN	interferon
IFTIM3	interferon-induced transmembrane protein 3
Ig	immunoglobulins
LB	Luria Bertani

LPAI	Low Pathogenic Avian influenza
LTR	long terminal repeat
M1	matrix proteins 1
mAb	monoclonal antibody
MCMC	Metropolis-Hastings Markov chain Monte Carlo
MCS	multiple cloning site
MDCK	Madin-Darby Canine Kidney
MEGA	Molecular Evolutionary Genetics Analysis
MHC	major histocompatibility complex
MLV	murine leukaemia virus
MN	microneutralization
mRNA	messenger ribonucleic acid
MVA	Modified Vaccinia Ankara
NA	neuraminidase
NCBI	National Center for Biotechnology Information
NEP	nuclear export proteins
NIBSC	National Institute for Biological Standards and Control
NK	Natural Killer
NP	nucleoprotein
NS1	non-structural protein 1
NS2	non-structural protein 2
NS3	non-structural protein 3
OIE	World Organization for Animal Health
ori	origin of replication
pA or poly A	polyadenylation
PA	polymerase acidic protein
PB1	polymerase basic protein 1
PB2	polymerase basic protein 2
PBS	Dulbecco's Phosphate Buffer Saline

PCR	Polymerase chain reaction
PDB	Protein Data Bank
PEI	polyethylenimine
pH	*potentia hydrogenii*
pp	pseudotype particles
pp-NT	pseudotype particle neutralization
PRNT	plaque-reduction neutralization test
PVDF	Polyvinylidene fluoride membrane
RBC	red blood cell
RBS	receptor binding site
Rev	reverse (primer)
RLU	relative luminescence unit
RNA	ribonucleic acid
rpm	revolutions per minute
RT	room temperature
SCR	seroconversion rate
$SCR_{(2\text{-fold})}$	seroconversion rate with 2-fold increase cut-off
$SCR_{(4\text{-fold})}$	seroconversion rate with 4-fold increase cut-off
SDS	sodium dodecyl sulphate
SDS-PAGE	sodium dodecyl sulphate-polyacrylamide gel electrophoresis
SEM	standard error of the mean
SFFV	Spleen Focus Forming virus
SNARE	Soluble N-ethylmaleimide-sensitive factor Attachment Protein Receptors
SOC	Super Optimal Broth with catabolite repression
SRH	Single Radial Haemolysis
SV40	Simian Vacuolating virus 40
TAE	Tris-Acetate-Ethylenediaminetetraacetic acid buffer
$TCID_{50}$	50% Tissue Culture Infectious Dose

TMPRSS2	type II Transmembrane Protease Serine 2
TMPRSS3	type II Transmembrane Protease Serine 3
TMPRSS4	type II Transmembrane Protease Serine 4
TMPRSS6	type II Transmembrane Protease Serine 6
TMPRSS11D	type II Transmembrane Protease Serine 11D
TMPRSS13	type II Transmembrane Protease Serine 13
TNS	Trypsin Neutralizing Solution
TPCK-Trypsin	L-tosylamido-2-phenyl ethyl chloromethyl ketone treated trypsin
UK	United Kingdom
UPGMA	Unweighted Pair Group Method with Arithmetic mean
USA	United States of America
v/v	volume per volume
VLP	virus-like particle
vRNA	viral ribonucleic acid
vRNP	viral ribonucleoprotein complex
VSV	vesicular stomatitis virus
w/v	weight per volume
WHO	World Health Organization
WPRE	Woodchuck hepatitis virus post-transcriptional regulatory element

CHAPTER 1
Introduction

1.1 Classification and nomenclature system of influenza viruses

Influenza viruses belong to the *Orthomyxoviridae* family as classified by the International Committee on Taxonomy of Viruses (International Committee on Taxonomy of Viruses ICTV 2013) and to the Group/Class V of the Baltimore classification (Baltimore 1971) since their genome is negative sense single-stranded segmented ribonucleic acid (RNA). Furthermore, considering the virion structure, influenza viruses are classified within the single enveloped viruses and their nucleocapsid has helical symmetry.

On the basis of internal protein antigenic and phylogenetic characteristics, three influenza virus *genera*/types, A, B and C, can be distinguished and are officially recognised (International Committee on Taxonomy of Viruses ICTV 2013). Recently, however, viruses homologous to influenza C viruses, but distinct from other *Orthomyxoviridae* influenza viruses were isolated and could represent a new *genus*/type, possibly Influenza D, when the official classification/nomenclature is implemented (Collin *et al.* 2014; Hause *et al.* 2014; Hause *et al.* 2013; Sheng *et al.* 2013).

Influenza A viruses are further classified into subtypes using antigenic characteristics (historical classification (Tumová and Schild 1972)) and phylogenetic characteristics (modern classification (Röhm *et al.* 1996)) of the envelope glycoproteins haemagglutinin (HA) and neuraminidase (NA). Currently 18 different HA subtypes are recognised and are divided into two lineages (**Figure 1A**): Group 1 (H1, H2, H5, H6, H8, H9, H11, H12, H13, H16, H17, H18) and Group 2 (H3, H4, H7, H10, H14, H15) (Tong *et al.* 2013; Tong *et al.* 2012; Fouchier *et al.* 2005). The NAs are also classified as 11 subtypes divided into two groups (**Figure 1B**) (N2, N3, N6, N7, N9 belong to one group; N1, N4, N5, N8 belong to the other group; N10 and N11 are not included in the classification) (J. Xu *et al.* 2012). However, there are doubts about considering N10 and N11 subtypes in the classical NA classification, since these proteins do not show the characteristic sialidase activity (Tong *et al.* 2013; García-Sastre 2012).

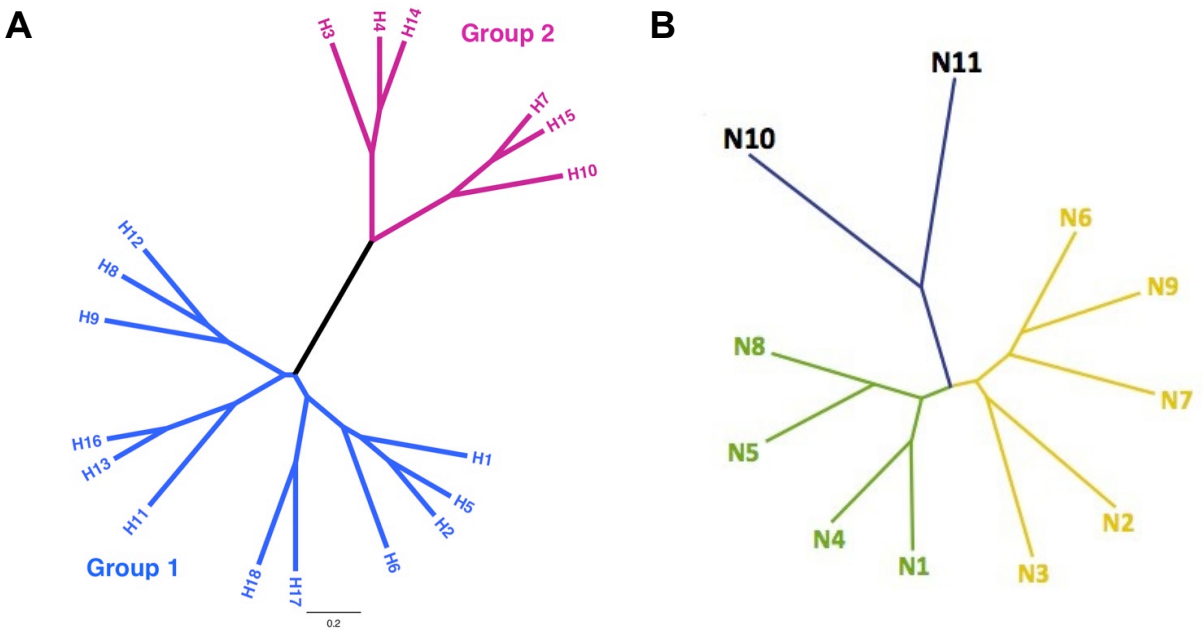

Figure 1: Phylogenetic tree of influenza HA and NA subtypes
A. HA phylogenetic tree (prepared using Molecular Evolutionary Genetics Analysis, MEGA); **B.** NA phylogenetic tree (adapted from Wu *et al.* 2014).

For influenza A viruses that infect the avian host, a further classification on the basis of the pathological phenotypes and biological properties is employed (Pantin-Jackwood and Swayne 2009): Highly Pathogenic Avian influenza (HPAI) and Low Pathogenic Avian influenza (LPAI) (clarification about this categorisation will be further discussed in Sections 1.2.1.1 and 1.4). Furthermore for HPAI H5N1 viruses (briefly discussed in Section 1.4.2) a clade nomenclature system based upon the phylogenetic characterisation of the H5 HA is employed (WHO/OIE/FAO H5N1 Evolution Working Group 2008).

The current nomenclature of influenza virus strains requires that the influenza type, the common or scientific name of the host species (if not human), the geographical origin, the isolate number, and the year of isolation are reported separated by slashes (e.g. B/Brisbane/60/2008, B/seal/Netherlands/1/1999, C/Johannesburg/1/1966). Furthermore, for influenza A virus, the HA and NA subtypes are also reported in brackets (e.g. A/Puerto Rico/8/1934 (H1N1), A/swine/Taiwan/1/70 (H3N2)) (World Health Organization 1980).

Finally, to minimise confusion, the World Health Organization (WHO) advises on the use of standardised terminologies in the case of influenza pandemics or outbreaks (e.g. A(H1N1)pdm09, A(H3N2)v) (World Health Organization, Food and Agriculture Organization, World Organization for Animal Health 2014; World Health Organization 2011).

1.2 Structure of influenza viruses

The intrinsic pleomorphic nature of influenza virions, determined by specific viral genes and by possible experimental 'artifacts', do not permit a straightforward description of native virus morphology (Noda 2012). The majority of influenza laboratory-adapted strains are pleomorphic particles of spherical (**Figure 2**) or elliptical shape with 120 nm (80-170 nm) average diameter (Noda 2012; Harris *et al.* 2006). Conversely, clinical isolates show a filamentous morphology with cylindrical shape reaching 20 μm in length (Elton *et al.* 2013; Seladi-Schulman, Steel and Lowen 2013; Calder *et al.* 2010). Irregular-shaped virions are also observed during negative-staining electron microscopy and cryoelectron microscopy experiments, but this is probably due to artefacts generated by sample preparation, such as air drying, 4°C storage, and ultracentrifugation (Sugita *et al.* 2013; Noda 2012).

Influenza virions are surrounded by an envelope acquired during viral budding and composed of a single lipid bilayer of cellular origin containing lipid rafts, enriched in sphingolipids and cholesterol, and depleted of glycerophospholipids (e.g. phosphatidylcholines), but not of phoshatidylserine (Gerl *et al.* 2012). In the envelope, the influenza virus harbours three different proteins: two spike glycoproteins, HA (Hirst 1942) and NA (Gottschalk 1957), and the transmembrane ion-channel M2 (Zebedee and Lamb 1988; Lamb, Zebedee and C. D. Richardson 1985). In influenza A virus it was estimated that each spherical or elliptical virion presents between 300-400 HAs, 38-50 NAs and 14-68 M2 (Harris *et al.* 2006; Zebedee and Lamb 1988) with a non-random distribution: protein clusters and single NA molecules surrounded by the more abundant HAs can be observed on the virion surface (Harris *et al.* 2006). In filamentous particles, the NA and M2 clusters are also positioned characteristically at one of the virion ends (the proximal end during the budding process) (Rossman and Lamb 2011; Calder *et al.* 2010). Furthermore HAs and NAs are usually localised in lipid rafts (Leser and Lamb 2005; M. Takeda *et al.* 2003), while M2 is not strictly associated with them (Rossman *et al.* 2010; Leser and Lamb 2005).

In the influenza C virus the two major glycoprotein functions are substituted by a single one, the haemagglutinin–esterase-fusion (HEF) protein, which possesses HA and NA activity (Rosenthal *et al.* 1998; Nakada *et al.* 1984). In influenza B and influenza C the transmembrane ion-channel is named B/M2 and C/M2 respectively (Kollerova and Betakova 2006). Furthermore, in influenza B virus, an additional transmembrane protein, denominated NB, is present on the envelope surface (Betakova, Nermut and Hay 1996).

In the internal core of influenza virus, there are the matrix proteins M1 (Baudin *et al.* 2001; Ruigrok, Calder and Wharton 1989), the nuclear export proteins (NEPs), and the

viral ribonucleoprotein complexes (vRNPs) in which the segmented negative sense RNA genome is associated with the nucleoproteins (NPs) and the polymerase complexes (each of them constituted by the polymerase acidic protein (PA), the polymerase basic protein 1 (PB1) and the polymerase basic protein 2 (PB2) (Area *et al.* 2004; Compans, Content and Duesberg 1972). The M1 protein, which principally but not exclusively determines the virus morphology, is in contact with the internal lipid layer, and is associated with small quantities of NEP. M1 interacts directly with the envelope proteins and with the NP of the vRNPs, connecting the two protein structures. The vRNPs are flexible, twisted rod-like structures (Compans, Content and Duesberg 1972). They differ in length depending on the molecular weight of the genome segment that they contain: the NPs surround each RNA strand which is folded then coiled in a regular double-helical arrangement forming a hairpin (Compans, Content and Duesberg 1972). Additionally a single polymerase complex associates with the 5' and 3' viral RNA (vRNA) ends, which partially complement with themselves. The vRNPs are arranged with a central vRNP surrounded by the others with the polymerase complexes that are differently orientated within virions (Sugita *et al.* 2013). In the filamentous particles, the vRNPs are opposite to the NA cluster in the distal end during viral budding, whilst the rest of the filament is empty as only one set of vRNPs is packed (Calder *et al.* 2010).

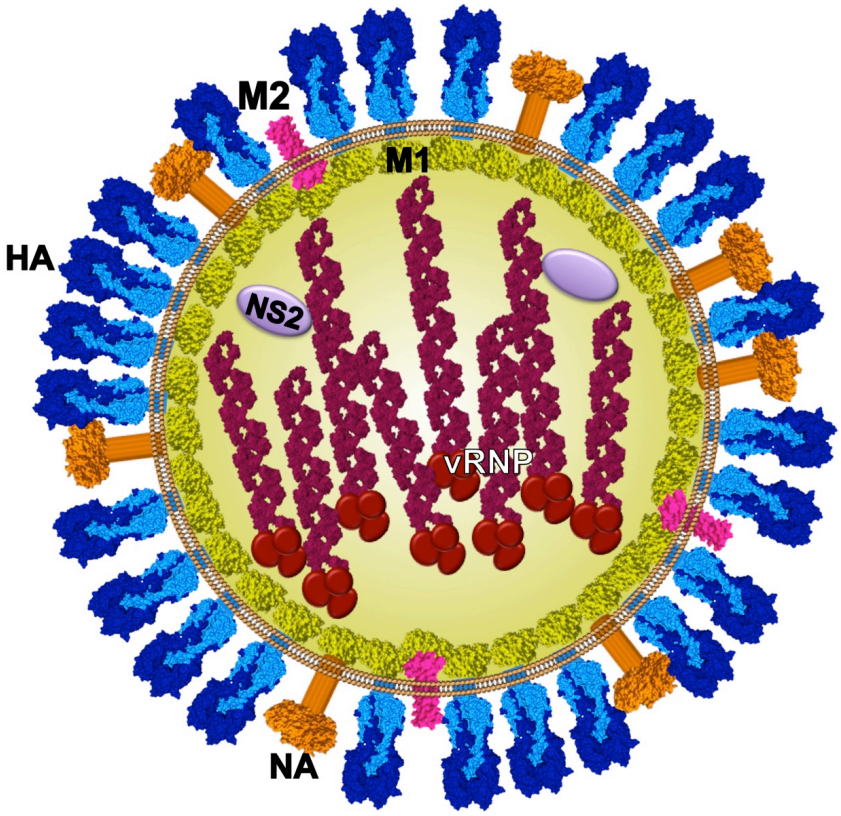

Figure 2: Influenza virus structure
The image was generated with Swiss PDB viewer, POV-Ray 3.7 and Microsoft® Power Point (Microsoft®).

The number of negative sense vRNA segments (and correspondingly vRNPs) in the virion varies depending on the influenza type. Influenza A and B viruses contain eight different segments, whereas influenza C has only seven segments (in relation to the presence of HEF glycoprotein instead of HA and NA). Each negative sense vRNA segment encodes one or more proteins through alternative splicing, leaky ribosomal scanning, re-initiation, and ribosomal frame-shifting mechanisms (Vasin *et al.* 2014). At the present time, 17 proteins have been mapped in the influenza A genome (**Table 1**), 10 in influenza B and 9 in influenza C (Vasin *et al.* 2014; Bouvier and Palese 2008).

The following sub-sections will be focused on the detailed description of the envelope proteins of influenza A, especially HA. The internal structural, the non-structural, and the accessory proteins will not be reviewed in detail, as they do not form an integral part of the work in this thesis. Details regarding influenza B envelope proteins will also be provided.

Table 1: Influenza A genome and proteome
Table adapted from Vasin *et al.* 2014 and Bouvier and Palese 2008. Genome segments were re-designed and adapted from ViralZone database (Swiss Institute of Bioinformatics).

Genome Segment	Organization of the protein-coding open reading frames	Encoded protein(s)	Protein function
1		PB2	Component of vRNPs mRNA cap recognition
2	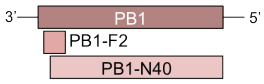	PB1	Component of vRNPs RNA elongation Endonuclease activity
		PB1-F2	Pro-apoptotic activity Virulence factor
		PB1-N40	Balance between PB1 and PB1-F2 expression
3	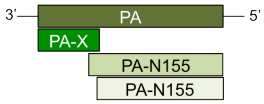	PA	Component of vRNPs Protease
		PA-X	Modulation of the host response
		PA-N155	?
		PA-N182	?
4		HA	Receptor binding Fusion activity
5		NP	Component of vRNPs RNA binding Nuclear import of vRNP
6		NA	Sialidase activity
7	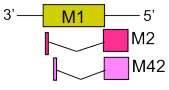	M1	Nuclear export of vRNPs Budding
		M2	Ion-channel Budding
		M42	Ion-channel Replace M2 in M2-null viruses
8	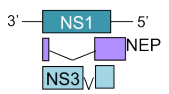	NS1 (non-structural 1)	Multifunctional Interferon antagonist
		NEP (non-structural 2)	Nuclear export of vRNPs
		NS3 (non-structural 3)	Adaptation to mouse host (?)

1.2.1 Haemagglutinin

The HA, a type I envelope glycoprotein, is crucial for biological activities during the viral life cycle (described in Section 1.3): receptor binding and envelope-endosome fusion. These two functions are mediated by the two regions that can be distinguished in the HA rod-like shaped structure: a globular head and a stalk region (**Figure 4(A and C)**). Besides the two regions that can be distinguished, the HA is composed of 3 identical polypeptide chains forming an homotrimer (Wilson, Skehel and Wiley 1981); in each monomer, the globular head is formed by loops, antiparallel β-sheets and small α-helixes, whereas the stalk is composed almost exclusively by α-helixes (**Figure 4B**).

The globular head is the region responsible for viral attachment to the cellular receptor, sialic acid (Weis *et al.* 1988). Sialic acids are a family of carboxylated sugars that constitute the terminal monosaccharides of animal protein glucidic residues (A. Varki 1992). They differ for the chemical substituents of their nine-carbon sugar ring and they are usually connected with other glucidic residues *via* α-glycoside linkage (**Figure 3**) (M. N. Matrosovich, Klenk and Kawaoka 2006; A. Varki 1992).

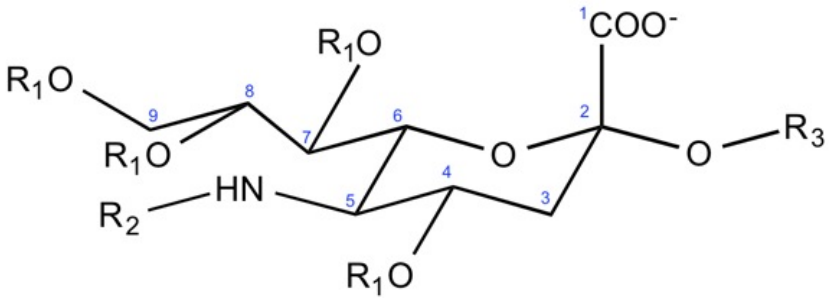

Figure 3: The sialic acids
The common sialic acid carbon ring is shown in the figure. R are the chemical substituents. The N-acetylneuraminic acid, possessing an N-acetyl in position 5 and hydrogen in all other substituents, is the most common sialic acid and a biosynthetic precursor of other sialic acids. R_3 is the α-glycoside linkage through which other sugars (D-galactose, N-acetyl-D-galactosamine, N-acetyl-D-glucosamine, and sialic acid) are attached, usually *via* their carbon 3 (α-2,3), 6 (α-2,6), and 8 (α-2,8) (M. N. Matrosovich, Klenk and Kawaoka 2006). Image adapted from (M. N. Matrosovich, Klenk and Kawaoka 2006) and (A. Varki 1992) using ChemBioDraw Ultra 14 (Perkin Elmer®).

The receptor binding site (RBS) is positioned in a pocket in the distal part of the HA head with the residues buried in the pocket tending to be conserved between different strains and subtypes (M. N. Matrosovich *et al.* 1997; Nobusawa *et al.* 1991; Weis *et al.* 1988). In contrast, residues forming the side of the pocket were shown to be responsible for receptor binding specificity, and can discriminate between different sialic acids (Gambaryan, Robertson and M. N. Matrosovich 1999; Govorkova *et al.* 1999; Vines *et al.* 1998; Rogers *et al.* 1983).

Usually the HA of avian origin viruses have higher affinity for α-2,3 sialic acids, whilst human viruses preferentially bind α-2,6 sialic acids (Meng, Marriott and Dimmock

2010; M. Matrosovich, J. Stech and Klenk 2009; Shinya *et al.* 2006; C. I. Thompson *et al.* 2006; M. N. Matrosovich, T. Y. Matrosovich, Gray, Roberts and Klenk 2004a; M. N. Matrosovich *et al.* 1997). This sialic acid HA specificity has important implications for influenza infection of human respiratory epithelial cells. In fact, in humans α-2,6 sialic acids are found in ciliated and non-ciliated cells, whereas ciliated cells present also α-2,3 sialic acids; additionally α-2,6 sialic acids are typical of the upper respiratory system (e.g. bronchi) cells, whereas α-2,3 sialic acids are found in alveoral cells (Shinya *et al.* 2006; M. N. Matrosovich, T. Y. Matrosovich, Gray, Roberts and Klenk 2004a). The virus binding affinity and specificity for sialic acid influences the infection site and the host range: avian origin viruses tend to infect non-ciliated cells and the lower respiratory system of humans (Shelton *et al.* 2011), whereas human viruses infect predominantly the upper respiratory system.

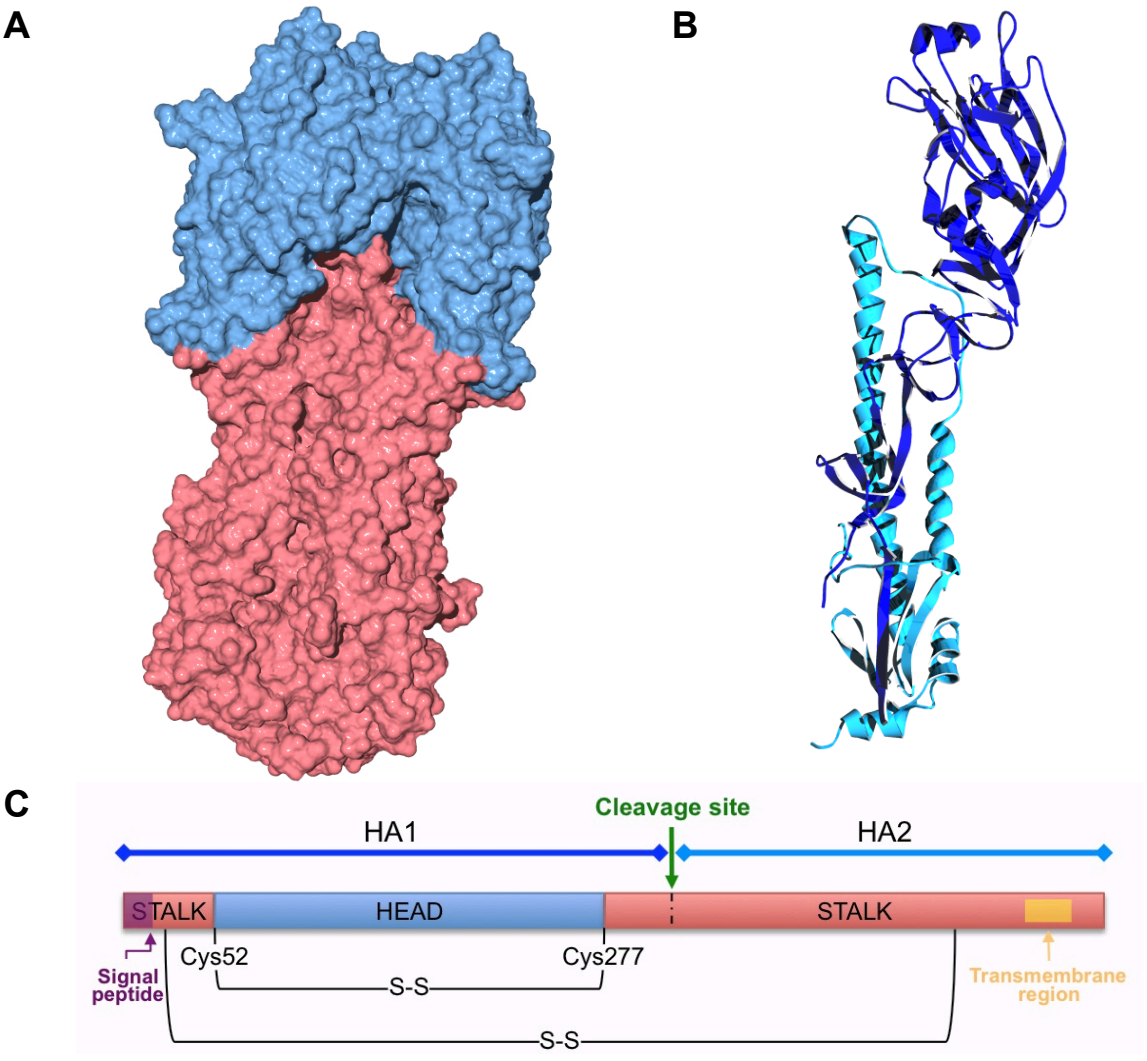

Figure 4: The influenza A HA
Three-dimensional structures were generated with Swiss PDB viewer and POV-Ray 3.7 using the structure of the recombinant virus A/Hong Kong/1/1968 X-31 H3 (PDB ID: 2VIU (Fleury *et al.* 1998)).
A. Three-dimensional structure of the influenza HA trimer, showing the HA surface of the head (blue) and stalk (red) regions; **B.** Three-dimensional ribbon structure of the influenza HA monomer showing HA1 (blue) and HA2 (light blue) subunits; **C.** Schematic of the HA polypeptide.

A second sialic acid binding site can be found in the central part of the HA head but the biological importance of this site is not clear since it does not seem to bind α-2,6 sialic acid (N. K. Sauter *et al.* 1992).

The role of HA in receptor binding and host specificity has been discussed, however, the property of binding sialic acid is not a feature common to all influenza A HA subtypes and strains. In fact, some strains were reported to be able to infect cells even in the absence of sialic acids where other proteins could mediate or facilitate the entry process instead (Londrigan *et al.* 2011; Reading, J. L. Miller and Anders 2000; Stray, Cummings and Air 2000). Furthermore, surprisingly, the HAs of the H17 and H18 subtypes show a putative RBS with different properties: the RBS base is relatively conserved with aromatic amino acids, but the other surrounding residues are substituted, resulting in a negatively charged region (Xiaoman Sun *et al.* 2013; Tong *et al.* 2013; Zhu *et al.* 2013). As a consequence H17 and H18 are not able to bind the canonical negatively charged receptors (α-2,3 and α-2,6 sialic acids), and other glycans (Xiaoman Sun *et al.* 2013). For these reasons, it was speculated that H17 and H18 could bind a protein receptor as the same switch is observed in viruses of the *Paramyxoviridae* family (Zhu *et al.* 2013).

Together with the receptor binding property, the HA mediates envelope-endosome fusion during infection, since a pH-mediated structural change exposes a α-helix fusion peptide present in the stalk region, and highly conserved between all influenza strains (**Figure 5A**) (X. Lin *et al.* 2014; Cross *et al.* 2001; C. Böttcher *et al.* 1999; Skehel *et al.* 1982). During this process (reviewed in Hamilton, Whittaker and Daniel 2012 and Skehel and Wiley 2000), the α-helices that compose the HA stalk rearrange and the stalk acquires the three dimensional structure of a rod-shaped α-helical bundle (Bullough *et al.* 1994). This structure is a common feature of other viral proteins that possess fusion activity, and also of the Soluble N-ethylmaleimide-sensitive factor Attachment Protein Receptors (SNARE) that mediate vesicle-membrane fusion (Skehel and Wiley 2000). The rod-shaped α-helical bundle is anchored by the C-terminal to the virus envelope membrane and the fusion peptide is free to insert itself into the endosome membrane, becoming anchored to it. Additional conformational changes to this structure permit to further bring together the two membranes, dehydrate the space between them and cause lipid mixing in a process called 'hemifusion'. Subsequentially, the membranes rupture forming a fusion pore, from which the internal proteins are released into the cytoplasm (**Figure 5B**) (Hamilton, Whittaker and Daniel 2012; Skehel and Wiley 2000).

Studies have now shown that a cluster of several HAs is necessary to mediate and complete the fusion process and HA amino acid residues can determine at which pH the conformational changes take place (Markovic *et al.* 2001).

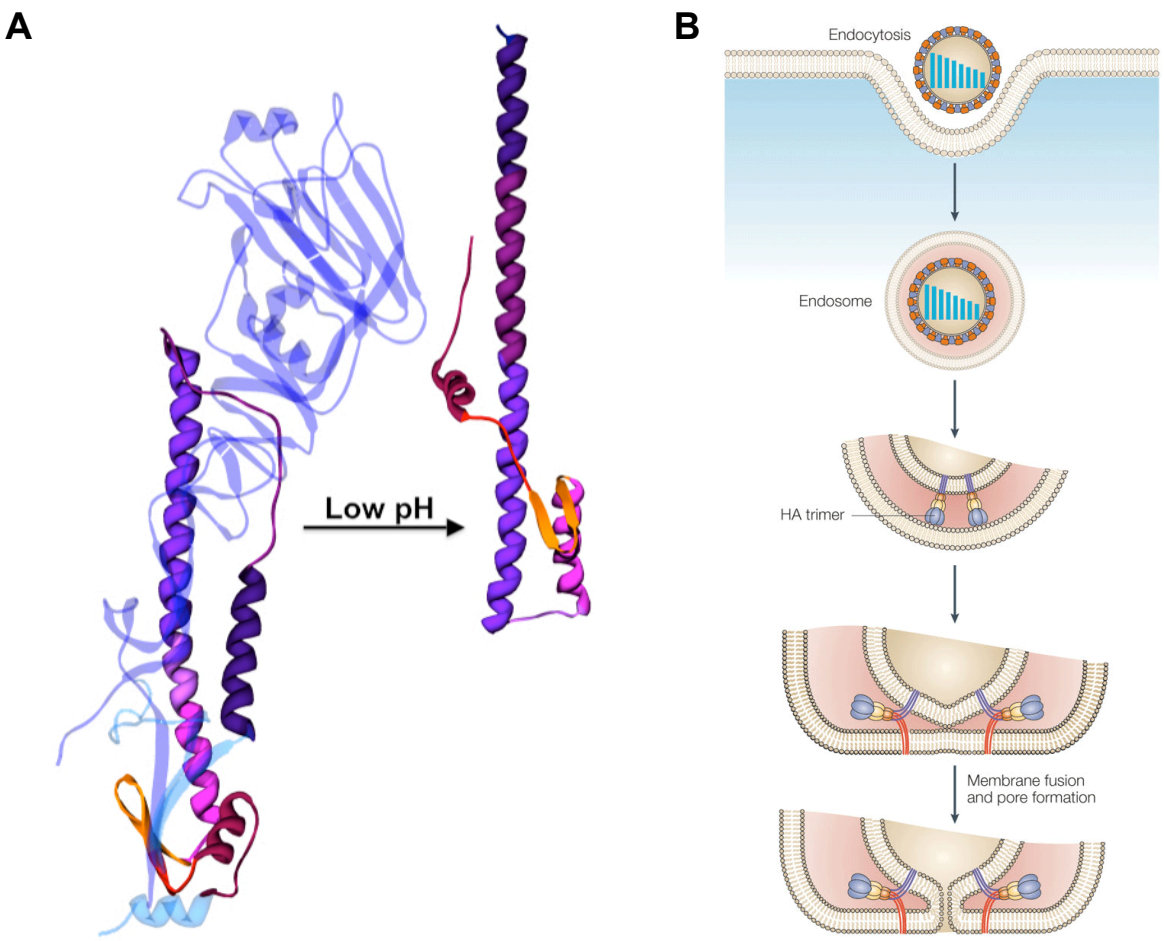

Figure 5: HA conformational change and fusion pore formation
A. Influenza HA (PDB ID: 2VIU (Fleury *et al.* 1998)) undergoes conformational changes (PDB ID: 1HTM (Bullough *et al.* 1994)) triggered by the low-pH environments of the endosome; **B.** The conformational change and fusion peptide permit the viral envelope and endosome membrane to be brought together and fuse (Figure adapted from Horimoto and Kawaoka 2005).

1.2.1.1 Haemagglutinin cleavage

To permit the conformational change at low pH, it is necessary that the HA is cleaved and the fusion peptide is exposed (Kido *et al.* 2008; J. Chen *et al.* 1998). The HA monomer is synthesised as a polypeptide precursor named HA0 (78kDa) which, after removal of a signal transport sequence in the N-terminal region, is cleaved into two subunits HA1 (50-58 kDa) and HA2 (28-22 kDa) during its maturation in the endoplasmic reticulum (ER), in the Golgi network or at the level of the plasma membrane. After cleavage, the two subunits remain connected with each other *via* a disulphide bond (Segal *et al.* 1992).

The HAs of influenza strains usually possess an arginine or a lysine immediately in front of the stalk fusion peptide. These residues are recognised by cellular proteases which then cleave the peptide bond between the arginine and the fusion peptide glycine, freeing the fusion peptide and activating the HA (**Figure 6A**) (J. Chen *et al.* 1998). The list of proteases that could be involved in HA cleavage is continuously expanding and it is

difficult to determine if only one protein is principally involved in HA activation (Böttcher-Friebertshäuser, Klenk and Garten 2013; Bertram, Glowacka, Steffen, *et al.* 2010). The soluble plasmin, tryptase Clara, and metalloproteases were described as able to activate HA, but other intracellular proteases, at the plasma membrane, or even secreted were described to be able to mediate the same process (Beaulieu *et al.* 2013; Hamilton and Whittaker 2013; Tse *et al.* 2013; Hamilton, Gludish and Whittaker 2012; Y. Chen *et al.* 2000; Kido *et al.* 1992). The cellular localisation of the proteases has important repercussions on HA activation. In fact, if the proteases have an intracellular expression, the HA cleavage occurs during HA synthesis; if the proteins are secreted or bound to the plasma membrane, HA activation can occur either during HA production or viral entry (Zmora and Pöhlmann 2014; Böttcher-Friebertshäuser *et al.* 2010). Proteins of the type II transmembrane serine proteases family, that have intracellular and plasma membrane expression, and also secreted forms, were extensively studied recently: especially the human airway trypsin-like protease (HAT, also known as type II Transmembrane Protease Serine 11D, TMPRSS11D), type II Transmembrane Protease Serine 2 (TMPRSS2), and type II Transmembrane Protease Serine 4 (TMPRSS4) were shown to be able to activate HA efficiently (Sakai *et al.* 2014; Tarnow *et al.* 2014; Baron *et al.* 2013; Bertram, Glowacka, Blazejewska, *et al.* 2010; E. Böttcher *et al.* 2006).

Furthermore, proteases of bacterial origin have been shown to be able to cleave HA, and this could have important implications for influenza morbidity related to secondary bacterial infection (Böttcher-Friebertshäuser, Klenk and Garten 2013). The HA cleavage site thus represents an important virulence determining factor (Steinhauer 1999).

Although it was noted above that influenza viruses usually possesses a single arginine at its cleavage site, during adaptation in poultry hosts they can develop a polybasic cleavage site characterised by several arginines and lysines and by a R-X-R/K-R consensus sequence (Horimoto *et al.* 1994). The proteases involved in the cleavage of a monobasic site have, in general, tissue-specific expression and influenza infection is usually restricted to the respiratory tract (in humans and avian species) and gastrointestinal tract (in avian species) (Bertram *et al.* 2012). However, the acquisition of a polybasic cleavage site results in a severe systematic infection since the virus is activated instead by ubiquitously expressed proteases such as furin and subtilisin-related protein convertase 5/6, and in certain cases, when a non-canonical site is present, by type II Transmembrane Protease Serine 13 (TMPRSS13) (Okumura *et al.* 2010; Stieneke-Gröber *et al.* 1992). Avian viruses that possess a polybasic cleavage site are usually named HPAI, whereas those that possess a single arginine (or lysine) are named LPAI (see Section 1.1) (**Figure 6B**). Nevertheless it should be noted that viruses harbouring HAs with a polybasic

cleavage site but showing a low pathogenic phenotype have been described (O. Stech *et al.* 2009).

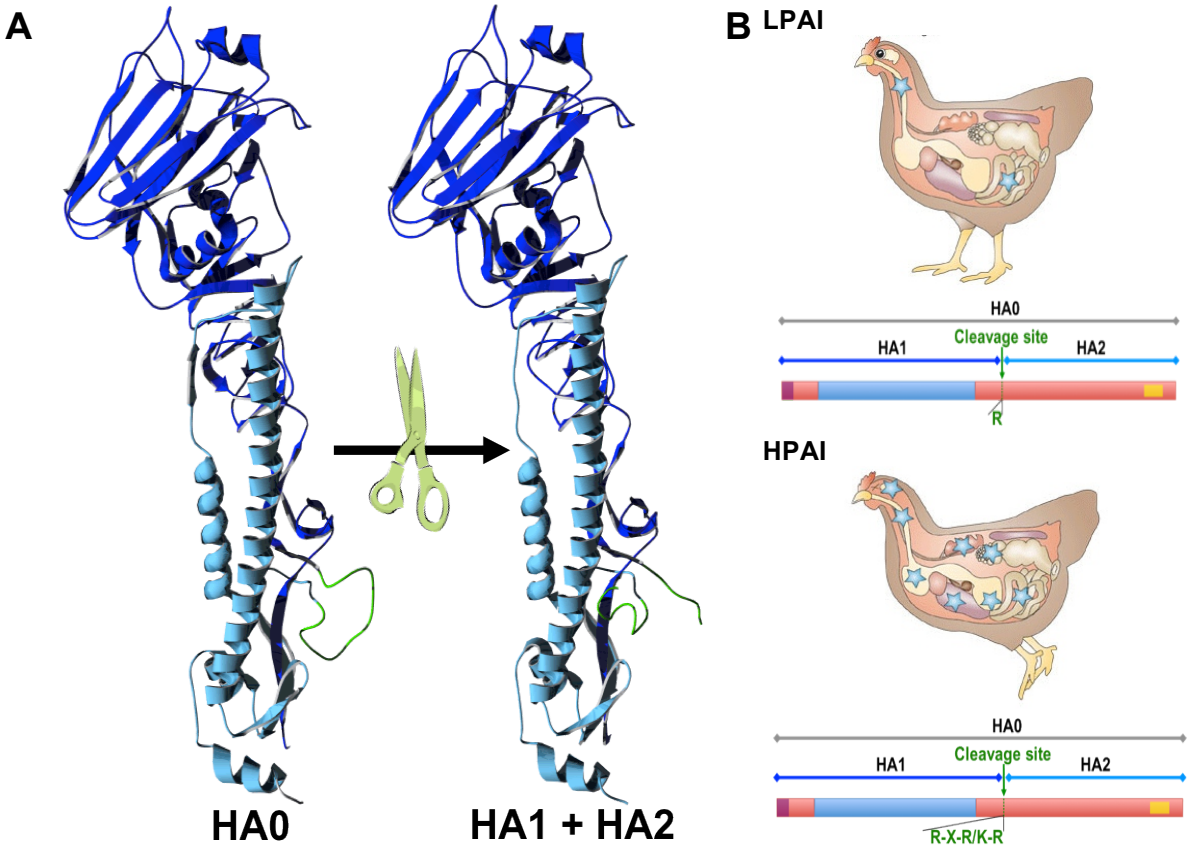

Figure 6: The HA cleavage
A. The HA0 monomer (PDB ID: 1HA0 (J. Chen *et al.* 1998)) is cleaved in the HA active form (PDB ID: 2VIU (Fleury *et al.* 1998)) by proteases; **B.** Differences in organ HA activation in HPAI and LPAI viruses. Image adapted from Horimoto and Kawaoka 2005.

The process by which the polybasic cleavage site is generated, and why only some HA subtypes efficiently support it are not yet clear. Recently, however, it was shown that it can result from recombination of the HA gene sequence with the viral NP gene or the even host ribosomal RNA (Orlich, Gottwald and Rott 1994; Khatchikian, Orlich and Rott 1989).

1.2.2 Neuraminidase

The NA (**Figure 7A**) is a mushroom-shaped homotetramer, a protein composed of four identical subunits; each monomer is anchored through the N-terminal transmembrane region to the viral envelope with a stalk region of variable length and a globular head domain, containing the active site (Shtyrya, Mochalova and Bovin 2009). Only the structure of the globular head has been resolved by crystallography (**Figure 7B**), since this region can be released and purified from the rest of the protein thanks to a cleavage site immediately after the stalk domain and before the globular head (Varghese *et al.* 1988).

In the influenza A NA a conserved N-terminal cytoplasmic tail is present in all NA subtypes, whilst in the influenza B NA it differs (Shtyrya, Mochalova and Bovin 2009).

The length of the NA stalk of influenza A viruses was recently shown to be associated with viral pathogenicity. Indeed upon transmission of virus from the avian wild bird reservoir to domestic poultry, NA short stalks are preferentially selected. Short NA stalks are also associated with enhanced replication and shedding of the virus in chickens but not in other animals (Hoffmann *et al.* 2011).

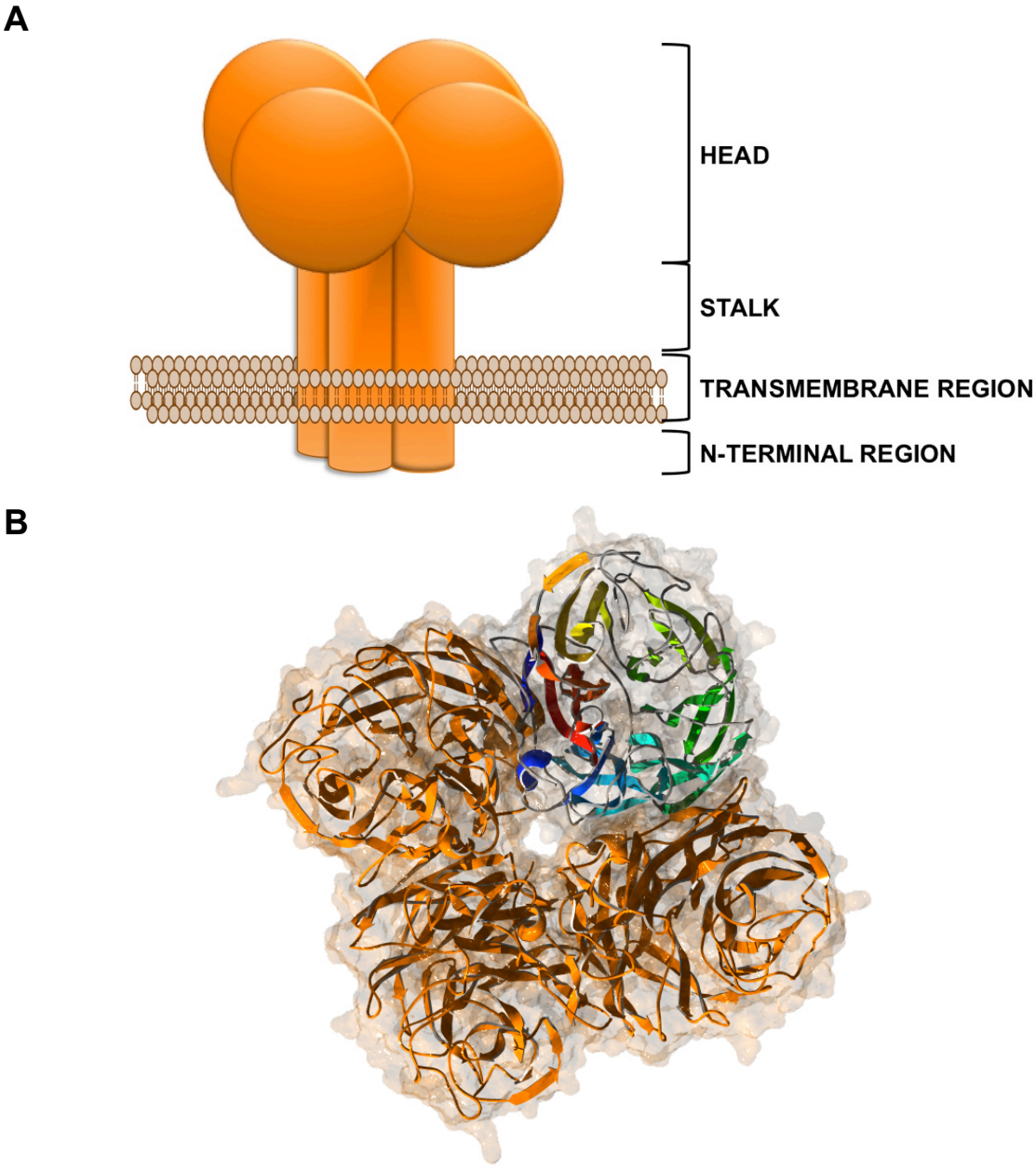

Figure 7: The structure of influenza A NA
A. Three-dimensional schematic of influenza NA; **B.** Three-dimensional structure of the NA head from A/Tokyo/3/1967 H2N2 (PDB ID:1NN2 (Varghese *et al.* 1988)). The image was obtained using Swiss PDB viewer and POV-Ray 3.7.

The NA globular head is a β-propeller in which six antiparallel β-sheets of four strands each are arranged around a nearly central symmetrical axis, with the active site positioned in a deep pocket near this region, at the side of the protein. The active site structure is generally conserved in all influenza A and B NAs but there are differences in

amino acid orientation near the active site cavity between the two influenza A NA groups (R. J. Russell *et al.* 2006).

The NA (Gottschalk 1957) is a sialidase that cleaves sialic acid from influenza infected cells to facilitate viral progeny release (Lentz and Air 1986; Palese *et al.* 1974). The NA was also shown to have a role in limiting influenza superinfection once expressed on the cell surface (I.-C. Huang *et al.* 2008).

For many years the activity of NA was exclusively associated with viral progeny release, and it was not clear if it could also influence viral binding to the receptor (Ohuchi *et al.* 2006). Only more recently was NA associated clearly with the viral entry process. In fact, *in vivo* its activity is also necessary to permit virus penetration of the mucus layer to arrive at the lung epithelia level (M. N. Matrosovich, T. Y. Matrosovich, Gray, Roberts and Klenk 2004b; Cohen *et al.* 2013). In addition, a more direct role of NA in receptor binding was also highlighted: circulating human H3N2 strains possess an NA mutation, D151G, near the active site that confers a remarkable sialic acid receptor-binding activity (Y. P. Lin *et al.* 2010). Recently other NA mutations have also been shown to mediate the same effect (Hooper and Bloom 2013).

As observed for the recently identified H17 and H18 subtypes, the associated NAs, N10 and N11, differ from the other influenza A NA subtypes since they do not possess sialidase activity, while maintaining three-dimensional structures similar to the other NAs (Tong *et al.* 2013; García-Sastre 2012; Qing Li *et al.* 2012; Zhu *et al.* 2012). However, the putative catalytic site is wider compared to the other NAs, and with largely substituted amino acid residues. It is possible that N10 and N11 possess a function not related to sialic acid cleavage or even viral progeny release (Tong *et al.* 2013; García-Sastre 2012).

The NA is extremely important, not only for its role in the viral replication cycle but also because it is the target of one of the influenza antiviral classes: the NA inhibitors (Moscona 2005; Gubareva, Kaiser and Hayden 2000).

NA inhibitors, osaltamivir and zanamivir, are sialic acid analogs that were designed on the basis of the NA globular head structure. They are able to block NA sialidase activity since they mimic the transition of the sialic acid structure during the cleavage reaction permitting the NA to be in a favourable energy state. Unfortunately the virus, through mutation of the NA, can develop resistance to NA inhibitors (Ferraris and Lina 2008). Another mechanism of resistance is mediated by mutation on HA to reduce affinity for the cellular receptor, enhancing viral particle release (Zambon, Hayden and Global Neuraminidase Inhibitor Susceptibility Network 2001).

The fact that HA mutations confer resistance to NA inhibitors indicates that the HA and NA are in a functional equilibrium that is necessary to permit viral entry and viral progeny release (Mitnaul *et al.* 2000; Kaverin *et al.* 1998).

1.2.3 The M2 ion channel

The M2 protein is a homotetramer in which four monomers of 96 amino acids are connected through disulphide bonds. Three domains can be identified: an N-terminal ectodomain of 23 amino acids, a 19 amino acid transmembrane domain, and a cytoplasmic tail of 54 amino acids (Lamb, Zebedee and C. D. Richardson 1985).

The M2 protein is an ion channel that permits the conductance of protons in an inward direction (from the extracellular domain to the intracellular) across the viral envelope (Pinto, Holsinger and Lamb 1992). Mutagenesis studies have shown that two residues present on the transmembrane region facing the internal surface of the channel pore, histidine 37 and tryptophan 41, are essential for proton selectivity and channel conductance (Tang *et al.* 2002; C. Wang, Lamb and Pinto 1995).

The M2 channel has numerous functions during the influenza virus replication cycle; some of these functions are mediated by its channel activity, others through its cytoplasmic tail (Pielak and J. J. Chou 2010b). Firstly, the M2 permits viral particle acidification after viral membrane-endosome fusion initiating viral uncoating, and release of vRNP (Pielak and J. J. Chou 2010b). Then it permits regulation of the pH of the Golgi network and the stabilisation of the native conformation of the HA during its transport through the network (Ciampor *et al.* 1992; Grambas and Hay 1992). Through its cytoplasmic tail, the M2 interacts with M1 and mediates the assembly of viral particles, especially in their filamentous form (Rossman *et al.* 2010). Furthermore, the M2 cytoplasmic tail, or to be precise, the amphipathic α-helix that permits cholesterol binding and localisation of the protein at the side of lipid rafts, was recently associated with viral membrane scission from the cellular membrane during virus release (Rossman *et al.* 2010).

The M2 it also important since it is the other viral protein targeted by antiviral drugs: amantadine and rimantadine. These two drugs are able to obstruct the ion channel pore, and they are effective in blocking viral replication (Cady *et al.* 2010). However, their use has been be discouraged since resistance arises quickly and tends to predominate in the viral population (Pielak and J. J. Chou 2010a).

Interestingly the M2 channel inhibitors do not have activity on the influenza B/M2, which is analogous and has similar functions to A/M2, demonstrating that the drug binding site differs between the two proteins (Pielak and J. J. Chou 2010a).

1.2.4 The NB ion channel

Influenza B virus possesses another ion channel on its envelope, in addition to B/M2, an ion channel called NB (Betakova, Nermut and Hay 1996; Brassard, Leser and Lamb 1996). NB is encoded by segment 6 of the influenza genome, along with NA (M. W. Shaw, Choppin and Lamb 1983). It has activity as a proton channel, but its conductance is lower than M2 and dependent on its oligomerisation (Kollerova and Betakova 2006; Fischer *et al.* 2000). NB appears unnecessary for viral replication but could have a role in determining replication efficiency (Hatta and Kawaoka 2003).

1.2.5 The M1 protein

The M1 protein is the most abundant protein in the virion, and mediates different but essential roles in the influenza replication cycle. Firstly it forms a matrix layer around the vRNPs and below the envelope, interacting with NEP, NP, HA, NA, M2, and the lipid bilayer. Only the N-terminal structure of the M1 is fully characterised, however, it has been shown that the M1 structure and oligomerisation properties are dependent on the pH of the biological environment (K. Zhang *et al.* 2012). This is not surprising since for the uncoating of the virus and the transport of the vRNPs into the nucleus (Section 1.3), it is necessary that the M1 dissociates from the vRNP, and this is mediated by the acidification of the internal viral environment.

In the cell nucleus, M1 is responsible for stopping RNA replication and, interacting with NEP, regulates the nuclear export of the vRNPs (Akarsu *et al.* 2003).

Furthermore, M1 allows viral particle assembly and shape, and it is the driving force of the budding process: its transfection into cells allows formation of virus-like particles (VLPs), particles harbouring the original envelope viral proteins and original viral core proteins but without genomic material (Gomez-Puertas *et al.* 2000).

1.2.6 The ribonucleoprotein complex

As explained earlier (Section 1.2), a vRNP is composed of the vRNA associated with the NPs and the polymerase complex.

The NP is a basic protein of 498 amino acids, arginine, serine and glycine-rich that confer a net positive charge at neutral pH (Ng, J. H. Wang and P. C. Shaw 2009). Each NP binds to the backbone of 25 nucleotide single-stranded vRNAs in a non-sequence-specific manner (Ortega *et al.* 2000; Baudin *et al.* 1994). Additionally NPs can also oligomerise with themselves and interact with PB1 and PB2 (Poole *et al.* 2004; Biswas, Boutz and D. P. Nayak 1998). Thanks to the presence of three nuclear localisation signals and to the fact that it interacts with filamentous actin and importins, NP is able to mediate the import of vRNP in the nucleus (Gabriel *et al.* 2011; Ng, J. H. Wang and P. C. Shaw 2009; Bullido *et*

al. 2000; Weber *et al.* 1998). Furthermore NP is also implicated in the regulation of vRNA transcription and replication (Momose *et al.* 2001).

Three different proteins, PB1, PB2, and PA, which interact with each other to mediate the transcription and replication of the vRNA, constitute the viral polymerase complex (Fodor 2013; Area *et al.* 2004). PB1 and PB2 interact *via* their N-terminal domains. PB1 interacts with PA through its C-terminal domain. Each protein has its specific function in vRNA replication and transcription (Fodor 2013). PB2 has a role in the vRNA replication process (Gastaminza *et al.* 2003) but also a fundamental function in the transcription of the viral messenger RNA (mRNA), because it binds the 5'-methylated cap of host cell RNAs that are then cut and utilised by the PB1 for elongating the viral transcript. In fact, PB1 is the protein that is homologous to other segmented negative-strand RNA-dependent polymerases and possesses polymerase activity catalysing the addition of ribonucleotides (Biswas and D. P. Nayak 1994; Poch *et al.* 1989). PB1 also mediates the interaction between the vRNA 5' and 3' terminii, permitting the initiation of transcription and replication (Gonzalez and Ortin 1999). On the other hand, the specific role of PA is not yet completely understood. It does however have a role in the 'cap-snatching' of the host mRNA (Dias *et al.* 2009).

The proteins of the polymerase complex are also associated with pathogenicity. For example, the amino acid in position 627 of PB2 is associated with viral replication efficiency in different hosts. Viruses possessing a lysine in this position are able to replicate more efficiently in mammalian cells at 33°C while viruses with a glutamic acid replicate better in the avian host (Massin *et al.* 2010; E. K. Subbarao, London and Murphy 1993).

1.2.7 Non-structural proteins

1.2.7.1 Non-structural protein 1

The non-structural protein 1 (NS1) is expressed at high levels in infected cells where it exhibits nuclear localisation (Krug and Etkind 1973). NS1 is multifunctional during viral replication (Hale *et al.* 2008). The main function is to antagonise the antiviral response mediated by interferon (IFN) especially by directly recognising the IFN induced MxA protein (see Section 1.6.1). The IFN antagonistic effect was discovered through studies with an influenza virus lacking the NS1 gene: this mutant virus was characterised by an attenuated phenotype, and could replicate efficiently only in absence of IFN (García-Sastre *et al.* 1998). The other functions in which NS1 is involved are the control of viral splicing, temporal regulation of vRNA synthesis, and enhancing translation of viral mRNA (Hale *et al.* 2008).

1.2.7.2 Nuclear export protein

The NEP, also known as non-structural protein 2 (NS2) was originally considered to be a non-structural protein, but it is now known that it is associated with M1 in the virion (J. C. Richardson and Akkina 1991). In infected cells, the subcellular localisation of NEP is both nuclear and cytoplasmic (Greenspan *et al.* 1985). In fact, NEP possesses a nuclear export signal that contains a region rich in leucine allowing the interaction with esportine protein family members, which are responsible for the transport from the nucleus to the cytoplasm (O'Neill, Talon and Palese 1998). Through interaction with M1, NEP allows the export of newly formed vRNP from the nucleus to the cytoplasm to permit virion assembly (Akarsu *et al.* 2003; Cros and Palese 2003; O'Neill, Talon and Palese 1998).

1.2.8 Accessory proteins

Among the recently identified accessory proteins only two are characterised in any detail: PB1-F2 and PA-X.

1.2.8.1 PB1-F2

PB1-F2 is encoded by the second segment of the influenza virus genome in a reading frame alternative to PB1. It is a protein of 87 amino acids produced early during the viral life cycle (W. Chen *et al.* 2001). It can be found in many avian and human isolates, although in viruses of swine origin the sequence coding for PB1-F2 is interrupted by a stop codon (W. Chen *et al.* 2001).

PB1-F2 induces apoptosis by depolarising the mitochondrial membrane due to a C-terminal mitochondrial localisation sequence composed of an amphipathic and positively charged α-helix (Chakrabarti and Pasricha 2013; Yamada *et al.* 2004; Gibbs *et al.* 2003). It was shown that occasionally, PB1-F2 can also have nuclear localisation and can regulate polymerase activity (Chakrabarti and Pasricha 2013). Furthermore PB1-F2 appears to be an important factor contributing to influenza virus pathogenicity (Chakrabarti and Pasricha 2013; Conenello and Palese 2007). Using mouse models, increasing pulmonary inflammation, higher incidence of secondary pneumonia, and increasing mortality rate were observed when a PB1-F2 expressing influenza virus was used compared to an influenza virus modified to reduce the expression of PB1-F2 (McAuley *et al.* 2007; Zamarin, Ortigoza and Palese 2006).

1.2.8.2 PA-X

PA-X was recently identified as the protein encoded by the second reading frame present in segment 3 (Jagger *et al.* 2012). PA-X is expressed during virus replication but it

does not possess a significant role in viral growth. PA-X is important in host mRNA degradation regulation and thus host gene expression, especially genes related to inflammation, immune response, apoptosis, cell differentiation, and tissue remodelling (Jagger *et al.* 2012).

1.3 Viral life cycle

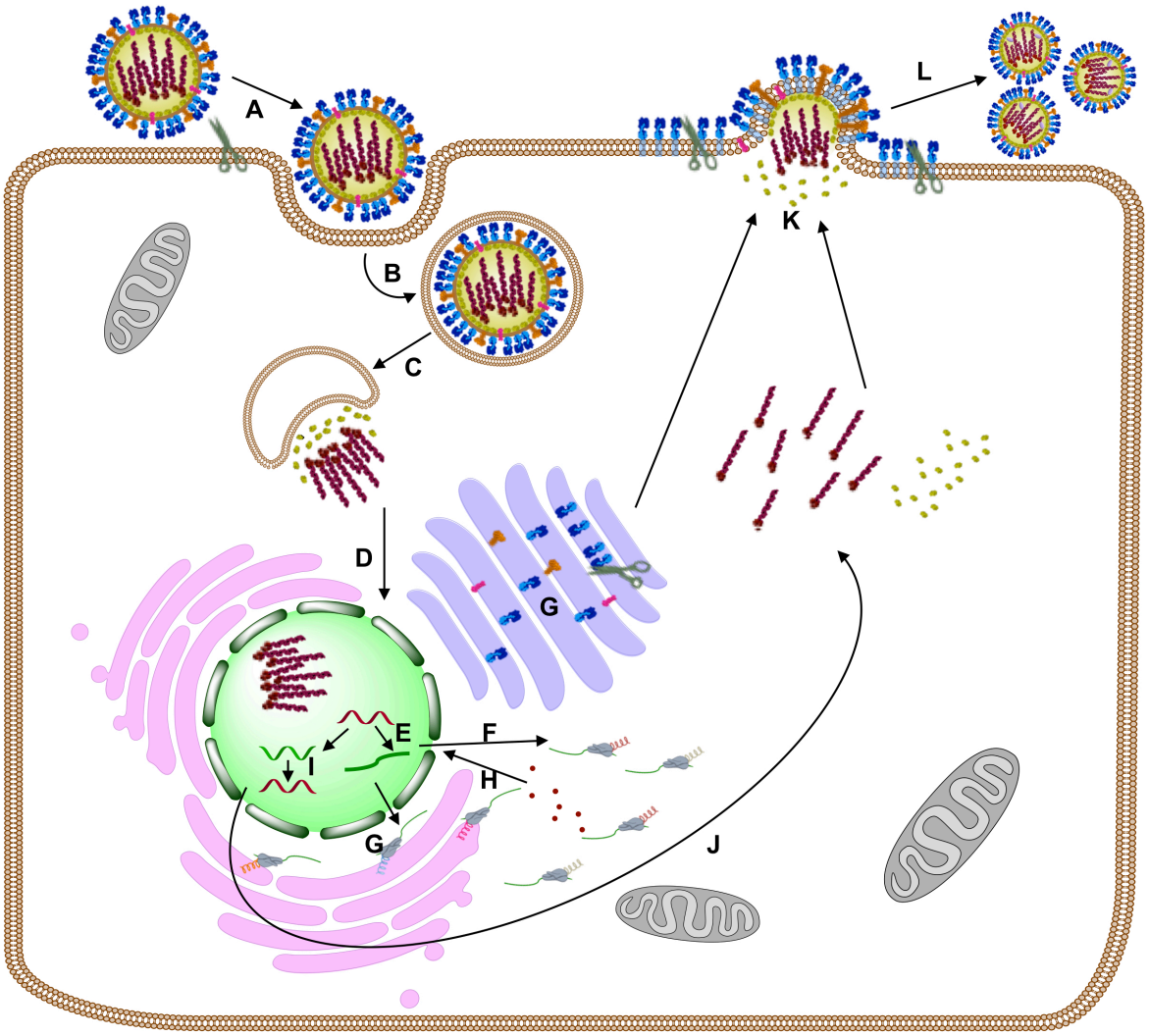

Figure 8: Influenza viral life cycle

A. Influenza virus binds the cellular receptor and its HAs can be activated by cellular proteases present on the cellular membrane; **B.** Influenza virus is endocytosed by cells and the low endosomal pH triggers HA conformational changes leading to envelope-endosome fusion; **C.** Uncoating of the virus with release of RNPs; **D.** The viral genome is transported to the nucleus; **E.** Transcription of viral protein genes take place; **F.** Transcripts are translated by ribosomes to produce viral proteins; **G.** Envelope proteins follow the endoplasmatic reticulum/Golgi pathway where post-translational modifications take place and HAs can be activated by proteases; **H.** NPs, polymerases, and NS2 proteins are instead translocated into the nucleus; **I.** Negative-sense viral genome is replicated through the synthesis of an RNA positive intermediate; **J.** NP, polymerases and NS2 assemble with the genome and RNPs are exported into the cytosol; **K.** Viral assembly takes place at the level of the cellular membrane and during this process HAs can be activated by cellular proteases. **L.** New virions are released thanks to M2 scission activity and NA sialidase activity.
The image was generated using ChemBioDraw Ultra 14 and Microsoft® Power Point.

The influenza virus binds, *via* the HAs, to the sialic acid residues on the surface of host cell glycoproteins (Hidari *et al.* 2013). Following binding to sialic acid, the influenza virus enters cells by receptor-mediated endocytosis usually by using clathrin-coated vesicles and dependent on dynamin (Edinger, Pohl and Stertz 2014; Lakadamyali *et al.* 2003). Recently, however it was shown that influenza virus can enter host cells also in a clathrin-independent manner as well as *via* macropinocytosis (Sieczkarski and Whittaker 2002; de Vries *et al.* 2011). After internalisation, the vesicle containing the virus fuses with primary endosomes, characterised by a mild acidic environment, which then progress to the late endosomes (Lakadamyali *et al.* 2003; Sieczkarski and Whittaker 2002). In general, the macromolecular complexes internalised by endocytosis, after crossing the endosomal compartment, are transported to lysosomes where they undergo degradation mediated by hydrolytic enzymes (Sieczkarski and Whittaker 2002). The influenza virus escapes degradation through the fusion of its envelope with the endosomal membrane. In fact, the low pH of the endosomes (5-6) promotes the start of the HA conformational changes (Doms, Helenius and J. White 1985; Yoshimura and Ohnishi 1984; Skehel *et al.* 1982) and the HA fusion peptide is inserted into the endosome membrane. In this way the HA becomes anchored to the viral membrane *via* the HA2 C-terminal, and to the endosomal membrane *via* the N-terminal part of HA2 (Hamilton, Whittaker and Daniel 2012; Skehel and Wiley 2000). This juxtaposition of the membranes involving a hemifusion process permits a pore to be generated and the genetic material is released into the cytoplasm (Hamilton, Whittaker and Daniel 2012; Skehel and Wiley 2000). The release of vRNP is also facilitated by the acidification of the interior of the virus particle mediated by the M2 ion channel (Bui, Whittaker and Helenius 1996), which weakens the interactions of M1 with the viral envelope and the vRNPs (Martin and Helenius 1991).

Since the processes of replication and transcription of vRNA occur in the nucleus, it is necessary for the vRNPs to be transported into the nucleus (Martin and Helenius 1991). This process, given the size of the complex vRNP, requires active transport: the vRNPs are recognised by the α-importin that by interacting with β-importin makes contact with the nuclear pore (Gabriel *et al.* 2011; P. Wang, Palese and O'Neill 1997; O'Neill *et al.* 1995). At this point other cellular proteins allow the transport of each vRNP through the nuclear pore complex, expending energy in the form of adenosine triphosphate (ATP) (Cros and Palese 2003).

In the host cell nucleus the processes of transcription and replication of the vRNA take place (Fodor 2013). The vRNA-dependent RNA-polymerase uses the negative sense RNA as template to synthesise the mRNAs, which are then transported into the cytoplasm to be used for the production of viral proteins. Transcription starts with the complex of the

viral polymerase bound to vRNA (Fodor, Pritlove and Brownlee 1994). This causes a conformational change that activates PB2. PB2 recruits cellular mRNA (M. L. Li, Ramirez and Krug 1998; Cianci, Tiley and Krystal 1995) of which the 5' cap is cleaved by PB1 and PA to be used as primer during transcription (Dias *et al.* 2009). This process is called 'cap snatching'. Subsequently, the PB1 starts to elongate the cap structure using the vRNA as template starting from the 3' end until the polymerase finds 5-7 uracils present at the 5' end of the vRNA: the polymerase transcribes these bases into a string of adenosines which forms the poly-adenosine tail (Robertson, Schubert and Lazzarini 1981). When splicing of mRNA is necessary to derive more mRNAs, such as for the production of the proteins encoded by segments 7 and 8, host cell proteins are usually exploited, but viral factors can also play a role (Lamb and C. J. Lai 1984; Lamb and C. J. Lai 1982). Since the mRNA synthesised is polyadenylated and possesses the cellular 5' cap, it can be exported out of the nucleus to allow the synthesis of viral proteins. The new polymerase proteins, the NPs, the M1, and the NEP are produced and imported into the nucleus. In fact, the replication of the vRNA starts only after an initial phase of transcription of mRNA and protein synthesis (Fodor 2013).

During replication, the viral polymerase copies the vRNA into complementary RNA (cRNA) that is then used as a template for the synthesis of new vRNA. Since, unlike the mRNA, the cRNA is exactly a positive polarity copy of the vRNA genome, the replication mechanism differs from transcription (Fodor 2013). It starts with the production of dinucleotide structures by the viral polymerase itself or by cellular enzymes. These dinucleotide structures are then exploited by the viral polymerase to start replication (Fodor 2013). It appears that newly synthesised NPs have a role in the transition from the synthesis of mRNAs to the primer-independent production of cRNA (Biswas, Boutz and D. P. Nayak 1998). Furthermore, recent studies have shown that the vRNA replication process is mediated by newly synthesised polymerases (Fodor 2013). When the replication of the vRNA is finished, new vRNP assemble in the nucleus and their nuclear export is mediated by the newly synthesised M1 and NS2 (D. P. Nayak *et al.* 2009; O'Neill, Talon and Palese 1998).

In the meantime, the envelope proteins are also synthesised by ribosomes associated with the membrane in the ER. This occurs outside the nucleus starting from the mRNA produced during the transcription phases. The envelope proteins then undergo maturation and folding, travelling through the Golgi network in which post-translational modification takes place (Doms *et al.* 1993). Since the three envelope proteins have a sorting signal in the transmembrane domain, they are directed, *via* the exocytosis

mechanism, towards the apical surface of the cell membrane (Rodriguez-Boulan, Paskiet and Sabatini 1983).

Once in the cytoplasm, all the internal components of the virion assemble, with the M1 acting as an adaptor between the cytoplasmic membrane, the envelope proteins, and the vRNP (D. P. Nayak *et al.* 2009). The new virions, in order to be infectious must contain all the eight genomic segments (Sugita *et al.* 2013). Evidence now suggests that the packaging is dependent on specific signals presented on all vRNA (Y.-Y. Chou *et al.* 2012). This enables the entire genome to be incorporated into most of the viral particles.

The mechanism of viral budding initiation is not yet clear, however, the final membrane scission is better understood (Rossman and Lamb 2011; D. P. Nayak *et al.* 2009). It seems that the envelope proteins permit the curvature of the membrane initiating the process (Rossman *et al.* 2010). Conversely, in the final budding steps, it is only M2 that, localising on the lipid raft borders, changes the curvature of the budding membrane and, due to its cytoplasmic tail, permits the membrane scission (Rossman *et al.* 2010).

Finally, to release the progeny viruses from the cell surface, the action of NA is required to remove sialic acid from the cell surface. This process prevents new virions sticking to the membrane or aggregating on the cell surface (Wagner, M. Matrosovich and Klenk 2002).

1.4 Ecology and epidemiology of influenza viruses

The three influenza virus types (A, B, and C) infect different mammalian and avian species. Influenza A viruses are disease-causing agents in mammals and birds, and the viruses harbouring the first sixteen HAs have a reservoir in wild birds, especially *Charadriiformes* (gulls) and *Anseriformes* (ducks) (Olsen *et al.* 2006; Webster *et al.* 1992). To date, viruses harbouring H17 and H18 have only been isolated in bats (Tong *et al.* 2013; Tong *et al.* 2012). In humans only influenza A viruses that harbour H1 or H3 HA in their envelope routinely circulate during winter seasons, causing annual epidemics (Graham-Rowe 2011; Monto 2008).

Influenza B infects humans causing seasonal epidemics (R. Chen and Holmes 2008). Influenza B has also been reported to infect other mammalian species, such as seals (Osterhaus *et al.* 2000).

Influenza C infects appears to exclusively[1] infect humans and, even if its spread is limited in the human population, it can cause severe disease (e.g. pneumonia) (Principi *et al.* 2013).

In wild avian species LPAI virus was believed to be avirulent. Recently, however, it has become clear that virus infection, even if it does not routinely cause an increase in mortality rates, can be associated with reduced body weight and slight increase of the body temperature. Histological findings of tissue damage at the level of the gastrointestinal or the respiratory tracts are also described. In contrast, chickens can show symptomatology such as diarrhoea, coughing, sneezing, and ocular discharge (Kuiken 2013; Pantin-Jackwood and Swayne 2009).

HPAI viruses in domestic poultry produce high mortality rates, associated with systemic disease comprising oedema, haemorrhage, and multiple organ failure (Swayne 2000). When transmitted to wild birds or other avian species they can occasionally be associated with mortality in these hosts (Swayne 2000).

In humans, influenza viruses cause respiratory disease with variable severity of clinical symptoms. The infection can be asymptomatic, limited to the respiratory tract or can be associated with extremely severe complications (e.g. pneumonia, myocarditis, influenza-associated myositis, rhabdomyolysis, encephalitis, Reye syndrome, and Guillain–Barré syndrome). Classic influenza symptoms includes: fever, cough, sore throat, runny or stuffy nose, muscle or body aches, headaches, fatigue (Centers for Disease Control and Prevention (CDC) n.d.; Monto *et al.* 2000). The sudden onset and presence of fever, myalgia, headaches, and fatigue allows differential clinical diagnosis and permits distinguishing influenza from the common cold (rhinoviruses) or from respiratory disease caused by other viral pathogens (e.g. coronaviruses, respiratory syncytial virus) (Eccles 2005). The clinical course of infection depends on the virulence and the infected individual: age (children or elder people), presence of previous morbidity affecting the heart (cardiopatic disease and/or hypertension) or lungs (e.g. asthma), diabetes, pregnancy, and immunosuppression are risk factors for influenza complications (Junge 2011; Monto 2008). Some genetic determinants can also play a role in the development of severe disease (T.-Y. Lin and Brass 2013; Horby *et al.* 2012).

[1] As mentioned in Section 1.1 the influenza virus distantly related to human influenza C virus isolated in swine and cattle, provisionally named C/swine/Oklahoma/1334/2011, could represent a new influenza *genus*/type (Collin *et al.* 2014; Hause *et al.* 2014; Hause *et al.* 2013; Sheng *et al.* 2013).

1.4.1 Antigenic shift and antigenic drift

The epidemiological success of influenza viruses is probably related to their two mechanisms of evolution of the two surface glycoproteins, HA and NA.

Due to the low replication fidelity of the vRNA dependent RNA polymerase, influenza A viruses and influenza B viruses undergo frequent mutations leading to the continuous appearance of new virus variants (Zambon 1999). When the virus variants are replication-competent and the mutations do not influence viral protein functions, they can be naturally selected, if due to these changes the virus can escape the host immune response, especially the antibody response. Since the antibodies are primarily directed against the envelope proteins these antigenic changes are found especially on the two surface glycoproteins, HA and NA. This evolutionary mechanism is referred to as antigenic drift, to indicate the progressive nature of the antigenic changes (**Figure 9A**).

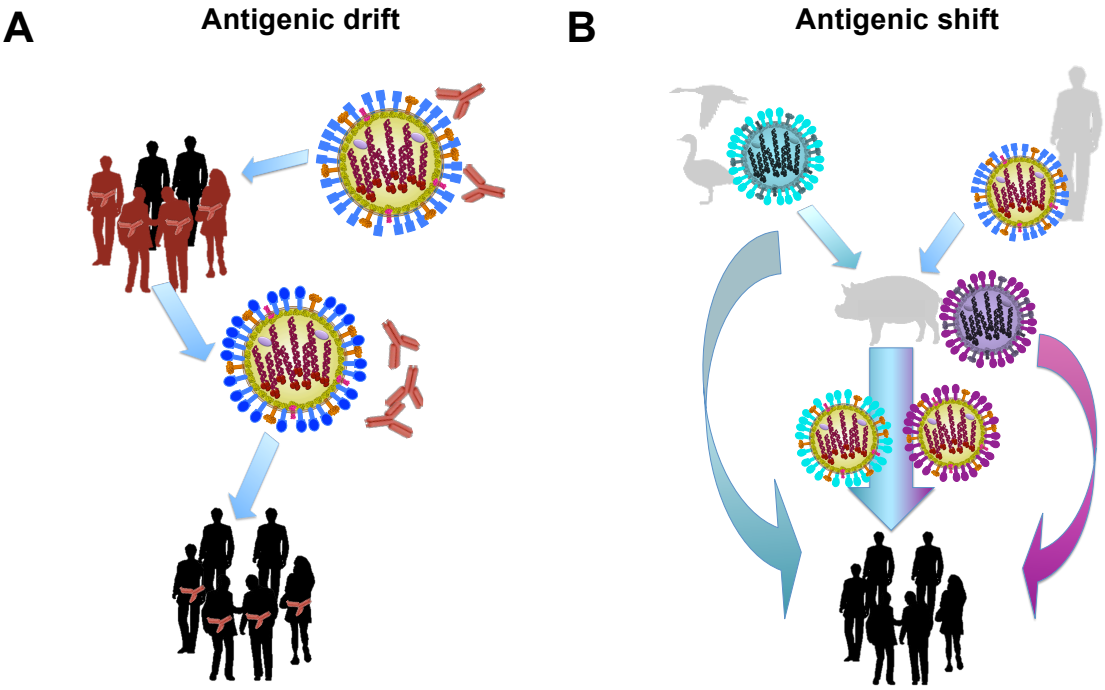

Figure 9: Antigenic drift and antigenic shift
A. A part of the human population possesses antibodies against the influenza virus; however the virus can escape this immune response via envelope protein mutations, leading to an epidemic in the humans now mostly naïve for the new antigenic variant virus; **B.** Avian and swine viruses that possess envelope proteins antigenically distinct from the ones circulating in the human population can infect humans directly or after recombination with human viruses in an intermediate host.

The ability of influenza viruses to undergo antigenic drift has particular implications for influenza vaccination in humans. Every year the WHO changes the seasonal vaccine composition on the basis of surveillance data in order to match the predicted circulating strain (Gerdil 2003). This choice is made twice each year: for the northern hemisphere in February (for the next winter), the other for the southern hemisphere in October (Gerdil 2003). The strains to be included in the vaccine are selected

in advance since for vaccine production, clinical trials, and stock piling, at least 6 months are necessary (Gerdil 2003; Wood and Levandowski 2003). Since the strain selection is made months before the onset of seasonal epidemics, occasionally the virus that circulates during the seasonal epidemic does not match the vaccine strains, impairing vaccine coverage.

It is now becoming evident, however, that even in the presence of a drift variant, the population is not completely immunologically naïve. This is due mainly to the presence of cross-reactive immune responses. These cross-reactive responses, mediated by T and B memory cells (see Section 1.6.2), are able to protect from or, at least, mitigate influenza infection. How widespread and how broad this cross-reactivity immunity is in the human population is however still unclear and numerous studies are now focusing on understanding its biological basis.

In addition to antigenic drift, influenza A viruses are subjected to a second evolution mechanism, named antigenic shift (**Figure 9B**). Since influenza viruses have a segmented genome, recombination between human, avian and/or swine virus, can occur if these viruses infect the same host (Freidl *et al.* 2014). Often these 'mixing vessels' are pigs since the swine respiratory epithelium possesses both α-2,6 and α-2,3 sialic acids, thus avian and human virus can infect them with similar efficiency (Trebbien, Larsen and Viuff 2011). Furthermore, the swine host also represents a way by which human strains are 'archived' and can re-emerge (Tharakaraman *et al.* 2013). Since swine are usually the host in which the original avian virus has adapted, this virus tends to circulate within the swine population (Tharakaraman *et al.* 2013). The virus then can re-infect humans, if it comes in contact with an immunologically naïve human population.

In certain cases, however, avian viruses are also able to directly infect the human host. This is due primarily to the fact that the human respiratory epithelia also possess the avian virus receptor, as previously mentioned (Section 1.2.1).

Often to permit efficient transmission and replication in the new host, influenza viruses need to undergo additional mutations, usually involving the HA RBS, and polymerase genes (see Section 1.2.6). This was recently highlighted by 'gain-of-function' experiments (Herfst *et al.* 2012; Imai *et al.* 2012). In these experiments, viruses, which have been shown previously to replicate in humans, were modified and passaged in the ferret animal model, acquiring efficient replication and transmission. This has permitted the identification of possible viral characteristics and molecular markers related to efficient replication and transmission in the human host (Tejeda and Capua 2013; C. A. Russell *et al.* 2012).

Since different antigenic envelope protein subtypes of influenza A circulate in the animal reservoirs, a virus with a new combination of HA and NA, if able to efficiently replicate, could spread in a completely immunological naïve human population, potentially causing a pandemic. In fact, the antigenic shift mechanism was the basis of the emergence of past influenza pandemics (G. J. D. Smith *et al.* 2009).

1.4.2 Influenza pandemics and pandemic preparedness

In 1918 an avian-like human-adapted H1N1 virus started to circulate in the human population causing the first pandemic of the twentieth century (Taubenberger and Morens 2006; Reid, Taubenberger and Fanning 2004). Subsequently the 1918 virus underwent antigenic drift mutations and then circulated as a seasonal strain until 1957 when a reassortment with an avian virus occurred (G. J. D. Smith *et al.* 2009). This new virus had acquired the avian origin envelope proteins of H2 and N2 subtypes. H2N2 viruses circulated for 10 years until, in 1968, they disappeared from the human population after a further reassortment event occurred and the H3N2 pandemic strain emerged (G. J. D. Smith *et al.* 2009). After the pandemic, H3N2 strains have continued circulating even after the reappearance of an H1N1 virus in 1976 (Scholtissek *et al.* 1978). This virus has subsequently become a seasonal strain (Both *et al.* 1983).

In addition to viruses with H1, H2 and H3 HA, viruses of avian origin from other HA subtypes (e.g. H5, H7, H9, and more recently H6 and H10) have been shown to directly infect humans (H. Chen *et al.* 2014; Gao *et al.* 2013; Yuan *et al.* 2013; Apisarnthanarak *et al.* 2004; Koopmans *et al.* 2004; Claas, de Jong, *et al.* 1998; Claas, Osterhaus, *et al.* 1998). If these viruses were to acquire efficient human-to-human transmission they could potentially cause pandemics.

At the start of the 21st century it was believed that the next pandemic could emerge either from a reassortment between human viruses and viruses belonging to HPAI H5 or H7 subtypes (predominantly circulating in poultry) or from an adaptation of these HPAI H5 or H7 viruses to the human host (Katz 2003; Horimoto and Kawaoka 2001). For this reason active surveillance, collaborative networks, vaccines and pandemic plans were developed to monitor and block the circulation of these subtypes in poultry populations around the world (Bogner *et al.* 2006). This in part led to the surveillance of other virus subtypes being neglected: for example, the emergence of new avian or swine-origin H1 or H3 viruses was believed not to be of particular concern since previously pandemics have originated from viruses with HA subtypes different from the subtype already circulating in the human population (Peiris, Poon and Guan 2012; Capua *et al.* 2009). Eventually a quadruple H1N1 reassortant virus emerged causing the first pandemic of the 21st century

after reassortment between two swine viruses: one was a Eurasian avian-like swine virus, the other originated previously through reassortment of north American avian, classical swine and human (H3N2) viruses (Neumann, Noda and Kawaoka 2009; Novel Swine-Origin Influenza A H1N1 Virus Investigation Team *et al.* 2009; Zimmer and Burke 2009).

In China, at the start of 2013, a recombinant LPAI H7N9 virus emerged (Gao *et al.* 2013). This can easily infect humans causing severe respiratory syndrome but does not have the capacity for efficient human-to-human transmission (Qun Li *et al.* 2013). Studies have shown that this virus and similar viruses have been circulating undetected in the avian reservoir and probably in poultry, and that this was ongoing for at least one year prior to the emergence of the human strains (Kageyama *et al.* 2013; Liu *et al.* 2013; Van Ranst and Lemey 2013). More recently, viruses belonging to the H10 and H6 subtypes have also been shown to infect humans creating concerns for possible diffusion (García-Sastre and Schmolke 2014; Montomoli and Maria 2014; G. Wang *et al.* 2014).

All these instances have shown that, to carry out effective pandemic preparedness of zoonotic viruses such as influenza, it is necessary to implement continuous surveillance. For example HPAI H7 and H5 viruses are symptomatic and are included in the diseases that need to be notified to the authorities; for this reason when outbreaks are registered, culling of poultry is rapidly implemented to block the spread of the disease and this has permitted a straightforward way to monitor the spread of this viruses (Peiris, Poon and Guan 2012). However, LPAI influenza and swine influenza are sometimes asymptomatic and they require the monitoring of both ill and healthy animals (especially live-stock) since these viruses can infect undetected for long periods of time (Peiris, Poon and Guan 2012).

For this reason it is necessary to monitor the viruses circulating in all animal reservoirs through virus isolation and identification (with classical and molecular biology methods reviewed in Belák, Kiss and Viljoen 2009, Cattoli and Terregino 2008, and Cattoli and Capua 2007), and with sero-epidemiology studies in animals and in humans to predict possible emerging viruses (Capua and Cattoli 2010). Another important monitoring aspect is the collection of viral gene sequences (Squires *et al.* 2012; Liu *et al.* 2009; Bao *et al.* 2008) since with bioinformatic analyses it is now possible to identify molecular markers that can help to recognise viruses that pose pandemic risks (Tejeda and Capua 2013; D. Smith 2003). This "One Health" approach (*"To improve health and well-being through the prevention of risks and the mitigation of effects of crises that originate at the interface between humans, animals and their various environments"* (One Health Global Network n.d.)) is now widely accepted by the international community and applied with common effort by Food and Agricultural Organization of the United Nations (FAO), and World

Organization for Animal Health (OIE), WHO, and Centers for Disease Control and Prevention (CDC).

1.5 Influenza virus pathogenicity: an equilibrium between viral diversity, host genetics and adaptive immunity

The pathogenicity of influenza virus in humans and in animals is primarily related to genetic factors of the virus. In Sections 1.2.1.1 and 1.4 it was previously shown how the property of the HA cleavage site can influence the pathogenesis and can cause systemic infection. Other factors, such as mutations in the polymerase proteins, in the HA RBS and related to the NA stalk length are known to determine a higher efficiency of viral replication in one host compared to another (Gambaryan, Robertson and M. N. Matrosovich 1999; E. K. Subbarao, London and Murphy 1993). Furthermore, the expression of accessory genes (or their variants) can be associated with increased disease severity (McAuley *et al.* 2007; Zamarin, Ortigoza and Palese 2006) .

However, recently, thanks to the use of animal models and genome-wide association studies in infectious disease research, it is becoming clear that host genetic factors play a role in determining influenza pathogenicity (T.-Y. Lin and Brass 2013). For example, the presence or absence of certain genes (some associated with the innate immune system) can confer resistance to influenza in animal models (Horby *et al.* 2012). Furthermore a polymorphism in a protein, interferon-induced transmembrane protein 3 (IFTIM3), which can interfere with influenza virus entry, was associated with increased influenza severity in humans (Everitt *et al.* 2012).

Nevertheless, host genetic characteristics are not the only host factors that can influence viral pathogenicity. The adaptive immune system of an individual is in fact shaped by the pathogens recognised during his/her lifetime, and its efficiency varies according to the age of the subject (Y.-C. Tan *et al.* 2014; Kucharski and Gog 2012). The presence of antibodies that can cross-neutralize, or T lymphocytes that can recognise different influenza strains is an important factor in determining protection from influenza virus infection and/or attenuation of pathology (Greenbaum *et al.* 2009; Hancock *et al.* 2009). On the contrary, abnormal immune responses (e.g. cytokine storms) are associated with mortality following influenza infection and are characteristics in pandemic influenza and in human infection with avian influenza virus, especially if HPAI (Morens and Fauci 2007; Chan *et al.* 2005).

It is for this reason essential to understand how the immune system in general, especially in humans, interacts with the influenza virus.

1.6 Immunological response to influenza virus

Influenza virus infection activates both the innate and adaptive components of the immune system. In fact, the virus is firstly detected and destroyed by the mechanisms of the innate immune response and secondly by specific adaptive immune responses (S.-I. Tamura and Kurata 2004).

The innate immunity is necessary to limit the initial influenza virus replication and to stimulate lymphocyte specific components (reviewed in Tripathi, M. R. White and Hartshorn 2014). Similarly, the adaptive immune response plays an important role in the containment and the elimination of the virus. The adaptive response, consisting in cellular (reviewed in Woodland, Hogan and Zhong 2001) and humoral immunity, is needed to establish the 'memory' response that results in long-term protection to infection with homologous virus, and sometimes also to drifted viruses.

1.6.1 Innate immune response

The respiratory mucosa is both the primary site of influenza infection and the first defense mechanism, as the mucous layer of the respiratory tract contains molecules that act as decoy receptors limiting the infection of the epithelium.

When the virus enters into cells and viral infection takes place, single-stranded and double-stranded RNA (produced during vRNA replication) act as pathogen-associated molecular patterns and can activate pattern recognition receptors, in particular the retinoic acid-inducible gene 1, the toll-like receptor 3, the toll-like receptor 7, and the Protein kinase RNA-activated (PKR) (Guillot *et al.* 2005). These receptors through signal pathways are able to activate the expression of IFN and pro-inflammatory cytokines.

Among the cytokines produced, IFNs play the major role in resistance to influenza infection. In fact, IFNs have a direct antiviral effect: they increase the expression of PKR, oligoadenylate synthetase, IFTIM3, and the MxA protein (Sadler and Williams 2008; Julkunen *et al.* 2000). IFTIM3 is able to interfere with viral membrane–endosome fusion (Desai *et al.* 2014). MxA directly interferes with influenza virus replication, preventing post-transcriptional processes that take place in the cytoplasm of infected cells and interacting with the polymerase subunits and NPs (Haller, Staeheli and Kochs 2009; Pavlovic, Haller and Staeheli 1992). IFN also plays a role in the activation of key components of the innate and adaptive immunity (K. Takeda and Akira 2004).

Alveolar macrophages constitute the first line of cellular defence, as they reside in the place of infection. They have an active role in clearance of influenza virus and infected cells, but also secrete chemokines and cytokines recruiting components of the innate and adaptive response (Tripathi, M. R. White and Hartshorn 2014).

Neutrophils are recruited in the first phase of influenza infection and play an important role in clearance *via* phagocytosis of influenza virus and other proteins, and also in activating the adaptive immune system. However, as they produce reactive oxygen species (ROS) they can also contribute to lung tissue damage (Tripathi, M. R. White and Hartshorn 2014).

Natural Killer (NK) cells have direct cytotoxic activity as well as playing a role in the activation of cytotoxic T lymphocytes and regulating the production of IFN-γ and of IL-2 (He *et al.* 2004). Further studies have also shown that the HAs expressed on infected cells are bound by NKp46 and NKp44 receptors expressed on NK cells resulting in the activation of the NK effector function (Mandelboim *et al.* 2001; T. I. Arnon *et al.* 2001).

Other classes of innate immune cells, such as NKT cells, γδ T cells, and T helper 17 cells, influence influenza infection and epithelial damage (Tripathi, M. R. White and Hartshorn 2014).

1.6.2 Adaptive immune response

Dendritic cells (DCs) represent the point of contact between the innate and the adaptive immune systems. They come into contact with influenza virus in two ways: by direct infection, or after phagocytosis of infected cells. These two processes, together with the mechanism of antigen cross-presentation, allow the presentation of viral antigens on the class I and II major histocompatibility complexes (MHCs). Upon uptake of the viral antigens, DCs mature, migrate to regional lymph nodes, and by interacting with $CD8^+$ T cells, $CD4^+$ T lymphocytes, and B lymphocytes, activate the adaptive immune response.

Influenza-specific, naïve or memory $CD8^+$ T cells are activated after recognition of the viral antigen presented by MHC class I, and subsequently migrate to the site of infection and inflammation (Cerwenka, Morgan and Dutton 1999). There they eliminate virus-infected cells by exocytosis of granules containing perforin and granzyme, which have cytolytic activity.

Memory $CD8^+$ T cells have the important role of mediating the protective cellular response following re-infection. These cells are able to respond to virus infection and mediate viral clearance more quickly compared to naïve T cells (S.-I. Tamura and Kurata 2004).

Virus-specific $CD4^+$ T cells also play an essential role in influenza defence since they induce the proliferation of $CD8^+$ T cells and B cells (Sant *et al.* 2007). The $CD4^+$ T cell component is essential since it was noted that their deficit can lead to a defect in the memory $CD8^+$ T cell response (Joseph C Sun and Bevan 2003). $CD4^+$ cells, once activated in the lymph nodes, tend to change toward a T helper 1 phenotype and migrate into the

lung. The T helper 1 cells contribute to viral clearance with the production of IFN that, as shown in Section 1.6.1, is able to limit the replication of the virus. Furthermore, the presence of cytokines such as IL-4 in infected lung tissues suggests that $CD4^+$ T cells acquire also a T helper 2 phenotype (S.-I. Tamura and Kurata 2004).

Influenza-specific B cells that are activated to become plasma cells, produce immunoglobulins (Ig, or antibodies) that are able to recognise influenza proteins, such as HA, NA, M2 and NP, and can neutralize the virus. Virus neutralization is the ability of an antibody to bind and inactivate the infectivity of a virus *in vitro* and *in vivo*. The majority of neutralizing antibodies are able to protect also *in vivo*, however, the mechanism by which they mediate the immune defence *in vivo* may involve the interaction with cells and molecules of the innate immune system to activate complement activation or Fragment crystallizable (Fc)-mediated processes. The mechanisms by which antibodies can neutralize influenza virus are now well characterised and explained in detail in Han and Marasco, 2011 review (Han and Marasco 2011).

The antibody response that develops following infection of Influenza A virus was initially studied by analysing and measuring the antibodies in sera, nasal and broncho-alveolar washes (Murphy *et al.* 1981). The mucosal B cell-mediated immune response is mainly characterised by the production of secretory IgA (Renegar *et al.* 2004). However, IgG isotope is primarily responsible for the protection of the lower respiratory tract. The mucosal levels of IgG correlate with serum levels, indicating passive diffusion from the systemic compartment. In contrast, IgA is produced locally and transported to the upper airways through the epithelium of the mucosa (Renegar *et al.* 2004; Palladino *et al.* 1995).

Antibodies directed against HA (see Section 1.6.2.1) are the major mediators of influenza neutralization since they can directly interfere with the virus entry process (Brandenburg *et al.* 2013).

Ig that recognise influenza NA are able to block viral replication and specifically to inhibit the release of new progeny virions from infected cells reducing shedding (reviewed in Wohlbold and Krammer 2014, and Marcelin, Sandbulte and Webby 2012). Antibodies directed against NA were associated with some degree of protection from influenza virus infection (Marcelin *et al.* 2011), and a recently isolated monoclonal antibody (mAb) was shown to inhibit the NA activity of different influenza subtypes (Doyle, Hashem, *et al.* 2013; Doyle, Li, *et al.* 2013).

Antibodies directed against M2 are elicited during natural infection and seasonal vaccination but until recently they were believed to be not long-lasting and present at low level (B. Nayak *et al.* 2010; Treanor *et al.* 1990). However, it was shown that since the M2

ectodomain region is conserved between different influenza subtypes, antibodies directed against this region confer heterosubtypic protection (Schotsaert *et al.* 2009).

During influenza infection antibody directed against NP can also be generated. These antibodies do not possess neutralizing activity but are able to augment cellular responses, *via* a mechanism not yet completely understood (Carragher *et al.* 2008).

In general the establishment of a memory B cell population has a crucial role in influenza re-infection since antibodies represent the first mechanism of protection from influenza virus (K. Y. A. Huang *et al.* 2014; Ellebedy and Ahmed 2012). This principle is the basis of the current influenza vaccines that aim to induce virus specific antibodies, especially directed against HA.

1.6.2.1 Influenza antibody response: from anti-haemagglutinin head to anti-haemagglutinin stalk antibodies

From the first studies on influenza antibody response, it was clear that antibodies against HA were able to prevent viruses binding to the cellular receptor, blocking viral infectivity (Jackson *et al.* 1982; Wiley, Wilson and Skehel 1981). Initially, considering the characteristic antigenic drift of influenza virus, haemagglutination inhibition (HI) assay[2] results, and isolation and characterisation of mAbs from human and animal models, it was thought that antibodies against HA were directed exclusively against immunodominant regions present in the HA head. In addition, it was believed that minimal mutation in this region could block the Ig binding and that antibody cross-reactivity between closely related strains was absent (Archetti and Horsfall 1950).

In the 1990s it became clear that antibodies able to neutralize different HA strains and subtypes could be generated *in vivo* and *in vitro* (Hoag presents an interesting historical perspective of this discovery (Hoag 2013)). Recently, mAbs showing a pan- and hetero-subtypic neutralization activity conferred by their ability to bind conserved regions on the HA stalk have been isolated, firstly from animal models and subsequently from humans (C179, CR6261, F10, CR8020, FI6v3, CR9114, CR8043) (Friesen *et al.* 2014; Dreyfus *et al.* 2012; Corti *et al.* 2011; Ekiert *et al.* 2011; Sui *et al.* 2009; Throsby *et al.* 2008; Okuno *et al.* 1993). These mAbs were shown to neutralize the virus, especially interfering with viral envelope-endosome membrane fusion but are also able to interfere with the HA activation process. Furthermore, it was highlighted that *in vivo* they are also able to mediate their neutralizing function by engaging the Fcγ receptor, explaining their high potency in protecting animal models from influenza infection (DiLillo *et al.* 2014).

[2] Explained in Section 1.8.1.

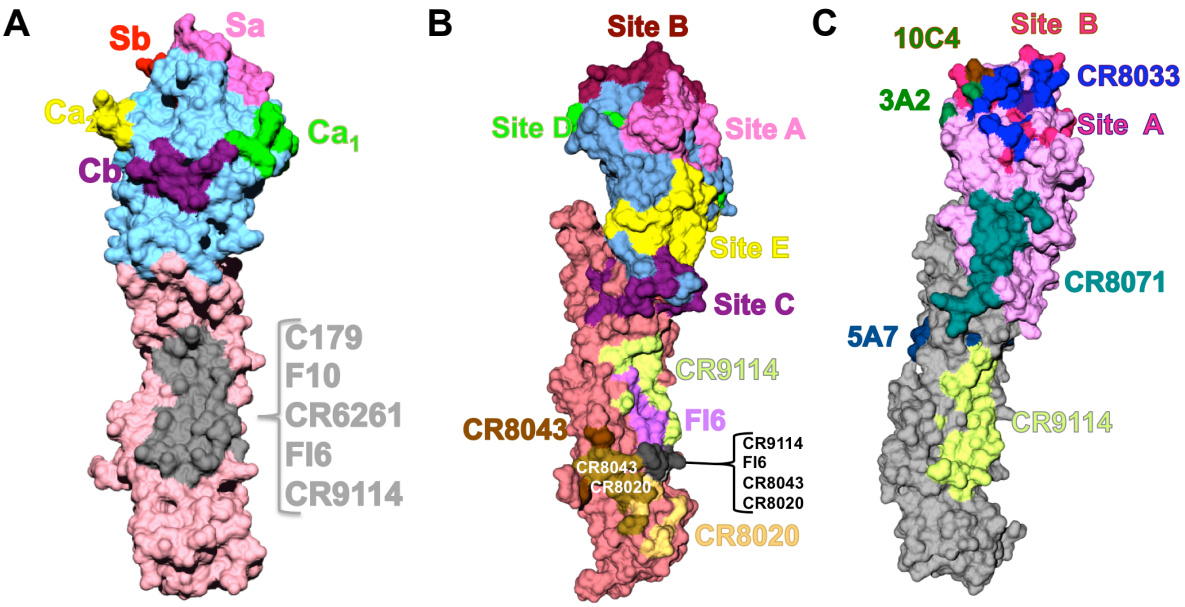

Figure 10: Immunodominant sites and mAb epitopes mapped on HA
The site and epitopes are reported using Swiss PDB viewer and POV-Ray 3.7 on the basis of Friesen *et al.* 2014; Dreyfus, Ekiert and Wilson 2013; Dreyfus *et al.* 2012; Corti *et al.* 2011; Ekiert *et al.* 2011; R. Xu *et al.* 2010; Ekiert *et al.* 2009; Sui *et al.* 2009; Berton, Naeve and Webster 1984; Both *et al.* 1983; Krystal *et al.* 1983; Caton *et al.* 1982; Underwood 1982; Wiley, Wilson and Skehel 1981.
A. Immunodominant sites and mAb epitopes on influenza A H1 HA (PDB ID: 1RU7 (Gamblin *et al.* 2004));
B. Immunodominant sites and mAb epitopes on influenza A H3 (PDB ID: 2VIU (Fleury *et al.* 1998));
C. Immunodominant sites and mAb epitopes on influenza B HA (PDB ID: 4FQM (Dreyfus *et al.* 2012)).

HA stalk-directed antibodies were believed extremely rare in the human population (Grebe, Yewdell and Bennink 2008). Only recently is it becoming clear that these antibodies could be widespread in humans (M. S. Miller, Gardner, *et al.* 2013; Wrammert *et al.* 2011). It is however still unclear if the levels found have an active role in protection against influenza infection. Understanding precisely if these HA stalk-directed antibodies, which can neutralize multiple influenza subtypes, are widespread in the human population and comprehend how they are generated, elicited, and augmented is of essential interest for pandemic preparedness and 'universal' influenza vaccination (see Section 1.7.4).

1.7 Influenza vaccines

Vaccines are considered the only tools that can prevent disease and death associated with influenza virus infection in humans.

In Section 1.4.1 it was explained that due to the influenza antigenic drift, different strains are selected each year to be included in seasonal vaccines. A trivalent vaccine containing one influenza A H1N1 strain, one influenza A H3N2 strain, and one influenza B strain is usually employed, but recently a quadrivalent vaccine containing an additional influenza B strain was also developed and is being used in the United States (Belshe 2010).

At the present time, two vaccine types, all containing three or four influenza strains, are available for administration to the human population: an inactivated virus vaccine and an attenuated virus vaccine. However, new vaccine approaches are being developed to overcome vaccine side effects and allergies, and to broaden the vaccine immunogenicity against viruses not included in the vaccine formulation (Wong and Webby 2013).

1.7.1 Inactivated virus vaccine

There are three different formulations of inactivated virus vaccine: whole virus, split virion, and subunit.

The inactivated whole virus vaccine was the first to be developed: originally influenza virus was grown in the allantoic cavity of embryonated chicken eggs and was subsequently purified using erythrocytes, then inactivated using formaldehyde or β-propiolactone. Nowadays, reassortant viruses that possess the envelope protein of the influenza strains of interest are used instead of native viruses, to obtain a high yield of antigen. Furthermore viruses are now purified using centrifugation and appropriate filter membranes, instead of erythrocytes (Wong and Webby 2013). The whole inactivated virus vaccine is immunogenic in children and adults; unfortunately it is sometimes associated with reactogenicity, especially in young children. For this reason split vaccines, in which virions are disrupted using detergents, and subunit vaccines, in which the HA and NA are purified and sometimes inserted on lipid micelles (virosomes), were developed (Moser *et al.* 2007). These vaccines can induce good responses in adults, but in naïve individuals and elderly they could require additional administrations after the first priming to induce adequate responses (Tricco *et al.* 2013; Lambert *et al.* 2012).

Inactivated influenza vaccines are generally administered intramuscularly, although presently other routes of administration, such as intradermal and mucosal (nasal), are being studied (Wong and Webby 2013; Sullivan *et al.* 2010).

1.7.2 Attenuated virus vaccine

In contrast to the inactivated virus vaccine, attenuated influenza vaccines can induce mucosal immunity since they are intranasally administered and they are able to replicate in a limited manner in the upper respiratory tract. Furthermore, they are able to induce not only antibody mediated responses but also cellular immunity. They were originally developed by growing the virus under suboptimal conditions, resulting in virus attenuation (Wong and Webby 2013). The attenuation, due to stable mutations of the polymerase-, NP-, and M1-encoding genes, permits the virus to replicate only at low temperatures (25°C-35°C), and for this reason the virus is usually termed cold-adapted. Nowadays the vaccine is developed using reassortment or reverse genetic systems, with the

envelope proteins (HA and NA) of the selected vaccine strains added to the genetic backbone of cold-adapted master donor viruses. The cold-adapted viruses are stable and are not able to revert back to their original phenotype (Buonagurio *et al.* 2006). Furthermore they do not induce influenza-like symptoms when administered, and they cannot be transmitted from vaccinated subjects to other people (Glezen 2004).

1.7.3 Vaccine adjuvants

Adjuvants are sometimes used in influenza vaccines to enhance their immunogenicity, especially if they are administered to high-risk groups, such as the elderly and children. Adjuvants are also dose-sparing since they are useful in reducing the quantity of antigen used in the vaccine (Even-Or *et al.* 2013). For example, the use of adjuvants during the 2009 pandemic enabled reduction in the quantity of antigen used in the single dose. Considering that the H1N1 pandemic virus did not propagate efficiently in eggs, this permitted the pandemic vaccine to become available in a relatively short period of time for a larger number of individuals (Robertson *et al.* 2011).

There are different types of adjuvants used in the commercial vaccine formulation: aluminium-based, virosome, and oil-in water emulsions. Other adjuvants are however being evaluated (Even-Or *et al.* 2013).

The use of adjuvants, especially of the oil-in water emulsion type, were also shown to increase the breath of immunological response against influenza viruses, permitting antibodies that are able to neutralize multiple influenza strains to be elicited (Vogel *et al.* 2009).

1.7.4 Future influenza vaccine and 'universal' influenza vaccine approaches

A major issue associated with current influenza vaccination is related to the fact that the vaccine is produced in eggs. In fact, certain human influenza viruses do not grow well in eggs, and in case of a shortage of eggs it will not be possible to produce the antigen quantities needed. Furthermore, people that have allergies to egg proteins cannot be vaccinated with egg-produced vaccine, as they can contain traces of these proteins (Hannoun 2013). For these reasons, different methods of vaccine production involving either the use of the reverse genetic system, VLPs or the production of recombinant proteins in mammalian, avian, insect cells, and plant systems are being developed (S.-M. Kang, M.-C. Kim and Compans 2012; Chichester, Haaheim and Yusibov 2009; Genzel and Reichl 2009; Neumann *et al.* 2005).

Vaccines to stimulate cellular immunity are being developed. These permit the expression and the presentation of viral proteins together with MHC class I, and are based either on plasmid deoxyribonucleic acid (DNA) or on vector expression systems (such as

adenoviruses, Modified Vaccinia Ankara (MVA) virus and Newcastle Disease Virus) (Kopecky-Bromberg and Palese 2009). These approaches are also used to stimulate immunity against more conserved influenza proteins such as NP, M1 and M2 and represent one of the ways by which protection against most subtypes ('universal' vaccination) could be achieved (Pica and Palese 2013).

'Universal' vaccines are vaccines that are able to induce an immune response against multiple, if not all, influenza subtypes. They will be useful since they will probably remove the necessity of annual vaccination and will also protect if a new pandemic arises. 'Universal' vaccines targeting the HA are at the moment being assessed using an epitope-based approach: specific epitopes in the influenza HA-stalk are recognised by antibodies that are able to neutralize multiple influenza subtypes (Section 1.6.2.1) and can be exploited to generate broad-neutralizing antibody responses (Pica and Palese 2013). Different approaches to present such epitopes efficiently to the immune system are being developed: some are based on the use of fragments of HA stalk, other use headless HAs, and more recently the use of HA nanoparticles and chimeric HAs was also described (Mallajosyula *et al.* 2014; Kanekiyo *et al.* 2013; Margine, Hai, et al. 2013; Steel *et al.* 2010).

1.8 Influenza serology and haemagglutinin antibody testing

The detection of serum antibodies directed against the HA is usually associated with the presence of protective immunity. For this reason, serological assays are commonly used to assess if such antibodies are present in the serum of a subject, for epidemiological purposes and to evaluate the immunogenicity of influenza vaccines, before their approval and licensing. However, routinely used serological assays present several issues when applied to the evaluation of the immunogenicity of 'universal' influenza vaccines that aim to elicit stalk-directed HA-responses.

The following sections will focus on the state-of-the-art of serological assays (comprehensively reviewed in Trombetta *et al.* 2014 and Katz, Hancock and X. Xu 2011) but also new assays that can be used to study antibody responses directed against influenza HA, and that could be useful to assess the immunogenicity of 'universal' HA-directed influenza vaccines.

1.8.1 Haemagglutination inhibition assay

The haemagglutination inhibition (HI) assay (Salk 1944; Hirst 1941) is based upon the principle that antibody binding to the HA globular head can inhibit the HA's ability to agglutinate red blood cells (RBCs). Since the agglutination process (Hirst 1941) is

mediated through the attachment of the HA RBSs to the erythrocytes' sialic acid residues creating a virus-RBC lattice, the ability of antibodies to block this binding is an indirect measure of the ability to block viral attachment to target cells and in this way inhibit viral infectivity.

In the HI assay two-fold serial dilutions of sera are prepared and a fixed amount of recombinant or viral origin HA antigen (previously measured through haemagglutination assay) are added. After 15 minutes incubation, RBCs (0.5% chicken and turkey, 0.75% guinea-pig and human type O or 1.0% horse RBCs) are added. Erythrocyte agglutination indicates absence of virus specific antibodies (negative, **Figure 11D**), and RBC precipitations show the presence of antibodies (positive, **Figure 11C**). Positive and negative reference antisera controls are always appropriately added to ensure a correct interpretation of the results and assay consistency: RBC in absence (**Figure 11A**) and in presence of HA antigens/viruses (**Figure 11B**) (Klimov *et al.* 2012; WHO Global Influenza Surveillance Network 2011).

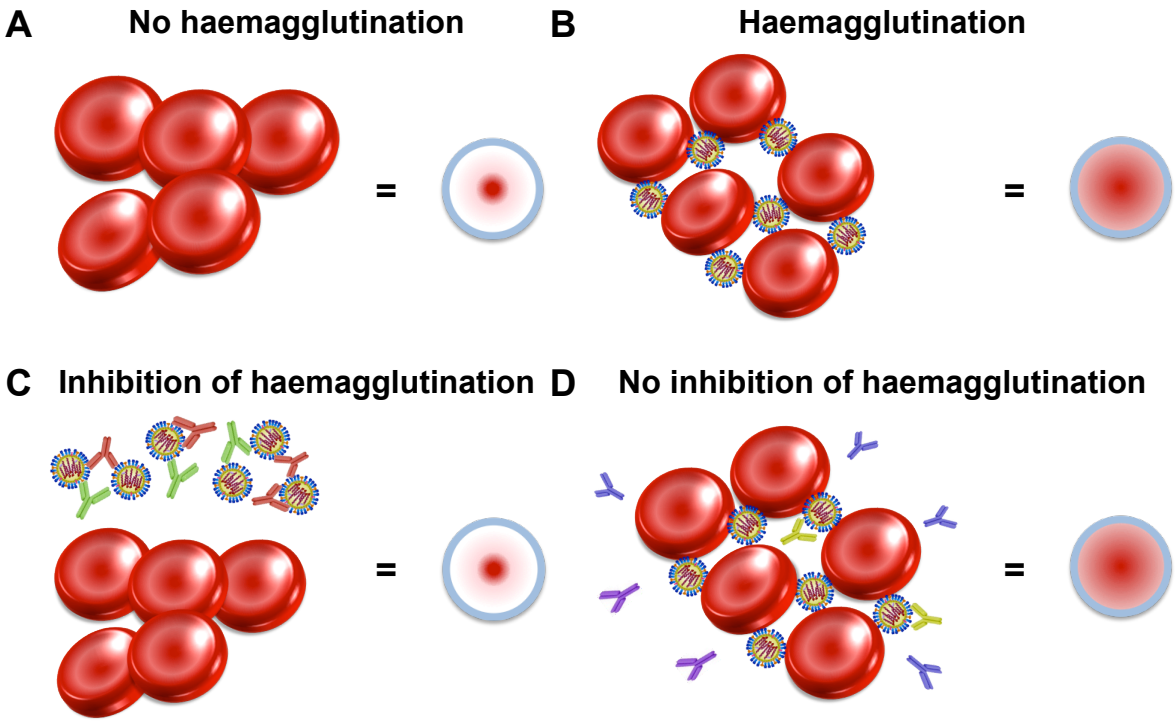

Figure 11: The haemagglutination inhibition assay
A-D show possible results with controls and test samples. In the left hand part of each figure the molecular mechanism is shown; in the right the assay results as they appear in a plate well are shown.
A. In absence of the virus/antigen, the RBCs precipitate and they appear at the bottom of the well; **B.** In presence of the virus, RBCs and virus form a lattice; **C.** The presence of antibodies directed against the virus HA head, inhibit the lattice formation and the RBCs precipitate; **D**. In absence of antibodies able to recognise the virus HA, the virus-RBCs lattice forms.

The major advantage of the HI assay is that correlation with protection against influenza has been determined. Different studies have shown that HI titers >40 are associated with at least 50% protection from infection in human adults (R. J. Cox 2013;

Al-Khayatt, Jennings and Potter 1984; Potter and Oxford 1979; Hobson *et al.* 1972). However, studies performed on children have shown that higher HI titers are necessary to attain 50% protection (Black *et al.* 2011; J R Davies 1989). Even if the complexity of influenza antibody response in humans is difficult to summarise using cut-off values, the correlates are widely accepted and recognised, and this has enabled its use as the preferred assay in vaccine evaluation studies (European Medicines Agency 2010).

However, as shown in different mAb studies, a disadvantage is that the HI assay cannot detect Ig that do not bind near the RBS, such as those binding to the HA stalk region (Corti *et al.* 2011; Ekiert *et al.* 2011; Ekiert *et al.* 2009; Sui *et al.* 2009; Okuno *et al.* 1993) and, for this reason, it cannot be effectively used in the evaluation of vaccines that aim to elicit these antibodies.

Another disadvantage is the fact that sera can contain non-specific inhibitors of haemagglutination that need to be inactivated using different chemical or enzymatic methods prior to the testing procedure (E. K. Subbarao *et al.* 1992).

Furthermore, the classic HI assay is less sensitive than microneutralization (MN) in detecting antibodies against avian influenza viruses (Rowe *et al.* 1999). This becomes a problem when the assay is applied for evaluating H5 pre-pandemic vaccines. For this reason a modified HI assay that uses horse instead of turkey erythrocytes was developed (Stephenson *et al.* 2003). Horse RBCs are richer in α-2,3 sialic acid and, for this reason, are bound with greater efficiency by avian influenza viruses. This modified version has shown good correlation with the MN assay for a vast range of avian influenza viruses (Kayali *et al.* 2008).

Even if the assay is widely used and easy to perform, problems with standardisation and inter-laboratory reproducibility/agreement still exist. In different collaborative studies (Wood *et al.* 2012; Stephenson *et al.* 2009; Stephenson *et al.* 2007; Wood *et al.* 1994) it was observed that the assay intra-laboratory variability is low, but the inter-laboratory variability is high. Nevertheless the same studies show that the use of an internal reference standard can improve the inter-laboratory results (Wood *et al.* 2012; Stephenson *et al.* 2009; Stephenson *et al.* 2007; Wood *et al.* 1994).

1.8.2 Single Radial Haemolysis Assay

The Single Radial Haemolysis (SRH) assay (S. M. Russell, McCahon and Beare 1975; Schild, Pereira and Chakraverty 1975) was developed as an antigen sparing modification of the single radial immunodiffusion test to offer an alternative to the more commonly used HI (Schild, Pereira and Chakraverty 1975). In this assay, virus-coated RBCs are mixed with agarose and guinea-pig complement to form gel immunoplates in

which, after cutting out circular wells, it is possible to add the de-complemented sera to be tested, usually undiluted. During the overnight incubation step if anti-HA antibodies are present, they can bind to the virus and, in the presence of complement, erythrocyte lysis occurs (Schild, Pereira and Chakraverty 1975). In this way the presence of the antibodies is indicated as as a zone of haemolysis around the well, the diameter of which is positively correlated to the quantity of antibody present (S. M. Russell, McCahon and Beare 1975; Schild, Pereira and Chakraverty 1975) (**Figure 12**).

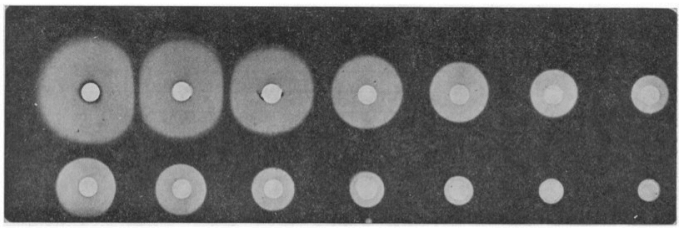

Figure 12: Single Radial Haemolysis reactions
Obtained from Schild, Pereira and Chakraverty 1975. The clear areas are zones of haemolysis produced by the presence of HA-directed antibodies in presence of guinea pig complement and A/Port Chalmers/1/1973 (H3N2) virus.

The SRH assay is robust and shows little intra-laboratory variation (S. M. Russell, McCahon and Beare 1975); also in inter-laboratory studies it has shown less variation than HI when results are expressed in the same format (e.g. surface area) (Stephenson *et al.* 2009; Wood *et al.* 1994). Furthermore it was observed that a >25 mm^2 SRH area usually correlates with protection (Al-Khayatt, Jennings and Potter 1984). Together with the fact that it does not require wild-type viruses, this makes the SRH one of the assays of choice for vaccine evaluation studies, especially for Influenza B since the HI assay is relatively insensitive compared to MN for this virus (European Medicines Agency 2010).

Disadvantages of SRH in detecting antibodies exist: the assay detects only Ig subclasses (IgG1, IgG3, and IgM) that bind the complement complex (the first protein in the complement cascade, C1q complement protein, to be precise) (Schroeder and Cavacini 2010) and, since Ig of class A do not bind C1q, applying this assay to study the mucosal IgA-mediated response is not possible (S. M. Russell, McCahon and Beare 1975). In addition, when performed against H5 viruses to test human sera, the samples should be pre-adsorbed against H1 and H3 viruses to remove possible cross-reactivity against viral internal proteins (Wood *et al.* 2001).

1.8.3 Plaque-reduction neutralization test and microneutralization

The plaque-reduction neutralization test (PRNT) and microneutralization (MN) are functional assays that directly evaluate the neutralizing antibody activity (Klimov *et al.* 2012).

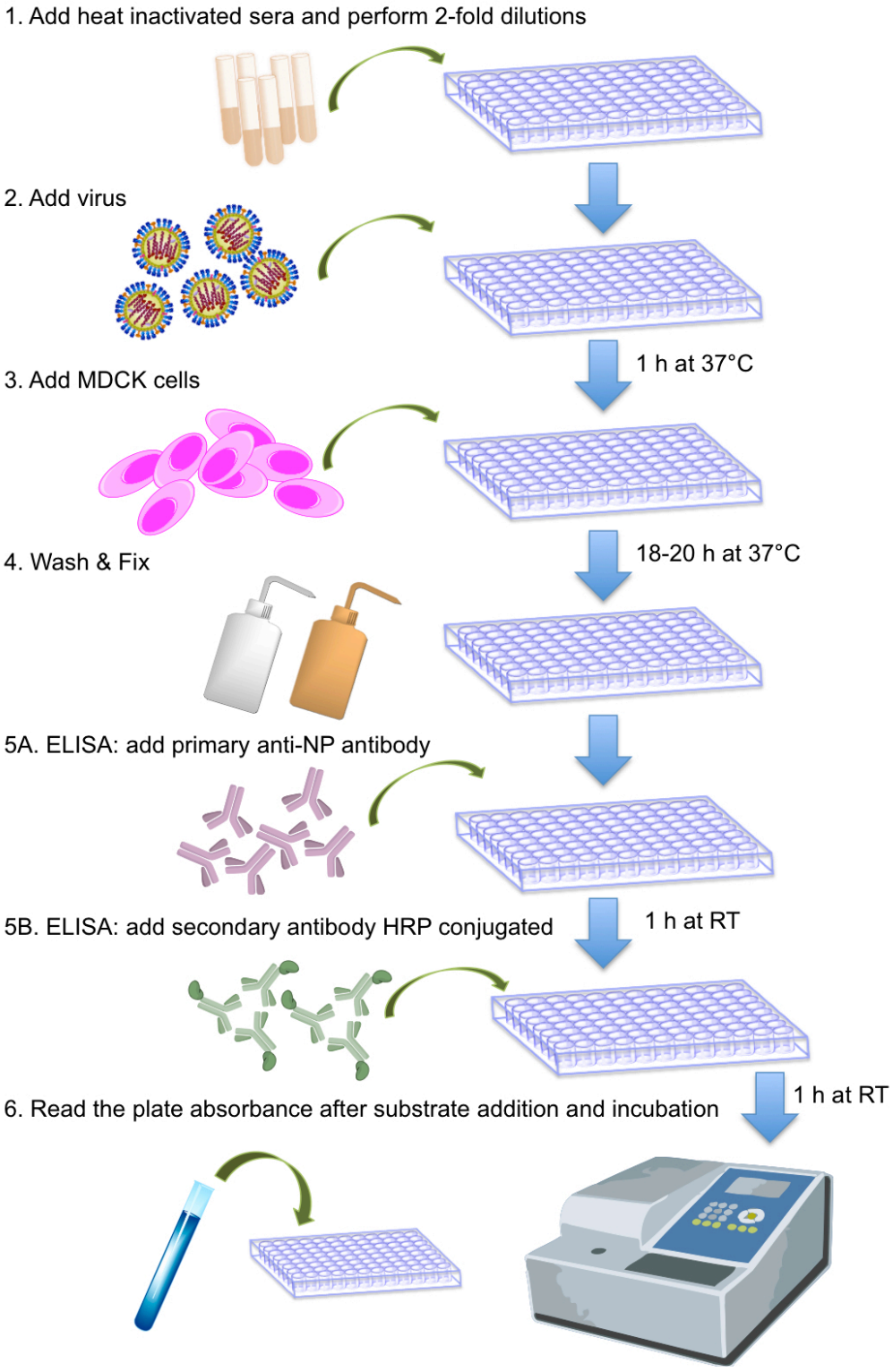

Figure 13: Overview of ELISA-MN assay
In step 1 and 2, serially-diluted sera are pre-incubated with a fixed amount of virus, previously determined by virus titration. In step 3, after 1 h incubation Madin-Darby canine kidney cells (MDCK) are added to each well and the plate is incubated overnight. In step 4, the plate is washed and fixed to perform the ELISA (step 5A-B) using a primary antibody directed against NP and a secondary antibody conjugated with horseradish peroxidase. In step 6 the plate absorbance is read using a spectrophotometer after addition and incubation of an appropriated horseradish peroxidase substrate (usually o-phenylenediamine).
Image adapted from Klimov *et al.* 2012 using ChemBioDraw Ultra 14 and Microsoft® Power Point.

In the PRNT, sera are diluted and incubated with virus. After incubation to permit antibody attachment, the antibody-virus mixture is added to a target cell monolayer. After 1 hour incubation in which the unbound virus can enter cells, which are covered with agarose to block the spreading of the viral progeny that will be produced after infection. In this way, instead of a generalised cytopathic effect (CPE), clear lysis plaques will appear after removing the agarose and staining with crystal violet. The neutralization is then evaluated as the reduction of the number of plaques in comparison to the virus infection control (in absence of antibodies) (Klimov *et al.* 2012).

The MN assay is performed in 96-well plates (Okuno *et al.* 1990). Since the plate-format does not permit the counting of the viral plaques, agarose is not used and the general viral CPE is evaluated. The neutralization activity is measured as the ability of the sera to reduce the CPE due to inhibition of viral entry and subsequent replication (World Health Organization 2002).

A more sensitive and quantitative approach is represented by the Enzyme-Linked Immunosorbent Assay (ELISA)-MN (**Figure 13**). In this assay (described in detail in World Health Organization International Avian Influenza Investigative Team 2010 and Klimov *et al.* 2012) the readout is quantitative: an ELISA to measure influenza NP is performed, and this correlates directly with viral infection.

Another approach (Martinez-Sobrido *et al.* 2010) is the use of recombinant viruses in the neutralization assay. This recombinant virus contains a Green Fluorescent Protein (GFP) gene instead of the HA gene in its genome and is produced by exploiting the reverse genetic system (in this case an HA-expressing plasmid is also necessary). Using this method it is unnecessary to use an extra detection step since the read-out is the GFP signal that is produced after viral infection. Furthermore the system is also safe since, lacking a proper HA genome segment, the recombinant virus cannot replicate in cells that do not express HA (Martinez-Sobrido *et al.* 2010).

Neutralization assays can detect antibodies that are able to inhibit/prevent viral attachment and viral entry and, for this reason, they are able to detect also antibodies binding to the HA stalk region (Okuno *et al.* 1993). Thus MN should represent the assay of choice to evaluate in its entirety the HA-directed antibody response. However, the main disadvantage of MN is the use of wild-type virus, which can require Biosafety Level 3 laboratories if HPAI or potentially pandemic strains are used. Furthermore, at the present time, a correlation of protection is not yet established. However, the WHO usually indicates the 1:80 titre as cut-off, or a 4-fold or greater increase in the neutralization titre between paired pre- and post-vaccination/infection as possible correlates of protection (European Medicines Agency 2010).

1.8.4 Cell-cell fusion inhibition assay

Infection with viruses harbouring proteins with fusion activity (such as *Paramyxoviridae* viruses) is usually evaluated by observing syncytia formation (Horvath *et al.* 1992). In its native state, influenza virus HA does not possess fusion activity but, when exposed to acid pH, it undergoes conformational changes and acquires fusion activity (Skehel and Wiley 2000). Since this function is mediated by the rearrangement of the stalk region, it is possible to evaluate antibodies that can bind to the HA stalk and block this conformational change. All the broadly neutralizing mAbs have been shown to inhibit this step, thus this assay (or its modification) represents a direct approach to assess stalk antibody function activity (Dreyfus *et al.* 2012; Corti *et al.* 2011; Ekiert *et al.* 2011; Friesen *et al.* 2010; Ekiert *et al.* 2009; Sui *et al.* 2009; Okuno *et al.* 1993).

Nevertheless, the assay (Okuno *et al.* 1993; J. White, Helenius and Gething 1982) is not easy to perform. Cells need to by transfected with HA or infected with influenza virus. After incubation to permit HA expression, cells are treated with L-tosylamido-2-phenyl ethyl chloromethyl ketone treated trypsin (TPCK-Trypsin)[3] to enable the HA cleavage necessary to trigger the conformational change and exposure of the fusion peptide. Cells are then incubated in the presence of mAbs or sera. After incubation, media is removed and low pH media added. Subsequentially formation of polykaryons (cells that possess more nuclei) is observed by microscopy; sometimes using tissue/cell staining can facilitate their visualisation (Vanderlinden *et al.* 2010; Sui *et al.* 2009). The presence of polykaryons indicates the absence of antibodies that block cell-cell fusion. Alongside the difficulty in reproduction of the technique, another complication is the fact that some HA mutations have been shown to change the HA fusion pH (Cotter, Jin and Z. Chen 2014; Reed *et al.* 2009), and fusion pH variations also exist between avian and human viruses (Shelton *et al.* 2013). Different groups (M. Takeda *et al.* 2003; Paterson, C. J. Russell and Lamb 2000) have tried to simplify the fusion assay using dyes or reporter gene systems, however the use of the assay is still not widespread.

1.8.5 Other functional assays

To study HA-directed antibody responses the application of the enzymatic VLP assay is a valid approach (Tscherne, Manicassamy and García-Sastre 2010). This assay is used to evaluate viral entry and performed using VLP in which the M1 protein is modified as a fusion protein with the β-lactamase enzyme. In this way when these particles enter into cells, a signal can be detected after adding the appropriate substrate. This assay is very

[3] The L-tosylamido-2-phenyl ethyl chloromethyl ketone removes possible chymotrypsin activity present in the trypsin preparation

rapid, since the incubation time is only required to permit viral entry and it is not necessary to wait for the expression of reporter genes. Furthermore Tscherne, Manicassamy and García-Sastre also showed that VLPs can be used as surrogate antigen in a HI assay (Tscherne, Manicassamy and García-Sastre 2010).

1.8.6 Haemagglutinin Enzyme-Linked Immunosorbent Assay

ELISAs are commonly used to detect antibodies against a protein of interest. In the influenza field, they are applied to detect antibody responses against HA and other influenza proteins in sample sera. The focus here is on ELISA for HA antibody detection.

In the most widely used approach (indirect ELISA) the HA is coated onto a 96-well plate. After a blocking step, dilutions of the sera to be tested are added and the plate is incubated. Then a labelled secondary antibody that can recognise the test antibodies is added. After further incubation, the assay is developed using an appropriate substrate and measured using a plate reader instrument. An advantage of the assay is that by using specific secondary antibodies it is possible to differentiate antibody subclasses and test other sample types (Madhun, R. J. Cox and Haaheim 1999), such as nasal washes. This is particularly useful for the detection of mucosal antibodies. The assay has high sensitivity but specificity needs to be improved. For example to distinguish between anti-head or anti-stalk responses other approaches, such as competitive ELISA (Corti *et al.* 2011; Postel *et al.* 2011; Throsby *et al.* 2008), need to be used. Furthermore, since ELISA detects only antibody binding, it cannot give information about the neutralizing activity of the antibodies detected (Plotkin 2008).

1.8.7 Other binding assays

Western blotting and immunofluorescence represent two classical methods to detect antibody response (Qiu *et al.* 1992). As with the ELISA assay, these assays can only detect the presence of binding antibodies and they do not give information about neutralization activity (Plotkin 2008).

Western blotting can be also used in the characterisation of epitopes recognised by antibodies: during electrophoresis in presence of reducing agents, the two HA subunits (HA1 and HA2) can be separated and antibodies against HA2 and HA1 can be distinguished. Antibodies that recognise stalk conformational epitopes can detect only the full HA protein (Corti *et al.* 2011; Throsby *et al.* 2008; Okuno *et al.* 1993).

Recently microarrays in which HAs of different influenza strains and subtypes are spotted on nitrocellulose coated slides or on activated glass surfaces were developed and they permit the evaluation of the breath of the antibody response (Baas *et al.* 2013; Desbien *et al.* 2013; Price *et al.* 2013; Koopmans *et al.* 2012).

1.8.8 Influenza pseudotype particles and their use in neutralization assays

In the past decade, to overcome the issues discussed different groups have tried to develop new assays that possess the advantages and characteristics of classical neutralization assays but without the risk associated with using native viruses. For this purpose surrogate recombinant pseudotype particles can be used. Pseudotypes or pseudotype particles (pp) are replication defective viruses that harbour on their envelope a protein of one virus, but their core is constituted of the internal proteins of another virus, and in their genome a reporter gene is encoded (**Figure 14**) (Temperton and Wright 2009).

The use of pp in serology for emerging and re-emerging viruses was recently reviewed in Mather *et al.* 2013. For influenza specifically, Garcia and J. C. C. Lai 2011 have reviewed their use in detail. Here, after explaining the history of influenza pp we will focus on the use of influenza lentiviral pp in neutralization assays, especially the detection of stalk-directed neutralizing antibody responses.

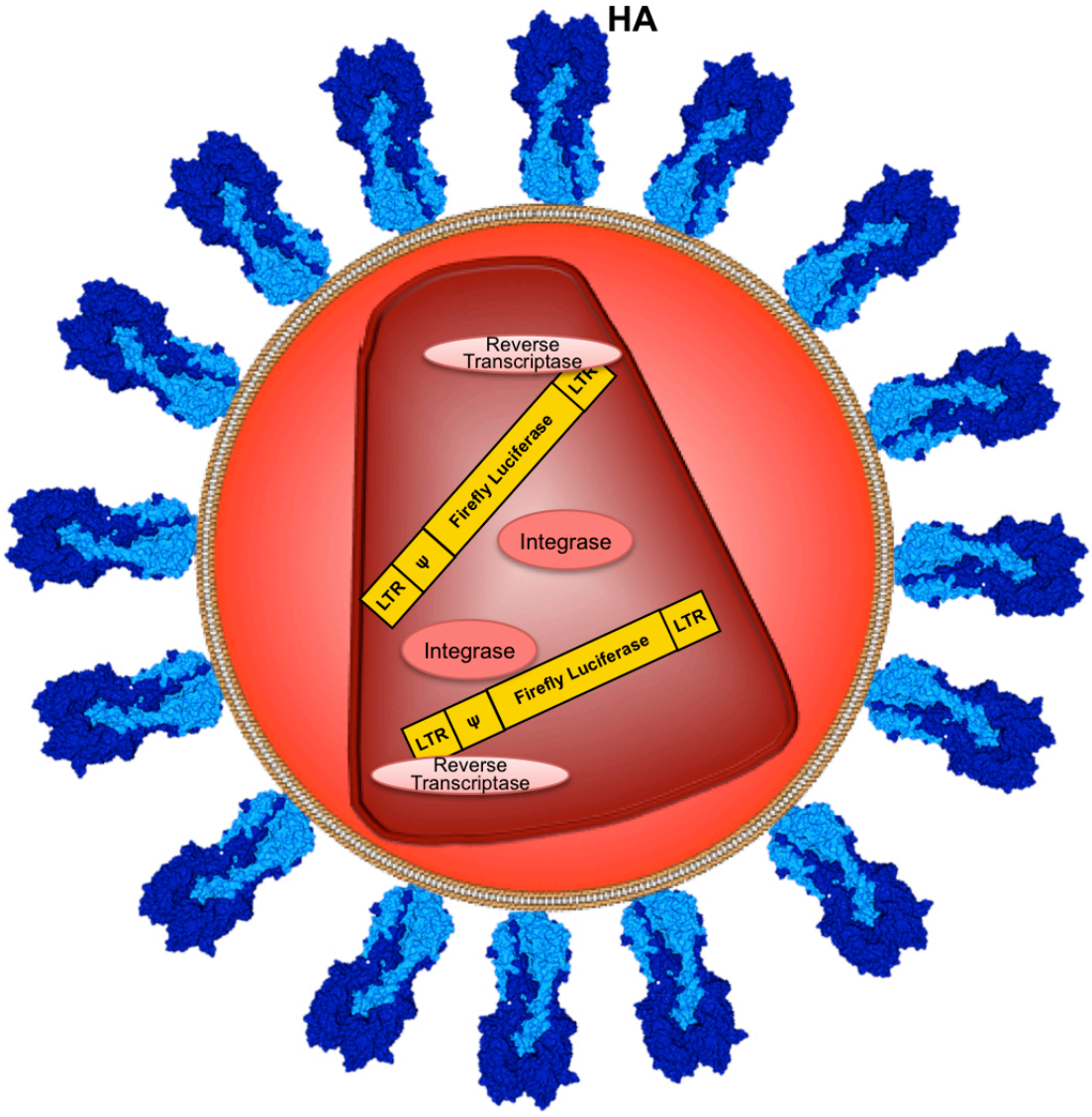

Figure 14: Influenza HA lentiviral pp structure

1.8.8.1 Influenza pseudotype particles: history

Different viral cores are commonly used to generate influenza pp: vesicular stomatitis virus (VSV) (Závada and Rosenbergová 1972), gammaretroviruses (e.g. murine leukaemia virus, MLV) (Hatziioannou *et al.* 1998), and lentivirus (e.g. human immunodeficiency virus type-1, HIV-1) (Ferrara *et al.* 2013; Molesti *et al.* 2013; Scott *et al.* 2012; Nefkens *et al.* 2007). Lentiviral cores are particularly popular and useful since lentiviruses can integrate in the cellular genome of dividing and non-dividing cells and this has led to their use in gene therapy. The application of lentiviral vectors to gene therapy has resulted in the development of many lentiviral vectors and packaging systems with different safety profiles (reviewed in Sakuma, Barry and Ikeda 2012). In **Figure 15** the different types of packaging systems and lentiviral vectors available are reported. The principle that has influenced the development of different generations of lentiviral system aimed to avoid the native virus being generated through accidental recombination (Schambach *et al.* 2013). For this reason, the packaging system viral elements and pathogenicity factors (if possible) were removed. When this was not possible, the gene was positioned in an additional plasmid (**Figure 15D**). For the production of lentiviral vectors expressing the transgene or the reporter gene of choice, viral genes were removed, just maintaining the viral elements necessary for vector packaging and integration (**Figure 15 (E-G)**).

Lentiviral pp are produced utilising highly transfectable cell lines (usually Human Embryonic Kidney (HEK) 293 cells or derivative cell lines) and introducing the plasmid constructs to produce the core proteins, the lentiviral genome encoding a reporter gene, and one encoding the envelope protein of the virus of interest. The pp generated acquire the cellular tropism of the virus that donated the envelope protein and the lentiviral capacity to integrate the genome into the target cell line (Cronin, X.-Y. Zhang and Reiser 2005). The reporter gene permits measurement of the virus transduction of target cells and quantification of the viral particles.

Since pp bear foreign proteins in their envelope, they are a useful tool to study viral entry and antibody response (Garcia and J. C. C. Lai 2011; Temperton and E. Wright 2009). Another major advantage associated with the use of pp is that, since they are replication defective viruses, they can be used in a low biosafety level laboratory (Garcia and J. C. C. Lai 2011; Temperton and Wright 2009).

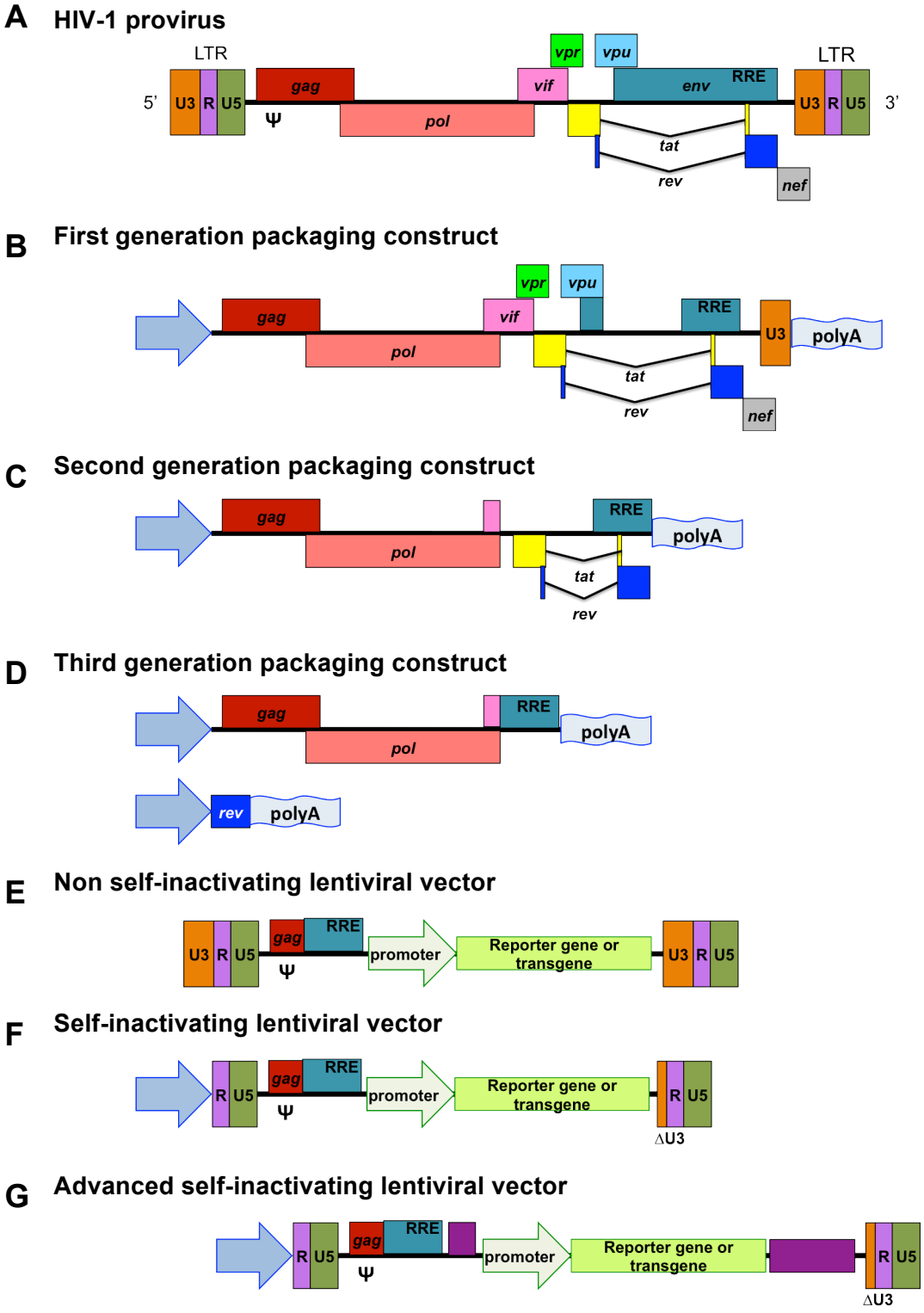

Figure 15: Lentiviral packaging systems and vectors
The figure is adapted from Escors *et al.* 2012 and Sakuma, Barry and Ikeda 2012.
A. The genome structure of the HIV-1 provirus is reported as guide;
B. In the first generation packaging system, the HIV-1 long terminal repeats (LTRs), composed of U3, R and U5, are removed. A strong constitutive promoter sequence (indicated by the sky blue arrow), and a polyadenylation signal (polyA) are introduced instead to permit the expression of the genes. The packaging signal Ψ is mutated, and the envelope gene deleted with the exception of the part of the gene encoding *rev*, *tat*, and *vpu*. The rev response element (RRE), which permits nuclear export, is also maintained;
C. In the second generation the accessory proteins encoded by *nef*, *vpr*, and *vpu* genes are removed.
D. In the third generation, *tat* is removed. Using an additional plasmid *rev* is expressed. The RRE is maintained in the *gagpol*-expressing plasmid;

E. In contrast to the packaging constructs, in the lentiviral vector, the LTRs and the Ψ are maintained, whilst the HIV-1 encoding genes are removed to be substituted by a transgene or reporter gene under the control of a promoter;
F. In self-inactivating lentiviral vectors the enhancer/promoter sequence in the 3' U3 is deleted as well as the 5' U3. It is thus necessary to add a strong constitutive promoter, to permit the expression of the lentiviral vector in the producer cell line. Subsequent to the deletion of the 3' U3 enhancer/promoter sequence, when integrating into the target cell line the lentiviral vector will not possess a functional U3 at the 5' end, since the 3' end region is copied at the 5' end during integration. This increases the safety of the construct by reducing the frequency of vector mobilisation;
G. Self-inactivating lentiviral vectors can be further modified to include enhancer elements for nuclear import and expression (purple).

1.8.8.2 Pseudotype particle neutralization assay

Pp can be used as surrogate antigens for MN assays. Serial dilutions of sera are incubated with pp. The mixture is subsequently tested for transduction activity on target cells. If the pp are not neutralized they will enter into cells, the viral genome will integrate and the reporter gene will be expressed. If neutralizing antibodies are present in test sera, the viral entry is reduced and the reporter gene signal will be lower. In other words, neutralization is indicated by absence of reporter gene signal (**Figure 16**).

Different groups have shown good correlation between the pseudotype particle neutralization (pp-NT) assay and the other serological assays described here using sera of different origins (Temperton *et al.* 2007; Molesti *et al.* 2013; Scott *et al.* 2012; Garcia *et al.* 2010; W. Wang, Xie, *et al.* 2010; Alberini *et al.* 2009; Garcia *et al.* 2009; Nefkens *et al.* 2007; Temperton *et al.* 2007). Furthermore, Alberini *et al*. have used the correlation between an H5 pp-NT assay and MN to infer a possible cut-off titre associated with protection in the pp-NT assay, which is 1:357. Similar studies are yet to be performed using other influenza pp strains.

As shown in different studies the pp-NT assay shows higher sensitivity in detecting HA stalk-directed antibodies, probably due to the lower HA density on pp surface in comparison with native influenza virus (Corti *et al.* 2011; Corti *et al.* 2010), thus removing some steric hindrance to antibody access to the stalk.

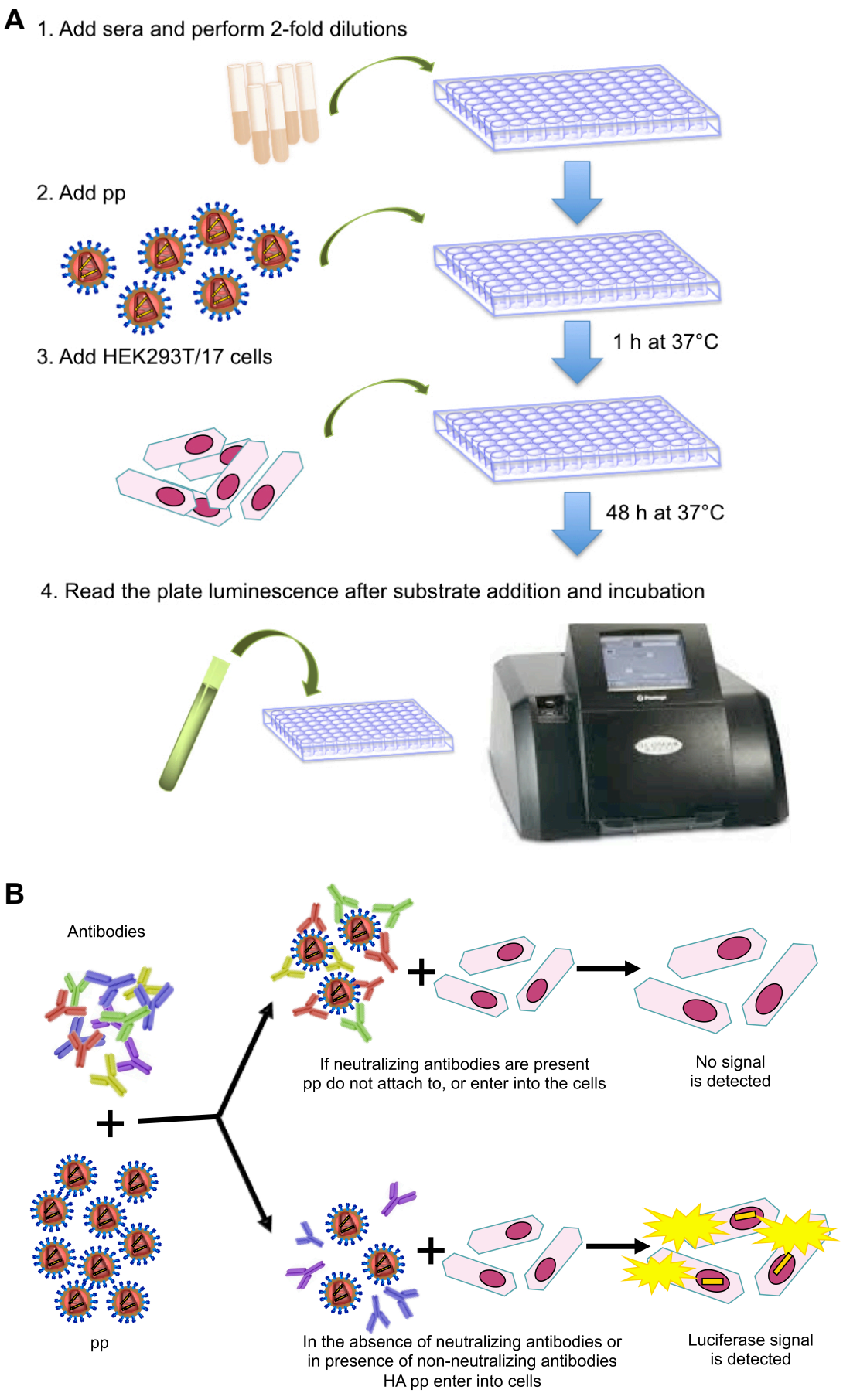

Figure 16: Pseudotype particle neutralization assay
Images were made using ChemBioDraw Ultra 14 and Power Point.
A. The protocol of a pp-NT assay performed using HA pp expressing firefly luciferase is shown (see Section 2.3.4 for detailed description); **B.** Representation of the principle at the basis of pp-NT assay.

1.8.8.3 Post-attachment pseudotype particle neutralization assay

Using pp as surrogate viruses Oh *et al.* 2010 have modified the post-attachment neutralization assay for influenza developed by Edwards and Dimmock 2001.

In this assay pp are incubated at 4°C with cells to permit the synchronisation of the virus binding to the cell surface and to block viral endocytosis. Diluted sera are then added, and following another 4°C incubation, plates are transferred to 37°C to permit transduction (Oh *et al.* 2010).

In the post-attachment pp-NT, neutralization is observed only when the antibody is blocking the endocytosis step and subsequent HA conformational changes necessary for virus-endosome fusion (Oh *et al.* 2010; Edwards and Dimmock 2001). Antibodies that have neutralizing activity through impeding viral attachment will produce negative results in this assay. For this reason the assay is useful for evaluation of stalk-directed antibodies that do not inhibit viral attachment (Oh *et al.* 2010).

1.8.8.4 Chimeric HA pseudotype particle neutralization assay

To study the antibody response directed against the HA stalk, the Palese group has developed pp and influenza viruses exhibiting a chimeric HA on their envelope. This chimeric HA has stalk region and globular head deriving from two different HA subtypes (or strains) (Hai *et al.* 2012). To create this chimeric construct they have exploited the presence in the influenza A HA of two cysteines, Cys52 and Cys277, that are engaged in a disulphide bond and separate the head and stalk regions (**Figure 4C**) (Hai *et al.* 2012). In fact the HA gene portion between the codons of Cys52 and Cys277 encodes for the amino acids that constitute the HA globular head and, for this reason it was possible using DNA recombinant technology to exchange the HA head of one virus with the HA head of another influenza strain (Hai *et al.* 2012). Additionally the same cysteines have been used to construct headless HAs used as a vaccine to induce stalk-directed antibodies (Steel *et al.* 2010).

The concept behind the idea of using these modified HAs to detect exclusively HA stalk-directed antibodies is that since the antibody response is principally directed against the HA head, testing sera against an HA that has a different head will permit easy detection of antibodies against the more conserved stalk region instead of the antibodies generated against the original HA globular head since they will not recognise an antigenically unrelated head. Furthermore these chimeric HAs can also be used as candidate vaccines to elicit stalk-directed antibodies (Krammer *et al.* 2013; Margine, Krammer, *et al.* 2013).

Table 2 lists the reported chimeric HA and their use in the pp system, neutralization assays, ELISA, and as vaccine candidates.

Table 2: Chimeric HAs described in the current literature

Head	Stalk	References
A/California/04/2009 H1	A/Puerto Rico/8/34 H1	(Hai et al. 2012)
A/Vietnam/1203/2004 H5	A/Puerto Rico/8/34 H1	(Hai *et al.* 2012) (Krammer *et al.* 2012) (Goff, Eggink, *et al.* 2013) (Krammer *et al.* 2013) (M. S. Miller, Tsibane, *et al.* 2013) (Krammer, Hai, *et al.* 2014) (Ryder *et al.* 2014)
A/Singapore/1-MA12E/1957 H2	A/Puerto Rico/8/34 H1	(Goff et al. 2015)
H9	A/Puerto Rico/8/34 H1	(Pica et al. 2012) (Goff, Eggink, et al. 2013) (Krammer et al. 2013) (Krammer, Hai, et al. 2014) (Nachbagauer et al. 2014)
A/mallard/Sweden/81/02 H6	A/Puerto Rico/8/34 H1	(Krammer *et al.* 2012) (Pica *et al.* 2012) (Goff, Eggink, *et al.* 2013) (Krammer *et al.* 2013) (M. S. Miller, Gardner, *et al.* 2013) (M. S. Miller, Tsibane, *et al.* 2013) (Sangster *et al.* 2013) (Krammer, Hai, *et al.* 2014) (Nachbagauer *et al.* 2014) (Ryder *et al.* 2014)
A/mallard/Alberta/24/2001 H7	A/Perth/16/2009 H3	(Hai *et al.* 2012) (Margine, Hai, *et al.* 2013) (Margine, Krammer, *et al.* 2013) (Goff, Krammer, *et al.* 2013) (Klausberger *et al.* 2014) (Krammer, Albrecht, *et al.* 2014)
A/Shanghai/1/13 H7	A/Perth/16/2009 H3	(G. S. Tan et al. 2014)
A/Vietnam/1203/2004 H5	A/Perth/16/2009 H3	(Hai *et al.* 2012) (Margine, Krammer, *et al.* 2013) (M. S. Miller, Gardner, *et al.* 2013) (Krammer, Margine, *et al.* 2014) (G. S. Tan *et al.* 2014)
A/duck/Czech/56 H4	A/Perth/16/2009 H3	(Margine, Hai, *et al.* 2013) (Margine, Krammer, *et al.* 2013) (Krammer, Margine, *et al.* 2014)

In different studies (M. S. Miller, Gardner, *et al.* 2013; Hai *et al.* 2012) the chimeric HA, even if not applied in the pp platform but in ELISA, has been demonstrated to be a useful approach to study and detect exclusively cross-reactive antibody responses directed against the stalk.

Thesis aims and structure

The primary purpose of this study is to assess the presence of influenza heterosubtypic neutralizing antibody in the human population before and after seasonal vaccination. Since classical serological assays are relatively insensitive for the detection of antibodies against the HA-stalk that are believed to be one of the main effectors of the heterosubtypic neutralizing immunity, pp-NT assays were exploited.

Since only H1, H3, H5, and H7 influenza pp were described in the literature at the start of the study, it was necessary firstly to generate pp harbouring different HA subtypes (Chapter 3), and then to evaluate their performance as surrogate antigens in neutralization and to establish appropriate controls (Chapter 4). Once pp-NT assays have been established, they were be used to assess the human antibody responses directed against human and non-human influenza virus (Chapter 5). The use of chimeric HA pp was also exploited to be able to discriminate the presence of HA stalk-directed antibodies.

Lastly (Chapter 6), influenza B HA pp were also generated and investigated, to establish if they could be used in pp-NT and if they represented a tool to study the heterotypic influenza neutralizing response.

CHAPTER 2

Materials and Methods

Detailed methodologies will be reported within each results chapter, whereas in this chapter common basic molecular biology, cell culture and protein detection techniques, reaction theory, reagents, and materials will be described. Furthermore, standard influenza pp protocols and reagents will be reported.

Throughout this thesis, when available, catalogue numbers (cat.no.) of materials and reagents used will be presented the first time they are mentioned, unless necessary for clarity.

2.1 Molecular biology reagents, materials and techniques

2.1.1 Plasmids

pI.18 (**Figure 17**) and phCMV1 plasmids (**Figure 18**) were used to clone HA genes (Chapters 3 and 6) used in this thesis.

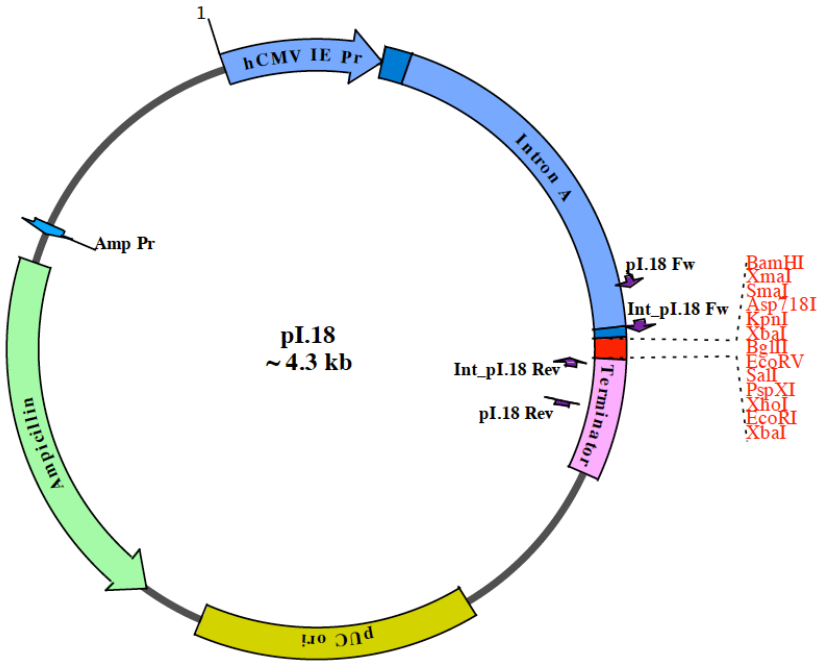

Figure 17: Plasmid map of pI.18
The plasmid map was designed with DNA Dynamo Sequence Analysis Software (Blue Tractor Software Ltd) with the sequence provided by Dr. Eleonora Molesti (Universities of Greenwich and Kent, Medway, UK). The expression of genes is permitted by the presence of the human cytomegalovirus immediate-early promoter (hCMV IE Pr) with the enhancer activity of the hCMV Intron A. The terminator sequence permits polyadenylation of the mRNA enhancing stability. The restriction enzyme sites in the multiple cloning site (MCS), in which the gene to be expressed needs to be cloned, are shown in red. In dark khaky yellow the pUC origin of replication (ori) necessary for plasmid amplification in bacterial cells is highlighted. β-lactamase, which mediates the resistance to ampicillin, is encoded by the ampicillin gene (green) driven by its own promoter (Amp Pr). Annealing region of sequencing primers (Table 3) are also reported.

pI.18 is an high-copy ampicillin resistant pUC-based plasmid that permits robust mammalian gene expression in various cell types by virtue of the human cytomegalovirus (hCMV) immediate-early gene promoter and the enhancer hCMV Intron A (R. J. Cox *et al.* 2002).

phCMV1 (Genlantis) is a 4.2 kb constitutive mammalian gene expression vector driven by a modified hCMV immediate-early promoter and enhancer/intron. Additionally, it possesses kanamycin and neomycin resistance that allows selection of plasmid-positive prokaryotic and eukaryotic cells, respectively.

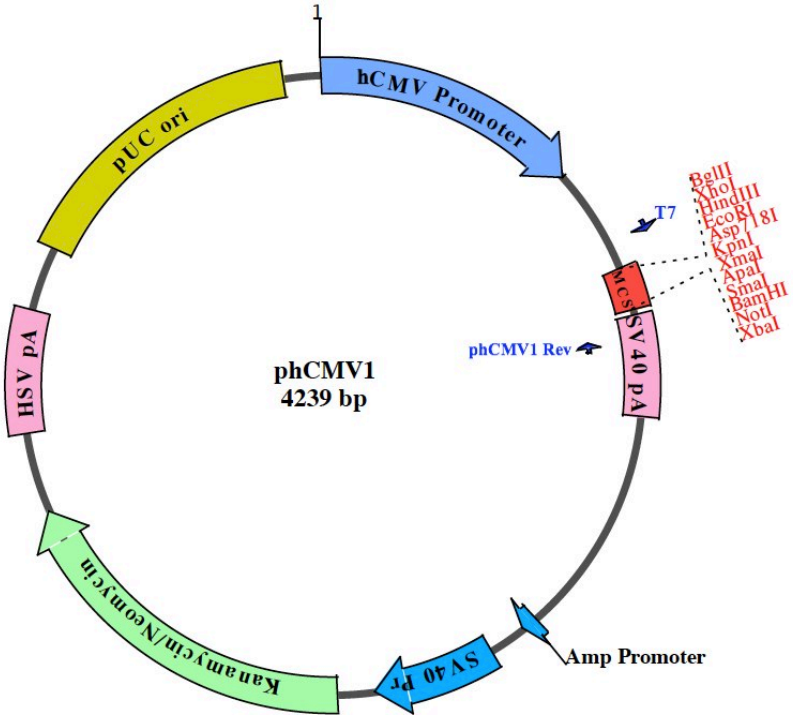

Figure 18: Plasmid map of phCMV1
The plasmid map was designed with DNA Dynamo Sequence Analysis Software (Blue Tractor Software Ltd) with the sequence downloaded from the Addgene database (http://www.addgene.org/). The modified hCMV promoter and the Simian Vacuolating virus 40 (SV40) polyadenylation signal (pA) permit the expression of the gene that is cloned in the multicloning site. The restriction enzyme sites in the multicloning site are reported in red. In dark khaky yellow is highlighted the pUC ori necessary for plasmid amplification in bacterial cells. The resistance to kanamycin and neomycin is encoded by the respective genes (green) under control of the ampicillin promoter (for bacterial expression) and the SV40 promoter (SV40 Pr, for mammilian cell expression). The expression of the resistance gene in the mammalian cell lines is also permitted by the polyadenylation signal of the of human Herpes Simplex Virus (HSV) type 1 thymidine kinase. Annealing regions of sequencing primers (Table 3) are also reported.

2.1.2 Antibiotic stocks, liquid and solid media

Ampicillin sodium salt (Fisher Scientific, cat.no. BP1760) and kanamycin sulphate (Fisher Scientific, cat.no. BP906) were dissolved in UltraPure™ DNase/RNase Free Distilled Water (Gibco®, Invitrogen™, cat.no. 10977-049) to produce a stock concentration of 100 mg/ml and 10 mg/ml respectively, and filtered through 0.22 µm filter (Merk Millipore®, cat.no. SLGP033RS). Ampicillin was used in a working solution

of 100 µg/ml in liquid medium and 200 µg/ml in solid medium, whereas kanamycin was always used at 50 µg/ml.

Ready-to-dissolve Luria Bertani (LB) Agar (Fisher Scientific, cat.no. BP1425, or Sigma-Aldrich, cat.no. L3147) and LB Broth (Fisher Scientific, cat.no. BP1426) were used for preparing bacterial liquid and solid media, dissolved in double distilled water following manufacturer's instruction (LB Agar: 16 g in 400 ml water; LB Broth: 12.5 g in 500 ml water) and autoclaved.

Super Optimal Broth with catabolite repression (SOC; Invitrogen™, cat.no. 15544-034) containing 2% tryptone (w/v), 0.5% yeast extract (w/v), 10 mM NaCl, 2.5 mM KCl, 10 mM $MgCl_2$, 10 mM $MgSO_4$, and 20 mM glucose was used as recovery medium in bacterial transformation to maximise the efficiency of the procedure.

2.1.3 Transformation of chemically induced competent *Escherichia coli* cells

Subcloning efficiency chemically induced competent *Escherichia coli* DH5α cells (Invitrogen™, cat.no. 18265-017) were used in a classic heat-shock transformation protocol when transformation was necessary for plasmid amplification or cloning purposes (ligation reactions).

An aliquot containing 12.5 µl or 25 µl of DH5α competent cells was defrosted from -80°C on ice. Then 1-2.5 µl (0.5-10 ng) of DNA was added to the cells that were further incubated on ice for 20 min. The aliquot was heat-shocked at 42°C in a water bath (Jouan, cat.no. 41093014) or in an AccuBlock™ Digital Dry Bath (Labnet International, cat.no. D1100-230 V) for 20 seconds and then placed for 2 min on ice. Subsequentially, 200-400 µl of SOC medium was added before recovery incubation. After 1 h incubation in a New Brunswick™ Scientific C25KC Incubator Shaker (Eppendorf) at 37°C shaking at 225 revolutions per minute (rpm), 100-200 µl was plated on LB Agar plates with the appropriate antibiotic selection and incubated in a laboratory incubator (Genlab, cat.no. INC/75) overnight at 37°C.

2.1.4 Isolation of plasmid DNA from bacterial culture

Amplification and purification of plasmid DNA for further analysis, sequencing or transfection of eukaryotic cells was performed using the commercial kits QIAprep Spin Miniprep Kit (QIAGEN, cat.no. 27104 or 27106) and HiSpeed Plasmid Midi Kit (QIAGEN, cat.no. 12643) that use a modified alkaline lysis with sodium dodecyl sulphate (SDS) method. Plasmid isolation was performed following manufacturer's instructions (QIAGEN 2012b; QIAGEN 2012a) and the protocol in brief is reported here.

For miniprep scale, a single colony transformed with the high-copy plasmid of interest was inoculated in 5 ml LB Broth with the addition of the appropriate antibiotic

solution and incubated overnight at 37°C, with shaking at 225 rpm. For low-copy plasmids a starting culture of 10 ml was used instead. 16 h later, the culture was pelleted using a table-top microcentrifuge (Thermo Fisher Scientific, cat.no. 10524723) for 3 min at 6800 gravity (g) or a standard Sorvall™ Legend™ RT centrifuge (Thermo Fisher Scientific, cat.no. 75004373) for 10 min at 2500 g. The pellet was then resuspended in 250 µl of Buffer P1 containing 100 µg/ml RNase A to remove the RNA during lysis. Next, 250 µl of a sodium hydroxide and SDS containing solution (Buffer P2) was added and incubated for 5 min before 350 µl of neutralization buffer (Buffer N3) was added. The neutralized and adjusted to high-salt binding conditions lysate was cleared *via* centrifugation for 10 min at 17000 g. Supernatant was added to the QIAprep Spin Column containing a silica membrane, which binds exclusively to DNA, and centrifuged for 1 min at 17000 g. Centrifugation flow-through was discarded and 750 µl of PE buffer containing ethanol was added to ensure salt removal. After 1 min of 17000 g centrifugation and discarding of the flow-through, an additional 2 min centrifugation at the same speed was performed to remove possible ethanol residue. Plasmid DNA was then eluted from the column using 50-100 µl of DNase/RNase free water previously warmed at 70°C, incubating for 1 min and centrifuged to elute in a clean 1.5 ml microtube (Greiner Bio-One, cat.no. 616201) at 17000 g for 1 min.

When a higher quantity of plasmid than the one obtained *via* miniprep protocol was necessary a midiprep scale was used instead. A single colony was inoculated into 5 ml LB Broth containing the appropriate antibiotic for plasmid selection and incubated for 8 h at 37°C shaking at 225 rpm. Then 100 µl of culture was sub-inoculated in 100 ml of LB Broth with antibiotic and incubated overnight at 37°C with shaking at 225 rpm. Growth culture was then pelleted in a Sorvall™ Legend™ RT centrifuge. After pelleting and resuspension with Buffer P1, cells were lysed with Buffer P2, then immediately neutralized with chilled Buffer P3. After 10 min incubation in a QIAfilter Cartridge, the lysate was cleared into a HiSpeed Midi tip, previously equilibrated with Buffer QBT. Once the cleared lysate entered the HiSpeed tip, washing with QC Buffer was performed, then DNA eluted using QF Buffer. Eluate containing DNA was precipitated using isopropanol in the QIAprecipitator. Using again the QIAprecipitator, DNA was washed with 70% ethanol and then eluted with pre-warmed TE Buffer.

2.1.5 Determination of nucleic acid concentration

DNA concentration and purity (260 nm/280 nm absorbance ratio) was measured by ultraviolet spectrophotometry using a NanoDrop™ 2000 Spectrophotometer (NanoDrop™

Products, Thermo Fisher Scientific) following manufacturer's instruction (Thermo Fisher Scientific 2009).

2.1.6 Oligonucleotide primers for molecular biology applications and sequencing

Primers were ordered from Eurofins MWG Operon or Invitrogen™ desalted in a 25 nmol synthesis scale and were delivered lyophilised. They were then reconstituted in DNase/RNase free water to a final concentration of 100 pmol/µl. When necessary primers were further diluted in DNase/RNase free water.

2.1.7 Sanger sequencing

Plasmids were sent for Sanger sequencing at GATC Biotech AG using the SUPREMErun™ sequencing or LIGHTrun™ sequencing options. For SUPREMErun™ sequencing 20 µl of 80 ng/µl plasmid were sent together with 20 µl (at 10 pmol/µl) of appropriate sequencing primers (with the exception of T7 that was a free universal primer offered at GATC Biotech AG), reported in **Table 3.** For LIGHTrun™ 5 µl of 80 ng/µl plasmid were mixed with an equal volume of 5 pmol/µl forward (Fw) or reverse (Rev) primer.

Table 3: Sequencing primer names, sequences, and descriptions
Nucleotide positions are referred to the 1 reported on the maps in Figure 17 and Figure 18.

Primer name	Primer sequence (5' to 3')	Primer description
pI.18 Fw	GGTGGAGGGCAGTGTAGTCT	Permits sequencing the gene cloned into the MCS of pI.18 plasmid in Fw direction, annealing at position 1134-1153.
pI.18 Rev	GCGAGGATGTCACCTGATGG	Permits sequencing the gene cloned into the MCS of pI.18 plasmid in Rev orientation, annealing at position 1430-1449.
Int_pI.18 Fw	TTCTGCAGTCACCGTCCTTGACA	Anneals upstream of the MCS, closer to the insert than pI.18 Fw.
Int_pI.18 Rev	GTATACAATAGTGACGTGGG	Anneals downstream of the MCS, closer to the insert than pI.18 Rev.
T7	TAATACGACTCACTATAGGG	Anneals to phCMV1 vector at position (759-778), permitting sequencing of the gene cloned into the MCS in Fw orientation.
phCMV1 Rev	TATGTTTCAGGTTCAGGG	Anneals to phCMV1 vector at position (986-1003), permitting sequencing of the gene cloned into the MCS in Rev orientation.

Resulting electropherograms were checked and edited using 4Peaks software (Nucleobytes.com); nucleotide and amino acid sequences were then aligned with the reference sequences using Jalview (Waterhouse *et al.* 2009) and the MUSCLE algorithm (Edgar 2004).

2.1.8 Polymerase chain reactions

Polymerase chain reaction (PCR) was used to amplify HA genes to be cloned into expression plasmids. Initially PCR using AccuPrime™ *Pfx* SuperMix was performed, however after problems with DNA amplification, such as low yield, it was decided to perform gradient PCRs.

Amplification of the DNA template was always verified by DNA gel electrophoresis before proceeding to other steps.

2.1.8.1 Polymerase chain reaction using AccuPrime™ Pfx SuperMix

For cloning it is necessary that the gene is amplified with maximum sequence accuracy and, for this reason, high-fidelity DNA polymerases with proofreading activity (3' end to 5' end exonuclease activity) were used. AccuPrime™ *Pfx* SuperMix (Invitrogen™, cat.no. 12344-040) is a ready-to-use mixture of DNA polymerase, accessory proteins, salts, magnesium, and deoxyribonucleotides (dNTPs) and has fidelity 26 times higher than Taq DNA polymerase, so it is suitable for amplification of genes that need to be cloned, expressed, and functionally studied.

To perform the amplification, a 25 µl reaction was set-up by adding to 22.5 µl of AccuPrime™ *Pfx* SuperMix, 2 µl of DNA template, and 0.3 µl of each Fw and Rev primers to have a final primer concentration of 200 nM. Then 0.2 ml microtubes (VWR International Ltd, cat.no. 732-0548) were transferred to the Mastercycler ep Gradient S (Eppendorf) or to the Mastercycler ep Gradient (Eppendorf) thermal cycler, and the PCR program reported in **Table 4** was run.

Table 4: PCR program used with AccuPrime™ Pfx SuperMix

Cycles	Temperature	Time	Step
	95°C	5 min	Initial denaturation
35 cycles	95°C	15 seconds	Denaturation
	51°C	30 seconds	Annealing
	68°C	2 min	Extension
	4°C	To conserve the reactions until they are removed from the thermocycler	

2.1.8.2 Gradient polymerase chain reaction using PfuUltra High-Fidelity DNA Polymerases

To achieve high levels of specific and sensitive amplification it is important to use an appropriate annealing temperature, which is usually 3-5°C less than the primer melting temperature. There are different formulae based on the nucleotide content that can be used to calculate the melting temperature of the primer sequence that anneal to the template; however other factors, such as the possibility of secondary structure in the sequences and primer-dimer formation between the Fw and Rev primers, should be considered when an annealing temperature is chosen. For these reasons, evaluation of appropriate annealing temperature using gradient PCR was employed. This method permits the testing of different annealing conditions simultaneously to determine empirically the best annealing temperature to have high levels of DNA amplification.

For gradient PCRs, *PfuUltra* High-Fidelity DNA Polymerase (Agilent Technologies, cat.no. 600382) was used and reactions were performed according to manufacturer's instruction: a 200 µl mix (50 µl/reaction) was prepared with 20 µl of 10X *PfuUltra* High-Fidelity reaction buffer containing Mg^{2+} (Agilent Technologies, cat.no. 600382), dNTPs (Thermo Fisher Scientific, cat.no. R0181) so that each was at a final concentration of 250 µM, 400 ng of Fw and Rev primers, complementary DNA (cDNA) template or DNA template (~10 ng), and 4 µL *PfuUltra* High-Fidelity DNA Polymerases (2.5 U/reaction). The mix was divided into four PCR microtubes that were positioned in columns 1, 4, 8, and 12 of a Mastercycler ep Gradient S or Mastercycler ep Gradient thermal cycler before running one of the gradient PCR protocols reported in **Table 5** and **Table 6**.

Table 5: Gradient PCR program with annealing temperature from 48°C to 55°C.

Cycles	Temperature	Time	Step
	95°C	2 min	Initial denaturation
30 cycles	95°C	30 seconds	Denaturation
	48°C-55°C*	30 seconds	Annealing
	72°C	2 min	Extension
	72°C	10 min	Final extension
	4°C	To conserve the reactions until they are removed from the thermocycler	

*Annealing temperatures are different in each thermocycler column: in column 1 48.2°C, in column 4 49.3°C, in column 8 52.6°C, in column 12 54.8°C

Table 6: Gradient PCR program with annealing temperature from 53°C to 62°C

Cycles	Temperature	Time	Step
	95°C	2 min	Initial denaturation
30 cycles	95°C	30 seconds	Denaturation
	53°C-62°C*	30 seconds	Annealing
	72°C	2 min	Extension
	72°C	10 min	Final extension
	4°C	To conserve the reactions until they are removed from the thermocycler	

*Annealing temperatures are different in each thermocycler column: in column 1 53°C, in column 4 54.5°C, in column 8 59°C, in column 12 61.8°C

2.1.9 DNA digestion using restriction endonucleases

DNA (plasmid and PCR product) digestions using restriction endonucleases were performed for preparative (cloning) and analytical purposes.

In general, for cloning purposes double digestions were set-up when the two restriction endonucleases (Thermo Fisher Scientific) to be used had 100% activity in a common buffer (Thermo Fisher Scientific); otherwise sequential digestions in the enzyme appropriate buffer (Thermo Fisher Scientific), with reaction purification (Section 2.1.13) between the first and the second reaction, were performed. Usually 800-1000 ng of plasmids or 500-800 ng of purified PCR products were digested. For the majority of the reactions, 10 U of each restriction enzyme was used; in sequential digestions, when the second reaction volume was bigger than 30 µl, 15 U of restriction enzyme was usually used. Since the restriction endonucleases used are suspended in a glycerol-containing buffer, to maintain the percentage of glycerol at less than or equal to 10% of the reaction (manufacturer's instruction) volume, single digestions were usually set-up in a total volume of 10 µl and double digestion in 20 µl, unless the low DNA concentration did not permit reactions in that volume. Reactions were incubated at 37°C in a water bath for at least 2 h, but never more than 3 h. Digestion reactions performed for cloning procedures were usually purified (Section 2.1.13) or subjected to preparative gel electrophoresis and DNA fragment extraction from agars gel (Sections 2.1.12 and 2.1.14).

For analytical purposes, such as screening of plasmid DNA, digestions were performed using FastDigest® enzymes (Thermo Fisher Scientific) when possible: usually 400-600 ng of plasmid DNA was digested in a total volume of 20 µl or 10 µl depending if double or single digestion was being performed. The universal FastDigest® Green Buffer (Thermo Fisher Scientific, cat.no. B72) and 10 U of FastDigest® enzymes were

used for these reactions. Reactions were incubated at 37°C for 20 min and subsequently run on agarose gel (Section 2.1.12).

2.1.10 DNA ligation

DNA ligation was used to ligate pI.18 or phCMV1 vector to the HA gene of interest. Reactions were set-up in the lowest volume possible, usually 10 µl, using 5 U of T4 DNA Ligase (Thermo Fisher Scientific, cat.no. EL0011) in its buffer (Thermo Fisher Scientific, cat.no. B69) and a vector to insert ratio of 1:3. A ligation control reaction (no insert) was also set-up to check the presence of undigested or re-ligated vector. Reactions were usually incubated for 68-72 h at room-temperature before being transformed into chemically competent DH5α *E. coli.*

2.1.11 Colony polymerase chain reaction for recombinant clone screening

Colony PCR is a fast and high-throughput method to discriminate if a bacterial transformant possesses plasmid DNA with certain characteristics (e.g. presence of a gene). Colony PCR amplification of a specific DNA sequence (in this case the MCS) permits identification of bacterial clones that possess a plasmid with an insert or not after gene cloning.

For colony PCR, each bacterial colony to be tested was diluted in 20 µl of DNase/RNase free water before streaking the colony on a grid on an appropriate LB Agar plate. Negative (colony with empty vector) and positive (colony with vector and insert) controls are inserted if available. Furthermore an additional control consisting of DNase/RNase free water was also added to evaluate if carry-over of DNA was present during the procedure. After a lysis step at 94°C for 3 min in a thermal cycler, 5 µl of each colony suspension was transferred to a PCR microtube in which a 20 µl of PCR mix was present. For the PCR mix, a stock was prepared and aliquoted into PCR microtubes; the stock mix was prepared calculating the samples to be screened and for each reaction adding 12.5 µl of DreamTaq Green PCR Master Mix (Thermo Fisher Scientific, cat.no. K1081 or K1082), 0.1 µl of each Fw and Rev primers (final concentration 400 nM). Usually vector specific sequencing primers (**Table 3**) were used since they anneal upstream and downstream of the MCS in which the gene of interest is cloned; however, in certain cases, gene-specific primers were used instead. Amplification of the target sequence was verified through analytical DNA gel electrophoresis, after the colony PCR program (**Table 7**).

Table 7: Colony PCR program

Cycles	Temperature	Time	Step
	94°C	2 min	Initial denaturation
30 cycles	94°C	30 seconds	Denaturation
	51°C	1 min	Annealing
	72°C	2 min	Extension
	72°C	5 min	Final extension
	4°C	To conserve the reactions until they are removed from the thermocycler	

2.1.12 DNA gel electrophoresis

DNA gel electrophoresis was performed principally for analytical purposes. Since analysed DNA usually ranged between 1 kb and 6 kb, 1% (w/v) agarose (Fisher Scientific, cat.no. BP1356) gel in 0.5X Tris-Acetate-Ethylenediaminetetraacetic acid (EDTA) buffer (TAE; 50X stock solution, Alpha Laboratories, cat.no. EL0077; or Fisher Scientific, cat.no. BP1332) was used as matrix. Ethidium bromide (Sigma-Aldrich, cat.no. 46067), a dye that intercalates between double-strand DNA and fluoresces orange-red when it adsorbs ultraviolet light, was added to the agarose gel to give a final concentration of 0.1 µg/ml.

Samples were loaded on the gel after addition of loading dyes: for PCR products, 4 µl or 5 µl was loaded after addition of 1 µl of 5X Loading Dye (QIAGEN, cat.no. 239901) or 6X DNA Loading Dye (Thermo Fisher Scientific, cat.no. R0611), respectively. Colony PCRs were performed using DreamTaq Green PCR Master Mix that contains tracking dyes and therefore were directly loaded onto the gel. When fast-digestion reactions were loaded on gel, FastDigest® Green Buffer, which permits direct loading, was used. At least one molecular weight marker/ladder was used per gel: GeneRuler 1 kb DNA Ladder Mix (Thermo Fisher Scientific, cat.no. SM0311), Fisher BioReagents™ exACTGene 1 kb Plus DNA Ladder (Fisher Scientific, cat.no. BP2579100) or 1 kb DNA Ladder (New England Biolabs, cat.no. N3232S).

When preparative gels were necessary (for subsequent DNA gel extraction), 1% low-melting agarose (Melford Laboratories Ltd, cat.no. L1204) or 1% UltraPure™ Agarose (Invitrogen™, cat.no. 6500-500) gels in 0.5X TAE were used. Samples for preparative gels were loaded on the gel using 6X DNA Loading Dye (Thermo Fisher Scientific).

Agarose gels were run in 0.5X TAE buffer using a power supply (Consort, cat.no. EV231) and electrophoretic chambers (SCIE-PLAS, cat.no. SVG-SYS Vari-gel MINI; or PEQLAB Biotechnologie GmbH, cat.no. 40-124 or 40-0911; or Sigma-Aldrich, cat.no. EP1101); analytical gels were run at 70-100 V for 1-2 h depending the voltage used, the gel length, resolution to be achieved and monitoring loading dye migration; preparative gels were run at 40 V to avoid over-heating.

A trans illuminator (UVItec, cat.no. BXT-26.MX) was used to observe gels and excise DNA bands; a G:Box Chemi XT Chemi XT Imaging System (Syngene) and GeneSnap software (Syngene) was used to acquire images.

2.1.13 Polymerase chain reaction and restriction digestion purification

To purify PCR and digestion reactions QIAquick PCR purification kit (QIAGEN, cat.no. 28104) was used following the manufacturer's instruction (QIAGEN 2012c). Briefly, 5 volumes of Buffer PB were added to the reaction, then 10 µl of 3 M sodium acetate pH 5.0 was added to permit acidification of the mixture since binding is optimal at pH 7.5. The mixture was then centrifuged in a QIAquick column at 17000 g for 1 min to permit specific DNA adsorption to the silica membrane. Flow-through was discarded and 750 µl of ethanol-containing Buffer PE was used to remove salt contaminant through another centrifugation at the same speed. Finally, after an additional 2 min centrifugation to remove ethanol residue, DNA was eluted from the column adding 30 µl of 70°C DNase/RNase free water, incubating for 1 min, and centrifuging into a clean 1.5 ml microtube for 1 min at 17000 g.

2.1.14 DNA fragment extraction from agarose gel

When it was necessary to gel purify DNA fragments, preparative agarose gel electrophoresis was performed, and the band of interest was excised from the gel using a scalpel. The DNA was extracted from the agarose gel slice using the QIAquick Gel Extraction Kit (QIAGEN, cat.no. 28704) or MinElute Gel Extraction Kit (QIAGEN, cat.no. 28604). Briefly, 3 volumes of Buffer QG, that permit gel melting, were added to 1 volume of gel slice and incubated at 50°C for 10 min with constant mixing to permit complete gel dissolution; pH was then adjusted to 7.5 using 3 M sodium acetate pH 5.0, and one volume of isopropanol (Fisher Scientific, cat.no. P/7500/17) was added. Then the mixture was loaded on a QIAquick or MiniElute spin column for 1 min with 17000 g centrifugation. Two centrifugation-wash steps were performed with Buffer QG and Buffer PE to remove traces of agarose and salt. After centrifugation at 17000 g for 2 min to remove ethanol residues, 30 µl or 10 µl of 70°C DNase/RNase free water was added to the QIAquick or MiniElute spin column. The column was incubated 1 min at room

temperature (RT) before proceeding to a final centrifugation step to elute DNA into a clean 1.5 ml microtube.

2.1.15 Site-directed mutagenesis of plasmid DNA

When it was necessary to correct a PCR-mediated nucleotide sequence mutation of a gene or for studies to analyse the role of a DNA sequence, site-directed mutagenesis was performed. Two different methods based on the same principle were used for this purpose: the first was a commercial QuikChange Lightning Site-direct mutagenesis kit (Agilent Technologies, cat.no. 210518); the second was an in-house protocol.

2.1.15.1 Site-directed mutagenesis with QuikChange Lightning Site-directed mutagenesis kit

For the QuikChange Lightning site-directed mutagenesis the manufacturer's protocol (Agilent Technologies n.d.), with slight modification was followed. Briefly, two reverse-complementary oligonucleotide primers that contain the desired mutation were designed using the QuikChange Primer Design web-tool (Agilent Technologies). These two primers (125 ng each) were then used in a 50 µl PCR reaction together with 140 ng of the plasmid DNA to be mutated, 5 µl of specific reaction buffer, 1.5 µl of QuikSolution reagent (an Agilent Technologies proprietary salt solution), and DNase/RNase free water. To this reaction, 1 µl of QuikChange Lightning Enzyme (an Agilent Technologies proprietary *Pfu*-based polymerase blend) was added. Subsequently, the PCR program in **Table 8** was run on the Mastercycler ep Gradient S or the Mastercycler ep Gradient thermal cycler.

During the amplification a mutation-containing double-nicked plasmid DNA is synthesised. The nick in this plasmid product is repaired after transformation in *E. coli* bacterial cells. However, before proceeding to the bacterial transformation, a step to eliminate the template DNA is required. For this, 2 µl of the provided *DpnI* restriction enzyme was added to the amplification reaction to digest the parental/template DNA. *DpnI* can cleave at its restriction site only in DNA that is methylated or hemimethylated, thus leaving the mutation-containing synthesised DNA untouched. Reactions were incubated at 37°C for 5 min to permit digestion. Then heat-shock transformation of *E. coli* XL10-Gold Ultracompetent cells was performed. This transformation differs from the one previously described (Section 2.1.3) for the incubation times, and for one step: before adding 2 µl of the *DpnI*-digested amplification reaction, XL10-Gold Ultracompetent cells were incubated on ice for 2 min with 2 µl of ß-mercaptoethanol to increase transformation efficiency. After adding the DNA, XL10-Gold Ultracompetent cells were incubated for 30 min on ice, 30 seconds at 42°C and 2 min on ice for recovery. The other transformation steps were

performed as previously described (Section 2.1.3). Mutagenesis success was verified through Sanger sequencing after isolation of plasmid DNA.

Table 8: QuikChange Lightning Site-directed mutagenesis PCR program

Cycles	Temperature	Time	Step
	95°C	2 min	Initial denaturation
18 cycles	95°C	20 seconds	Denaturation
	60°C	10 seconds	Annealing
	68°C	3 min	Extension
	68°C	5 min	Final extension
	4°C	To conserve the reactions until they are removed from the thermocycler	

2.1.15.2 Site-directed mutagenesis with in-house protocol

In order to reduce cost, an in-house protocol, based on the same principle as the QuikChange Lightning Site-direct mutagenesis kit, was optimised. This method takes a little longer than the kit version since additional steps are necessary between one stage and another, but has a similar efficacy.

For primer design the QuikChange Primer Design web-tool was used. Then amplification was performed using the site-direct mutagenesis PCR protocol reported in **Table 9** and preparing an amplification reaction with 25 µl of ACCUZYME™ Mix (Bioline, cat.no. BIO-25028), 125 ng of each primer, 130 ng of plasmid DNA to be mutated, and DNase/RNase free water to a final volume reaction of 50 µl.

Table 9: In-house site-directed mutagenesis PCR protocol

Cycles	Temperature	Time	Step
	98°C	3 min	Initial denaturation
25 cycles	98°C	20 seconds	Denaturation
	60°C	15 seconds	Annealing
	72°C	12 min	Extension
	72°C	20 min	Final extension
	4°C	To conserve the reactions until they are removed from the thermocycler	

Amplification was verified by analytical DNA gel electrophoresis; the amplicons were purified, before 200-400 ng were digested for 20 min at 37°C in a 10 µl reaction with

10 U of FastDigest® *DpnI* (Thermo Fisher Scientific, cat.no. FD1703) in 1X FastDigest® Buffer (Thermo Fisher Scientific, cat.no. B64). The *DpnI* reaction was heat-inactivated for 5 min at 80°C, before being used to transform *E. coli* DH5α cells. Also in this case the success of the mutagenesis protocol was verified through Sanger sequencing after isolation of plasmid DNA from bacterial cultures.

2.2 Cell culture reagents, materials and techniques

General cell culture protocols and maintenance of cell lines are described below.

All the procedures were performed in a MSC-Advantage™ Class II Biological Safety Cabinet (Thermo Fisher Scientific, cat.no. 51028226) and using a Heracell™ 150i humidified CO_2 Incubator (Thermo Fisher Scientific) for incubations at 37°C 5% CO_2.

2.2.1 Cell line characteristics and maintenance

The Human Embryonic Kidney (HEK) 293T/17 (ATCC®: CRL-11268™) cell line is a highly transfectable cell line that was selected from a clone of HEK293T cells and is widely used for the production of retroviral and lentiviral vectors.

HEK293T/17 cells were maintained in Dulbecco's Modified Eagle Medium (DMEM) with high glucose and GlutaMAX™[4] (Gibco®, Invitrogen™, cat.no. 31966-021) or equivalent media (Sigma-Aldrich, cat.no. D6429, or PAN-Biotech, cat.no. P04-04510). The medium was supplemented depending on the application with 15% (v/v) or 10% (v/v) of European Union approved origin heat-inactivated Fetal Bovine Serum (FBS; Gibco®, Invitrogen™, cat.no. 10500-064, or PAN-Biotech, cat.no. P30-8500) and 1% (v/v) penicillin/streptomycin (Sigma-Aldrich, cat.no. P4333).

HEK293T/17 cells were cultured at 37°C 5% CO_2 in 10 cm sterile ΔNunclon® surface cell culture dishes (Thermo Fisher Scientific, cat.no. 150350) using 15% FBS-DMEM media three times a week, maintaining a constant subculture ratio of 1:4, 1:4, and 1:8 respectively. Briefly, old medium was removed from the cells that were rinsed with 2 ml of 0.05% (w/v) Trypsin-0.53 mM EDTA solution (Sigma-Aldrich, cat.no. T3924, or PAN-Biotech, cat.no. P10-040100) and then incubated with 2 ml of fresh Trypsin-EDTA solution at 37°C 5% CO_2 until the cells were completely detached from the dish. Subsequently, cells were resuspended by adding 6 ml of 15% FBS-DMEM medium that also neutralized the trypsin. Finally, 2 ml (1:4 ratio) or 1 ml (1:8 ratio) of cell suspension was added to 10 ml of fresh medium in a new 10 cm dish.

[4]L-alanine-L-glutamine, a more stable derivate of L-glutamine, which does not degrade to ammonia.

Madin-Darby Canine Kidney (MDCK) cells were kindly provided by Prof. Sarah Gilbert (Jenner Institute, University of Oxford, UK). These canine kidney epithelial cells are widely used for the propagation of influenza viruses. MDCK cells were cultured in DMEM (Sigma-Aldrich, cat.no. D6429) with 5% heat-inactivated FBS (PAN Biotech) and 1% penicillin-streptomycin and subcultured twice a week to a ratio of 1:5.

A549 cell line (ATCC®: CCL-185™), kindly provided by Prof. Paul Kellam (Wellcome Trust Sanger Institute, UK), is a human lung carcinoma epithelial cell line (Giard *et al.* 1973) and it was chosen for its origin, as the human lung represents the natural target of influenza viruses. A549 cells were cultured in DMEM/F12 media (Hyclone, cat.no. SH30023.02) with 10% FBS and 1% penicillin-streptomycin, maintained at 37°C 5% CO_2, and subcultured to a 1:5 ratio twice a week.

MDCK and A549 subculturing protocol was similar to the one described above for HEK293T/17 cells with the following differences: cells were maintained in T75 flasks (Thermo Fisher Scientific, cat.no. 156499) in presence of their cell-line specific culture media, volumes were adapted to the culture format, and Dulbecco's Phosphate Buffer Saline (PBS; Sigma-Aldrich, cat.no. D8537) was used instead of Trypsin-EDTA solution to wash the cells.

2.2.2 Freezing and thawing of cell lines

Cells were frozen when they reached 80% confluence: for a 10 cm dish one cryovial (Corning®, cat.no. 430915) was prepared, whereas for a T75 flask three vials were set up. Briefly, cells were detached by trypsinization as previously described (Section 2.2.1) and centrifuged at 1000 g for 5 min using Rotor 6M of ELMI CM-6MT Centrifuge (Spectra Services) and then resuspended in freezing media, which is the culture media with addition of 10% (v/v) dimethyl sulfoxide (DMSO; VWR International Ltd, BDH Prolabo GPR RECTAPUR®, cat.no. 282164K). Cells were then transferred into cryovials (1 ml/cyovial) that were placed in a Mr. Frosty™ Freezing Container (Thermo Fisher Scientific, cat.no. 5100-0001) at -80°C to have a 1°C/min cooling rate, and stored at -80°C until this temperature was reached. Subsequently, they were maintained at -80°C in a cryobox (Thermo Fisher Scientific, cat.no. 1417563).

When cells were required, a cryovial was thawed at 37°C in a water bath. The cell suspension was then transferred into 15 ml tubes (Greiner Bio-One, cat.no. 188271) with 7 ml of appropriate medium, centrifuged at 1000 g for 5 min and supernatant was removed to eliminate traces of DMSO. Cells were then resuspended in 5 ml or 10 ml of appropriate medium and transferred to a 10 cm dish or a T25 flask (Thermo Fisher Scientific, cat.no. 156367). When cells had attached to the cell culture vessel, the medium was

changed; when cells were confluent, subculturing was performed (cells usually kept in T75 flask were transferred from T25 to T75 flask in the first passage).

2.3 Influenza lentiviral pseudotype protocols

2.3.1 Pseudotype production plasmids

p8.91 (originally named pCMVΔR8.91 (Zufferey *et al.* 1997)) is a second generation packaging plasmid construct that expresses HIV-1 *gagpol* under a hCMV promoter but has HIV-1 accessory genes *vif*, *vpr*, *vpu* and *nef* deleted; it was kindly provided by Dr. Nigel Temperton (Universities of Greenwich and Kent, Medway, UK).

pCSFLW, provided by Dr. Nigel Temperton, is a self-inactivating lentiviral vector with Ψ packaging signal, the central polypurine tract *cis*-active sequence (cPPT), an internal promoter constituted by the U3 part of the Spleen Focus Forming virus (SFFV) long terminal repeat sequence, and a Woodchuck hepatitis virus post-transcriptional regulatory element (WPRE) to enhance reporter gene expression. pCSFLW was originally modified from pCSGW (originally pHR'SIN-cPPT-SE (Demaison *et al.* 2002)) inserting firefly luciferase-encoding gene as a reporter system instead of enhanced GFP-encoding gene.

pI.18-A/Vietnam/1194/2004 H5 (Temperton *et al.* 2007) was kindly provided by the National Institute for Biological Standards and Control (NIBSC, London, UK), pI.18-A/Hong Kong/156/1997 was kindly provided by Novartis Vaccines and Diagnostics, and pI.18-A/turkey/Turkey/1/2005 H5 was kindly provided by Dr. Nigel Temperton who subcloned the gene originally provided in another plasmid by the National Institute for Medical Research (Mill Hill, London, UK).

The ampicillin-resistant pCAGGS-HAT and pCAGGS-TMPRSS2 plasmids (E. Böttcher *et al.* 2006), expressing HAT and TMPRSS2 proteases under the control of a chicken β-actin promoter, were used for influenza HA pp production (Chapters 3 and 6). They were kindly provided by Prof. Hans-Dieter Klenk and Dr. Eva Böttcher-Friebertshäuser (Institute of Virology, Philipps University Marburg, Germany).

The kanamycin-resistant pCMV-Tag3 TMPRSS4 (ECD)-myc expressing the TMPRSS4 extracellular domain (ECD) (Jung *et al.* 2008), the ampicillin-resistant pcDNA3.1-TMPRSS3 and pcDNA3.1-TMPRSS6, expressing type II Transmembrane Protease Serine 3 (TMPRSS3) and type II Transmembrane Protease Serine 6 (TMPRSS6) respectively (Bertram, Glowacka, Blazejewska, *et al.* 2010), were provided by Prof. Stefan Pöhlmann (Infection Biology Unit, German Primate Center, Germany).

2.3.2 Production of Highly Pathogenic Avian influenza haemagglutinin pseudotypes

2.3.2.1 Production of H5 and H7 pseudotypes using FuGENE® 6 transfection reagent

Production of HPAI H5pp and HPAI H7pp was essentially as described in Temperton *et al.* 2007 and in Molesti *et al.* 2013.

For production of HPAI pp a DNA mix containing 1 µg of p8.91, 1.5 µg of pCSFLW and 1 µg of HA-expressing plasmid (pI.18 backbone) was set-up in DNase/RNase free water with total volume 15 µl and a plasmid ratio 1:1.5:1. To transfect the DNA mix into HEK293T/17 cells, 18 µl of FuGENE® 6 (Promega, cat.no. E2692) was diluted directly in 200 µl of OptiMEM® I reduced serum medium (Gibco®, Invitrogen™, cat.no. 31985-047) with care to not touch the plastic 1.5 ml microtube, as contact between undiluted FuGENE® 6 and plastic limits transfection efficiency (Jacobsen 2004). After 5 min incubation at RT, the 15 µl DNA mix was added resulting in a FuGENE® 6-DNA ratio of approximately 5.2:1; then the microtube was further incubated at RT for 15 min to enable DNA-FuGENE® 6 complex formation. Finally, the mixture was added dropwise to an 80% confluent HEK293T/17 10 cm dish, in which 7 ml of fresh 15% FBS-DMEM was previously added after the original medium had been removed. Subsequently, the transfection dish was incubated at 37°C 5% CO_2.

After 24 h, the transfection medium was removed, and 7 ml of fresh 15% FBS-DMEM and 1 U of exogenous NA from *Clostridium perfringens* (Sigma-Aldrich, cat.no. N2876) were added to facilitate pp release from the producer cells, since NA activity is lacking in these pp. Cells were then incubated at 37°C 5% CO_2 for an additional 24 h before pp harvesting, by removal of cell supernatant using a 20 ml syringe and filtration using a 0.45 µm mixed cellulose ester membrane filter (Merck Millipore, cat.no. SLHA033SB). Pp were then directly titrated and stored at -80°C. When direct titration was not possible, a 130 µl aliquot of pp was prepared and conserved at -80°C until titration was performed to minimise the freeze-thawing of this original batch.

2.3.2.2 Production of H5 and H7 influenza pseudotypes using polyethylenimine

FuGENE® 6 is a mixture of lipids/cationic amphiphiles in 80% ethanol that coat the DNA. After interaction with and disruption of the negative cell membrane, the coated DNA can enter into target cells (Jacobsen 2004; Behr 1994). FuGENE6® has been shown to be a highly efficient low-cytotoxicity transfection reagent (Jacobsen 2004; Yamano, Dai and Moursi 2010) and is used widely for small scale production of lentiviral vectors. However, its relatively high cost can limit its use in large optimisation or lentiviral

production experiments. For this reason another reagent was evaluated for pp production. The use of polycationic polymer polyethylenimine (PEI) in transfection and in production of lentiviral vectors has been described as being as efficient as lipofection reagents (Yamano, Dai and Moursi 2010; Segura *et al.* 2007) or the calcium phosphate method (Toledo *et al.* 2009). PEI mediates transfection of DNA through condensing DNA forming cationic nanosized complexes (polyplexes) that can interact with the membrane and enter cells through endocytosis (Hanzlíková *et al.* 2011); subsequently, by virtue of PEI intrinsic buffering activity, it destabilizes the endosome permitting DNA delivery into the cytosol (Toledo *et al.* 2009).

An already optimised transfection protocol for routine pp production was kindly provided by Dr. Edward Wright (University of Westminster) and was adapted for the production of influenza pp. Firstly, branched 25 kDa PEI (Sigma-Aldrich, cat.no. 408727) was dissolved in water to 50 mg/ml and then diluted to 1 mg/ml adjusting the pH to 7 with hydrochloric acid (Fisher Scientific, cat.no. H/1200/PB17). The solution was sterilised through filtration with a 0.22 µm filter, aliquoted, and conserved at -20°C. The working aliquot once thawed and opened was conserved at 4°C for 2 months. Then a DNA mix of p8.91, pCSFLW and HA-expressing plasmid at ratio 1:1.5:1 as previously described was prepared in 200 µl of OptiMEM® I. At the same time, in another microtube, 35 µl of 1 mg/ml PEI was added to 200 µl of OptiMEM® I. After 5 min incubation the PEI-OptiMEM® I mixture was transferred to the DNA mix microtube and further incubated for 20 min to permit the formation of DNA-PEI polyplexes, before adding dropwise to a 80% confluent HEK293T/17 10 cm dish, in which the medium was previously changed with 7 ml of 10% FBS-DMEM. The plate was then incubated and the procedure for pp production was continued as described in the previous section and using 10% FBS-DMEM instead of 15% FBS-DMEM.

Before the PEI protocol was extensively used for pp production, it was tested and compared with the FuGENE® 6 protocol for the production of influenza pp: a bridge-experiment was performed producing in parallel A/Hong Kong/156/1997 H5pp using the FuGENE® 6 protocol and the PEI protocol which showed that the two production methods are comparable ($p = 0.6809$) (**Figure 19**).

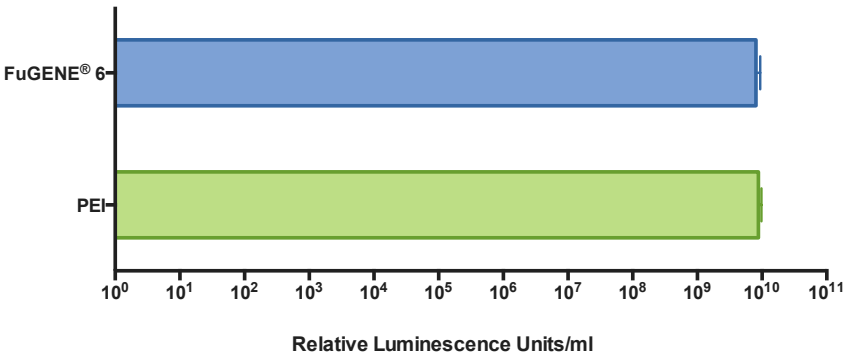

Figure 19: Comparison of A/Hong Kong/156/1997 pp titres produced using two different transfection methods

2.3.3 Pseudotype titration protocol

Titration experiments were performed in Nunc™ F96 MicroWell™ white polystyrene plates (Thermo Fisher Scientific, cat.no. 136101), using reagent reservoirs (Corning®, cat.no. 4870, or Dutscher Scientific, cat.no. 006793) to hold the culture medium, and 8- or 12-channel pipettes (PZ HTL, cat.no. 5123 and 5127) to perform dilutions.

The pp titre was evaluated by transducing HEK293T/17 cells with 2-fold serial dilutions of neat pp supernatants performed in a total mixing volume of 100 µl, discarding 50 µl from the last dilution. Next, a cell suspension was added to each well (details below). Control wells in which pp were not present were set-up in every titration as an indirect cell viability measurement.

To prepare the cell suspension to be added to the titration plate, a 10 cm dish of confluent HEK293T/17 cells was washed with 2 ml of Trypsin-EDTA solution, before 2 ml of fresh trypsin were added, and incubation at 37°C 5% CO_2 was performed to permit cell detachment. After adding 6 ml of 10% FBS-DMEM, cells were resuspended to have a single-cell suspension to be counted under the light microscope (Medline scientific, cat.no. Inverso-TC100) using a FastRead 102™ counting slide (Immune Systems, cat.no. BVS100) following manufacturer's instructions (Immune Systems n.d.). Finally, a 1.5×10^4 cells/50 µl suspension in 15% FBS-DMEM was prepared and 50 µl (1.5×10^4 cells) were added to each well of the plate that was then incubated at 37°C 5% CO_2 to allow pp transduction of cells and luciferase gene expression.

Firefly luciferase gene expression was evaluated and quantified after 48 h by luminometry using the Bright-Glo™ assay system (Promega, cat.no. E2650, **Figure 20**) and GloMax Multi detection system luminometer (Promega, cat.no. E7031 and E7041): 50 µl of Bright-Glo™ Luciferase Assay System solution was added to each well and, after incubation for 5 min at RT, the plate was read using the standard Bright-Glo™ protocol pre-installed on the luminometer.

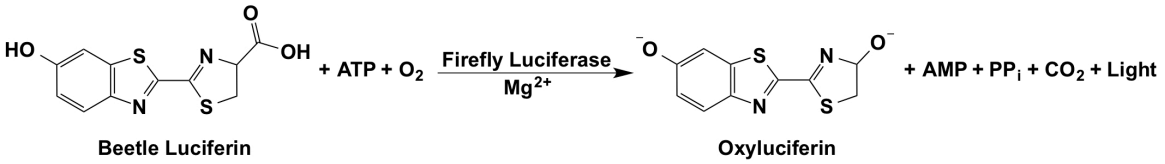

Figure 20: The firefly luciferase reaction used in the Bright-Glo™ Luciferase Assay System
In the presence of Mg^{2+}, firefly luciferase catalyses the mono-oxygenation of beetle luciferin using ATP and molecular oxygen to produce oxyluciferin and light. The figure was adapted using ChemBioDraw Ultra 14 from the Bright-Glo™ Luciferase Assay System Technical Manual, Promega (Promega 2011).

2.3.4 Pseudotype particle neutralization assay

To perform the pp neutralization assay (pp-NT), Nunc™ F96 MicroWell™ white polystyrene plates and reagent reservoirs were used; human sera were always handled using 200 µl MultiGuard NX Barrier tips (Sorenson BioScience, cat.no. 30550T), 20 µl MultiGuard Barrier tips (Sorenson BioScience, cat.no. 35220), or 10 µl MultiGuard E Barrier tips (Sorenson BioScience, cat.no. 15020T) and dilutions were performed using 8- or 12-channel pipettes.

For the pp-NT, 2-fold serial dilutions of 2 µl, 2.5 µl or 5 µl serum samples and neutralization controls (positive and negative) were performed in a total mixing volume of 100 µl and, in the last dilution, 50 µl was discarded. The plate was centrifuged for 1 min at 500 g using an ELMI CM-6MT Centrifuge and rotor 6M04 and then 50 µl of a pp solution with a concentration 1×10^6 RLU/50 µl was added to each well. Four or eight wells were also used for the viral input control, in which no sera was present; another four or eight wells were kept antibody and virus-free (50 µl of 10% FBS-DMEM was added instead of the pp solution) as a cell-only control. The plate was centrifuged for 1 min at 500 g before 1 h incubation at 37°C 5% CO_2. Finally, 1.5×10^4 HEK293T/17 cells, prepared as described in the previous section, were added to each well and incubated at 37°C 5% CO_2 after a final 1 min centrifugation at 500 g. 48 h later, 50 µl of Bright-Glo™ solution were added to each well and, after 5 min incubation at RT, the plate was read using a GloMax® Multi detection system luminometer as previously described in Section 2.3.3.

2.4 Protein detection reagents, materials and techniques

2.4.1 Sera, primary antibodies and secondary antibodies.

The characteristics of each serum sample, primary antibody or secondary antibody used in this thesis are reported in **Table 10**.

Table 10: Antibodies and reference sera

Name	Antigen used in immunization	Specificity	Origin	Produced by	Cat. no.	Other characteristics	Used in
C179	A/Okuda/57 (H2N2)	H1N1 H2N2	BALB/c mouse	TaKaRa Clonthec	M145	mAb, IgG2a subclass Recognise a conformational epitope on HA stalk (H1, H2, H5, H6, H10)	Chapter 3 Chapter 5
H1 reference antisera	A/duck/Italy/1447/2005 (H1N1)	Avian H1	Chicken (pathogen-free)	OIE	Not applicable	Hyperimmune Approved for HI assay, Agar Gel Immunodiffusion test, and Agar Gel Precipitation test	Chapter 3 Chapter 4
H2 reference antisera	A/duck/Germany/1215/1973 (H2N3)	Avian H2	Chicken (pathogen-free)	OIE	Not applicable	Hyperimmune Approved for HI assay, Agar Gel Immunodiffusion test, and Agar Gel Precipitation test	Chapter 4
H3 reference antisera	A/psittacine/Italy/2873/2000 (H3N8)	H3	Chicken (pathogen-free)	OIE	Not applicable	Hyperimmune Approved for HI assay, Agar Gel Immunodiffusion test, and Agar Gel Precipitation test	Chapter 4
H4 reference antisera	A/cockatoo/England/1972 (H4N8)	H4	Chicken (pathogen-free)	OIE	Not applicable	Hyperimmune Approved for HI assay, Agar Gel Immunodiffusion test, and Agar Gel Precipitation test	Chapter 4 Chapter 5
H6 reference antisera	A/turkey/Canada/1965 (H6N2)	H6	Chicken (pathogen-free)	OIE	Not applicable	Hyperimmune Approved for HI assay, Agar Gel Immunodiffusion test, and Agar Gel Precipitation test	Chapter 4 Chapter 5
H8 reference antisera	A/turkey/Ontario/6118/1968 (H8N4)	H8	Chicken (pathogen-free)	OIE	Not applicable	Hyperimmune Approved for HI assay, Agar Gel Immunodiffusion test, and Agar Gel Precipitation test	Chapter 4 Chapter 5
H9 reference antisera	A/mallard/Italy/3817-34/2005 (H9N2)	H9	Chicken (pathogen-free)	OIE	Not applicable	Hyperimmune Approved for HI assay, Agar Gel Immunodiffusion test, and Agar Gel Precipitation test	Chapter 4 Chapter 5
H10 reference antisera	A/ostrich/South Africa/2001 (H10N1)	H10	Chicken (pathogen-free)	OIE	Not applicable	Hyperimmune Approved for HI assay, Agar Gel Immunodiffusion test, and Agar Gel Precipitation test	Chapter 4 Chapter 5

Name	Antigen used in immunization	Specificity	Origin	Produced by	Cat. no.	Other characteristics	Used in
H11 reference antisera	A/duck/Memphis/546/1974 (H11N9)	H11	Chicken (pathogen-free)	OIE	Not applicable	Hyperimmune Approved for HI assay, Agar Gel Immunodiffusion test, and Agar Gel Precipitation test	Chapter 4 Chapter 5
H12 reference antisera	A/duck/Alberta/60/1976 (H12N5)	H12	Chicken (pathogen-free)	OIE	Not applicable	Hyperimmune Approved for HI assay, Agar Gel Immunodiffusion test, and Agar Gel Precipitation test	Chapter 4 Chapter 5
H13 reference antisera	A/gull/Maryland/704/1977 (H13N6)	H13	Chicken (pathogen-free)	OIE	Not applicable	Hyperimmune Approved for HI assay, Agar Gel Immunodiffusion test, and Agar Gel Precipitation test	Chapter 4
H14 reference antisera	A/mallard/Gurjev/263/1982 (H14N5)	H14	Chicken (pathogen-free)	OIE	Not applicable	Hyperimmune Approved for HI assay, Agar Gel Immunodiffusion test, and Agar Gel Precipitation test	Chapter 4 Chapter 5
H15 reference antisera	A/shearwater/Australia/2576/1979 (H15N9)	H15	Chicken (pathogen-free)	OIE	Not applicable	Hyperimmune Approved for HI assay, Agar Gel Immunodiffusion test, and Agar Gel Precipitation test	Chapter 4 Chapter 5
H16 reference antisera	A/gull/Denmark/68110/2002 (H16N3)	H16	Chicken (pathogen-free)	OIE	Not applicable	Hyperimmune Approved for HI assay, Agar Gel Immunodiffusion test, and Agar Gel Precipitation test	Chapter 4
H5N1 reference antisera	A/chicken/Scotland/1959 (H5N1)	H5	Chicken (pathogen-free)	APHA*	RAB7000	Hyperimmune	Chapter 4
H7N1 reference antisera	A/African starling/England/983/1979 (H7N1)	H7	Chicken (pathogen-free)	APHA*	RAB7004	Hyperimmune	Chapter 4
H7N2 reference antisera	A/chicken/Wales/1306/2007 (H7N2)	H7	Chicken (pathogen-free)	APHA*	Not applicable	Hyperimmune	Chapter 4 Chapter 5
H7N3 reference antisera	A/chicken/England/4054/2006 (H7N3)	H7	Chicken (pathogen-free)	APHA*	Not applicable	Hyperimmune	Chapter 4
H7N7 reference antisera	A/England/268/1996 (H7N7)	H7	Chicken (pathogen-free)	APHA*	Not applicable	Hyperimmune	Chapter 4

Name	Antigen used in immunization	Specificity	Origin	Produced by	Cat. no.	Other characteristics	Used in
H7N7 reference antisera	A/turkey/England/647/1977 (H7N7)	H7	Chicken (pathogen-free)	APHA*	RAB7005	Hyperimmune	Chapter 4
NIBSC anti-A/England/427/1988 (H3N2)	A/England/427/1988 (H3N2) HA purified from virus particle after bromelain treatment	Human H3 Influenza	Sheep	NIBSC	Not applicable	Hyperimmune Animal immunized multiple times Approved for single radial diffusion assay Treated by manufacture with pH5.5 or lower for 30 min	Chapter 3 Chapter 5
NIBSC 11/136 anti-B/Brisbane/60/2008	B/Brisbane/60/2008 HA purified from virus particle after bromelain treatment	Victoria lineage Influenza	Sheep	NIBSC	NIBSC 11/136	Hyperimmune Animal immunized multiple times Approved for single radial diffusion assay Treated by manufacture with pH5.5 or lower for 30 min	Chapter 6
anti-mouse IgG (whole molecule)–FITC	Mouse IgG	Mouse IgG	Goat	Sigma-Aldrich	F9006	Secondary antibody Fluorescein isothiocyanat (FITC) conjugated	Chapter 3
anti-chicken IgG (H+L) - Fluorescein	Chicken IgY (IgG) (H+L)	Chicken IgY (IgG) (H+L)	Goat	Sigma-Aldrich	SAB3700197	Secondary antibody Fluorescein conjugated	Chapter 3
Alexa Fluor® 680-AffiniPure donkey anti-chicken IgY	Chicken IgY (IgG) (H+L)	Chicken IgY (IgG) (H+L)	Donkey	Stratech Scientific Ltd	703-625-155	Secondary antibody Alexa Fluor® 680 conjugated	Chapter 3
anti-sheep/goat IgG Dylight®800	Sheep IgG	Sheep / Goat IgG	Donkey	AbD Serotec®,	STAR88D800GA	Secondary antibody Dylight®800 conjugated	Chapter 3 Chapter 6

*Animal and Plant Health Agency (APHA)

OIE hyperimmune chicken reference antisera were produced by inoculation of specific pathogen-free chickens with whole influenza viruses, in accordance with OIE guidelines (World Organization for Animal Health n.d.). If necessary, sera were pre-adsorbed with chicken RBCs. Other pre-treatments (e.g. decomplementation at 56°C for 30 min, treatment with receptor destroying enzymes) were not performed.

NIBSC sheep antisera were produced by multiple immunizations with HA protein of the selected influenza virus. The HA protein is missing the transmembrane domain and it is obtained after digestion of virus particles with bromelain and its purification. Sera are decomplemented for SRH use.

2.4.2 Immunofluorescence

Immunofluorescence was performed to evaluate the expression of HAs after plasmid transfection.

HEK293T/17 cells were seeded in a 24-well plate within which poly-lysine coated glass coverslips (VitroCam, cat.no. 1290-P01) had been positioned under 1 ml of 10% FBS-DMEM. After overnight incubation at 37°C 5% CO_2, 200 ng HA-expressing plasmids were transfected using 2.3 µl of the 1 mg/ml PEI solution following a protocol similar to the one described in Section 2.3.2.2 for pp production but with OptiMEM® I volumes reduced to 50 µL in each DNA and PEI microtube. After 24 h, medium was changed with 1 ml of fresh 10% FBS-DMEM. 48 h post-transfection media was removed, cells were washed with PBS (Sigma-Aldrich, cat.no. D8537), fixed and permeabilised for 10 min using 1 ml of methanol (Sigma-Aldrich, cat.no. 32213) previously stored at -20°C. Fixed cells were maintained at 4°C overnight, before protein detection was undertaken. Non-transfected cells were also kept during the transfection procedure as controls and immunofluorescence was performed on them.

Firstly, cells were washed using PBS and then 500 µl of solutions containing the primary antibody were incubated with the cells for 1 h at 37°C. At the end of the incubation, cells were washed with 1 ml of PBS four times: the first wash was for 1 min, the successive washes for 5 min each. Subsequently, 500 µl of a secondary antibody solution was incubated for 1 h at 37°C. Cells were washed again using the previous described washing protocol, and then incubated for 20 min at RT with 500 µl of 1 drop/ml NucBlue® Live ReadyProbes® reagent (Molecular Probes®, cat.no. R37605) in PBS to permit nuclear staining with Hoechst 33342. Cells were washed with PBS for 5 min one last time before coverslips were mounted on slides using a RT Mowiol® solution and observed using an epifluorescence microscope Eclipse 50i (Nikon) with a charge-coupled device digital camera QICAM Fast 1394 (QImaging).

The Mowiol® solution was prepared by mixing 6 ml of glycerol, 2.4 g of Mowiol® 40-88 (Sigma-Aldrich, cat.no. 324590), and 6 ml of DNAase/RNase free water for at least 2 h. Then 12 ml of 0.2 M Tris pH 8.5 was added and the solution warmed at 50-60°C till the Mowiol® was dissolved. The solution was then centrifuged at 5000 g for 15 min to remove any undissolved Mowiol® before being aliquoted and stored at -20°C.

2.4.3 Western blotting

Western blotting experiments were performed to verify the presence of the envelope-located HAs in the produced pp.

2.4.3.1 SDS-polyacrylamide gel electrophoresis and Western blotting solutions

Tris-glycine-SDS buffer was used as running buffer for SDS-polyacrylamide gel electrophoresis (SDS-PAGE). It was prepared by dissolving the components in water to a concentration of 25 mM Tris base (Fisher Scientific, cat.no. BPE152-1), 192 mM glycine (Sigma-Aldrich, cat.no. G8898), and 0.1% (w/v) SDS (Fisher Scientific, cat.no. BP166-500).

The Western transfer buffer was prepared to a final concentration of 25 mM Tris base, 192 mM glycine, and 20% (v/v) methanol (Sigma-Aldrich, cat.no. 32213). The buffer was prepared by dissolving Tris base and glycine in water and storing at 4°C; methanol was added only before use.

To block the Western blotting membrane and to dissolve the primary and secondary antibody, solutions were prepared in PBS (Fisher Scientific, cat.no. BPE9739-1) to a final concentration of 10% (w/v) or 5% (w/v) dried milk (Marvel), and 0.01% (v/v) Tween20 (Sigma-Aldrich, cat.no. P1379).

2.4.3.2 SDS-polyacrylamide gel electrophoresis and Western blotting

The first Western blotting experiments were performed using pp that were simply filtered through a 0.45 μm filter and were still in the cell culture medium (DMEM GlutaMAX with 10% FBS and 1% penicillin-streptomycin); however, significant background due to the presence of bovine serum albumin (BSA) was observed. Since the single HA monomer (~78 kDa) has a similar molecular weight to BSA and could have been partially obscured by the large BSA band (66.5 kDa), to partially remove the BSA low-speed centrifugation was employed. Low-speed centrifugation was chosen firstly because a specific antibody that could be used as a blocking reagent was unavailable. Low speed centrifugation is a widely used method for concentration/purification of lentiviral vectors, and for p120 HIV-1, VSV glycoprotein (VSV-G), and other pp it has been demonstrated to be a suitable approach since it does not disrupt the envelope proteins and

the virion itself (Strang *et al.* 2004; Cepko 2001; B. Zhang *et al.* 2001; Darling *et al.* 2000). For these reasons 2 ml of pp were centrifuged on a fixed angle centrifuge at 3000 g and 4°C for 24 h. Then 1.95 ml of supernatant was removed and 150 µl of OptiMEM® I reduced serum medium were added to the 2 ml tubes (Thermo Fisher Scientific, cat.no. 11519934) that were incubated overnight at 4°C to permit pp resuspension. After resuspension, pp were preserved at -80°C before proceeding to prepare the samples for SDS-PAGE.

Samples for SDS-PAGE were prepared by adding 6 µl of pp to 2 µl of 4X Laemmli buffer (Bio-Rad Laboratories, cat.no. 161-0747) and 0.4 µl of ß-mercaptoethanol (Bio-Rad Laboratories, cat.no. 161-0710), producing a final concentration of 5% v/v. All the samples were boiled in an AccuBlock™ Digital Dry Bath at 100°C for 10 min before spinning them for 1 min at 17000 g and loading them on a 4-15% Mini-PROTEAN® TGX™ precast polyacrylamide gel (Bio-Rad Laboratories, cat.no. 456-1083). MagicMark™ XP Western Protein Standard was also loaded on a gel to estimate the molecular weight of the proteins of interest.

The gel was run in a Mini-PROTEAN® Tetra Cell (Bio-Rad Laboratories, cat.no. 165-8004EDU) with Tris-Glycine-SDS running buffer for 10 min at 100 V and then 50 min at 130 V. The gel was transferred on an Immuno-Blot® low fluorescence Polyvinylidene fluoride membrane (PVDF, Bio-Rad Laboratories, cat.no. 162-0262) for 60 min at 100 V using the Mini Trans-Blot Module (Bio-Rad Laboratories, cat.no. 170-3935) and 4°C Western transfer buffer. To keep the electrophoretic/blotting chamber and the buffer cold, an ice block was inserted in the Mini-PROTEAN® cell; a magnetic anchor and a IKA® Big Squid magnetic stirrer (Sigma-Aldrich, cat.no. Z342033) were also used to keep the Western transfer buffer uniform.

The membrane was blocked overnight with shaking at RT using 25ml of a solution containing 10% (w/v) dried milk + 0.01% (v/v) Tween20-PBS. After removing the blocking buffer, the primary antibody was diluted in 5% (w/v) dried milk-0.01% (v/v) Tween20-PBS and 10 ml of the primary antibody solution were incubated with the membrane for 1 h at RT with shaking. Before adding the secondary antibody, the membrane was washed 4 times (first wash of 1 min, then three subsequent washes for 10 min) with 0.01% (v/v) Tween20-PBS. The membrane was then incubated for 1 h at RT with shaking and with an appropriate secondary antibody conjugated with infrared dyes compatible with Odyssey® Sa Infrared Imaging System (LI-COR Bioscience, cat.no. 9260) and diluted in 5% (w/v) dried milk-0.01% (v/v) Tween20-PBS.

Finally, the membrane was washed four times with 0.01% (v/v) Tween20-PBS and one time with PBS before imaging using the Odyssey® Sa Infrared Imaging System at 700 nm or 800 nm and intensity 4 (on a scale of 1 to 10) was performed.

2.5 Statistical analysis

2.5.1 Evaluation of pseudotype titres

Using Microsoft® Excel 2011 (Microsoft®) each relative luminescence unit (RLU) value obtained during titration at different pp dilution points (n=8) was transformed into RLU/ml; the arithmetic mean of these concentrations was considered as the pp titre (expressed as RLU/ml). Titres were also graphed using GraphPad Prism® version 6 (GraphPad Software) together with standard error of the mean (SEM).

The origin of the graph was taken as 9×10^4 RLU/ml to normalize the data in relation to the value obtained when a pp without envelope protein is analysed using the same methodology.

A blue dotted line at 2×10^7 RLU/ml was also reported on each graph. This line represents the pp titre necessary to perform pp-NT assays without the need for additional processing steps (e.g. concentration, purification, etc.).

Since biological replicates were performed only in certain cases and for this reason excluded from the analysis, statistical tests were not applied. In fact, statistical test should be applied only in presence of biological replicates and not in presence of multiple measures. Titres were only compared graphically.

2.5.2 Calculation of serum neutralizing titres

Unless otherwise stated, pp-NT assays were performed only once since sufficient sera volume was not available to perform replicate assays.

Data analysis on each pp-NT assay was performed using Microsoft® Excel 2011 and GraphPad Prism® version 6 (GraphPad Software). To measure neutralization activity, RLU results were normalised, expressed as the percentage of neutralization (inhibition of pp entry into cells as indicated by reduction in luminescence) using the arithmetic mean of the RLU values of viral input control and of the cell control as 0% and 100% neutralization values, respectively. The half maximal inhibitory concentration (IC_{50}, **Figure 21**), expressed as the dilution factor in which the sample shows 50% neutralization activity, was calculated using a non-linear regression method (GraphPad Prism® "logarithm of inhibitor versus normalised response – variable slope") in which the slope factor was constrained to be less than zero to better fit the neutralization curves (GraphPad Software n.d.).

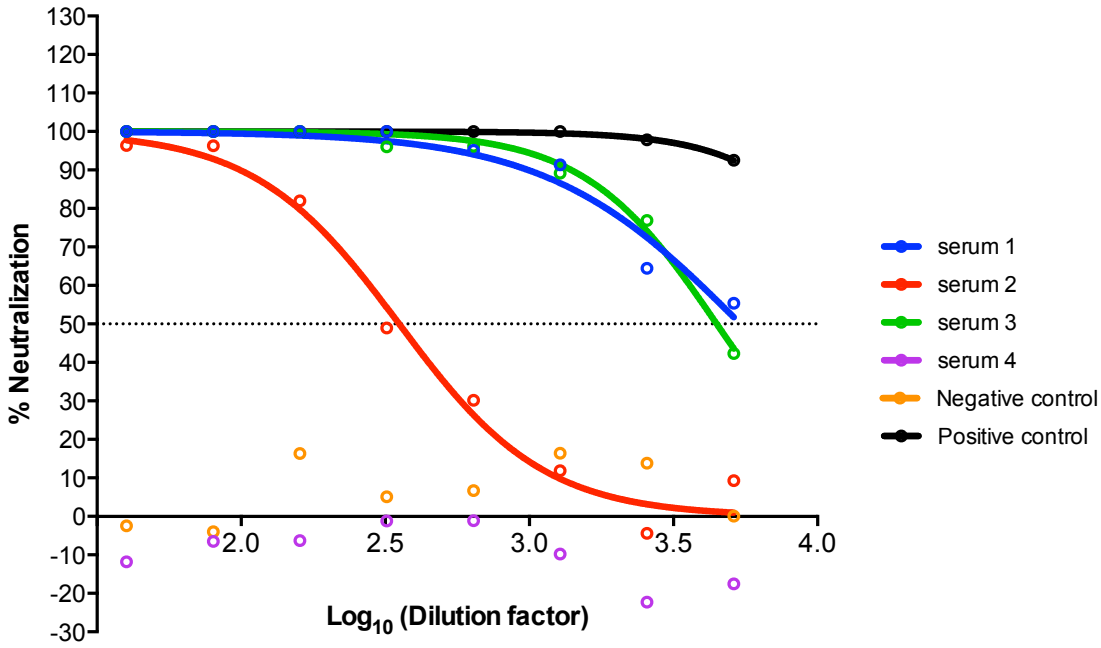

Figure 21: Example of pp-NT results after GraphPad Prism® 6 analysis
Normalised percentage neutralization values are plotted against the logarithm of the dilution factors and neutralization curves are inferred by the software that calculates the IC_{50}. In this example, sera 1, 2 and 3 are able to neutralize the pp tested with different potency (IC_{50} serum 1 = 5402, IC_{50} serum 2 = 353.3, IC_{50} serum 3 = 4468), whereas serum 4 does not neutralize the pp with a result comparable to the negative control.

The IC_{50} calculated with GraphPad Prism® were or directly used for further statistical analisis or transformed in the nearest dilution range. In all cases, appropriate tests on the basis of the experimental design were performed. Specific information about each analysis is reported in each chapter. In general, non-parametric tests were used since the data do not follow a normal distribution.

CHAPTER 3

Production of low pathogenic avian and human influenza A haemagglutinin pseudotypes

3.1 Introduction

As illustrated earlier (Section 1.8.8), pp are useful tools to study HA-directed antibody responses. However, the main limitation is generating these reagents. In fact, to produce pp it is necessary to understand the characteristics of the protein of interest, in this case the HA. Influenza HA was already described in Section 1.2.1; here some aspects and information that were necessary in order to design the correct strategies for influenza A pp production will be discussed.

The HA is encoded by the 4th segment gene of the eight segmented negative strand RNA genome of influenza A virus. The mechanisms that regulate HA expression during the viral life cycle are still not completely understood but the conserved regions flanking the HA gene are known to play an important role (Gomila *et al.* 2013). In fact, sequences essential for the viral polymerase binding the promoter sequence, and the polyadenylation signal are situated at the 5' end and 3'end regions of the HA segment.

The HA is then synthesised as a single polypeptide precursor HA0 by ribosomes. HA folding starts during its synthesis and translocation to the ER (W. Chen and Helenius 2000; Segal *et al.* 1992; Braakman *et al.* 1991). During its synthesis and passage to the ER and within the Golgi, the HA is also subjected to post-translational modification, such as glycosylation and palmitoylation (Brassard and Lamb 1997; Veit and Schmidt 1993; Hurtley *et al.* 1989). Glycosylation is an essential step in HA folding and expression, as it was observed that blocking the glycosylation machinery results in retention of the influenza HA rather than expression at the plasma membrane (Brassard and Lamb 1997; Hurtley *et al.* 1989). Acquisition or loss of a glycosylation site was shown to be related to an increase or decrease in HA folding (Hebert *et al.* 1997). In addition, palmitolylation (S-acetylation) of three cytosolic cysteines is necessary for HA localisation in the lipid raft membrane domains and expression at the plasma membrane, representing an important trafficking signal (Kordyukova *et al.* 2008; B. J. Chen, M. Takeda and Lamb 2005).

During its passage within the Golgi or at the level of the plasma membrane, influenza HA is also cleaved into two active subunits HA1 and HA2 by tissue-specific or ubiquitously expressed proteases (see Section 1.2.1.1) *via* specific single or multiple

arginine or/and lysine residues. This process is essential to activate the HA: without this cleavage the HA cannot undergo the structure change necessary for virus envelope-endosome membrane fusion. Consequentially, influenza virus with uncleaved HA is replication-defective, since it cannot complete the cell entry process.

The N-Terminal region (of different length between different HA subtypes) of the HA0 polypeptide presents a hydrophobic signal peptide that has an essential role in trafficking of the HA to the plasma membrane surface (Sekikawa and C. J. Lai 1983). This sequence is not present in the membrane-integrated HA, since it is removed during HA maturation (Wilson, Skehel and Wiley 1981).

Another peptide sequence important for HA trafficking is situated in the transmembrane region of the C-Terminal region (Engel *et al.* 2012; Scheiffele, Roth and Simons 1997). This sequence is especially involved in the HA sorting from the ER to the Golgi network and between different parts (*cis*, *medial*, and *trans*) of the Golgi network (Engel *et al.* 2012).

Thus, regulatory sequences, glycosylation, cleavage, and trafficking signals are necessary for the synthesis, correct folding and activation of influenza HA in the virus-cell cycle and need to be taken into account when influenza pp are produced. In this chapter the focus is investigation into protease-mediated activation of influenza HA for the production of high titre pp.

In particular, three proteases were investigated to enable the production of pp: TMPRSS2, HAT, and TMPRSS4. As previously discussed in Section 1.2.1.1, TMPRSS2, HAT, and TMPRSS4 are serine protease with trypsin-like activity that belong to the family of type II transmembrane serine proteases. This family is characterized by an N-terminal transmembrane region, a highly variable stem region containing domains specific for each protease and a catalytic domain that can recognise and cleave at single arginine residues (Böttcher-Friebertshäuser, Klenk and Garten 2013). Between the type II transmembrane serine protease family only some members have shown the ability to activate HA *in-vitro* through cleavage. It is not yet clear why not all the members possess this activity even in the presence of functional catalytic domains.

TMPRSS2, HAT and TMPRSS4 were shown to activate the HA of numerous influenza strains *in-vitro*. Furthermore, it was also demonstrated that TMPRSS2 can have HA cleavage activity *in-vivo*, since studies on the knock-out mouse for this protein have shown that the animal is partially resistant to influenza virus infection (Böttcher-Friebertshäuser, Klenk and Garten 2013).

Since the proteases present a transmembrane domain, they are expressed either at the level of the plasma membrane or at the level of the Golgi system. TMPRSS2 is

expressed and active intracellularly at the level of the Golgi system, HAT intracellularly and at the plasma membrane, whereas TMPRSS4 is expressed at the plasma membrane (Zamora and Pöhlmann 2014). These data also show that the protease(s) can be found in the cellular department in which the HA is also present.

Furthermore, all the proteases are expressed in the respiratory or gastrointestinal system (Bertram *et al*. 2012, E. Böttcher *et al*. 2006), which represent the tissues for which influenza virus has tropism.

All these elements render TMPRSS2, HAT, and TMPRSS4, and especially their catalytic domain, suitable targets for experimental analysis. Since TMPRSS2 and HAT soluble forms do not posses HA activation properties (E. Böttcher *et al.* 2006), their addition post-transfection as recombinant proteins was excluded and it was decided to co-transfect protease-encoding plasmids instead.

Additionally, treatment with TPCK-trypsin, which is the family member routinely used to activate and cleave influenza HA enabling influenza virus replication, was used on pp and considered as control and indicator of efficient HA activation. Furthermore, it has similar catalytic activity to the three proteases investigated. However, even if promising, activation with TPCK-trypsin was excluded as a routine method for pp production since it requires additional protocol steps to be performed for the pp-NT assay.

3.2 Materials and Methods

To express a foreign protein in a eukaryotic cell system specific promoter sequences and polyadenylation signals are necessary to permit gene transcription into mRNA, its nuclear export, and its stability. These sequences have already been engineered into the two vectors, pI.18 and phCMV1 that were used to express the HA gene (Section 2.1.1). However sequences that control mRNA translation into protein are also important. Together with the starting codon AUG, the Kozak consensus sequence is essential to determine the initiation of the translation process (Kozak 2005). The plasmids that are used for the production of H5pp contain prior to the 5' end of the HA coding sequence a Kozak sequence GTCAAA that was recommended by NIBSC for inclusion. This sequence will be referred here and in other chapters as "Influenza A Kozak sequence".

3.2.1 Influenza A haemagglutinin-expressing plasmids

Different HA-expressing plasmids already containing the influenza Kozak sequence and a terminator sequence are reported in **Table 11** and were kindly provided by Dr. Nigel

Temperton and Dr. Simon Scott (Universities of Greenwich and Kent, Medway, UK), and by Dr. Davide Corti (Institute for Research in Biomedicine, Bellinzona, Switzerland).

Table 11: HA-encoding plasmids

Plasmid backbone	HA	Codon optimisation	HA accession number	Source
phCMV1	A/South Carolina/1/1918 H1	Yes	AF117241.1	Dr. Davide Corti
pI.18	A/Puerto Rico/8/1934 H1*	No	CY105896.1	Dr. Temperton Dr. Scott
phCMV1	A/New Caledonia/20/1999 H1	Yes	CY033622.1	Dr. Davide Corti
pI.18	A/Udorn/307/1972 H3*	No	DQ508929.1	Dr. Temperton Dr. Scott
phCMV1	A/duck/Czechoslovakia/1956 H4	Yes	D90302.1	Dr. Davide Corti
phCMV1	A/chicken/Germany/N49 H10	Yes	CY014671.1	Dr. Davide Corti
phCMV1	A/duck/Memphis/546/1974 H11	Yes	AB292779.1	Dr. Davide Corti
phCMV1	A/duck/Alberta/60/1976 H12	Yes	CY130078.1	Dr. Davide Corti
phCMV1	A/gull/Maryland/704/1977 H13	Yes	D90308.1	Dr. Davide Corti
phCMV1	A/mallard/Astrakhan/263/1982 H14	Yes	AB289335.1	Dr. Davide Corti
phCMV1	A/shearwater/West Australia/2576/1979 H15	Yes	CY130102.1	Dr. Davide Corti
phCMV1	A/black-headed gull/Sweden/2/1999 H16	Yes	AY684888.1	Dr. Davide Corti

*HA genes provided by Dr. David Woodhall (Novartis, Boston, USA)

3.2.2 Cloning and subcloning influenza A haemagglutinin genes into pI.18 or phCMV1 expression vectors

In **Table 12**, sequence characteristics, accession numbers and sources of starting material (cDNA or plasmids) used to clone influenza A HAs are reported.

For the plasmids encoding HAs that were ordered from GenScript, appropriate restriction enzyme cleavage site, Kozak sequence and termination sequence were included at the 5' and 3' termini/ends at the point of purchase. The synthesised gene was cloned in pUC17 and delivered lyophilised by GenScript. The plasmids were then resuspended in DNase/RNase free water to a final concentration of 200 ng/µl.

Table 12: HA genes cloned or subcloned in pI.18 or phCMV1 expression vectors

HA	Starting material	Codon optimisation	HA accession number	Source
A/Solomon Islands/3/2006 H1	**Plasmid**	Yes	EU124177.1	Prof. Sarah Gilbert*
A/Brisbane/59/2007 H1	**cDNA**	Not Applicable	CY163864.1	Dr. Katja Hoeschler**
A/Texas/05/2009 H1	**Plasmid**	Yes	FJ966959.1	Prof. Sarah Gilbert *
A/duck/Italy/1447/2005 H1	**cDNA**	Not Applicable	HF563054.1	Istituto Zooprofilattico delle Venezie
A/Korea/426/1968 H2	**Plasmid**	No	CY125846.1	Ordered from GenScript
A/duck/Germany/1215/1973 H2	**cDNA**	Not Applicable	CY014710.1	Dr. Davide Corti
A/Wisconsin/67/2005 H3	**Plasmid**	Yes	CY034116.1	Prof. Sarah Gilbert*
A/California/7/2004 H3	**cDNA**	No	CY114373.1	Dr. Davide Corti
A/Shanghai/2/2013 H7	**Plasmid**	No	KF021597.1	Ordered from GenScript
A/turkey/Ontario/6118/1968 H8	**cDNA**	Not Applicable	CY014659.1	NIBSC
A/Hong Kong/1073/1999 H9	**cDNA**	Not Applicable	AJ404626.1	NIBSC

* Jenner Institute, University of Oxford, Oxford, UK
** Respiratory Virus Unit, Public Health England, London, UK

Since different cloning/subcloning strategies were applied for each separate cloning, considering the different nature of the starting material and the different problematic aspects encountered during the cloning procedure, the methodology and troubleshooting for each are here reported as flow charts[5]. Examples of cloning and subcloning flow charts are shown in **Figure 22** and **Figure 23**. All other flow charts are reported in **Appendix Figure 2-8**. To better understand and follow the flowcharts a legend is reported in **Appendix Figure 1**. The protocols of the methods presented in the flowcharts were described in Chapter 2 unless otherwise stated.

[5] A detailed example of a cloning procedure will be reported only in Chapter 6.

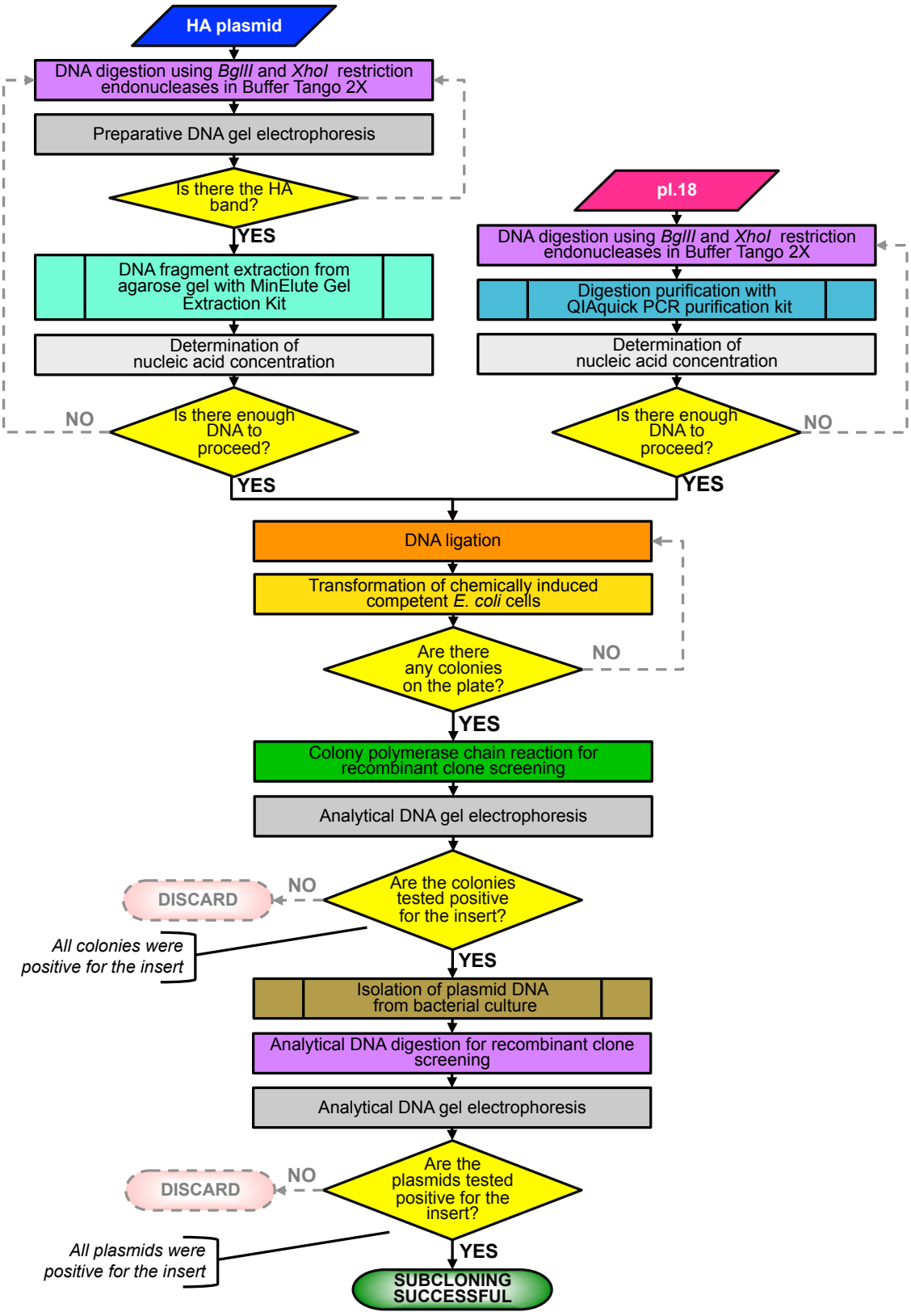

Figure 22: Flow chart representing the subcloning of A/Korea/426/1968 H2 and A/Shanghai/2/2013 H7 into pI.18 vector

This flow chart represents an example of subcloning strategies and of all the steps that need to be followed in the absence of experimental issues.

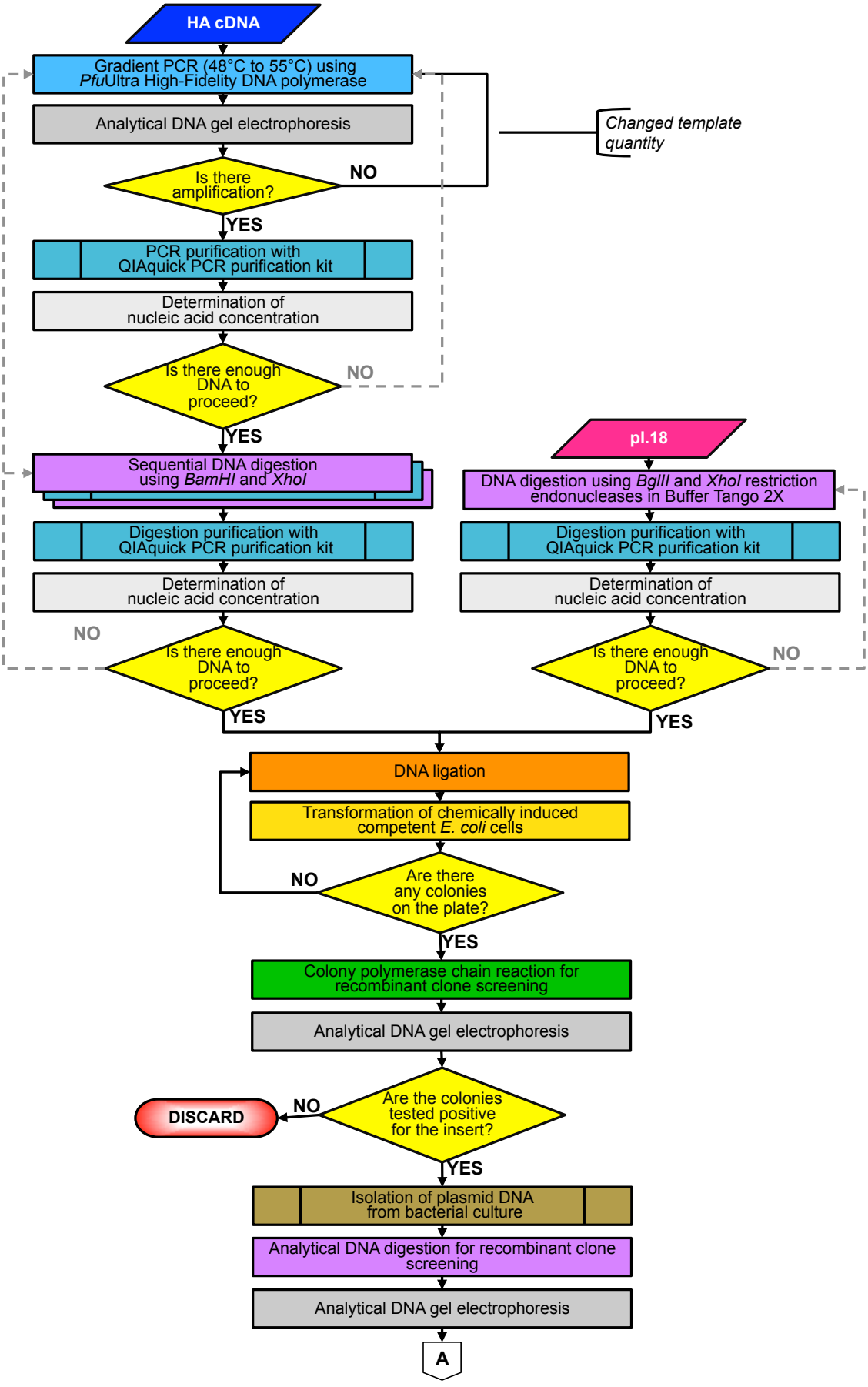
HA cDNA
Gradient PCR (48°C to 55°C) using PfuUltra High-Fidelity DNA polymerase
Analytical DNA gel electrophoresis
Is there amplification?
NO
YES
Changed template quantity
PCR purification with QIAquick PCR purification kit
Determination of nucleic acid concentration
Is there enough DNA to proceed?
NO
YES
Sequential DNA digestion using BamHI and XhoI
Digestion purification with QIAquick PCR purification kit
Determination of nucleic acid concentration
NO
Is there enough DNA to proceed?
YES
pI.18
DNA digestion using BglII and XhoI restriction endonucleases in Buffer Tango 2X
Digestion purification with QIAquick PCR purification kit
Determination of nucleic acid concentration
Is there enough DNA to proceed?
NO
YES
DNA ligation
Transformation of chemically induced competent E. coli cells
NO
Are there any colonies on the plate?
YES
Colony polymerase chain reaction for recombinant clone screening
Analytical DNA gel electrophoresis
DISCARD
NO
Are the colonies tested positive for the insert?
YES
Isolation of plasmid DNA from bacterial culture
Analytical DNA digestion for recombinant clone screening
Analytical DNA gel electrophoresis
A

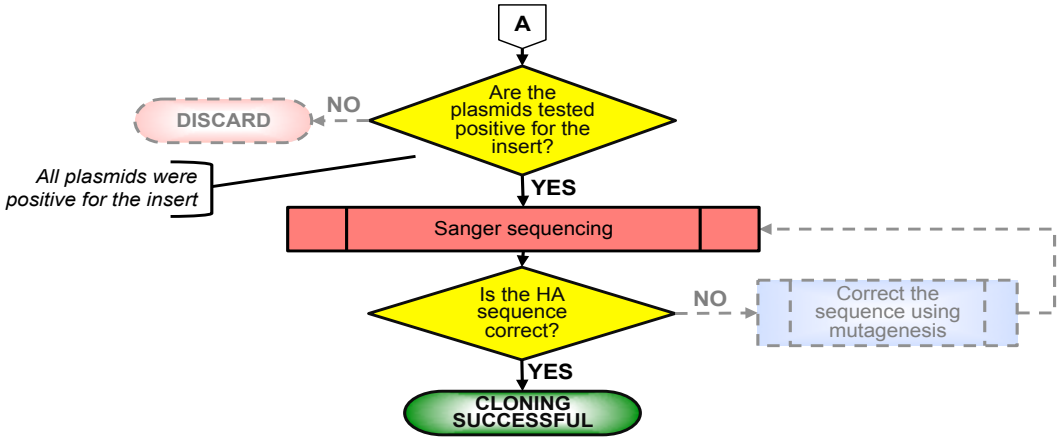

Figure 23: Flow chart representing the cloning of A/Hong Kong/1073/1999 H9 into pI.18 vector

This flow chart represents an example of HA cloning strategies starting from cDNA. It also shows the minimal number of steps required for HA cloning. Only two experimental issues have required the repeat of two experimental steps (HA amplification and DNA ligation)

Table 13: Primer names, restriction enzyme, and primer sequences used for Influenza A HA cloning

Within the sequences, restriction enzyme cleavage sites are reported in red, influenza Kozak sequence in bold, 5' end HA sequence in green, influenza A termination sequence in bold and italics, the reverse complement stop codon (UAA) in pink, and 3' end HA reverse complement sequence in blue.

Primer name	Primer sequence (5' to 3')	Restriction enzyme
SolomonH1_Fw	GCGCGCAGATCT**GTCAAA**ATGAAGGTCAAGCTG	*BglII*
SolomonH1_Rev	GCGCGCGAATTC***AAT***TTAGATGCAGATCCGGCA	*EcoRI*
BrisbaneH1_Fw	GGCGGATCC**GTCAAA**ATGAAAGTAAAACTA	*BamHI*
BrisbaneH1_Rev	GGCCTCCGA***AAT***TTAGATGCATATTCTACA	*XhoI*
TexasH1_Fw	GCGCGCAGATCT**GTCAAA**ATGAAGGCTATCCTG	*BglII*
TexasH1_Rev	GCGCGCGAATTC***AAT***TTAAATACAGATCCGGCA	*EcoRI*
H1duck_Fw	GCGCGCAGATCT**GTCAAA**ATGGAAGCAAAACTACTC	*BglII*
H1duck_Rev	GGCGCGCTCCGA***AAT***TTAAATGCATATTCTGC	*XhoI*
H2duck_Fw	GCGCGCAGATCT**GTCAAA**ATGGCCATCATTTAT	*BglII*
H2duck_Rev	GCGCGCGGTACC***AAT***TCATATGCAGATTCTG	*KpnI*
CaliforniaH3_Fw	GGCGGTACC**GTCAAA**ATGAAGACTATCATT	*KpnI*
CaliforniaH3_Rev	GGCGTCGAC***AAT***TCAAATGCAAATGTTGCA	*SalI*
WisconsinH3_Fw	GCGCGCAGATCT**GTCAAA**ATGAAGACCATCATT	*BglII*
WisconsinH3_Rev	GCGCGCGTCGAC***AAT***TTAGATGCAGATGTTGC	*SalI*
TkOntarioH8_Fw	GCGCGCCTCGAG**GTCAAA**ATGGAGAAATTCATC	*XhoI*
TkOntarioH8_Rev	GCGCGCGAATTC***AAT***TTAAATACAGAACATGCATC	*EcoRI*
HongKongH9_Fw	GCGCGCGGATCC**GTCAAA**ATGGAAACAATA	*BamHI*
HongKongH9_Rev	GCGCGCCTCGAG***AAT***TTATATACAAATGTT	*XhoI*

The primers used to amplify the HA-encoding sequences were designed as reported in **Table 13** using GenBank database sequences of influenza gene segment 4. Fw primers were designed to possess a GC-rich flanking region to facilitate restriction digestion, an appropriate restriction enzyme cleavage site to clone the amplified HA into the vector of interest (pI.18 or phCMV1), the influenza A Kozak sequence, and the HA 5' terminal encoding region sequence. Rev primers possessed the GC-rich flanking region, appropriate restriction enzyme cleavage sites, the reverse complement stop codon, influenza A termination sequence, and the reverse complement HA 3' terminal encoding sequence. All the primers were analysed to ensure absence of secondary structure with Sigma-Aldrich OligoEvaluator™ tool.

3.2.3 Mutagenesis to correct haemagglutinin sequences

After sending the cloned HAs for Sanger sequencing, the A/California/7/2004 H3 cloned using PCR was found to contain the nucleotide mutation A to C leading to amino acid mutation N205H. To correct this mutation, *in vitro* mutagenesis was performed as described in Section 2.1.15.1. The primers used are reported in **Table 14**.

Table 14: Primer names and sequences used for A/California/7/2004 H3 mutagenesis
The primers were used to change the histidine at position 205 to asparagine and correct the cloned A/California/7/2004 H3 sequence. The primer annealing schematics are reported below the primer sequences. In these schematics primer sequences are in bold, gene sequence is in black, and in grey the translated gene sequence (5' to 3') corresponding to the primer (Fw) or the original gene (Rev) is shown. The nucleotide that corrects the mutation is highlighted in red in the primer sequence and in the schematic.

Primer name	Primer sequence (sequence in 5' to 3') and annealing scheme
H3Cal H205N	CACCCGGGTACGAACAATGACCAAATCAGCC H P G T N N D Q I S 5' **C A C C C G G G T A C G A A C A A T G A C C A A A T C A G C C** 3' T G G T G G G C C C A T G C T T G G T A C T G G T T T A G T C G G A
H3Cal H205N_Rev	GGCTGATTTGGTCATTGTTCGTACCCGGGTG H P G T N H D Q I S A C C A C C C G G G T A C G A A C C A T G A C C A A A T C A G C C T 3' **G T G G G C C C A T G C T T G T T A C T G G T T T A G T C G G** 5'

Furthermore, after sequencing of pI.18-A/Puerto Rico/8/1934 H1, two single nucleotide mutations (Q341R and S342R) and an insertion (S342_R343insRR) near the cleavage site were also identified (**Figure 27**). To revert the sequence to the original amino acid database entry QuikChange Lightning Site-direct mutagenesis kit was used again. However, since the QuikChange Primer Design web-tool does not permit the design of primers that introduce a mutation, and perform a deletion simultaneously, the primers were designed manually, combining the information of two sets of primers designed by the tool:

one set was designed with the software to correct the insertion, the other set to perform the mutations. The primers that were used for the mutagenesis, and the two original sets of primers that were designed are shown in **Table 15**.

Table 15: Primer names and sequences used for A/Puerto Rico/8/1934 H1 mutagenesis
The primers were used to change the A/Puerto Rico/8/1934 H1 incorrect cleavage sequence. Two set of primers were designed (R341Q_S342R and del343-344) and then combined into a third set (PR8_mut). The primer annealing schematics are reported below the primer sequences. In these schematics primer sequences are in bold, gene sequence is in black, and in grey the translated gene sequence (5' to 3') corresponding to the primer (Fw) or the original gene (Rev) is shown. The nucleotide that corrects the mutation is highlighted in red in the primer sequence and in the schematic.

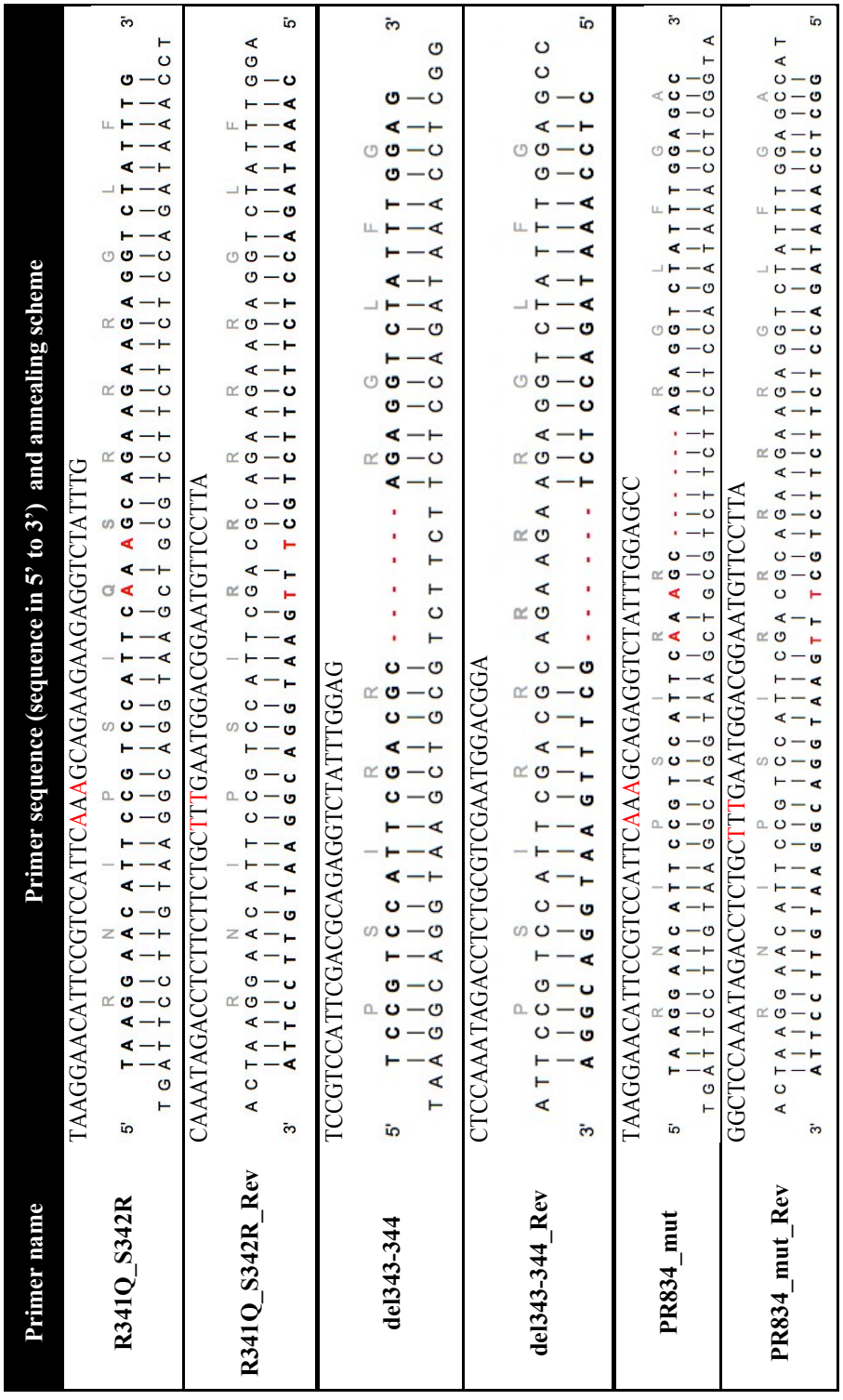

3.2.4 Production optimisation of low pathogenic avian and human influenza A haemagglutinin pseudotypes

In order to produce influenza A HA pp, it is necessary to activate the HA *via* proteolytic cleavage. If the HA is not cleaved the pp will not be able to complete the entry process (**Figure 24**). For HPAI H5 and HPAI H7pp, HA cleavage is mediated by ubiquitously expressed proteases, such as furin, that are expressed in the producer cell line (Böttcher-Friebertshäuser, Klenk and Garten 2013). However, for low pathogenic avian and human influenza HA, tissue-specific proteases are necessary (Böttcher-Friebertshäuser, Klenk and Garten 2013). Since these proteases are not expressed (or are expressed at low level) in the producer HEK293T/17 cells, they need to be expressed *via* transfection of protease-encoding plasmids (**Figure 25**).

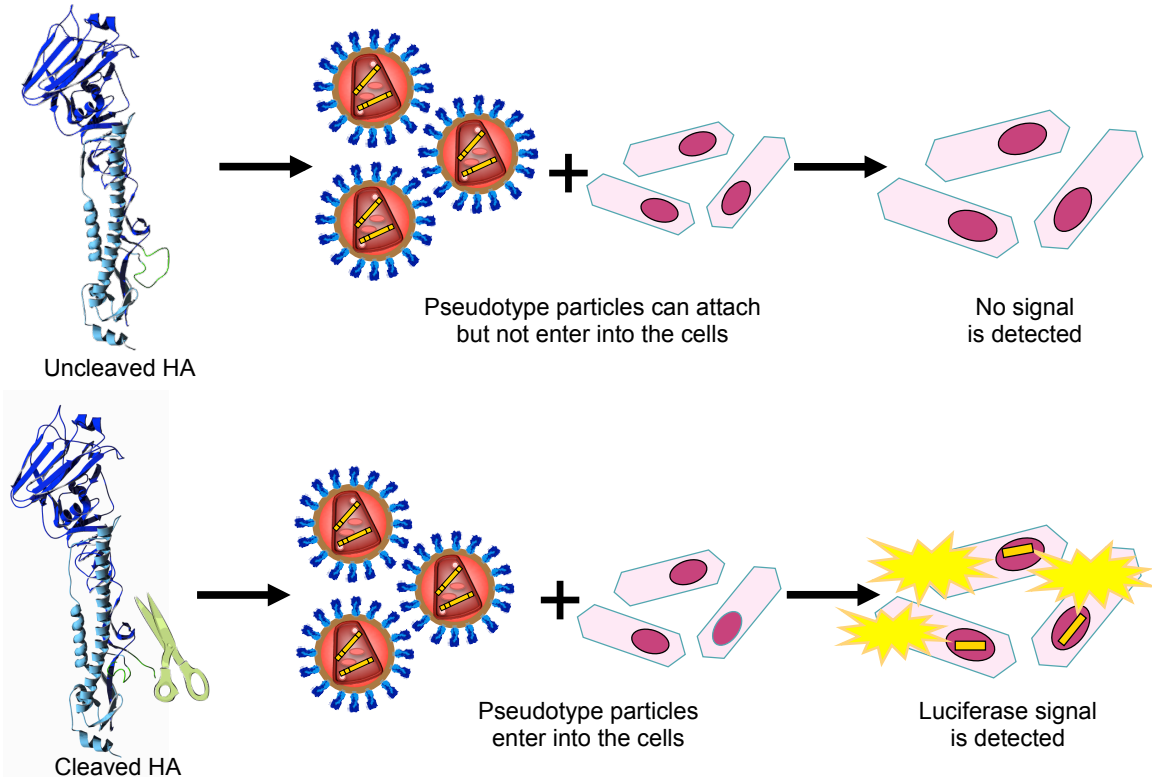

Figure 24: Evaluation of the protease activity using pp
If the HA is uncleaved, pp can bind the sialic acid on the cell surface, but cannot complete the entry process since the uncleaved HA does not possess fusion activity. As a consequence, the lentiviral genome doesn't integrate into cells, the reporter gene luciferase is not expressed, and its signal cannot be detected after adding an appropriate substrate. On the other hand, if the HA is cleaved during pp production, the pp completes the entry process and luminescence signal is detected.

To test different protease types and quantity, and the resultant pp production efficiency, the protocol described in Section 2.3.2.2 was modified to a down-sized format: transfection reactions were performed in the wells of 6-well plates in 2 ml volumes and all the OptiMEM® I volumes, plasmids quantities were halved to maintain a fixed plasmid ratio of 1:1.5:1. Briefly, a DNA mix containing 500 ng of p8.91, 750 ng of pCSFLW and 500 ng of HA-expressing plasmid was prepared and then a protease-encoding

plasmid (Section 2.3.1: pCAGGS-HAT, pCAGGS-TMPRSS2 or pCMV-Tag3 TMPRSS4 (ECD)-myc) was added to permit HA cleavage/activation and test the activity of HAT, TMPRSS2 and TMPRSS4. In some cases (A/gull/Maryland/704/1977 H13pp) since the above proteases had not produced positive results, a further two proteases, TMPRSS3 and TMPRSS6, were also tested, by adding the appropriate encoding plasmid (Section 2.3.1) to the mix. In general, two quantities of protease-encoding plasmids were tested (250 ng and 125 ng). In certain cases, a higher (500 ng) and/or a lower quantity (75 ng) were also tested. A transfection in the absence of protease-encoding plasmid (Δ protease) was also included in all experiments as a control.

For the production of A/gull/Maryland/704/1977 H13pp and A/Texas/5/2009 H1pp optimisation of the production conditions was performed by evaluating additional quantities (1000 ng and/or 250 ng) of the HA-encoding plasmids and consequentially changing the ratios between HIV-1 core, lentiviral vector, and envelope protein.

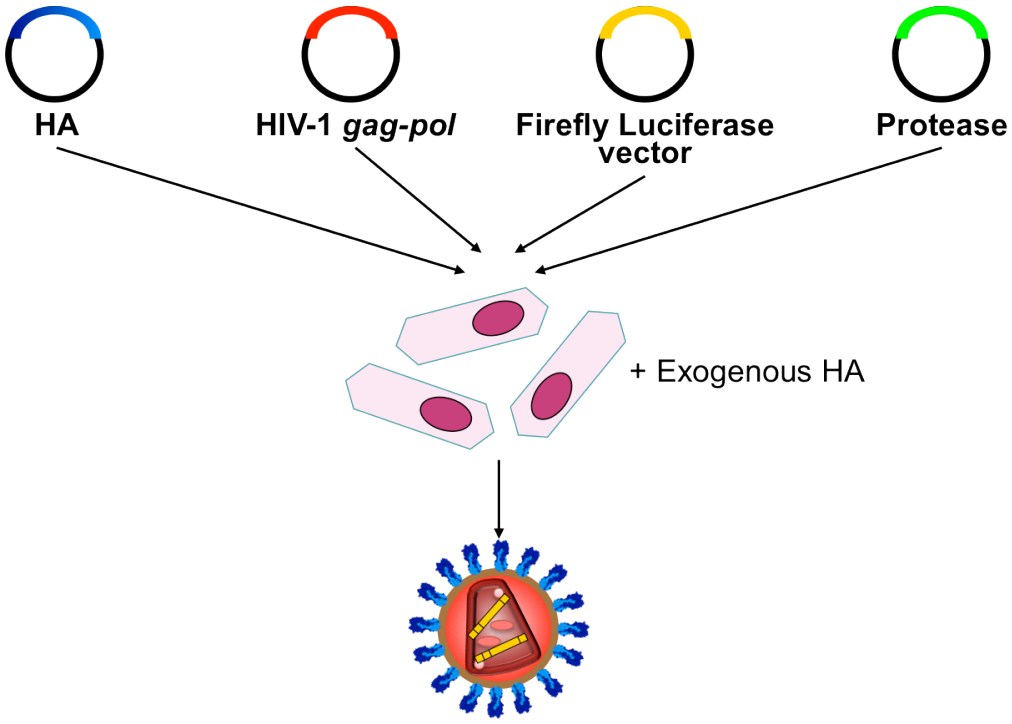

Figure 25: Production of low pathogenic avian and human influenza A HA pp by four-plasmid co-transfection

OptiMEM® I (50 µl) was then added to the DNA mix and in the meantime a tube containing 50 µl OptiMEM® I and 20 µl of 1 mg/ml PEI was prepared and incubated for 5 min. The OptiMEM® I-PEI mix was then added to the OptiMEM® I-DNA mix and incubated for 20 min.

The transfection mix was subsequently added dropwise to the well of a 6 well plate, in which the previous day 1×10^6 HEK293T/17 cells had been plated to reach 80% confluence on the transfection day. After 24 h, 0.5 U of exogenous NA from *Clostridium perfringens* was added when the transfection media was changed.

3.2.5 Titration of influenza pseudotypes and trypsin-treatment to mediate haemagglutinin activation

Influenza pp produced in the presence or absence of the protease-encoding plasmids were titrated following the protocol described in Section 2.3.3.

As control, the Δ proteases HA pp were also activated post-transfection using TPCK-Trypsin (Sigma-Aldrich, cat.no. T1426). To perform the TPCK-Trypsin activation, 2-fold serial dilutions of neat Δ protease pp supernatants were carried out in a total volume of 100 µl 10% FBS-DMEM, discarding 50 µl in the last dilution. Then 30 µl of a ~133.3 µg/ml TPCK-Trypsin solution in 10% FBS-DMEM were added to each well to produce a final concentration of 50 µg/ml.

After 30 min incubation at 37°C 5% CO_2, 50 µl of Trypsin Neutralizing Solution (TNS, Lonza, cat.no. CC-5002) was added to each well to stop TPCK-Trypsin activity; then 1.5×10^4 cells (in 50 µl) were added to allow pp transduction of cells and luciferase gene expression. Firefly luciferase gene expression and pp titre were evaluated and quantified after 48 h incubation at 37°C 5% CO_2 by luminometry as described in Section 2.3.3.

3.2.6 Mutagenesis to study the role of H16 cleavage sequences

Recently Lu *et al.* 2012 described the first crystal structure of an H16 HA. In their study, they show that, since an α-helix is present before the cleavage arginine, the cleavage arginine is facing the protein surface and remains buried in a cavity instead of being exposed to the solvent (Lu *et al.* 2012). To investigate the role of this structure in HA cleavage and pp production, mutagenesis (Section 2.1.15.1) of the A/black-headed gull/Sweden/2/1999 H16 HA was conducted to remove the α-helix and render the cleavage site more similar to the cleavage site of an H1 HA. Primers were designed as described in Section 2.1.15.1 and shown in **Table 16**.

The mutated H16-encoding plasmid was then used to produce pp and evaluate different proteases as described in Section 3.2.4.

Table 16: Primer names and sequences used for A/black-headed gull/Sweden/2/1999 H16 mutagenesis

The primers were used to disrupt the α-helix at the level of the cleavage site. The primer annealing schematics are shown below the primer sequences. In these schematics primer sequences are in bold, gene sequence is in black, and in grey the translated gene sequence (5' to 3') corresponding to the primer (Fw) or the original gene (Rev) is shown. The mutated nucleotide is highlighted in red in the primer sequence and in the schematic.

Primer name	Primer sequence (sequence in 5' to 3') and annealing scheme
H16cl_Fw	GCGGAATGTGCCAAGCATCCAGTCGAGAGGACTGTTCGGCGCT 
H16cl_Rev	AGCGCCGAACAGTCCTCTCGACTGGATGCTTGGCACATTCCGC 

3.2.7 Evaluation of the role of the receptor-binding site and of glycosylation in expression of A/Texas/05/2005 H1

Elsewhere (Nicolson *et al.* 2012; Z. Chen *et al.* 2010; W. Wang, Castelán-Vega, *et al.* 2010) it was noted that two mutations, one introducing a glycosylation site, the other at the level of the RBS, in the HA of 2009 H1 pandemic strains could improve the 2009 monovalent vaccine production and pp transduction activity. Since initial experiments to produce A/Texas/05/2009 H1pp failed to result in production of high titre pp, these two mutations K136N and Q240R (A/Texas/05/2009 H1 numbering) were investigated to see if the HA expression could be improved and if so, to use this mutated HA to produce a 2009 pandemic pp.

For this reason the producer pI.18-A/Texas/05/2009 H1 plasmid was mutated. Primers (**Table 17**) were designed and mutagenesis was performed as described in Section 2.1.15.2.

The mutated HA-encoding plasmids were used in immunofluorescence experiments (Section 3.2.9) to compare HA expression with the wild-type. This permitted evaluation, together with data in the literature, to decide if these strategies should be implemented for effective pp production.

Table 17: Primer names and sequences used for A/Texas/05/2009 H1 mutagenesis
Primers were used to change the lysine at position 136 to asparagine introducing a glycosylation site, and to change the RBS introducing an arginine instead of a glutamine. The primer annealing schematics are reported below the primer sequences. Primer sequences are in bold, gene sequence is in black, and in grey the translated gene sequence (5' to 3') corresponding to the primer (Fw) or the original gene (Rev) is shown. The mutated nucleotide is highlighted in red in the primer sequence.

Primer name	Primer sequence (sequence in 5' to 3') and annealing scheme
Texas_K136N	CGGTTCGAGATTTTCCCCAATACCAGCTCCTGGC R F E I F P N T S S W 5' **CGGTTCGAGATTTTCCCCAATACCAGCTCCTGGC** 3' TCGCCAAGCTCTAAAAGGGGTTCTGGTCGAGGACCGGG
Texas_K136N_Rev	GCCAGGAGCTGGTATTGGGGAAAATCTCGAACCG R F E I F P K T S S W AGCGGTTCGAGATTTTCCCCAAGACCAGCTCCTGGCCC 3' **GCCAAGCTCTAAAAGGGGTTATGGTCGAGGACCG** 5'
Texas_Q240R	AAAGTGCGGGACCGGGAAGGCCGGATG 5' **AAAGTGCGGGACCGGGAAGGCCGGATG** 3' GGTTTCACGCCCTGGTCCTTCCGGCCTACTT
Texas_Q240R_Rev	CATCCGGCCTTCCCGGTCCCGCACTTT CCAAAGTGCGGGACCAGGAAGGCCGGATGAA 3' **TTTCACGCCCTGGCCCTTCCGGCCTAC** 5'

3.2.8 Evaluation of the role of neuraminidase in pseudotype production

Recently it was noted that the circulating H3 HAs are losing affinity for α-2,6 sialic acids and to maintain the entry function the virus supplies the lost affinity for the receptor using the NA (Y. P. Lin *et al.* 2010) . Since co-transfection of NA was shown to be an important aspect to produce high titre pp (Molesti *et al.* 2013; F. Zhang *et al.* 2011; W. Wang, Castelán-Vega, *et al.* 2010; Bosch *et al.* 2001), it was decided to evaluate if the presence of the NA could affect production of the pp harbouring the HA of more recently circulating H3N2 strains.

For this reason A/Wisconsin/67/2005 H3pp were produced with an A/Udorn/307/1972 N2 NA on their envelope. For this purpose, the transfection protocol described in Section 3.2.4 was modified and 125 ng of pI.18-A/Udorn/307/1972 N2 plasmid (kindly provided by Dr. David Woodhall, Novartis, Boston, USA) was added to the DNA mixes. As a control A/Wisconsin/67/2005 H3pp were also produced following Section 3.2.4 protocol using 0.5 U, 1 U or absence of exogenous NA from *Clostridium perfringens*.

3.2.9 Immunofluorescence

To control the expression location of the HA following transfection of HA-encoding plasmids immunofluorescence was performed as described in Section 2.4.2.

For the immunofluorescence of the H13 HA, the OIE reference antisera produced by inoculation of A/gull/Maryland/704/1977 (H13N6) in specific pathogen-free chicken, kindly provided by Dr. Giovanni Cattoli (Istituto Zooprofilattico delle Venezie, OIE, Legnaro, Padua, Italy), was used as primary antibody at a dilution of 1:500, whereas the goat anti-chicken IgG (H+L)-Fluorescein antibody (Sigma-Aldrich, cat.no. SAB3700197) diluted at 1:1000 was used as the secondary antibody.

For immunofluorescence of cells transduced with A/Texas/05/2009 H1 wild-type and mutant pp, C179 mAb (TaKaRa Clonthec, cat.no. M145) was used at a working concentration of 1 µg/ml; the secondary goat anti-mouse IgG (whole molecule)–Fluorescein isothiocyanate (FITC) antibody (Sigma-Aldrich, cat.no. F9006) was used at a 1:500 dilution.

3.2.10 Western blotting

To confirm HA cleavage of A/duck/Italy/1447/2005 H1pp and A/Udorn/307/1972 H3pp by the test proteases, Western blotting was performed (as described in Section 2.4.3.2) using the pp produced in the presence of a protease-encoding plasmid. As controls, Δ protease pp was used and TPCK-Trypsin treatment was performed: 45 µl of Δ protease pp was digested with 1 mg/ml TPCK-Trypsin to have a final concentration of 50 µg/ml. After 30 min at 37°C, 50 µl of TNS was added to block the TPCK-Trypsin activity: in this case, to maintain the quantity proportion of loaded samples, 12 µl, instead of 6 µl, of treated pp were mixed with Laemmli Buffer and ß-mercaptoethanol to have a 1X and 5% v/v concentration respectively.

For A/duck/Italy/1447/2005 H1pp, the A/duck/Italy/1447/2005 H1N1 reference chicken antiserum, kindly provided by Dr.Giovanni Cattoli (Istituto Zooprofilattico delle Venezie, World Organization for Animal Health, Legnaro, Padua, Italy), was used diluted to 1:500 as primary antibody. To detect the binding of this avian serum, an Alexa Fluor® 680-AffiniPure donkey anti-chicken IgY (IgG) (H+L) (Stratech Scientific Ltd., cat.no. 703-625-155) secondary antibody was diluted at 1:20000.

For A/Udorn/307/1972 H3pp, the sheep antiserum A/England/427/1988 (H3N2) provided by NIBSC was diluted to 1:500 and used as the primary antibody; the donkey anti-sheep/goat IgG Dylight®800 antibody (AbD Serotec®, Bio-Rad, cat.no. STAR88D800GA) diluted to 1:20000 was used as the secondary antibody.

The Western blot membranes were detected using the Odyssey® Sa Infrared Imaging System at 700 nm for A/duck/Italy/1447/2005 H1pp and at 800 nm with A/Udorn/307/1972 H3pp.

3.3 Results

3.3.1 Cloning, subcloning and mutation correction of influenza A haemagglutinin genes

All the cloning procedures reported in the flow charts were successful. In certain cases troubleshooting was necessary since different problems, such as absence of amplification of the HA gene from the cDNA, incorrect design of primers (resulting in unexpected primer dimer formation or the presence of uncorrected restriction enzyme site), problems with gel extraction, or unsuccessful ligation, were encountered. As a result, the following HA-encoding plasmids were generated to permit pp production: pI.18-A/Solomon Islands/3/2006 H1, pI.18-A/Brisbane/59/2007 H1, pI.18-A/Texas/05/2009 H1, pI.18-A/duck/Italy/1447/2005 H1, pI.18-A/Korea/426/1968 H2, phCMV1-A/duck/Germany/1215/1973 H2, pI.18-A/Wisconsin/67/2005 H3, pI.18-A/California/7/2004 H3, pI.18-A/Shanghai/2/2013 H7, phCMV1-A/turkey/Ontario/6118/1968 H8, pI.18-A/Hong Kong/1073/1999 H9.

For pI.18-A/California/7/2004 H3, a mutation was present after cloning and was successfully corrected by site-directed mutagenesis (sequences shown in **Figure 26**).

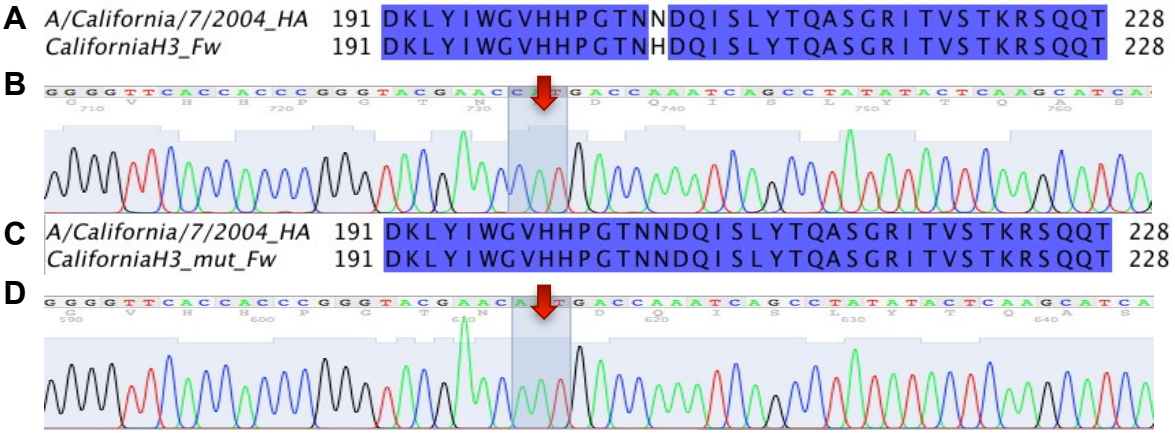

Figure 26: Site-direct mutagenesis of A/California/7/2004 H3
A. A/California/7/2004 H3 gene sequence showing the N205H mutation; **B.** Electropherograms of A/California/7/2004 H3 gene sequence showing the N205H mutation; **C.** A/California/7/2004 H3 gene sequence after mutagenesis showing the correction of the mutation; **D.** Electropherograms of corrected A/California/7/2004 H3 sequence.

Of the plasmids already available at the beginning of the studies (Section 3.2.1) the pI.18-A/Puerto Rico/8/1934 H1 contained a mutation at the level of the cleavage site. As

shown in **Figure 27**, the cleavage site of A/Puerto Rico/8/1934 H1 was successfully restored *via* mutagenesis, permitting the use of this plasmid to produce pp.

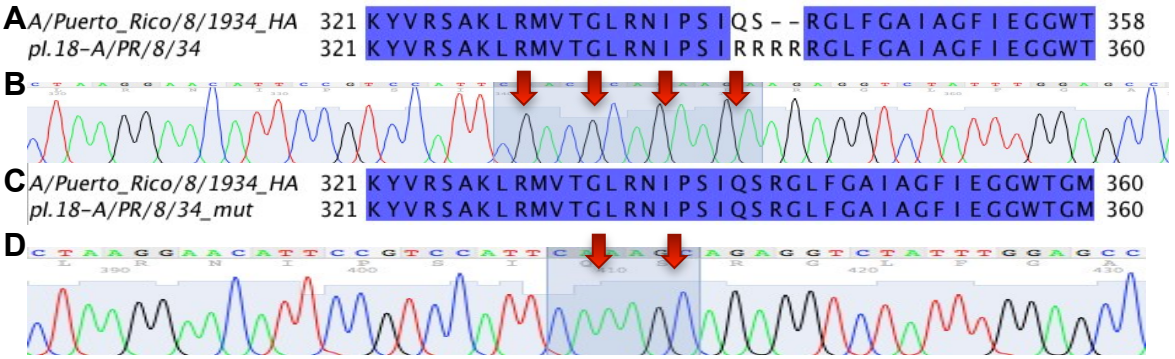

Figure 27: Site-direct mutagenesis of A/Puerto Rico/8/1934 H1
A. A/Puerto Rico/8/1934 H1 gene sequence showing the cleavage site mutation; **B.** Electropherograms of A/Puerto Rico/8/1934 H1 gene sequence showing the cleavage site mutation; **C.** A/Puerto Rico/8/1934 H1 gene sequence after mutagenesis showing the correct cleavage site; **D.** Electropherograms of corrected A/Puerto Rico/8/1934 H1 gene sequence.

3.3.2 Optimised protease conditions are necessary for the production of different influenza haemagglutinin pseudotypes

Cloned or donated HAs were used in influenza HA pp production experiments and to test the activity of different proteases. In general in the absence of proteases (Δ protease) all the pp titres are negligible (1×10^4-1×10^5 RLU/ml), and only when a protease plasmid is co-transfected during pp production do titres increase significantly (**Figures 28-32**). This demonstrates that proteases are essential for the production of low pathogenic avian and human influenza pp.

In **Figure 28** the H1pp titres obtained testing different types and quantities of protease-encoding plasmid are presented. It can be noticed that for all the H1pp, in general, higher titres were observed when the lower quantities of the TMPRSS4-encoding plasmid was used. HAT was also able to mediate H1 HA activation and produce high titre pp. TMPRSS2 seems to mediate cleavage activation less efficiently, with the exception of A/Puerto Rico/8/1934 H1pp (**Figure 28B**) and A/Brisbane/59/2007 H1pp (**Figure 28E**), in which this protease permitted the production of pp preparations with titre equal or higher than the ones produced with HAT. Generally, when low quantities of protease-encoding plasmids were used higher titres were observed, however some exceptions were observed, especially when the HAT was involved (**Figure 28 (B and C)**).

As a control, Δ protease pp were also titrated with concomitant TPCK-Trypsin treatment. In general TPCK-Trypsin treatment permitted the rescue of the Δ protease pp titre, however, when the A/duck/Italy/1447/2005 H1 Δ protease pp was similarly treated the titres did not increase (**Figure 28F**).

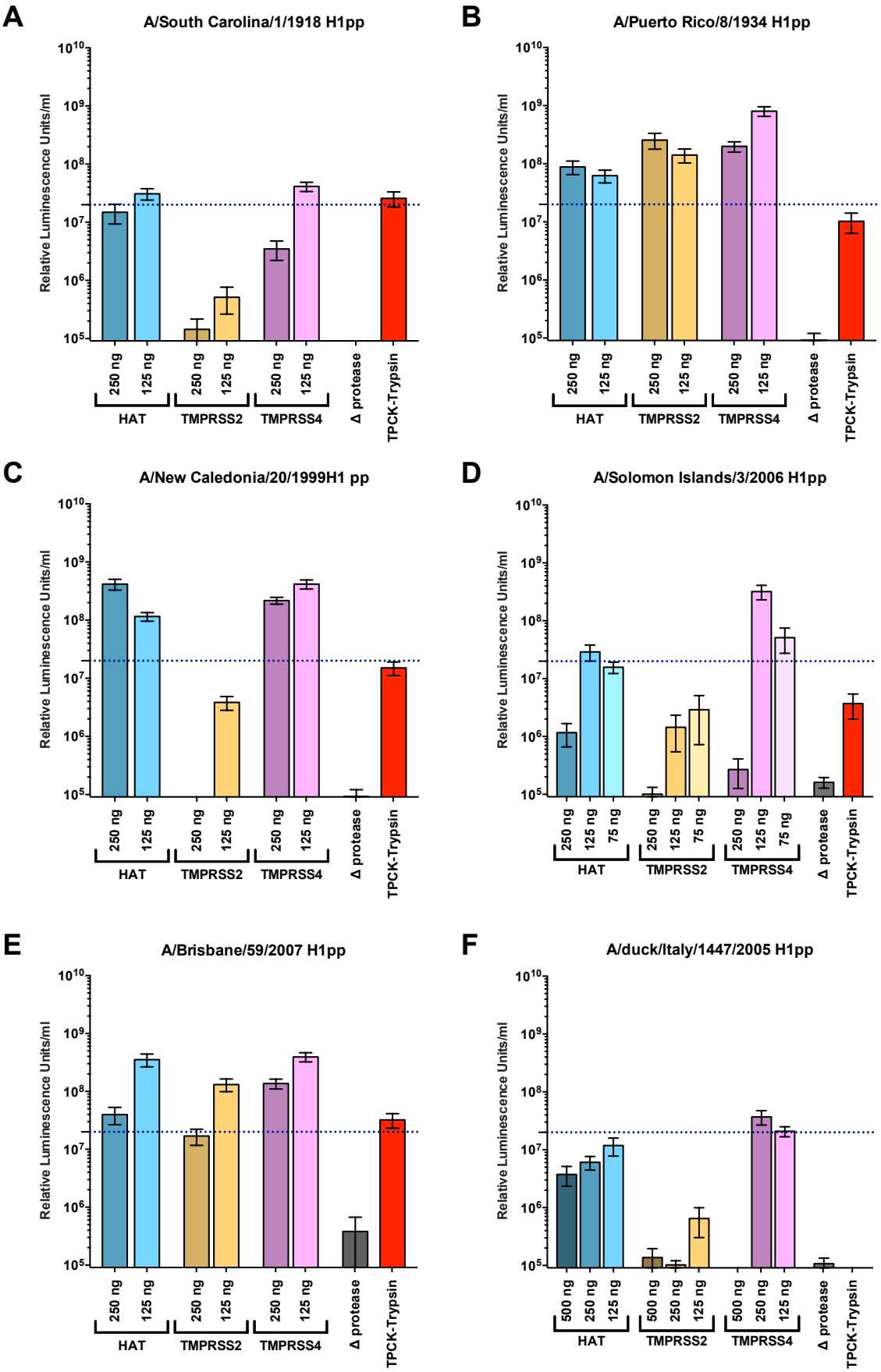

Figure 28: Role of HAT, TMPRSS2, and TMPRSS4 proteases in H1pp production
Titres of pp generated during an individual transfection experiment are reported in RLU/ml with SEM (n=8 titre measurements). A line corresponding to 2×10^7 RLU/ml is drawn to indicate the minimum titre necessary to effectively perform neutralization assays. **A.** A/South Carolina/1/1918 H1pp; **B.** A/Puerto Rico/8/1934 H1pp; **C.** A/New Caledonia/20/1999 H1pp; **D.** A/Solomon Islands/3/2006 H1pp; **E.** A/Brisbane/59/2007 H1pp; **F.** A/duck/Italy/1447/2005 H1pp.

Figure 29 shows the production of H2pp. All the proteases, including TPCK-Trypsin, were able to mediate the cleavage of the human H2, permitting the production of high titre (>1×10^8 RLU/ml) pp. The pp bearing the H2 of avian origin (**Figure 29B**) exhibited lower titres compared to the human H2pp, and also a different protease activation pattern: A/Korea/426/1968 H2pp showed lower titres when the TMPRSS2- and TMPRSS4-encoding plasmids were used at 250 ng, whereas the opposite result is observed for A/duck/Germany/1215/1973 H2pp.

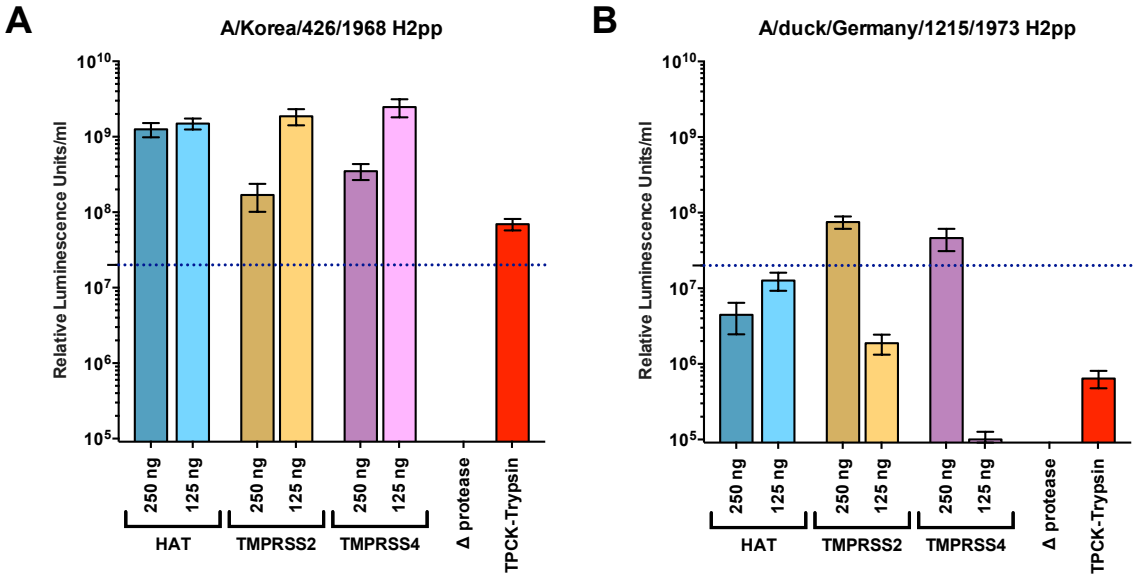

Figure 29: Role of HAT, TMPRSS2, and TMPRSS4 proteases in H2pp production
Titres of pp generated during an individual transfection experiment are reported in RLU/ml with SEM (n=8 titre measurements). A line corresponding to 2×10^7 RLU/ml is drawn to indicate the minimum titre necessary to effectively perform neutralization assays. **A.** A/Korea/426/1968 H2pp; **B.** A/duck/Germany/1215/1973 H2pp.

In **Figure 30 (A and B)**, the production of H3pp is reported. For A/Udorn/307/1972 H3pp (**Figure 30A**) it can be observed that high pp titres were obtained when the TMPRSS2 protease was used. HA cleavage and activation was also mediated by TMPRSS4 and at a lower level also by HAT. TPCK-Trypsin can also rescue Δ protease pp titre. For A/California/7/2004 H3pp (**Figure 30B**), the pp titres failed to exceed 1×10^7 RLU/ml. Cleavage was observed when 75 ng of pCAGGS-HAT, 500 ng and 125 ng of pCAGGS-TMPRSS2, and 250 ng, 125 ng and 75 ng of pCMV-Tag3 TMPRSS4 (ECD)-myc were used. Also TPCK-Trypsin was able to mediate HA cleavage but the effect was moderate in comparison to the Δ protease pp titre.

Figure 30C shows the production of A/duck/Czechoslovakia/1956 H4pp. High titre pp were produced when 250 ng of pCAGGS-TMPRSS2 was used; also when lower quantities (125 ng) of the encoding plasmid were used titres remained high. TMPRSS4 and HAT were also able to mediate HA activation and, interestingly, higher pp titres were

observed when less plasmid was used in the co-transfection. HA activation was also observed when TPCK-Trypsin treatment was performed.

In **Figure 30D** the titres of pp harbouring the HA of the potentially pandemic H7N9 virus is shown. A/Shanghai/2/2013 H7 was cleaved by all the proteases tested. Higher titres were observed when TMPRSS4 was used but also when 250 ng of HAT-encoding plasmid was used. Other conditions showed moderate pp titres (1×10^7-1×10^8 RLU/ml).

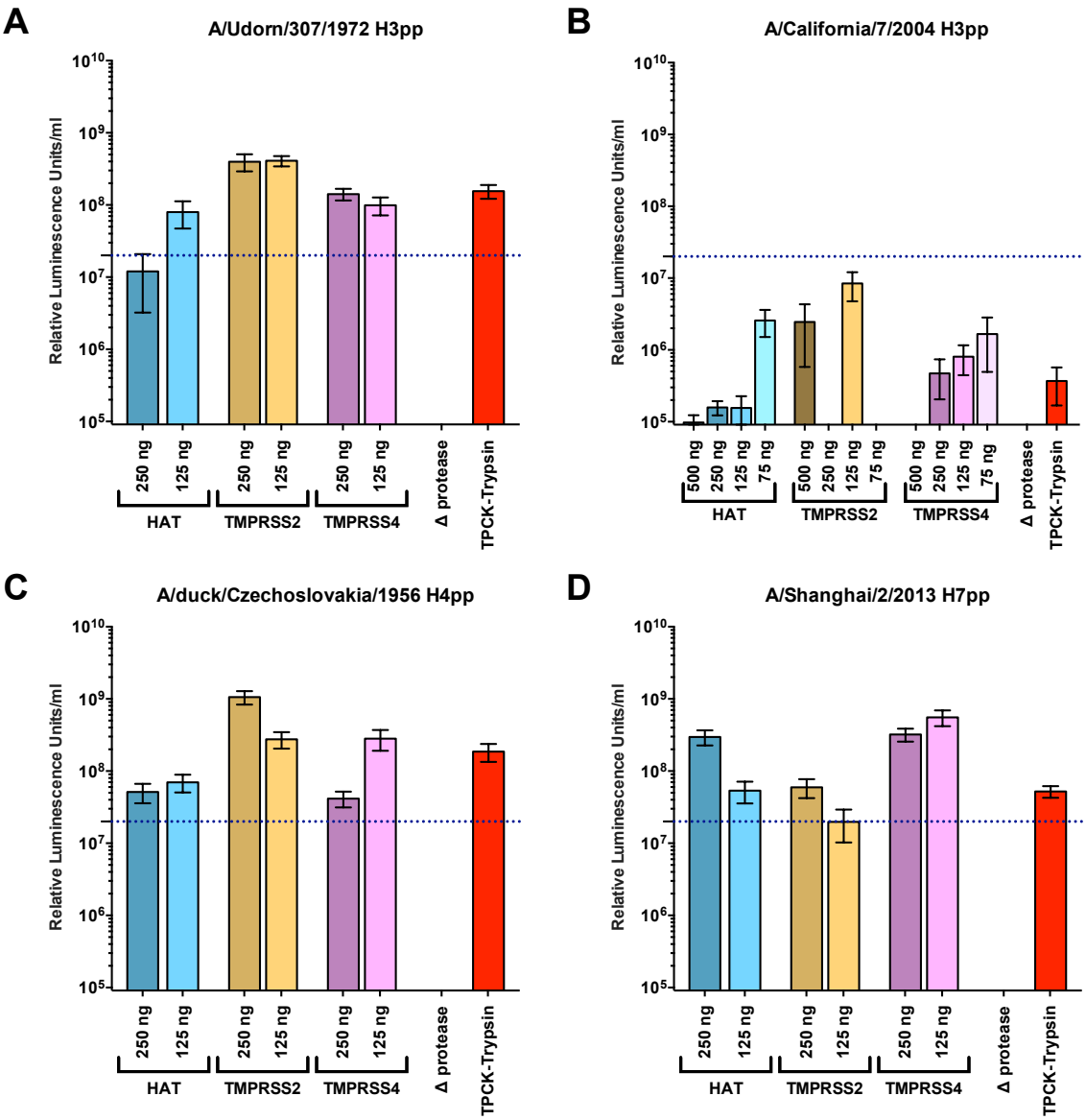

Figure 30: Role of HAT, TMPRSS2, and TMPRSS4 proteases in H3pp, H4pp, and H7pp production

Titres of pp generated during an individual transfection experiment are reported in RLU/ml with SEM (n=8 titre measurements). A line corresponding to 2×10^7 RLU/ml is drawn to indicate the minimum titre necessary to effectively perform neutralization assays. **A.** A/Udorn/307/1972 H3pp; **B.** A/California/7/2004 H3pp; **C.** A/duck/Czechoslovakia/1956 H4pp; **D.** A/Shanghai/2/2013 H7pp.

The production optimisation of H8pp is shown in **Figure 31A**. High titre pp were produced when the pCMV-Tag3 TMPRSS4 (ECD)-myc plasmid was co-transfected into producer cells. The use of pCAGGS-HAT permitted the production of H8pp of moderate

titre, whereas lower titres were observed when pCAGGS-TMPRSS2 was used during the transfection or when TPCK-Trypsin treatment was performed post-supernatant harvesting.

Figure 31B shows the production of another Group 1 HA bearing pp, A/Hong Kong/1073/1999 H9pp. As observed for H8pp, the highest titres were obtained when TMPRRSS4 was used, followed by HAT. TMPRSS2 failed to activate the H9 HA and pp titres were lower than for the Δ protease pp. TPCK-Trypsin treatment also permitted the rescue of Δ protease pp titre.

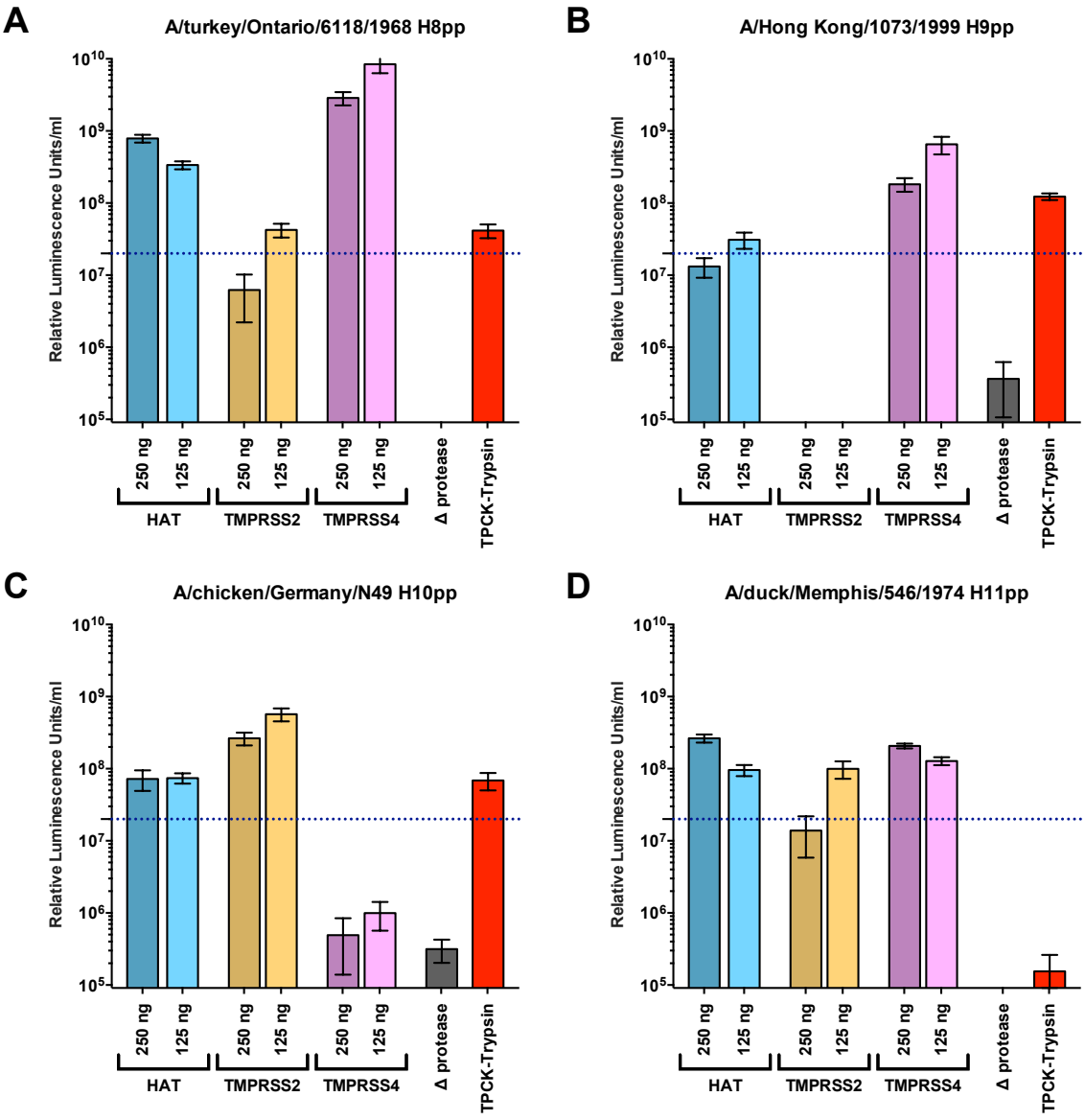

Figure 31: Role of HAT, TMPRSS2, and TMPRSS4 proteases in H8pp, H9pp, H10pp, and H11pp production
Titres of pp generated during an individual transfection experiment are reported in RLU/ml with SEM (n=8 titre measurements). A line corresponding to 2×10^7 RLU/ml is drawn to indicate the minimum titre necessary to effectively perform neutralization assays. **A.** A/turkey/Ontario/6118/1968 H8pp; **B.** A/Hong Kong/1073/1999 H9pp; **C.** A/chicken/Germany/N49 H10pp; **D.** A/duck/Memphis/546/1974 H11pp.

In **Figure 31C**, titres obtained during the optimisation of the H10pp are reported. The optimisation has shown that high pp titres can be obtained when TMPRSS2 is used;

alternatively HAT permits high titre pp (>1×10^8 RLU/ml) production. However, the use of TMPRSS4 failed to produce high titre pp.

The production optimisation of A/duck/Memphis/546/1974 H11pp is reported in **Figure 31D**. It was possible to produce moderate titre (>1×10^7 RLU/ml) pp using all the three proteases tested. Higher titres were observed when 250 ng of pCAGGS-HAT and pCMV-Tag3 TMPRSS4 (ECD)-myc were used, whereas the titres of TMPRSS2-produced pp resulted in at least a half log lower titre. The Δ protease H11pp titre was not rescued by the TPCK-Trypsin treatment.

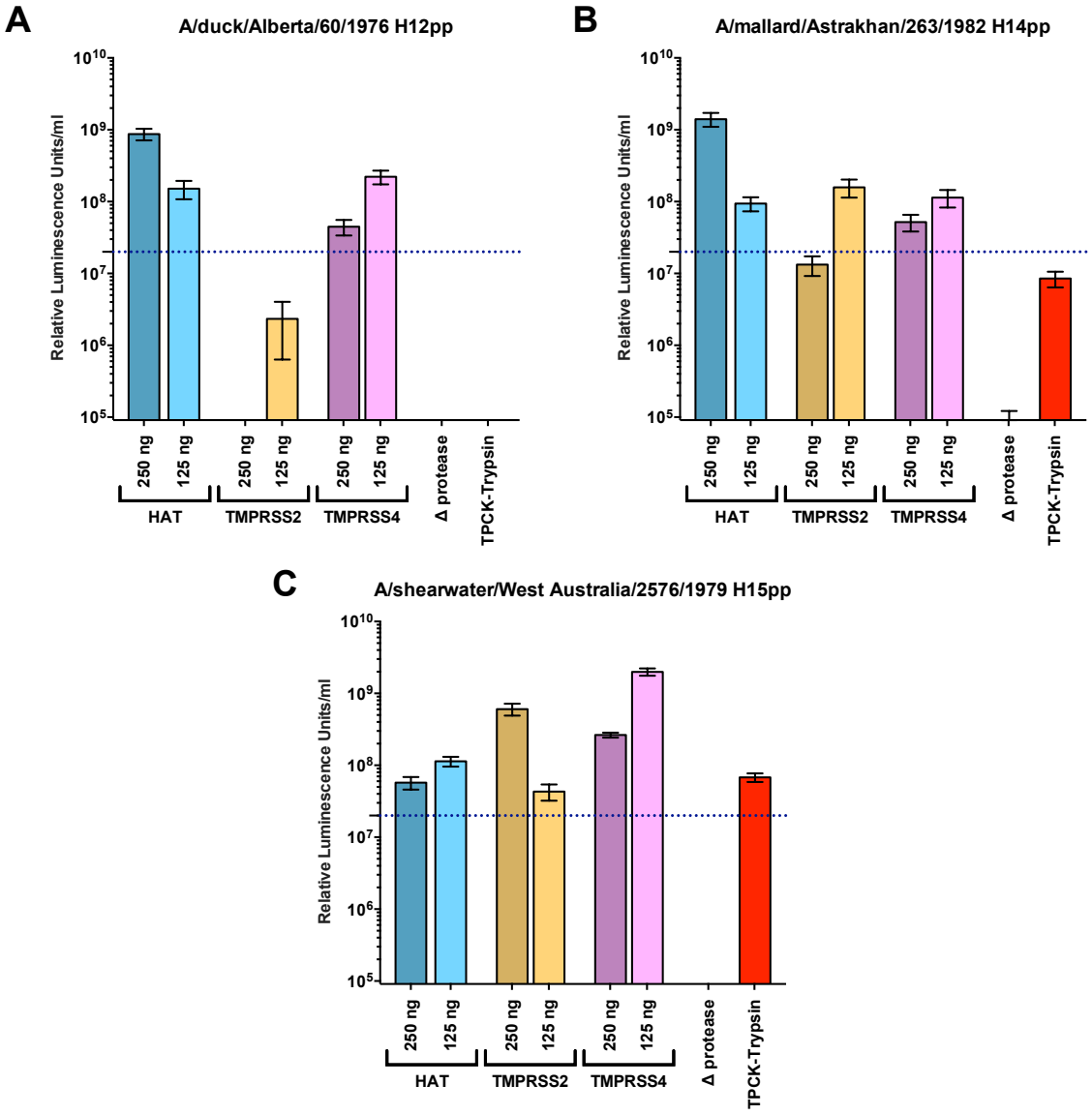

Figure 32: Role of HAT, TMPRSS2, and TMPRSS4 proteases in H12pp, H13pp, and H14pp production

Titres of pp generated during an individual transfection experiment are reported in RLU/ml with SEM (n=8 titre measurements). A line corresponding to 2×10^7 RLU/ml is drawn to indicate the minimum titre necessary to effectively perform neutralization assays. **A.** A/duck/Alberta/60/1976 H12pp; **B.** A/mallard/Astrakhan/263/1982 H14pp; **C.** A/shearwater/West Australia/2576/1979 H15pp.

Figure 32A shows the production optimisation of H12pp. High titre pp were obtained using HAT and TMPRSS4. The co-transfection of pCAGGS-TMPRSS2 permitted the production of an active pp when 125 ng was used but not when 250 ng was transfected. As observed for the H11pp, the TPCK-Trypsin does not activate the H12 HA.

The production of H14pp is reported in **Figure 32B**. H14pp were generated through HA activation, especially mediated by HAT, subsequentially by TMPRSS4 and TMPRSS2. Activation of HA pp was also achieved using TPCK-Trypsin treatment.

In **Figure 32C** H15pp are reported. High titre H15pp were generated by co-transfection of pCMV-Tag3 TMPRSS4 (ECD)-myc. Also the use of TMPRSS2 permitted the production of high titre pp, especially when 250 ng of plasmid was used. HAT and TPCK-Trypsin mediate HA activation and pp production to a lower extent than the other two proteases.

To verify that the HA cleavage is mediated by the co-transfected proteases, Western blotting was performed on the A/duck/Italy/1447/2005 H1pp and A/Udorn/307/1972 H3pp. The two Western blot membranes are shown in **Figure 33** and **Figure 34.**

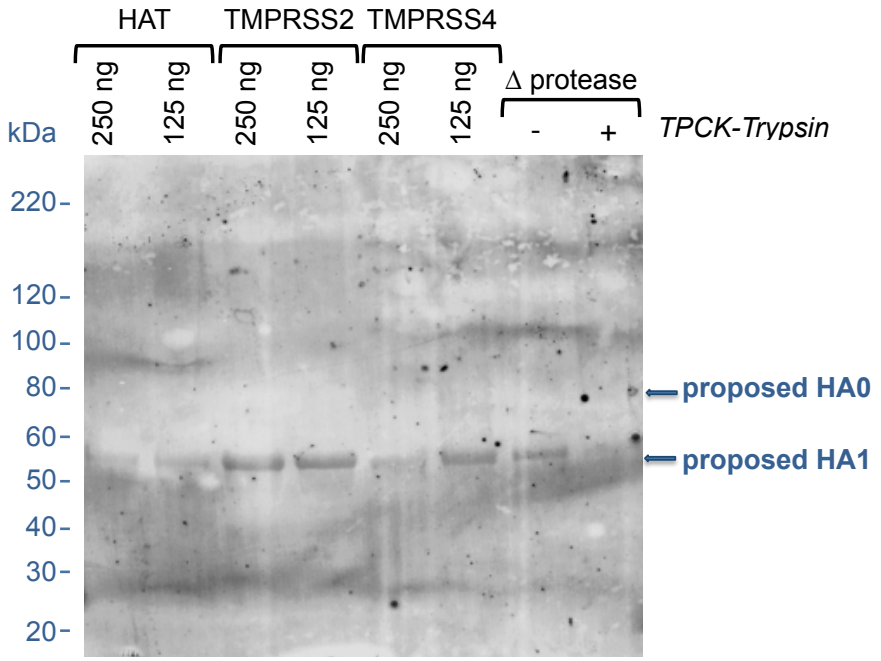

Figure 33: Western blot of A/duck/Italy/1447/2005 H1pp obtained using different proteases
HA was detected using 1:500 A/duck/Italy/1447/2005 H1N1 OIE reference chicken antiserum and 1:20000 Alexa Fluor® 680-AffiniPure donkey anti-chicken IgY (IgG) (H+L) secondary antibody. Membrane was acquired using the 700nm channel. Molecular weight size marker lane was not shown as acquired using sensitivity parameters that differed from the rest of the membrane. An HA control, that could be used to better identify the bands detected, was not used as a recombinant HA was unavailable for the subtype tested (other HA subtypes, e.g. H5, would have not be recognised by the antisera used).

Unfortunately, the poor quality of the A/duck/Italy/1447/2005 H1pp Western blot (**Figure 33**) does not permit the clear visualisation and quantification of the bands,

however it is possible to observe the presence of bands at 55 kDa, corresponding to HA1, for all the pp produced using protease co-transfection, indicating successful cleavage of the HAs. The HA1 band is also present in the Δ protease pp indicating that producer cells possess proteases that were able to cleave the HA generating functional pp. Bands corresponding to the uncleaved HA0 are undetectable in the membrane, indicating that by far the majority of the HAs are active. However, this does not correlate with the titration results in which the Δ protease pp had a lower titre (**Figure 28F**), indicating the presence of uncleaved HA.

In the Δ protease pp subjected to TPCK-Trypsin an HA1 band cannot be observed. The absence of the HA1 after the TPCK-Trypsin treatment could indicate that this treatment was too harsh and has resulted in HA degradation and non-specific cleavage. This result correlates with the observation that TPCK-Trypsin treatment cannot rescue the Δ protease A/duck/Italy/1447/2005 H1pp titre that was diminished after this cleavage treatment (**Figure 28F**).

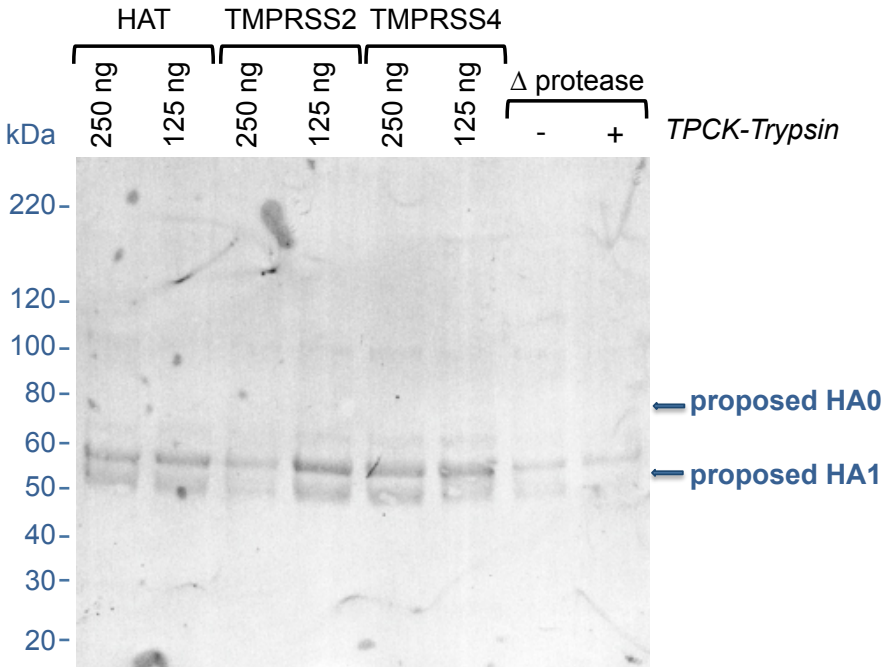

Figure 34: Western blot of A/Udorn/307/1972 H3pp obtained using different proteases
HA was detected using 1:500 A/England/427/1988 (H3N2) NIBSC sheep antiserum and 1:20000 anti-sheep/goat IgG Dylight®800 secondary antibody. Membrane was acquired using the 800nm channel. Molecular weight size marker lane was not shown as acquired using sensitivity parameters that differed from the rest of the membrane. An HA control, that could be used to better identify the band detected, was not used as a recombinant HA was unavailable for the subtype tested (other HA subtypes, e.g. H5, would have not be recognised by the antisera used).

In the A/Udorn/307/1972 H3pp Western blot (**Figure 34**), two bands between 50 kDa and 60 kDa are observed. Since in each sample these two bands are observed at a molecular weight corresponding to HA1, this could indicate that HA1 presents two different glycosylation patterns. As observed in the A/duck/Italy/1447/2005 H1pp Western blot, the HA0 bands are not observed. Nevertheless, it is clear that the HAs present on the

pp surface were cleaved by the HAT, TMPRSS2 and TMPSS4 since the HA1 bands are visible. Furthermore the presence of the HA1 bands in the A/Udorn/307/1972 H3 Δ protease pp demonstrates that these or other proteases that are involved in HA cleavage are expressed in the HEK293T/17 producer cells.

3.3.3 Residues near the cleavage arginine play a role in protease haemagglutinin activation

A/black-headed gull/Sweden/2/1999 H16pp was also produced following the protease optimisation protocol. However, to test the role of an α-helix present at the level of the cleavage arginine in the H16 HA (Lu *et al.* 2012), pp were produced and optimised using a wild-type and a mutant H16. In this mutant H16, produced by site-direct mutagenesis, the amino acids near the H16 cleavage arginine were changed to resemble the ones present in H1 (**Figure 35**). In this way the α-helix should be disrupted.

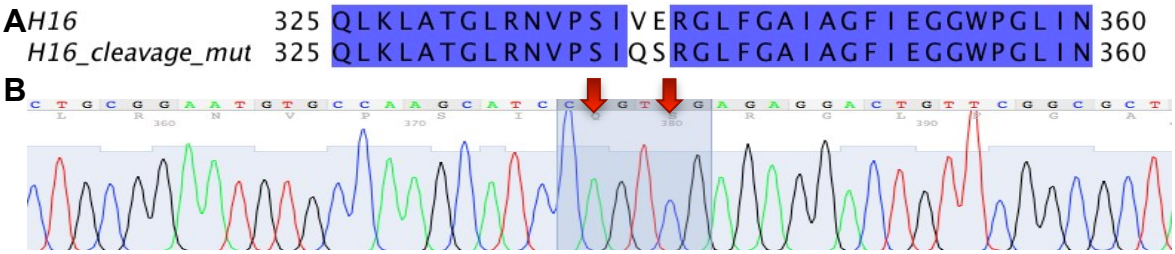

Figure 35: Site-direct mutagenesis of A/black-headed gull/Sweden/2/1999 H16
A. A/black-headed gull/Sweden/2/1999 H16 gene sequence after mutagenesis showing the mutated cleavage site; **B.** Electropherograms of mutated A/black-headed gull/Sweden/2/1999 H16 gene sequence.

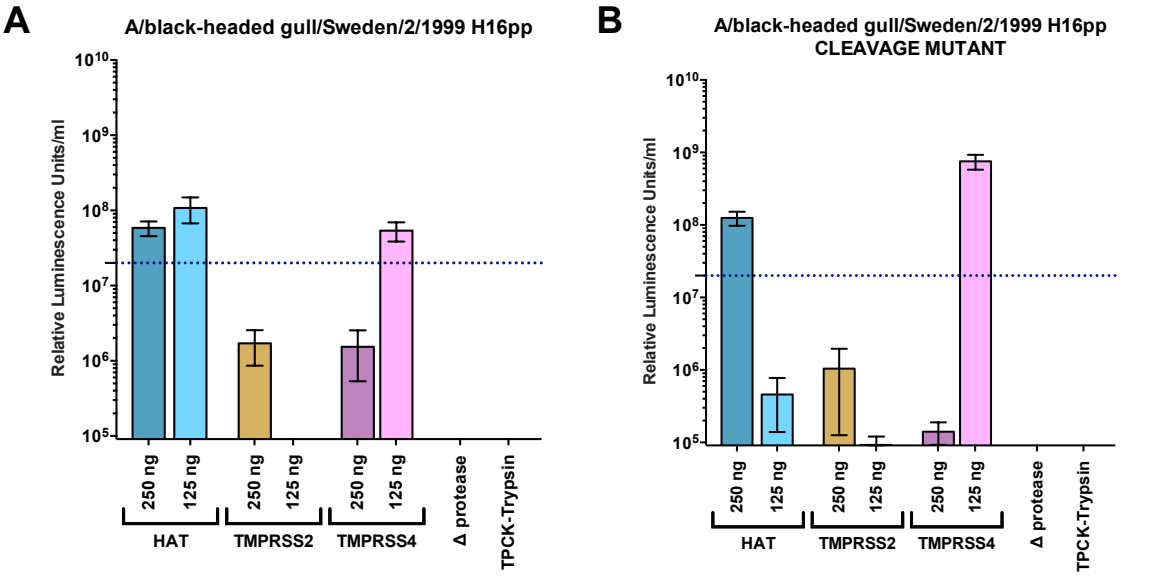

Figure 36: Role of HAT, TMPRSS2, and TMPRSS4 proteases in the production of wild-type and mutated A/black-headed gull/Sweden/2/1999 H16pp
Titres of pp generated during an individual transfection experiment are reported in RLU/ml with SEM (n=8 titre measurements). A line corresponding to 2×10^7 RLU/ml is drawn to indicate the minimum titre necessary to effectively perform neutralization assays. **A.** Wild-type A/black-headed gull/Sweden/2/1999 H16pp**; B.** A/black-headed gull/Sweden/2/1999 H16pp with cleavage mutation.

The protease-activation profiles of the H16pp and its mutant (**Figure 35**) have many similarities but also some differences. In fact, the protease activation profile of the H16 cleavage mutant pp is more similar to the one observed with H1pp: high titres are observed when high quantities of HAT were used and especially when lower quantities of TMPRSS4 were used, as observed for some of the H1pp (**Appendix Table 1**).

Both H16 and its cleavage mutant were not activated by TPCK-Trypsin, possibly indicating that the disruption of the α-helix is not sufficient to permit the TPCK-Trypsin cleavage as observed with H1pp. Therefore other factors could be involved to explain this cleavage pattern.

3.3.4 Production of A/Texas/05/2009 H1 pseudotypes is dependent on the quantity of the haemagglutinin-encoding plasmid used

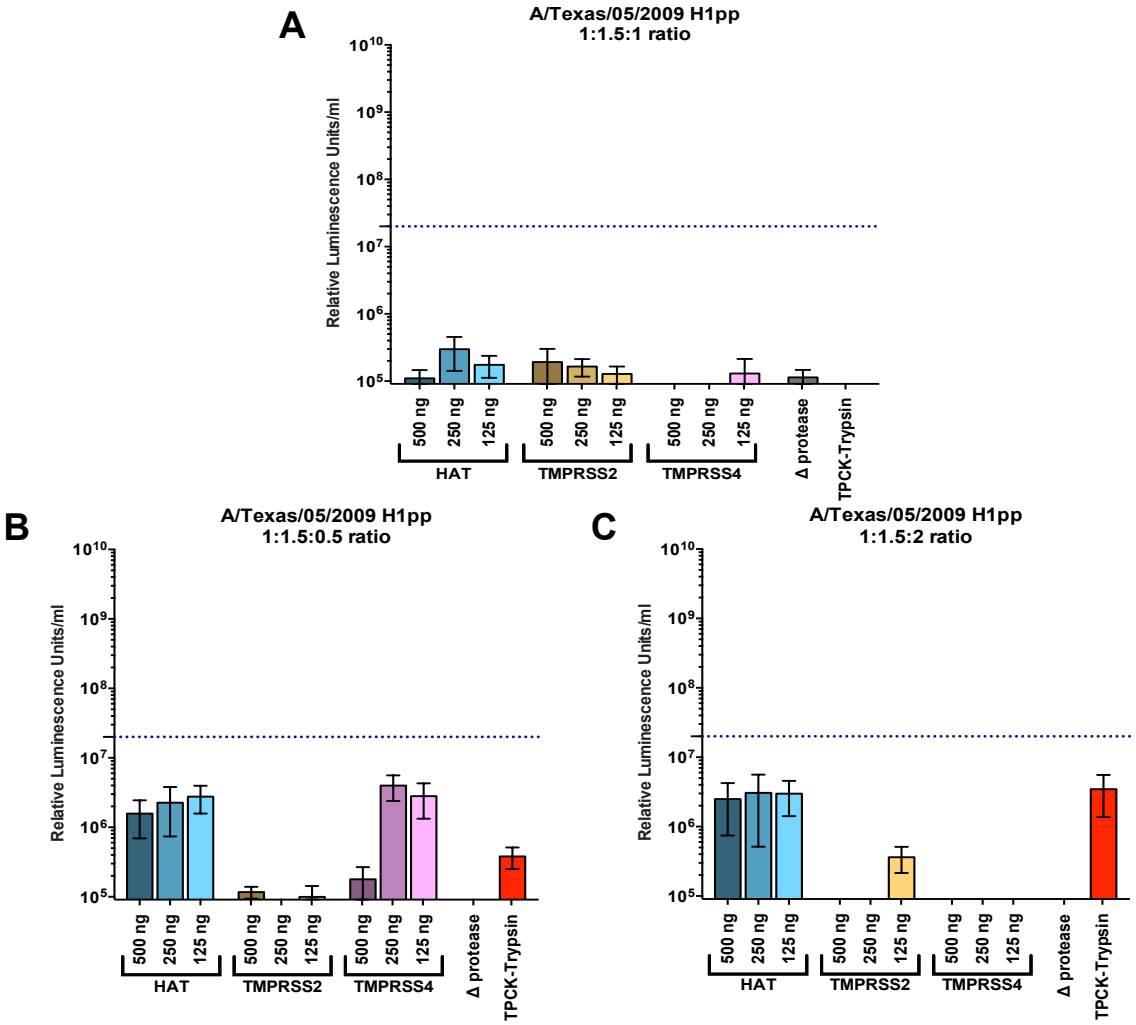

Figure 37: Production of A/Texas/05/2009 H1pp
The role of HAT, TMPRSS2, and TMPRSS4 proteases in the production of A/Texas/05/2009 H1pp was evaluated concomitantly to the optimisation of pp production ratios. Titres are reported in RLU/ml with SEM (n=8 titre measurements). A line corresponding to 2×10^7 RLU/ml is drawn to indicate the minimum titre necessary to effectively perform neutralization assays. **A.** A/Texas/05/2009 H1pp produced using standard ratio of p8.91, pCSFLW and pI.18-A/Texas/05/2009 H1; **B.** A/Texas/05/2009 H1pp produced halving the amount of pI.18-A/Texas/05/2009 H1; **C.** A/Texas/05/2009 H1pp produced doubling the amount of pI.18-A/Texas/05/2009 H1.

To produce A/Texas/05/2009 H1pp, the optimisation of type and quantity of the protease-encoding plasmid was performed (**Figure 37A**). However, the pp titres, obtained using proteases or TPCK-Trypsin treatment, were not different from Δ protease pp.

Initially a problem with the expression of the envelope protein was hypothesised. However, having confirmed the expression of A/Texas/05/2009 H1 on the producer cell surface by immunofluorescence (**Figure 40**), this explanation was excluded.

Suspecting a toxic effect due to the expression of this particular HA or a less efficient expression in comparison to other HAs, and knowing that evaluating different HIV-1 core, lentiviral vector and envelope protein plasmid ratios could help the optimisation of pp production (Garcia and J. C. C. Lai 2011), the effect of changing quantities of HA-encoding plasmid during co-transfection was tested. Two conditions were tested: the quantity of the HA-encoding plasmid was halved (250 ng) or doubled (1000 ng) changing the plasmid ratio to 1:1.5:0.5 and 1:1.5:2 respectively. When less pI.18-A/Texas/05/2009 H1 was used (**Figure 37B**), HAT- and TMPRSS4-generated pp showed an increase in titres in comparison to the Δ protease pp, indicating that the two proteases were able to activate the HA permitting the production of transduction-efficient pp. When the HA-encoding plasmid quantity was doubled an increase in transduction activity was observed when HAT-encoding plasmid was used and when 125 ng of pCAGGS-TMPRSS2 was used (**Figure 37C**). In both cases TPCK-Trypsin treatment permitted HA cleavage and the consequential increase of the Δ protease pp titre.

However, the titres of the A/Texas/05/2009 H1pp remain comparatively low ($<1\times10^7$ RLU/ml) and further optimisation will be necessary to produce a pp that can be efficiently used for other applications (e.g. pp-NT assay).

Recently two mutations of the influenza 2009 pandemic HA were reported to be able to increase virus production/replication and pp titre (Nicolson *et al.* 2012; Z. Chen *et al.* 2010; W. Wang, Castelán-Vega, *et al.* 2010). To investigate the feasibility of using this knowledge in pp production, mutagenesis was performed on the pI.18-A/Texas/05/2009 H1 plasmid. **Figure 38** and **Figure 39** show the successful mutagenesis and the introduction of the K136 and Q240 amino acid mutations.

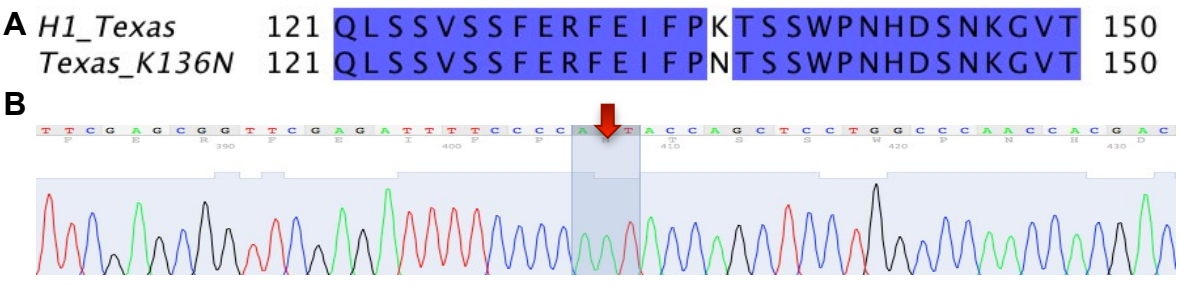

Figure 38: Site-direct mutagenesis K136N of A/Texas/05/2009 H1pp
A. A/Texas/05/2009 H1 gene sequence after mutagenesis showing the K135N mutation; **B.** Electropherograms of mutated A/Texas/05/2009 H1 gene sequence.

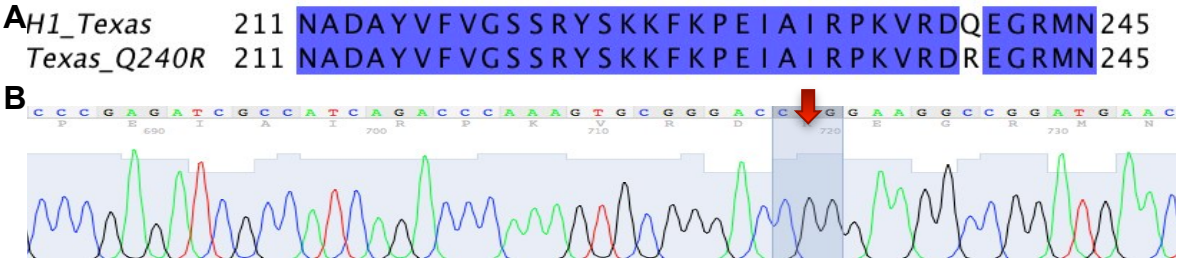

Figure 39: Site-direct mutagenesis Q240R of A/Texas/05/2009 H1pp
A. A/Texas/05/2009 H1 gene sequence after mutagenesis showing the Q240R mutation; **B.** Electropherograms of mutated A/Texas/05/2009 H1 gene sequence.

Before evaluating these new mutant HAs in the pp generation system, immunofluorescence was performed to verify protein expression following simple plasmid transfection. In **Figure 40**, the immunofluorescence shows that the two mutated HAs were expressed on the HEK293T/17 cells, with no significant differences in expression observed in comparison with the wild-type HA. For this reason and the fact that possible antigenic differences between the mutated HAs and the wild-type HA could be present (García-Barreno *et al.* 2014; Job *et al.* 2013; Koel *et al.* 2013), it was decided to not proceed in the evaluation of these HA in the pp producing system.

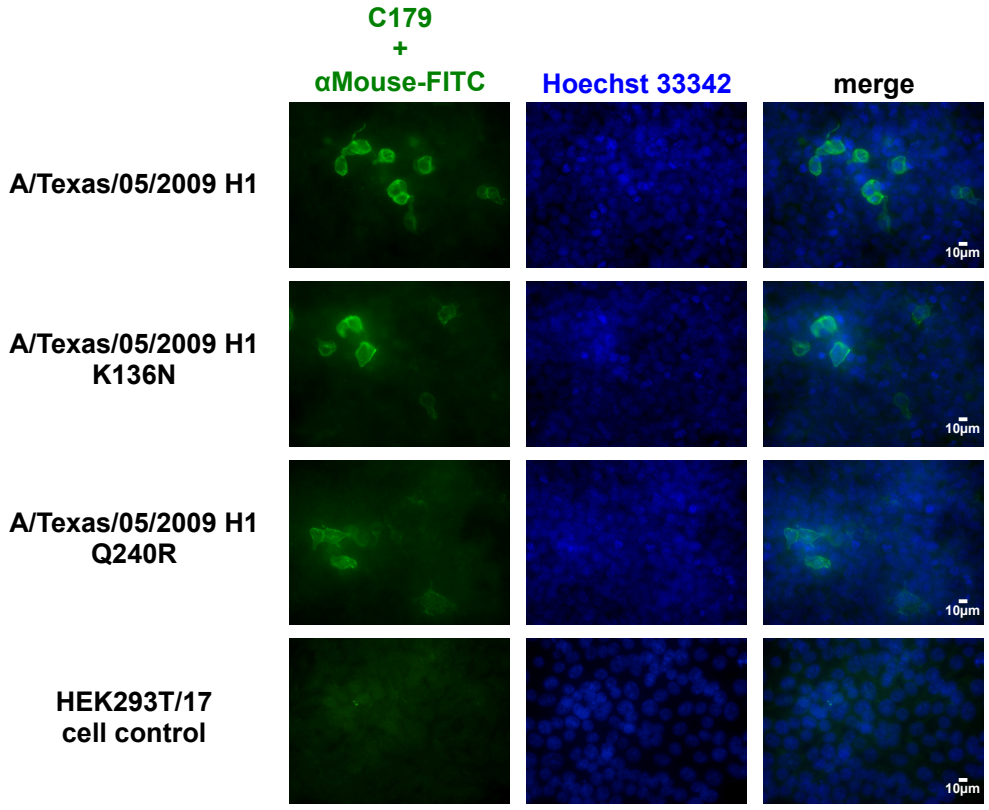

Figure 40: Immunofluorescence of the wild-type A/Texas/6/2009 H1, and the K136N and Q240R mutants
The immunofluorescence was performed using C17 as primary antibody and anti-mouse IgG (whole molecule)–FITC antibody as secondary antibody. Images were acquired using 20X magnification and the scale bar (10µm) is shown in the figure. The immunofluorescence shows the plasma membrane expression of A/Texas/6/2009 H1 wild-type and mutated HAs compered to the cell control, in which minimal background is detected. Hoechst 33342 was used to highlight the HEK293T/17 nuclei.

3.3.5 Presence of neuraminidase in the pseudotype membrane increases the titre of A/Wisconsin/67/2005 H3 pseudotype

Firstly, to produce A/Wisconsin/67/2005 H3pp, different protease types and quantities were evaluated. The results, showed in **Figure 41A**, demonstrate that the use of pCAGGS-TMPRSS2 and pCMV-Tag3 TMPRSS4 (ECD)-myc resulted in only slight increase in titres compared to Δ protease pp titre; however, HAT was able to activate the HA permitting the production of functional pp with titre reaching the 1×10^7 RLU/ml.

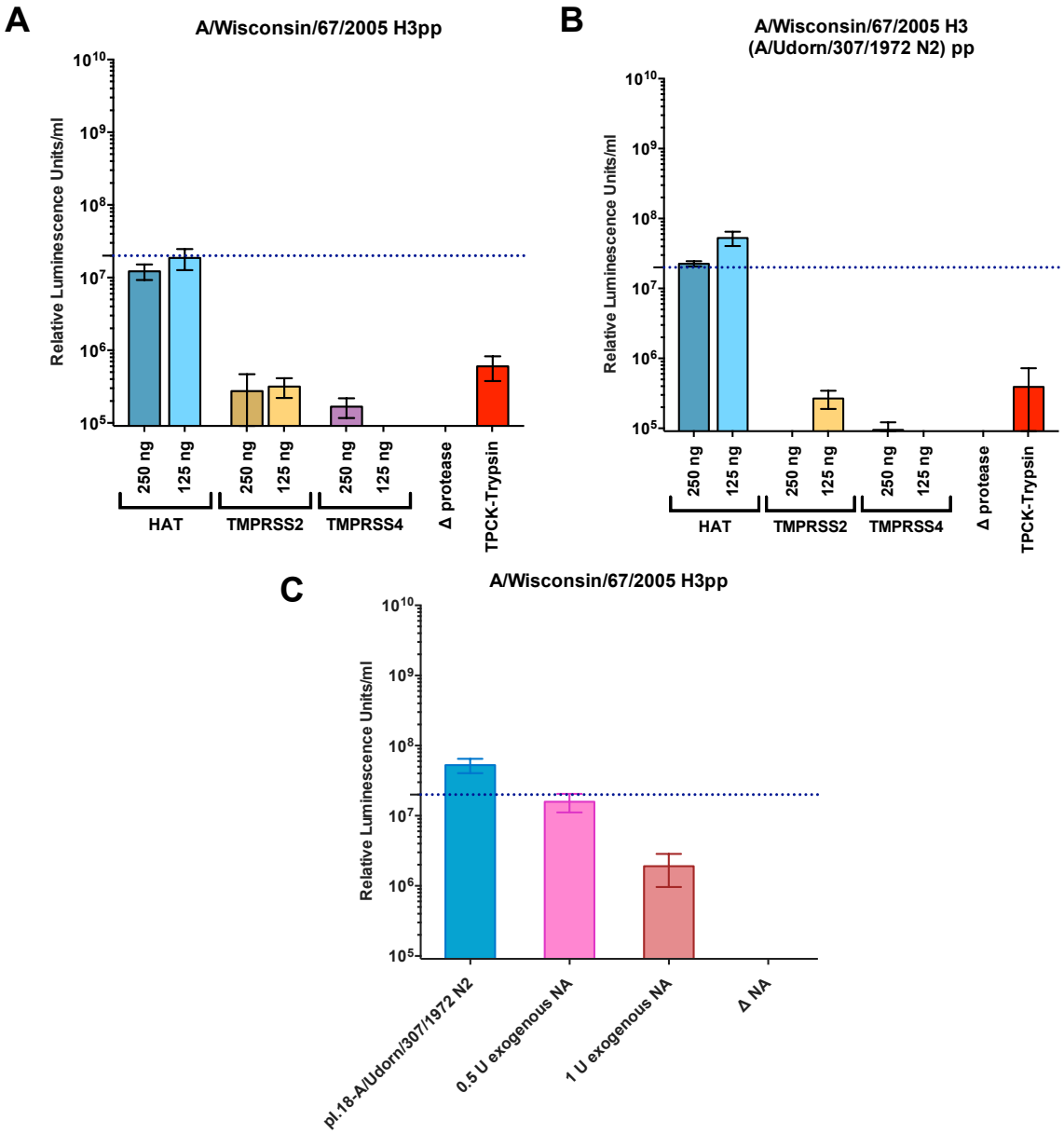

Figure 41: Production of A/Wisconsin/67/2005 H3pp
Titres of pp generated during an individual transfection experiment are reported in RLU/ml with SEM (n=8 titre measurements). A line corresponding to 2×10^7 RLU/ml is drawn to indicate the minimum titre necessary to effectively perform neutralization assays. **A.** Evaluation of HAT, TMPRSS2, and TMPRSS4 protease on the production of A/Wisconsin/67/2005 H3pp; **B.** Evaluation of HAT, TMPRSS2, and TMPRSS4 protease role on production of A/Wisconsin/67/2005 H3pp in which the A/Udorn/307/1972 N2 was also expressed. **C.** Role of the A/Udorn/307/1972 N2 and exogenous NA on A/Wisconsin/67/2005 H3pp production.

Since recently it was demonstrated that H3 bearing influenza A viruses show a lower affinity for short and branched sialylated glycan receptors (Gulati *et al.* 2013) and that the N2 NA can acquire significant receptor-binding activity following mutation (Y. P. Lin *et al.* 2010), it was decided to evaluate, in the pp system, the effect of the co-transfection of an N2 NA-expressing plasmid.

When the A/Udorn/307/1972 N2 was added to the pp surface by co-transfection of the encoding plasmid, the HA protease cleavage pattern did not change, but a slight increase in the titres of pp produced using HAT was observed (**Figure 41B**).

Further analysis shows that the H3N2pp titre was higher than the titre of the H3pp produced using both the standard (0.5 U) and double (1U) amount of exogenous NA. As expected, the lowest titre is observed in NA absence, indicating that NA activity is necessary for pp production (**Figure 41C**).

3.3.6 For production of A/gull/Maryland/704/1977 H13 pseudotype further strategies should be implemented

Initial experiments performed to produce the A/gull/Maryland/704/1977 H13pp did not yield positive results since in all the cases pp titres lower than 5×10^5 RLU/ml were obtained (**Figure 43A**).

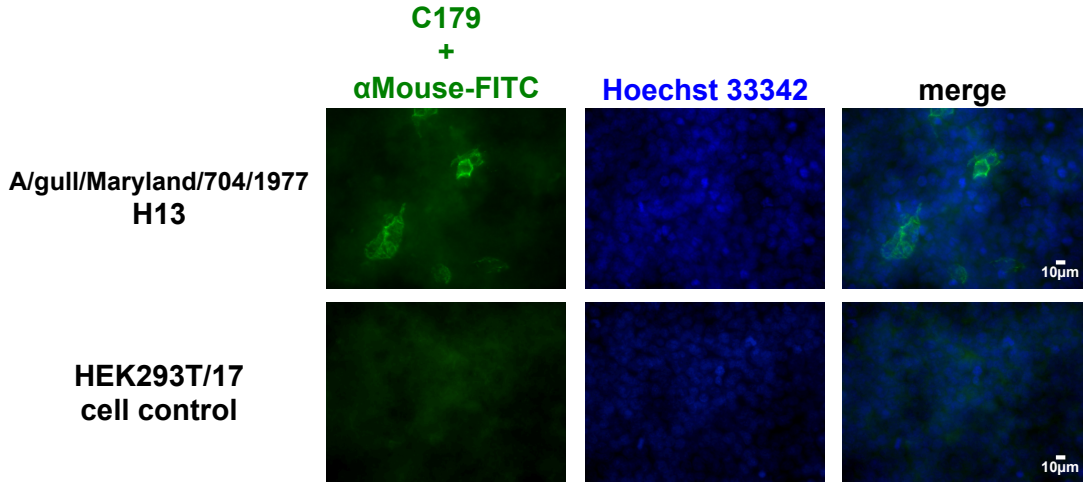

Figure 42: Immunofluorescence of the wild-type A/gull/Maryland/704/1977 H13
The immunofluorescence was performed using A/gull/Maryland/704/1977 (H13N6) antisera as primary antibody and the anti-chicken IgG (H+L)-Fluorescein antibody as secondary antibody. Images were acquired using 20X magnification and the scale bar (10µm) is shown in the figure. The immunofluorescence shows the plasma membrane expression of A/gull/Maryland/704/1977 H13 compered to the cell control, in which minimal background is detected. Hoechst 33342 was used to highlight the HEK293T/17 nuclei.

Since also TPCK-Trypsin treatment failed to activate H13pp, a problem with the expression of the envelope protein was suspected and thus immunofluorescence was performed. However, the immunofluorescence (**Figure 42**) clearly showed that the H13

HA was expressed on the plasma cell membrane when the encoding plasmid was transfected into cells.

For this reason, in order to produce the H13pp, two strategies were investigated. The first strategy consisted of decreasing the amount of HA-encoding plasmid used, as was done for A/Texas/05/2009 H1, in case that a toxic effect following the expression of the HA had occurred. This strategy did not result in any improvement in the pp titre (**Figure 43B).**

The second strategy used was evaluating two additional proteases, TMPRSS3 and TMPRSS6. Testing these two proteases (**Figure 43C**), an increase in the H13pp titre was observed when 125 ng of TMPRSS6-encoding plasmid was co-transfected during pp production, indicating a possible role of this protease in the cleavage of the H13 HA.

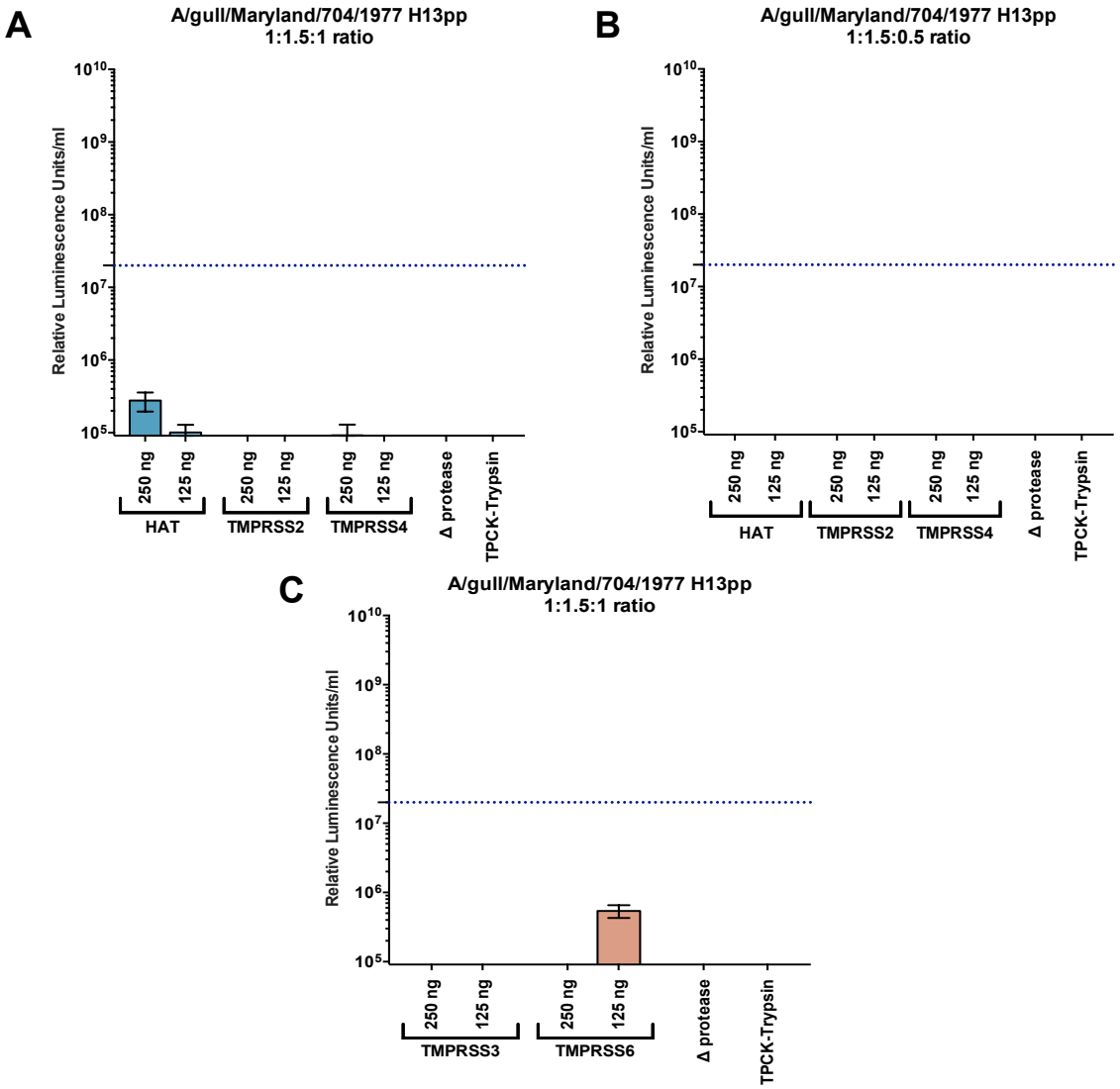

Figure 43: Production of A/gull/Maryland/704/1977 H13pp
Titres of pp generated during an individual transfection experiment are reported in RLU/ml with SEM (n=8 titre measurements). A line corresponding to 2×10^7 RLU/ml is drawn to indicate the minimum titre necessary to effectively perform neutralization assays. **A.** Role of HAT, TMPRSS2, and TMPRSS4 proteases in the production of A/gull/Maryland/704/1977 H13pp; **B.** Role of HAT, TMPRSS2, and TMPRSS4 proteases in the production of A/gull/Maryland/704/1977 H13pp in with the amount of HA-encoding plasmid used during transfection was halved; **C.** Role of TMPRSS3 and TMPRSS6 proteases in the production of A/gull/Maryland/704/1977 H13pp.

3.4 Discussion

To permit entry into cells, influenza viruses or pp need to harbour on their envelope trimerised and correctly folded HAs. Furthermore, it is necessary that the fusion peptide is exposed. This is mediated by HA0 cleavage at the level of basic residue/residues preceding the fusion peptide sequence itself.

Influenza HPAI H5 and HPAI H7pp are usually straightforward to produce, since HA cleavage is mediated by proteases that are expressed in producer cell lines (Garcia and J. C. C. Lai 2011). On the other hand, production of pp harbouring the human or low pathogenic avian HA is more problematic since cleavage is mediated by tissue-specific proteases.

Recently, different proteases putatively involved in HA cleavage were isolated and exploited to produce pp and study HA cleavage using pp (Zmora *et al.* 2014; Sawoo *et al.* 2014; Ferrara *et al.* 2013; Galloway *et al.* 2013; Bertram *et al.* 2012; Bertram *et al.* 2011; Bertram, Glowacka, Blazejewska, *et al.* 2010; W. Wang *et al.* 2008). However, these studies have mainly concentrated on human H1 and H3 HA subtypes. In this chapter the essential role of three proteases HAT, TMPRSS2, and TMPRSS4 to cleave HAs and thus produce low pathogenic avian and human influenza pp is shown. In fact, when protease-encoding plasmid is co-transfected into HEK293T/17 with HIV-1 *gagpol*-encoding plasmid, HA-encoding plasmid, and lentiviral vector, pp can be obtained. This process is not straightforward: optimisation of the type and the quantity of protease used is necessary to obtain high titre pp.

Before proceeding to discuss the data in detail, it should be noted that to calculate the pp titre, which is used as surrogate measure of protease activity, a method that does not consider the mathematical relationship between the titration dilution points was used. Alternatively and perhaps more relevant, the titration results could have been fitted with a curve and then the titre in RLU/ml should have been interpolated on the basis of the curve equation. However it was impossible to find a curve fitting the data. This curve-fitting methodology would have been more appropriate especially to calculate the titre of the pp produced without envelope protein, which were used to normalize the data (Section 1.5.1). In fact the method used here tends to intrinsically overestimate the background level, with the risk of masking significant results. However the method used permits an effective evaluation of pp titre for further experimental procedures (i.e. pp-NT assay) and for this reason was considered more appropriate for the final use of pp. In future other mathematical methods to calculate the titre should be evaluated.

Another important factor that should be considered is the fact that pp are produced with equal amounts of transfected DNA that may or may not result in an equal amount of

protein being expressed. If the elements encoded by p8.91 and pCSFLW are identical in each transfection, and could be considered expressed at the same level in each transfection, the same is not true for the HA and the protease encoding plasmid: even if expression controlling elements are similar, the genes are inherently different and this is a factor that can contribute to protein expression. In fact each gene could be codon- or not codon-optimized and specific sequences could interfere with mRNA stability and translation. For this reason caution should be exercised when comparing different pp.

Additionally if the p8.91, pCSFLW, and the plasmid encoding the HA should also be present at the same time in the same cells to produce pp, for the proteases the process is more complicated. For example TMPRSS2 needs to be expressed in the cell in which HA is expressed since it mediates cleavage intracellulary, whereas HAT could activate HA in trans since it is also expressed at the plasma membrane. The cellular localization in which TMPRSS4 mediates its activity is not clear.

Taking in consideration the points discussed, in general, from the results obtained, it can be noticed that TMPRSS4 shows a broad cleavage activity since it is able to activate HAs belonging to different Group 1 and Group 2 subtypes, permitting the production of high titre pp. Furthermore, Group 1 HAs are preferentially cleaved by HAT rather than TMPRSS2, whilst for Group 2 HAs the opposite is true. More specifically, it appears clear that different subtypes exhibit different cleavage patterns. This was also noted by Galloway *et al.* 2013; however, the results reported here differ from those previously described. For example, in Galloway *at al.* TMPRSS2 had a greater and broader cleavage activity compared to the results presented here. However, these dissimilarities could be explained by different experimental conditions. In fact, the results presented here show that not only the type, but also the quantity of the protease-encoding plasmid needs to be investigated to have optimal cleavage conditions and high pp titres. In relation to this, it could be that a HA-protease equilibrium is necessary to produce high titre pp. In fact it could be that, when overexpressed, proteases mediate aspecific degradation of the HA.

Unfortunately, the poor quality of the Western blots performed and the absence of normalisation of pp loading do not permit the quantification of the ratio of uncleaved: cleaved HA and comparison of different preparations. Nevertheless, the Western blot performed on A/duck/Italy/1447/2005 H1pp shows that after TPCK-Trypsin treatment of Δ protease pp the HA is degraded since an HA1 band is not visible. Furthermore, the A/duck/Italy/1447/2005 H1pp activated by TPCK-Trypsin has a titre lower than the Δ protease. This indicates that TPCK-Trypsin treatment conditions also need to be optimised for each pp and reinforces the concept that an equilibrium between HAs and proteases is needed to permit optimal cleavage/activation and to not cause HA degradation.

Degradation could also be the cause of the double bands (corresponding to the proposed HA1) observed in the Western blot performed on A/Udorn/307/1972 H3pp, however other effects such as different HA glycosylation could also exhibit with this pattern. The optimisation and standardisation of Western blotting using pp is necessary to understand if degradation, differential glycosylation or other artefacts can affect the results observed. Furthermore, it will reveal deeper insight into protease-HA equilibrium and should be investigated in future. Furthermore, the ability to assess the protease kinetic in relation to HA as substrate using purified proteins could be useful to understand this equilibrium (Ferrara *et al.* 2013).

In regards to the protease-HA equilibrium hypothesis, the A/Texas/05/2009 H1pp production experiments permit some elucidation of this mechanism. In fact, A/Texas/05/2009 H1pp production using 500 ng of HA-encoding plasmid resulted in low titre pp. However, when the plasmid quantity was increased or decreased, pp with higher titres were obtained. The experiments have also shown that using different HA quantities, the cleavage pattern changed.

In **Appendix Table 1** the pp production optimisation results were reported and the best conditions were highlighted. In general it was always possible to determine the best protease for cleavage, however when two different quantities of the same protease-encoding plasmid permit the production of a pp, the lower quantity should be used to minimise the toxic effect of the expressed protease. In fact, during optimisation experiments and pp production, it was observed that, when transfecting protease-encoding plasmids, high titre pp are obtained only 48 h post-transfection; if pp are collected 72 h post-transfection the titre is at least 10 fold lower (**Appendix Figure 9**). This effect appears to be associated with acidification, as noted by colour change, of the cell culture media and change of producer cell morphology. To support the hypothesis of the toxic effect of protease expression, it should be noted that HAT and TMPRSS2 are expressed under the control of inducible promoters in the MDCK-HAT and MDCK-TMPRSS2 cell lines (E. Böttcher *et al.* 2009) and the use of an inducible promoter is highly recommended when toxic proteins need to be produced (Kaufman 2000).

An interesting result was obtained when pp were produced in the absence of protease-expressing plasmids: pp titration and Western blot indicates that Δ protease pp are partially able to enter into the target cell line and they present a cleaved HA on their surface, confirmed by the presence of the HA1 band. Surprisingly, in the Western blot the HA0 band is not observed, indicating that the majority of HAs are activated. However, since Δ protease pp titre is lower than the protease-activated pp titre (indicating the presence of uncleaved HA) the absence of the HA0 band, especially in Δ protease pp,

could be an artefact due to the sample preparation (e.g. low-speed centrifugation). As mentioned, titration data suggest that Δ protease pp could harbour some cleaved HA. In regards to this observation, it is likely that HAT, TMPRSS2 and TMPRSS4 are expressed at low levels in the HEK293T/17 cells. Recently, it has been shown that TMPRSS2 and HAT are expressed at different levels in different human respiratory and gastrointestinal tissues (Bertram *et al.* 2012) and expression profiles of TMPRSS2 and TMPRSS4 show that they are expressed also at the level of the kidney (**Appendix Figure 10-12**). It is for this reason likely that these two proteases at least are expressed in the producer cell, but unfortunately data concerning protease expression in HEK293T/17 cells are not currently available to confirm this theory. Nevertheless, it should be possible to investigate expression of the proteases using immunofluorescence and appropriate primary antibodies. It will be also interesting to perform knockdown experiments and subsequently produce pp to evaluate if cleaved HA is still present. In fact it cannot be excluded that other proteases could also be involved in the HA cleavage observed in the Δ protease pp. Recently, matriptase 1 was shown to be able to activate HA (Baron *et al.* 2013; Beaulieu *et al.* 2013; Hamilton, Gludish and Whittaker 2012). Also kallikrein 5 and kallikrein 12 have been associated with the cleavage of H1, H2 and H3 HAs (Hamilton and Whittaker 2013).

The fact that human proteases are able to cleave and activate the HAs of different influenza A subtypes highlights that HA cleavage is a conserved process between avian species and humans, which was underlined after the observation that TMPRSS2 homologous proteins are able to cleave human influenza HAs (Bertram *et al.* 2012). However, it is necessary to understand which of the HA amino acid residues are involved in the recognition of the HA by the proteases. In this chapter the role of amino acid residues preceding the cleavage arginine was investigated briefly.

Recently the structure of an H16 subtype HA was resolved and it was observed that some amino acid residues upstream of the cleavage site are important in determining the surface accessibility of the cleavage arginine (Lu *et al.* 2012). Previously it was observed that TPCK-Trypsin is not able to mediate H16 cleavage (Galloway *et al.* 2013), a result that is confirmed by this study. In fact, in H16 the arginine remains buried since an α-helix is present preceding it (Lu *et al.* 2012). To test the effect of this structure in HA cleavage, the wild-type and a mutant H16, in which the α-helix was disrupted, were used to produce pp using different proteases. The results show that different cleavage patterns are observed in the two H16 HAs, indicating that amino acids near the cleavage arginine play an important role in determining protease specificity: the proteases, even if they are all serine proteases and should recognise the same cleavage arginine, could activate HA on the basis of specific proximal sequence differences. From the results observed it is not clear which

residues are important for each protease, however this could be further investigated via mutagenesis studies. Residues distal from the cleavage arginine could also play a role in determining protease specificity, when considering protein interactions. Supporting this, H1, H2, and H3 HAs present slightly different cleavage patterns, although they possess subtype specific cleavage motifs (Galloway *et al.* 2013). These indicate that other residues, possibly in the stalk or in regions proximal to the stalk, could play a role in the determination of protease-mediated cleavage.

The study of HA mutants could help to elucidate which residues are involved, and will generate data that can permit at least the prediction of the protease type that should be used to activate a determinant HA, and thus enable production of high titre pp. Furthermore, the resolving of the protease structures and co-crystallization of the proteases with human and/or avian HA could be valuable to delineate the amino acid residues involved in the cleavage process (Ferrara *et al.* 2013). This would not only enhance understanding of the HA activation mechanism, but importantly may aid development of potential protease inhibitors (Dahms *et al.* 2014; Hamilton *et al.* 2014; Becker *et al.* 2012; Böttcher-Friebertshäuser *et al.* 2012; Sielaff *et al.* 2011; Zhirnov *et al.* 2011; Zhirnov, Ovcharenko and Bukrinskaya 1984), in a similar manner to NA inhibitor design , for treatment of severe influenza virus infections. In theory, if miniaturised and optimised, the pp producing protocol could also be exploited to screen compounds that can block protease-mediated cleavage.

In this chapter, only optimisation of the protease quantity and type used was investigated to activate the HA and produce high titre pp. However, another possible strategy to produce pp could have been modifying the cleavage site from a single arginine or lysine to a multibasic cleavage site (Sawoo *et al.* 2014). Different groups have investigated the role of the multiple lysines and arginines introduced in the HA cleavage site of native viruses especially to evaluate if subtypes other than H5, H7 and H9 can support a multibasic cleavage site and the effect that this has on virus pathogenicity (Veits *et al.* 2012; Schrauwen *et al.* 2011; Munster *et al.* 2010; Szécsi *et al.* 2006). This literature reveals that only some subtypes/strains can support a multibasic cleavage site, implicating that this strategy may not be applicable to all influenza strains.

From the data presented here, differences in pp titre between strains and subtypes are observed: certain pp tend to always produce higher titres, others lower. In this regard, differential HA expression and maturation (glycosylation, folding and trafficking) in the HEK293T/17 producer cell line could play an important role as mentioned in Section 3.1 of this chapter. It is probable that certain HAs are expressed in lower quantities than others and this results in a lower number of pp produced (Hai *et al.* 2012). In relation to this, the

quantity of HA in each preparation should be evaluated to determine if pp of different strains harbour the same amount of HAs on their surfaces.

Furthermore, regarding the role of glycosylation in HA expression, in the current study the A/Texas/05/2009 H1 K136N mutant, which possesses a glycosylation site in position 136 in comparison to the wild-type, was investigated by immunofluorescence. This was to see if any differences in expression were evident, since this mutation was reported to increase vaccine yield (Nicolson *et al.* 2012). Results have shown that expression differences are not apparent and it is probably necessary to use other techniques (e.g. Western blotting) to highlight any. The production of pp harbouring this mutation present some concerns, as recently, antigenic differences compared with the wild-type caused by this same mutation were reported (García-Barreno *et al.* 2014; Job *et al.* 2013) and this is an issue if pp are to be used in neutralization assays.

To increase the titre of A/Texas/05/2009 H1pp another mutant was investigated. In this mutant the receptor-binding site was modified to introduce an arginine instead of glutamine at position 246 (A/Texas/05/2009 numbering). As mentioned, this mutant was associated with an increase of pp titre and of vaccine yield (Z. Chen *et al.* 2010; W. Wang, Castelán-Vega, *et al.* 2010). In immunofluorescence experiments, this mutant does not appear to be differentially expressed compared to the wild-type HA. However, this HA mutation is also related to sialic acid receptor recognition (W. Wang, Castelán-Vega, *et al.* 2010), and for this reason to test its effect, pp should be produced and tested on target cells. Unfortunately, viruses with mutated receptor-binding sites were recently associated with the presence of antigenic differences compared to the wild-type HA (Koel *et al.* 2013). For this reason, before proceeding to generate this mutant pp, further evaluation of the advantages and disadvantages of producing a mutated HA pp to be used in neutralization assays should be performed. At present, other strategies involving the optimisation of HA quantity and cleavage seems to be more suitable, considering also that, from immunofluorescence experiments, the wild-type A/Texas/05/2009 H1 HA appears to be strongly expressed.

The two H3pp bearing more recently circulating HAs, A/California/7/2004 H3pp and the A/Wisconsin/67/2007 H3pp, exhibit lower titres compared to the A/Udorn/307/1972 H3pp. Recently it was recognised that currently circulating H3N2 strains are losing receptor-binding activity (Gulati *et al.* 2013). It was recently demonstrated that in response to this loss the NA have acquired a compensating mutation (Y. P. Lin *et al.* 2010). This is not surprising since HA and NA coevolve and an equilibrium between the two opposite activities is necessary to have efficient replication (Mitnaul *et al.* 2000; Kaverin *et al.* 1998). In this case the NA mutation permits

increase of the binding activity of the virus (Y. P. Lin *et al.* 2010). Furthermore, the use of a NA-encoding plasmid was shown to increase the pp titre (Molesti *et al.* 2013; F. Zhang *et al.* 2011; W. Wang, Castelán-Vega, *et al.* 2010; Bosch *et al.* 2001). For these reasons it was decided to evaluate the NA role in the production of the A/Wisconsin/67/2007 H3pp. Unfortunately, the associated strain N2 NA was not available and for this reason the N2 of A/Udorn/307/1972 (H3N2) was used instead. The data produced support the observation that the presence of an endogenous NA increases pp titre (Molesti *et al.* 2013; F. Zhang *et al.* 2011; W. Wang, Castelán-Vega, *et al.* 2010; Bosch *et al.* 2001). To understand better if this effect was dependent on an increased release of pp, production experiments were also performed doubling the amount of exogenous NA usually used. Results show that increasing amount of exogenous NA does not have a positive effect in pp production. This seems to indicate that is not the sialidase activity that increase pp titre but the binding activity itself. Since the NA used does not possess the mutation associated with increased binding activity, a hypothesis is that the presence of NAs could influence the avidity of pp for their receptor (Ohuchi *et al.* 2006). The study of pp harbouring NA and a headless HA, which confers fusion activity to these pp, could have been useful to verify if NA could possess binding activity.

Furthermore, NA and HA plasmids were used in a ratio 1:4 but, as previously mentioned, this may not directly represent the NA:HA protein ratio. It is possible that the two plasmids were transfected into different cells and for this reason pp harbouring only NA or only HA could also be present. To analyse NA expression on the viral surface, immunofluorescence on transfected cells and protein quantification of pp though ELISA and Western Blot could have been useful. Confocal immunofluorescence imaging of pp (Pizzato *et al.* 1999) could also have been used for this purpose.

Lastly, it was not possible to produce the A/gull/Maryland/704/1977 H13pp even using TPCK-Trypsin treatment as observed previously (Galloway *et al.* 2013). Immunofluorescence has confirmed that the H13 HA is expressed on the producer cell surface, indicating that the absence of pp titre could be related to the fact that the HA is uncleaved or not properly cleaved. Reducing the amount of HA used did not permit to increase the pp titre as observed for A/Texas/05/2009 H1pp. Interesting, when testing two different proteases, TMPRSS3 and TMPRSS6, an increase in titre compared to the Δ protease was observed using TMPRSS6. This protease, like TMPRSS3, was not previously associated with HA cleavage (Zmora *et al.* 2014; Bertram *et al.* 2011; Bertram, Glowacka, Blazejewska, *et al.* 2010), so further experiments (e.g. Western blotting) are necessary to confirm this data. Simultaneous optimisation of HA quantity and the protease quantity could perhaps elucidate if this protease is involved. It should also be noticed that

an asparagine is present near the cleavage arginine (Galloway *et al.* 2013). This asparagine is not present in other subtypes, and should be further investigated using mutagenesis since it could potentially be glycosylated. This interpretation, is in contrast with the recently resolved H13 structure that shows only one glycosylation site (Lu *et al.* 2013); however, the recombinant protein used for structure characterisation was produced using a baculovirus system, and insect cell differs for glycosylation in comparison with mammalian cells (Contreras-Gómez *et al.* 2013).

H13 HA was also previously reported to have specific characteristics of receptor binding and recognises exclusively α-2,3 sialic acids (Lu *et al.* 2013; Shelton *et al.* 2011; Nobusawa *et al.* 1991). For this reason it is obligatory to test the ability of the pp to enter into the target cells used but also into other cell lines using pp encoding for GFP as reporter gene, since this reporter permits a qualitative evaluation of pp entry.

In this chapter it was shown that influenza HA pp production is a process that requires optimisation of the protease-mediate HA cleavage, of HA expression, and in certain cases the addition of other influenza envelope proteins (i.e. NA). Despite these limitations, pp are important tools to elucidate all biological processes involving HA (e.g. receptor-recognition, cleavage, antibody responses).

CHAPTER 4

Evaluation of reference antisera cross-reactivity for establishment of reference standards for employment in pseudotype particle neutralization assays

4.1 Introduction

The advantages of the use of pp-NT assays were described in Chapter 1 and the production of novel influenza pp in Chapter 3. However, before proceeding to use them as tools to study immune responses, it is necessary to investigate more thoroughly their use as surrogate antigens in neutralization assays. It is necessary to identify appropriate neutralization controls to be used with the pp produced. Usually sera collected from previously infected or vaccinated animals/individuals can be useful for this purpose, especially if positivity for specific influenza antibody was confirmed by another serological assay (e.g. HI, MN or SRH). Additionally, established positive sera would represent a useful tool to optimise, validate, and monitor an assay. The International Organization for Standardization, the International Conference on Harmonisation of Technical Requirements for Registration of Pharmaceuticals for Human Use (ICH), the WHO, the OIE, and the United States Pharmacopeia describe reference materials as critical reagents supporting the use of numerous bioassays for standardisation and control of different biological products. The same organizations also extensively established how such material should be produced, characterised, and maintained (Health:2008tk World Health Organization 2006; P. F. Wright 1998). Appropriate reference standards are especially useful when the specificity, sensitivity, precision, and accuracy of an assay are evaluated for the first time (Jacobson 1998) but are also essential when other assay aspects, such as dilution range or calibration curves, are established (The United States Pharmacopeial Convention 2010b). Furthermore they have an essential role when the Westgard quality control rules[6] are applied to monitor assay stability and consistency over different analytical sessions (e.g. days) (J. J. Gray *et al.* 1995).

[6] Westgard rules are a set of criteria used for laboratory quality control. These rules help to establish if the results of an analytic session should be ignored: in fact an analytic session can be accepted only if the measured value of a control/reference standard is in accordance with the value established during assay validation. The Westgard rules state the statistical criteria of accordance (T. A. Carroll, Pinnick and W. E. Carroll 2003; Westgard *et al.* 1977).

Reference materials are also useful when multisite validation of an assay is performed. For example the use of reference standard sera has been shown to be extremely useful to increase consistency between laboratories using HI and SRH (Wood *et al.* 1994).

Reference antisera against all the HA subtypes are commonly generated and used for influenza virus typing in the HI assay (World Organization for Animal Health 2012; Dwyer *et al.* 2006), and for this reason they represent suitable material to be investigated as possible controls and reference standards in pp-NT assays.

For this reason, the neutralization activity and cross-reactivity of reference antisera was evaluated to identify appropriate controls that can be used in proof-of-principle experiments with pp-NT assays. This will also permit understanding of which steps will be necessary to optimise and validate the pp-NT assay, and to certify its use in product release and stability control (if, in future, HA stalk-directed mAbs will be licensed) and in evaluating antibody responses elicited by current and 'next-generation universal' influenza vaccines.

4.2 Material and methods

4.2.1 Haemagglutinin-expressing plasmids and pseudotype production

pI.18-A/duck/Italy/1447/2005 H1, phCMV1-A/duck/Germany/1215/1973 H2, pI.18-A/Udorn/307/1972 H3, phCMV1-A/duck/Czechoslovakia/1956 H4, phCMV1-A/turkey/Ontario/6118/1968 H8, pI.18-A/Hong Kong/1073/1999 H9, phCMV1-A/chicken/Germany/N/49 H10, phCMV1-A/duck/Memphis/546/1974 H11, phCMV1-A/duck/Alberta/60/1976 H12, phCMV1-A/mallard/Astrakhan/263/1982 H14, phCMV1-A/shearwater/West Australia/2576/1979 H15, phCMV1-A/black-headed gull/Sweden/2/1999 H16 were used for pp production as described in Section 2.3.2.2, with addition of an appropriate protease-encoding plasmid to the transfection mix, based on Chapter 3 results.

pI.18-A/Vietnam/1194/2004 H5 (Accession number: ABP51976.1) was used for production of H5pp, as described in Chapter 2.

pI.I8-A/chicken/Italy/1082/1999 H7 (Accession number: ABR37396.1) was kindly provided by Dr. Eleonora Molesti (Universities of Greenwich and Kent, Medway, UK), and the H7pp was produced as described elsewhere (Molesti *et al.* 2013; Ferrara *et al.* 2013) following the protocol reported in Chapter 2, but with the addition of 250 ng of pCAGGS-TMPRSS2 in the transfection mix.

4.2.2 Reference sera

The OIE avian reference hyperimmune sera used for these studies were kindly provided by Dr. Giovanni Cattoli (Istituto Zooprofilattico delle Venezie, OIE, Legnaro, Padua, Italy) and are reported in **Table 18**.

Table 18: OIE avian influenza reference antisera for HI assay, Agar Gel Immunodiffusion test, and Agar Gel Precipitation test

Antigen strain name	Subtype	HA accession number	HI titre
A/duck/Italy/1447/2005	H1N1	HF563054.1	1:512
A/duck/Germany/1215/1973	H2N3	CY014710.1	1:512
A/psittacine/Italy/2873/2000	H3N8	GQ247846.1*	1:256
A/cockatoo/England/1972	H4N8	GQ247847.1*	1:128
A/turkey/Canada/1965	H6N2	GQ247851.1*	1:256
A/turkey/Ontario/6118/1968	H8N4	CY014659.1	1:512
A/mallard/Italy/3817-34/2005	H9N2	Not Applicable	1:256
A/ostrich/South Africa/2001	H10N1	GQ247860.1*	1:512
A/duck/Memphis/546/1974	H11N9	AB292779.1	1:1024
A/duck/Alberta/60/1976	H12N5	CY130078.1	1:128
A/gull/Maryland/704/1977	H13N6	D90308.1	1:1024
A/mallard/Gurjev/263/1982	H14N5	M35997	1:512
A/shearwater/Australia/2576/1979**	H15N9	CY130102.1	1:2048
A/gull/Denmark/68110/2002	H16N3	GQ247872.1*	1:256

*Partial sequence
**Also known as A/shearwater/West Australia/2576/1979

Reference avian sera against H5 and H7 influenza strains were provided by the Animal and Plant Health Agency (APHA, previously Animal Health and Veterinary Laboratories Agency) and are reported in **Table 19**.

Table 19: APHA avian influenza reference antisera

Antigen strain name	Subtype	HA accession number	HI titre
A/chicken/Scotland/1959	H5N1	CY015081.1	Not available
A/African starling/England/983/1979	H7N1	AF202232.1	Not available
A/chicken/Wales/1306/2007	H7N2	EF675618.1	Not available
A/chicken/England/4054/2006	H7N3	EF467826.1	Not available
A/England/268/1996	H7N7	AF028020.1	Not available
A/turkey/England/647/1977	H7N7	AF202247.1	Not available

4.2.3 Pseudotype particle neutralization assays

The pp-NT assays were performed as described in Section 2.3.4, using 5 µl of each serum sample (starting dilution 1:40) and using a pp input of 1×10^6 RLU/well.

IC_{50} neutralization titres were calculated using GraphPad Prism® expressed as dilution factor; then for further statistical analysis they were categorised into 17 groups according to the dilution tested and as reported in **Table 20**.

Table 20: Category of IC_{50} used for statistics

Group	IC_{50} values	Dilution Factor
0	<35	<40
1	35-45	40
2	45-75	40-80
3	75-85	80
4	85-150	80-160
5	150-170	160
6	170-310	160-320
7	310-330	320
8	330-630	320-640
9	630-670	640
10	670-1270	640-1280
11	1270-1290	1280
12	1290-2550	1280-2560
13	2550-2570	2560
14	2570-5100	2560-5120
15	5100-5140	5120
16	>5140	>5120

A cross-reactivity map (pp versus reference antisera), completed using the neutralization groups for further statistical analysis, was designed in a Microsoft® Excel 2011 spread sheet and then saved as a comma-separated value (csv) file.

4.2.4 Bioinformatic analysis

Percentage identity between HA amino acid sequences of pp and reference sera antigens were calculated to check if cross-reactivity could be explained by overall sequence similarity. Amino acid sequences of the HA used in neutralization assays, and used to generate the reference antisera, were downloaded from the Influenza Virus

Resource, the Influenza Research database and the Global Initiative on Sharing Avian Influenza Data (GISAID) Epi-Flu™ platform. The accession numbers of the HAs used in pp-NT assays are reported in Chapter 3 **Table 11** and **Table 12**, and in Section 4.2.1; HA accession numbers of the reference antisera are reported in **Table 18** and **Table 19**. For A/mallard/Italy/3817-34/2005 (H9N2) the HA sequence was not available and for this reason the pp sequence was used as reference.

Unfortunately some of the sequences are not complete, which complicates the analysis. To avoid this problem it was decided to evaluate the percentage identity only for the amino acids that constitute the extracellular part of the HA (amino acids from 24 to 547 - H3 numbering), which were available for all HAs used.

All sequences were aligned using MUSCLE algorithm (Edgar 2004) and Jalview software (Waterhouse *et al.* 2009). Subsequently the sequences were trimmed of their N-Terminal signal sequence, the transmembrane region, and the cytoplasmic tail. Percentage identities between amino acid sequences were calculated by pair-wise alignments using Jalview, before being reported in a Microsoft® Excel 2011 spread sheet and saved as csv file.

The phylogenetic trees shown alongside the cross-reactivity and the percentage identity tables were generated using Molecular Evolutionary Genetics Analysis (MEGA) software (K. Tamura *et al.* 2011): the aligned sequences were imported and trees derived using Unweighted Pair Group Method with Arithmetic mean (UPGMA), the simplest method of tree construction based on pairwise evolutionary distances. The trees generated were manually modified using MEGA and FigTree (http://tree.bio.ed.ac.uk/software/figtree/).

4.2.5 Statistical analysis

Cross-reactivity tables for the IC_{50} neutralization titres, expressed as group (**Table 20**), and for percentage amino acidic identity, were completed using Microsoft® Excel 2011. The R statistical software was then used to analyse the data and design a 'heat-map' which colour codes the neutralization titres and the percentage identity. The precise codes used to produce the maps are reported in Appendix Section A.2. These codes are based on the use of the software package "RColorBrewer", which permits building of a personalised colour palette, and "gplots", a package that contains functions for the graphical interface. The "heatmap.2" function was eventually used to assign to each IC_{50} group or percentage identity value a colour.

Kendall τ (tau) statistics ("Kendall" package) was also run using R software to check if association/correlation between measured IC_{50} titres and percentage identity was present.

4.3 Results

Pp-NT assays were performed against a panel of reference standard antisera using pp bearing HAs of a representative strain, where possible of avian origin, for each HA subtype. The resulting neutralization data, expressed as $IC_{50,}$ were then added to a Microsoft® Excel 2011 spreadsheet that was analysed with the statistical software R. The analysis with R permitted the colour-coding of the neutralization titre calculated. In this way a 'heat-map', or in this case a cross-reactivity map, in which a darker colour represents a higher neutralization activity of the sera against the pp analysed, is designed.

This cross reactivity map is shown in **Figure 44** and should be read positioning the page in landscape orientation. In the cross-reactivity map each pp is compared with a matching antisera (same subtypes and often strains) and other 19 non-matching reference antisera. The phylogenetic relationship between each pp and between each antigen used to produce the antisera was also taken into consideration, and phylogenetic trees are indicated on the x-axis for reference antisera and on the y-axis for the pp.

Observing the **Figure 44**, some features of the cross-reactivity map become immediately discernable: in the top left there are Group 1 HA pp against Group 1 reference antisera, bottom right there are Group 2 HA pp against Group 2 reference antisera, and in bottom left and top right there are the results of pp tested with reference antisera from a different Group. The cross-reactivity map diagonal represents pp that were tested against matching antisera, and as expected the higher neutralization titres are usually found in this part of the table. It can also be noticed that two map-shifts are present since the H6pp and H13pp are missing.

A definite symmetry can be visualised using the diagonal as symmetry axis and, in general, high neutralization titres are found when pp are tested with antisera of the same group (top left and bottom right). Conversely, sometimes antisera neutralize pp that harbour HAs of a completely different subtype/group.

Other important features are that pp were usually neutralized by antisera generated against closely related viruses: in fact using the two phylogenetic tree as guides, it is possible to identify clusters of darker green in relation to phylogenetic clades, for example the H2-H5, H12-H8-H9, H11-H16-H13, H4-H14, and H7-H15.

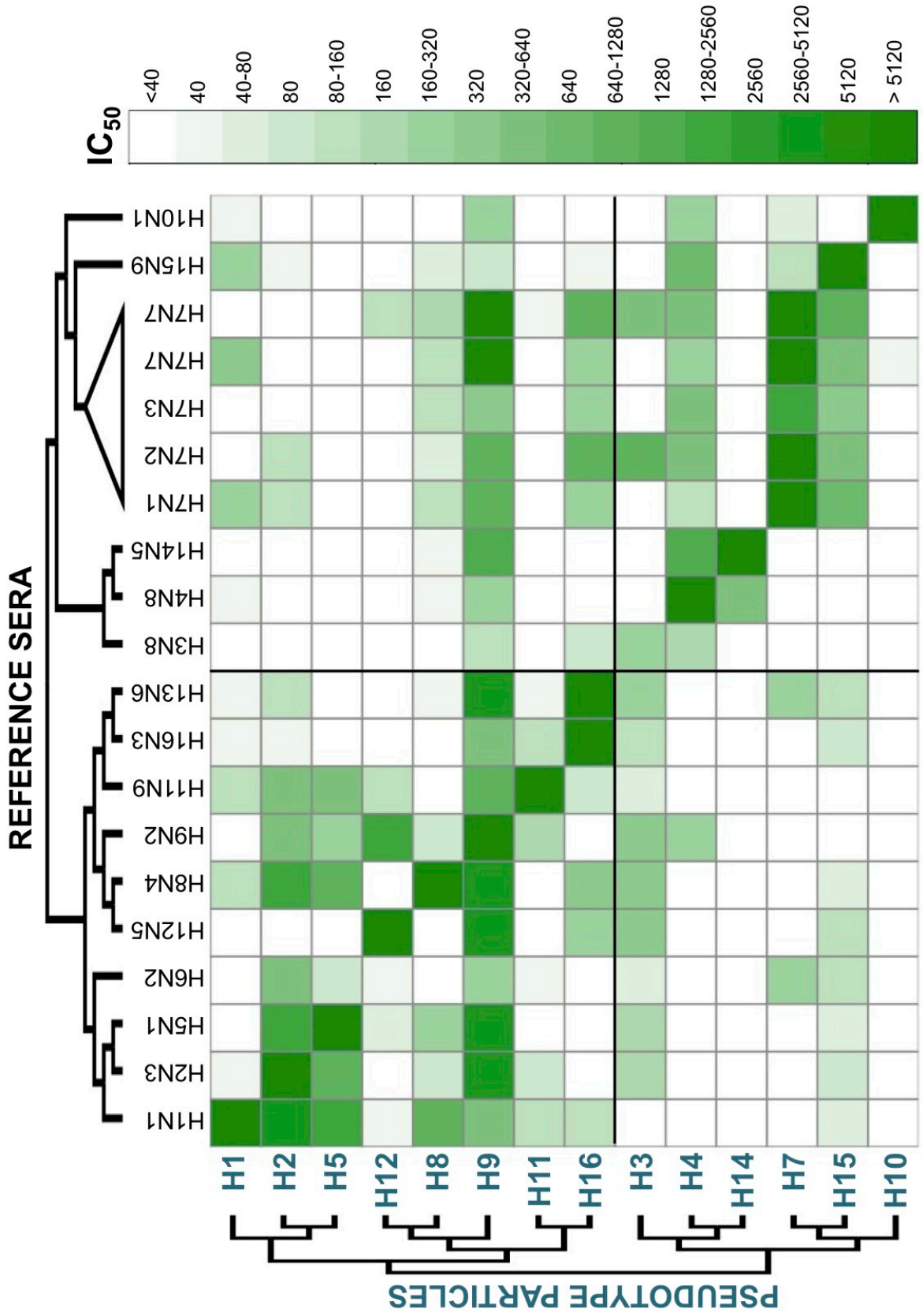

Figure 44: Cross-reactivity map of pp and reference sera based on IC_{50}

Analysing **Figure 44** in detail, it is possible to notice additional distinctive topographies. H1pp was highly neutralized by the matched antisera, but not by antisera generated against closely related HAs (same clade); however, it was neutralized by some Group 1 antisera (H8N4 and H11N9) and additionally by three Group 2 antisera. The H2pp

and H5pp were neutralized by the each others' antisera, by the antisera generated against the most closed related HAs (H1 and H6) but also by H8N4, H9N2 and H11N9 antisera.

H8pp and H12pp, even if closely related, did not exhibit neutralization by each others antisera; however, they were neutralized by the antisera generated against the closely related H9N2. Furthermore, H8pp was also neutralized by the antisera generated against the H1-H2-H5 clade, and by some antisera of Group 2, especially the ones generated against H7 viruses.

All the antisera, without distinction of HA subtype, neutralized H9pp: higher neutralization activities were detected for Group 1 antisera, for H14N5 and H7 antisera, especially anti-H7N7.

H11pp and H16pp were neutralized by their matched antisera and by antisera generated against other closely related HA, and by H1N1 antisera. For H16pp, neutralization activity was detected also when H12N5, H8N4, and H7 antisera were used.

For Group 2 pp, A/Udorn/207/1972 H3pp (a human isolate) was poorly neutralized by the matched avian antisera, but was neutralized by the anti-H7N2 sera, one of the H7N7 antisera, and by numerous Group 1 antisera.

H4pp was neutralized by all Group 2 antisera and by the H9N2 antisera. H14pp was neutralized by the matching antisera and by the antisera generated against the closely related H4.

H7pp and H15pp were neutralized by their matched antisera and by each others antisera; Group 1 sera were also found to cross-react with H15pp and some (H6N2 and H13N9) also with H7pp.

H10pp was only neutralized by its matching antisera and not by any others.

Since phylogenetic relationships did not completely explain the cross-reactivity pattern detected, percentage of amino acid identity was evaluated. Considering that the pp used exhibit only the HA in the envelope, the analysis was performed using only this protein. A percentage-identity map was designed and reported in **Figure 45**. This map shows a similar pattern to the one previously described (**Figure 44**): there is a symmetry following the diagonal, the darker green is concentrated in the top left and bottom right sectors of the map. However, compared to the previous map (**Figure 44**), dark green cannot be observed in the two other sectors of the maps, thus, as expected, the similarity between strains belonging to different groups is low.

Since it is difficult to highlight all the differences and all the similarities by eye, statistical analysis was performed to see whether any concordance or association between the maps was present. Kendall τ test shows that there is low association between

percentage identity and neutralization titres (τ = 0.269, $p \leq 2.22\ 10^{-16}$). This means that additional factors could influence the neutralization titres obtained.

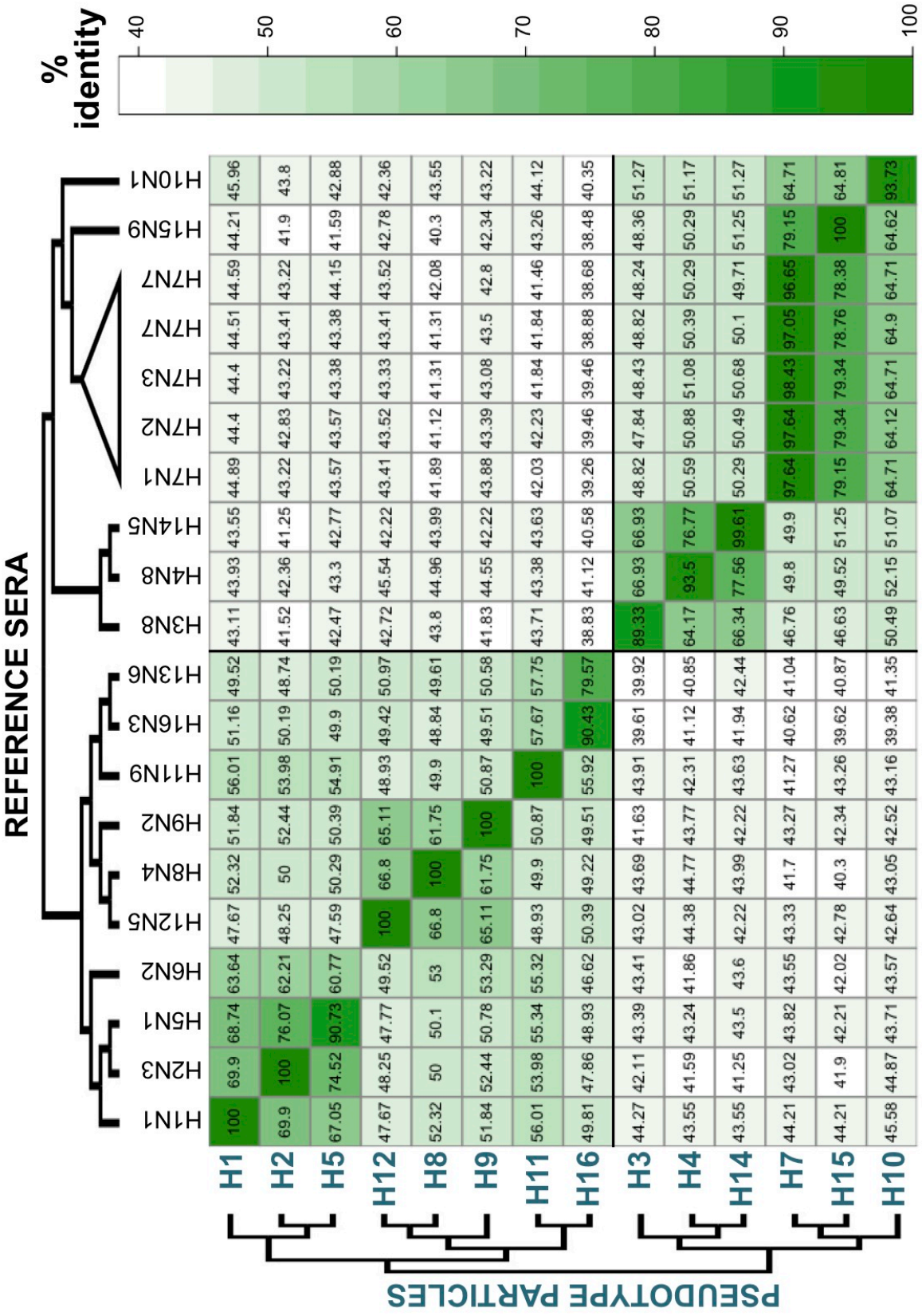

Figure 45: Cross-reactivity map of pp and reference sera based on percentage of amino acid identity

4.4 Discussion and Conclusion

Serological methods, such as HI and MN, are cost-effective and widely-used methodologies to monitor the circulation and the prevalence of influenza viruses and are also employed in vaccine immunogenicity studies (Cattoli and Terregino 2008). However, as described in Chapter 1, these assays are subject to numerous shortcomings.

It has been previously demonstrated that influenza pp-NT assays correlate with other classical serological assays (Garcia *et al.* 2010; W. Wang, Xie, *et al.* 2010; Alberini *et al.* 2009; Temperton *et al.* 2007) and thus may become the technique of choice for HPAI H5 virus serology. Since pp are replication-defective, they offer a safe alternative to wild-type virus methods that require Biosafety Level 3 containment, and the detection of antibody responses is not influenced by the variability of blood-based reagents as observed in other assays (i.e. RBC in HI) (Stephenson *et al.* 2003; Rowe *et al.* 1999). Furthermore the pp-NT appears to be more effective than other functional assays to detect the antibody response directed against the HA stalk (Corti *et al.* 2011).This is most likely due to the fact that, with the absence of NA on the pp membrane surface, glycoprotein density is reduced and the HA stalk becomes more accessible to antibodies. Consequently, pp could be used to effectively study heterosubtypic antibody responses directed against the HA stalk region (Chapter 5).

The pp-NT assay is becoming used more frequently for HPAI H5 virus and more recently also for H7 viruses and human seasonal H1N1 and H3N2, however its use with other influenza antigens is limited. Here, after the production of different avian influenza HA pp (Chapter 3), the possible use of pp in neutralization assay as surrogate antigen was evaluated through testing a panel of reference antisera. For this study a panel of chicken reference antisera was used. This panel was chosen because sera recognising all different HA were available. Mammalian (e.g. ferret) reference antisera could represent a more appropriate control for assays applied for human serology however only antisera against strains of human importance (e.g. H1, H3, H5, H7, and H9) are readily available, and for other subtypes appropriate antisera need to be generated. Since pp-NT assay can be used for avian serological studies as well as for human serological ones, the chicken antisera panel was considered acceptable for a first analysis of cross-reactivity in reference sera. In future, further studies could be designed to assess mammalian antisera and subtype-specific mAbs for cross-reactivity. Additionally it should be noted that chicken sera are more prone to cross-reactivity responses and could better help to identify possible drawbacks of the pp-NT assay.

In this study it was shown that influenza reference antisera are usually able to efficiently neutralize HA-paired pp. However, interestingly, the human A/Udorn/307/1972

H3pp is not efficiently neutralized by its paired (H3N8) avian antisera. This may be due to the fact that H3 avian viruses belong to a different lineage with respect to the human H3 (W. Zhang, Jiang and Y. Chen 2007) as can also be observed by the percentage of identity between the A/Udorn/307/1972 H3 and the A/psittacine/Italy/2873/2000 H3, that is lower (89.33%) than other paired HAs.

Variation in the antiserum neutralizing titres against the HA-paired pp is also observed when H7 antisera are tested. This could be related to the origin of the antisera reflecting intra-subtype antigenic differences among H7 strains and to the fact that different antisera preparations most likely have different neutralizing titres.

However, pp were also tested against antisera generated using non-matched viruses. This analysis has shown that cross-reactive responses can be detected not only when phylogenetic relationships are present between the HA of the pp tested and the HA used as antigens to generate the antisera, but also between HA and antisera that share less similarity. Conversely these cross-reactivity responses do not follow an explainable pattern.

Many authors have previously observed that chicken antisera generated using whole virus in comparison to the ones generated through HA-expressing DNA vaccination or recombinant HA1 vaccination present a lower specificity in HI and/or immunodot-blot assays: this is primarily due to the fact that antisera produced using whole virus also includes NA- and M2-directed antibodies (Shahsavandi *et al.* 2011; C.-W. Lee, Senne and Suarez 2006). However, since a certain level of cross reactivity is observed also with DNA or recombinant protein vaccination, cross-reactive HA-directed antibodies are involved (C.-W. Lee, Senne and Suarez 2006). Similarly, cross-reactive responses were detected using reference antisera in pp-NT assays.

The fact that reference antisera show high neutralizing responses and cross-reactivity between different strain/subtypes could be problematic not only for HI typing, but especially for pp-NT assays. In fact the results show that these antisera can be efficiently used as controls to neutralize pp, but when matched-pp are tested the IC_{50} is usually exceeding the examined dilution range (1:40-1:5120), and therefore cannot permit the direct implementation of quality controls and used as reagents for checking the robustness of the assay. Furthermore, the high cross-reactivity and absence of specificity observed in the pp-NT assay is problematic since it cannot discriminate between two pp. Preparation of the standard material through dilution of the commonly used reference standard, or the use of mAb mixtures (with or without the presence of a serum matrix) showing high specificity could be more effective approaches to establish reference materials to be used to validate, standardise, and control the pp-NT assay.

To better understand the factors contributing to the cross-reactivity results, and to investigate if similarity present between HAs could explain the cross-reactivity results observed, percentage of amino acid identity was calculated between HA tested and HA used to generate the antisera. Statistical analysis has shown that there is a low association between HA similarity and neutralization activity of the sera observed, however other factors could also explain the results observed.

An influence that needs to be accounted for to explain the cross-reactivity observed is that proteins are flexible. Immunoglobulins, especially the complementarity determining regions, can be adapted to different epitopes, thus an epitope that is similar but not completely conserved between two HAs could potentially still be bound by the same antibody (Dreyfus *et al.* 2012). Other factors could also be dependent on the serum origin: for example the chicken IgY are comparable with mammalian IgG but have some unique characteristics. IgY heavy chain is longer due to the presence of an additional constant region and the presence of glycine and proline residues between the constant region boundaries limits the antibody flexibility (Davison *et al.* 2008; Narat 2003). All these properties could have an impact in antigen recognition, especially considering the three dimensional structure of influenza HA on the virus surface: for example the longer heavy chain could impair the recognition of the HA stalk, which is less accessible especially in the wild-type viruses (Wasilewski *et al.* 2012). Supporting this hypothesis is the fact that avian antibodies directed against the HA stalk are not yet described.

Furthermore, the percentage of amino acid identity is a good approach to evaluate similarity between proteins since it is easy to perform with standard bioinformatics tools (multiple alignment and pair-wise alignment), however it does not take into account the insertion or the deletion of glycosylation sites. Glucidic residues attached to the protein through linking to asparagine residues can influence antigen recognition masking or modifying an epitope and, for this reason, should be taken into account when similarity is evaluated (J. I. Kim and Park 2012). There are different tools (Chauhan, Rao and Raghava 2013) that are able to score and detect which residues have a higher probability to be glycosylated. They could be useful when two different HAs are compared, however they cannot yet predict which are the glycans that are linked to the proteins, and the glycan length could also have a role in antigen recognition. Furthermore glycosylation varies between different producer cells and this can influence antigenicity (viruses used as antigens to generate antisera are usually propagated in eggs, whereas pp are produced in a mammalian cell line) (Jacobs and Callewaert 2009).

To understand and explain the cross-reactivity detected, evaluating the structural similarity between the HAs could be a useful approach. Different methods were developed

for this purpose: some of them use structural alignments, and others use approaches such as distance matrix or secondary structure matching (Choi, Kwon and S.-H. Kim 2004; Carugo and Pongor 2002). However, these methods are either time-consuming or computationally intensive; furthermore the software solutions require the protein structures as input and this could be problematic (Choi, Kwon and S.-H. Kim 2004) since, for influenza A virus only 9 HA influenza subtypes are available and, especially for strains that have no human impact, the number of resolved HA structures within each subtype is minimal.

Methodologies that were developed to understand antigenic characteristics of influenza HA could perhaps be the most useful to explain the cross-reactivity pattern observed. Recently antigenic cartography has been used to evaluate the antigenic evolution/drift of different influenza viruses and to help vaccine strain selection (Fouchier and D. J. Smith 2010; de Jong *et al.* 2007). In antigenic cartography, different strains of the same subtypes are usually analysed using HI, MN, and ELISA using reference sera generated against the different strains. In this way matrices/cross-reactivity maps are built and using mathematical analysis, antigenic distance between strains is represented on a graphical map. This methodology could, in theory, be used to analyse the data presented here and can potentially elucidate some of the antigenic characteristics highlighted in these studies, or at least show a new representation of the antigenic interplays between different pp.

Overall, the results presented here reinforce the greater sensitivity of the pp-NT assays described previously (Garcia *et al.* 2010; Temperton *et al.* 2007). Nonetheless, these results point out some features and characteristics that need to be improved and investigated further, such as the specificity, quality control, and the robustness of the assay.

In this study only positive sera were evaluated but an important aspect of diagnostic assay development is also identifying an appropriate negative control. At the moment FBS (data not shown) is used as control in each assay, however it is not a perfect control: an appropriate negative control should possess the same matrix of the samples tested in absence of the analytes, in this case influenza HA-directed antibodies (The United States Pharmacopeial Convention 2010a; The United States Pharmacopeial Convention 2010b). As an additional control, chicken antisera against Newcastle disease virus (data not shown) was used in some of the assays as a more appropriate reference control (produced using the same methodology as OIE reference antisera). This control was not used in all the assays since it was not available at the start of the study. Another appropriate control for the study could have been sera from pre-immunised chicken, however this was not available.

In general for selecting an appropriate control is straightforward if immunological-naïve experimental animals are used. However, this is difficult with humans since influenza circulates in the population and the presence of cross-reactive antibodies, easily detected by pp-NT assays (Molesti, Ferrara, *et al.* 2014; Corti *et al.* 2010), can render the identification of such sera difficult for all the pp produced (Jacobson 1998). In this case a good approach could be to utilise artificially generated sera or ferret antisera. The identification of such materials will also be essential to define sensitivity and specificity of the pp-NT assay.

In the absence of appropriate controls and presence of high cross-reactivity responses, it will be difficult to assess the specificity of the assay. Some important parameters should be evaluated to understand which factors could interfere with the pp-NT assay. For example the presence of virus-attachment inhibitors in the sera and serum treatments (e.g. heat-inactivation, pre-treatment with receptor-destroying enzymes) can be assessed to optimise pp-NT assay conditions and to reduce non-specific neutralization if present. Also the evaluation of possible haemolysis or other contaminants (e.g. lipids) of the serum samples is an aspect that needs to be taken in consideration when the assay is optimised and validated (Jacobson 1998).

Furthermore using RLU as a fixed input for each pp is an optimal approach since it permits direct comparison with MN assays (in neutralization assays 50% Tissue Culture Infectious Dose, $TCID_{50}$, is used as indicator of viral infectivity). However, research groups have emphasised the need to normalise on the basis of the HA content or by other methods to permit comparison between results (Garcia and J. C. C. Lai 2011). Knowing the HA content could be important to complete the analysis reported here but it is not essential. For a final standardisation and validation of the pp-NT assay, a fine characterisation of pp input using HA quantity measures, preferentially the amount of cleaved and uncleaved HA simultaneously, will be necessary to support any statistical analysis performed, but at the moment this is beyond the study remit and will require further studies (e.g. quantification method development and standardisation). In relation to the studies presented here and in the following chapters, the possible unfeasibility (Chapter 7) of quantifying cleaved and uncleaved HA content in pp preparations could result in the impossibility of a direct comparison between the IC_{50} obtained using different HA subtypes or strains, since IC_{50} is related to antibody affinity, which is dependent also on the antigen content used. For example, it appears from the data reported here that certain pp could be intrinsically easier to neutralize (e.g. H9pp) than others (e.g. H10pp): it could be that this is due to the fact that some display a smaller number of HA molecules on their surface. However, it should be noted that in classic

neutralization and MN assays the HA content of the viral input is not routinely evaluated and the same problem therefore exists. At present, the use of RLU for normalisation is the only reasonable way to proceed and can still permit comparison between results if normalisation is performed to calculate the IC_{50} values.

To conclude, the results presented here show that the high sensitivity and the propensity of the pp-NT assay to detect cross-reactive responses permit the use of OIE reference standard antisera as positive neutralization controls, but not as reference standards to validate the assay. More appropriate standards (e.g. mAb mixtures) need to be developed to further progress optimisation and validation of the pp-NT assay.

CHAPTER 5

Use of influenza A pseudotypes to study heterosubtypic antibodies pre- and post- vaccination

5.1 Introduction

The study of antibody responses induced by natural infection and vaccination directed against influenza A HAs is an important facet of pandemic preparedness, since it permits the evaluation of whether a population is subclinically infected, and can identify the geographical spread of circulating viruses. Furthermore, understanding how the immune response against influenza works is of paramount importance for the design of vaccines with higher efficacy (M. A. Rose, Zielen and Baumann 2012; G. L. Chen and K. Subbarao 2009; Olive TW Li and Poon 2009; Ben-Yedidia and R. Arnon 2007;).

In Chapter 1, it was discussed how human mAbs that exhibit pan-, hetero-, or homo-subtypic neutralization activity, conferred by their ability to bind conserved regions on the HA stalk, have been isolated (Friesen *et al.* 2014; Dreyfus *et al.* 2012; Corti *et al.* 2011; Ekiert *et al.* 2011; Sui *et al.* 2009; Throsby *et al.* 2008; Okuno *et al.* 1993). The discovery of these cross-reactive antibodies has opened up the possibility not only for the use of these as therapeutic agents in antiviral therapy (Clementi *et al.* 2012; N. Mancini *et al.* 2011; Friesen *et al.* 2010; Marasco and Sui 2007), but has also increased interest in understanding how they are generated by natural infection and vaccination, in addition to stimulating production of such neutralizing antibodies using novel 'universal' vaccine approaches (G. L. Chen and K. Subbarao 2009; T. T. Wang and Palese 2009).

In Section 1.7, present and future influenza vaccines were already discussed. Inactivated and attenuated influenza vaccines are in general unable to induce strong cross-reactive protective immune responses. In contrast, 'universal' vaccines should be able to induce a protective immune response against multiple influenza A subtypes and strains. There are different approaches to reach this target: broaden the immune response induced by traditional vaccines using adjuvants, aim to induce antibodies against conserved regions of HA, induce responses against the conserved membrane external domain of the M2 protein or the NA, and induce T-cell (cytotoxic and helper) responses (Babon *et al.* 2012; Sommerfelt 2011; Song *et al.* 2011; Steel *et al.* 2010; Ulmer *et al.* 1998). However, since the various parts of the immune system are strictly interconnected, vaccination strategies have also aimed to elicit responses at T-cell level and at B-cell/antibody level simultaneously. One of the strategies used for this purpose is the use of vectors as delivery

systems. This permits the expression of influenza proteins and subsequent activation of a T-cell response and in certain cases also of the B-cell response. For example, MVA, which is a highly attenuated pox vector, permits the infection of host cells, the transient expression of viral (envelope or internal) proteins of interest, and the presentation of viral peptides on MHC of both classes inducing T- and B- cell responses. Furthermore, through intrinsic adjuvant and immunostimulating activities, it recalls on site components of the innate immune system and stimulates the production of interferons, inflammatory cytokines and chemokines. This results in a local inflammatory environment that helps the onset of a robust immune response.

The development and evaluation of these 'universal' vaccines is however problematic. For example, some protein regions are often poorly immunogenic or exposed and need to be correctly presented to trigger an efficient immune response; the vaccine needs to induce a long lasting immunity; clinical trials are essential since it is not possible to evaluate the role of pre-existing immunity in animal models (Krammer and Palese 2014). For antibody-inducing vaccines it is necessary to evaluate if the antibodies elicited are able to bind and neutralize different influenza viruses and potential pandemic strains, and especially for the latter, strict biosafety containment is necessary. Subsequently, especially for a vaccine whose aim is to elicit HA stalk-directed antibodies, other problems exist: firstly it is necessary to precisely evaluate whether antibodies that can bind to different influenza viruses are already present in the human population and, if present, determine at what level. Subsequentially it is necessary to assess whether these new vaccines will be able to induce or boost a heterosubtypic, preferentially stalk-directed, neutralizing antibody-mediated response.

As discussed in Chapter 1, classical serological assays, such as SRH, HI and MN assays, have unfortunately demonstrated low sensitivity for the detection of cross-neutralizing antibodies, especially those directed against epitopes in the HA stalk region (Corti *et al.* 2011; Ekiert *et al.* 2011; Ekiert *et al.* 2009; Sui *et al.* 2009; Okuno *et al.* 1993). The use of binding assays (e.g. ELISA, immunofluorescence, Western blotting, microarray) permits the detection of HA specific antibodies present in sera and other samples (e.g. nasal wash, throat wash) (Reber and Katz 2013) but they cannot differentiate whether these antibodies can neutralize influenza virus infection, since they evaluate binding ability only, and not antibody function (Plotkin 2008).

Many studies and the results reported in Chapter 4 have shown that the pp-NT is more prone to detect cross-reactive antibody responses than the classic neutralization assay. Furthermore the use of pp exhibiting on their envelope a chimeric HA (Section

1.8.8.4) permits a more direct evaluation of stalk-directed antibody presence in serum samples.

From this perspective, the panel of HA pp lentiviral vectors generated in Chapter 3 was next used to understand the presence and the breadth of heterosubtypic immunity in humans, and to evaluate/investigate how seasonal vaccination or new influenza experimental vaccines can affect these responses. Furthermore, to be able to demonstrate that the heterosubtypic responses detected are mediated by stalk-specific HA antibodies, a chimeric HA pp was generated and used in neutralization assays.

5.2 Materials and Methods

5.2.1 Production of a chimeric haemagglutinin pseudotype

Head and stalk regions of the chimeric pp studied were chosen on the basis of the high pp titre of the two parental HA pp (Chapter 3), the phylogenetic relationships between the two HAs, the epidemiological importance of the original virus strain and the cross-reactivity map reported in Chapter 4, in order to minimise responses directed against the HA head. Consequently, it was decided to produce a chimeric HA with the head of A/duck/Memphis/546/1974 H11 and the A/South Carolina/1/1918 H1 stalk: H11 was chosen primarily for its low cross-reactivity, whereas A/South Carolina/1/1918 H1 stalk was considered of interest since the virus is representative of the 1918 influenza pandemic and has antigenic characteristics similar to the 2009 pandemic strain (Wei *et al.* 2010).

5.2.1.1 Cloning of a H11 head/H1 stalk chimeric haemagglutinin

The original protocol (Hai *et al.* 2012; Pica *et al.* 2012) for generating chimeric HAs requires the amplification of the regions of interest using primers containing *SapI* sites and then cloning into pDZ plasmid (a pCAGGS derivative plasmid), however it was decided to not follow this protocol since it requires multi-segment ligation and was considered more error-prone in the primer design. Instead, Gibson Assembly Cloning (New England Biolabs, cat.no. E5510) was used for assembling the chimeric HA. The Gibson methodology permits the fast assembly of multiple overlapping DNA fragments through a reaction in which three different enzymes are used at the same time: an exonuclease to create 3' overhangs, a polymerase to fill gaps, and DNA ligase to close the nicks in the assembled DNA (Gibson *et al.* 2009).

The schematic representation of the chimeric HA cloning strategy utilising Gibson Assembly is shown in **Figure 46**: the head region of the H11 HA is PCR amplified and flanking sequences complementary to A/South Carolina/1/1918 H1 stalk are inserted, while the stalk sequence A/South Carolina/1/1918 H1 in the backbone vector is also

amplified. Then the two PCR products are added to the Gibson Assembly reaction and a chimeric HA is generated.

To create a chimeric HA the two cysteines Cys52 and Cys277 that separate the head and the stalk, need to be identified. For this purpose an alignment with the two amino acid sequences of interest, A/South Carolina/1/1918 H1 (Accession Number: AAD17229.1) and A/duck/Memphis/546/1974 H11 (Accession Number: BAF47125.1) was conducted using the MUSCLE algorithm (Edgar 2004) in Jalview (Waterhouse et al. 2009) (**Appendix Figure 13**). DNA Dynamo (Blue Tractor Software Ltd) and plasmid DNA sequences were then used to identify the nucleotide sequence corresponding to the three regions of interest: N-terminal and C-terminal stalk region of A/South Carolina/1/1918 H1, and head region of H11. With this identification completed, the hypothetical chimeric HA sequence was assembled and primers, reported in **Table 21**, were designed using the NEBuilder® online tool (New England Biolabs).

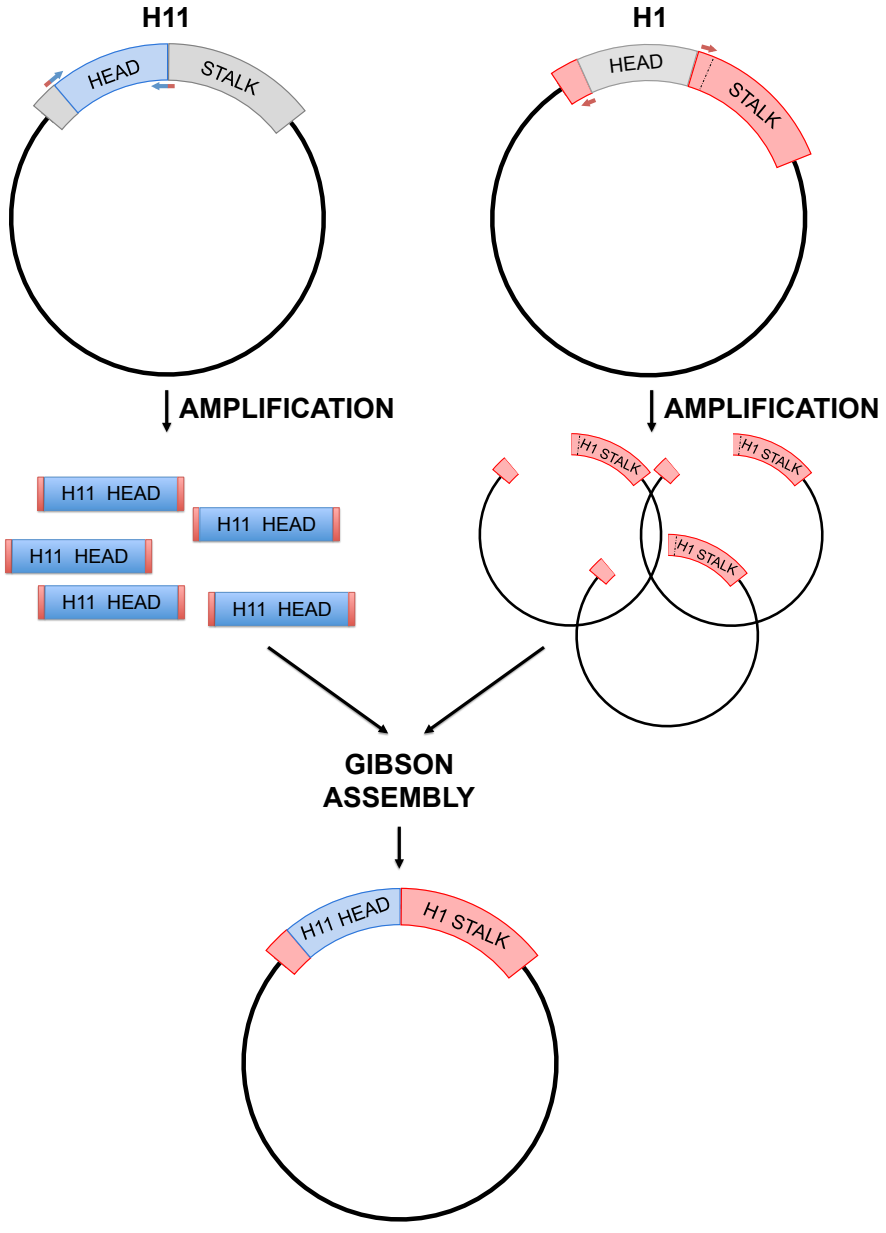

Figure 46: Schematic representation of chimeric HA cloning using Gibson Assembly

Table 21: Primer sequences and annealing temperatures for cloning of the H11 head/H1 stalk chimeric HA
Sequences annealing with H1 stalk are shown in red, the ones annealling with H11 head in blue. Annealing temperatures were calculated by NEBuilder.

Primer name	Primer sequence (5' to 3')	Annealing Temperature
H1_stalk_Rev	GCACAGCTTTCCATTATG	58.9°C
H1_stalk_Fw	AACACCAAGTGTCAGACAC	58.9°C
H11_head_Fw	ATAATGGAAAGCTGTGCAGCATCGACGGAAAAGCAC	63.6°C
H11_head_Rev	GTCTGACACTTGGTGTTGCAAGACTCGATATTCAGGTC	63.6°C

NEBuilder® designs primers that are suitable for amplification using the Q5® High-Fidelity DNA Polymerase and for this reason 25 µl PCR reactions were set-up as follows: dNTPs at a final concentration of 200 µM, 0.5 µM of each primers, 1X Q5® Reaction Buffer, 0.005 U of Q5® High-Fidelity DNA Polymerase, and 1 ng of plasmid DNA (phCMV1-A/South Carolina/1/1918 H1 or phCMV1-A/duck/Memphis/546/1974 H11) used as template. For the amplification of the A/South Carolina/1/1918 H1 stalk domain in the backbone phCMV1 vector, 5 µl of Q5® High GC Enhancer was also added to the reaction mix. PCRs were run in Mastercycler ep Gradient S and in the Mastercycler ep Gradient thermal cyclers using the programs reported in **Table 22** and **Table 23**.

Table 22: PCR program for the amplification of the H1 stalk-encoding sequence in the phCMV1 vector

Cycles	Temperature	Time	Step
	98°C	3 min	Initial denaturation
30 cycles	98°C	30 seconds	Denaturation
	58.9°C	30 seconds	Annealing
	72°C	6 min	Extension
	72°C	8 min	Final extension
	4°C	To conserve the reactions until removed from the thermocycler	

Table 23: PCR program for the amplification of the H11 head-encoding sequence

Cycles	Temperature	Time	Step
	98°C	3 min	Initial denaturation
30 cycles	98°C	15 seconds	Denaturation
	63.6°C	30 seconds	Annealing
	72°C	1 min	Extension
	72°C	2 min	Final extension
	4°C	To conserve the reactions until removed from the thermocycler	

Amplification of the H1 stalk in the phCMV1 backbone (~5.3 kb) and of the H11 head (~640 bp) were verified by DNA electrophoresis using a 0.8% agarose gel (Section 2.1.12). PCR products were purified using the QIAquick PCR purification kit (Section 2.1.13), measured by NanoDrop™, and then ~500 ng DNA digested in a total volume of 20 µl using 10 U of FastDigest® DpnI in 1X FastDigest® buffer and DNase/RNase free water. This digestion was performed to destroy the parental DNA and thus increase Gibson Assembly efficiency. After digestion, purification to remove buffer salts and enzyme was carried out, then samples were measured by NanoDrop™ and, to join the two overlapping fragments, a 20 µl Gibson Assembly reaction was set up in DNase/RNase free water using 10 µl of 2X Gibson Assembly mix, 80 ng of the stalk fragment, and 29 ng of the head fragment to produce a vector (phCMV1 H1 South Carolina stalk) to insert (H11 head) ratio of 1:3. After 15 min at 50°C in the Mastercycler ep Gradient S thermocycler, 2 µl of assembled product was added to 50 µl NEB 5-α competent *E. coli* (New England Biolabs, cat.no. C2987) for transformation according to the protocol presented in Section 2.1.3, adjusting the heat-shock incubation times according to the New England Biolabs instructions: 30 min in ice, 30 seconds at 42°C, and 2 min in ice again; then 950 µl of SOC medium was added and bacterial cells were incubated for recovery before plating 100 µl on a kanamycin-LB Agar plate.

After overnight incubation at 37°C, 20 of the colonies present on the plates were screened using T7 and phCMV1 Rev primers in colony PCRs (Section 2.1.11) to assess the presence of a 1.7 kb band corresponding to the assembled chimeric HA. After PCR amplification and purification of plasmid DNA, some of the positive clones were then additionally screened *via* restriction enzyme digestion (Section 2.1.9) with FastDigest® *HindIII*: this enzyme linearises the phCMV1 vector and the template plasmid phCMV1-A/South Carolina/1/1918 H1, but cleaves phCMV1-A/duck/Memphis/546/1974

H11, and the phCMV1-H11 head/H1 stalk creating two fragments of 400 bp and 5.6 Kb. Lastly, two clones were sent for Sanger sequencing to confirm the phCMV1-H11 head/H1 stalk.

After the amino acid sequence of the HA construct was confirmed through alignment using MUSCLE algorithm (Edgar 2004) in Jalview (Waterhouse *et al.* 2009), the chimeric HA was used for pp production.

5.2.1.2 Optimisation of the production of a H11 head/H1 stalk haemagglutinin pseudotype

Before producing the chimeric pp, optimisation experiments in 6-well plates (Section 3.2.4) were performed to determine quantity and quality of the proteases that need to be used in pp production. These experiments were executed as described in Chapter 3 testing two different quantities (250 ng and 125 ng) of HAT, TMPRSS2 and TMPRSS4 protease-expressing plasmids in transfection mixes. Protease controls (Δprotease and TPCK-trypsin activation) were also included.

5.2.2 Sera and antibodies

Sera from 18-60 year old people (n=13) and from elderly >60 (n=9), collected before and after the 2007-2008 seasonal vaccination with A/Wisconsin/67/2005 (H3N2), A/Solomon Island/3/2006 (H1N1) and B/Malaysia/2506/2004, were a kind gift form Prof. Emanuele Montomoli (University of Siena, Italy). The samples were previously decomplemented at 56°C for 30 min. For these sera, Prof. Emanuele Montomoli provided serological results from SRH using as antigens A/Wisconsin/67/2005 (H3N2), A/Solomon Island/3/2006 (H1N1) and A/New Caledonia/20/1999 (H1N1).

Another set of sera was evaluated against representative influenza pp strains. Human sera from clinical trial NCT00942071 (Antrobus *et al.* 2013) were kindly provided by Prof. Sarah Gilbert (Jenner Institute, University of Oxford, UK). These sera were collected from adults aged 50 years and over pre- and post- administration of an Influenza split virion vaccine (Sanofi Pasteur MSD, France) containing HAs of A/California/7/2009 (H1N1), A/Perth/16/2009 (H3N2), and B/Brisbane/60/2008. Nine subjects also received an injection of MVA vectors expressing the A/Panama/2007/1999 (H3N2) NP and M1 antigens as a single fusion protein (Antrobus *et al.* 2013; Berthoud *et al.* 2011) (MVA-NP+M1), meanwhile the other remaining subjects (n=8) received a saline placebo (Antrobus *et al.* 2013). These sera were not subjected to any pre-treatment

C179 mAb (TaKaRa Clonthec, cat.no. M145) was used as neutralization control at a starting concentration of 10 μg/ml in H1 and H2 pp-NT assays and as an additional control in pp-NT assay performed using the chimeric HA pp.

Reference sheep serum against A/England/427/1988 (H3N2) was provided by the NIBSC and used as positive control in H3 pp-NT.

The OIE avian reference hyperimmune sera and the reference avian serum against A/chicken/Wales/1306/2007 (H7N2) (APHA, UK), which were described in Section 4.2.2, were used as appropriate positive neutralization controls in the pp-NT assays. The anti-H11 serum was also used as positive control in the chimeric HA pp-NT assay.

5.2.3 Haemagglutinin-expressing plasmids and pseudotype production

The pp A/Vietnam/1194/2004 H5, A/turkey/Turkey/1/2005 H5, and A/Netherlands/219/2003 H7 used for screening the 2007-2008 seasonal vaccination sera were generated by Dr. Nigel Temperton and Dr. Eleonora Molesti (Universities of Greenwich and Kent, Medway, UK) using a protocol equivalent to the one described in Section 2.3.2.1.

For the other pp presented here and used in neutralization assays, the HA-expressing plasmids were provided, obtained or cloned to produce pp as described in Chapters 2-4.

Lentiviral pp were produced as described in Section 2.3.2.2, adding to the transfection mixes an appropriate quantity of protease-expressing plasmid based on the data shown in **Appendix Table 1**, the result of optimisation experiments performed in Chapter 3. For the chimeric pp, produced with the HA-encoding plasmid, the quantity and quality of proteases to be used were chosen after optimisation.

As in Chapter 3, the pI.18-A/Udorn/307/1972 N2 plasmid was added to the transfection mix used to produce the A/Wisconsin/67/2005 H3pp.

5.2.4 Pseudotype particle neutralization assays

The 2007-2008 seasonal vaccination serum panel was tested in neutralization assays using the following pp: A/Solomon Islands/3/2006 H1, A/New Caledonia/1/1918 H1, A/South Carolina/1/1918 H1, A/Korea/426/1968 H2, A/Wisconsin/67/2005 H3 (with A/Udorn/307/1972 N2), A/Udorn/307/1972 H3, A/duck/Czechoslovakia/1956 H4, A/Vietnam/1194/2004 H5, A/turkey/Turkey/1/2005 H5, A/Shanghai/2/2013 H7, A/chicken/Italy/1082/1999 H7, A/Netherlands/219/2003 H7, A/Hong Kong/1073/1999 H9, A/chicken/Germany/N/49 H10, A/duck/Memphis/546/1974 H11, A/duck/Alberta/60/1976 H12, A/mallard/Astrakhan/263/1982 H14, A/shearwater/West Australia/2576/1979 H15, and the chimeric H11 head/H1 stalk HA pp.

For 2007-2008 seasonal vaccination sera, the pp-NT neutralization assay using as antigens A/Vietnam/1194/2004 H5, A/turkey/Turkey/1/2005 H5, and A/Netherlands/219/2003 H7pp were kindly performed by Dr. Eleonora Molesti. The raw data were re-analysed here and reported in the **Appendix Figure 15** and **Appendix Figure 16** and should be taken into consideration when interpreting the results presented in this chapter.

Pp-NT were performed as described in Section 2.3.4 using a fixed pp input of 1×10^6 RLU/well and 2.5 µl of sera in the first dilution well (starting dilution 1:80).

The aforementioned pp, with the exception of A/Solomon Islands/3/2006 H1, A/Netherlands/219/2003 H7, and A/duck/Alberta/60/1976 H12, were also used to test the neutralization activity of the clinical trial sera panel: in this case the starting dilution was 1:100 (2 µl of sera), since the samples provided were of limited volume.

Analysis was performed as described in Section 2.3.4. When the IC_{50} value could not be calculated, since all the dilution points tested showed 100% neutralization, an arbitrary value corresponding to the distribution mean plus three standard deviations was assigned.

5.2.5 Statistical analysis

To evaluate the correlation of the pp-NT assay with a classical serological assay, SRH assay, Pearson correlation between the SRH titres and the logarithm IC_{50} values was calculated.

IC_{50} values (expressed as reciprocal of serial dilution) obtained from pp-NT assays were also reported in Box-and-Whisker plots for comparison; in the **Appendix Table 2-5**, quartiles and medians of the IC_{50} distributions were also reported. A non-parametric Wilcoxon matched-pairs signed rank test to assess statistical significance between pre- and post- vaccination time-points in the 2007-2008 vaccination study and day 0 and day 21 in the clinical trial was applied considering that the data were not following Gaussian distributions.

Data obtained from the 2007-2008 vaccination study were subsequently stratified into two groups, adults and elderly, considering the age of the subject, to highlight if differences in seroconversion and titres were present between these two groups.

Clinical trial data were stratified on the basis of the vaccine regimen: TIV + placebo or TIV + MVA-NP+M1, to evaluate the effect of the MVA-NP+M1 in broadening the heterosubtypic antibody response.

At this point, if the data were normally distributed, a mixed Analysis of Variance (ANOVA) should have been used for further analysis; unfortunately the data did

not follow a parametric distribution, and a non-parametric version of this test does not exist. Consequently for the first dataset, resulting from the 2007-2008 vaccination study, Wilcoxon matched-pairs signed rank test and Mann-Whitney U test were performed. Then, to counteract the problem of multiple comparisons, p values were corrected using the Bonferroni correction (significance $p \leq 0.0125$[7]).

For the second dataset, since the stratification was applied to understand the MVA-NP+M1 vaccination effect and to avoid multiple comparisons, it was decided to compare the result graphically to see if it was possible to identify differences and then perform statistical analysis comparing the IC_{50} fold-increase between TIV + placebo and the TIV + MVA-NP+M1groups using a Mann-Whitney U test. The graphs showing the IC_{50} fold-increase are reported in **Appendix Figure 17**.

Seroconversion rates (SCRs) were also calculated as a percentage or fraction of subjects showing a 4-fold increase ($SCR_{(4\text{-fold})}$) or a 2-fold increase ($SCR_{(2\text{-fold})}$) in the IC_{50} titre post-vaccination or at day 21. For the 2007-2008 vaccination study, to see if age is a factor in determining the responses, SCRs of each age-group expressed as fractions were added together and then compared using a contingency table and the chi-squared test. The same procedure was performed for the clinical trial study, this time to identify whether differences were present between TIV + placebo and TIV + MVA-NP+M1.

All the analyses were performed using GraphPad Prism® version 6 and Microsoft® Excel 2011.

5.3 Results

5.3.1 Cloning of a H11 head/H1 stalk chimeric haemagglutinin

A chimeric HA comprising the head region of A/duck/Memphis/546/1974 H11 and the stalk region of A/South Carolina/1/1918 H1 was successfully cloned using Gibson Assembly. Firstly the two regions of interest, the H11 head and the H1 stalk, were successfully amplified using the Q5® High-Fidelity DNA Polymerase as shown in **Figure 47**.

[7] In the Bonferroni correction, the p value significance cut-off is calculated dividing the p value 0.05 for the number of comparisons performed, in this case four.

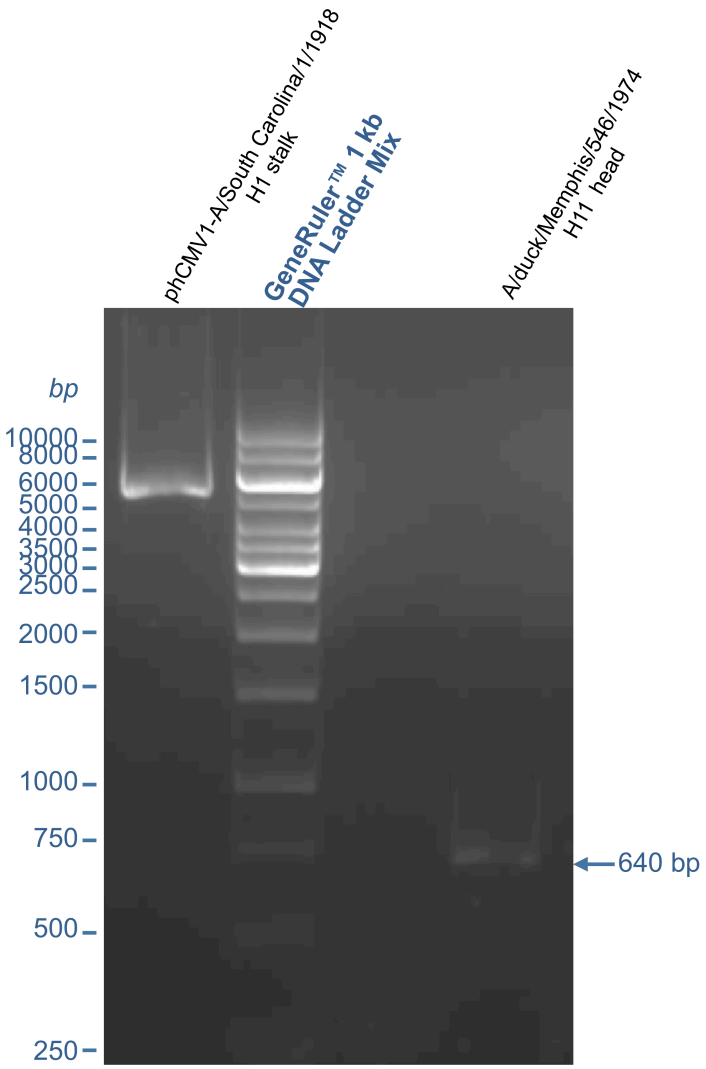

Figure 47: Amplification of the H1 stalk in the phCMV1 backbone (~5.3 kb) and of the H11 head (~640 bp)

Subsequently, after PCR purification, *DpnI* digestion was conducted to remove the bacterial methylated plasmid template, then further purification to remove the restriction enzyme, and finally the Gibson Assembly reaction was set-up. Following transformation of *E. coli* and overnight incubation, numerous colonies were present on the selection plate. Twenty of these colonies (#1-#20) were screened through colony PCRs. As shown in **Figure 48**, 18 colonies were positive for a band at ~1.7 kb corresponding to a full length HA. Of these colonies, 6 were grown overnight, and the plasmid DNA purified for further analysis.

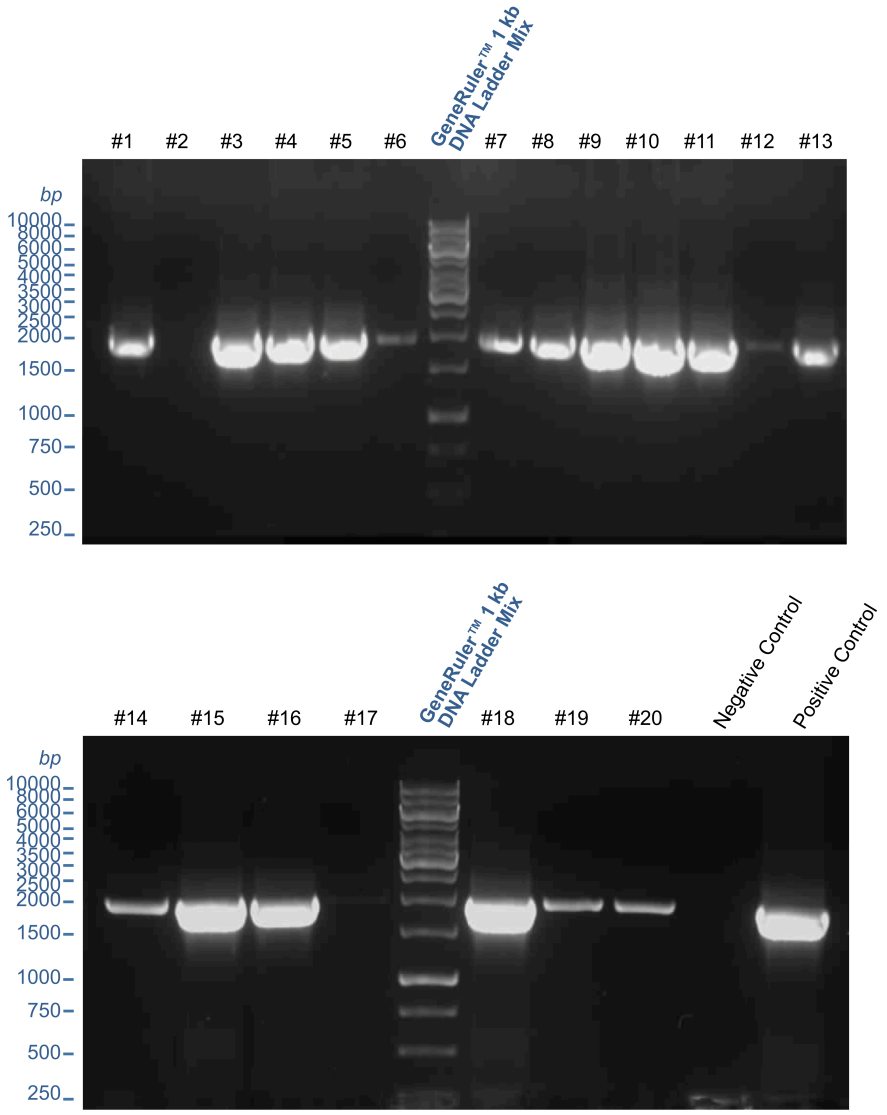

Figure 48: Colony PCR screening after Gibson Assembly of the chimeric HA
Twenty colonies (#1-#20) were screened by colony PCR; phCMV1 and phCMV1-A/duck/Memphis/546/1974 H11 were used as negative and positive controls.

The six plasmid clones were analysed by digestion with HindIII followed by analytical DNA gel electrophoresis. *HindIII* cleaves phCMV1, the vector backbone, and H11 head in the middle. In this way if the plasmid encodes the chimeric HA or H11 two bands at 400 bp and at 5.6 Kb will be visible, if it encodes for the H1 a band at 6 Kb will be observed, and if phCMV1 is empty a band at 4.3 kb will be visualised (**Figure 49A**).

As shown in **Figure 49B**, all the clones showed a band at 400 bp and a band at 5.6 kb, confirming the presence of the H11 head in a plasmid encoding an HA. However, it cannot be concluded that all six clones carried a chimeric HA as the use of the *HindIII* restriction enzyme permitted only the discrimination between H1 and the H11 head/H1 stalk HA, but not between H11 and the chimeric HA. To differentiate between these two (since satisfactory restriction enzyme analysis was unavailable), clones #3 and #5 were sent for Sanger sequencing and, after checking the electropherogram, these two clones

were confirmed chimeric HA. However, since clone #3 contained a mutation (probably introduced during amplification of the H1 stalk), it was decided to produce pp with clone #5.

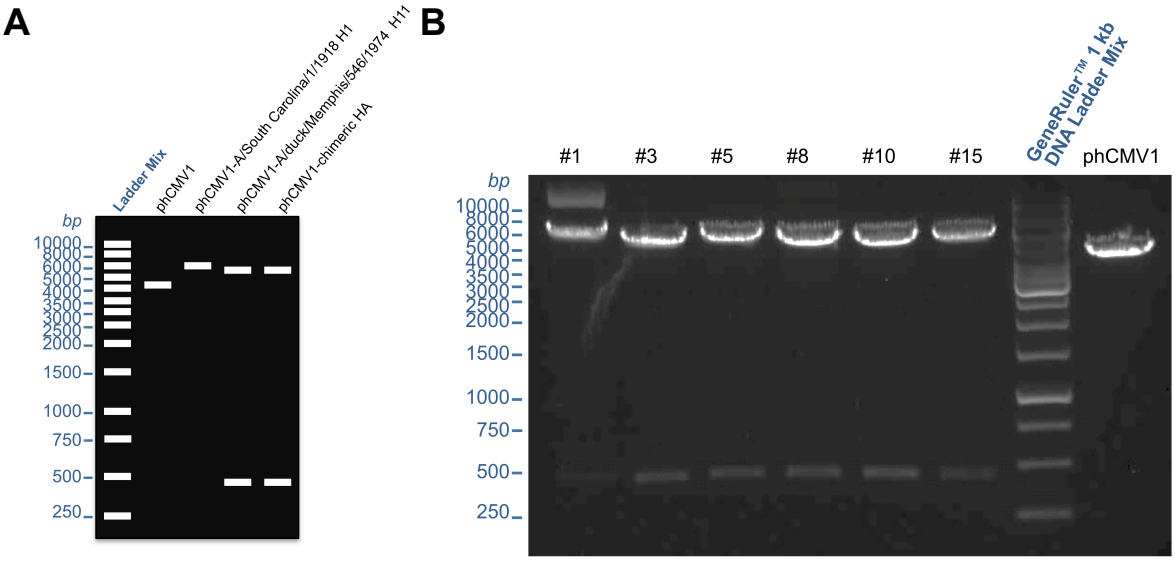

Figure 49: Digestion screening of chimeric HA-encoding plasmids
A. Schematic representation of potential results of the screening with HindIII restriction enzyme; **B.** Screening of six possible chimeric HA-encoding plasmids with phCMV1 control.

The above results show that Gibson Assembly is a rapid and efficient method to construct chimeric HA, however sequences need to be verified carefully since mutations can be introduced during PCR amplification steps.

5.3.2 Production of the H11 head/H1 stalk chimeric haemagglutinin pseudotype

With the chimeric HA sequence confirmed (**Appendix Figure 14**), production of the chimeric HA pp was investigated. As shown in Chapter 3, to produce influenza A pp it is necessary to define the quantity and quality of the proteases that mediate HA cleavage and, even for closely related HAs, protease-cleavage specificity cannot yet be predicted. Therefore the 6-well transfection protocol (Section 3.2.4) was applied to identify the appropriate production conditions.

TPCK-Trypsin is not efficient in activating and cleaving the chimeric HA, but the protease-optimisation showed (**Figure 50**) that the chimeric HA was activated by HAT and TMPRSS4, especially when low quantities (i.e. 125 ng) of plasmids were used. However, only when 125 ng of pCAGGS-HAT were added to the transfection mix was the pp titre adequate ($\geq 2\times10^7$ RLU/ml) to perform neutralization assays. Since the pp-production optimisation is performed in a 6-well format, the protease plasmid quantity found here would have to be doubled (i.e. 250 ng) when producing pp for neutralization assay in a 10 cm plate transfection format (Chapter 2).

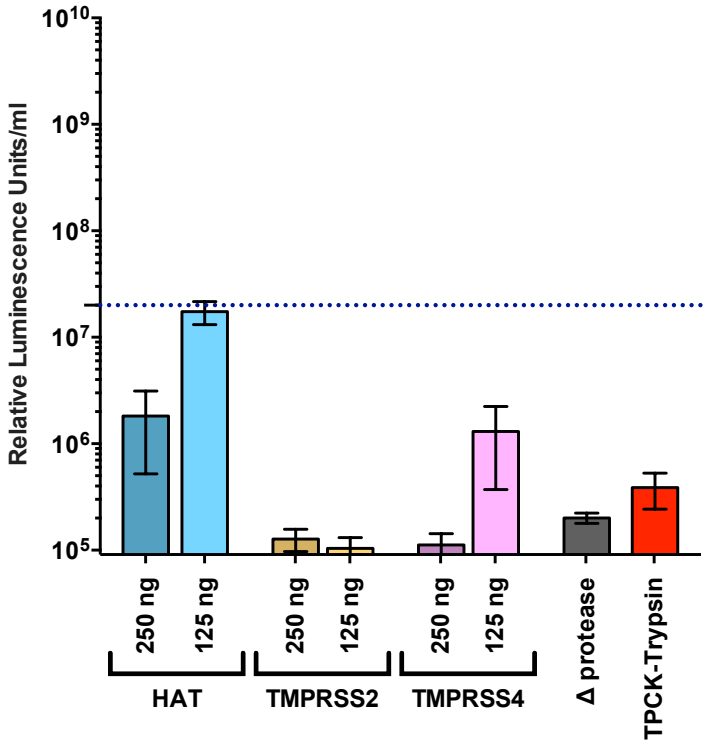

Figure 50: Production optimisation of the chimeric HA pp
Titres are reported in RLU/ml with SEM (n=8 titre measurements). A line corresponding to 2×10^7 RLU/ml is drawn to indicate the minimum titre necessary to effectively perform neutralization assays.

5.3.3 Pseudotype particle neutralization assay correlates with Single Radial Haemolysis assay

Before analysing the heterosubtypic antibody response in the 2007-2008 vaccinated subjects, the suitability of the pp-NT assays was evaluated through comparison with the SRH assay. A/Solomon Island/3/2006 (H1N1), A/Wisconsin/67/2005 (H3N2), A/New Caledonia/20/1999 (H1N1) SRH titres and the logarithm IC_{50} values obtained by pp-NT assay were graphed in a Scatter plot (**Figure 51**) and the Pearson coefficient for correlation was calculated.

In general, antibody responses detected by pp-NT assay were higher than the ones detected by SRH, with discordance between the two assays when SRH titres were <10 mm^2. Statistical analysis shows that the pp-NT assay correlates with SRH when the H1 and H3 antigens are used (A/Solomon Island/3/2006 H1: $r = 0.5110$, A/Wisconsin/67/2005 H3: $r = 0.6048$, A/New Caledonia/20/1999 H1: $r = 0.0.6875$) and all the correlations were statistically significant (A/Solomon Island/3/2006 H1: $p = 0.0004$, A/Wisconsin/67/2005 H3 and A/New Caledonia/20/1999 H1: $p < 0.0001$).

These results demonstrate that pp-NT assays are suitable for vaccine immunogenicity evaluation studies.

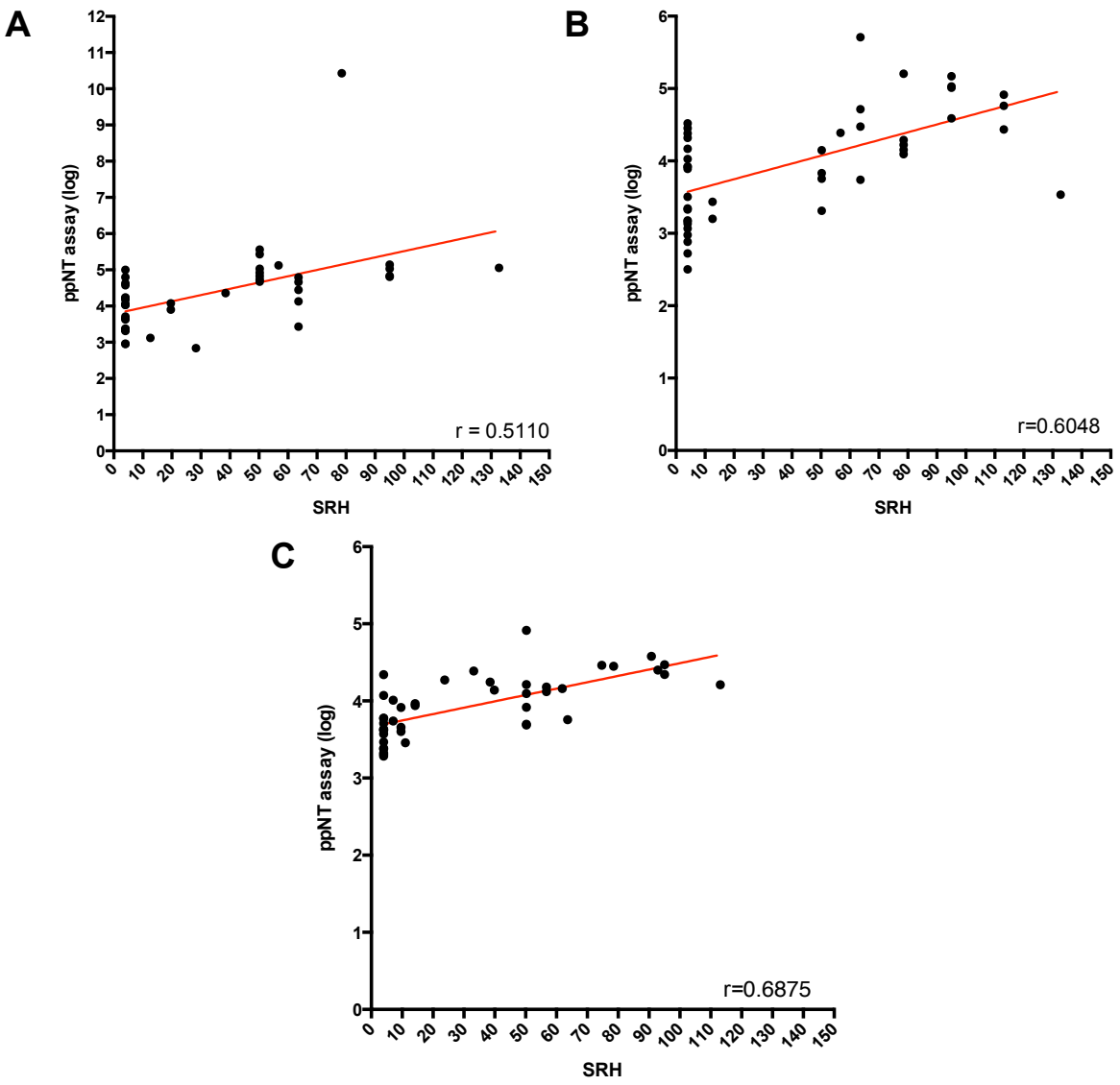

Figure 51: Correlation of SRH and pp-NT
Correlation was performed using three different antigens including the two vaccine strains: **A.** A/Solomon Islands/3/2006 (H1N1); **B.** A/Wisconsin/67/2005 (H3N2); **C.** A/New Caledonia/20/1999 (H1N1).

5.3.4 Heterosubtypic haemagglutinin stalk-directed antibody responses are present pre- and post- 2007-2008 seasonal vaccination in an Italian population

After evaluating the correlation between pp-NT assay and SRH assay, different pp were used as surrogate antigens in neutralization assays to study if heterosubtypic neutralizing antibody responses were present in the 2007-2008 vaccination sera. For each pp tested, the IC_{50} distributions were depicted in Box-and-Whisker plots. The Box-and-Whisker plot is a suitable graphical representation for a population distribution, especially if non-parametric, because it depicts the median, the first and third quartiles as a plot, the variability outside the interquartile range as whiskers, and the outliers as single dots. Consequently, it allows a graphical comparison, which enriches the statistical analysis.

The overall results, obtained when each pp was tested, were stratified based on the collection date: pre- and post-vaccination (**Figures 52-56 (A and B), Figures 57 and 59**). Subsequently, the sub-populations of adults (18-60 years old) and elderly (> 60 years old) were analysed (**Figures 52-56 (A and D)**, **Figures 58 and 60**).

Firstly the two vaccine strains, A/Solomon Island/3/2006 (H1N1) and A/Wisconsin/67/2005 (H3N2), were considered. For A/Solomon Island/3/2006 H1 high responses were detected pre-vaccination, which increased following vaccine administration (**Figure 52A**). This increase was statistically significant ($p < 0.0001$) and at least 72.7% of the total population presented a 4-fold increase in the neutralizing titres with a further 9.1% of the population presenting a 2-fold increase (**Table 24**). When the population is stratified by age (**Figure 52C**) it can be noticed that only the differences between pre- and post-vaccination titres in adults ($p = 0.0002$) were significant using the Wilcoxon matched-pairs signed rank test and after applying the Bonferroni correction for multiple comparison: in fact in elderly ($p = 0.0195$) the differences were not significant when the p-value cut-off 0.0125 was applied. When comparing by Mann-Whitney U test the IC_{50} titres in the pre-vaccination adults and elderly groups, the differences observed ($p = 0.0304$) are not significant. Likewise, IC_{50} titres post-vaccination in the two groups are not statistically significant ($p = 0.5949$).

For the other vaccine strain A/Wisconsin/67/2005 H3N2 (**Figure 52B**), a pp bearing a non-cognate NA (A/Udorn/307/1972 N2) in conjunction with the H3 was used for neutralization. Neutralization titres were detected pre-vaccination and were augmented ($p = 0.0029$) by the administration of the seasonal vaccine. When age-stratification (**Figure 52D**) was applied and multiple comparison was implemented, statistical significance was not reached for the comparison of pre- and post-vaccination titres of adults and of elderly groups, nevertheless differences ($p = 0.0273$) between pre- and post-vaccination titres could be present in elderly in the absence of the Bonferroni correction. Also, when comparing neutralization titres at the same time-point between age-groups statistically significant differences were not detected.

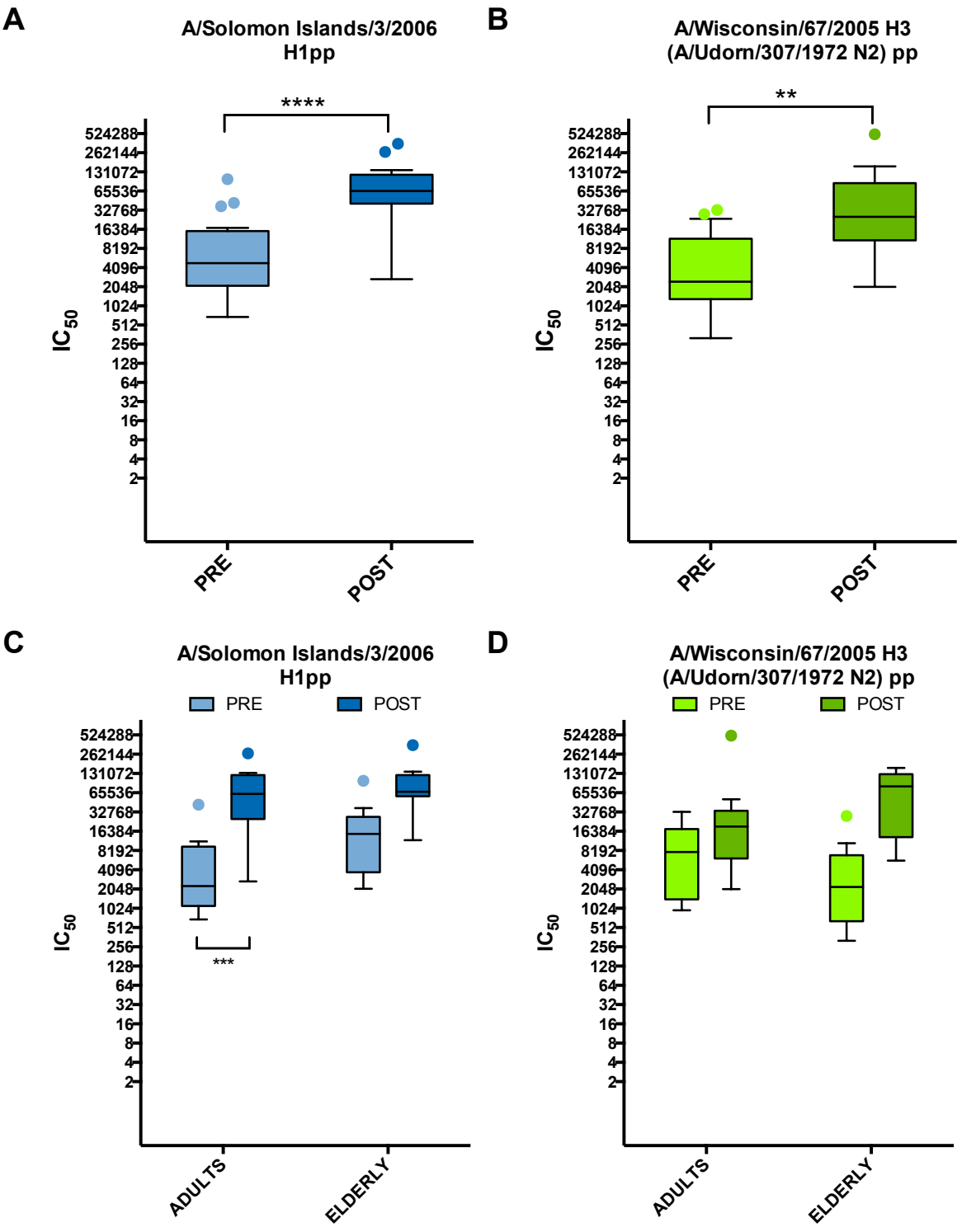

Figure 52: IC_{50} of sera tested with A/Solomon Island/3/2006 H1 and A/Wisconsin/67/2005 H3 (A/Udorn/307/1972 N2) pp-NT assays

Comparison in the overall population and after age-stratification of IC_{50} measured pre- and post-vaccination with A/Wisconsin/67/2005 (H3N2), A/Solomon Island/3/2006 (H1N1) and B/Malaysia/2506/2004. Quartiles and medians of the distributions are reported in Appendix Table 2 and Appendix Table 3. **A.** Results against A/Solomon Island/3/2006 H1pp; **B.** Results against A/Wisconsin/67/2005 H3 (A/Udorn/307/1972 N2) pp; **C.** Results of A/Solomon Island/3/2006 H1 pp-NT after stratification of age groups; **D.** Results of A/Wisconsin/67/2005 H3 A/Udorn/307/1972 N2 pp-NT after stratification of age groups.

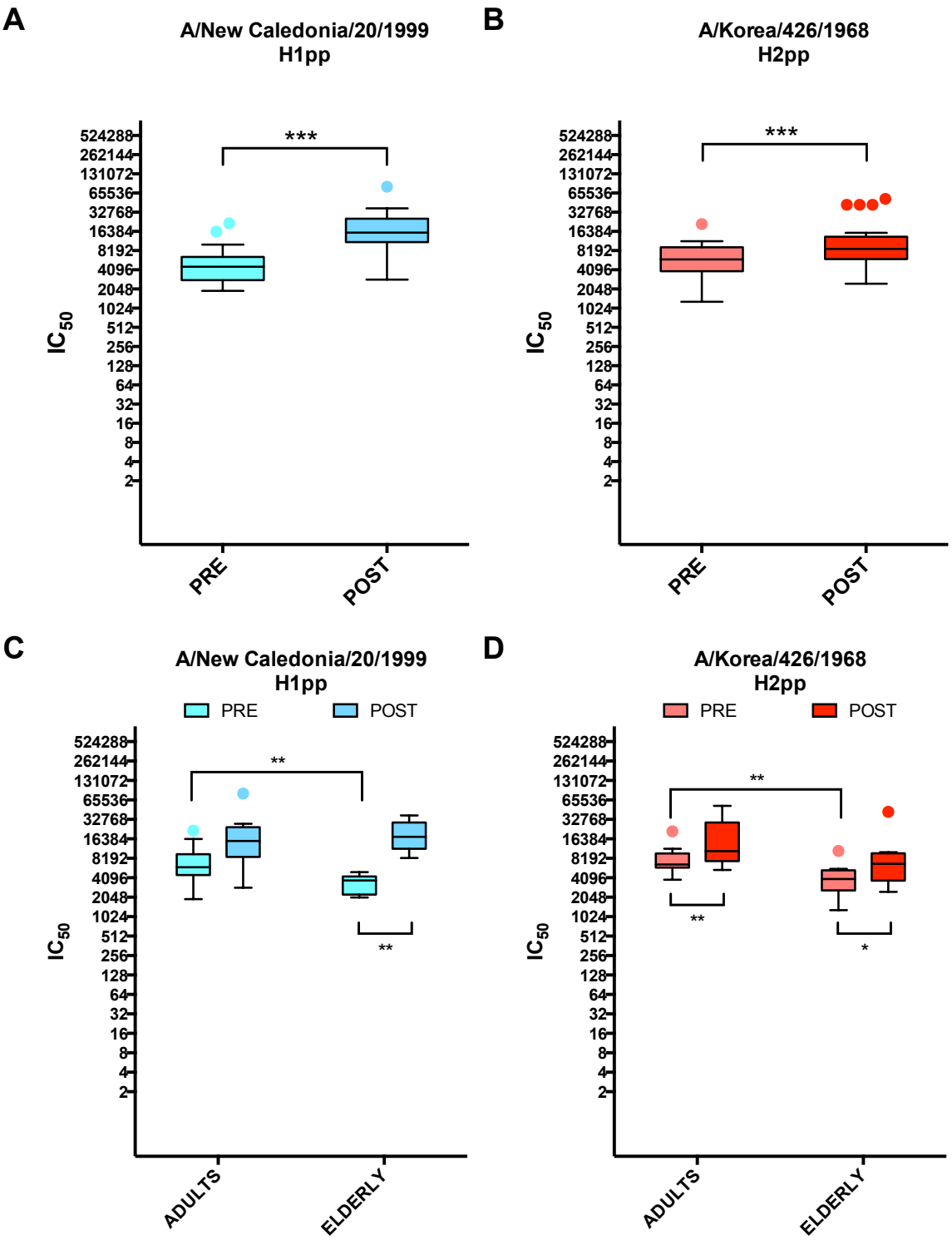

Figure 53: IC_{50} of sera tested with A/New Caledonia/20/1999 H1 and A/Korea/426/1968 H2 pp-NT assays

Comparison in the overall population and after age-stratification of IC_{50} measured pre- and post-vaccination with A/Wisconsin/67/2005 (H3N2), A/Solomon Island/3/2006 (H1N1) and B/Malaysia/2506/2004. Quartiles and medians of the distributions are reported in Appendix Table 2 and Appendix Table 3. **A.** Results against A/New Caledonia/20/1999 H1pp; **B.** Results against A/Korea/426/1968 H2pp; **C.** Results of A/New Caledonia/20/1999 H1 pp-NT after stratification of age groups; **D.** Results of A/Korea/426/1968 H2 pp-NT after stratification of age groups.

After analysis of the two vaccine strains, neutralizing titres were evaluated for the other HAs. When A/New Caledonia/20/1999 H1pp was used in a neutralization assay, statistically significant differences ($p = 0.0001$) were observed post-vaccination, even if high titres were detected pre-vaccination (**Figure 53A**), but this was not surprising because the strain has abundantly circulated before 2007. When the time-point analysis was performed after age-group stratification (**Figure 53C**), statistically significant differences in antibody titres were observed in elderly ($p = 0.0039$), but not in adults ($p = 0.0327$). Furthermore the elderly tend to have lower starting antibody titres than adults ($p = 0.0070$), but this difference disappeared after vaccination.

The results obtained in the H2 (A/Korea/426/1968) pp-NT assay (**Figure 53B**) show that strong neutralizing antibody responses were present in pre-vaccination sera and that they were boosted ($p = 0.0001$) post-vaccination. After data stratification based on age groups and collection date (**Figure 53D**), comparing pre- and post-vaccination data inside the same age-group, increasing IC_{50} titres were observed with statistical significance in adults ($p = 0.0046$) and in elderly ($p = 0.0117$) while, using a Mann-Whitney test to compare both adults and elderly a significant difference was obtained pre-vaccination ($p = 0.0043$) but not post-vaccination ($p = 0.0511$).

For A/Udorn/307/1972 H3, a significant difference ($p = 0.0127$) between pre-vaccination and post-vaccination responses was identified (**Figure 54A**). After data stratification and considering the Bonferroni correction, statistical significance was lost in the adult group ($p = 0.0479$) and in the elderly ($p = 0.2383$). Also using Mann-Whitney U test, no significant differences between age groups were observed (**Figure 54C**).

As shown in **Figure 54B**, pre-vaccination sera neutralized H4pp with an overall increased response ($p < 0.0001$) detected in post-vaccination samples. This difference was significant in adults ($p = 0.0012$) but not in elderly ($p = 0.0547$) (**Figure 54D**). In addition, no differences were observed between age-stratified cohorts.

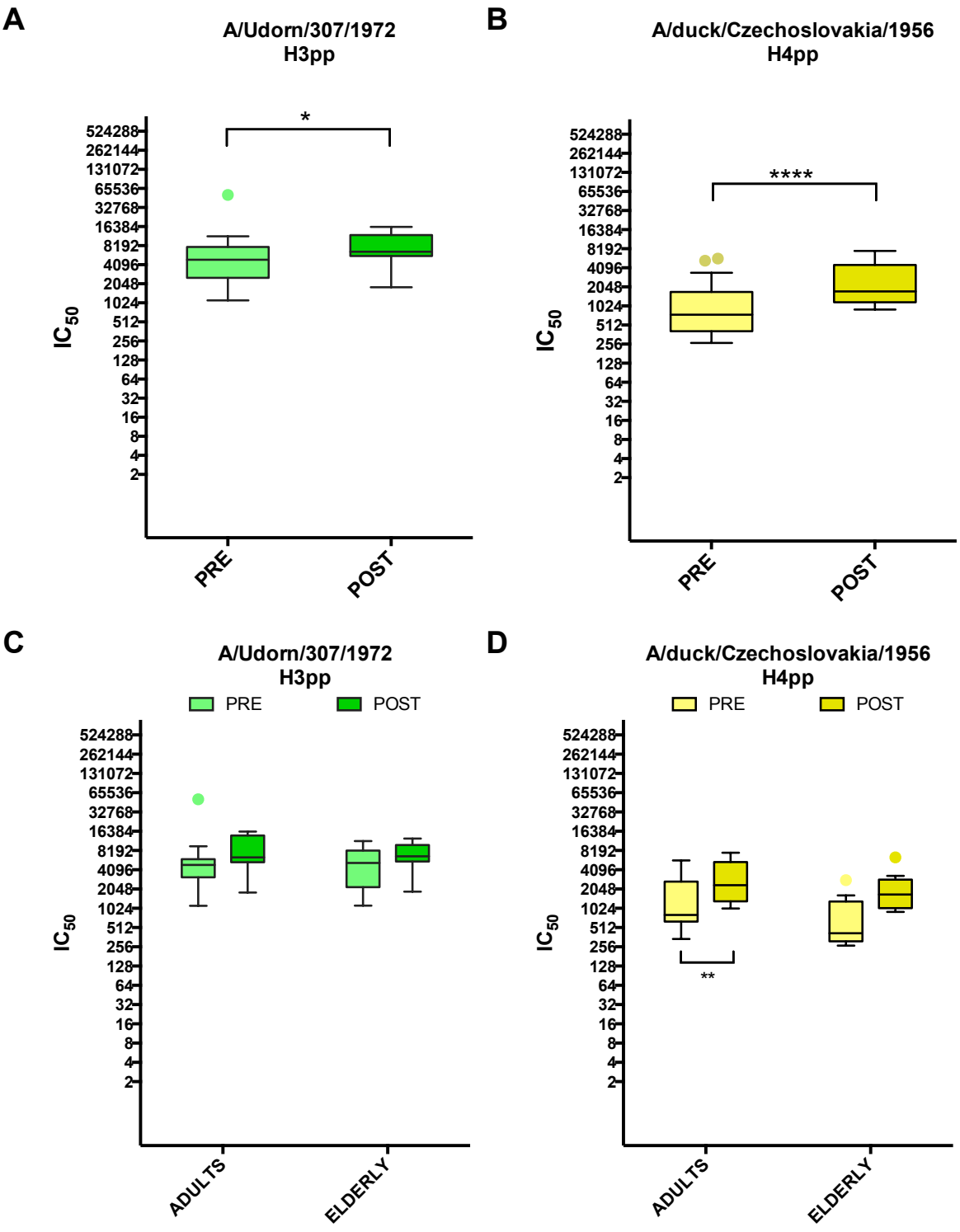

Figure 54: IC_{50} of sera tested with A/Udorn/307/1972 H3 and A/duck/Czechoslovakia/1956 H4 pp-NT assays

Comparison in the overall population and after age-stratification of IC_{50} measured pre- and post-vaccination with A/Wisconsin/67/2005 (H3N2), A/Solomon Island/3/2006 (H1N1) and B/Malaysia/2506/2004. Quartiles and medians of the distributions are reported in Appendix Table 2 and Appendix Table 3. **A.** Results against A/Udorn/307/1972 H3pp; **B.** Results against A/duck/Czechoslovakia/1956 H4pp; **C.** Results of A/Udorn/307/1972 H3 pp-NT after stratification of age groups; **D.** Results of A/duck/Czechoslovakia/1956 H4 pp-NT after stratification of age groups.

Following the re-analysis (**Appendix Figure 15** and **Appendix Figure 16**) of the neutralization assays performed using A/Vietnam/1194/2004 H5, A/turkey/Turkey/1/2005 H5, and A/Netherlands/219/2003 H7pp, it can be noticed that, when the two H5pp were used, neutralizing antibody responses were detected in pre-vaccination sera, but in post-vaccination only the responses against A/turkey/Turkey/1/2005 are boosted ($p < 0.0001$) (**Appendix Figure 15B**). A similar pattern was observed using age-group stratification with A/turkey/Turkey/1/2005 (**Appendix Figure 16B**): adults ($p = 0.0061$) and elderly ($p = 0.0039$) having a statistical significant increase in the neutralizing responses. For H5 A/Vietnam/1194/2004, the comparison between age groups at the same collection time is not statistically significant pre-vaccination $p = 0.0142$ when the Bonferroni correction was applied, but it was statistically significant post-vaccination ($p = 0.0089$) (**Appendix Figure 15A**). On the contrary to A/turkey/Turkey/1/2005, only pre-vaccination ($p = 0.0089$) there were significant differences between adults and elderly (**Appendix Figure 16A**).

When A/Netherlands/219/2003 H7 HPAI pp was used (**Appendix Figure 15C**), a low neutralizing antibody response was detected pre-vaccination and was boosted ($p = 0.002$) by vaccine administration. In age-cohorts (**Appendix Figure 16C**), differences were observed ($p = 0.0017$) only in adults between the two time-points.

The other two H7pp used in neutralization assays carry the HA of LPAI viruses. When A/Shanghai/2/2013 H7 was used (**Figure 55**A), neutralizing titres higher than the ones detected against other H7pp were observed pre-vaccination as well as post-vaccination when they increased ($p = 0.0032$). Furthermore, a post-vaccination increase of antibody titre against A/Shanghai/2/2013 H7pp is observed in adults ($p = 0.0017$) but not in elderly (**Figure 55C**). For A/chicken/Italy/1082/1999 H7 influenza pp (**Figure 55B**) neutralizing antibody responses were detected in pre-vaccination sera and they were raised ($p = 0.0462$) in post-vaccination; however, with age-stratification the significance was lost (**Figure 55D**).

Differences ($p < 0.0001$) between pre-vaccination and post-vaccination sera were observed for H9pp (A/Hong Kong/1073/1999) (**Figure 56A**). Stratified data showed significant variations between pre- and post-vaccination titres (adults: $p = 0.0012$, elderly: $p = 0.0039$) while comparison between the adults and the elderly group showed significance only in pre-vaccination ($p = 0.0026$) (**Figure 56C**).

Against H10pp, a neutralizing antibody response was measured in pre-vaccination sera, but no significant variation ($p = 0.4245$) was detected in post-vaccination sera (**Figure 56B**). Also the subsequent age stratification showed the same statistical pattern (**Figure 56D**).

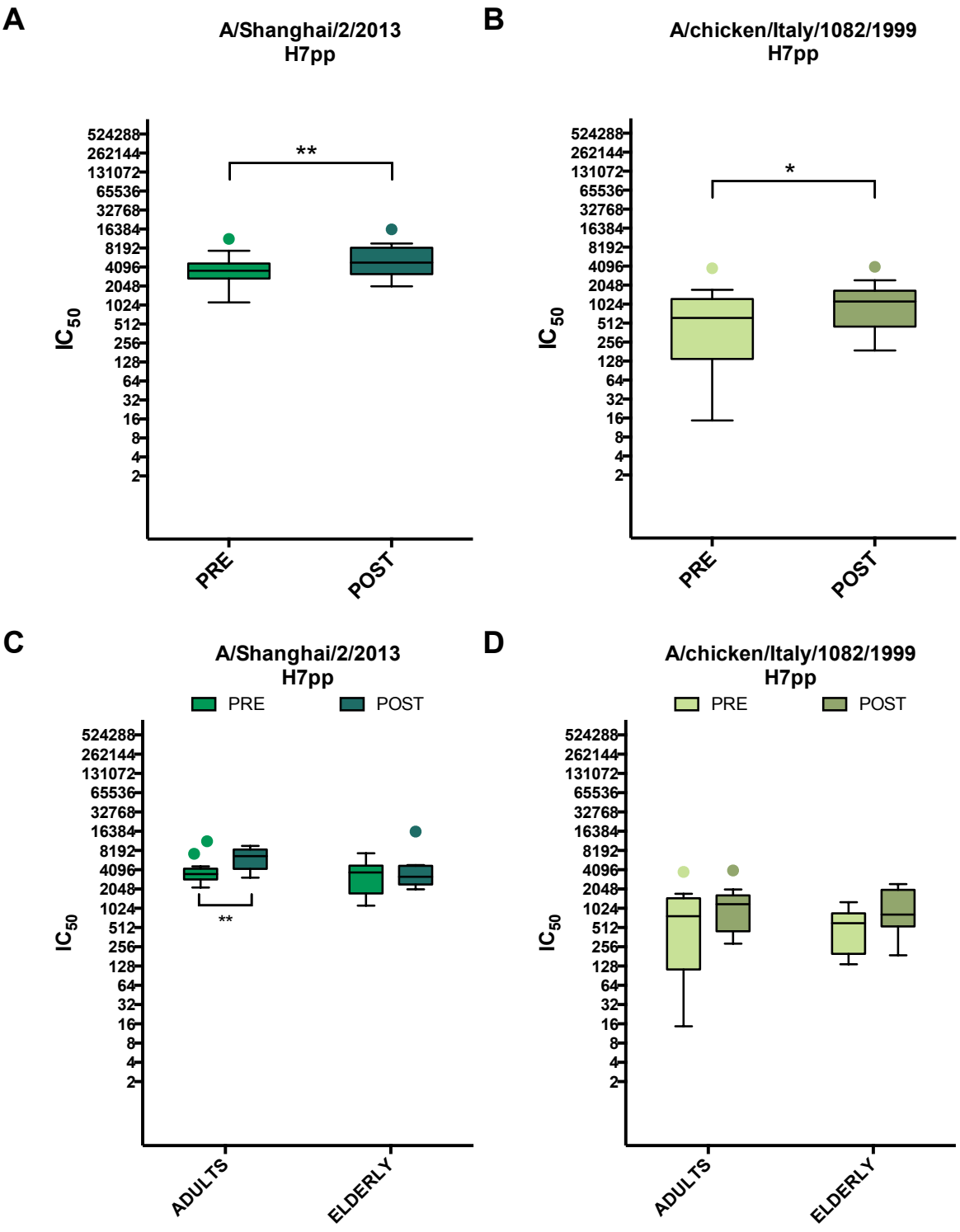

Figure 55: IC_{50} of sera tested with A/Shanghai/2/2013 H7 and A/chicken/Italy/1082/1999 H7 pp-NT assays

Comparison in the overall population and after age-stratification of IC_{50} measured pre- and post- vaccination with A/Wisconsin/67/2005 (H3N2), A/Solomon Island/3/2006 (H1N1) and B/Malaysia/2506/2004. Quartiles and medians of the distributions are reported in Appendix Table 2 and Appendix Table 3. **A.** Results against A/Shanghai/2/2013 H7pp; **B.** Results against A/chicken/Italy/1082/1999 H7pp; **C.** Results of A/Shanghai/2/2013 H7 pp-NT after stratification of age groups; **D.** Results of A/chicken/Italy/1082/1999 H7 pp-NT after stratification of age groups.

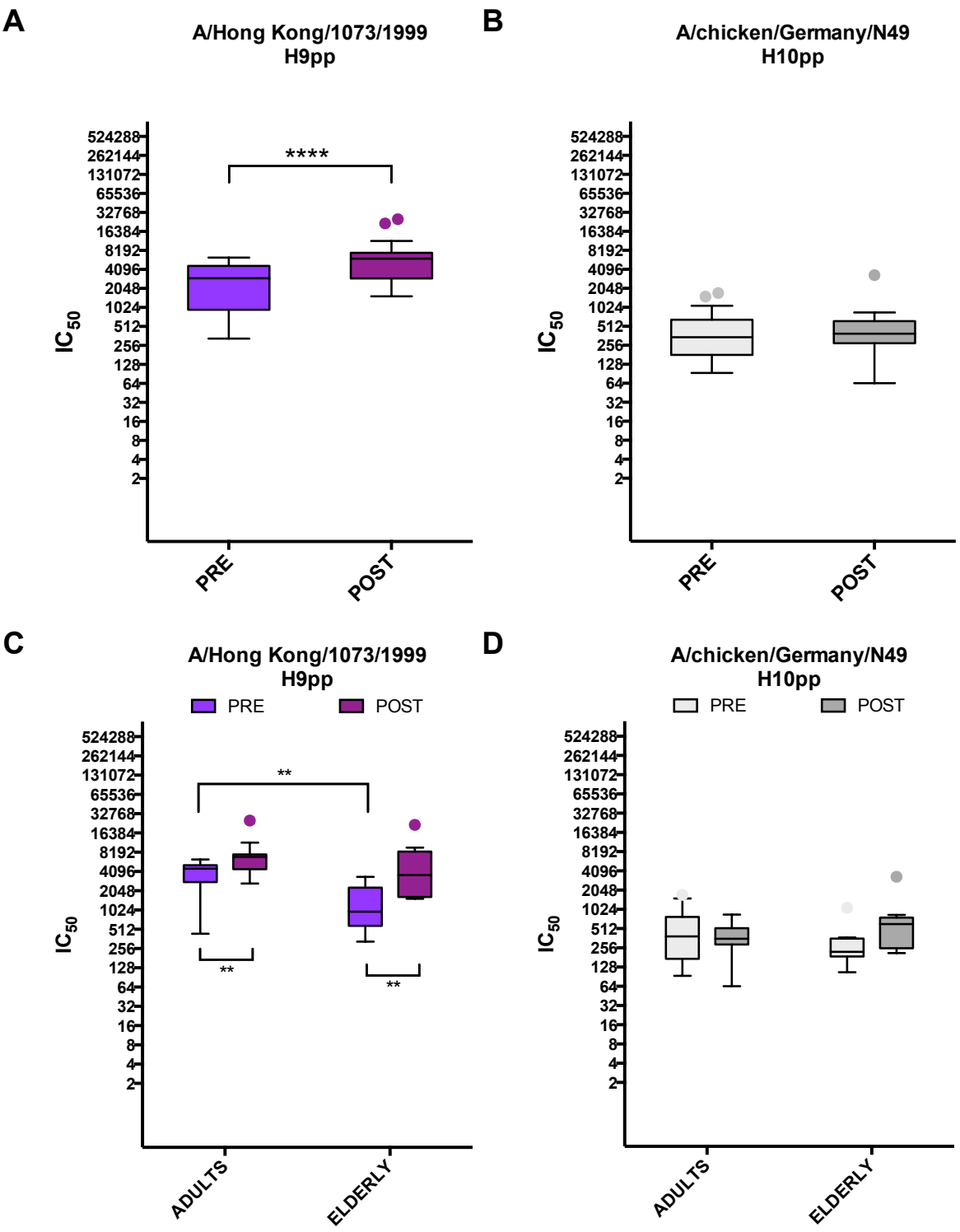

Figure 56: IC_{50} of sera tested with A/Hong Kong/1073/1999 H9 and A/chicken/Germany/N49 H10 pp-NT assays

Comparison in the overall population and after age-stratification of IC_{50} measured pre- and post-vaccination with A/Wisconsin/67/2005 (H3N2), A/Solomon Island/3/2006 (H1N1) and B/Malaysia/2506/2004. Quartiles and medians of the distributions are reported in Appendix Table 2 and Appendix Table 3. **A.** Results against A/Hong Kong/1073/1999 H9pp; **B.** Results against A/chicken/Germany/N49 H10p; **C.** Results of A/Hong Kong/1073/1999 H9 pp-NT after stratification of age groups; **D.** Results of A/chicken/Germany/N49 H10 pp-NT after stratification of age groups.

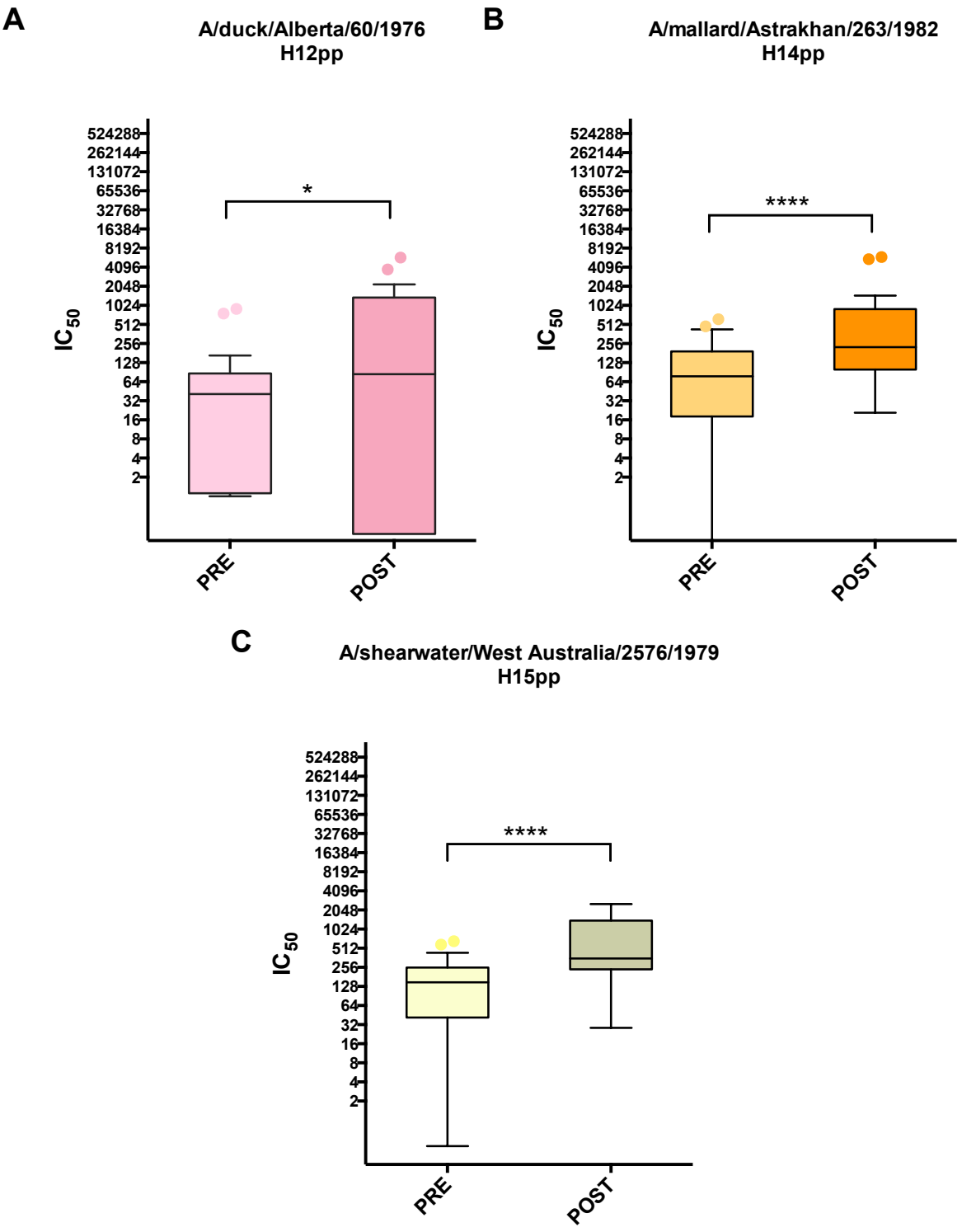

Figure 57: IC_{50} of sera tested with A/duck/Alberta/60/1976 H12, A/mallard/Astrakhan/263/1982 H14, and A/shearwater/West Australia/2576/1979 H15 pp-NT assays

Comparison between IC_{50} measured pre- and post-vaccination with A/Wisconsin/67/2005 (H3N2), A/Solomon Island/3/2006 (H1N1) and B/Malaysia/2506/2004. Quartiles and medians of the distributions are reported in Appendix Table 2. **A.** Results against A/duck/Alberta/60/1976 H12pp; **B.** Results against A/mallard/Astrakhan/263/1982 H14pp; **C.** Results against A/shearwater/West Australia/2576/1979 H15pp.

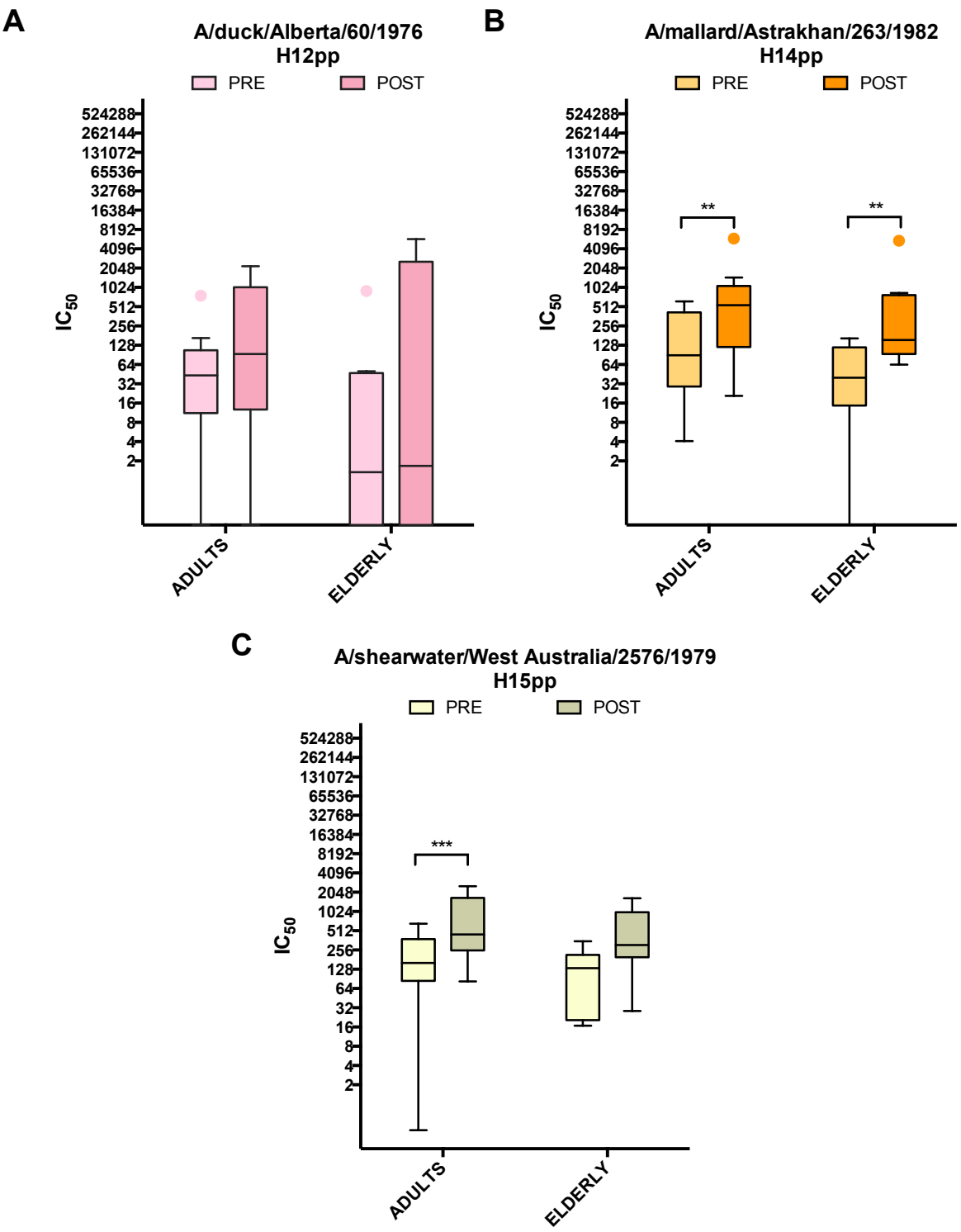

Figure 58: Age-stratified IC_{50} of sera tested A/duck/Alberta/60/1976 H12, A/mallard/Astrakhan/263/1982 H14, and A/shearwater/West Australia/2576/1979 H15 pp-NT assays

Comparison between IC_{50} measured pre- and post-vaccination with A/Wisconsin/67/2005 (H3N2), A/Solomon Island/3/2006 (H1N1) and B/Malaysia/2506/2004. Quartiles and medians of the distributions are reported in Appendix Table 3. **A.** Results against A/duck/Alberta/60/1976 H12pp; **B.** Results against A/mallard/Astrakhan/263/1982 H14pp; **C.** Results against A/shearwater/West Australia/2576/1979 H15pp.

In the A/duck/Alberta/60/1976 H12 pp-NT assay (**Figure 57A**) low responses were detected and they were augmented by vaccination ($p = 0.0275$). However, when age-stratification was applied, the statistical significance was lost in adults as well as the elderly. Comparing the responses between groups at the same time-point did not show any differences (**Figure 58A**).

Neutralizing antibody responses against H14 and H15pp in pre-vaccination individuals were boosted ($p < 0.0001$) post-vaccination (**Figure 57 (B and C)**). Age group stratification showed the same pattern with post-vaccination responses of higher magnitude for adults (H14 $p = 0.0017$; H15 $p = 0.0002$) but for elderly only against H14 ($p = 0.078$). In the IC_{50} comparison between the two age-groups, variations were not significant (**Figure 58 (B and C)**).

Before proceeding to the use of the chimeric HA in pp-NT assay, it was important to test the two parental HA pp to be able to compare the IC_{50} titres and understand if antibodies are directed against the stalk or the head of the HA. In A/South Carolina/1/1918 pp-NT assay (**Figure 59A and 60A**), high neutralizing responses were detected pre-vaccination but a statistically significant increase ($p < 0.0001$) was observed in post-vaccination titres. When comparing pre- and post-vaccination data in adults and in elderly, titre increase at the two time-points was significant (adults: $p = 0.0002$; elderly: $p = 0.0039$). No differences were detected between adults and elderly at the two time-points using the Mann-Whitney U test.

When the H11pp was used (**Figure 59B and 60B**), very low neutralization titres were detected pre-vaccination but increased ($p = 0.0007$) post-vaccine administration. Using the Bonferroni correction, differences between pre- and post-vaccination titres in adults ($p = 0.0151$) and in elderly ($p = 0.0313$) were not detected. When comparing the two time-points between the two groups variations were not significant.

Lastly, the chimeric HA pp was tested (**Figure 59C and 60C**): high responses were detected pre- and post-vaccination though differences were statistically significant ($p = 0.0002$). However, when data stratification and Bonferroni correction were applied, differences between pre- and post-vaccination titres were observed in the elderly ($p = 0.0039$) but not in adults ($p = 0.0215$). No difference between the adults and elderly IC_{50} titres were detected pre- or post-vaccination.

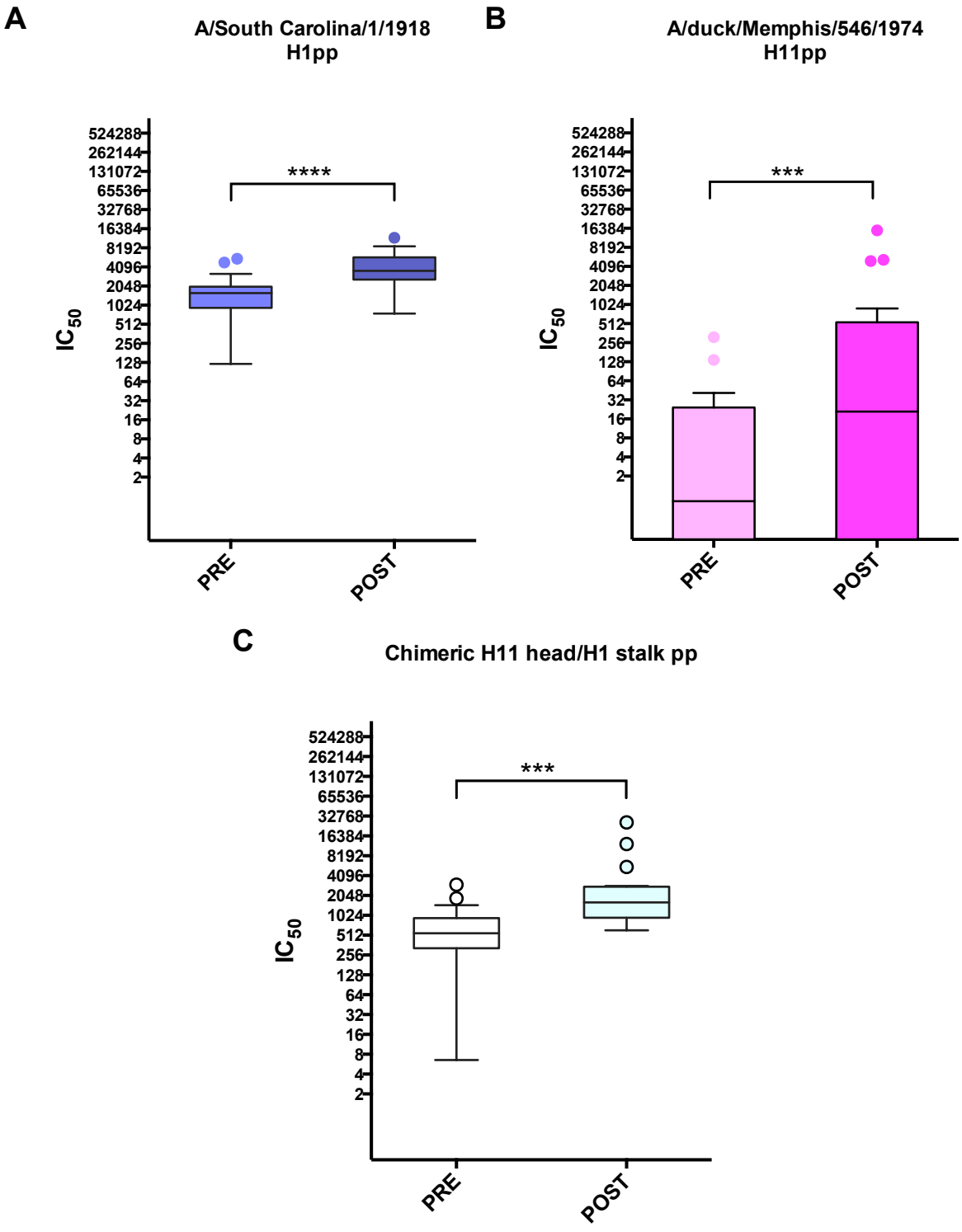

Figure 59: IC_{50} of sera tested with A/South Carolina/1/1918 H1, A/duck/Memphis/546/1974 H11, and the chimeric HA pp-NT assays

Comparison between IC_{50} measured pre- and post-vaccination with A/Wisconsin/67/2005 (H3N2), A/Solomon Island/3/2006 (H1N1) and B/Malaysia/2506/2004. Quartiles and medians of the distributions are reported in Appendix Table 2. **A.** Results against A/South Carolina/1/1918 H1pp; **B.** Results against A/duck/Memphis/546/1974 H11pp; **C.** Results against the chimeric H11 head/H1 stalk HA pp.

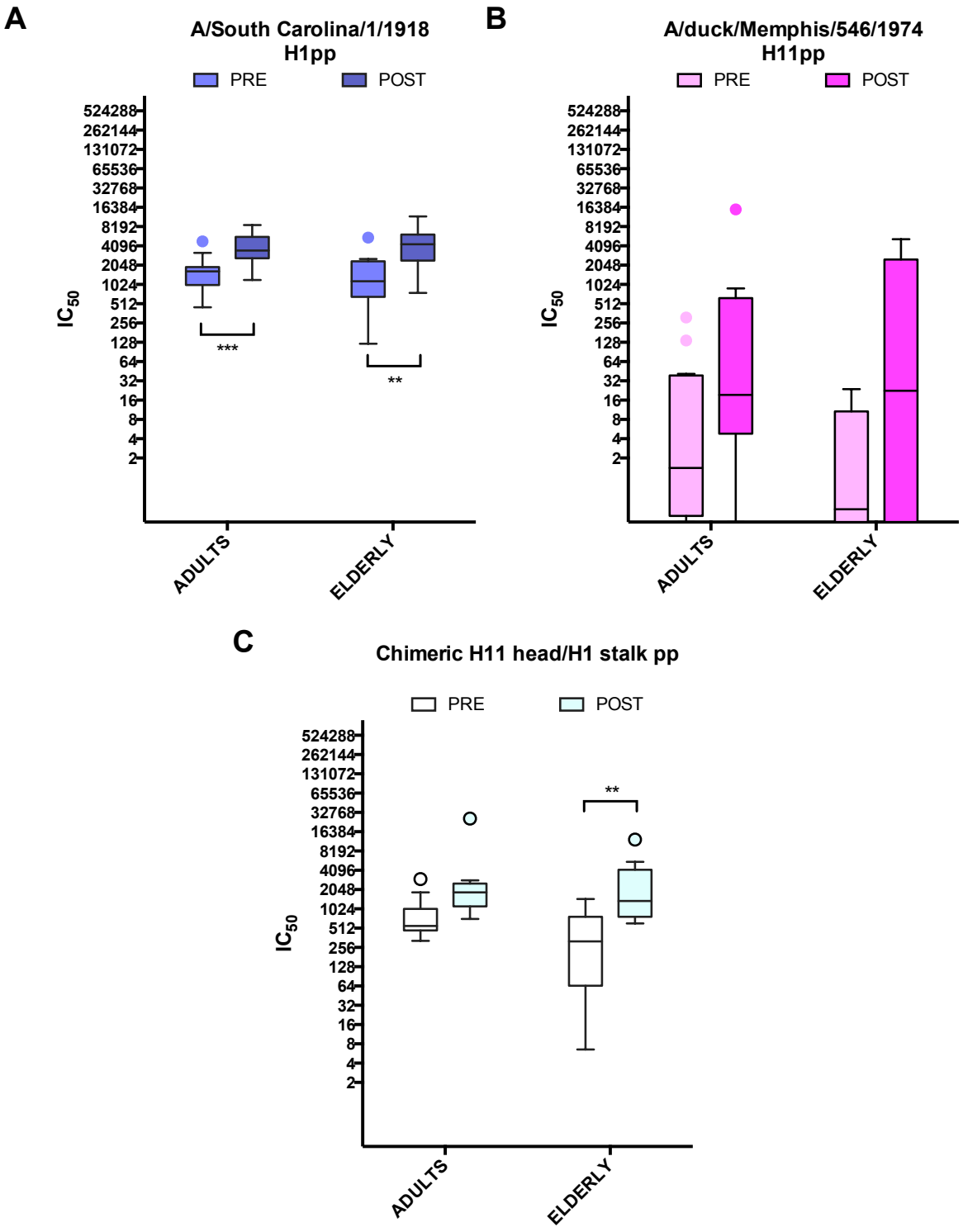

Figure 60: Age-stratified IC_{50} of sera tested with A/South Carolina/1/1918 H1, A/duck/Memphis/546/1974 H11, and the chimeric HA pp-NT assays
Comparison between IC_{50} measured pre- and post-vaccination with A/Wisconsin/67/2005 (H3N2), A/Solomon Island/3/2006 (H1N1) and B/Malaysia/2506/2004. Quartiles and medians of the distributions are reported in Appendix Table 3. **A.** Results against A/South Carolina/1/1918 H1pp; **B.** Results against A/duck/Memphis/546/1974 H11pp; **C.** Results against the chimeric H11 head/H1 stalk HA pp.

The IC_{50} values obtained when the chimeric HA pp was employed were higher than the ones detected against H11 (the pp that has donated the head region) but lower than the ones detected with A/South Carolina/1/1918 H1pp, which has donated the stalk region. This indicates that the presence of the A/South Carolina/1/1918 H1 stalk mediates an increase in neutralizing titres, demonstrating that antibodies against this region were present in the samples pre-vaccination. Likewise these antibody responses increased post-seasonal vaccination, since a statistical difference was observed between the two time-points. Nevertheless, since the A/South Carolina/1/1918 H1 pp-NT IC_{50} values are higher than the ones detected in the chimeric HA pp-NT assay, a response against the head was also involved. Since A/South Carolina/1/1918 (H1N1) was not present in the vaccine but this HA is related to A/Solomon Islands/3/2006 (H1N1) (same HA subtype), it is clear that at the basis of the neutralization detected there is homosubtypic cross-reactivity.

To better analyse the magnitude of the responses detected and to understand if there are changes between the two populations analysed, the data analysis was enriched by calculating SCRs, which are reported in **Table 24**. SCRs were calculated pre- and post- age-stratification, and two cut-off values (2-fold and 4 fold) were used to determine the SCRs. It can be noticed that $SCR_{(4\text{-fold})}$ for the H1 vaccine strains were > 40% and/or > 30%, which are the two vaccine immunogenicity criteria cut-offs for adults and elderly when the HI assay is used (Committee for Proprietary Medicinal Products 1997), whereas for the H3 vaccine strains only the elderly $SCR_{(4\text{-fold})}$ exceed the cut-off percentage. Interesting, viewing the SCRs for the two vaccine strains, it is noticeable that the majority of adults had a seroconversion for the H1 strain but not for the H3, whereas in elderly it was the opposite.

In the previous analyses, the elderly had lower antibody titres pre-vaccination but SCRs revealed that these increased to levels that were comparable to the IC_{50} values of adult subjects post-vaccination. In fact, using chi-squared statistics, it was possible to verify that $SCR_{(4\text{-fold})}$ and $SCR_{(2\text{-fold})}$ were influenced by the age of subjects ($\chi^2 = 10.16$, $df = 1$, $p = 0.0014$, and respectively $\chi^2 = 3.912$, $df = 1$, $p = 0.0479$) indicating that the elderly had better qualitative and quantitative cross-reactive antibody response than adults.

Taken together the data presented show that heterosubtypic stalk-directed antibody responses were present in this Italian population and they increased post-seasonal vaccination; the data also suggested that homosubtipic and/or heterosubtypic head-directed responses were sometimes present.

Table 24: SCRs using cut-off values of 4-fold IC_{50} ($SCR_{(4\text{-fold})}$) or 2-fold IC_{50} increase ($SCR_{(2\text{-fold})}$)

	ADULTS n=13				ELDERLY n=9				TOTAL n=22			
	$SCR_{(2\text{-fold})}$ %		$SCR_{(4\text{-fold})}$ %		$SCR_{(2\text{-fold})}$ %		$SCR_{(4\text{-fold})}$ %		$SCR_{(2\text{-fold})}$ %		$SCR_{(4\text{-fold})}$ %	
Vaccine strains												
A/Solomon Islands/3/2006 H1	92.3	(12/13)	84.6	(11/13)	66.7	(6/9)	55.6	(5/9)	81.8	(18/22)	72.7	(16/22)
A/Wisconsin/67/2005 H3 (A/Udorn/307/1972 N2)	53.8	(7/13)	38.5	(5/13)	77.8	(7/9)	77.8	(7/9)	63.6	(14/22)	54.5	(12/22)
Group 1 strains												
A/New Caledonia/20/1999 H1	46.2	(6/13)	30.8	(4/13)	88.9	(8/9)	66.7	(6/9)	63.6	(14/22)	45.5	(10/22)
A/South Carolina/1/1918 H1	69.2	(9/13)	7.7	(1/13)	77.8	(7/9)	33.3	(3/9)	72.7	(16/22)	18.2	(4/22)
A/Korea/426/1968 H2	23.1	(3/13)	7.7	(1/13)	22.2	(2/9)	11.1	(1/9)	22.7	(5/22)	9.1	(2/22)
A/Viet Nam/1194/2004 H5	46.2	(6/13)	30.8	(4/13)	77.8	(7/9)	55.6	(5/9)	59.1	(13/22)	40.9	(9/22)
A/turkey/Turkey/1/2005 H5	53.8	(7/13)	15.4	(2/13)	100	(9/9)	77.8	(7/9)	72.7	(16/22)	40.9	(9/22)
A/Hong Kong/1073/1999 H9	46.2	(6/13)	15.4	(2/13)	66.7	(6/9)	44.4	(4/9)	54.5	(12/22)	27.3	(6/22)
A/duck/Memphis/546/1974 H11	53.8	(7/13)	46.2	(6/13)	55.6	(5/9)	55.6	(5/9)	54.5	(12/22)	50	(11/22)
A/duck/Alberta/60/1976 H12	38.5	(5/13)	38.5	(5/13)	44.4	(4/9)	44.4	(4/9)	40.9	(9/22)	40.9	(9/22)
Group 2 strains												
A/Udorn/307/1972 H3	23.1	(3/13)	7.7	(1/13)	33.3	(3/9)	22.2	(2/9)	27.3	(6/22)	13.6	(3/22)
A/duck/Czechoslovakia/1956 H4	53.8	(7/13)	23.1	(3/13)	66.7	(6/9)	33.3	(3/9)	59.1	(13/22)	27.3	(6/22)
A/chicken/Italy/1082/1999 H7 (LPAI)	46.2	(6/13)	23.1	(3/13)	33.3	(3/9)	22.2	(2/9)	40.9	(9/22)	22.7	(5/22)
A/Shanghai/2/2013 H7	30.8	(4/13)	0	(0/13)	22.2	(2/9)	0	(0/9)	27.3	(6/22)	0	(0/22)
A/chicken/Netherlands/1/2003 H7 (HPAI)	61.5	(8/13)	53.8	(7/13)	66.7	(6/9)	66.7	(6/9)	63.6	(14/22)	59.1	(13/22)
A/chicken/Germany/N49 H10	15.4	(2/13)	0	(0/13)	66.7	(6/9)	11.1	(1/9)	36.4	(8/22)	4.5	(1/22)
A/mallard/Astrakhan/263/1982 H14	76.9	(10/13)	61.5	(8/13)	66.7	(6/9)	55.6	(5/9)	72.7	(16/22)	59.1	(13/22)
A/shearwater/West Australia/2576/1979 H15	84.6	(11/13)	30.8	(4/13)	55.6	(5/9)	44.4	(4/9)	72.7	(16/22)	36.4	(8/22)
Chimeric haemagglutinin												
H11 head/H1 South Carolina stalk	76.9	(10/13)	30.8	(4/13)	88.9	(8/9)	55.6	(5/9)	81.8	(18/22)	40.9	(9/22)

5.3.5 Heterosubtypic haemagglutinin antibody responses are detected and partially augmented after the administration of a trivalent vaccine with or without the co-administration of a MVA-NP+M1 vaccine

The small volumes of samples available for the 2007-2008 vaccination study prevented repeats of the pp-NT assays being conducted. For this reason and to investigate whether the results observed were specific to the population, another set of sera was evaluated with the same methodology. These sera were collected at day 0 and at day 21 of the NCT00942071 clinical trial (Antrobus *et al.* 2013) in which subjects were firstly vaccinated with a trivalent 2011-2012 seasonal influenza vaccine and immediately after with placebo or with a MVA-NP+M1 vaccine.

Since all the subjects have received a trivalent seasonal vaccine, it was decided to perform the first analysis comparing the two time-points regardless of the kind of regimen that the subject had received. Subsequently, data were stratified for the regimen to see if the MVA-NP+M1 vaccine has had an effect in increasing the heterosubtypic antibody responses, if they are present.

All the subjects were older adults aged 50 years and above and no age-difference were observed between the two experimental groups (Antrobus *et al.* 2013), therefore a age-stratification was not performed for this study.

In the trivalent vaccine, A/California/7/2009 H1N1 and A/Perth/16/2009 H3N2 were included and, unfortunately, two matching or related pp were not available to evaluate neutralizing responses: in fact A/Texas/05/2009 H1pp, which is related by subtype to A/California/7/2009 H1, was not produced at a titre high enough to perform neutralization assays (Chapter 3). However, the response against the vaccine strains and seroconversion of the subjects were previously evaluated though ELISA and HI (Antrobus *et al.* 2013). Therefore, in the current study, sera were directly evaluated against different representative strains of human and avian influenza.

Considering human influenza viruses, the A/New Caledonia/20/1999 H1 pp-NT assay (**Figure 61A**), detected high responses at day 0 but a statistically significant increase was not detected at day 21. The same was observed when A/Korea/426/1968 H2pp was used: high responses were detected but the vaccine failed to increase them (**Figure 61B**). On the contrary when the two H3pp were used in neutralization assay, pre-vaccine administrations showed higher responses when the older A/Udorn/307/1972 H3 was used (**Figure 61C**), than when the more recent A/Wisconsin/67/2005 H3 but in both cases, these responses increased ($p = 0.0001$) at day 21 (**Figure 61D**).

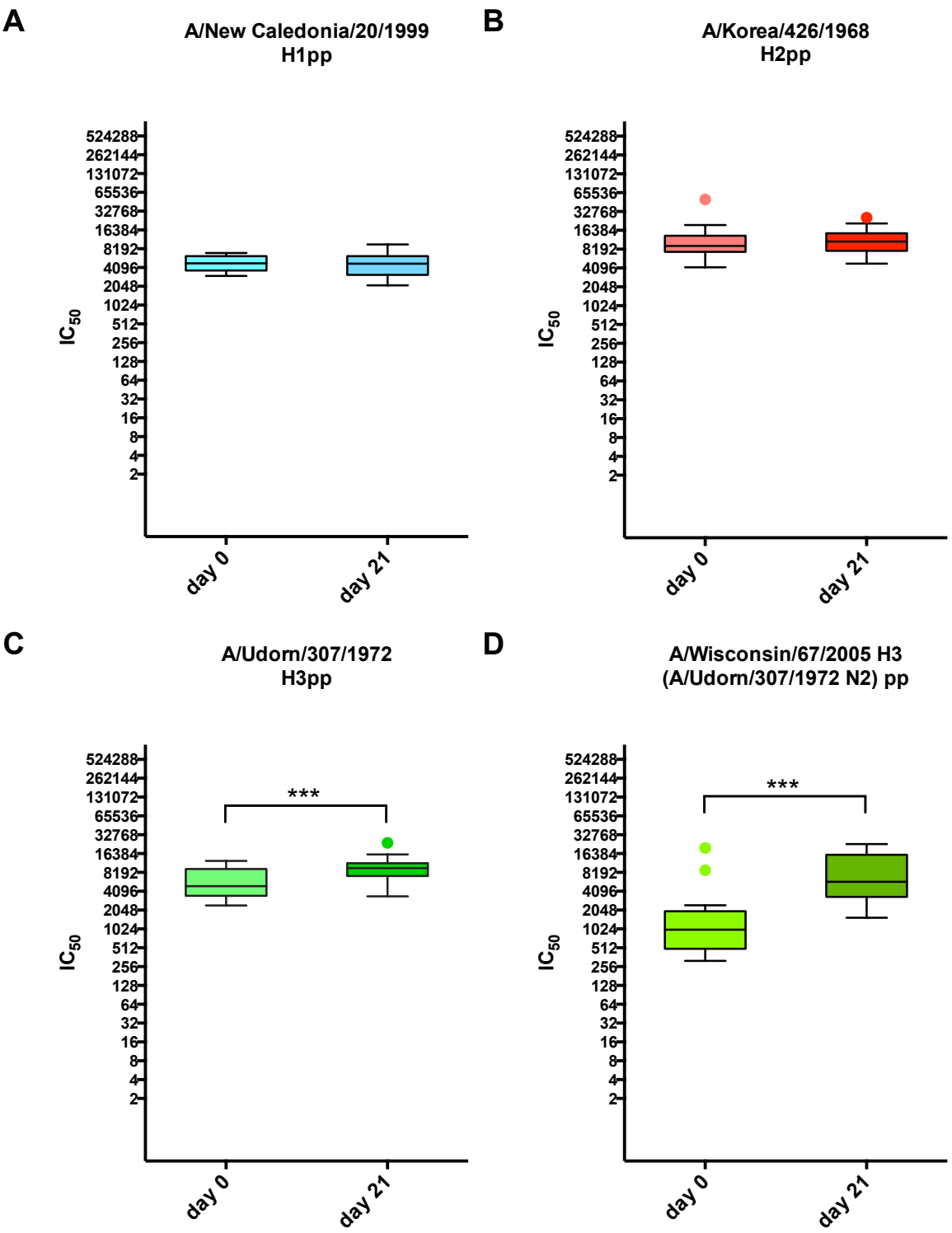

Figure 61: IC_{50} of NCT00942071 clinical trial sera tested with pp-NT assays (1)
Comparison between IC_{50} measured at day 0 and at day 21 of the NCT00942071 clinical trial. Quartiles and medians of the distributions are reported in Appendix Table 4. **A.** Results against A/New Caledonia/20/1999 H1pp; **B.** Results against A/Korea/426/1968 H2pp; **C.** Results against A/Udorn/307/1972 H3pp; **D.** Results against A/Wisconsin/67/2005 H3 (A/Udorn/307/1972 N2) pp.

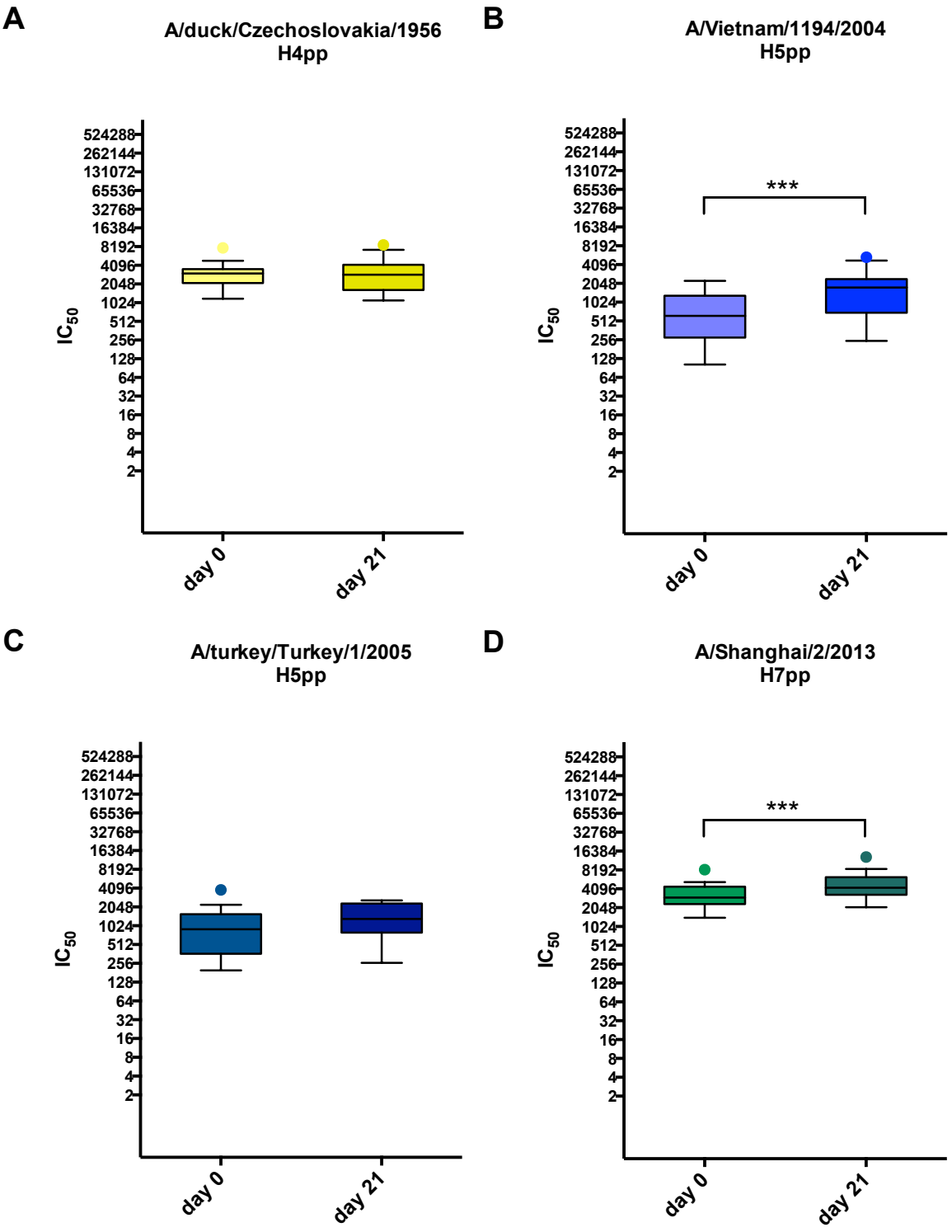

Figure 62: IC_{50} of NCT00942071 clinical trial sera tested with pp-NT assays (2)
Comparison between IC_{50} measured at day 0 and at day 21 of the NCT00942071 clinical trial. Quartiles and medians of the distributions are reported in Appendix Table 4. **A.** Results against A/duck/Czechoslovakia/1956 H4pp; **B.** Results against A/Vietnam/1194/2004 H5pp. **C.** Results against A/turkey/Turkey/1/2005 H5pp; **D.** Results against A/Shanghai/2/2013 H7pp.

Analysing the neutralization data obtained using H4pp (**Figure 62A**), it can be observed that high neutralization activity are detected at day 0 and remained high also post-vaccination. On the other hand, in H5 pp-NT assays (**Figure 62 (B and C)**) antibody responses were observed before vaccination but they increased at day 21 only for A/turkey/Turkey/1/2005 H5 ($p < 0.001$), whereas A/Vietnam/1194/2004 H5 remained unchanged.

In the sera analysed, neutralizing antibody responses against A/Shanghai/2/2013 H7 (**Figure 62D**) were already present at day 0 but titres increased ($p = 0.0002$) at day 21. The same was observed for A/Hong Kong/1073/1999 H9 (**Figure 63A**) with IC_{50} values that increased ($p < 0.0001$) post-vaccine administration. In contrast, in the A/chicken/Germany/N49 pp-NT assay (**Figure 63B**), low antibody responses were detected at the first time-point and they did not increase at the second. Also for H14 and H15 pp-NT assays, neutralizing antibodies were identified but they failed to be boosted by vaccination (**Figure 63 (C and D)**).

Lastly, as for the 2007-2008 vaccination study, the chimeric HA pp and the two parental HAs, A/South Carolina/1/1918 H1 and A/duck/Memphis/546/1974 H11, were used in neutralization assays as surrogate antigens. In A/South Carolina/1/1918 H1 pp-NT (**Figure 64A**) responses were detected at day 0 and they were augmented ($p = 0.0150$) by vaccination. Similarly, but at lower magnitude, responses for H11 were detected pre-vaccine administrations and they increased ($p = 0.0202$) post-vaccination (**Figure 64B**). As shown in the 2007-2008 vaccination study, and in this case, neutralizing antibody responses against the chimeric HA were detected (**Figure 64C**). These were of intermediate magnitude when compared with those measured against the donor H1 (**Figure 64A**) and they increased ($p = 0.0046$) during the two time-points.

The results obtained with the chimeric HA clearly show that, as already underlined in the 2007-2008 vaccination study (Section 5.3.4), stalk-directed and head-directed cross-reactive antibody responses are present in the human population and are partially boosted by vaccination. In contrast to the results reported previously (Section 5.3.4), the effect of the vaccine regimens noted was less broad in the current study, with the IC_{50} distribution against some the pp analysed not changing post-vaccine administration.

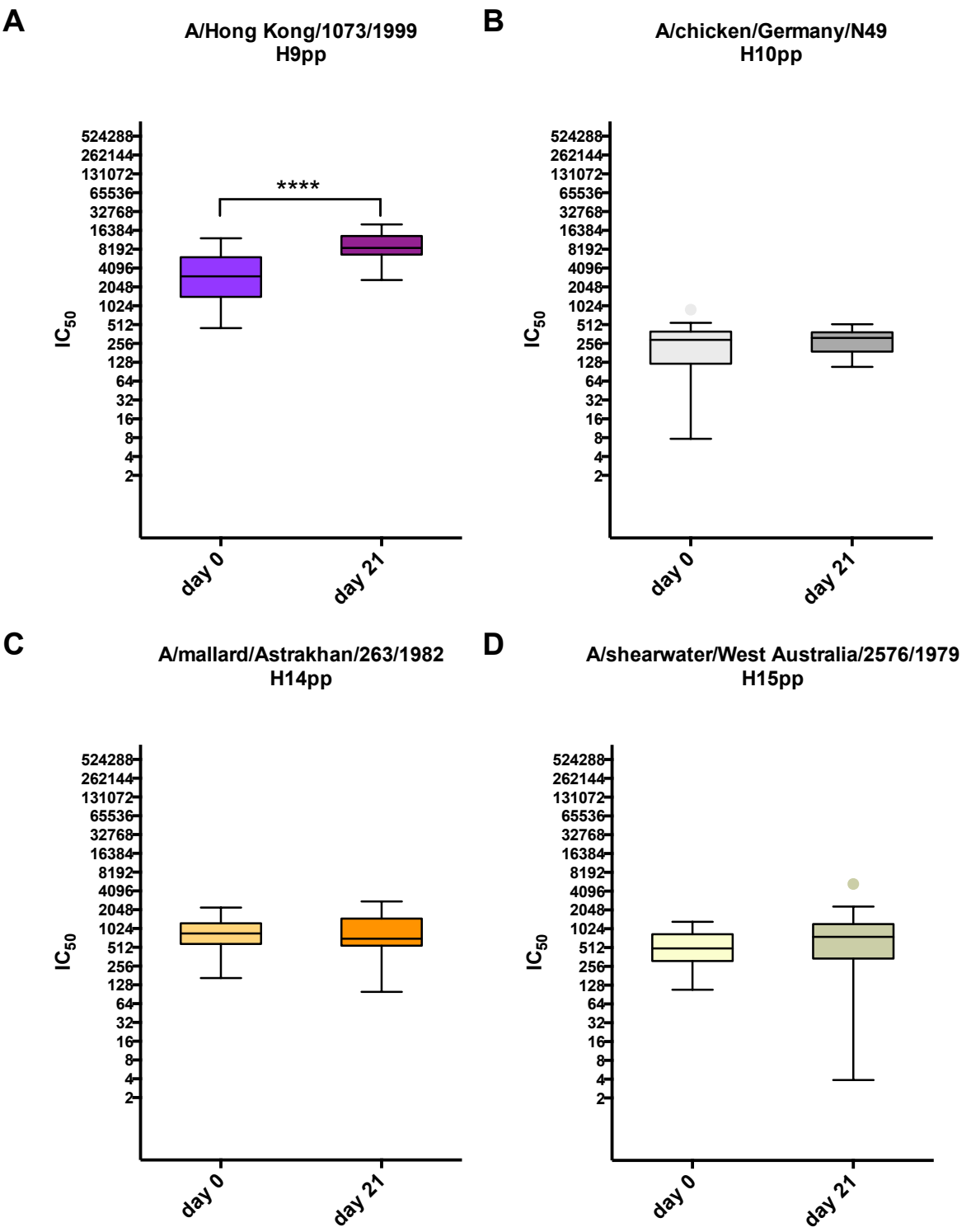

Figure 63: IC_{50} of NCT00942071 clinical trial sera tested with pp-NT assays (3)
Comparison between IC_{50} measured at day 0 and at day 21 of the NCT00942071 clinical trial. Quartiles and medians of the distributions are reported in Appendix Table 4. **A.** Results against Hong Kong/1073/1999 H9pp; **B.** Results against A/chicken/Germany/N/49 H10pp; **C.** Results against A/mallard/Astrakhan/263/1982 H14pp; **D.** Results against A/shearwater/West Australia/2576/1979 H15pp.

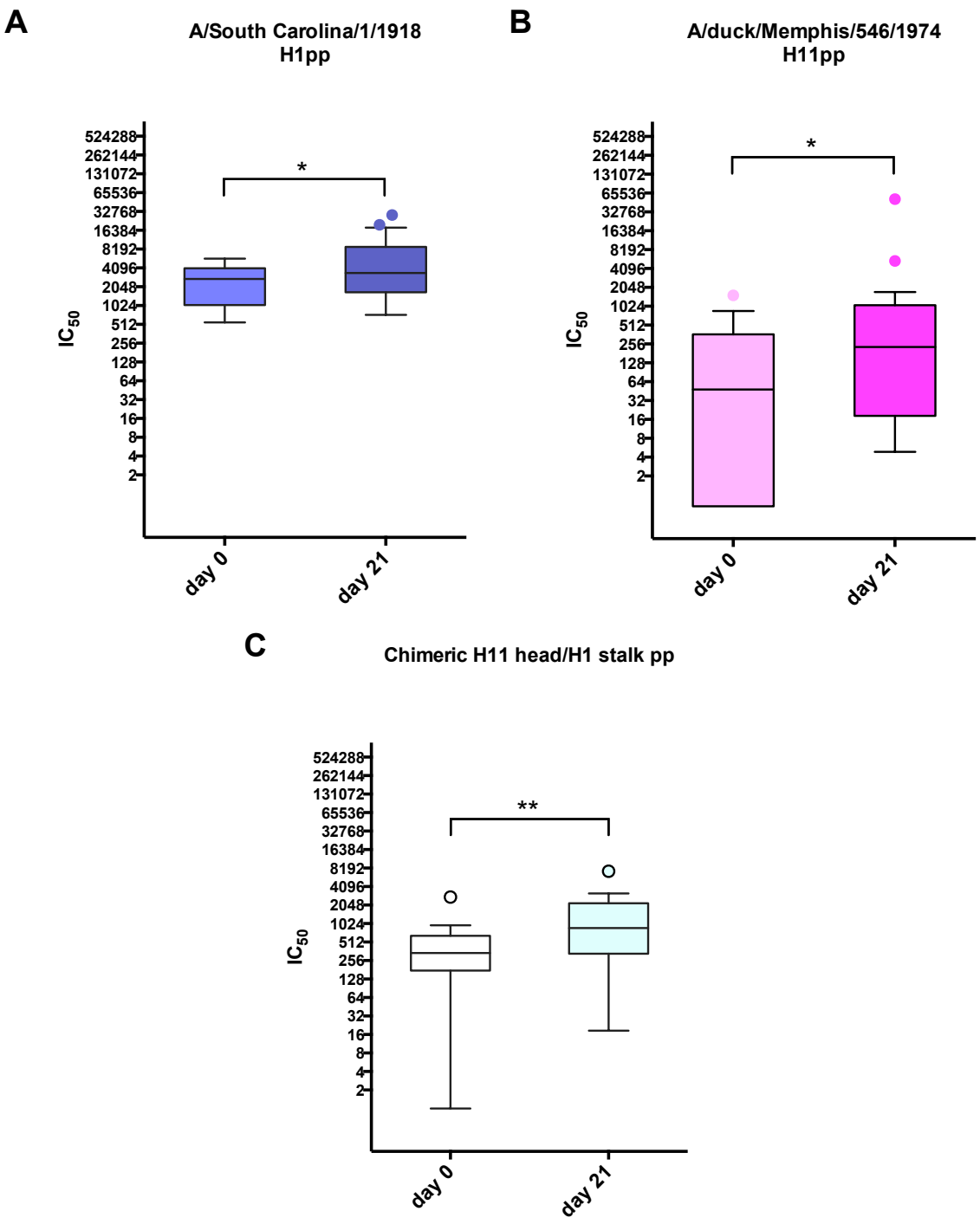

Figure 64: IC_{50} of NCT00942071 clinical trial sera tested with pp-NT assays (4)
Comparison between IC_{50} measured at day 0 and at day 21 of the NCT00942071 clinical trial. Quartiles and medians of the distributions are reported in Appendix Table 4. **A.** Results against A/South Carolina/1/1918 H1pp; **B.** Results against A/duck/Memphis/546/1974 H11pp; **C.** Results against H11 head/H1 stalk chimeric HA peudotype.

To compare the two different vaccine regimens (TIV + placebo and TIV + MVA-NP+M1) and avoid multiple comparisons, a strategy different to the one used in the 2007-2008 vaccination study was followed. Firstly the data were graphed in Box-and-Whisker plots after regimen-stratification (**Figures 65-69**) in order to compare the distributions. Subsequently, IC_{50} fold-increases (**Appendix Figure 17**) were calculated for each subject and they were compared on the basis of the regimen-stratification. In only

two cases were statistically significant differences found in the IC_{50} fold-increase comparing TIV + placebo and TIV + MVA-NP+M1. This was when A/Wisconsin/67/2005 H3 (A/Udorn/307/1972 N2) pp (p = 0.0359) (**Figure 65D** and **Appendix Figure 17D**) and H15pp (p = 0.0152) was used (**Figure 67D** and **Appendix Figure 17L**).

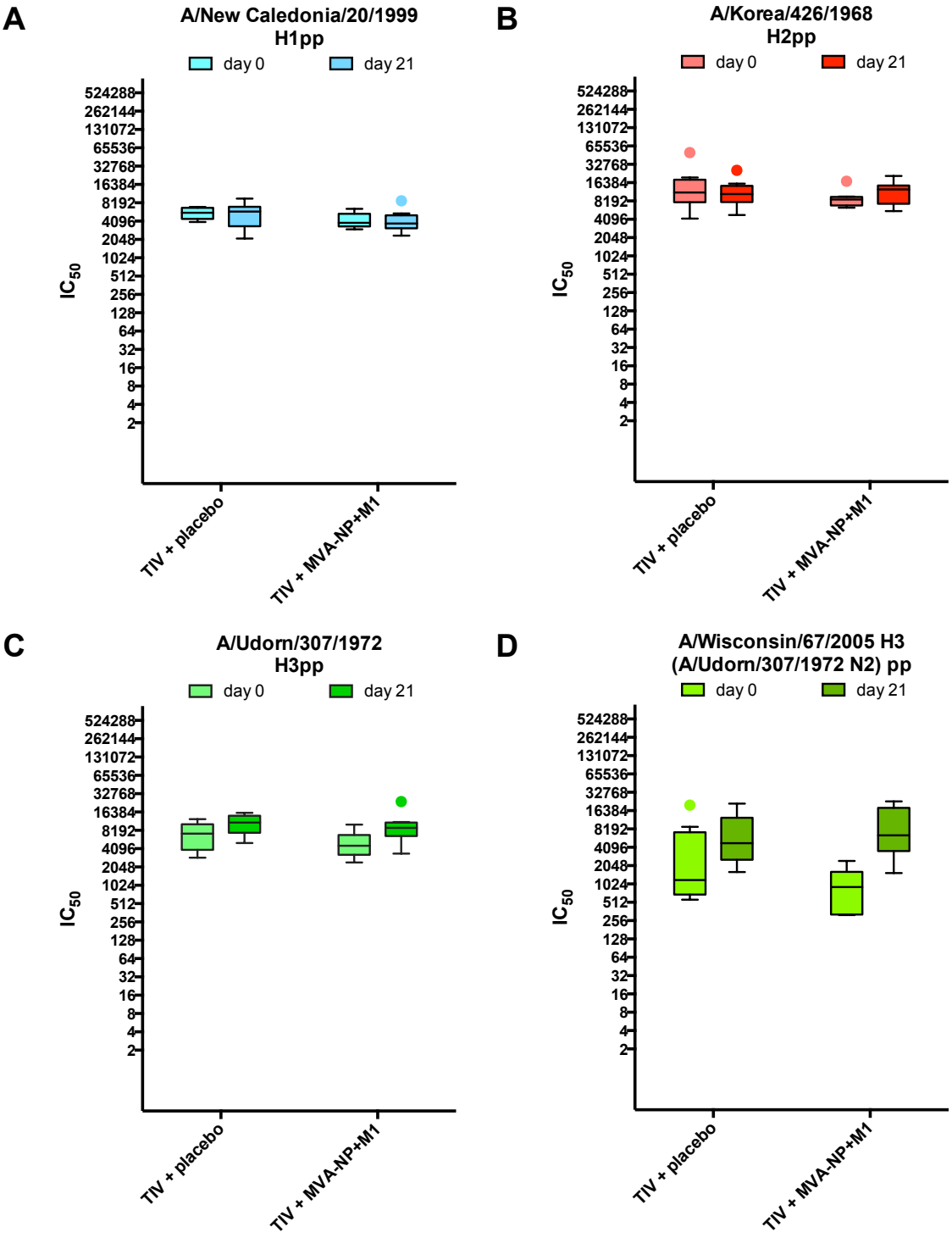

Figure 65: Comparison of TIV + placebo and TIV + MVA-NP+M1 vaccine combinations using pp-NT IC_{50} (1)

IC_{50} measured pre- and post-vaccination and stratified considering the vaccine combinations from NCT00942071 clinical trial were reported on Box-and-Whisker plots for comparison. Quartiles and medians of the distributions are reported in Appendix Table 5. **A.** Results against A/New Caledonia/20/1999 H1pp; **B.** Results against A/Korea/426/1968 H2pp; **C.** Results against A/Udorn/307/1972 H3pp; **D.** Results against A/Wisconsin/67/2005 H3 (A/Udorn/307/1972 N2) pp.

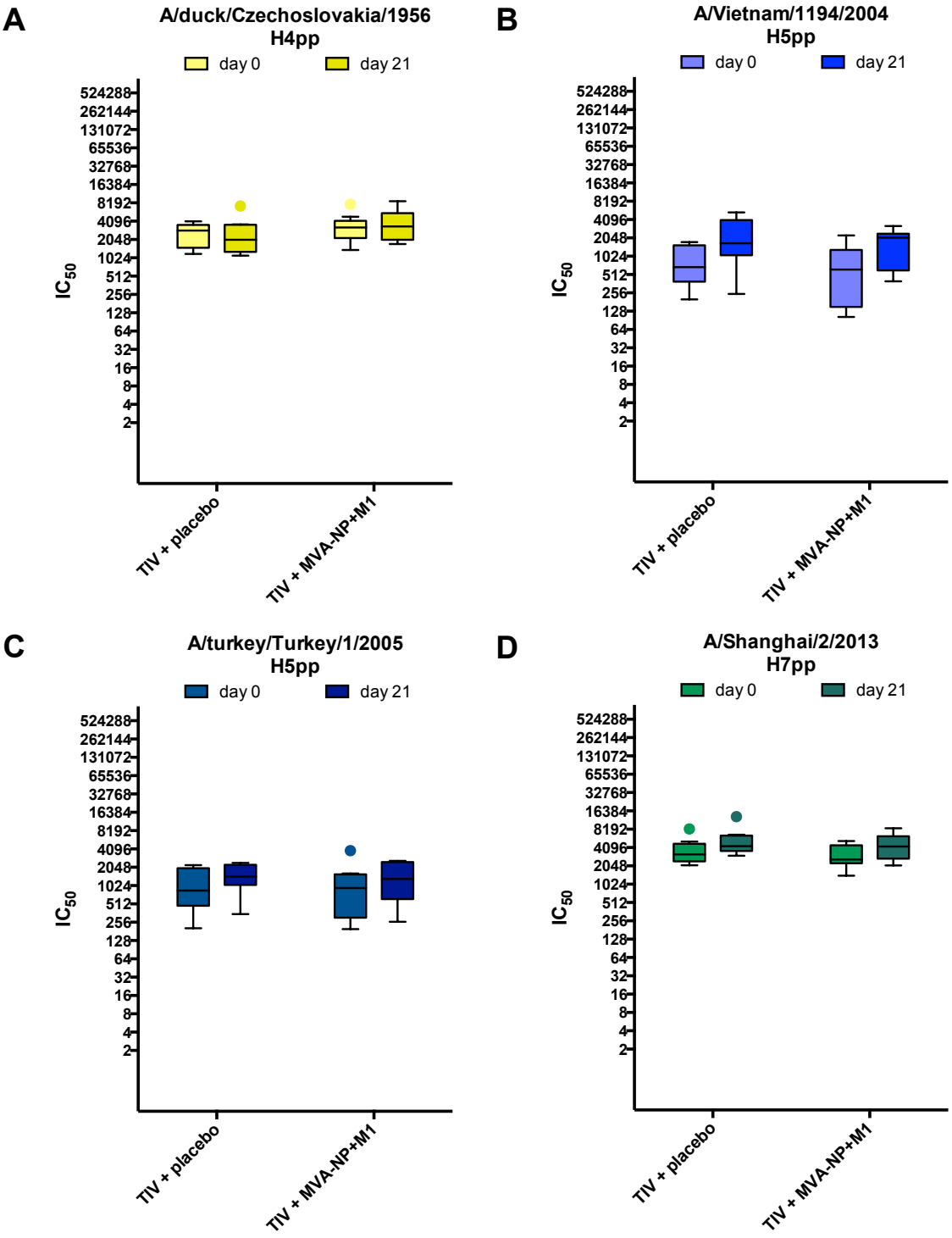

Figure 66: Comparison of TIV + placebo and TIV + MVA-NP+M1 vaccine combinations using pp-NT IC_{50} (2)

IC_{50} measured pre- and post-vaccination and stratified considering the vaccine combinations from NCT00942071 clinical trial were reported on Box-and-Whisker plots for comparison Quartiles and medians of the distributions are reported in Appendix Table 5. **A.** Results against A/duck/Czechoslovakia/1956 H4pp; **B.** Results against A/Vietnam/1194/2004 H5pp. **C.** Results against A/turkey/Turkey/1/2005 H5pp; **D.** Results against A/Shanghai/2/2013 H7pp.

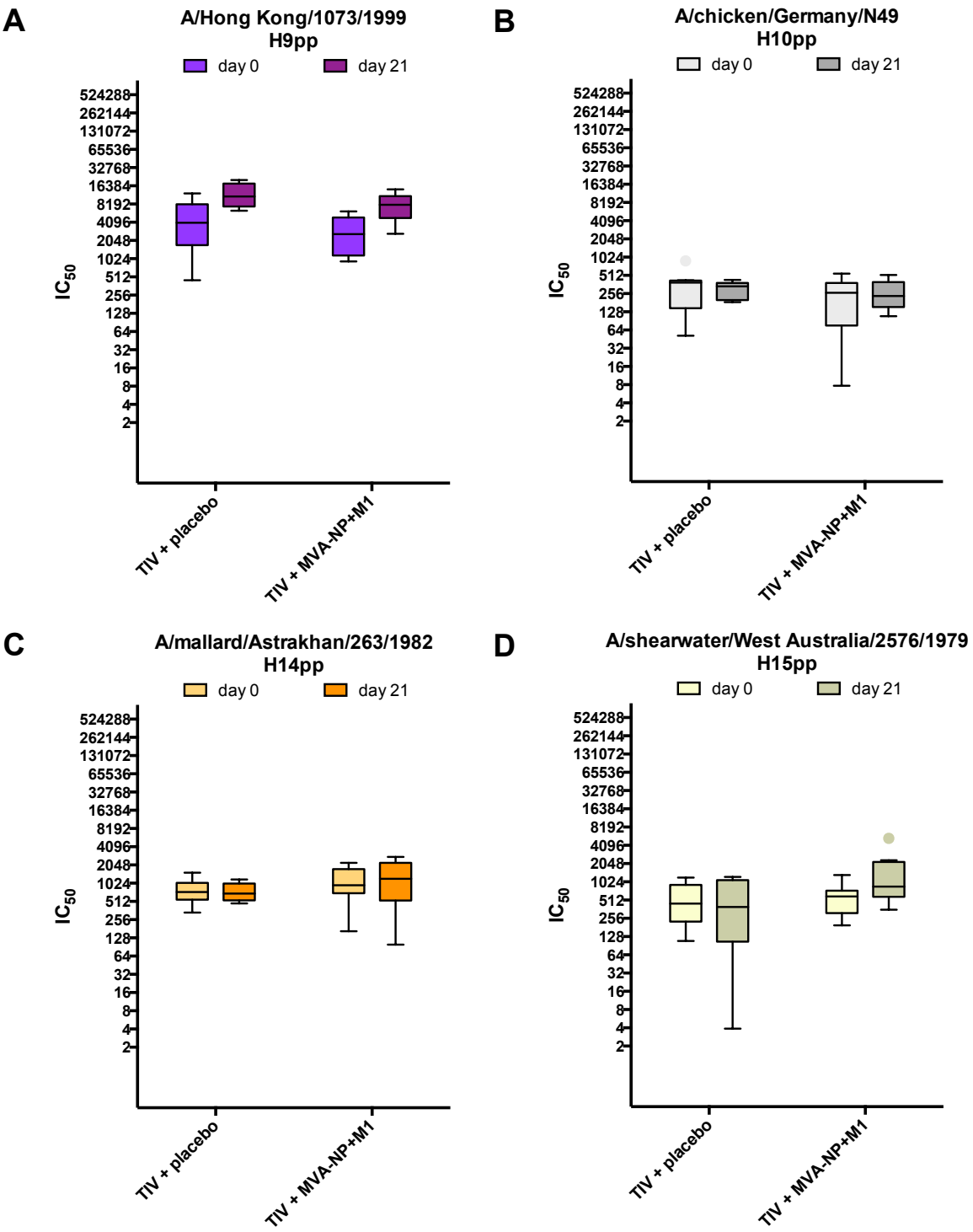

Figure 67: Comparison of TIV + placebo and TIV + MVA-NP+M1 vaccine combinations using pp-NT IC_{50} (3)

IC_{50} measured pre- and post-vaccination and stratified considering the vaccine combinations from NCT00942071 clinical trial were reported on Box-and-Whisker plots for comparison. Quartiles and medians of the distributions are reported in Appendix Table 5. **A.** Results against Hong Kong/1073/1999 H9pp; **B.** Results against A/chicken/Germany/N/49 H10pp; **C.** Results against A/mallard/Astrakhan/263/1982 H14pp; **D.** Results against A/shearwater/West Australia/2576/1979 H15pp.

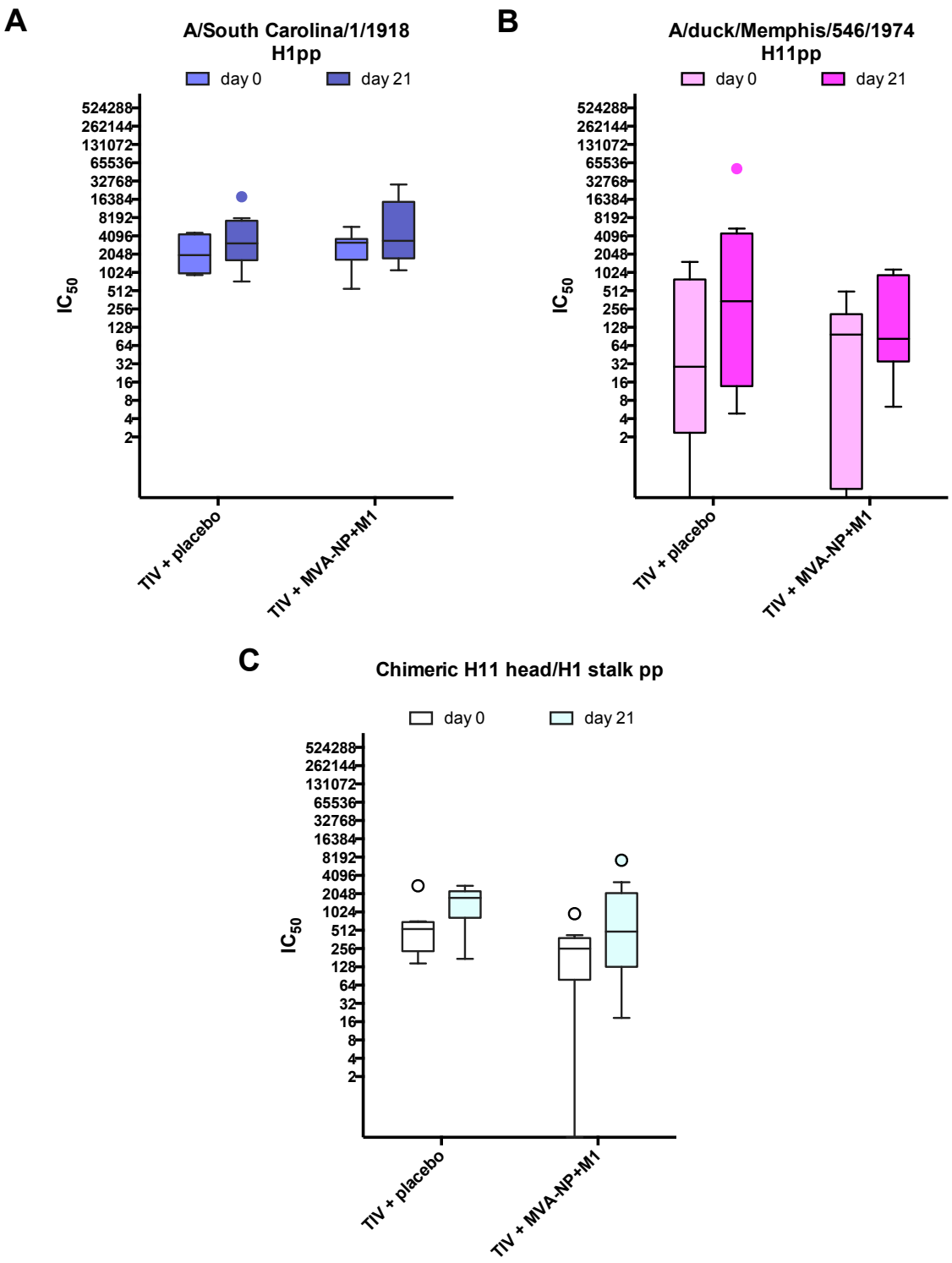

Figure 68: Comparison of TIV + placebo and TIV + MVA-NP+M1 vaccine combinations using pp-NT IC_{50} (4)

IC_{50} measured pre- and post-vaccination and stratified considering the vaccine combinations from NCT00942071 clinical trial were reported on Box-and-Whisker plots for comparison. Quartiles and medians of the distributions are reported in Appendix Table 5. **A.** Results against A/South Carolina/1/1918 H1pp; **B.** Results against A/duck/Memphis/546/1974 H11pp; **C.** Results against H11 head/H1 stalk chimeric HA peudotype.

Table 25: SCRs using cut-off values of 4-fold IC_{50} ($SCR_{(4\text{-fold})}$) or 2-fold IC_{50} increase ($SCR_{(2\text{-fold})}$)

	TIV + placebo n=8				TIV + MVA-M1+NP n=9				TOTAL n=17			
	$SCR_{(2\text{-fold})}$		$SCR_{(4\text{-fold})}$		$SCR_{(2\text{-fold})}$		$SCR_{(4\text{-fold})}$		$SCR_{(2\text{-fold})}$		$SCR_{(4\text{-fold})}$	
	%		%		%		%		%		%	
Group 1 strains												
A/New Caledonia/20/1999 H1	0	(0/8)	0	(0/8)	0	(0/9)	0	(0/9)	0	(0/17)	0	(0/17)
A/South Carolina/1/1918 H1	37.5	(3/8)	25	(2/8)	33.3	(3/9)	22.2	(2/9)	35.3	(6/17)	23.5	(4/17)
A/Korea/426/1968 H2	12.5	(1/8)	0	(0/8)	11.1	(1/9)	0	(0/9)	11.8	(2/17)	0	(0/17)
A/Viet Nam/1194/2004 H5	75	(6/8)	12.5	(1/8)	66.7	(6/9)	33.3	(3/9)	70.6	(12/17)	23.5	(4/17)
A/turkey/Turkey/1/2005 H5	37.5	(3/8)	12.5	(1/8)	33.3	(3/9)	0	(0/9)	35.3	(6/17)	5.9	(1/17)
A/Hong Kong/1073/1999 H9	50	(4/8)	50	(4/8)	77.8	(7/9)	44.4	(4/9)	64.7	(11/17)	47.1	(8/17)
A/duck/Memphis/546/1974 H11	62.5	(5/8)	62.5	(5/8)	66.7	(6/9)	66.7	(6/9)	64.7	(11/17)	64.7	(11/17)
Group 2 strains												
A/Udorn/307/1972 H3	25	(2/8)	0	(0/8)	55.6	(5/9)	0	(0/9)	41.2	(7/17)	0	(0/17)
A/Wisconsin/67/2005 H3 (A/Udorn/307/1972 N2)	62.5	(5/8)	37.5	(3/8)	88.9	(8/9)	77.8	(7/9)	76.5	(13/17)	58.8	(10/17)
A/duck/Czechoslovakia/1956 H4	12.5	(1/8)	0	(0/8)	0	(0/9)	0	(0/9)	5.9	(1/17)	0	(0/17)
A/Shanghai/2/2013 H7	0	(0/8)	0	(0/8)	11.1	(1/9)	0	(0/9)	5.9	(1/17)	0	(0/17)
A/chicken/Germany/N49 H10	25	(2/8)	0	(0/8)	33.3	(3/9)	22.2	(2/9)	29.4	(5/17)	11.8	(2/17)
A/mallard/Astrakhan/263/1982 H14	0	(0/8)	0	(0/8)	22.2	(2/9)	0	(0/9)	11.8	(2/17)	0	(0/17)
A/shearwater/West Australia/2576/1979 H15	12.5	(1/8)	0	(0/8)	44.4	(4/9)	22.2	(2/9)	29.4	(5/17)	11.8	(2/17)
Chimeric haemagglutinin												
H11 head/H1 South Carolina stalk	62.5	(5/8)	37.5	(3/8)	55.6	(5/9)	44.4	(4/9)	58.8	(10/17)	41.2	(7/17)

SCRs were also calculated and reported in **Table 25**. Using chi-squared statistics to compare the $SCR_{(4\text{-fold})}$ and $SCR_{(2\text{-fold})}$ between the two vaccine groups, a statistically significant difference was identified for the $SCR_{(2\text{-fold})}$ ($\chi^2 = 4.416$, df = 1, p = 0.0356) but not for the $SCR_{(4\text{-fold})}$ ($\chi^2 = 1.670$, df = 1, p = 0.1962). These, along with the fold-increase results previously evaluated, could indicate that that MVA-NP+M1 vaccine increases the responses of subjects that usually have a low response to the traditional vaccine, or that influenza immune responses differ from those induced by classic TIV.

These last two analyses have shown that differences were not present between the TIV + placebo and TIV + MVA-NP+M1 vaccine combinations, however since the number of participants in the clinical trial was limited and some dissimilarities were identified between the two groups, bigger differences could be identified if a diverse study with a larger number of subjects in which individuals have more specific characteristics (e.g. low pre-vaccination neutralizing titre) will be designed.

5.4 Discussion and Conclusion

In the recent years it has become clear that antibodies that are able to neutralize different influenza virus subtypes can be generated in animal models, exist in nature and can be isolated in humans (Friesen *et al.* 2014; Dreyfus *et al.* 2012; Corti *et al.* 2011; Ekiert *et al.* 2011; Sui *et al.* 2009; Throsby *et al.* 2008; Okuno *et al.* 1993). The discovery of these antibodies has stimulated investigations into their frequency, characteristics, and how they are generated, with a view to designing new vaccine strategies that can stimulate them. However, one of the problematic aspects in the study of these responses is to identify appropriate diagnostic and serological tools. As already reported in Section 1.8, classical assays such as HI and SRH are frequently used in seroepidemiological and vaccine immunogenicity studies. These two assays are extremely useful to charachterize influenza directed antibodies responses but have drawbacks when applied to the evaluation of cross-reactive antibodies: HI is unable to detect antibodies directed against the HA stalk, whereas SRH could potentially detect these antibodies but only if they are of specific Ig classes (i.e. the ones that can activate the complement system). Furthermore, if sera are not properly pre-adsorbed, SRH can also detect antibodies that recognise internal proteins, which can be the cause of detected cross-reactivity since they are more conserved between different influenza strains.

In contrast, MN and influenza pp-NT assay have been successfully applied to identification and characterisation of broadly-reactive mAbs directed against the HA and to study immunological response to natural infection and vaccines (Corti *et al.* 2010; Alberini *et al.* 2009; Garcia *et al.* 2009; Temperton *et al.* 2007). However, studies on the breadth of

the cross-reactive response have been predominantly focused on seasonal and potentially pandemic (H5, H7 and H9) strains. Evaluation of serological responses against other avian influenza viruses is usually limited to defined populations (such as farmers and animal workers) and often performed using HI assay, which does not give information on the cross-reactive HA stalk-directed antibodies (Oshansky *et al.* 2014; G. C. Gray *et al.* 2011; Kayali *et al.* 2011).

To address this issue, a study using pp-NT assays was implemented using a panel of HA subtypes representative of avian and human viruses, to detect the antibody response pre- and post-seasonal vaccination. Two collections of pre- and post-vaccination sera (2007-2008 vaccination study and NCT00942071 clinical trial (Antrobus *et al.* 2013)) were tested using a broad panel of influenza pp in neutralization assays to assess whether cross-reactive antibody responses can be detected in the human populations and, if present, whether they can be boosted by current seasonal vaccination. Furthermore using different HA subtypes the breadth of the response was also evaluated.

The results reported here indicate that pp-NT assays are able to detect different magnitudes of neutralizing antibody responses against human and avian influenza viruses pre-vaccine administration. Considering the age and the geographical origin of the two populations tested, it is unlikely that these people have been in contact or were infected by avian influenza viruses harbouring HAs antigenically-related to some of the HAs tested (such as H4, H7, H9, H10, H11, H12, H14, and H15) and for this reason it is likely that a cross-reactive antibody response is responsible for the measured IC_{50}.

However, it should be noticed that some of the H1, H2 and H3 strains used in pp-NT have previously circulated in the human population: in fact A/New Caledonia/20/1999 (H1N1) abundantly circulated from 1999 to at least 2006, A/South Carolina/1/1918 is the prototype for the 1918 influenza pandemic but related viruses have circulated until 1957, H2 viruses circulated between 1957 and 1968, A/Udorn/307/1972 H3 is from a virus isolated 40 years ago. Probably at least part of the population tested (elderly >60 years old and/or the older subjects in the adult group in the 2007-2008 seasonal vaccination study, and the clinical trial subjects) could have been naturally infected by these viruses or by antigenically-related viruses and thus the responses detected could be partially explained. Furthermore for the 2007-2008 vaccination studies in which it was possible to analyse the neutralizing antibody response for the vaccine strains prior to vaccination, high neutralization titres were detected against A/Solomon Islands/3/2006 H1 and A/Wisconsin/67/2005 H3: this can only be explained if cross-reactive antibodies are being detected, since these viruses did not circulate abundantly previously.

At this point it is fundamental to understand which HA epitopes are involved in this cross-reactivity. For H1 and H3, since common epitopes between the HA head exist, antibodies that can neutralize more than one strain could be present (R. Xu *et al.* 2010; Yamashita *et al.* 2010), but between different HA subtypes the head variation is bigger. Since the HA stalk is the most conserved region between the different HAs tested, the response measured here against non-seasonal strains (such as H4, H7, H9, H10, H11, H12, H14, and H15) are probably mediated by stalk-directed cross-neutralizing antibodies in the majority of cases.

Recently it has been shown that the use of chimeric HAs on pp or virus surfaces is a useful tool to study cross-reactive antibody responses and, more precisely, antibody directed against the HA stalk region (Hai *et al.* 2012; Pica *et al.* 2012). For this reason, in this study a pp harbouring a chimeric HA was generated and used in neutralization assays. The use of a chimeric HA in neutralization assays has permitted the delineation of cross-reactivity firstly mediated by stalk-directed antibodies and secondarily by head-directed antibodies.

In the 2007-2008 study, comparing pre-vaccination neutralization titres with post-vaccination values has shown statistically significant differences. It also showed that heterosubtypic antibody responses are partially boosted during seasonal vaccination. In fact with the exception of A/Vietnam/1194/2004 and A/chicken/Germany/N49 H10, increases in antibody responses are always detected, with SCRs that can exceed 40% when the 4-fold increase cut-off is used.

This is not the first time that seasonal vaccination has been reported to induce cross-reactive antibodies: in the past it was shown that mAbs that neutralize different Group 1 viruses can be isolated after seasonal vaccination (Corti *et al.* 2010) and that seasonal vaccination can induce antibodies and T-cell responses that cross-neutralize H5 viruses (Ding *et al.* 2011; Gioia *et al.* 2008). Furthermore a recent longitudinal study (M. S. Miller, Gardner, *et al.* 2013) has shown that influenza antibodies against previously encountered strains increase over time and that cross-reactive stalk antibodies increase even in the absence of an antigenic shift, which is considered the major stimuli for generation of the heterosubtypic antibody subsets (Pica *et al.* 2012; Palese and T. T. Wang 2011). The increase in stalk-directed cross-reactive antibody responses post-seasonal vaccination described here mirrors the one observed by Miller, Gardner, *et al.* over a more expanded period of time. Unfortunately precise age information, vaccination and medical history of the subjects were not known in the 2007-2008 study and it is not possible to perform an epidemiological study breaking down the data into specific subject age and seasonal strains encountered.

However, the increase in antibody responses observed could be explained not only by the boosting of an already present immune response. An interesting hypothesis, considering that the pp-NT assay is a potency assay[8], is that the higher response detected post-vaccination could be mediated by the 'affinity maturation' of the pre-existing antibodies following seasonal vaccination, and to a consequential increase in the potency of these antibodies, more than merely an increase in quantities of the same. Different studies have now shown that a small number of somatic mutations in germline antibodies with low HA binding activity are required for the acquisition of a stalk-directed broad-neutralization activity (Avnir *et al.* 2014; Pappas *et al.* 2014; Lingwood *et al.* 2012; Corti *et al.* 2011).

Another important finding in the 2007-2008 vaccination study, was that pre-vaccination neutralizing antibody responses, when significant, were higher in adults compared to the elderly, but usually these responses resulted in the equivalent magnitude post-vaccine administration. This can be explained by the decline of the antibody response in the elderly (N. Lee, Shin and I. Kang 2012; Weksler and Szabo 2000). Surprisingly in the elderly population it was observed that the post-vaccination titres against all subtypes increase more than the antibody response in the 18-60 group. The elderly are usually less able to generate antibody responses against newly encountered epitopes since B-cell diversification is lower in the elderly than in the young (Weksler and Szabo 2000). Also the decreasing of $CD4^+$ and $CD8^+$ naïve cell population with aging impairs the ability to mount an immune response against new antigens (N. Lee, Shin and I. Kang 2012). However, their antibody responses were high and broad post-vaccination: this could be explained by the fact that seasonal vaccination in the elderly does not create new antibodies, but can recall memory responses directed against conserved or semi-conserved epitopes. This highlights the seasonal vaccination importance in this high-risk population since it can potentially confer a partial protection to unmatched-vaccine viruses through cross-reactivity.

The other set of sera that was evaluated was collected during the NCT00942071 clinical trial (Antrobus *et al.* 2013). In this trial the effect of a trivalent vaccine containing antigens was evaluated in the absence or presence of a co-administration of a MVA-NP+M1 vaccine. Firstly the total effect of the trivalent vaccination was evaluated and subsequently the effect of the co-administration.

[8] A potency assay is an assay that permits to evaluate the activity of a biological substance: the pp-NT evaluates the biological (neutralization) activity of an antibody mixture. The neutralization activity is dependent on the quantity and on the affinity of the antibodies present in the mixture (Klasse and Sattentau 2002). For this reason when an increase in the activity is detected, it could be related to an enrichment of antibody quantities and/or to a change in the affinity of the antibody mixture.

Different research groups have demonstrated that H1N1 2009 pandemic infection and vaccination has generated a higher cross-reactivity response by inducing stalk-directed antibodies (Mahallawi *et al.* 2013; Sangster *et al.* 2013; Krammer *et al.* 2012; Pica *et al.* 2012; Perera *et al.* 2011; W. Wang *et al.* 2011). Here, analysing the antibody response against different human and avian strains, antibodies neutralizing previously encountered strains (e.g. H1, H2, and H3) and avian strains were detected, but only in certain cases were these antibodies boosted post-vaccination. Statistically significant increases were detected only for the two H3 stains, for the A/Vietnam/1194/2004 H5pp, for A/South Carolina/1/1918 H1pp, A/Shanghai/2/2013 H7pp, H9pp and H11pp. These data in part seem to contradict previous findings that vaccination with pandemic 2009 HA confers high cross-reactive antibodies, since the 2007-2008 seasonal vaccination seems here to result in higher and broader responses. The use of chimeric HA demonstrates that stalk-directed antibodies were boosted, however the increase does not appear to be as high as in the other study. It could be that different antibodies were boosted in these two studies: for example in the NCT00942071 clinical trial they could be directed versus certain subtypes (e.g. Group 2) and not against others, as heterosubtypic antibodies with different specificity exist (Ekiert *et al.* 2011; Ekiert *et al.* 2009; Throsby *et al.* 2008; Varecková, N. Cox and Klimov 2002). To test this hypothesis it would be interesting to generate and use a different chimeric HA in pp-NT assays, for example a Group 2 chimeric HA, since high cross-reactive titres were detected against H3 strains after vaccination.

In the NCT00942071 clinical trial a MVA-NP+M1 vaccine was also co-administered in nine subjects to induce a T-cell response together with an antibody response. MVA is a modified and highly attenuated smallpox vector, that can transduce different cells, including DCs, and permits the expression of the protein of interest and the subsequent presentation of peptides *via* MHC molecules. This enhances and induces $CD8^+$ and $CD4^+$ T-cell responses. Influenza MVA-based vaccines have been shown to be able to induce $CD8^+$ and $CD4^+$ T-cell responses, and humoral responses, depending on the proteins that are expressed (e.g. HA, NA, NP) (Rimmelzwaan and Sutter 2009).

Recently the administration of MVA alone or MVA-NP+M1 has been shown also to be able to induce an adjuvant effect on antibody response (Mullarkey *et al.* 2013; Berthoud *et al.* 2011). Since other adjuvants (e.g. MF59) have been shown to have an effect in enhancing and broadening the antibody response (Khurana *et al.* 2014; Banzhoff *et al.* 2009), it would be interesting to evaluate if MVA-NP+M1 has an effect on heterosubtypic HA-directed antibody responses.

In this study, as already highlighted in Antrobus et al., with MVA-NP+M1 vaccine significant variations in the antibody titres post-vaccination compared to placebo were not

detected. Only when A/Wisconsin/67/2005 H3pp and H15pp were tested, increasing neutralizing titres were detected following MVA-NP+M1 vaccine administration. Nevertheless, analysis of the SCRs has highlighted the possibility of differences between placebo and MVA-NP+M1 vaccine that could have been too small to be detected by non-parametric tests (in relation to the statistical power and the limited number of subjects analysed) and thus further studies will be necessary to understand the possible effect of the MVA-NP+M1 co-administration.

The adjuvant effect of MVA-NP+M1 vaccine did not generate high variation in the HA-directed heterosubtypic cross-reactive responses in comparison to the placebo administration; however this vaccine could have generated other classes of cross-reactive antibodies, which were not evaluated in this study. For example, antibodies against the NP could have been induced and should be evaluated. NP is more conserved than the envelope proteins since it is internal to the virion and therefore less subject to selective pressures. In fact, antibodies against NP have been shown to have an important role *in vivo* conferring protection against influenza virus infection (LaMere *et al.* 2011; Carragher *et al.* 2008; Zheng *et al.* 2007). These antibodies do not possess neutralization activity and the mechanism by which they confer protection is not yet clear, but it is believed to have a role in enhancement of DC function and interaction with T-cell responses (LaMere *et al.* 2011; Carragher *et al.* 2008; Zheng *et al.* 2007).

In contrary to past studies in which HA cross-reactive antibodies were considered extremely rare (Grebe, Yewdell and Bennink 2008), the two studies presented here show that cross-reactive antibody responses could be more frequent in the human population than was previously believed. Similar findings are becoming more common now that methodologies (e.g. isolation of mAbs and plasma cells, pp-NT, chimeric HA ELISA) able to detect stalk-directed antibodies are becoming more widely used (Molesti, Ferrara, *et al.* 2014; M. S. Miller, Gardner, *et al.* 2013; Wrammert *et al.* 2011; Labrosse *et al.* 2010). Nevertheless the frequency of these antibodies is still controversial. The possibility of multiplexing (Molesti, Wright, *et al.* 2014) and automatisation the pp-NT assay should be investigated (see Chapter 7) since this will permit the evaluation of responses against more subtypes simultaneously. Also testing of larger panels of samples would permit the verification of the real frequency of these cross-reactive antibodies in the human population.

It is also possible that geographical origin of the analysed subjects could play an important role in explaining the dissimilarity observed in different studies. This may also determine the basal level of certain cross-reactive antibodies: in fact in different regions of the world different pathogens and immunological stimuli (e.g. vaccine, allergens) are

encountered at different times during the human lifespan, and that alone can shape the immune system in different ways (Kucharski and Gog 2012). Also genetic polymorphisms could play a role in modulating the antibody response: for example it is now accepted that the majority of cross-neutralizing antibodies against influenza HA uses the variable heavy chain segment VH1-69. Furthermore, it was shown how a polymorphism in the germline version of this locus could impair the generation of stalk-directed antibodies (Pappas *et al.* 2014; Lingwood *et al.* 2012). Since other cross-reactive antibodies use different segments, it is important that studies focusing on evolution of antibodies from the germlines are performed and it is also essential that genome-wide association studies are implemented. This is not only to identify important factors in influenza susceptibility and pathogenesis (Everitt *et al.* 2012; Zhou *et al.* 2012), but also to highlight genetic factors that could explain differences in immune responses between individuals.

These studies have shown that cross-reactive antibody responses can be detected in the human population. However, the detection of cross-reactive antibodies through pp-NT assays does not give information on possible protection that they can mediate. In fact correlates of protection are not established for pp-NT, and in the literature there is only one report in which a cut-off value was calculated using correlation with MN for H5 viruses (Alberini *et al.* 2009). It is unlikely that the same cut-off could be used for other influenza strains, as the correlation experiment with SRH described here demonstrates that correlation coefficient varied in relation to the antigen tested. However, the need for clinical trials to evaluate 'universal' vaccines (Krammer and Palese 2014) and the fact that only with MN and pp-NT is it possible to evaluate efficiently stalk-directed antibodies, could permit the establishment of a cut-off for this assay in the future.

Recently stalk-directed neutralizing antibodies have been shown to be able to mediate protection from influenza infection in the mouse model engaging the Fcγ receptors (DiLillo *et al.* 2014), and also this will be need to be evaluated in the future as an explanation as to why numerous mAbs show an enhanced activity *in vivo* than *in vitro*.

It is also important to bear in mind possible bias in the data presented here. Firstly, as already discussed in Chapter 4, the pp-NT assay was performed normalising on the basis of the transduction activity (RLU) of each pp and not on the basis of HA content. Secondarily the populations analysed are of limited numbers. Especially when analysing stratified data in the 2007-2008 vaccination study, populations had been reduced and statistical power was lost due to the Bonferroni correction, resulting in the absence of statistical significance in presence of a graphical difference when comparing pre- and post-vaccination neutralization titres. However, since a conservative approach was used in the statistical analysis, overall the data strongly suggest that influenza seasonal vaccination

is able to mediate the increase of heterosubtypic antibody responses in certain cases. Similar studies with a larger population sample size will need to be undertaken to finally confirm and to improve understanding of the heterosubtypic responses detected here.

Furthermore in these two studies, certain factors were not controlled or investigated. For example, the effect of sera pre-treatment was not considered. The sera from the 2007-2008 vaccination study, being previously used for SRH, were subjected to complement inactivation, whereas the sera from the NCT00942071 clinical trial were not. This could potentially explain differences between the two studies. Additionally, the treatment of sera with receptor destroying enzymes was also not investigated. This treatment is necessary in HI and MN to avoid the detection of aspecific inhibiting and neutralizing responses caused by non-specific inhibitors such as sera lectins. The absence of this treatment could be the factor underlying the high neutralization responses here detected and should be considered for future optimization and validation of pp-NT (see Chapter 7)

Another important factor that was not controlled for in the experimental design is that in the current study pp producer cell lines, target cells and sera are all of human origin. For classical neutralization assays that are usually performed using MDCK cells as virus producer cells and as target, concerns about this usually do not exist but this cell line is of canine origin. In the pp-NT assays performed, all the components are of the same origin (i.e. human) and it is not clear if neutralization titres could be affected, but should be a concern and investigated in future. For example, it is possible that antibodies against phospholipids, or other antibodies could interfere in the neutralization process causing an overestimation of the neutralization titre. Some authors perform neutralization assays against non-related pp (e.g. VSV-G, HIV-1 or Hepatitis C pp) to avoid possible problems of non-specific neutralization: this method is highly valid but it is better and necessary to know the immunological status of the subject with respect to the control virus.

If the findings presented here are confirmed by further serological testing in larger populations, they could have important implications for seasonal vaccination and vaccine development. For this purpose it will also be necessary to understand whether stalk antibodies exclusively mediate the heterosubtypic HA-directed responses and which HA epitopes are shared between different subtypes. For example, antibodies recognising the RBS have shown homosubtypic and heterosubtypic neutralization activity (Whittle *et al.* 2011). Adding data about the response at the single B-cell level, differentiating between memory responses and plasma cells, and isolating mAbs can be also useful for this purpose. Slight modifications of the pp-NT assay, involving increasing incubation times and the amount of the samples tested, could be effectively used to test antibody content in

the medium of isolated and cultured cells (Mahallawi *et al.* 2013), permitting these types of experiments to be performed easily.

The use of bioinformatic approaches can also represent a useful tool to analyse neutralization data and design precise experiments. Simple alignments can permit the identification of conserved regions; more complex approaches, involving the analysis and comparison of antibody-HA binding complex to identified residues subjected to immunological pressure and/or the prediction of the regions subjected to evolutionary pressure evaluating the prevalence of circulating strains (Wikramaratna *et al.* 2013; Sivalingam and Shepherd 2012; Lees, Moss and Shepherd 2011), can also give information that can be used to study precise epitopes, especially if conformational.

It is shown here that a pp-NT assay performed with a panel of pp is a useful, safe and simple tool to study cross-reactive antibody responses, and that a chimeric HA pp-NT assay is useful to discriminate if the cross-reactive antibody responses are directed against the HA stalk or head region. However, other modifications of the pp-NT assay could be additionally useful to confirm whether the cross-reactive antibodies are directed against the stalk and to finely characterise the epitopes that are involved. Post-attachment neutralization assay has also shown the ability to differentiate stalk-directed antibodies from head-directed antibodies (Edwards and Dimmock 2001) and could be used to confirm the presence of stalk antibodies. Another possible approach could be the use of chimeric HA, or HA pp bearing mutated HA stalks mimicking the one of broadly neutralizing mAbs escape-mutant viruses. This latter approach may also give precise information about the epitopes recognised: if the antibodies that present in the serum recognise the same epitopes of broadly neutralizing mAbs, serum will not be able to neutralize the mAb escape-mutant HA pp.

To conclude, the studies here described represent the first employment of a comprehensive panel of influenza pp to detect heterosubtypic antibody responses pre- and post- influenza seasonal vaccinations in human populations. Furthermore the use of a chimeric HA has permitted the origin of the cross-reactive response detected to be established: it is primarily mediated by antibodies directed against the HA stalk region but heterosubtypic or homosubtypic responses directed against the HA head could be present and need further investigation. In general, the data presented here highlight that the knowledge on influenza cross-reactive response is still lacking and even if it has notably improved over the last twenty-five years, more systematic studies are still necessary to understand the complex interaction between immune system and influenza viruses.

CHAPTER 6
Production of influenza B haemagglutinin lentiviral pseudotype particles and their use in neutralization assays

6.1 Introduction

It is generally accepted that influenza A virus represents a health burden that needs to be monitored by surveillance and prevented using vaccination. However, influenza A virus is not the only virus that causes seasonal influenza epidemics in the human populations. In fact, influenza B viruses cause, especially in children and young adults, respiratory disease with intermediate but significant mortality rates in comparison to influenza A (pandemic H1N1 and H3N2 influenza A infections were usually associated with higher mortality rates but seasonal H1N1 infection had lower mortality rates than influenza B infection in the last 20 years) (Glezen *et al.* 2013; Ellis *et al.* 2011; W. W. Thompson *et al.* 2003; P. F. Wright, Bryant and Karzon 1980). Influenza B death, when occurring, is extremely rapid and frequently, but not exclusively, associated with myocarditis or with pneumonia caused by bacterial superinfection (Rein *et al.* 2014; Paddock *et al.* 2012; Frank *et al.* 2010; Yusuf, Soraisham and Fonseca 2007).

Influenza B virus (prototype virus B/Lee/40) was first isolated after a human epidemic in 1940, but was demonstrated to have caused epidemics from at least 1936 (Francis 1940) and since then it has continued to cause cyclic seasonal epidemics.

After years in which the influenza B burden has been underestimated by the clinical and public-health community, recently it has become evident that it is necessary to raise awareness of influenza B virus infection, especially by increasing epidemiological surveillance and seasonal vaccination coverage (Glezen *et al.* 2013). An influenza B strain is routinely included in the seasonal vaccine, but frequently the strain presented in the trivalent vaccine had not matched the circulating strain, leaving the population (usually the high-risk one) unprotected (Dolin 2013). This is partially due to the fact that, in the late 1970s, a large-scale genomic reassortment event involving all eight influenza B segments led to the generation of two distinct influenza B lineages: the Victoria lineage (prototype virus B/Victoria/2/1987) and the Yamagata lineage (prototype virus B/Yamagata/16/88) (R. Chen and Holmes 2008; Rota *et al.* 1990). These two lineages

continue to diverge, are subject to reassortment, and to co-circulation, even if one tends to dominate over the other for a determinate period of time (R. Chen and Holmes 2008).

To resolve the vaccine mismatch issue, quadrivalent vaccines containing one representative strain for each influenza B lineage together with the influenza A H1N1 and H3N2 viruses were developed and were recently licensed (Tinoco *et al.* 2014; Beran *et al.* 2013; Pepin *et al.* 2013). Despite the improved vaccine coverage, epidemiological surveillance and rigorous vaccine testing are still needed (Eichner *et al.* 2014; Beran *et al.* 2013).

The use of serological methods for the evaluation of influenza epidemiological distribution and vaccine immunogenicity was already discussed in Chapter 1. Unfortunately, there are concerns when classical serological assays are used for influenza B epidemiological studies and vaccine evaluation. In fact, several authors have independently shown that the classical HI assay is insensitive for the measurement of seroconversion, since it routinely underestimates antibody titres in comparison to SRH (Wood *et al.* 1994; G. Mancini *et al.* 1983; Oxford, Yetts and Schild 1982). Ether-treatment of the antigen (virus) during HI was shown to increase sensitivity (Pyhälä, Kleemola and Visakorpi 1985; Kendal and Cate 1983; Monto and Maassab 1981), however this increase is insufficient to attain SRH and MN consistency (Ansaldi *et al.* 2004; Kendal and Cate 1983; G. Mancini *et al.* 1983).

Furthermore, with the evidence that antibodies that are able to neutralize the two influenza B lineages and, in some cases, also influenza A viruses (CR9114, pan-neutralizing mAb) could exist in humans (Yasugi *et al.* 2013; Dreyfus *et al.* 2012), interest in studying the cross-neutralizing response from an influenza B perspective has increased. In this case, classic serological methods do not provide assistance, since they usually do not detect HA stalk-directed antibodies (Dreyfus *et al.* 2012; Corti *et al.* 2011; Ekiert *et al.* 2011; Ekiert *et al.* 2009; Sui *et al.* 2009; Okuno *et al.* 1993), as mentioned in the previous chapter.

Since pp are useful tools to study heterosubtypic antibodies, with the know-how acquired during the production of influenza A HA pp (Chapters 2 and 3) it was decided to produce a panel of influenza B HA pp. These newly developed influenza B reagents, which have hitherto not been reported in the literature, were then investigated for their feasibility of use as surrogate antigens in neutralization assays and to study cross-neutralizing antibody responses.

6.2 Materials and Methods

6.2.1 Cloning B/Brisbane/60/2008 and B/Bangladesh/3333/2007 haemagglutinins into the pI.18 expression vector

In order to clone influenza B HAs, influenza B cDNA and HA sequences of B/Bangladesh/3333/2007 (Accession number: CY115255.1) and B/Brisbane/60/2008 (Accession number: FJ766840.1) were kindly provided by Prof. Paul Kellam (Wellcome Trust Sanger Institute, UK).

An outline of the cloning protocol used is reported in **Appendix Figure 18** as a flow chart. In this chapter the detailed cloning protocol and results are given.

6.2.1.1 Primer design

Primers to amplify influenza B HA were designed using the protocol outlined in Section 3.2.2: inclusion of a GC-rich flanking region to facilitate restriction digestion, appropriate restriction enzyme cleavage sites, influenza A Kozak sequence (GTCAAA) and sequence of the HA 5' end encoding region (Fw primer), or reverse complement stop codon, influenza A termination sequence (ATT) and reverse complement HA 3' end encoding sequence (Rev primer). Considering the high titre pp obtained using the influenza A Kozak sequence, it was decided to evaluate this sequence instead of a putative influenza B Kozak in the first instance (Section 6.2.2) Since the Influenza B strains used have 100% nucleotide identity in the region used to design the primers, HA 5' and 3' end encoding sequences (**Appendix Figure 19**), only one set of primers was designed to permit HA amplification (**Table 26**).

Table 26: Primer names, restriction enzyme, and primer sequences used for Influenza B HA cloning into p.I.18 vector
Within the sequences, restriction enzyme cleavage sites are reported in red, influenza Kozak sequence in bold, 5' end HA sequence in green, the influenza A termination sequence in bold and italics, the reverse complement stop codon (UAA) in pink, and 3' end HA reverse complement sequence in blue.

Primer name	Primer sequence (5' to 3')	Restriction enzyme
FluB_*SalI*_Fw	GCGCGCGTCGAC**GTCAAA**ATGAAGGCAATAA	*SalI*
FluB_*EcoRI*_Rev	GCGCGCGAATTC***AAT***TTATAGACAGATGGAGCA	*EcoRI*

6.2.1.2 Polymerase chain reactions

A gradient PCR using *PfuUltra* High-Fidelity DNA Polymerase was performed for each Influenza B HA as previously described in Section 2.1.8.2 using 2 µl/reaction of cDNA template, previously diluted 1:50, and a range of annealing temperatures of 48.2°C, 49.3°C, 52.6°C and 54.8°C.

Before proceeding to PCR purification, the PCRs were checked for successful amplification by agarose gel electrophoresis as described in Section 2.1.12 (**Figure 69A**).

Since on first attempt HA amplification was not observed, the gradient PCR was repeated, increasing the amount of cDNA template (10 µl/reaction) previously diluted 1:50, and decreasing the water volume to maintain the same PCR volume. HA specific amplification was checked on a 1% agarose-TAE gel (**Figure 69B**).

From the positive PCR results, the sample obtained using the highest annealing temperature (for better primer specificity) was selected for purification and further processing. The other PCRs were stored at -20°C as backups.

6.2.1.3 PCR product and vector digestion using restriction endonucleases

After PCR purification using QIAquick PCR purification kit (Section 2.1.11), 627.6 ng B/Brisbane/60/2008 and 515.2 ng of B/Bangladesh/3333/2007 PCR products were digested in a reaction volume of 20 µl for 2 h at 37°C using 10 U *EcoRI* (Thermo Fisher Scientific, cat.no. ER0271) and 10 U *SalI* (Thermo Fisher Scientific, cat.no. ER0641) in 1X Buffer O (Thermo Fisher Scientific, cat.no. BO5), in which the two enzymes have 100% activity. Alongside the PCR product digestions, 1 µg of pI.18 vector was also digested for 2 h at 37°C using 10 U *EcoRI* and 10 U *SalI* in 1X Buffer O. After the incubations, the digestions were purified to remove enzymes and buffer salts, and were quantified by NanoDrop™.

6.2.1.4 Ligation

Ligation was performed using T4 DNA Ligase as previously described in Section 2.1.10: 20 ng of vector (pI.18 *EcoRI-SalI* digested, 4.3 kb) and 25 ng of insert (Influenza B HA *EcoRI-SalI* digested, 1.7 kb) were used for the 10 µl reactions, corresponding to a vector:insert ratio of 1:3.

After 72 h, 25 µl aliquots of chemically competent DH5α *E. coli* were transformed with 2.5 µl of control and ligation reactions following the standard transformation protocol (Section 2.1.3). Lastly, 100 µl of the ligation-transformed bacteria were plated on ampicillin-LB Agar plates.

6.2.1.5 Recombinant clone screening: colony PCR, digestion and Sanger sequencing

After overnight 37°C incubation of the ligation plates, 10 colonies for each HA strain (B/Bangladesh/3333/2007: B#1-B#10; B/Brisbane/60/2008: B#11-B#20) were screened by colony PCRs using pI.18 Fw and pI.18 Rev sequencing primers, as previously described (Section 2.1.11). HA positive (pI.18-A/Korea/426/1968 H2) and negative (pI.18) DH5α *E. coli* colonies were also included as colony PCR controls.

Positive colonies were inoculated in 5 ml of 100 µg/ml ampicillin-LB Broth and incubated overnight at 37°C with constant shaking (225 rpm). Plasmid preparation was then performed as described in Section 2.1.4. Subsequently 600 ng of plasmid DNA was digested by FastDigest® *EcoRI* (Thermo Fisher Scientific, cat.no. FD0274) in FastDigest® Green buffer for 20 min at 37°C before being run on 1% agarose-TAE gel (**Figure 71**).

The positive recombinant clones were sent for Sanger sequencing at GATC Biotech AG (Section 2.1.7) using pI.18 Fw and pI.18 Rev sequencing primers.

6.2.1.6 Site-direct mutagenesis of B/Brisbane/60/2008 to correct N212S mutation

The alignment of the cloned B/Brisbane/60/2008 HA shows a missense nucleotide mutation corresponding to the amino acid mutation N212S (**Figure 72 (A and B)**). Instead of repeating the cloning starting from the PCR (the mutation could have been inserted during cDNA amplification), it was decided to correct the mutation by performing mutagenesis on the cloned HA, since it could not be excluded that the mutation was inserted during the reverse transcription-PCR[9] (retro transcription of the extracted viral RNA into cDNA) and that the cDNA already contained the mutation.

To revert the mutation, the QuikChange Lightning Site-direct mutagenesis kit was used as described in Section 2.1.15.1. Primers were designed using the QuikChange Primer Design web-tool and are reported in **Table 27**.

Table 27: Primer names and sequences used for B/Brisbane/60/2008 HA mutagenesis
The primers were used to change the serine at position 212 to asparagine and correct the cloned B/Brisbane/60/2008 HA sequence. The primer annealing schematics are reported below the primer sequences. In these schematics primer sequences are in bold, gene sequence is in black, and in grey the translated gene sequence (5' to 3') corresponding to the primer (Fw) or the original gene (Rev) is shown. The nucleotide that corrects the mutation is highlighted in red in the primer sequence and in the schematic.

Primer name	Primer sequence (sequence in 5' to 3') and annealing schematic
S212N	TGGGGGTTCCACTCTGACAACGAGACCCAA W G F H S D N E T Q 5' **T G G G G G T T C C A C T C T G A C A A C G A G A C C C A A** 3' A A A C C C C C A A G G T G A G A C T G T C G C T C T G G G T T T A
S212N_Rev	TTGGGTCTCGTTGTCAGAGTGGAACCCCCA W G F H S D E T Q T T T G G G G G T T C C A C T C T G A C A G C G A G A C C C A A A T 3' **A C C C C C A A G G T G A G A C T G T T G C T C T G G G T T** 5'

[9] This is highly probable considering that RNA-dependent DNA polymerase has lower proofreading activity compared to *PfuUltra* High-Fidelity DNA Polymerase (and all DNA-dependent DNA polymerases in general).

6.2.2 Site-direct mutagenesis of B/Bangladesh/3333/2007 Kozak sequence to evaluate the role of the influenza B Kozak

Considering the importance of the Kozak sequence for expression of influenza A HA and pp production, and the fact that the 5' and 3' non-coding regions are highly conserved in the influenza B genome, it was decided to evaluate the role of the Kozak sequence in producing influenza B pp.

A putative influenza B Kozak sequence CACAAA that is highly conserved in the 5' non-coding region of Influenza B HA cDNA was identified using Clustal X (Larkin *et al.* 2007) and Jalview (Waterhouse *et al.* 2009) through multiple alignment of the first 100 nucleotides of the circulating influenza B segment 4 (i.e. HA), after downloading the sequences from the National Center for Biotechnology Information (NCBI) Influenza Virus Resource database (**Appendix Figure 20**).

The QuikChange Primer Design web-tool and the QuikChange Lightning Site-direct mutagenesis kit (Section 2.1.15.1) were again used to perform the mutagenesis and design the primers (**Table 28**).

Table 28: Primer names and sequences used for B/Bangladesh/3333/2007 Kozak sequence mutagenesis

The region of the primer that anneals to pI.18 is highlighted in green; the Kozak sequence is highlighted in red; the nucleotides that are modified to generate the influenza B Kozak sequence are in bold; the region of the primer that anneals to the HA 5' end encoding sequence is highlighted in blue.

Primer name	Primer sequence (5' to 3')
FluB_KozakFw	CTAGAAGATCTGATATCGTCGAC**CA**CAAAATGAAGGCAATAATTGTAC
FluB_KozakRev	GTACAATTATTGCCTTCATTTTG**TG**GTCGACGATATCAGATCTTCTAG

6.2.3 Preparation of other influenza B haemagglutinin-encoding plasmids

phCMV1-B/Hong Kong/8/1973 HA, phCMV1-B/Victoria/2/1987 HA, phCMV1-B/Yamagata/16/1988 HA, phCMV1-B/Florida/4/2006 HA plasmid clones were provided by Dr. Davide Corti (Institute for Research in Biomedicine, Bellinzona, Switzerland). Each expression plasmid encodes a codon-optimised HA gene flanked by the influenza A Kozak enabling its use in pp production. The plasmids were diluted 1:100 and 1 µl was used to transform DH5α *E. coli* as previously described (Section 2.1.3). Transformed colonies were inoculated in 5 ml kanamycin-LB Broth and were grown overnight at 37°C with shaking at 225 rpm; then plasmids were prepared using QIAprep Spin Miniprep Kit as described in Section 2.1.4.

6.2.4 Production of influenza B pseudotypes

Influenza B HA, like the influenza A HA, is synthesised as a polypeptide precursor that needs to be activated through cleavage by tissue-specific proteases that recognise a single conserved arginine. Exactly as implemented during the production and optimisation of influenza A pp (Chapter 3) to permit influenza B HA cleavage and activation, the three proteases HAT, TMPRSS2, and TMPRSS4 were evaluated by adding the encoding plasmid to 6-well transfection mixes of 750 ng of pCSFLW, 500 ng of p8.91, and 500 ng of the appropriate HA-encoding plasmid. Three protease plasmid quantities (500 ng, 250 ng and 125 ng) were tested for B/Bangladesh/3333/2007 pp, whereas only two quantities (250 ng and 125 ng) were used with the other influenza B pp. As controls, pp were also produced in the absence of proteases.

Furthermore to visualise the pp entry into target cell lines directly, influenza B pp expressing emerald GFP (emGFP) were also produced in 6-well plates: 750 ng of the self inactivating lentiviral vector encoding emGFP (pCSemGW, kindly provided by Prof. Greg Towers, University College London, UK), 500 ng of p8.91, 500 ng of HA-encoding plasmid and 250 ng of pCAGGS-HAT were used according to the optimisation results obtained. All the 6-well transfections were performed as previously described in Section 3.2.4.

6.2.5 Titration of influenza B pseudotypes

The newly generated pp were titrated on HEK293T/17 cells as outlined in Section 2.3.3; treatment with TPCK-Trypsin was also performed as previously described (Section 3.2.5) using a final TPCK-Trypsin concentration of 100 µg/ml.

Influenza B pp were also tested for their ability to enter into two further target cell lines: MDCK and A549.

Titrations of luciferase lentiviral pp onto MDCK and A549 were performed using the standard HEK293T/17 titration protocols (Section 2.3.3), maintaining the same quantity of virus and cells, and the same incubation time (48 h).

For evaluation of influenza B pp expressing emGFP, poly-lysine coated glass coverslips were positioned in the wells of a 24-well plate and covered with 5×10^4 cells (HEK293T/17, MDCK or A549) and 1 ml of cell-line specific culture media (Section 2.2.1). Then 300 µl of pp was added to each well. After 48 h, cells were removed from the incubator, washed with 1 ml of PBS (Sigma, cat.no. D8537), fixed with 1 ml of 4% (w/v) paraformaldehyde (Fisher Scientific, cat.no. P/0840/53) in PBS pH 7.4 for 15 min, and washed again with 1 ml of PBS. Cells were then incubated for 20 min at RT with 1 drop/ml NucBlue® Live ReadyProbes® reagent in PBS. Coverslips were then

washed again with 1 ml PBS and mounted on glass slides using 10 µl of Mowiol® 40-88 solution (Section 2.4.2).

6.2.6 Western blotting

To study the activity of the proteases on the pp HAs and confirm HA cleavage, a Western blot was performed using B/Brisbane/60/2008 pp since a suitable primary antibody, NIBSC 11/136 anti-B/Brisbane/60/2008 serum (NIBSC), was available.

Samples were prepared as described in Section 2.4.3.2 and in Section 3.1.9. To check HA activation, TPCK-Trypsin treatment on the Δ protease pp was accomplished mixing 45 µl of pp produced and 1 mg/ml TPCK-Trypsin to have a final concentration of 100 µg/ml.

Western Blotting was performed as described in Sections 2.4.3.2. The anti-B/Brisbane/60/2008 serum was used diluted 1:500 and a donkey anti-sheep/goat IgG Dylight®800 antibody diluted 1:20000 was used as secondary antibody to detect the sheep-origin antisera. The membrane was detected using the Odyssey® Sa Infrared Imaging System at 800 nm.

6.2.7 Pseudotype particle neutralization assays

B/Brisbane/60/2008, B/Hong Kong/8/1973, and B/Florida/4/2006 pp used for neutralization assays were produced in 10 cm dishes as previously described in Section 2.3.2.2 with the addition of 500 ng of HAT-encoding plasmid. Titration was performed according to the standard protocol (Section 2.3.3).

Firstly, the neutralization activity of a positive control NIBSC 11/136 anti-B/Brisbane/60/2008 serum was evaluated against the three different pp (B/Brisbane/60/2008, B/Hong Kong/8/1973, and B/Florida/4/2006) by performing pp-NT in quadruplicate (starting dilution 1:100 and pp input 1×10^6 RLU/well).

The human sera from clinical trial NCT00942071 (Antrobus *et al.* 2013) described in Section 5.1.2 were used to investigate the suitability of influenza B pp-NT assays in a vaccine immunogenicity study, to determine if the assay correlates with standard serological assays (e.g. HI), and to investigate if it is possible to detect cross-reactive responses to influenza B as observed for influenza A (Chapter 5). B/Brisbane/60/2007 HI data were kindly provided by Prof. Sarah Gilbert and Dr. Teresa Lambe (Jenner Institute, University of Oxford, UK). Using these sera, pp-NT assays against B/Brisbane/60/2008, B/Hong Kong/8/1973, and B/Florida/4/2006 were performed as previously described in Section 2.3.4 using 2 µl of sera (1:100 starting dilution) and 1×10^6 RLU/well pp input.

6.2.8 Statistical analysis

Statistical analysis for pp-NT assays was performed as previously described in Sections 2.3.4 and 5.2.5. IC_{50} titres were reported in Box-and-Whisker plots to allow a graphical comparison of the results; in the **Appendix Table 7** and **Appendix Table 8**, quartiles and medians of the IC_{50} distributions were also reported.

SCRs for pp-NT assays were also calculated on the basis of the percentage of subjects showing a $SCR_{(4\text{-fold})}$ or a $SCR_{(2\text{-fold})}$ in the IC_{50} titre at day 21.

Pearson correlation between the $\log_{10}$ HI assay titres and the $\log_{10}$ IC_{50} values was performed using GraphPad Prism®.

6.2.9 Bioinformatic analysis

Influenza B HA nucleotide sequences of genes used in the production of pp were used for a phylogenetic analysis. Firstly, HA-encoding sequences were downloaded from the Influenza Virus Resource database, then codon-based alignment was performed on the sequence using the MUSCLE algorithm (Edgar 2004) in MEGA (K. Tamura *et al.* 2011).

A Bayesian inference of phylogeny method was used to build the phylogenetic tree. This method allows the concurrent calculation of the phylogenetic tree and its credibility. The principles on which it is based are explained in a user-friendly but detailed manner by Huelsenbeck *et al.* 2001 and by Huelsenbeck, Rannala and Masly 2000. Here only a summary of the method will be reported.

The Bayesian statistical inference is based on the concept of posterior probability, which is the probability of an event occurring after taking into consideration relevant evidences, described by the prior probability. In phylogenetics, this is the probability of a given tree when considered in terms of the sequence alignment. For this reason, before performing Bayesian analysis, a fundamental requirement is to establish the evolutionary model based on the sequence alignment. The evolutionary models describe, through parameters, the rates with which one nucleotide replaces another during evolution. To find the best nucleotide substitution model, Jmodeltest (Posada 2008) was used: this software calculates the evolutionary model that best fits the sequence alignment evaluating a likelihood for each substitution model given the data in the alignment, and then comparing the likelihood of multiple models to determine the most likely model (Posada and Buckley 2004).

The Bayesian phylogenetic analysis was performed using Bayesian evolutionary analysis by sampling trees (BEAST) (Drummond *et al.* 2012; Drummond and Rambaut 2007) software package. The Hasegawa, Kishino and Yano (HKY) + Gamma model, which was determined as the best fit model by the Jmodetest analysis, was used as

nucleotide substitution model; furthermore the year of strain isolation was added as parameters to permit the software to evaluate the time-dependent rates of molecular evolution (molecular clock), calculate branch length and incorporate a time-scale in the tree. The Metropolis-Hastings Markov chain Monte Carlo (MCMC) algorithm at the basis of BEAST was then run. The first tree is generated randomly; then the algorithm generates a new tree changing a parameter, and accepts or rejects it based on its probability and the probability of the tree generated previously. The tree with the highest probability is then used for the next iteration of the algorithm. Every fixed number of iterations (e.g. 1000), the software saves the tree. In this way the algorithm evaluates different trees but with the increase of the iterations will tend to consider trees that are in a stationary phase of the probability distribution and that should be more similar to each other. Once a user-specified number (e.g. 10000000) of iterations is reached, the software stops.

Lastly, the maximum clade credibility tree was calculated by the software discarding (burn-in) the first 25% of saved trees, which for the characteristics of the algorithm used are usually more divergent between each other, and using a majority-rule to combine the remaining trees. Posterior probability for each tree node are then calculated on the basis of how many trees analysed have that node. The maximum clade credibility tree generated was then graphically elaborated adding colour and formatting with FigTree (http://tree.bio.ed.ac.uk/software/figtree/).

The HA amino acid sequence of B/Brisbane/60/2008, B/Hong Kong/8/1973 and B/Florida/4/2006 were aligned using MUSCLE algorithm (Edgar 2004) in Jalview (Waterhouse *et al.* 2009), and non-conserved amino acids were highlighted using the Zapo colour system[10]. The alignment was then manually annotated. Percentages of identity between amino acid sequences were calculated by pair-wise alignments using Jalview.

B/Brisbane/60/2008 HA structure (PDB ID: 4FQM (Dreyfus *et al.* 2012)) was downloaded from the Protein Data Bank (PDB) (Bernstein *et al.* 1977) and analysed using Swiss PDB Viewer software (Guex and Peitsch 1997): monomer surface was calculated, non-conserved residues between B/Brisbane/60/2008 and B/Hong Kong/8/1973 or B/Florida/4/2006 were mapped and highlighted on the B/Brisbane/60/2008 HA surface. The HA structure of B/Hong Kong/8/1973 (PDB ID: 2RFU (Q. Wang *et al.* 2007)) was also downloaded from the PDB database and non-conserved residues between B/Hong Kong/8/1973 or B/Florida/4/2006 were mapped on its surface; the position of the residues of B/Florida/4/2006 HA that were not present in B/Hong Kong/8/1973 were

[10] In the Zapo colour system the amino acid residues are coloured on the basis of their physiochemical properties.

highlighted after superimposing (fit) the B/Florida/4/2006 structure HA (PDB ID: 4FQJ (Dreyfus *et al.* 2012)).

6.3 Results

6.3.1 Cloning B/Brisbane/60/2008 and B/Bangladesh/3333/2007 haemagglutinins into pI.18 expression vector

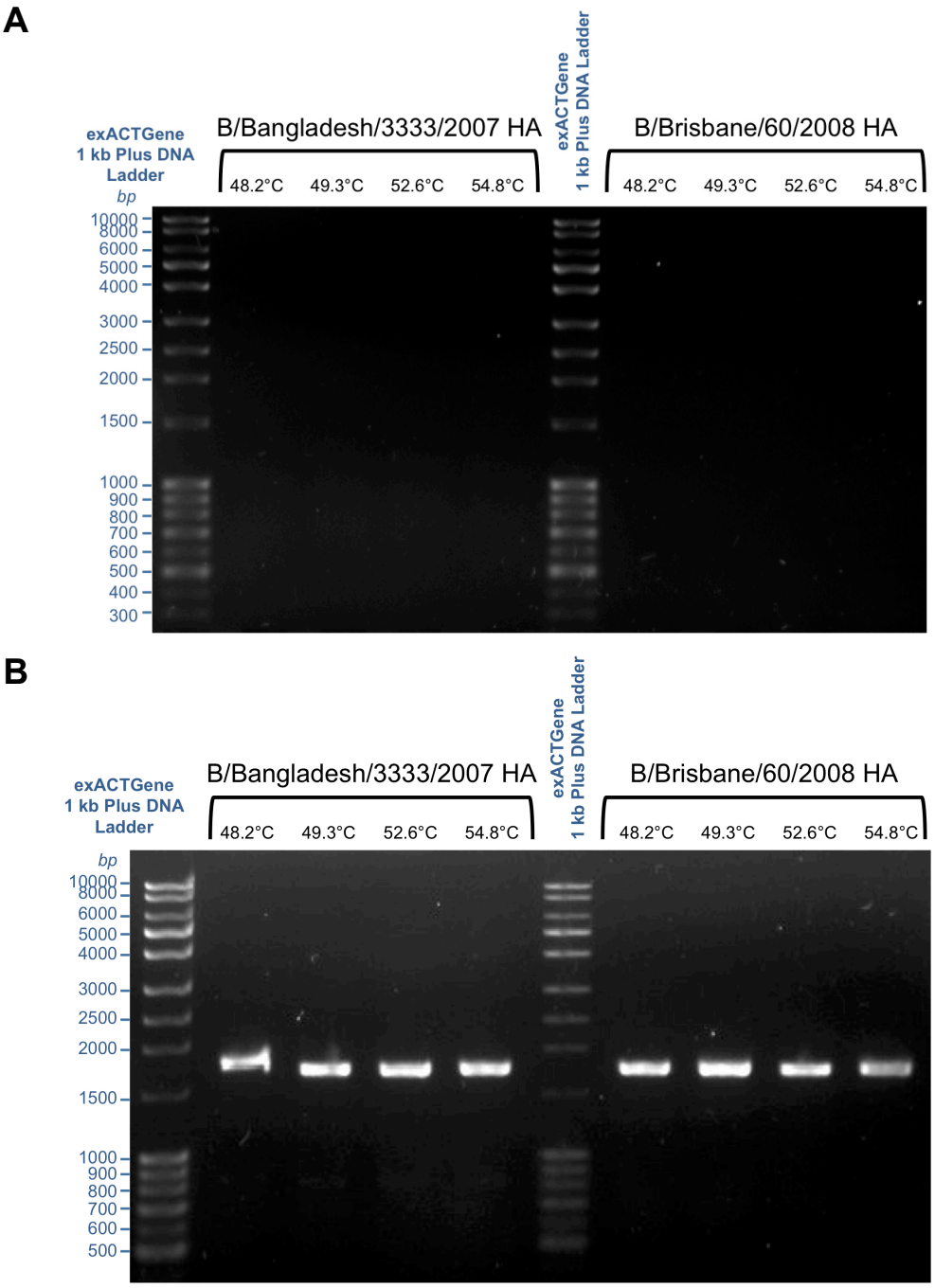

Figure 69: Gel electrophoresis of B/Bangladesh/3333/2007 and B/Brisbane/60/2008 HA amplicons
Four different annealing temperatures were tested in a gradient PCR to amplify influenza B HA. **A.** The gel shows that HA amplification was not achieved when 2 µl/reaction of 1:50 cDNA dilution was used as template. **B.** The gel shows amplification of influenza B HA using 10 µl/reaction of 1:50 cDNA dilution as template at the four different annealing temperatures.

To clone B/Brisbane/60/2008 and B/Bangladesh/3333/2007 HAs, cDNA was used as template in a gradient PCR. The concentration of the cDNA material was unknown and considering the limited volume and the fact that it contains the genetic material of all 8 influenza B genome segments, it was decided to use a 1:50 cDNA dilution. When the first PCR performed (**Figure 69A**) gave negative results, the PCR was repeated by increasing the template quantity of 5-fold. These second PCRs resulted in positive amplification for the two strains at all the annealing temperatures tested (**Figure 69B**). The amplicons obtained using an annealing temperature of 54°C (the highest tested) were then used for the subsequent cloning steps: digestion and ligation into pI.18 vector.

After ligation and transformation, colonies grew on the "vector plus insert" ligation plate. However, since colonies were present also in the control (no insert) plate, demonstrating the presence of undigested or re-ligated pI.18 vector, colony PCRs were performed on the "vector plus insert" colonies to screen more recombinant clones and to identify positive ones. Of the 20 colonies (10 for each strain) screened *via* colony PCR, only three (B/Bangladesh/3333/2007 B#4, B/Brisbane/60/2008 B#11, and B#16) were positive (**Figure 70**). To confirm that the recombinant clones identified were not false positives, the colonies were further cultured, the plasmid purified, and final screening achieved *via EcoRI* restriction digestion. After vector linearization with Fast Digest *EcoRI*, the expected band size of 6 kb (pI.18 vector 4.3 kb plus the insert 1.7 kb) was obtained (**Figure 71**).

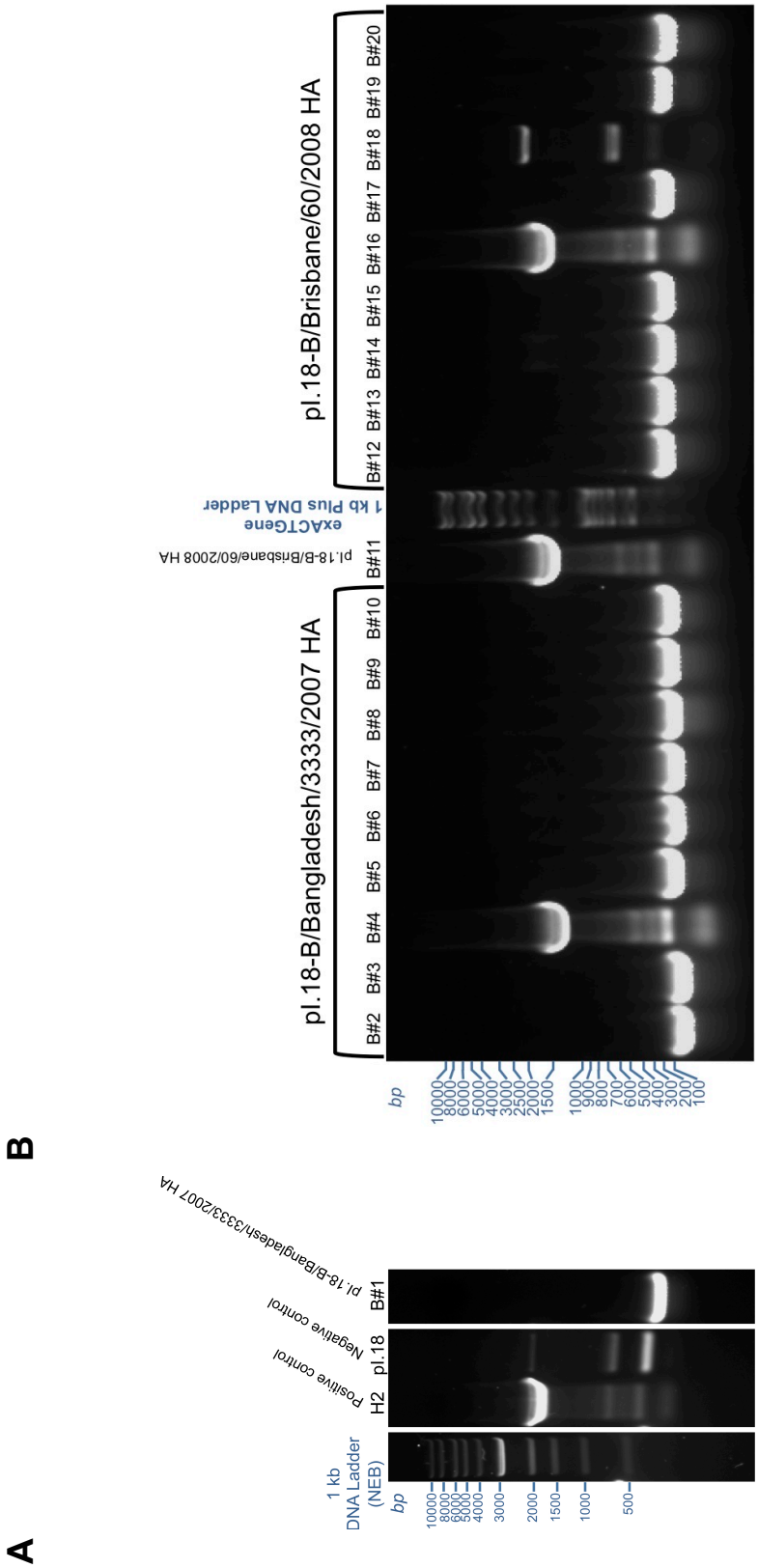

Figure 70: Gel electrophoresis of pI.18-B/Bangladesh/3333/2007 and pI.18-B/Brisbane/60/2008 HA colony PCR screenings

A band corresponding to ~1.7 kb indicates successful cloning. Bands <100 bp indicate the amplification of the pI.18 empty multicloning site and an insert-negative clone.

A. Colony PCR of pI.18-B/Bangladesh/3333/2007 B#1, together with the DNA ladder, positive (A/Korea/ H2) and negative control (pI.18) are shown. **B.** PCR of pI.18-B/Bangladesh/3333/2007 B#2-B#10 colonies and of pI.18-B/Brisbane/60/2008 B#11-#B20 colonies.

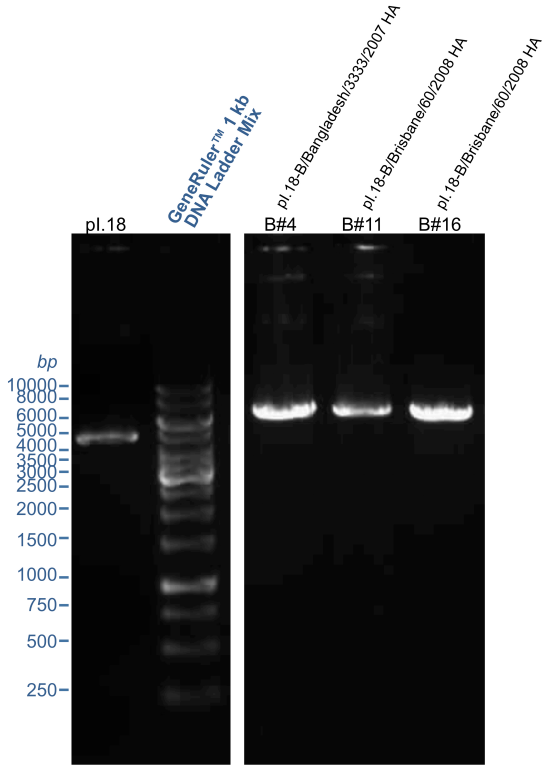

Figure 71: Gel electrophoresis of positive clone digestions using *EcoRI*
Control pI.18 vector (4.3 kb) is compared with positive clones that contain influenza B HA-encoding gene (6 kb).

The positive plasmids pI.18-B/Bangladesh/3333/2007 B#4, pI.18-B/Brisbane/60/2008 B#11 and B#16 were then sent for sequencing to confirm HA insertion and identity. The B/Bangladesh/3333/2007 B#4 HA had 100% identity with the database HA sequence (**Appendix Figure 21**); however in the two B/Brisbane/60/2008 HAs the mutation N212S was present (**Figure 72 (A and B)**).

The mutation was then successfully corrected using the QuickChange Lightning Site-direct mutagenesis kit as shown in **Figure 72 (C and D)**.

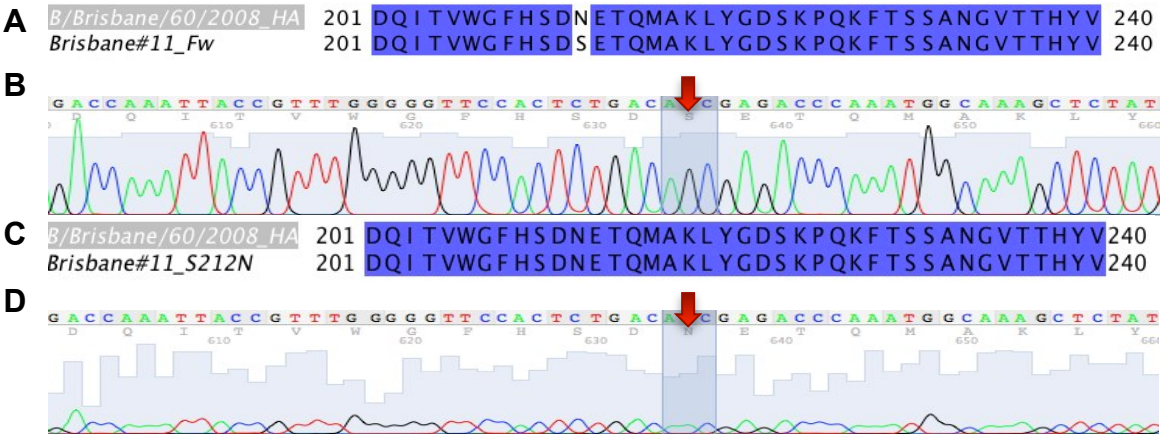

Figure 72: Site-direct mutagenesis of B/Brisbane/60/2008 HA
A. B/Brisbane/60/2008 HA gene sequence showing the N212S mutation; **B.** Electropherograms of B/Brisbane/60/2008 HA gene sequence showing the N212S mutation, corresponding to the nucleotide substitution 635°>G, **C.** B/Brisbane/60/2008 HA gene sequence after mutagenesis showing the correction of the mutation; **D**. Electropherograms of corrected B/Brisbane/60/2008 HA gene sequence.

6.3.2 Proteases are necessary for production of high titre influenza B pseudotypes

Once correct cloned influenza B HAs were obtained, the production of Influenza B pp was investigated by testing the effect that different types and quantities of proteases had on HA activation.

Using this methodical approach, pp with high titre were obtained for all the tested HAs: B/Bangladesh/3333/2007 (**Figure 73**), B/Hong Kong/8/1973 (**Figure 74A**), B/Victoria/2/1987 (**Figure 74B**), B/Yamagata/16/1988 (**Figure 75A**), B/Florida/4/2006 (**Figure 75B**), and B/Brisbane/60/2008 (**Figure 76**).

In general, higher pp titres (>1×10^9 RLU/ml) can be achieved by co-transfection of the HAT or the TMPRSS4 protease-expressing plasmid (**Appendix Table 6**). However, it can be observed that there are not significant differences when using 125 ng or 250 ng of HAT or TMPRSS4, whereas using lower quantities of TMPRSS2 usually improves pp production.

All the pp produced in the absence of proteases had low titres (<1×10^6 RLU/ml). However, titres were increased significantly after treatment with TPCK-Trypsin permitting the pp to transduce target cells.

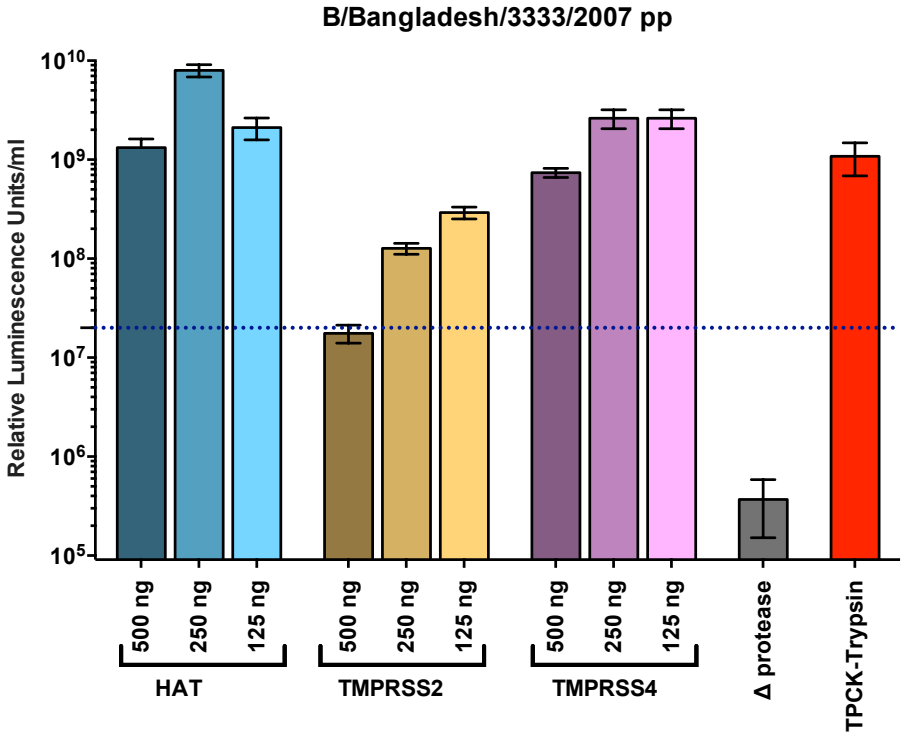

Figure 73: Role of HAT, TMPRSS2, and TMPRSS4 proteases in B/Bangladesh/3333/2007 pp production
Titres are reported in RLU/ml with SEM (n=8 titre measurements). A line corresponding to 2×10^7 RLU/ml is drawn to indicate the minimum titre necessary to perform neutralization assays.

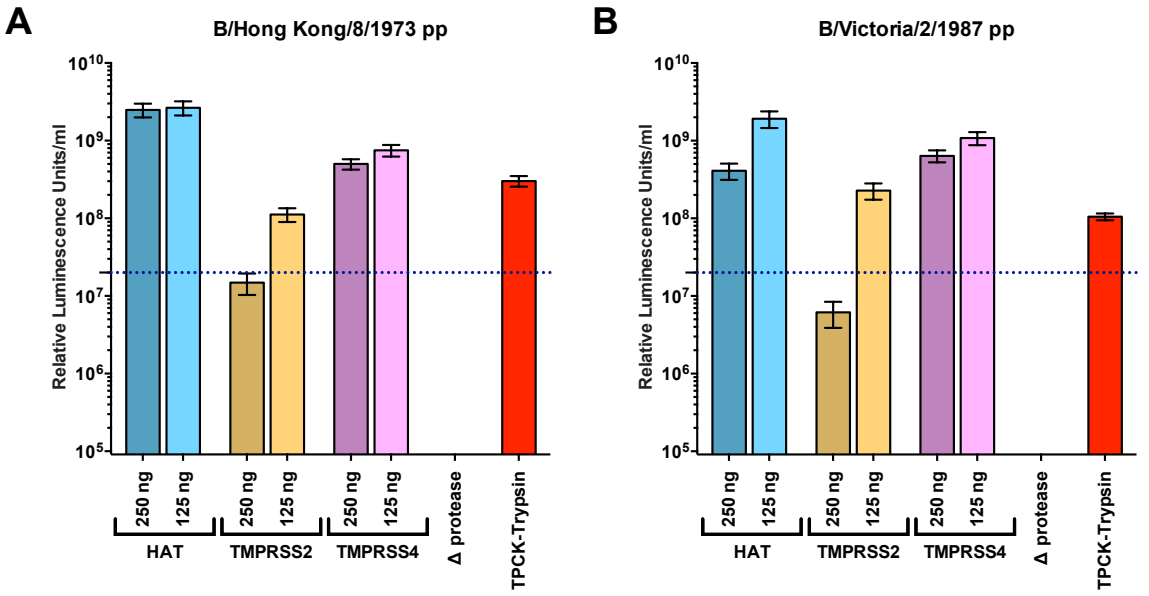

Figure 74: Role of HAT, TMPRSS2, and TMPRSS4 proteases in B/Hong Kong/8/1973 pp and B/Victoria/2/1987 pp production
Titres are reported in RLU/ml with SEM (n=8 titre measurements). A line corresponding to 2×10^7 RLU/ml is drawn to indicate the minimum titre necessary to perform neutralization assays.
A. B/Hong Kong/8/1973 pp; **B.** B/Victoria/2/1987 pp.

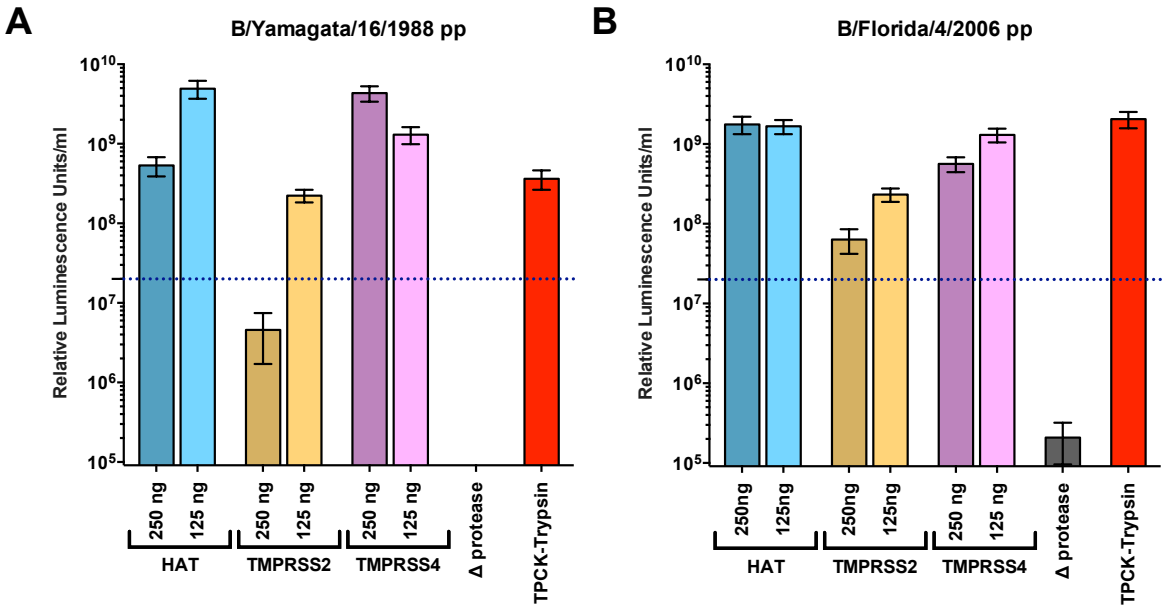

Figure 75: Role of HAT, TMPRSS2, and TMPRSS4 proteases in B/Yamagata/16/1988 pp and B/Florida/4/2006 pp production
Titres are reported in RLU/ml with SEM (n=8 titre measurements). A line corresponding to 2×10^7 RLU/ml is drawn to indicate the minimum titre necessary to perform neutralization assays.
A. B/Yamagata/16/1988 pp; **B.** B/Florida/4/2006 pp.

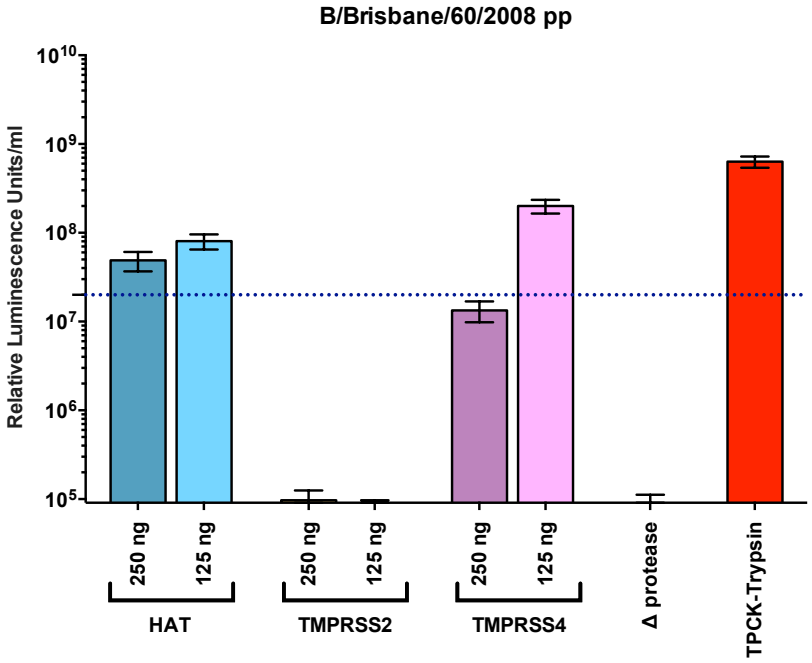

Figure 76: Role of HAT, TMPRSS2, and TMPRSS4 proteases in B/Brisbane/60/2008 pp production
Titres are reported in RLU/ml with SEM (n=8 titre measurements). A line corresponding to 2×10^7 RLU/ml is drawn to indicate the minimum titre necessary to perform neutralization assays.

A Western blot was performed on B/Brisbane/60/2008 pp, following low-speed centrifugation, to confirm that HA activation and pp entry are dependent on HA cleavage. In all the B/Brisbane/60/2008 pp produced through protease addition, bands at 51-55 kDa corresponding to HA1 can be observed in the Western blot (**Figure 77**). HAT and TMPRSS4 produced pp displaying a thicker HA1 band, whereas the bands observed when TMPRSS2 is used are thinner. The band intensities correlate with the pp titres in which TMPRSS2 viruses show lower titres compared to HAT and TMPRSS4 produced pp (**Figure 76**). Furthermore, in the Western blot, the Δ protease pp shows not only a band at ~78 kDa corresponding to HA0, but also a small band at ~55 kDa. The presence of the HA1 band is likely to be related to the presence of proteases in the producer HEK293T/17 cells and explains the entry of Δ protease pp into HEK293T/17 target cell line observed during titration experiments. The Western blot shows that the HA cleavage mediated by proteases can also be reproduced through TPCK-trypsin treatment of the Δ protease pp: in fact the HA0 band disappeared and instead the HA1 was observed. These results clearly support the hypothesis that the three proteases and TPCK-trypsin cleave the HA0 into the two subunits HA1 and HA2.

Interestingly, in the Western blot, the HAs activated by HAT, TMPRSS2 and TMPRSS4 present heterogeneous glycosylation characteristics: more than one band between 50 kDa and 60 kDa, all corresponding to HA1, are present. Instead, in the

Δ protease pp before and after TPCK-trypsin treatment only a single band at 55 kDa is observed.

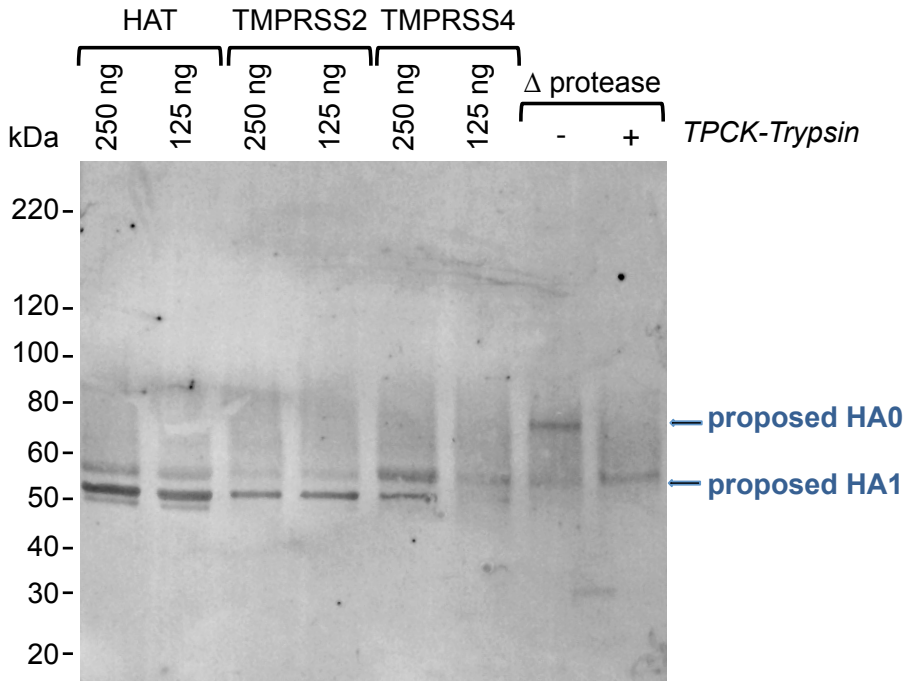

Figure 77: Western blot of B/Brisbane/60/2008 pp obtained using different proteases
HA was detected using 1:500 NIBSC 11/136 anti-B/Brisbane/60/2008 serum and 1:20000 anti-sheep/goat IgG Dylight®800 secondary antibody. Membrane was acquired using the 800nm channel. Molecular weight size marker lane was not shown as acquired using sensitivity parameters that differs from the rest of the membrane. An HA control, that could be used to better identify the band detected, was not used as a recombinant HA was unavailable for the Influenza B HA tested.

6.3.3 Influenza B Kozak is as efficient as influenza A Kozak for pseudotype production

To test the role of the putative influenza B Kozak sequence and to see if it can improve the pp titre *via* increased expression of HA, mutagenesis was successfully performed on the B/Bangladesh/3333/2007 to change the initial influenza A Kozak (**Figure 78**).

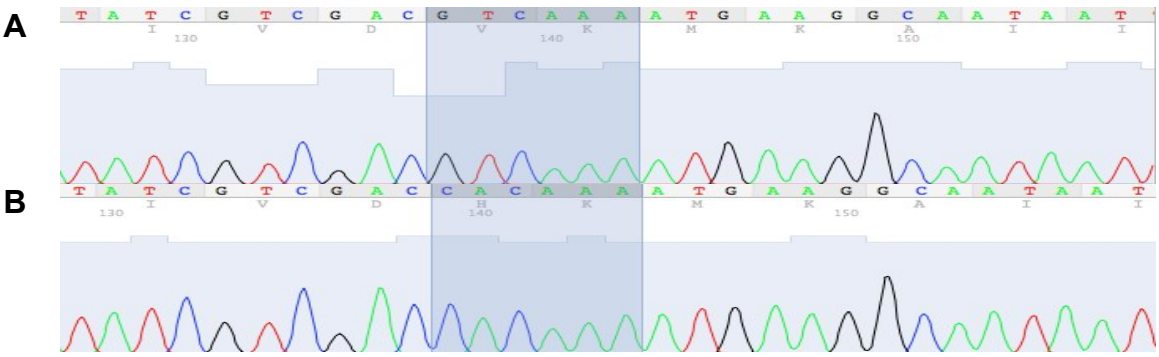

Figure 78: Electropherograms showing B/Bangladesh/3333/2007 HA Kozak sequence before and after mutagenesis
The Kozak sequence is highlighted. **A.** Influenza A Kozak sequence (GTCAAA) in pI.18 B/Bangladesh/3333/2007 HA; **B.** Influenza B Kozak sequence (CACAAA) in pI.18 B/Bangladesh/3333/2007 HA after successful mutagenesis.

Influenza B Kozak-B/Bangladesh/3333/2007 pp were produced employing HAT, TMPRSS2, TMPRSS4 and TPCK-Trypsin treatment and the titres of these pp were then compared with the B/Bangladesh/3333/2007 pp produced using the influenza A Kozak sequence. The results (**Figure 79**) show that there are no clear differences between the titres of the pp produced using the influenza A or influenza B Kozak sequence. Furthermore the influenza B Kozak-B/Bangladesh/3333/2007 pp shows the same cleavage/activation pattern to the non-mutated B/Bangladesh/3333/2007 pp.

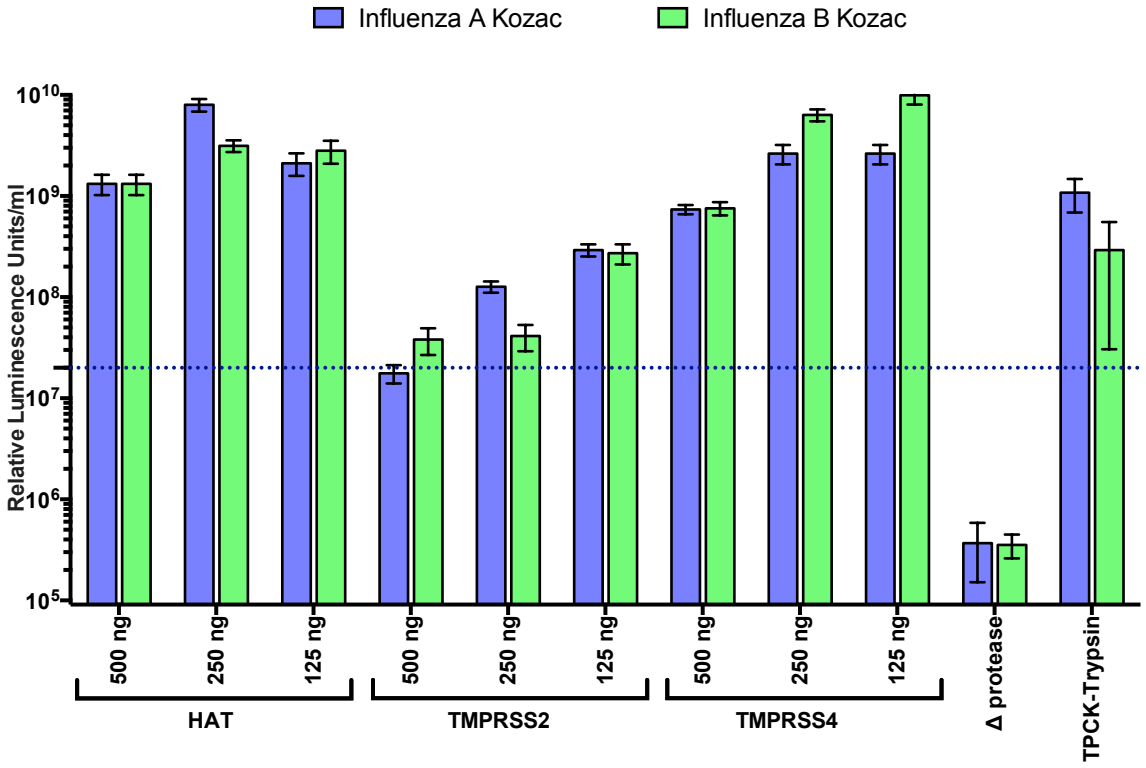

Figure 79: The role of influenza B Kozak sequence in pp production
Titre of B/Bangladesh/3333/2007 pp obtained using the standard influenza A Kozak sequence (GTCAAA) are compared with the ones obtained using Influenza B Kozak sequence (CACAAA).
Titres are reported in RLU/ml with SEM (n=8 titre measurements). A line corresponding to 2×10^7 RLU/ml is drawn to indicate the minimum titre necessary to perform neutralization assays.

6.3.4 Influenza B pseudotypes enter into different target cell lines

The influenza B pp produced were also tested for their ability to transduce MDCK and A549 cells. All the influenza B pp tested can transduce the target cell lines examined showing higher transduction activity for MDCK compared to A549 (**Figure 80**). However, the best target was found to be the HEK293T/17 cell line. In fact, in the quantitative results obtained using firefly luciferase-expressing pp, it is clear that the highest pp titres are obtained when HEK293T/17 cell line is used as transduction target, whereas using MDCK and A549 the pp titres can be considered low ($<1\times10^7$ RLU/ml) especially for certain strains (B/Victoria/2/1987, B/Yamagata/16/1988, B/Brisbane/60/2008).

These results were also confirmed using emGFP-expressing influenza B pp and epifluorescent microscopy, to have a qualitative approach, demonstrating that the influenza B pp can transduce both MDCK and A549 cells (**Figure 81**).

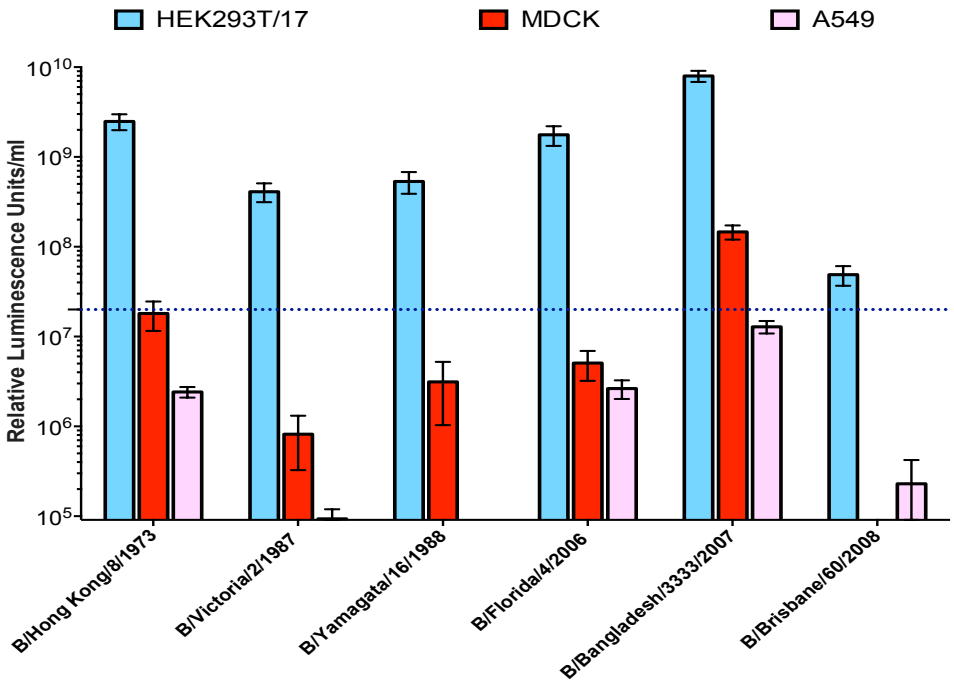

Figure 80: Transduction of HEK293T/17, MDCK, and A549 cells with Influenza B pp expressing firefly luciferase
Titres are reported in RLU/ml with SEM (n=8 titre measurements). A line corresponding to 2×10^7 RLU/ml is drawn to indicate the minimum titre necessary to perform neutralization assays.

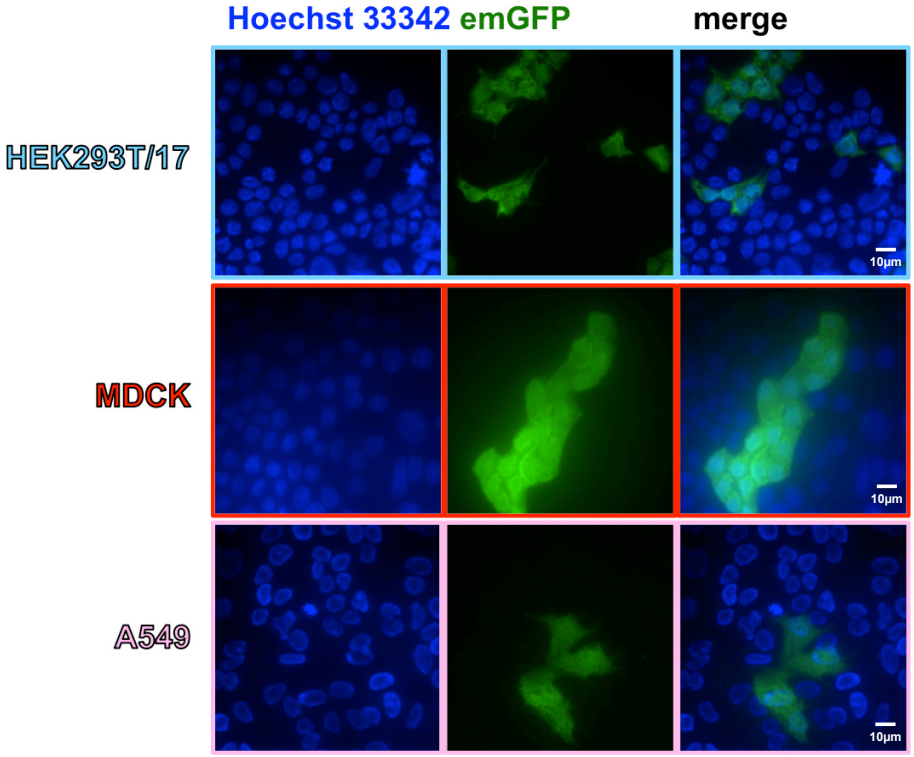

Figure 81: Transduction of HEK293T/17, MDCK, and A549 cells with influenza B/Florida/4/2006 pp expressing emGFP
Images were acquired with 40X objective. The scale bar (10µm) is shown in the figure. Transduction results for the other pp are comparable to the examples presented here.

6.3.5 Influenza B pseudotypes are neutralized by reference antiserum

To evaluate if the influenza B pp could be used as surrogate antigens in neutralization assays, pp-NT assays were undertaken using a reference antisera and three different pp: B/Brisbane/60/2008 (Victoria lineage), B/Hong Kong/8/1973 and B/Florida/4/2006 (Yamagata lineage) (**Figure 82**).

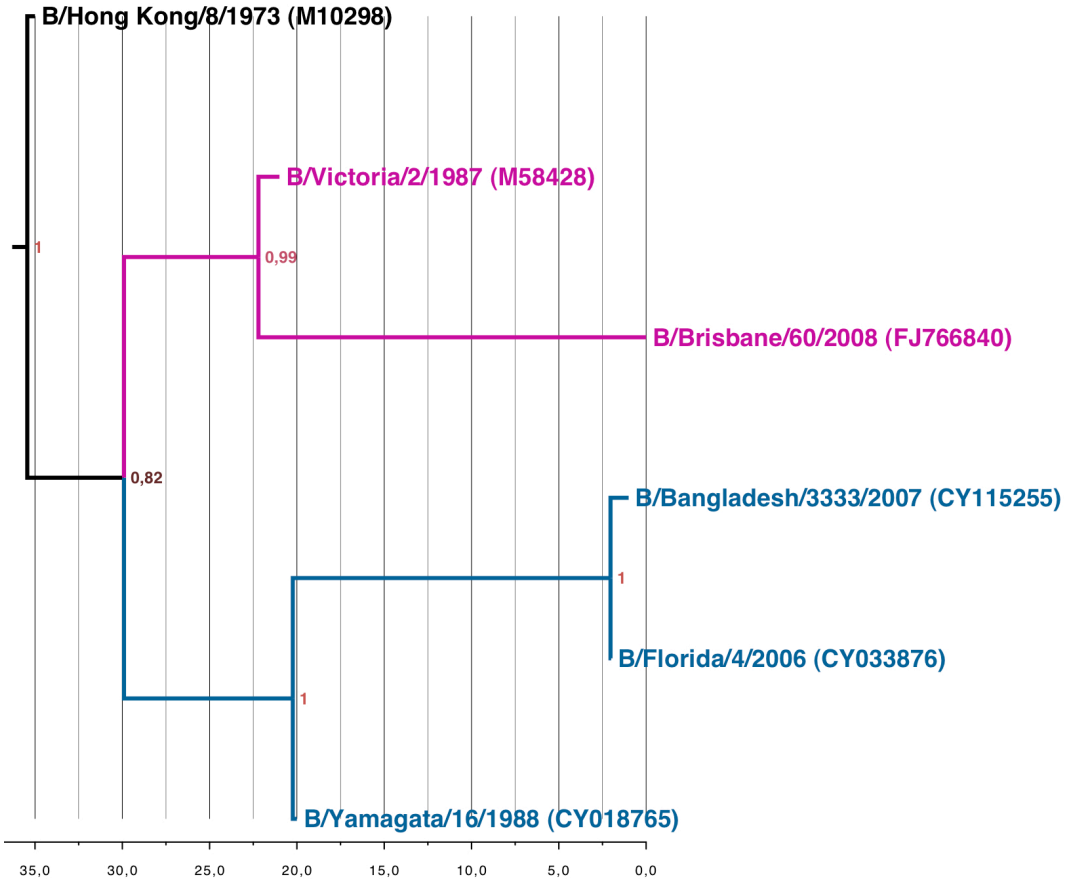

Figure 82: Phylogenetic tree of the HAs used for pp production
Victoria lineage strains are in fuchsia, whereas Yamagata strains are in lagoon. B/Hong Kong/8/1973 is reported in black as circulating before the lineage division. Accession numbers are reported with the strain name on the tree tips. Posterior probabilities (Section 6.2.9) are reported on the nodes. Axes represent time scales with origin at the most recent circulating strain (B/Brisbane/60/2008).

The results, reported in **Figure 83**, show that the anti-B/Brisbane/60/2008 serum can neutralize not only the matched pp (IC_{50}=20761), but also, at a lower level, pp bearing the HA of the other influenza B lineage (B/Florida/4/2006, IC_{50}=10582) or the HA of a strain that was circulating before the lineage division (B/Hong Kong/8/1972, IC_{50}=18404).

This indirectly demonstrates that influenza B pp-NT assay has a high sensitivity but a low specificity since reference serum should not cross-react and neutralize viruses of different lineages.

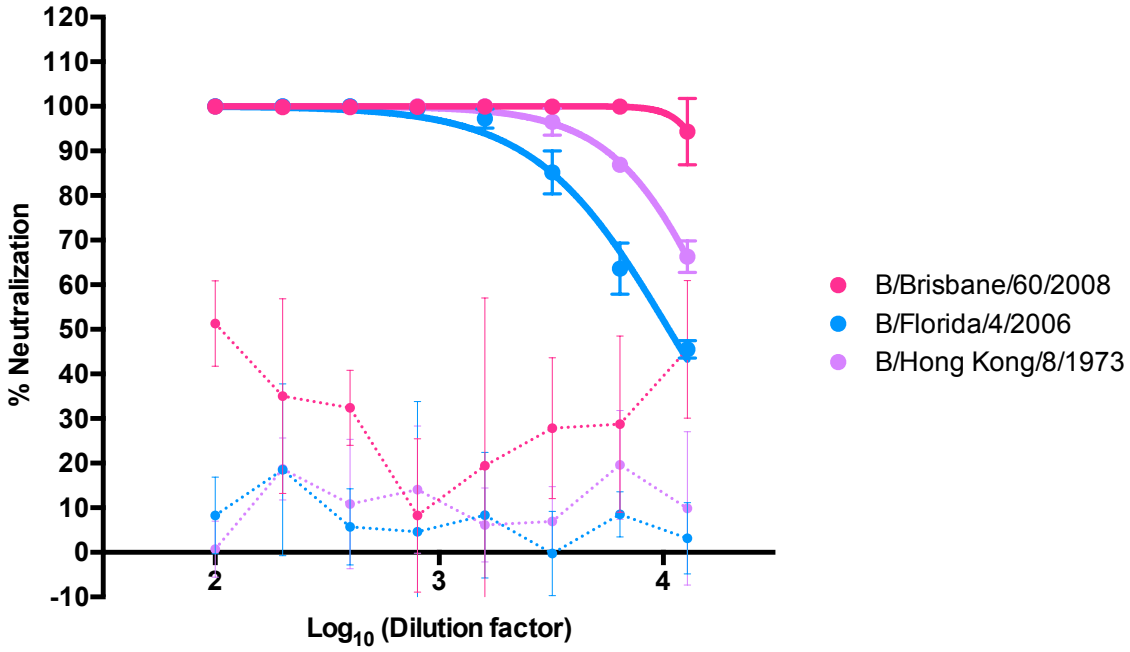

	IC_{50}
B/Brisbane/60/2008	20761
B/Florida/4/2006	10582
B/Hong Kong/8/1973	18404

Figure 83: Neutralization activity of NIBSC 11/136 anti-B/Brisbane/60/2008 HA serum and of the negative control

On the X axis the logarithm of the sera dilution factor is reported; on the Y axis percentage neutralization is reported. Assays were performed in quadruplicate (n=4) and SD is reported for each dilution point. Neutralization activity of the NIBSC 11/136 serum (continuous line) against matched B/Brisbane/60/2008 (fuchsia), B/Florida/4/2006 (blue), and B/Hong Kong/8/1973 (lilac) pp. Neutralization activity of the negative control (FBS) is also reported. Calculated IC_{50} values for the NIBSC 11/136 serum are also reported in the associated table. IC_{50} of the negative control are equal to 0.

6.3.6 Influenza B pseudotype particle neutralization assay does not correlate with haemagglutination inhibition assay

Human sera from NCT00942071 clinical trial were screened against the vaccine matching B/Brisbane/60/2008 in a pp-NT assay and $\log_{10}(IC_{50})$ and IC_{50} values were calculated. Log_{10} (IC_{50}) values were then compared with the $\log_{10}$ HI titres. In **Figure 84**, show that HI and pp-NT assay results do not correlate with each other ($r = 0.1632$, $p = 0.3563$).

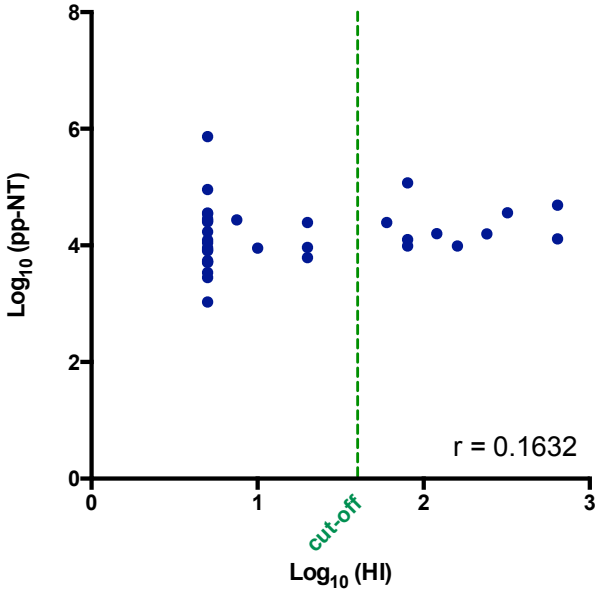

Figure 84: Correlation of HI assay and pp-NT assay performed with B/Brisbane/60/2008 influenza strain
The cut-off reported on the $\log_{10}$ (HI) axis corresponds to $\log_{10}(40)$.

6.3.7 Influenza B pseudotype particle neutralization assays detect cross-reactive antibody response between Victoria and Yamagata lineage

Human clinical trial NCT00942071 sera collected at day 0 and day 21 after vaccination with A/California/7/2009 H1N1, A/Perth/16/2009 H3N2, and B/Brisbane/60/2008, and placebo or MVA-NP+M1, were tested in pp-NT assays using B/Brisbane/60/2008 pp, B/Hong Kong/8/1973 pp and B/Florida/4/2006 pp.

Data obtained in pp-NT assay using B/Brisbane/60/2008 show that strong neutralizing antibody responses are present already pre-vaccination and that the vaccination itself fails ($p = 0.5791$) to induce higher antibody responses (**Figure 85A**). However, a shift of the IC_{50} distribution first quartile can be observed post-vaccination.

Sera were tested also against B/Hong Kong/8/1973 pp that have antigenic characteristics typical of influenza B strains circulating before the lineage division: antibody responses were detected at vaccination day 0 and at day 21; the post-vaccination neutralizing titres exhibit a significant increase ($p = 0.0046$) (**Figure 85B**).

Finally, sera were also analysed against a strain of the Yamagata lineage (B/Florida/4/2006) that was un-matched to the vaccine administered to the recruited subjects: day 0 shows responses that increase significantly ($p = 0.0129$) at day 21 (**Figure 85C**).

Overall titres obtained against B/Brisbane/60/2008 pp were higher than those measured using B/Hong Kong/8/1973 pp and B/Florida/4/2006 pp.

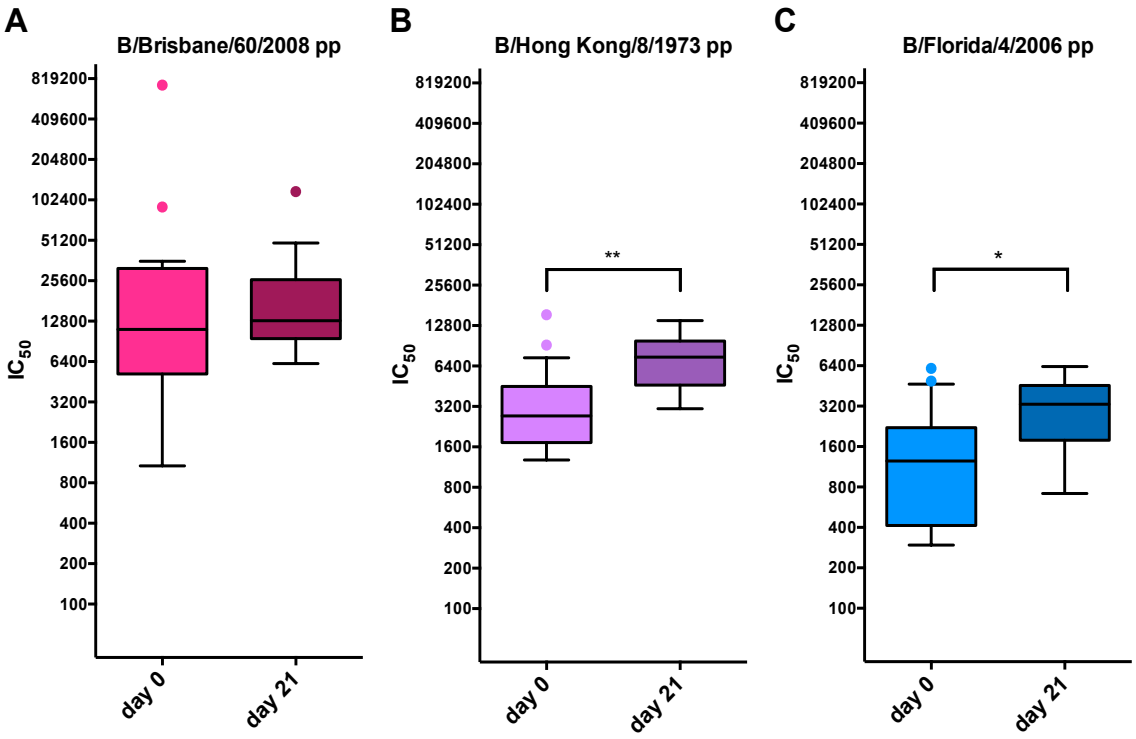

Figure 85: IC_{50} of sera tested with pp-NT assay reported in a Box-and-Whisker plot
Comparison between IC_{50} measured pre- (day 0) and post- (day 21) vaccination. Quartiles and medians are reported in Appendix Table 7. **A.** IC_{50} against B/Brisbane/60/2008 pp; **B.** IC_{50} against B/Hong Kong/8/1973 pp; **C.** IC_{50} against B/Florida/4/2006 pp.

SCRs using two cut-off values (4-fold and 2-fold increase) for the three strains were also calculated: B/Brisbane/60/2008 and B/Hong Kong/8/1973 have an 17.6% $SCR_{(4\text{-fold})}$ (3/17 subjects), whereas the B/Brisbane/60/2008 $SCR_{(2\text{-fold})}$ is 29.4% (5/17 subjects) and the B/Hong Kong/8/1973 $SCR_{(2\text{-fold})}$ is 58.8% (10/17 subjects); the B/Florida/4/2006 $SCR_{(4\text{-fold})}$ is 29.4% (5/17 subjects) and the $SCR_{(2\text{-fold})}$ is 58.8% (10/17 subjects).

During the NCT00942071 clinical trial, placebo or MVA-NP+M1 was co-administered with the seasonal TIV. Considering the B/Brisbane/60/2008 HI titre, Antrobus *et al.* found no difference between the TIV + placebo and the TIV + MVA-NP+M1 groups. Since pp-NT is more sensitive than HI and the two assays did not correlate in this case, the pp-NT IC_{50} obtained were stratified and were analysed graphically to see if any difference was present between the two vaccination regimen groups. The IC_{50} fold-increases of each group were also compared statistically.

From the graphs (**Figure 86**) it appears that at day 0 the subjects of the TIV + MVA-NP+M1 group have lower IC_{50} values than the TIV + placebo group. However, at day 21 the IC_{50} titres of the TIV + MVA-NP+M1 group have a distribution comparable to the one measured in the TIV + placebo. These results, together with the small number of subjects recruited and the non-parametric distribution of the IC_{50} titres, render any statistical analysis problematic. For this reason only the fold-increase in the IC_{50}

titres (**Figure 87**) for each pp were compared after treatment-stratification using a Mann-Whitney U test: the results show that differences in IC_{50} fold-increase between TIV + placebo and TIV + MVA-NP+M1 are not statistically significant for all the pp tested.

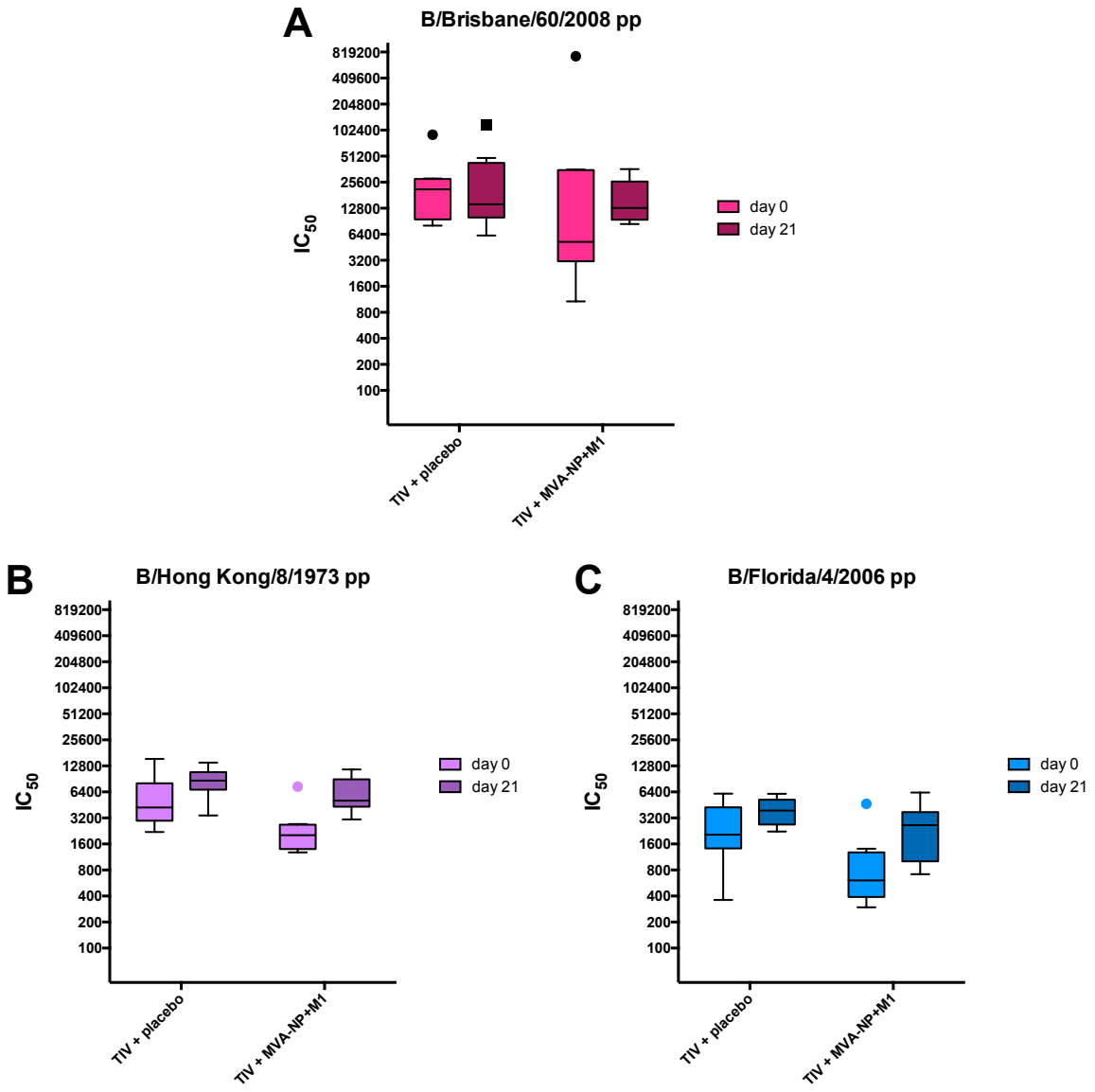

Figure 86: IC_{50} of sera tested with pp-NT assay reported in a Box-and-Whisker plot after stratification using vaccination regimens
Comparison between IC_{50} measured before (day 0) and after (day 21) vaccination after stratification using vaccine regimens (TIV + placebo and TIV + MVA-NP+M1). Quartiles and medians are reported in Appendix Table 8. **A.** IC_{50} against B/Brisbane/60/2008; **B.** IC_{50} against B/Hong Kong/8/1973; **C.** IC_{50} against B/Florida/4/2006.

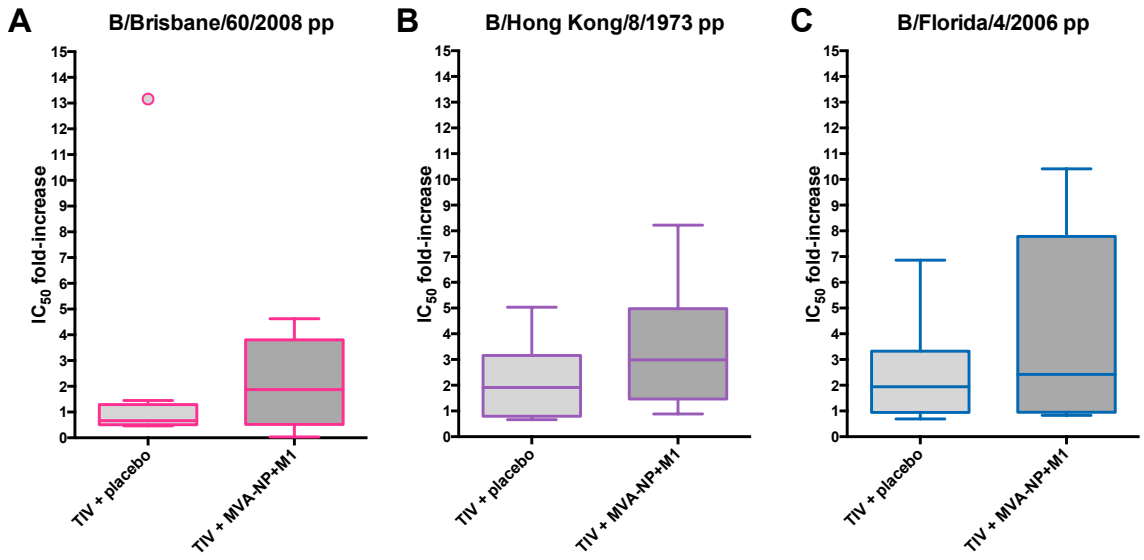

Figure 87: Fold-increase in the IC_{50} titres of the TIV + placebo and the TIV + MVA-NP+M1 groups
A. IC_{50} fold-increase against B/Brisbane/60/2008 pp; **B.** IC_{50} fold-increase against B/Hong Kong/8/1973 pp; **C.** IC_{50} fold-increase against B/Florida/4/2006 pp.

6.3.8 Influenza B haemagglutinin antigenic differences can be related to the HA head region

The pair-wise amino acid alignments, performed on the three HAs used in the pp-NT, show that between B/Brisbane/60/2008 and B/Hong Kong/8/1973 HAs there is 94.9% of amino acidic identity, whereas between B/Brisbane/60/2008-B/Florida/4/2006 there is 93.5% identity. B/Hong Kong/8/1973 HA is also similar to B/Florida/4/2006 HA with a percentage identity of 94.4%. Bioinformatics analysis also shows that non-conserved amino acids are located in the head region, especially in the outer surface part, traditionally implicated in antigenic differences between different HAs (**Figure 88** and **Figure 89**).

Of particular relevance is the fact that B/Hong Kong/8/1973 HA possesses an amino acid deletion in the head region near the sialic acid binding-site and corresponding to antigenic site B, that can be clearly visualised in the comparison of B/Hong Kong/8/1973 and B/Florida/4/2006 HA structures (the deleted residues are added in orange to the B/Hong Kong/8/1973 HA structure in **Figure 89 (E and F)**). These deleted residues are positioned near and probably involved in the binding region of the CR8033 mAb (Dreyfus *et al.* 2012), and the 3A2 and 10C4 mAbs (Yasugi *et al.* 2013). This indicates that the B/Hong Kong/8/1973 HA could not be bound by these antibodies.

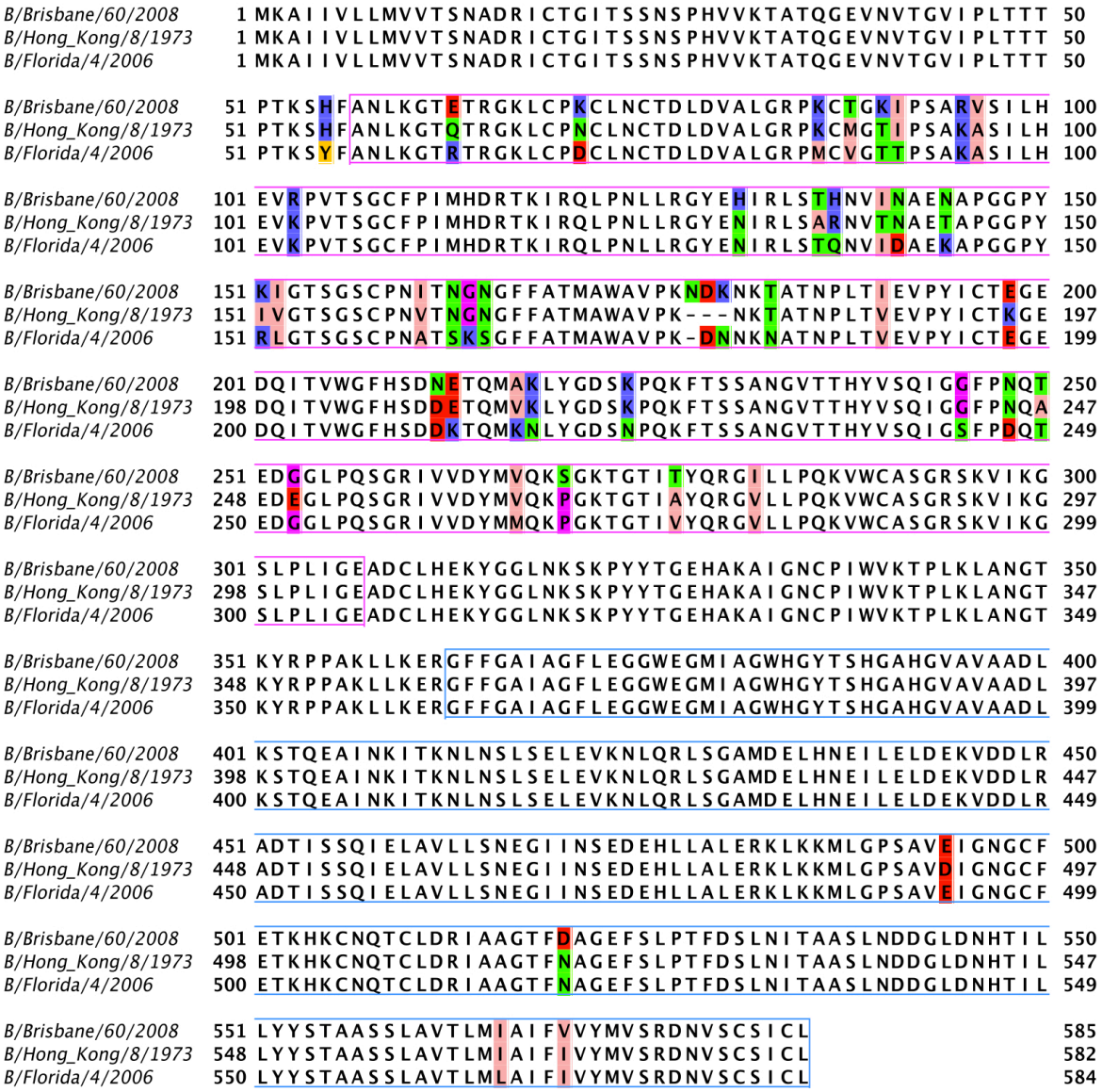

Figure 88: Amino acid alignment of B/Brisbane/60/2008, B/Hong Kong/8/1973, and B/Florida/4/2006 HAs

The sequences of B/Brisbane/60/2008 (ACN29380), B/Hong Kong/8/1973 (AAA43717), and B/Florida/4/2006 (ACF54246) HA were aligned and annotated using Jalview. The amino acids corresponding to the head region are boxed in pink. The HA2 subunit is boxed in light blue. The amino acids that differ between the three sequences are highlight using the Zapo colour system based on amino acid physiochemical properties.

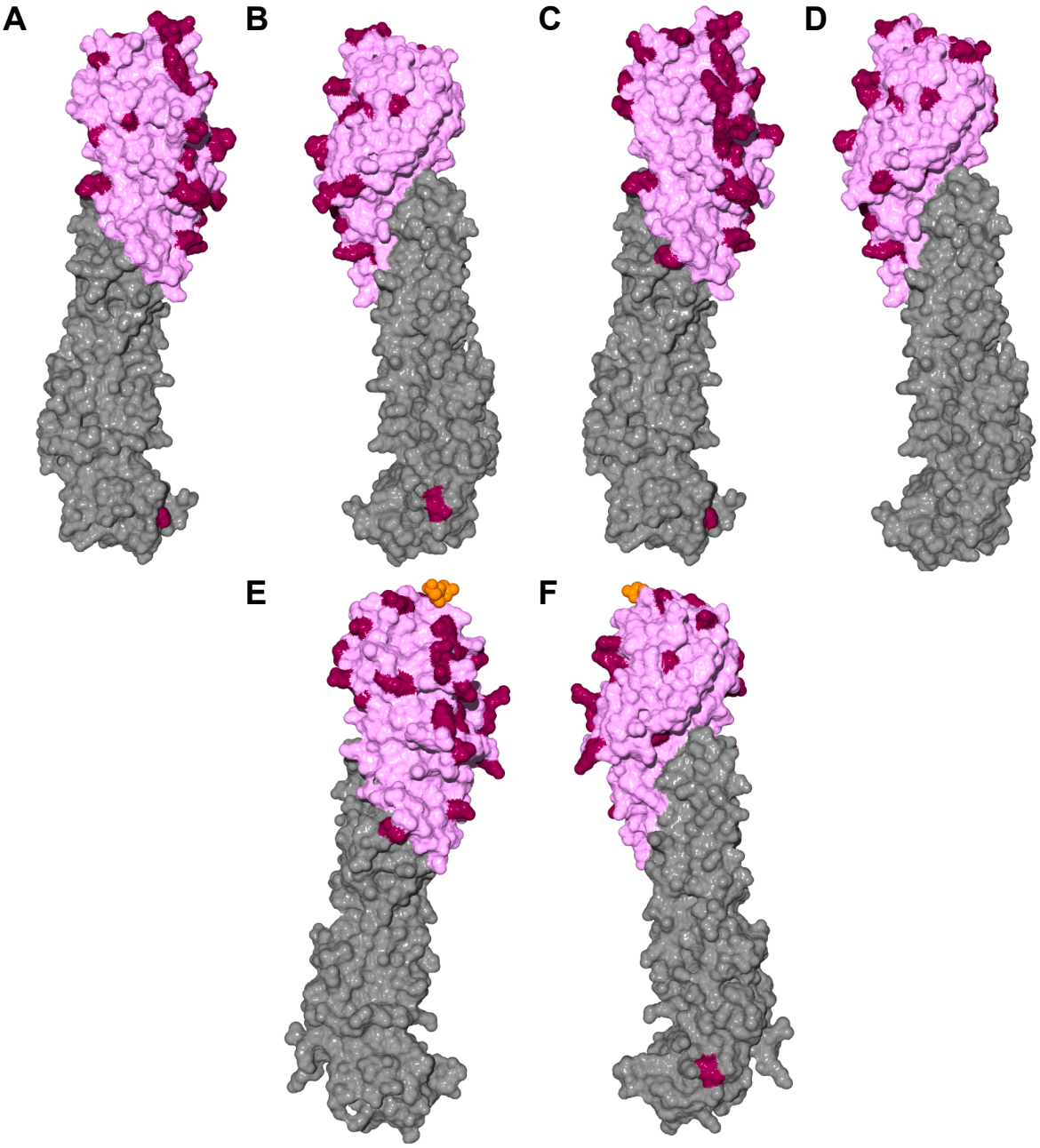

Figure 89: Differences between B/Brisbane/60/2008, B/Hong Kong/8/1973, and B/Florida/4/2006 HAs

The HA head is shown in pink and the stalk in grey. In dark red the non-conserved residues are highlighted.

A and B. Outer-surface view and inner-surface view of B/Brisbane/60/2008 HA (PDB ID: 4FQM) in which the residues that differ from B/Hong Kong/8/1973 HA are highlighted; **C and D**. Outer-surface view and inner-surface view of B/Brisbane/60/2008 HA in which the residues that differ B/Florida/4/2006 HA are highlighted; **E and F.** Outer-surface view and inner-surface view of B/Hong Kong/8/1973 HA (PDB ID: 2RFU) in which non-conserved residues in comparison to B/Florida/4/2006 HA are highlighted. The B/Florida/4/2006 HA structure (PDB ID: 4FQJ) was superimposed on B/Hong Kong/8/1973 HA to highlight in orange the residues present in B/Florida/4/2006 HA but deleted in B/Hong Kong/8/1973 HA. Images produced using Swiss PDB Viewer.

Non-conserved amino acids in the stalk HA domain (**Figure 88** and **Figure 89**) were found proximal to the viral envelope and in the HA transmembrane region. The only exception is the mutation H55Y (B/Brisbane/60/2008 numbering) in the B/Florida/4/2006

HA. This mutation is positioned in the stalk region adjacent to the head and it is included in the epitope recognised by the influenza pan-neutralizing mAb CR8071 (Dreyfus *et al.* 2012). This indicates that CR8071 and potentially similar antibodies are able to bind and neutralize B/Brisbane/60/2008, B/Hong Kong/8/1973, and B/Florida/4/2006.

6.4 Discussion and Conclusion

Influenza B virus is an important human pathogen that causes severe annual epidemics, however its study is frequently neglected in comparison to Influenza A. Nonetheless, recently with the failure of the vaccine coverage and with the development of a quadrivalent vaccine, the interest in this virus from an epidemiological prospective is growing, and the need for new assays for diagnosis and vaccine evaluation, as a consequence of severe limitation of classical serological assays, is compelling. To respond to this request, the production of influenza B pp, their characterisation and their use in neutralization assays as surrogate antigens was investigated and described here.

As shown in Chapter 3, a prerequisite to be able to produce high titre pp is to pinpoint the important elements of and understand the life cycle of the virus that will donate the envelope protein. HA activation through specific-cleavage has an essential role in the influenza virus life cycle since it permits low-pH dependent fusion with the endosome-membrane after attachment and endocytosis of the virus, permitting the release into the cytosol of the vRNP complexes. For influenza B HA activation has been observed in chicken embryonated eggs (Zhirnov, Golyando and Ovcharenko 1994), and in a trypsin-dependent and independent way in MDCK cells (Lugovtsev, Melnyk and Weir 2013; Noma *et al.* 1998). Furthermore, experiments have shown that the NA could also have a role in HA activation by removing glucidic residues on the HA surface (Yamamoto-Goshima and Maeno 1994; Shibata *et al.* 1993) and it was shown that influenza B can be cleaved by porcine pancreatic elastase when the cleavage arginine is substituted with an alanine or a valine (J. Stech *et al.* 2011). Influenza B HA can also partially support a poly-basic cleavage site that permits the cleavage by subtilisin-like proteases (Brassard and Lamb 1997). More recently, HAT and TMPRSS2 have been shown to be able to cleave and activate influenza B HA in *in vitro* models (Böttcher-Friebertshäuser *et al.* 2012). However, data on other proteases that could be involved in the influenza B HA cleavage in nature are lacking.

As already shown in Chapter 3 and elsewhere (Sawoo *et al.* 2014; Ferrara *et al.* 2013; Bertram *et al.* 2012; Bertram, Glowacka, Blazejewska, *et al.* 2010), pp are useful tools to study HA cleavage mediated by proteases: the optimisation of pp production through testing of different protease-expressing plasmids gives indirect information about

protease-cleavage specificity. Here the three proteases HAT, TMPRSS2 and TMPRSS4, described in the literature for their ability to activate influenza A HAs (Sakai *et al.* 2014; Tarnow *et al.* 2014; Baron *et al.* 2013; Galloway *et al.* 2013; Bertram *et al.* 2012; Bertram, Glowacka, Blazejewska, *et al.* 2010; E. Böttcher *et al.* 2009; E. Böttcher *et al.* 2006), were tested for cleavage of influenza B HAs to produce high titre pp. Interestingly, the results reported here correlate with the ones previously observed (Böttcher-Friebertshäuser *et al.* 2012): high titre pp are dependent on abundant and specific HAT-mediated HA cleavage as confirmed by Western blotting (**Figure 77**). In contrast, the TMPRSS2-activated pp have lower transduction titres even though the protease does mediate HA cleavage. For the first time, the role of TMPRSS4 in influenza B HA cleavage/activation is shown, since the transfection of the encoding plasmid during pp production is associated with high pp titres and HA cleavage, as observed in Western blot analysis.

It was already stated that pp transduction titres appear to correlate with Western blot results: it can also be noticed in the overall quantity of HA in each pp seems to differ. This is especially evident in the TMPRSS2-activated pp in which the HA1 bands are thinner but the HA0 bands do not appear, and by the fact that all the TMPRSS2-activated pp result in a lower transduction titre in comparison with pp produced by HAT and TMPRSS4 co-transfection. It seems unlikely that the results observed are due to transfection errors because the TMPRSS2-activated pp always exhibit lower titres independently of the influenza B HA used. These results could be explained by the fact that, to produce high titre pp, a protease-HA equilibrium could be important as a high quantity of protease usually results in a lower pp titres for all the influenza B HAs tested. This could be due to degradation of HA following the presence of a high quantity and/or highly active protease, probably related to the fact that it is known that the pp envelope displays less HA in comparison to wild-type virus (Corti *et al.* 2010). Additionally, other mechanisms could be implicated in the digestion pattern observed: for example it has been shown that protease activity is also dependent on other cellular factors, such as anti-protease/protease equilibrium and oxidative-stress (Kesic *et al.* 2012; Kesic, Hernandez and Jaspers 2012), that were not controlled in this study. As alluded to in Chapter 3 other approaches, especially biochemical, to evaluate protease activity and protease-HA affinity, will be necessary to better understand the HA cleavage mechanism and to be able to better predict type and quantity of the protease that can be used to obtain high titre pp.

Another important point to further investigate is that in the Western blot a heterogeneous HA glycosylation pattern seems to be present, as HA1 is represented by more than one band. Elsewhere it was noted that exogenous bacterial NA can also play a

role in removing glucidic residues from the HA surface, to enhance viral attachment to the receptor (Brassard and Lamb 1997). Furthermore, it was noted that the proteases, especially TMPRSS2, that mediate HA cleavage including intracellularly (E. Böttcher *et al.* 2009), could interact with the cell glycosylation machinery (Walker *et al.* 1992). The implication of this should be further investigated as it can potentially have repercussions on the pp-NT assay since glycosylation represents an important antigenic influence. To understand better the glycosylation pattern of the pp HA it will be necessary to perform further analysis that involve Peptide-N-glycosidase F and/or Endoglycosidase H treatment followed by Western blotting to highlight differences in the HA molecular weight after removal of specific oligosaccharide molecules. Potential characterisation of pp using Western and lectin blotting, and *via* mass spectrometry (Kordyukova and Serebryakova 2012; Downard, Morrissey and Schwahn 2009) would be useful to understand which glycosylation residues are lost, which are maintained, and in what proportion.

To investigate the production of influenza B pp, the role of the Kozak sequence in the influenza B HA expression was evaluated. Reverse genetic system studies performed for influenza B viruses (Jackson, Elderfield and Barclay 2010; Jackson *et al.* 2002; Barclay and Palese 1995) have previously shown that specific 5' and 3' vRNA non-coding regions, containing the Kozak sequence, are of essential importance for production of viruses, and correct sequences must always be included in this system to permit vRNA packaging, vRNA transcription and translation, and protein expression. In an analogous manner, it was previously highlighted (Chapter 3) that the presence of a Kozak sequence is necessary to express the HA and produce high-titre pp, and even if this requisite for pp production is less stringent than the reverse genetic system requirements, the presence of the Kozak sequence is an important aspect that should be evaluated. In this chapter, the use of two different Kozak sequences to permitted HA expression and production of influenza B HA pp to be investigated. Results show that the influenza A Kozak sequence GTCAAA and the influenza B Kozak sequence CACAAA are equally efficient for the expression of HA and the production of high titre pp. In fact B/Bangladesh/3333/2007 pp exhibit the same titres and cleavage pattern independently of the Kozak sequence used (**Figure 79**). These data, and literature show that it could be interesting to test the effect of the absence of the influenza Kozak sequence, or of the presence of other Kozak sequences (e.g. human) in the influenza B pp production model, perhaps also using direct qualitative and quantitative evaluation of HA expression by immunofluorescence, Western blotting or by fluorescence-activated cell sorting analysis. Furthermore it could be of interest to see if the influenza B Kozak sequence CACAAA could be used to express other viral proteins and

produce influenza A and non-influenza pp. Unfortunately, this is beyond the scope of this study.

After optimisation of the production of influenza B pp through analysis of HA cleavage and Kozak sequence, the pp were characterised for their activity to transduce different cell lines. Influenza B pp are able to transduce HEK293T/17, MDCK and A549 cell lines: higher transduction titres were obtained when the producer cells HEK293T/17 were used, whereas the classical influenza producing cell lines MDCK and the human lung carcinoma A549 show lower transduction titres. There are two major factors that could explain why different HAs show better entry capacity than others in different cell lines. Firstly, influenza B HA recognises different sialoglycan residues present on the glycoprotein surface to mediate cell entry, and different strains/viruses can have different preferences (Y.-F. Wang *et al.* 2012; G. Xu *et al.* 1994; M. N. Matrosovich *et al.* 1993); secondly cells can present a different proportion of sialic acid combinations (Lugovtsev, Melnyk and Weir 2013; N. M. Varki and A. Varki 2007; Svennevig, Prydz and Kolset 1995). A further factor, in the light of the results observed during the production of recent H3pp (Chapter 3), is that if pp have a lower density of HAs in their surface, a lower pp avidity could consequently result. This could be important for the entry into certain cell lines, in relation to differential sialic acid distribution between cells (Sieben *et al.* 2012).

However, these elements alone cannot explain the differences in titre observed, especially taking into consideration that MDCK should be a highly susceptible cell line since it is routinely used for influenza virus infection and amplification. Considering that HEK293T/17 are used as producer cells and subsequentially as target cells, exhibiting higher transduction efficiency compared to the other cell lines tested, it is reasonable to enquire if the identical origin of the pp lipid bilayer and of the target cell plasma membrane can influence the transduction activity. In fact, the lipid bilayer and the characteristics of the membrane lipids can play an important role in the attachment of the virus particle and lipid properties have been shown to play an important role in membrane fusion (Heaton and Randall 2011; Xiangjie Sun and Whittaker 2003; Chernomordik *et al.* 1998). Furthermore it was demonstrated that HIV-1 and influenza viruses present lipid bilayer envelopes showing different characteristics in comparison to the producer cell lines (Lorizate *et al.* 2013; Gerl *et al.* 2012; Aloia, Tian and Jensen 1993). To assess membrane role in pp transduction the study of the pp envelope lipids in comparison with the ones of the producer and target cell lines could help to elucidate the factors that can interfere with viral attachment. Furthermore performing experiments in which different cell lines are used as producer cells and as target cell lines could also be helpful to understand the lipid roles in membrane attachment and fusion.

With a first characterisation of the pp complete, the use of the generated influenza B pp in neutralization assays was investigated. Firstly, the ability of a reference antiserum to neutralize the pp generated. Only an anti-B/Brisbane/60/2008 reference serum was available, and it was tested successfully in neutralization assays against three different viruses: B/Brisbane/60/2008, B/Florida/4/2006, and B/Hong Kong/8/1973. Next, pp-NT assays were used to evaluate the neutralization activity of a set of pre- and post-vaccination sera for which the HI titre against B/Brisbane was known.

The reference serum used could neutralize all the pp tested and it could also differentiate between them showing correlation with amino acid identity through different neutralization activities: in fact the serum neutralizes the homologous B/Brisbane/60/2008 most efficiently, followed by B/Hong Kong/8/1973, which shares 94.9% amino acid identity with B/Brisbane/60/2008, and B/Florida/4/2006 (93.5% amino acidic identity). This could indicate that, as already observed with influenza A (Molesti, Ferrara, *et al.* 2014; Corti *et al.* 2011; Corti *et al.* 2010; Garcia *et al.* 2009), the pp-NT assay is more sensitive in detecting cross-neutralizing antibody responses.

Furthermore, it should be noted that the reference sheep antisera used is hyperimmune and for this reason more prone to cross-react in presence of similar strains and therefore not recommended for antigenic analysis. This could explain why such high cross-reactivity was detected between strains of different lineages using pp-NT assay. Additionally cross-reactivity between influenza B lineage is sometime reported using similar serum. Additionally, absence of serum pre-treatment should also be considered as possible cause of the cross-reactivity detected, as discussed in Chapter 4.

Here, using a panel of vaccination sera in the analysis of IC_{50} results obtained with the pp-NT assay and the HI titres against B/Brisbane/60/2008, discordant correlation was observed between the HI and pp-NT assays (**Figure 84**). However, this observation does not represent a problem in the reliability of the pp-NT assay, since influenza B HI assay is already known to not be sensitive (Wood *et al.* 1994; G. Mancini *et al.* 1983; Oxford, Yetts and Schild 1982), whereas pp-NT is highly sensitive (Garcia *et al.* 2010; W. Wang *et al.* 2008; Temperton *et al.* 2007). The HI insensitivity is also demonstrated by the fact that it was unable to detect antigenic differences between influenza B viruses until the 1980s (Rota *et al.* 1990) meanwhile phylogenetic analyses have shown that the two distinct lineages were present already in the second part of the 1970s (R. Chen and Holmes 2008). Furthermore SRH and classical HI have also been shown to correlate poorly (Oxford, Yetts and Schild 1982). More recently, it was reported that discordant correlation could be observed between SRH, MN, HI, and pp-NT, since all these assays measure different kind of antibody responses (Molesti, Ferrara, *et al.* 2014). For this reason, it will be also

necessary to test other sets of sera to understand the correlation characteristics of the Influenza B pp-NT with HI. For the same reason, it will be necessary also to see if the pp-NT assay correlates with SRH or MN. Of special interest would be the correlation study with MN since pp-NT and MN are based on the same principle, differing essentially in sensitivity, and are able to detect stalk-directed cross-neutralizing antibodies.

Considering that reference sera neutralization has shown some level of cross-reactivity and that it was demonstrated (Chapter 5) that Influenza A pp-NT is able to detect cross-reactive stalk-directed antibodies, Influenza B pp-NT assays ability to detect Influenza B cross-reactive responses in this set of vaccination sera was also investigated. This took the form of neutralization assays with viruses not included in the trivalent vaccine that was originally administered to the test subjects. In fact, as already mentioned, if the influenza B pp-NT assay is more prone to detect stalk-directed antibody responses, this alone can partially explain the discordant correlation with the HI assay previously observed. As explained in Chapter 5 for the analysis it was decided firstly to consider simply the differences in time-points (day 0 and day 21), secondly the differences in vaccination regimens (TIV + placebo and TIV + MVA-NP+M1) were evaluated, despite that the limited number of subjects recruited in each group restricts the statistical analysis that can be performed.

Surprisingly, high neutralization responses were detected against the vaccination strain B/Brisbane/60/2007 and for B/Florida/4/2006 and B/Hong Kong/8/1973 HA pp, and for the last two strains analysed, these neutralization titres also increased after vaccine administration. With regard to the age of the participants in this clinical trial (50 years and above) (Antrobus *et al.* 2013), it is likely that the subjects have encountered the two strains (B/Florida/4/2006 and B/Hong Kong/8/1973) previously so it is expected that a certain level of antibody against theses two strains could already be present; however the high titre observed, especially against the B/Hong Kong/8/1973 pp, and the increase in the neutralization titre after vaccination indicate that a certain level of cross-reactivity could be present. This is not surprising especially for influenza B viruses. Before the Yamagata and Victoria lineage division, SRH was shown to be able to detect seroconversion also for strains not encountered previously and not included in the administered vaccines (Oxford, Yetts and Schild 1982). In that case, this was not interpreted as lower specificity of the assay, but as a characteristic of influenza B virus to be able to induce a cross-reactive response (Oxford, Yetts and Schild 1982). Recently it was shown that seroconversion and increase in antibody responses was obtained against a Yamagata strain, when a trivalent vaccine containing a Victoria lineage strain was used if the subjects were previously primed with a Yamagata-strain containing vaccine (Skowronski *et al.* 2012). Here,

analogously, when a Victoria-strain based vaccine (B/Brisbane/60/2008) is administered, a significant increase in the neutralizing antibody response against a Yamagata strain (B/Florida/4/2006) and a pre-lineage division strain (B/Hong Kong/8/1973) is observed, whereas the increase against the vaccine strain if present is not statistically significant.

A bioinformatic analysis to investigate similarity between the HAs used in the pp-NT assays was performed to understand possible epitopes underlining the cross-reactive response observed. The three HAs used differ especially for residues present within epitopes located on HA head. The region corresponding to antigenic site A and B are the ones with the greatest differences between the three HAs tested. The HA stalk and the central part of the HA head appear conserved. When differences are observed in the stalk, these are usually in positions proximal to the membrane or in the transmembrane region itself, and it is unlikely that they have an antigenic role since known stalk epitopes are usually less proximal (Dreyfus *et al.* 2012; Corti *et al.* 2011; Ekiert *et al.* 2011; Ekiert *et al.* 2009; Sui *et al.* 2009). Furthermore, the parts of the HA that are more conserved correspond roughly to the epitope regions of mAbs that show broader neutralization activity against influenza B viruses (also inter-lineage neutralization) (Yasugi *et al.* 2013; Dreyfus *et al.* 2012). With the knowledge that the influenza A pp-NT neutralization assay is able to detect antibodies directed to the stalk region, a hypothesis is that the influenza B pp-NT is also able to recognise antibodies directed against the conserved characterised epitopes (Yasugi *et al.* 2013; Dreyfus *et al.* 2012). These antibodies are the ones that in B/Florida/4/2006 and B/Hong Kong/8/1973 pp-NT increase post-vaccination, as it is unlikely that the seasonal vaccine would be able to increase or generate antibody that recognise the non-conserved regions of these unrelated HAs.

Furthermore, using classical epitope mapping methods, site B seems to be the one for which influenza B antibody response is directed in the majority of cases (Rivera *et al.* 1995; Berton, Naeve and Webster 1984; Krystal *et al.* 1983). It will not be surprising if, as observed for Yamagata-lineage (Yasugi *et al.* 2013; Dreyfus *et al.* 2012), broad neutralizing Victoria-lineage specific antibodies directed against site B were present in the human population and were not yet described. The presence of these antibodies, for example, could explain the decrease in antibody titre observed between B/Brisbane/60/2008 HA and B/Hong Kong/8/1973 HA that possess a different antigenic site B, as a deletion is present, while other sites appear more conserved. These show that epitopes generating cross-reactive responses to influenza B are more readily exposed than influenza A ones, and in the light of the results and the literature reported here, they could potentially drive the antibody response against the virus. A cross-reactive response, also

stalk-directed, probably plays a more predominant role in protecting against influenza B viruses than the one usually observed with influenza A viruses. For the moment, the ability to detect stalk-directed antibody responses *via* the pp-NT assay is the only tool to verify the spread of this cross-reactive response. In addition, to test this hypothesis a convenient approach could be using chimeric influenza B HA that present the stalk of influenza B and the head of influenza A HA. Unfortunately such hybrid HA is potentially more difficult to construct than others, since influenza B HA lack the two cysteines of the disulphide bond that are exploited for creating the chimeric protein (Pica *et al.* 2012). Another possible approach is to insert influenza B epitopes into the influenza A HA frame, however this could potentially result in protein misfolding. Since the influenza B reservoir is principally restricted to humans, the influenza B strains that are found in other animals (i.e. seals) usually have antigenic characteristics similar to human influenza B strains (Bodewes *et al.* 2013; Osterhaus *et al.* 2000), and considering that two influenza B lineages co-circulate, the use of influenza B HAs that present a single-mutation or switching of small epitopes between non-related influenza B strains could be of help, on condition that the influenza B assay is sensitive enough to distinguish between single amino acid mutations.

Despite this, there is a result that remains difficult to interpret using this cross-reactive theory without need for additional explanation: the fact that, using the B/Brisbane/60/2008 pp-NT, an increase in neutralizing titres are not detected post-vaccination. It was previously pointed out that an original antigenic-sin could explain higher responses to non-related HAs than the vaccine HA; an interesting additional hypothesis is that B/Brisbane/60/2008-specific antibodies were already present at high level in the population analysed and that the vaccine has simply not boosted an already high and specific antibody response, boosting only a cross-reactive one that was lower. This could be partially explained in the light of influenza B HA evolution: in 2013 a new influenza B virus has started to circulate causing increased seasonal epidemics and it was pointed out that herd immunity could play a big role in determining influenza B evolution (R. Chen and Holmes 2008; Air *et al.* 1990), triggering the emergence of new influenza B strains. The higher sensitivity of the pp-NT in comparison to classical serological assays (e.g. HI) could have potentially emphasised this underlying herd immunity.

In the second part of the analysis of the neutralization responses in vaccination sera, differences between the two vaccination regimen groups were evaluated. By graphical comparison it could be observed that TIV + MVA-NP+M1 group seems to have lower antibody responses at day 0 compared to the TIV + placebo group (**Figure 86**). Graphical results also appear to indicate that an underling role of MVA vaccine in increasing

antibody responses against influenza B could be present, as the IC_{50} fold-increase observed (**Figure 87**) in the TIV + MVA-NP+M1 group appears to be greater than the one of the TIV + placebo group. However, statistical analysis does not confirm this observation. In Chapter 5, the advantage of MVA vaccination was discussed. If a role of this vaccine in increasing influenza B specific response will be proved by other analysis and experiments with a larger number of subjects, it could pose numerous questions. Is it the adjuvant effect of MVA that mediates the increase in antibody responses observed? Is there a role of influenza A NP and M1 protein-specific T-cell response in influenza B response? How are influenza A and B specific responses connected in nature? These are questions that remain unanswered for the moment, but are undeniably of biological interest, especially for the generation of 'universal' vaccines. It was suggested that the response against influenza A virus could influence influenza B virus response and consequentially influenza B virus evolution, facilitating the shift of dominance between the two lineages in different seasons (R. Chen and Holmes 2008; Air *et al.* 1990). However, how or if this happens is not yet clear and should be investigated. It could be that HA stalk-directed antibodies play an important role in this and pp will be effective tools to assess it.

To conclude, the data presented here demonstrate that influenza B pp, which are produced at higher titre using proteases, could be useful tools to study influenza B HA directed specific and cross-reactive antibody responses. However, more experiments are necessary to understand the advantages and disadvantages of the influenza B pp-NT assay in comparison with classical serological methods.

CHAPTER 7
Discussion

The studies presented in this thesis detail the generation of new influenza pseudotype particles (pp) and the investigation of their use in neutralization assays to study human antibody responses.

In Chapters 3 and 6, pp expressing the haemagglutinins (HAs) of different influenza A and B strains and subtypes on their surface were produced. Firstly this involved an optimisation procedure to identify proteases that were able to efficiently mediate HA cleavage/activation. As is shown, the production of pp using these proteases has two advantages: it is possible to study a critical process in which HA is involved and that is a determinant in viral pathogenicity, and to produce important reagents that can be used for evaluating antibody responses.

As shown in Chapter 3, certain pp were more problematic to produce, especially to high titres, and different strategies involving additional adjustments of the HA encoding plasmid were necessary to increase the pp titre. In another case it was necessary to add a neuraminidase (NA) encoding plasmid to the transfection mix in order to increase pp titre. Probably this was due to the fact that HA did not have sufficient affinity for the cellular receptor, and that the presence of NA permitted to compensate for absence of HA affinity (Gulati *et al.* 2013; de Vries *et al.* 2012; Y. P. Lin *et al.* 2010). This demonstrates that pp production system can be improved and can also help to elucidate processes underlying aspects of the co-evolution of the influenza envelope proteins. Another utility of pp is the ability to generate mutants and to evaluate different combinations of HA and NA subtypes without the risk of creating potentially dangerous/pandemic viruses, since pp are replication defective.

The work presented demonstrates that it is becoming important to better characterise the pp produced, especially in relation to specific HA attributes. In Chapters 3 and 6, when HA cleavage was evaluated through Western blotting, a potential problem in the glycosylation characteristics of influenza pp was noted. In fact, HAs processed by the tested proteases seem to present a more heterogeneous glycosylation (indicated by the presence of double band corresponding to HA1) compared to HAs produced in absence of proteases and treated with L-tosylamido-2-phenyl ethyl chloromethyl ketone treated trypsin (TPCK-Trypsin). These glycosylation ‘problems’ should be investigated to not only improve the pp production methodology but also to understand the pp antigenic characteristics. In fact, such pp glycosylation differences/characteristics have important

repercussions as they expose usually hidden epitopes (usually masked by glycosylation), explaining the high sensitivity (sometimes at the expense of specificity) observed during pp neutralization (pp-NT) assays.

In Chapters 4-6 it was shown that the pp-NT assay is particularly sensitive compared to Single Radial Haemolysis (SRH) and haemagglutination inhibition (HI) assays. Other authors have also discussed the high sensitivity of pp-NT in comparison to microneutralization (MN) assay (Molesti, Ferrara, *et al.* 2014; Hai *et al.* 2012; Corti *et al.* 2010; Garcia *et al.* 2010; Alberini *et al.* 2009; Sui *et al.* 2009; W. Wang *et al.* 2008), however it is not yet clear if this sensitivity is related to pp characteristics (i.e. lower density/quantity of envelope proteins on the surface) or there are other factors, such as non-specific inhibitors (e.g. lectins) present in antisera that could influence neutralization (E. K. Subbarao *et al.* 1992). The results reported in Chapters 4 and 5 indicate that some influenza A pp (e.g. H4pp and H9pp) are more readily neutralized than others by the reference antisera tested and by human pre- and post-seasonal vaccination sera. These neutralization profiles do not appear to be non-specific, since the negative control used does not neutralize the pp, but they are of concern. It could be that epitopes described to be involved in cross-reactivity between HAs are more exposed in these more readily neutralized HAs. However, there is no evidence of this at the moment but further investigation involving the characterisation of pp and optimisation of pp-NT assay should be pursued.

In Chapter 5 a particular advantage of pp was shown: using different pp and especially using chimeric HA pp, it was possible to directly study stalk-directed antibodies and confirm their presence in human sera. Whether the cross-reactive antibodies detected using pp-NT have a protective role *in vivo* is not yet clear, especially since correlates of protection are not yet established for pp-NT. Furthermore, since stalk-directed antibodies are believed to mediate their function in vivo through Fragment crystallizable (Fc) γ receptor engagement (DiLillo *et al.* 2014), it is not clear if the stalk-directed antibodies detected here could have an activity *in vivo*. In fact, pp-NT does not permit discrimination between immunoglobulins (Ig) classes, and only certain classes/subclasses binds efficiently to the Fcγ receptor. Additional experiments using antibody preparations that have been purified to obtain Ig of one specific class may better elucidate the biological significance of the cross-reactive responses detected here.

7.1 Future work

Future developments of this project in light of the results reported in this thesis are extensive and can be summarised in the following categories:

- Generation of other influenza pp, including influenza C and D;
- Optimisation of the pp production system;
- Study and prediction of HA protease-mediated activation and cleavage;
- Characterisation of pp using microscopy and proteomics techniques;
- Optimisation and standardisation of the pp-NT, including the establishment of reference standards and controls;
- Evaluation of heterosubtypic antibody response and its evolution over time in different human populations (with particular focus on newborn infants, children, immunocompromised people, etc.) using the panel of pp described here, and novel chimeric HA pp;
- Use of pp in other serological/immunological assays (e.g. HI, Enzyme-Linked Immunosorbent Assay 'ELISA', post-attachment neutralization assay);
- Application of influenza HA pp/lentiviral vectors in novel vaccine and gene therapies.

Below some of these potential project developments are discussed in relation to results reported in this thesis. In addition, some other preliminary experiments that were performed during the study period will be briefly mentioned.

7.1.1 Generation of other influenza pseudotypes, including influenza C and D

In Chapter 3, new pp belonging to different subtypes never before pseudotyped were described. Nevertheless, pp representative of certain subtypes, such as H6 and H13, were not able to be generated since either the HA-encoding plasmid was non available or the current protocols resulted to be unsuccessful. These two pp need to be developed as soon as possible. In fact, since influenza viruses bearing H6 HA have been shown to infect humans (Freidl *et al.* 2014; Yuan *et al.* 2013; Kayali *et al.* 2009), H6 viruses can pose a pandemic threat (G. Wang *et al.* 2014). H6pp could be used in neutralization assays to highlight if the human population possess antibodies that can mitigate or protect from H6 viruses in case of a pandemic. Additionally, H13pp could be useful to study the characteristics of H13 HA (i.e. receptor specificity) since this HA has been shown to possess peculiar receptor binding activity (i.e. different amino acid residues in the

receptor-binding site compared to other HA subtypes and unclear affinity for α-2,3 sialic acids) (Lu *et al.* 2013; Nobusawa *et al.* 1991; Chambers *et al.* 1989).

Furthermore, the production of pp bearing HAs of the most recent human H1 and H3 circulating influenza strains (e.g. A/California/04/2009 (H1N1)-like, A/Perth/16/2009 (H3N2)-like, and A/Victoria/361/2011(H3N2)-like) should be further investigated, since some of these reagents are already described in the literature (Sawoo *et al.* 2014; Yang *et al.* 2014; Margine, Krammer, *et al.* 2013; W. Wang, Castelán-Vega, *et al.* 2010), whereas in this thesis their production was more problematic (i.e. difficulties in production of A/Texas/05/2009 H1pp, and A/Wisconsin/67/2005 H3pp compared to pp bearing H1 and H3 of past circulating viruses).

Of particular interest would be the production of pp expressing HAs of H1 and H3 avian and swine strains, too. Producing such tools will allow pp neutralization (pp-NT) assays to be carried out, and to understand how much cross-reactivity is present in the human population against avian and swine strains from which pandemics have started in the past, and for which the human population was previously reported to be naïve (Capua *et al.* 2009).

Recently H17 and H18 influenza A viruses were detected by polymerase chain reaction (PCR) in bats and different studies have now highlighted the fact that it is not possible to cultivate these viruses and that the HAs do not recognise sialic acids as receptors (Xiaoman Sun *et al.* 2013; Tong *et al.* 2013). The production of pp harbouring these novel HAs could permit elucidation of their biologic characteristics, to identify the cellular receptor, to investigate the spread of these viruses in the bat/animal population using serological methods, and to understand if they have potential to cause pandemics taking into account the immunological status of the human population.

Amongst the influenza viruses, influenza C tends to be neglected even if it is the only type that is exclusively circulating in humans. Since the lentiviral pp production protocol reported in this thesis was efficient for the generation of influenza B pp, the production of influenza C pp using the same method could be evaluated. Production of influenza C pp using vesicular stomatitis virus (VSV) core is described in the literature (Hanika *et al.* 2005). However, influenza C pp using a lentiviral core are not yet described. Lentiviral vectors have the advantage to be able to transduce non-dividing and dividing cells (Sakuma, Barry and Ikeda 2012; Durand and Cimarelli 2011). Furthermore compared to VSV, lentiviral pseudotyping usually do not require engineering the cytoplasmic tail of the donor envelope protein, consequentially it is in general a more straightforward process (Owens and J. K. Rose 1993). Lastly, they have a higher safety profile than VSV since more recombination events are necessary to reproduce the native

virus (especially if second or third generation packaging systems are used). In the light of the protocols described here for Influenza A and B pp, and considering the characteristics of the Haemagglutinin-esterase-fusion (HEF) envelope protein, which possesses sialidase activity (Pekosz and Lamb 1999; Rosenthal *et al.* 1998; Herrler *et al.* 1988), to produce influenza C pp exogenous NA will not be necessary; however proteases able to activate influenza C are not yet described, and the optimisation protocol (as described in Chapters 3 and 6) will be important to elucidate HEF activation.

Lastly, with the very recent discovery of a possible influenza D virus (Hause *et al.* 2014; Hause *et al.* 2013; Sheng *et al.* 2013), pp could be utilised to study this new virus, understanding the similarities and differences of the envelope proteins compared with the other influenza types. Furthermore, the use of an influenza D pp-NT will permit to evaluate how wide spread the immunity to this virus is in animal and human populations.

7.1.2 Optimisation of the pseudotype production system

In the literature there are regular reports of the development of novel packaging cell lines to produce lentiviral vectors for gene therapy (Ni *et al.* 2005; Sinn, S. L. Sauter and McCray 2005; Strang *et al.* 2004; Farson *et al.* 2001; Pacchia *et al.* 2001). Packaging cell lines are extremely useful as they permit continuous production of lentiviral vectors and the reduction of the number of plasmids that need to be transfected (Sinn, S. L. Sauter and McCray 2005; Strang *et al.* 2004). However, these cell lines present different problems, for example the partial toxicity of the human immunodeficiency virus type-1 (HIV-1) structural proteins expressed (Sinn, S. L. Sauter and McCray 2005; Farson *et al.* 2001). In case of influenza pp, considering that different envelope proteins are used, a packaging cell line expressing (probably under an inducible promoter) only the HIV-1 structural proteins would be very useful to investigate. A packaging cell line expressing only HIV-1 structural proteins and not the lentiviral vector or the envelope surface proteins would permit the maintenance of pp production flexibility. In fact, different envelope protein-encoding plasmid and lentiviral vector expressing different reporter genes could be transiently transfected into this producer cells, consequently permitting the generation of pp with different envelope-reporter combinations.

Furthermore, in Chapters 3 and 6, it was shown that proteases are necessary for production of high titre pp. Generation of a cell line expressing such proteases as a pp producer could be investigated. Since the results reported seem to indicate that an accurate optimisation of the protease quantity is necessary to obtain HA activation, inducible cell lines, utilising different gene promoters, could be developed. Since inducible cells expressing type II Transmembrane Protease Serine 2 (TMPRSS2) and human airway

trypsin-like protease (HAT) have been produced, testing these cell lines for pp production before generating protease-expressing Human Embryonic Kidney (HEK) 293T/17 cells may help to understand if the approach is suitable.

7.1.3 Study and prediction of haemagglutinin protease-mediated activation and cleavage

In Chapters 3 and 6, it was shown that optimisation of the type and quantity of protease is necessary to activate HA, however it is not yet clear which are the factors that influence protease-HA recognition. The cleavage data acquired during the current study using different HA/protease combinations, and generation of new data with new combinations, will permit the use of bioinformatic methods to understand and possibly predict which proteases will be able to cleave a specific HA. Bioinformatics prediction tools have been specifically generated to predict different aspects of protein characteristics, such as protein sorting, glycosylation, and secondary structures (Chauhan, Rao and Raghava 2013; B. Eisenhaber and F. Eisenhaber 2010; Krogh *et al.* 2001; Nakai 2000).

Furthermore, using bioinformatic approaches and pp-derived data will make it possible to identify potential critical residues for HA cleavage and to test their role through mutagenesis and pp production, and thus confirm the reliability of the bioinformatics tool generated.

7.1.4 Characterisation of pseudotype particles using microscopy and proteomics techniques

In this thesis different pp were produced and characterised only for their ability to transduce target cell lines. In Chapters 3 and 6 the need to optimise Western blotting using pp was highlighted, which has shown mixed results to date. This would permit quantification of the particles, characterisation of the HA cleavage, study of pp HA glycosylation characteristics, and evaluation of batch-to-batch variations.

Confocal microscopy has been used to evaluate the concomitant presence of the core protein and the envelope protein on the pp surface (Pizzato *et al.* 1999), and could be an extremely useful tool to evaluate what proportion of particles present HA on their surface.

Electromicroscopy and cryoelectromicroscopy are also useful tools to characterise virus particles and recently they were used to understand the distribution of HA on the influenza virus surface and to understand how stalk-directed antibodies interact and recognise the HAs (Wasilewski *et al.* 2012; Corti *et al.* 2011; Bonnafous *et al.* 2010). These kinds of studies will be extremely valuable for pp since they could help to elucidate if the high sensitivity of pp-NT is due to a lower density of HA on pp surface.

Recently mass spectrometry has begun to be used for virus characterisation and typing (Kordyukova and Serebryakova 2012). For this reason, it represents a technique that should be investigated to characterise pp; furthermore it will also permit the evaluation of glycosylation characteristics of the HAs expressed on the pp surface.

7.1.5 Optimisation and standardisation of the pseudotype particle neutralization assay, including the establishment of reference standards and controls

The work presented using pp-NT is still at a research level and proof-of-principle stage. The pp-NT assay is not optimised, standardised or validated according to the International Conference on Harmonisation of Technical Requirements for Registration of Pharmaceuticals for Human Use (ICH), and the United States Pharmacopeia. In Chapter 4 it was discussed that establishing adequate positive, negative controls and reference standards are essential, but other aspects should be evaluated to standardise and validate an assay.

As in all cell-based assays, cell input is an important aspect in standardisation (The United States Pharmacopeial Convention 2010a; The United States Pharmacopeial Convention 2010b): the use of an automatic cell counter, cell viability (e.g. using trypan blue), and evaluation of α-2,3:α-2.6 sialic acid ratios present on the cell surface, are all aspects that should be taken into account and investigated since they could be important for the consistency of the assay during different analytical sessions.

Another important aspect of optimisation and standardisation is the viral input used in the pp-NT assay. The measure of the transduction activity of pp, as performed in this thesis, evaluating the expression of reporter genes is the most straightforward technique to evaluate pp titres. However, this method cannot discriminate between cells with single or multiple integration events (due to multiplicity of infection) (Geraerts *et al.* 2006). Furthermore, especially when using enzymes as reporters (e.g. firefly luciferase), the titres can also depend on the level of reporter protein expression, which could be related to the vector integration in more or less active regions of the chromatin (Geraerts *et al.* 2006).

Different research groups exploiting pp of influenza virus and other viruses determine the viral input evaluating the number of viral particles. These quantification methods usually consist on evaluation of the HIV-1 viral core protein p24 amount (directly correlating with number of particles), or in quantification of pp genomes through reverse transcription real-time or quantitative PCR, or evaluating pp reverse transcriptase activity (Geraerts *et al.* 2006). Evaluation of p24 protein content and of reverse transcriptase

activity can be readily achieved using commercial kits that are commonly used in HIV-1 testing (Geraerts *et al.* 2006).

Instruments able to track and characterise nanoparticles can also be employed for evaluation of viruses and vaccines. These instruments are able to evaluate not only the number of particles but also their dimension, and if they aggregated (Carr and M. Wright 2013). These instruments can potentially help to differentiate defective pp. Firstly it can discriminate if the pp harbour on their surface HAs, since their presence should change the diameter of the pp. Secondarily, if coupled with reverse transcription real-time or quantitative PCR it permits to establish the ratio of genome-containing or empty pp (Filipe, Jiskoot and Hawe 2011). Preliminary experiments (**Appendix Table 9**) performed using Nanosight LM10, one of these instruments, show that the number of pp is of the same order of magnitude in the preparations of different HA pp and in pp without envelope glycoproteins, but the two differ for particle dimensions. This means that evaluating pp titre using simply particle number does not correlate with viral entry since particles without envelope glycoproteins cannot enter into cells, or if they enter, do not integrate their genome since they remain trapped in the endosomes to be subsequently degraded (Voelkel *et al.* 2012). If this Nanosight result will be confirmed by further experiments, it will underline the impossibility to normalise viral input using p24 measurement or quantitative reverse transcription PCR, since these methods are related to the particle number and not to the ability of the particle to enter into cells, the factor that is evaluated in a pp-NT assay.

A good compromise used by different groups (Hai *et al.* 2012; W. Wang, Xie, *et al.* 2010), in relation to the use of pp in neutralization or other assays, is also to standardise the pp input using HA content. However, technical problems can be encountered. In fact, the HA content could be expressed by different measures: HA content can be the total HA protein amount, the amount of only the active (cleaved) HA, or the haemagglutinating units. Evaluation of total HA quantity can be easily achieved using ELISAs that are already commercially available or that can be developed in-house; however it could be necessary to use a specific kit for each HA subtype or strain. Quantification of haemagglutinating units can be easily performed with the haemagglutination assay (World Health Organization 2002). However, it has been shown that normalising the virus input using haemagglutination units instead of reporter gene expression can result in lower reporter signal levels for some pp since a lower number of particles is used (Hai *et al.* 2012). This is probably due either to HA differential expression on the viral surface (some HA can be more expressed than others (Hai *et al.* 2012)) or to the decrease of HA affinity for sialic acid and consequentially reduction in viral entry (Hai *et al.* 2012).

To quantify cleaved and uncleaved HA, quantitative Western blotting using densitometry needs to be performed (Taylor and Posch 2014; Changgui Li *et al.* 2010). This assay requires complex development and standardisation: internal loading controls need to be used, membrane transfer needs to be consistent between different experiments, quantity standards (e.g. different amount of recombinant HA) need to be prepared and validated. Furthermore this assay requires the use of specific antibodies against the protein of interest, and for this reason it will be necessary to isolate at least two antibodies (recognising HA1 and HA2) or a suitable polyclonal preparation for each HA subtype that needs to be tested.

Ultimately, establishing cut-off values for pp-NT to be used to discriminate between positive or negative sera (Garcia *et al.* 2010) and subsequently for correlation with protection (Alberini *et al.* 2009) will be necessary.

7.1.6 Use of pseudotype particles in other serological/immunological assays

Different groups have now used pp as surrogate antigens not only in neutralization but also in HI: they have shown that serological results are comparable with the classic HI performed using native viruses (Yang *et al.* 2014; W. Wang, Xie, *et al.* 2010). However, studies have focussed only on Highly Pathogenic Avian influenza (HPAI) and human seasonal strains and for this reason it will be of interest to evaluate the new pp described in Chapter 3.

A rudimentary experimental ELISA using pp was investigated: in preliminary experiments it was observed that an influenza H5 pp fails to coat the wells of a standard ELISA plate, which was possible using recombinant HAs (Protein Sciences, cat.no. 3006 A/Vietnam/1203/2004) (**Appendix Figure 22**). The presence of Fetal Bovine Serum (FBS) in the pp production media may contribute to this effect. A potential solution that should be investigated further was found in a sandwich ELISA. This will not require removal of FBS protein (i.e. albumin), which was a problem (Chapters 2, 3 and 6) when purification methods are not used (e.g. gel-filtration and commercial available kits). In this sandwich ELISA an antibody directed against the specific HA head will be coated on the well surface and it should be able to capture strain/subtype specific pp, permitting the use of sera or other monoclonal or polyclonal preparations. However, to be able to apply this format, HA-head specific antibodies need to be used, and a precise optimisation for each pp will be necessary, with particular attention paid to the origin of the antibodies used during the coating (they should be of a different species to avoid cross-reactivity with the ones that require testing).

In Chapter 1, the use of pp in post-attachment neutralization assays (Oh *et al.* 2010) was described. This allows specific detection of antibodies that inhibit virus-endosome fusion. However, the method is scarcely used. The development and optimisation of a post-attachment neutralization assay that does not require incubation at 4°C could be an advantage and it was partially investigated. Preliminary results have shown that neutralization occurs when HA head-directed antibodies are added 1 h after HEK293T/17 cells and HA pp were mixed together at room temperature (**Appendix Figure 23**). A possible solution is to investigate centrifugation (spinoculation) to facilitate and enhance attachment of the pp to the cell surface, a necessary step to discriminate between head-directed and stalk directed antibodies.

Recently multiplexing of HA pp-NT using avian sera was also described (Molesti, Wright, *et al.* 2014). The major advantage of multiplexing includes the possibility to test sera against two or more different pp at the same time, reducing the quantity of sample to be used. However, a disadvantage could be the fact that in the presence of cross-reactive antibodies, which are present in human sera according to the results presented in Chapters 5 and 6, the pp could compete during the neutralization. It will be necessary for this reason to perform the multiplexed pp-NT using stalk-directed monoclonal antibodies and see if any differences in neutralizing titres are detected in comparison to single pp-NT.

7.1.7 Application of influenza haemagglutinin pseudotype particles/lentiviral vectors in vaccine and gene therapies

Recently lentiviral vectors bearing HA on their surface were used as gene therapy vectors, as they are able to efficiently transfer a gene to the airways of a mouse model (Ostrowski *et al.* 2014; Patel *et al.* 2013). This would be a promising development, especially for pathology of the respiratory system (e.g. Cystic Fibrosis, Primary Ciliary Dyskinesia) (Ostrowski *et al.* 2014; Patel *et al.* 2013). Nevertheless, the potential application of these vectors in humans has one problematic aspect: humans, unlike laboratory mice, can encounter influenza HA during their lifetime, and can express mucosal-derived antibodies that are potentially able to stop the entry of the lentiviral vectors into the target cells and thus prevent gene transfer. In this case, age and immunological status of the patient could be an important aspect for gene therapy and the possibility to choose between different avian and animal HA lentiviral vectors/pp on the basis of prevalence of the antibodies in potential patients could be an advantage. In fact, immunological tests (i.e. pp-NT assay) can be used as tools to select an HA to which a lowered or absent antibody response is detected and that can be safely and effectively used in gene therapy. Even if this strategy appears over complicated, the same principle is used

when adenoviral and adeno-associated gene therapy is applied (Ahi, Bangari and Mittal 2011).

Influenza virus-like particles (VLPs) are being investigated as influenza vaccines by different groups since they permit the presentation of proteins in their natural conformation (S.-M. Kang, M.-C. Kim and Compans 2012; Haynes 2009; Bright *et al.* 2007). In addition, VLPs possessing the HA as the envelope and lentiviral or retroviral *gag* as the core have been used successfully as vaccines in animal models (Haynes 2009; Guo *et al.* 2003). Furthermore, VSV bearing influenza HAs on their envelope were also shown to be a successful candidate vaccines (Ryder *et al.* 2014). With adequate precautions, lentiviral pp could therefore be used as vaccines too. For example, recently, non-integrating lentiviral vectors have been described (Farazmandfar *et al.* 2012; Banasik and McCray 2010). These vectors permit the transduction of target cell lines, however the genes within the vector are expressed but not integrated. They can for this reason be used efficiently as a vaccine permitting the expression of proteins of interest after entry, potentially also inducing T-cell responses, in a similar manner to that observed using adenoviral and Modified Vaccinia Ankara (MVA) vectors.

CHAPTER 8
Conclusion

In this thesis the production of influenza HA lentiviral pp as novel reagents for the study of influenza HA specific antibody responses is described. The generation of pp bearing HA on their surface was shown to require optimisation, particularly of the proteases used to activate the HA and the quantity of envelope protein used.

The pp were used to investigate amino acid residues that could influence HA cleavage, demonstrating that they are useful tools to study the basic biology of the influenza virus. Furthermore, with the addition of a NA-encoding plasmid to the transfection mixes, it is possible to study the co-dependency and potentially evolution of HA and NA functions.

The use of pp as surrogate antigens in neutralization assays was also shown to be extremely useful to detect cross-reactive antibody responses in vaccine immunogenicity studies. This was particularly notable when using pp harbouring a chimeric HA, where it was possible to distinguish the presence of antibodies that were stalk- or head-directed.

Lastly, it was also shown that it is still necessary to evaluate different aspects of pp characterisation and pp-NT optimisation/standardisation. Nevertheless, the results presented in this thesis provide additional incentive to optimise, standardise, and validate the pp technology as a method to evaluate vaccine immunogenicity and for the surveillance of influenza viruses in animals and humans.

References

Ahi, Y.S., Bangari, D.S. and Mittal, S.K. (2011). Adenoviral vector immunity: its implications and circumvention strategies. *Current gene therapy* **11**:307–320.

Air, G.M. *et al.* (1990). Evolutionary changes in influenza B are not primarily governed by antibody selection. *Proceedings of the National Academy of Sciences of the United States of America* **87**:3884–3888.

Agilent Technologies *QuikChange Lightning Site-Directed Mutagenesis Kit*.

Akarsu, H. *et al.* (2003). Crystal structure of the M1 protein-binding domain of the influenza A virus nuclear export protein (NEP/NS2). *The EMBO journal* **22**:4646–4655.

Al-Khayatt, R., Jennings, R. and Potter, C.W. (1984). Interpretation of responses and protective levels of antibody against attenuated influenza A viruses using single radial haemolysis. *The Journal of hygiene* **93**:301–312.

Alberini, I. *et al.* (2009). Pseudoparticle neutralization is a reliable assay to measure immunity and cross-reactivity to H5N1 influenza viruses. *Vaccine* **27**:5998–6003.

Aloia, R.C., Tian, H. and Jensen, F.C. (1993). Lipid composition and fluidity of the human immunodeficiency virus envelope and host cell plasma membranes. *Proceedings of the National Academy of Sciences of the United States of America* **90**:5181–5185.

Ansaldi, F. *et al.* (2004). Antigenic characterisation of influenza B virus with a new microneutralisation assay: comparison to haemagglutination and sequence analysis. *Journal of medical virology* **74**:141–146.

Antrobus, R.D. *et al.* (2013). Coadministration of Seasonal Influenza Vaccine and MVA-NP+M1 Simultaneously Achieves Potent Humoral and Cell-Mediated Responses. *Molecular therapy : the journal of the American Society of Gene Therapy* **22**:233–238.

Apisarnthanarak, A. *et al.* (2004). Atypical avian influenza (H5N1). *Emerging infectious diseases* **10**:1321–1324.

Archetti, I. and Horsfall, F.L. (1950). Persistent antigenic variation of influenza A viruses after incomplete neutralization in ovo with heterologous immune serum. *The Journal of experimental medicine* **92**:441–462.

Area, E. *et al.* (2004). 3D structure of the influenza virus polymerase complex: localization of subunit domains. *Proceedings of the National Academy of Sciences of the United States of America* **101**:308–313.

Arnon, T.I. *et al.* (2001). Recognition of viral hemagglutinins by NKp44 but not by NKp30. *European journal of immunology* **31**:2680–2689.

Avnir, Y. *et al.* (2014). Molecular Signatures of Hemagglutinin Stem-Directed Heterosubtypic Human Neutralizing Antibodies against Influenza A Viruses. *PLoS pathogens* **10**:e1004103.

Baas, D.C. *et al.* (2013). Detection of influenza A virus homo- and heterosubtype-specific memory B-cells using a novel protein microarray-based analysis tool. *Journal of medical virology* **85**:899–909.

Babon, J.A.B. *et al.* (2012). A human CD4+ T cell epitope in the influenza hemagglutinin is cross-reactive to influenza A virus subtypes and to influenza B virus. *Journal of virology* **86**:9233–9243.

Baltimore, D. (1971). Expression of animal virus genomes. *Bacteriological reviews* **35**:235–241.

Banasik, M.B. and McCray, P.B. (2010). Integrase-defective lentiviral vectors: progress and applications. *Gene Therapy* **17**:150–157.

Banzhoff, A. *et al.* (2009). MF59-adjuvanted H5N1 vaccine induces immunologic memory and heterotypic antibody responses in non-elderly and elderly adults. *PloS one* **4**:e4384.

Bao, Y. *et al.* (2008). The Influenza Virus Resource at the National Center for Biotechnology Information. *Journal of virology* **82**:596–601.

Barclay, W.S. and Palese, P. (1995). Influenza B viruses with site-specific mutations introduced into the HA gene. *Journal of virology* **69**:1275–1279.

Baron, J. *et al.* (2013). Matriptase, HAT, and TMPRSS2 activate the hemagglutinin of H9N2 influenza A viruses. *Journal of virology* **87**:1811–1820.

Baudin, F. *et al.* (2001). In vitro dissection of the membrane and RNP binding activities of influenza virus M1 protein. *Virology* **281**:102–108.

Baudin, F. *et al.* (1994). Structure of influenza virus RNP. I. Influenza virus nucleoprotein melts secondary structure in panhandle RNA and exposes the bases to the solvent. *The EMBO journal* **13**:3158–3165.

Beaulieu, A. *et al.* (2013). Matriptase Proteolytically Activates Influenza Virus and Promotes Multicycle Replication in the Human Airway Epithelium. *Journal of virology*.

Becker, G.L. *et al.* (2012). Highly potent inhibitors of proprotein convertase furin as potential drugs for treatment of infectious diseases. *Journal of Biological Chemistry* **287**:21992–22003.

Behr, J.-P. (1994). Gene Transfer with Synthetic Cationic Amphiphiles: Prospects for Gene Therapy. *Bioconjugate Chemistry* **5**:382–389.

Belák, S., Kiss, I. and Viljoen, G.J. (2009). New developments in the diagnosis of avian influenza. *Revue scientifique et technique (International Office of Epizootics)* **28**:233–243.

Belshe, R.B. (2010). The need for quadrivalent vaccine against seasonal influenza. *Vaccine* **28 Suppl 4**:D45–53.

Ben-Yedidia, T. and Arnon, R. (2007). Epitope-based vaccine against influenza. *Expert review of vaccines* **6**:939–948.

Beran, J. *et al.* (2013). Immunogenicity and safety of quadrivalent versus trivalent inactivated influenza vaccine: a randomized, controlled trial in adults. *BMC infectious diseases* **13**:224.

Bernstein, F.C. *et al.* (1977). The Protein Data Bank: a computer-based archival file for macromolecular structures. *Journal of Molecular Biology* **112**:535–542.

Berthoud, T.K. *et al.* (2011). Potent CD8+ T-cell immunogenicity in humans of a novel heterosubtypic influenza A vaccine, MVA-NP+M1. *Clinical Infectious Diseases* **52**:1–7.

Berton, M.T., Naeve, C.W. and Webster, R.G. (1984). Antigenic structure of the influenza B virus hemagglutinin: nucleotide sequence analysis of antigenic variants selected with monoclonal antibodies. *Journal of virology* **52**:919–927.

Bertram, S. *et al.* (2011). Cleavage and Activation of the Severe Acute Respiratory Syndrome Coronavirus Spike Protein by Human Airway Trypsin-Like Protease. *Journal of virology* **85**:13363–13372.

Bertram, S. *et al.* (2012). Influenza and SARS-Coronavirus Activating Proteases TMPRSS2 and HAT Are Expressed at Multiple Sites in Human Respiratory and Gastrointestinal Tracts. *PloS one* **7**:e35876.

Bertram, S., Glowacka, I., Blazejewska, P., *et al.* (2010). TMPRSS2 and TMPRSS4 Facilitate Trypsin-Independent Spread of Influenza Virus in Caco-2 Cells. *Journal of virology* **84**:10016–10025.

Bertram, S., Glowacka, I., Steffen, I., *et al.* (2010). Novel insights into proteolytic cleavage of influenza virus hemagglutinin. *Reviews in medical virology* **20**:298–310.

Betakova, T., Nermut, M.V. and Hay, A.J. (1996). The NB protein is an integral component of the membrane of influenza B virus. *The Journal of general virology* **77 (Pt 11)**:2689–2694.

Biswas, S.K. and Nayak, D.P. (1994). Mutational analysis of the conserved motifs of influenza A virus polymerase basic protein 1. *Journal of virology* **68**:1819–1826.

Biswas, S.K., Boutz, P.L. and Nayak, D.P. (1998). Influenza virus nucleoprotein interacts with influenza virus polymerase proteins. *Journal of virology* **72**:5493–5501.

Black, S. *et al.* (2011). Hemagglutination Inhibition Antibody Titers as a Correlate of Protection for Inactivated Influenza Vaccines in Children. *The Pediatric infectious disease journal* **30**:1081–1085.

Bodewes, R. *et al.* (2013). Recurring Influenza B Virus Infections in Seals. *Emerging infectious diseases* **19**:511–512.

Bogner, P. *et al.* (2006). A global initiative on sharing avian flu data. *Nature* **442**:981–981.

Bonnafous, P. *et al.* (2010). Characterization of hepatitis C virus pseudoparticles by cryo-transmission electron microscopy using functionalized magnetic nanobeads. *Journal of General Virology* **91**:1919–1930.

Bosch, V. *et al.* (2001). Inhibition of release of lentivirus particles with incorporated human influenza virus haemagglutinin by binding to sialic acid-containing cellular receptors. *The Journal of general virology* **82**:2485–2494.

Both, G.W. *et al.* (1983). Antigenic drift in influenza virus H3 hemagglutinin from 1968 to 1980: multiple evolutionary pathways and sequential amino acid changes at key antigenic sites. *Journal of virology* **48**:52–60.

Bouvier, N.M. and Palese, P. (2008). The biology of influenza viruses. *Vaccine* **26**:D49–D53.

Böttcher, C. *et al.* (1999). Structure of influenza haemagglutinin at neutral and at fusogenic pH by electron cryo-microscopy. *FEBS letters* **463**:255–259.

Böttcher, E. *et al.* (2009). MDCK cells that express proteases TMPRSS2 and HAT provide a cell system to propagate influenza viruses in the absence of trypsin and to study cleavage of HA and its inhibition. *Vaccine* **27**:6324–6329.

Böttcher, E. *et al.* (2006). Proteolytic Activation of Influenza Viruses by Serine Proteases TMPRSS2 and HAT from Human Airway Epithelium. *Journal of virology* **80**:9896–9898.

Böttcher-Friebertshäuser, E. *et al.* (2010). Cleavage of Influenza Virus Hemagglutinin by Airway Proteases TMPRSS2 and HAT Differs in Subcellular Localization and Susceptibility to Protease Inhibitors. *Journal of virology* **84**:5605–5614.

Böttcher-Friebertshäuser, E. *et al.* (2012). Hemagglutinin activating host cell proteases provide promising drug targets for the treatment of influenza A and B virus infections. *Vaccine* **30**:7374–7380.

Böttcher-Friebertshäuser, E., Klenk, H.-D. and Garten, W. (2013). Activation of influenza viruses by proteases from host cells and bacteria in the human airway epithelium. *Pathogens and disease*.

Braakman, I. *et al.* (1991). Folding of influenza hemagglutinin in the endoplasmic reticulum. *The Journal of cell biology* **114**:401–411.

Brandenburg, B. *et al.* (2013). Mechanisms of hemagglutinin targeted influenza virus neutralization. *PloS one* **8**:e80034.

Brassard, D.L. and Lamb, R.A. (1997). Expression of influenza B virus hemagglutinin containing multibasic residue cleavage sites. *Virology* **236**:234–248.

Brassard, D.L., Leser, G.P. and Lamb, R.A. (1996). Influenza B virus NB glycoprotein is a component of the virion. *Virology* **220**:350–360.

Bright, R.A. *et al.* (2007). Influenza virus-like particles elicit broader immune responses than whole virion inactivated influenza virus or recombinant hemagglutinin. *Vaccine* **25**:3871–3878.

Bui, M., Whittaker, G. and Helenius, A. (1996). Effect of M1 protein and low pH on nuclear transport of influenza virus ribonucleoproteins. *Journal of virology* **70**:8391–8401.

Bullido, R. *et al.* (2000). Several protein regions contribute to determine the nuclear and cytoplasmic localization of the influenza A virus nucleoprotein. *The Journal of general virology* **81**:135–142.

Bullough, P.A. *et al.* (1994). Structure of influenza haemagglutinin at the pH of membrane fusion. *Nature* **371**:37–43.

Buonagurio, D.A. *et al.* (2006). Genetic stability of live, cold-adapted influenza virus components of the FluMist®/CAIV-T vaccine throughout the manufacturing process. *Vaccine* **24**:2151–2160.

Cady, S.D. *et al.* (2010). Structure of the amantadine binding site of influenza M2 proton channels in lipid bilayers. *Nature* **463**:689–692.

Calder, L.J. *et al.* (2010). Structural organization of a filamentous influenza A virus. *Proceedings of the National Academy of Sciences* **107**:10685–10690.

Capua, I. and Cattoli, G. (2010). One Flu for One Health. *Emerging infectious diseases* **16**:719a–719.

Capua, I. *et al.* (2009). Pandemic Vaccine Preparedness—Have We Left Something Behind? Rall, G. F. ed. *PLoS pathogens* **5**:e1000482.

Carr, B. and Wright, M. (2013). *Nanoparticle Tracking Analysis—a Review of Applications and Usage 2010–2012*. NanoSight.

Carragher, D.M. *et al.* (2008). A novel role for non-neutralizing antibodies against nucleoprotein in facilitating resistance to influenza virus. *Journal of immunology (Baltimore, Md.: 1950)* **181**:4168–4176.

Carroll, T.A., Pinnick, H.A. and Carroll, W.E. (2003). Probability and the Westgard Rules. *Annals of clinical and laboratory science* **33**:113–114.

Carugo, O. and Pongor, S. (2002). Protein fold similarity estimated by a probabilistic approach based on C(alpha)-C(alpha) distance comparison. *Journal of Molecular Biology* **315**:887–898.

Caton, A.J. *et al.* (1982). The antigenic structure of the influenza virus A/PR/8/34 hemagglutinin (H1 subtype). *Cell* **31**:417–427.

Cattoli, G. and Capua, I. (2007). Diagnosing avian influenza in the framework of wildlife surveillance efforts and environmental samples. *Journal of Wildlife Diseases* **43**:S35–S39.

Cattoli, G. and Terregino, C. (2008). New Perspectives in Avian Influenza Diagnosis. *Zoonoses and Public Health* **55**:24–28.

Centers for Disease Control and Prevention (CDC) *CDC - Flu Symptoms & Severity | Seasonal Influenza (Flu)* [Online]. Available at: http://www.cdc.gov/flu/about/disease/symptoms.htm [Accessed: 20 March 2014].

Cepko, C. (2001). Large-scale preparation and concentration of retrovirus stocks. *Current protocols in molecular biology / edited by Frederick M. Ausubel ... [et al.]* **Chapter 9**:Unit9.12.

Cerwenka, A., Morgan, T.M. and Dutton, R.W. (1999). Naive, effector, and memory CD8 T cells in protection against pulmonary influenza virus infection: homing properties rather than initial frequencies are crucial. *Journal of immunology (Baltimore, Md.: 1950)* **163**:5535–5543.

Chakrabarti, A.K. and Pasricha, G. (2013). An insight into the PB1F2 protein and its multifunctional role in enhancing the pathogenicity of the influenza A viruses. *Virology* **440**:97–104.

Chambers, T.M. *et al.* (1989). Antigenic and molecular characterization of subtype H13 hemagglutinin of influenza virus. *Virology* **172**:180–188.

Chan, M.C. *et al.* (2005). Proinflammatory cytokine responses induced by influenza A (H5N1) viruses in primary human alveolar and bronchial epithelial cells. *Respiratory research* **6**.

Chauhan, J.S., Rao, A. and Raghava, G.P.S. (2013). In silico Platform for Prediction of N-, O- and C-Glycosites in Eukaryotic Protein Sequences. *PloS one* **8**:e67008.

Chen, B.J., Takeda, M. and Lamb, R.A. (2005). Influenza virus hemagglutinin (H3 subtype) requires palmitoylation of its cytoplasmic tail for assembly: M1 proteins of two subtypes differ in their ability to support assembly. *Journal of virology* **79**:13673–13684.

Chen, G.L. and Subbarao, K. (2009). Attacking the flu: Neutralizing antibodies may lead to 'universal' vaccine. *Nature medicine* **15**:1251–1252.

Chen, H. *et al.* (2014). Clinical and epidemiological characteristics of a fatal case of avian influenza A H10N8 virus infection: a descriptive study. *Lancet* **383**:714–721.

Chen, J. *et al.* (1998). Structure of the hemagglutinin precursor cleavage site, a determinant of influenza pathogenicity and the origin of the labile conformation. *Cell* **95**:409–417.

Chen, R. and Holmes, E.C. (2008). The Evolutionary Dynamics of Human Influenza B Virus. *Journal of Molecular Evolution* **66**:655–663.

Chen, W. and Helenius, A. (2000). Role of ribosome and translocon complex during folding of influenza hemagglutinin in the endoplasmic reticulum of living cells. *Molecular biology of the cell* **11**:765–772.

Chen, W. *et al.* (2001). A novel influenza A virus mitochondrial protein that induces cell death. *Nature medicine* [Online] **7**:1306–1312. Available at: http://www.nature.com/doifinder/10.1038/nm1201-1306.

Chen, Y. *et al.* (2000). Mast cell tryptase from pig lungs triggers infection by pneumotropic Sendai and influenza A viruses. Purification and characterization. *European journal of biochemistry / FEBS* **267**:3189–3197.

Chen, Z. *et al.* (2010). Generation of live attenuated novel influenza virus A/California/7/09 (H1N1) vaccines with high yield in embryonated chicken eggs. *Journal of virology* **84**:44–51.

Chernomordik, L.V. *et al.* (1998). The pathway of membrane fusion catalyzed by influenza hemagglutinin: restriction of lipids, hemifusion, and lipidic fusion pore formation. *The Journal of cell biology* **140**:1369–1382.

Chichester, J.A., Haaheim, L.R. and Yusibov, V. (2009). Using plant cells as influenza vaccine substrates. *Expert review of vaccines* **8**:493–498.

Choi, I.-G., Kwon, J. and Kim, S.-H. (2004). Local feature frequency profile: a method to measure structural similarity in proteins. *Proceedings of the National Academy of Sciences of the United States of America* **101**:3797–3802.

Chou, Y.-Y. *et al.* (2012). One influenza virus particle packages eight unique viral RNAs as shown by FISH analysis. *Proceedings of the National Academy of Sciences* **109**:9101–9106.

Ciampor, F. *et al.* (1992). Regulation of pH by the M2 protein of influenza A viruses. *Virus research* **22**:247–258.

Cianci, C., Tiley, L. and Krystal, M. (1995). Differential activation of the influenza virus polymerase via template RNA binding. *Journal of virology* **69**:3995–3999.

Claas, E.C., de Jong, J.C., *et al.* (1998). Human influenza virus A/HongKong/156/97 (H5N1) infection. *Vaccine* **16**:977–978.

Claas, E.C., Osterhaus, A.D.M.E., *et al.* (1998). Human influenza A H5N1 virus related to a highly pathogenic avian influenza virus. *Lancet* **351**:472–477.

Clementi, N. *et al.* (2012). Broad-range neutralizing anti-influenza A human monoclonal antibodies: new perspectives in therapy and prophylaxis. *The new microbiologica* **35**:399–406.

Cohen, M. *et al.* (2013). Influenza A penetrates host mucus by cleaving sialic acids with neuraminidase. *Virology Journal* **10**:321.

Collin, E.A. *et al.* (2014). Co-circulation of two distinct genetic and antigenic lineages of proposed influenza D virus in cattle. *Journal of virology*.

Committee for Proprietary Medicinal Products, The European Agency for Evaluation of Medicinal Products (1997). *Note for Guidance on Harmonization of Requirements for Influenza Vaccines.* :18.

Compans, R.W., Content, J. and Duesberg, P.H. (1972). Structure of the ribonucleoprotein of influenza virus. *Journal of virology* **10**:795–800.

Conenello, G.M. and Palese, P. (2007). Influenza A virus PB1-F2: a small protein with a big punch. *Cell host \& microbe* **2**:207–209.

Contreras-Gómez, A. *et al.* (2013). Protein production using the baculovirus-insect cell expression system. *Biotechnology Progress* **30**:1–18.

Corti, D. *et al.* (2011). A Neutralizing Antibody Selected from Plasma Cells That Binds to Group 1 and Group 2 Influenza A Hemagglutinins. *Science* **333**:850–856.

Corti, D. *et al.* (2010). Heterosubtypic neutralizing antibodies are produced by individuals immunized with a seasonal influenza vaccine. *The Journal of clinical investigation* **120**:1663–1673.

Cotter, C.R., Jin, H. and Chen, Z. (2014). A single amino acid in the stalk region of the H1N1pdm influenza virus HA protein affects viral fusion, stability and infectivity. *PLoS pathogens* **10**:e1003831.

Cox, R.J. (2013). Correlates of protection to influenza virus, where do we go from here? *Human vaccines & immunotherapeutics* **9**:405–408.

Cox, R.J. *et al.* (2002). Non-lethal viral challenge of influenza haemagglutinin and nucleoprotein DNA vaccinated mice results in reduced viral replication. *Scandinavian journal of immunology* **55**:14–23.

Cronin, J., Zhang, X.-Y. and Reiser, J. (2005). Altering the tropism of lentiviral vectors through pseudotyping. *Current gene therapy* **5**:387–398.

Cros, J.F. and Palese, P. (2003). Trafficking of viral genomic RNA into and out of the nucleus: influenza, Thogoto and Borna disease viruses. *Virus research* **95**:3–12.

Cross, K.J. *et al.* (2001). Studies on influenza haemagglutinin fusion peptide mutants generated by reverse genetics. *The EMBO journal* **20**:4432–4442.

Dahms, S.O. *et al.* (2014). X-ray structures of human furin in complex with competitive inhibitors. *ACS chemical biology* **9**:1113–1118.

Darling, D. *et al.* (2000). Low-speed centrifugation of retroviral vectors absorbed to a particulate substrate: a highly effective means of enhancing retroviral titre. *Gene Therapy* **7**:914–923.

Davison, F. *et al.* (2008). Structure and evolution of avian immunoglobulins. *Avian immunology* **1**:107–127.

de Jong, J.C. *et al.* (2007). Antigenic and Genetic Evolution of Swine Influenza A (H3N2) Viruses in Europe. *Journal of virology* **81**:4315–4322.

de Vries, E. *et al.* (2011). Dissection of the Influenza A Virus Endocytic Routes Reveals Macropinocytosis as an Alternative Entry Pathway. *PLoS pathogens* **7**:e1001329.

de Vries, E. *et al.* (2012). Influenza A virus entry into cells lacking sialylated N-glycans. *Proceedings of the National Academy of Sciences* **109**:7457–7462.

Demaison, C. *et al.* (2002). High-level transduction and gene expression in hematopoietic repopulating cells using a human immunodeficiency [correction of imunodeficiency] virus type 1-based lentiviral vector containing an internal spleen focus forming virus promoter. *Human Gene Therapy* **13**:803–813.

Desai, T.M. *et al.* (2014). IFITM3 restricts influenza A virus entry by blocking the formation of fusion pores following virus-endosome hemifusion. *PLoS pathogens* **10**:e1004048.

Desbien, A.L. *et al.* (2013). Development of a high density hemagglutinin protein microarray to determine the breadth of influenza antibody responses. *BioTechniques* **54**:345–348.

Dias, A. *et al.* (2009). The cap-snatching endonuclease of influenza virus polymerase resides in the PA subunit. *Nature* **458**:914–918.

DiLillo, D.J. *et al.* (2014). Broadly neutralizing hemagglutinin stalk–specific antibodies require FcγR interactions for protection against influenza virus in vivo. *Nature medicine* **20**:143–151.

Ding, H. *et al.* (2011). Heterosubtypic Antibody Response Elicited with Seasonal Influenza Vaccine Correlates Partial Protection against Highly Pathogenic H5N1 Virus Doherty, T. M. ed. *PloS one* **6**:e17821.

Dolin, R. (2013). The quadrivalent approach to influenza vaccination. *Journal of Infectious Diseases* **208**:539–540.

Doms, R.W. *et al.* (1993). Folding and assembly of viral membrane proteins. *Virology* **193**:545–562.

Doms, R.W., Helenius, A. and White, J. (1985). Membrane fusion activity of the influenza virus hemagglutinin. The low pH-induced conformational change. *The Journal of biological chemistry* **260**:2973–2981.

Downard, K.M., Morrissey, B. and Schwahn, A.B. (2009). Mass spectrometry analysis of the influenza virus. *Mass Spectrometry Reviews* **28**:35–49.

Doyle, T.M., Hashem, A.M., *et al.* (2013). Universal anti-neuraminidase antibody inhibiting all influenza A subtypes. *Antiviral Research* **100**:567–574.

Doyle, T.M., Li, C., *et al.* (2013). A monoclonal antibody targeting a highly conserved epitope in influenza B neuraminidase provides protection against drug resistant strains. *Biochemical and biophysical research communications* **441**:226–229.

Dreyfus, C. *et al.* (2012). Highly Conserved Protective Epitopes on Influenza B Viruses. *Science* **337**:1343–1348.

Dreyfus, C., Ekiert, D.C. and Wilson, I.A. (2013). Structure of a classical broadly neutralizing stem antibody in complex with a pandemic H2 influenza virus hemagglutinin. *Journal of virology* **87**:7149–7154.

Drummond, A.J. and Rambaut, A. (2007). BEAST: Bayesian evolutionary analysis by sampling trees. *BMC Evolutionary Biology* **7**:214.

Drummond, A.J. *et al.* (2012). Bayesian phylogenetics with BEAUti and the BEAST 1.7. *Molecular biology and evolution* **29**:1969–1973.

Durand, S. and Cimarelli, A. (2011). The Inside Out of Lentiviral Vectors. *Viruses* **3**:132–159.

Dwyer, D.E. *et al.* (2006). Laboratory diagnosis of human seasonal and pandemic influenza virus infection. *The Medical journal of Australia* **185**:S48–53.

Eccles, R. (2005). Understanding the symptoms of the common cold and influenza. *The Lancet infectious diseases* **5**:718–725.

Edgar, R.C. (2004). MUSCLE: multiple sequence alignment with high accuracy and high throughput. *Nucleic acids research* **32**:1792–1797.

Edinger, T.O., Pohl, M.O. and Stertz, S. (2014). Entry of influenza A virus: host factors and antiviral targets. *Journal of General Virology* **95**:263–277.

Edwards, M.J. and Dimmock, N.J. (2001). Hemagglutinin 1-specific immunoglobulin G and Fab molecules mediate postattachment neutralization of influenza A virus by inhibition of an early fusion event. *Journal of virology* **75**:10208–10218.

Eichner, M. *et al.* (2014). 4Flu - an individual based simulation tool to study the effects of quadrivalent vaccination on seasonal influenza in Germany. *BMC infectious diseases* **14**:365.

Eisenhaber, B. and Eisenhaber, F. (2010). Prediction of posttranslational modification of proteins from their amino acid sequence. *Methods in molecular biology (Clifton, N.J.)* **609**:365–384.

Ekiert, D.C. *et al.* (2011). A Highly Conserved Neutralizing Epitope on Group 2 Influenza A Viruses. *Science* **333**:843–850.

Ekiert, D.C. *et al.* (2009). Antibody Recognition of a Highly Conserved Influenza Virus Epitope. *Science* **324**:246–251.

Ellebedy, A.H. and Ahmed, R. (2012). Re-engaging cross-reactive memory B cells: the influenza puzzle. *Frontiers in immunology* **3**:53.

Ellis, J. *et al.* (2011). Virological analysis of fatal influenza cases in the United Kingdom during the early wave of influenza in winter 2010/11. *Eurosurveillance* **16**.

Elton, D. *et al.* (2013). The genetics of virus particle shape in equine influenza A virus. *Influenza and Other Respiratory Viruses* **7 Suppl 4**:81–89.

Engel, S. *et al.* (2012). Mutation of a raft-targeting signal in the transmembrane region retards transport of influenza virus hemagglutinin through the Golgi. *FEBS letters* **586**:277–282.

Escors, D. *et al.* (2012). *Lentiviral Vectors and Gene Therapy*. Springer Science & Business Media.

European Medicines Agency (2010). *Report From Scientific Workshop on Serology Assays and Correlates of Protection for Influenza Vaccines*. European Medicines Agency.

Even-Or, O. *et al.* (2013). Adjuvanted influenza vaccines. *Expert review of vaccines* **12**:1095–1108.

Everitt, A.R. *et al.* (2012). IFITM3 restricts the morbidity and mortality associated with influenza. *Nature* **484**:519–523.

Farazmandfar, T. *et al.* (2012). Use of integrase-minus lentiviral vector for transient expression. *Cell journal* **14**:76–81.

Farson, D. *et al.* (2001). A new-generation stable inducible packaging cell line for lentiviral vectors. *Human Gene Therapy* **12**:981–997.

Ferrara, F. *et al.* (2013). The human Transmembrane Protease Serine 2 is necessary for the production of Group 2 influenza A virus pseudotypes. *Journal of molecular and genetic medicine : an international journal of biomedical research* **7**:309–314.

Ferraris, O. and Lina, B. (2008). Mutations of neuraminidase implicated in neuraminidase inhibitors resistance. *Journal of clinical virology : the official publication of the Pan American Society for Clinical Virology* **41**:13–19.

Filipe, V., Jiskoot, W. and Hawe, A. (2011). *Understanding Virus Preparations Using Nanoscale Particle Characterization* [Online]. Available at: http://www.bioprocessintl.com/downstream-processing/separation-purification/understanding-virus-preparations-using-nanoscale-particle-characterization-309342/ [Accessed: 12 January 2015].

Fischer, W.B. *et al.* (2000). Transmembrane peptide NB of influenza B: a simulation, structure, and conductance study. *Biochemistry* **39**:12708–12716.

Fleury, D. *et al.* (1998). Antigen distortion allows influenza virus to escape neutralization. *Nature Structural & Molecular Biology* **5**:119–123.

Fodor, E. (2013). The RNA polymerase of influenza A virus: mechanisms of viral transcription and replication. *Acta virologica* **57**:113–122.

Fodor, E., Pritlove, D.C. and Brownlee, G.G. (1994). The influenza virus panhandle is involved in the initiation of transcription. *Journal of virology* **68**:4092–4096.

Fouchier, R.A.M. and Smith, D.J. (2010). Use of antigenic cartography in vaccine seed strain selection. *Avian diseases* **54**:220–223.

Fouchier, R.A.M. *et al.* (2005). Characterization of a Novel Influenza A Virus Hemagglutinin Subtype (H16) Obtained from Black-Headed Gulls. *Journal of virology* **79**:2814–2822.

Francis, T. (1940). A New Type of Virus From Epidemic Influenza. *Science (New York, N.Y.)* **92**:405–408.

Frank, H. *et al.* (2010). Lethal influenza B myocarditis in a child and review of the literature for pediatric age groups. *Infection* **38**:231–235.

Freidl, G.S. *et al.* (2014). Influenza at the animal-human interface: a review of the literature for virological evidence of human infection with swine or avian influenza viruses other than A(H5N1). *Euro surveillance : bulletin europeen sur les maladies transmissibles = European communicable disease bulletin* **19**.

Friesen, R.H. *et al.* (2010). New class of monoclonal antibodies against severe influenza: prophylactic and therapeutic efficacy in ferrets. *PloS one* **5**.

Friesen, R.H.E. *et al.* (2014). A common solution to group 2 influenza virus neutralization. *Proceedings of the National Academy of Sciences* **111**:445–450.

Gabriel, G. *et al.* (2011). Differential use of importin-α isoforms governs cell tropism and host adaptation of influenza virus. *Nature Communications* **2**:156.

Galloway, S.E. *et al.* (2013). Influenza HA subtypes demonstrate divergent phenotypes for cleavage activation and pH of fusion: implications for host range and adaptation. *PLoS pathogens* **9**:e1003151.

Gambaryan, A.S., Robertson, J.S. and Matrosovich, M.N. (1999). Effects of egg-adaptation on the receptor-binding properties of human influenza A and B viruses. *Virology* **258**:232–239.

Gamblin, S.J. *et al.* (2004). The structure and receptor binding properties of the 1918 influenza hemagglutinin. *Science (New York, N.Y.)* **303**:1838–1842.

Gao, R. *et al.* (2013). Human infection with a novel avian-origin influenza A (H7N9) virus. *The New England journal of medicine* **368**:1888–1897.

Garcia, J.-M. and Lai, J.C.C. (2011). Production of influenza pseudotyped lentiviral particles and their use in influenza research and diagnosis: an update. *Expert Review of Anti-infective Therapy* **9**:443–455.

Garcia, J.-M. *et al.* (2009). Heterosubtype Neutralizing Responses to Influenza A (H5N1) Viruses Are Mediated by Antibodies to Virus Haemagglutinin Ho, P. L. ed. *PloS one* **4**:e7918.

Garcia, J.-M. *et al.* (2010). Optimization and evaluation of an influenza A (H5) pseudotyped lentiviral particle-based serological assay. *Journal of clinical virology : the official publication of the Pan American Society for Clinical Virology* **47**:29–33.

García-Barreno, B. *et al.* (2014). Exploring the antigenic relatedness of influenza virus haemagglutinins with strain-specific polyclonal antibodies. *Journal of General Virology* **95**:2140–2145.

García-Sastre, A. (2012). The neuraminidase of bat influenza viruses is not a neuraminidase. *Proceedings of the National Academy of Sciences* **109**:18635–18636.

García-Sastre, A. and Schmolke, M. (2014). Avian influenza A H10N8-a virus on the verge? *Lancet*.

García-Sastre, A. *et al.* (1998). Influenza A virus lacking the NS1 gene replicates in interferon-deficient systems. *Virology* **252**:324–330.

Gastaminza, P. *et al.* (2003). Mutations in the N-terminal region of influenza virus PB2 protein affect virus RNA replication but not transcription. *Journal of virology* **77**:5098–5108.

Genzel, Y. and Reichl, U. (2009). Continuous cell lines as a production system for influenza vaccines. *Expert review of vaccines* **8**:1681–1692.

Geraerts, M. *et al.* (2006). Comparison of lentiviral vector titration methods. *BMC biotechnology* **6**:34.

Gerdil, C. (2003). The annual production cycle for influenza vaccine. *Vaccine* **21**:1776–1779.

Gerl, M.J. *et al.* (2012). Quantitative analysis of the lipidomes of the influenza virus envelope and MDCK cell apical membrane. *The Journal of cell biology* **196**:213–221.

Giard, D.J. *et al.* (1973). In vitro cultivation of human tumors: establishment of cell lines derived from a series of solid tumors. *Journal of the National Cancer Institute* **51**:1417–1423.

Gibbs, J.S. *et al.* (2003). The influenza A virus PB1-F2 protein targets the inner mitochondrial membrane via a predicted basic amphipathic helix that disrupts mitochondrial function. *Journal of virology* **77**:7214–7224.

Gibson, D.G. *et al.* (2009). Enzymatic assembly of DNA molecules up to several hundred kilobases. *Nature methods* **6**:343–345.

Gioia, C. *et al.* (2008). Cross-subtype immunity against avian influenza in persons recently vaccinated for influenza. *Emerging infectious diseases* **14**:121–128.

Glezen, W.P. (2004). Cold-adapted, live attenuated influenza vaccine. *Expert review of vaccines* **3**:131–139.

Glezen, W.P. *et al.* (2013). The burden of influenza B: a structured literature review. *American journal of public health* **103**:e43–51.

Goff, P.H. *et al.* (2015). Synthetic TLR4 and TLR7 ligands as influenza virus vaccine adjuvants induce rapid, sustained and broadly protective responses. *Journal of virology*.

Goff, P.H., Eggink, D., *et al.* (2013). Adjuvants and immunization strategies to induce influenza virus hemagglutinin stalk antibodies. *PloS one* **8**:e79194.

Goff, P.H., Krammer, F., *et al.* (2013). Induction of cross-reactive antibodies to novel H7N9 influenza virus by recombinant Newcastle disease virus expressing a North American lineage H7 subtype hemagglutinin. *Journal of virology*.

Gomez-Puertas, P. *et al.* (2000). Influenza virus matrix protein is the major driving force in virus budding. *Journal of virology* **74**:11538–11547.

Gomila, R.C. *et al.* (2013). Improving influenza virus backbones by including terminal regions of MDCK-adapted strains on hemagglutinin and neuraminidase gene segments. *Vaccine* **31**:4736–4743.

Gonzalez, S. and Ortin, J. (1999). Distinct regions of influenza virus PB1 polymerase subunit recognize vRNA and cRNA templates. *The EMBO journal* **18**:3767–3775.

Gottschalk, A. (1957). Neuraminidase: the specific enzyme of influenza virus and Vibrio cholerae. *Biochimica et biophysica acta* **23**:645–646.

Govorkova, E.A. *et al.* (1999). Selection of receptor-binding variants of human influenza A and B viruses in baby hamster kidney cells. *Virology* **262**:31–38.

Graham-Rowe, D. (2011). Epidemiology: Racing against the flu. *Nature* **480**:S2–3.

Grambas, S. and Hay, A.J. (1992). Maturation of influenza A virus hemagglutinin--estimates of the pH encountered during transport and its regulation by the M2 protein. *Virology* **190**:11–18.

GraphPad Software *GraphPad Curve Fitting Guide - Hill Slope* [Online]. Available at: http://www.graphpad.com/guides/prism/6/curve-fitting/index.htm?reg_hill_slope.htm [Accessed: 21 December 2014].

Gray, G.C. *et al.* (2011). A national study of US bird banders for evidence of avian influenza virus infections. *Journal of clinical virology : the official publication of the Pan American Society for Clinical Virology* **51**:132–135.

Gray, J.J. *et al.* (1995). Internal quality assurance in a clinical virology laboratory. II. Internal quality control. *Journal of clinical pathology* **48**:198–202.

Grebe, K.M., Yewdell, J.W. and Bennink, J.R. (2008). Heterosubtypic immunity to influenza A virus: where do we stand? *Microbes and Infection* **10**:1024–1029.

Greenbaum, J.A. *et al.* (2009). Pre-existing immunity against swine-origin H1N1 influenza viruses in the general human population. *Proceedings of the National Academy of Sciences* **106**:20365–20370.

Greenspan, D. *et al.* (1985). Expression of influenza virus NS2 nonstructural protein in bacteria and localization of NS2 in infected eucaryotic cells. *Journal of virology* **54**:833–843.

Gubareva, L.V., Kaiser, L. and Hayden, F.G. (2000). Influenza virus neuraminidase inhibitors. *Lancet* **355**:827–835.

Guex, N. and Peitsch, M.C. (1997). SWISS-MODEL and the Swiss-PdbViewer: an environment for comparative protein modeling. *ELECTROPHORESIS* **18**:2714–2723.

Guillot, L. *et al.* (2005). Involvement of toll-like receptor 3 in the immune response of lung epithelial cells to double-stranded RNA and influenza A virus. *The Journal of biological chemistry* **280**:5571–5580.

Gulati, S. *et al.* (2013). Human H3N2 Influenza Viruses Isolated from 1968 To 2012 Show Varying Preference for Receptor Substructures with No Apparent Consequences for Disease or Spread Pekosz, A. ed. *PloS one* **8**:e66325.

Guo, L. *et al.* (2003). Enhancement of mucosal immune responses by chimeric influenza HA/SHIV virus-like particles. *Virology* **313**:502–513.

Hai, R. *et al.* (2012). Influenza viruses expressing chimeric hemagglutinins: globular head and stalk domains derived from different subtypes. *Journal of virology* **86**:5774–5781.

Hale, B.G. *et al.* (2008). The multifunctional NS1 protein of influenza A viruses. *The Journal of general virology* **89**:2359–2376.

Haller, O., Staeheli, P. and Kochs, G. (2009). Protective role of interferon-induced Mx GTPases against influenza viruses. *Revue scientifique et technique (International Office of Epizootics)* **28**:219–231.

Hamilton, B.S. and Whittaker, G.R. (2013). Cleavage activation of human-adapted influenza virus subtypes by kallikrein-related peptidases 5 and 12. *Journal of Biological Chemistry* **288**:17399–17407.

Hamilton, B.S. *et al.* (2014). Inhibition of influenza virus infection and hemagglutinin cleavage by the protease inhibitor HAI-2. *Biochemical and biophysical research communications* **450**:1070–1075.

Hamilton, B.S., Gludish, D.W.J. and Whittaker, G.R. (2012). Cleavage activation of the human-adapted influenza virus subtypes by matriptase reveals both subtype and strain specificities. *Journal of virology* **86**:10579–10586.

Hamilton, B.S., Whittaker, G.R. and Daniel, S. (2012). Influenza Virus-Mediated Membrane Fusion: Determinants of Hemagglutinin Fusogenic Activity and Experimental Approaches for Assessing Virus Fusion. *Viruses* **4**:1144–1168.

Han, T. and Marasco, W.A. (2011). Structural basis of influenza virus neutralization. *Annals of the New York Academy of Sciences* **1217**:178–190.

Hancock, K. *et al.* (2009). Cross-reactive antibody responses to the 2009 pandemic H1N1 influenza virus. *The New England journal of medicine* **361**:1945–1952.

Hanika, A. *et al.* (2005). Use of influenza C virus glycoprotein HEF for generation of vesicular stomatitis virus pseudotypes. *The Journal of general virology* **86**:1455–1465.

Hannoun, C. (2013). The evolving history of influenza viruses and influenza vaccines. *Expert review of vaccines* **12**:1085–1094.

Hanzlíková, M. *et al.* (2011). Mechanisms of polyethylenimine-mediated DNA delivery: free carrier helps to overcome the barrier of cell-surface glycosaminoglycans. *The Journal of Gene Medicine* **13**:402–409.

Harris, A. *et al.* (2006). Influenza virus pleiomorphy characterized by cryoelectron tomography. *Proceedings of the National Academy of Sciences of the United States of America* **103**:19123–19127.

Hatta, M. and Kawaoka, Y. (2003). The NB Protein of Influenza B Virus Is Not Necessary for Virus Replication In Vitro. *Journal of virology* **77**:6050–6054.

Hatziioannou, T. *et al.* (1998). Incorporation of fowl plague virus hemagglutinin into murine leukemia virus particles and analysis of the infectivity of the pseudotyped retroviruses. *Journal of virology* **72**:5313–5317.

Hause, B.M. *et al.* (2014). Characterization of a novel influenza virus in cattle and Swine: proposal for a new genus in the orthomyxoviridae family. *mBio* **5**.

Hause, B.M. *et al.* (2013). Isolation of a novel swine influenza virus from Oklahoma in 2011 which is distantly related to human influenza C viruses. *PLoS pathogens* **9**:e1003176.

Haynes, J.R. (2009). Influenza virus-like particle vaccines. *Expert review of vaccines* **8**:435–445.

He, X.S. *et al.* (2004). T cell-dependent production of IFN-gamma by NK cells in response to influenza A virus. *The Journal of clinical investigation* **114**:1812–1819.

Heaton, N.S. and Randall, G. (2011). Multifaceted roles for lipids in viral infection. *Trends in microbiology* **19**:368–375.

Hebert, D.N. *et al.* (1997). The number and location of glycans on influenza hemagglutinin determine folding and association with calnexin and calreticulin. *The Journal of cell biology* **139**:613–623.

Herfst, S. *et al.* (2012). Airborne Transmission of Influenza A/H5N1 Virus Between Ferrets. *Science* **336**:1534–1541.

Herrler, G. *et al.* (1988). The Glycoprotein of Influenza C Virus Is the Haemagglutinin, Esterase and Fusion Factor. *Journal of General Virology* **69**:839–846.

Hidari, K.I.P.J. *et al.* (2013). Influenza virus utilizes N-linked sialoglycans as receptors in A549 cells. *Biochemical and biophysical research communications* **436**:394–399.

Hirst, G.K. (1942). Adsorption of Influenza Hemagglutinins and Virus by Red Blood Cells. *The Journal of experimental medicine* **76**:195–209.

Hirst, G.K. (1941). The Agglutination of Red Cells by Allantoic Fluid of Chick Embryos Infected with Influenza Virus. *Science (New York, N.Y.)* **94**:22–23.

Hoag, H. (2013). A universal problem. *Nature medicine* **19**:12–14.

Hobson, D. *et al.* (1972). The role of serum haemagglutination-inhibiting antibody in protection against challenge infection with influenza A2 and B viruses. *The Journal of hygiene* **70**:767–777.

Hoffmann, T.W. *et al.* (2011). Length Variations in the NA Stalk of an H7N1 Influenza Virus Have Opposite Effects on Viral Excretion in Chickens and Ducks. *Journal of virology* **86**:584–588.

Hooper, K.A. and Bloom, J.D. (2013). A mutant influenza virus that uses an N1 neuraminidase as the receptor-binding protein. *Journal of virology*.

Horby, P. *et al.* (2012). The role of host genetics in susceptibility to influenza: a systematic review. *PloS one* **7**:e33180.

Horimoto, T. and Kawaoka, Y. (2005). Influenza: lessons from past pandemics, warnings from current incidents. *Nature reviews.Microbiology* **3**:591–600.

Horimoto, T. and Kawaoka, Y. (2001). Pandemic Threat Posed by Avian Influenza A Viruses. *Clinical microbiology reviews* **14**:129–149.

Horimoto, T. *et al.* (1994). Proprotein-processing endoproteases PC6 and furin both activate hemagglutinin of virulent avian influenza viruses. *Journal of virology* **68**:6074–6078.

Horvath, C.M. *et al.* (1992). Biological activity of paramyxovirus fusion proteins: factors influencing formation of syncytia. *Journal of virology* **66**:4564–4569.

Huang, I.-C. *et al.* (2008). Influenza A Virus Neuraminidase Limits Viral Superinfection. *Journal of virology* **82**:4834–4843.

Huang, K.Y.A. *et al.* (2014). Virus-Specific Antibody Secreting Cell, Memory B-cell, and Sero-Antibody Responses in the Human Influenza Challenge Model. *Journal of Infectious Diseases* **209**:1354–1361.

Huelsenbeck, J.P. *et al.* (2001). Bayesian inference of phylogeny and its impact on evolutionary biology. *Science (New York, N.Y.)* **294**:2310–2314.

Huelsenbeck, J.P., Rannala, B. and Masly, J.P. (2000). An Introduction to Bayesian Inference of Phylogeny. *Science* [Online]:1–7. Available at: http://www.sciencemag.org/site/feature/data/1050262.pdf.

Hurtley, S.M. *et al.* (1989). Interactions of misfolded influenza virus hemagglutinin with binding protein (BiP). *The Journal of cell biology* **108**:2117–2126.

Imai, M. *et al.* (2012). Experimental adaptation of an influenza H5 HA confers respiratory droplet transmission to a reassortant H5 HA/H1N1 virus in ferrets. *Nature* **486**:420–428.

Immune Systems *FastRead 102*™.

International Committee on Taxonomy of Viruses ICTV (2013). *ICTV Virus Taxonomy 2013* [Online]. Available at: http://www.ictvonline.org/virusTaxonomy.asp [Accessed: 19 June 2014].

J R Davies, E.A.G. (1989). Natural or vaccine-induced antibody as a predictor of immunity in the face of natural challenge with influenza viruses. *Epidemiology and infection* **102**:325.

Jackson, D. *et al.* (2002). A reverse genetics approach for recovery of recombinant influenza B viruses entirely from cDNA. *Journal of virology* **76**:11744–11747.

Jackson, D., Elderfield, R.A. and Barclay, W.S. (2010). Molecular studies of influenza B virus in the reverse genetics era. *Journal of General Virology* **92**:1–17.

Jackson, D.C. *et al.* (1982). Enumeration of antigenic sites of influenza virus hemagglutinin. *Infection and immunity* **37**:912–918.

Jacobs, P. and Callewaert, N. (2009). N-glycosylation Engineering of Biopharmaceutical Expression Systems. *Current Molecular Medicine* **9**:774–800.

Jacobsen, L. (2004). FuGENE 6 Transfection Reagent: the gentle power. *Methods* **33**:104–112.

Jacobson, R.H. (1998). Validation of serological assays for diagnosis of infectious diseases. *Revue scientifique et technique (International Office of Epizootics)* **17**:469–526.

Jagger, B.W. *et al.* (2012). An Overlapping Protein-Coding Region in Influenza A Virus Segment 3 Modulates the Host Response. *Science* **337**:199–204.

Job, E.R. *et al.* (2013). Addition of Glycosylation to Influenza A Virus Hemagglutinin Modulates Antibody-Mediated Recognition of H1N1 2009 Pandemic Viruses. *Journal of immunology (Baltimore, Md.: 1950)* **190**:2169–2177.

Julkunen, I. *et al.* (2000). Inflammatory responses in influenza A virus infection. *Vaccine* **19 Suppl 1**:S32–7.

Jung, H. *et al.* (2008). TMPRSS4 promotes invasion, migration and metastasis of human tumor cells by facilitating an epithelial-mesenchymal transition. *Oncogene* **27**:2635–2647.

Junge, C. (2011). Morbidity: A personal response. *Nature* **480**:S14–5.

Kageyama, T. *et al.* (2013). Genetic analysis of novel avian A(H7N9) influenza viruses isolated from patients in China, February to April 2013. *Euro surveillance : bulletin europeen sur les maladies transmissibles = European communicable disease bulletin* **18**.

Kanekiyo, M. et al. (2013). Self-assembling influenza nanoparticle vaccines elicit broadly neutralizing H1N1 antibodies. Nature 499:102–106.

Kang, S.-M., Kim, M.-C. and Compans, R.W. (2012). Virus-like particles as universal influenza vaccines. *Expert review of vaccines* **11**:995–1007.

Katz, J.M. (2003). The Impact of Avian Influenza Viruses on Public Health. *Avian diseases* **47**:914–920.

Katz, J.M., Hancock, K. and Xu, X. (2011). Serologic assays for influenza surveillance, diagnosis and vaccine evaluation. *Expert Review of Anti-infective Therapy* **9**:669–683.

Kaufman, R.J. (2000). Overview of vector design for mammalian gene expression. *Molecular Biotechnology* **16**:151–160.

Kaverin, N.V. *et al.* (1998). Postreassortment changes in influenza A virus hemagglutinin restoring HA-NA functional match. *Virology* **244**:315–321.

Kayali, G. *et al.* (2011). Evidence of Infection with H4 and H11 Avian Influenza Viruses among Lebanese Chicken Growers Smith, G. J. D. ed. *PloS one* **6**:e26818.

Kayali, G. *et al.* (2009). Evidence of Previous Avian Influenza Infection among US Turkey Workers. *Zoonoses and Public Health* **57**:265–272.

Kayali, G. *et al.* (2008). Testing human sera for antibodies against avian influenza viruses: Horse RBC hemagglutination inhibition vs. microneutralization assays. *Journal of Clinical Virology* **43**:73–78.

Kendal, A.P. and Cate, T.R. (1983). Increased sensitivity and reduced specificity of hemagglutination inhibition tests with ether-treated influenza B/Singapore/222/79. *Journal of clinical microbiology* **18**:930–934.

Kesic, M.J. *et al.* (2012). Exposure to Ozone Modulates Human Airway Protease/Antiprotease Balance Contributing to Increased Influenza A Infection Pekosz, A. ed. *PloS one* **7**:e35108.

Kesic, M.J., Hernandez, M. and Jaspers, I. (2012). Airway protease/antiprotease imbalance in atopic asthmatics contributes to increased Influenza A virus cleavage and replication. *Respiratory research* **13**:82.

Khatchikian, D., Orlich, M. and Rott, R. (1989). Increased viral pathogenicity after insertion of a 28S ribosomal RNA sequence into the haemagglutinin gene of an influenza virus. *Nature* **340**:156–157.

Khurana, S. *et al.* (2014). Heterologous prime-boost vaccination with MF59-adjuvanted H5 vaccines promotes antibody affinity maturation towards the hemagglutinin HA1 domain and broad H5N1 cross-clade neutralization. *PloS one* **9**:e95496.

Kido, H. *et al.* (2008). Host envelope glycoprotein processing proteases are indispensable for entry into human cells by seasonal and highly pathogenic avian influenza viruses. *Journal of molecular and genetic medicine : an international journal of biomedical research* **3**:167–175.

Kido, H. *et al.* (1992). Isolation and characterization of a novel trypsin-like protease found in rat bronchiolar epithelial Clara cells. A possible activator of the viral fusion glycoprotein. *The Journal of biological chemistry* **267**:13573.

Kim, J.I. and Park, M.-S. (2012). N-Linked Glycosylation in the Hemagglutinin of Influenza A Viruses. *Yonsei Medical Journal* **53**:886.

Klasse, P.J. and Sattentau, Q.J. (2002). Occupancy and mechanism in antibody-mediated neutralization of animal viruses. *The Journal of general virology* **83**:2091–2108.

Klausberger, M. *et al.* (2014). One-shot vaccination with an insect cell-derived low-dose influenza A H7 virus-like particle preparation protects mice against H7N9 challenge. *Vaccine* **32**:355–362.

Klimov, A. *et al.* (2012). Influenza Virus Titration, Antigenic Characterization, and Serological Methods for Antibody Detection. In: *Link.Springer.com*. Totowa, NJ: Humana Press, pp. 25–51.

Koel, B.F. *et al.* (2013). Substitutions Near the Receptor Binding Site Determine Major Antigenic Change During Influenza Virus Evolution. *Science* **342**:976–979.

Kollerova, E. and Betakova, T. (2006). Influenza viruses and their ion channels. *Acta virologica*:7–16.

Koopmans, M. *et al.* (2012). Profiling of humoral immune responses to influenza viruses by using protein microarray. *Clinical Microbiology and Infection* **18**:797–807.

Koopmans, M. *et al.* (2004). Transmission of H7N7 avian influenza A virus to human beings during a large outbreak in commercial poultry farms in the Netherlands. *Lancet* **363**:587–593.

Kopecky-Bromberg, S.A. and Palese, P. (2009). Recombinant vectors as influenza vaccines. In: Compans, R. W. and Orenstein, W. A. eds. *Vaccines for Pandemic Influenza*. Current topics in microbiology and immunology, pp. 243–267.

Kordyukova, L.V. and Serebryakova, M.V. (2012). Mass spectrometric approaches to study enveloped viruses: New possibilities for structural biology and prophylactic medicine. *Biochemistry (Moscow)* **77**:830–842.

Kordyukova, L.V. *et al.* (2008). S Acylation of the Hemagglutinin of Influenza Viruses: Mass Spectrometry Reveals Site-Specific Attachment of Stearic Acid to a Transmembrane Cysteine. *Journal of virology* **82**:9288–9292.

Kozak, M. (2005). Regulation of translation via mRNA structure in prokaryotes and eukaryotes. *Gene* **361**:13–37.

Krammer, F. and Palese, P. (2014). Universal influenza virus vaccines: need for clinical trials. *Nature immunology* **15**:3–5.

Krammer, F. *et al.* (2013). Chimeric hemagglutinin influenza virus vaccine constructs elicit broadly protective stalk-specific antibodies. *Journal of virology* **87**:6542–6550.

Krammer, F. *et al.* (2012). Hemagglutinin Stalk-Reactive Antibodies Are Boosted following Sequential Infection with Seasonal and Pandemic H1N1 Influenza Virus in Mice. *Journal of virology* **86**:10302–10307.

Krammer, F., Albrecht, R.A., *et al.* (2014). Divergent H7 immunogens offer protection from H7N9 virus challenge. *Journal of virology* **88**:3976–3985.

Krammer, F., Hai, R., *et al.* (2014). Assessment of influenza virus hemagglutinin stalk-based immunity in ferrets. *Journal of virology* **88**:3432–3442.

Krammer, F., Margine, I., *et al.* (2014). H3 stalk-based chimeric hemagglutinin influenza virus constructs protect mice from H7N9 challenge. *Journal of virology* **88**:2340–2343.

Krogh, A. *et al.* (2001). Predicting transmembrane protein topology with a hidden markov model: application to complete genomes. *Journal of Molecular Biology* **305**:567–580.

Krug, R.M. and Etkind, P.R. (1973). Cytoplasmic and nuclear virus-specific proteins in influenza virus-infected MDCK cells. *Virology* **56**:334–348.

Krystal, M. *et al.* (1983). Sequential mutations in hemagglutinins of influenza B virus isolates: definition of antigenic domains. *Proceedings of the National Academy of Sciences of the United States of America* **80**:4527–4531.

Kucharski, A.J. and Gog, J.R. (2012). The role of social contacts and original antigenic sin in shaping the age pattern of immunity to seasonal influenza. *PLoS Computational Biology* **8**:e1002741.

Kuiken, T. (2013). Is low pathogenic avian influenza virus virulent for wild waterbirds? *Proceedings of the Royal Society B: Biological Sciences* **280**:20130990–20130990.

Labrosse, B. *et al.* (2010). Detection of Extensive Cross-Neutralization between Pandemic and Seasonal A/H1N1 Influenza Viruses Using a Pseudotype Neutralization Assay Zhang, L. ed. *PloS one* **5**:e11036.

Lakadamyali, M. *et al.* (2003). Visualizing infection of individual influenza viruses. *Proceedings of the National Academy of Sciences of the United States of America* **100**:9280–9285.

Lamb, R.A. and Lai, C.J. (1984). Expression of unspliced NS1 mRNA, spliced NS2 mRNA, and a spliced chimera mRNA from cloned influenza virus NS DNA in an SV40 vector. *Virology* **135**:139–147.

Lamb, R.A. and Lai, C.J. (1982). Spliced and unspliced messenger RNAs synthesized from cloned influenza virus M DNA in an SV40 vector: expression of the influenza virus membrane protein (M1). *Virology* **123**:237–256.

Lamb, R.A., Zebedee, S.L. and Richardson, C.D. (1985). Influenza virus M2 protein is an integral membrane protein expressed on the infected-cell surface. *Cell* **40**:627–633.

Lambert, N.D. *et al.* (2012). Understanding the immune response to seasonal influenza vaccination in older adults: a systems biology approach. *Expert review of vaccines* **11**:985–994.

LaMere, M.W. *et al.* (2011). Contributions of antinucleoprotein IgG to heterosubtypic immunity against influenza virus. *Journal of immunology (Baltimore, Md.: 1950)* **186**:4331–4339.

Larkin, M.A. *et al.* (2007). Clustal W and Clustal X version 2.0. *Bioinformatics (Oxford, England)* **23**:2947–2948.

Lee, C.-W., Senne, D.A. and Suarez, D.L. (2006). Development and application of reference antisera against 15 hemagglutinin subtypes of influenza virus by DNA vaccination of chickens. *Clinical and vaccine immunology : CVI* **13**:395–402.

Lee, N., Shin, M.S. and Kang, I. (2012). T-Cell Biology in Aging, With a Focus on Lung Disease. *The Journals of Gerontology Series A: Biological Sciences and Medical Sciences* **67A**:254–263.

Lees, W.D., Moss, D.S. and Shepherd, A.J. (2011). Analysis of Antigenically Important Residues in Human Influenza A Virus in Terms of B-Cell Epitopes. *Journal of virology* **85**:8548–8555.

Lentz, M.R. and Air, G.M. (1986). Loss of enzyme activity in a site-directed mutant of influenza neuraminidase compared to expressed wild-type protein. *Virology* **148**:74–83.

Leser, G.P. and Lamb, R.A. (2005). Influenza virus assembly and budding in raft-derived microdomains: a quantitative analysis of the surface distribution of HA, NA and M2 proteins. *Virology* **342**:215–227.

Li, Changgui *et al.* (2010). Application of deglycosylation and electrophoresis to the quantification of influenza viral hemagglutinins facilitating the production of 2009 pandemic influenza (H1N1) vaccines at multiple manufacturing sites in China. *Biologicals : journal of the International Association of Biological Standardization* **38**:284–289.

Li, M. L., Ramirez, B.C. and Krug, R.M. (1998). RNA-dependent activation of primer RNA production by influenza virus polymerase: different regions of the same protein subunit constitute the two required RNA-binding sites. *The EMBO journal* **17**:5844–5852.

Li, Olive TW and Poon, L.L. (2009). One step closer to universal influenza epitopes. *Expert Review of Anti-infective Therapy* **7**:687–690.

Li, Qing *et al.* (2012). Structural and functional characterization of neuraminidase-like molecule N10 derived from bat influenza A virus. *Proceedings of the National Academy of Sciences* **109**:18897–18902.

Li, Qun *et al.* (2013). Preliminary Report: Epidemiology of the Avian Influenza A (H7N9) Outbreak in China. *The New England journal of medicine*.

Lin, T.-Y. and Brass, A.L. (2013). Host genetic determinants of influenza pathogenicity. *Current Opinion in Virology* **3**:531–536.

Lin, X. *et al.* (2014). Order and disorder control the functional rearrangement of influenza hemagglutinin. *Proceedings of the National Academy of Sciences*.

Lin, Y.P. *et al.* (2010). Neuraminidase Receptor Binding Variants of Human Influenza A(H3N2) Viruses Resulting from Substitution of Aspartic Acid 151 in the Catalytic Site: a Role in Virus Attachment? *Journal of virology* **84**:6769–6781.

Lingwood, D. *et al.* (2012). Structural and genetic basis for development of broadly neutralizing influenza antibodies. *Nature*:1–6.

Liu, D. *et al.* (2013). Origin and diversity of novel avian influenza A H7N9 viruses causing human infection: phylogenetic, structural, and coalescent analyses. *Lancet* **381**:1926–1932.

Liu, D. *et al.* (2009). Website for avian flu information and bioinformatics. *Science in China Series C: Life Sciences* [Online] **52**:470–473. Available at: http://www.springerlink.com/index/10.1007/s11427-009-0065-9.

Londrigan, S.L. *et al.* (2011). N-linked glycosylation facilitates sialic acid-independent attachment and entry of influenza A viruses into cells expressing DC-SIGN or L-SIGN. *Journal of virology* **85**:2990–3000.

Lorizate, M. *et al.* (2013). Comparative lipidomics analysis of HIV-1 particles and their producer cell membrane in different cell lines. *Cellular Microbiology* **15**:292–304.

Lu, X. *et al.* (2012). Insights into avian influenza virus pathogenicity: the hemagglutinin precursor HA0 of subtype H16 has an alpha-helix structure in its cleavage site with inefficient HA1/HA2 cleavage. *Journal of virology* **86**:12861–12870.

Lu, X. *et al.* (2013). Structure and receptor binding specificity of the hemagglutinin H13 from avian influenza A virus H13N6. *Journal of virology*.

Lugovtsev, V.Y., Melnyk, D. and Weir, J.P. (2013). Heterogeneity of the MDCK cell line and its applicability for influenza virus research. *PloS one* **8**:e75014.

Madhun, El, A.S., Cox, R.J. and Haaheim, L.R. (1999). The Effect of Age and Natural Priming on the IgG and IgA Subclass Responses after Parenteral Influenza Vaccination. *Journal of Infectious Diseases* **180**:1356–1360.

Mahallawi, W.H. *et al.* (2013). Infection with 2009 H1N1 influenza virus primes for immunological memory in human nose-associated lymphoid tissue, offering cross-reactive immunity to H1N1 and avian H5N1 viruses. *Journal of virology* **87**:5331–5339.

Mallajosyula, V.V.A. *et al.* (2014). Influenza hemagglutinin stem-fragment immunogen elicits broadly neutralizing antibodies and confers heterologous protection. *Proceedings of the National Academy of Sciences* **111**:E2514–23.

Mancini, G. *et al.* (1983). Comparison of haemagglutination-inhibition and single radial haemolysis techniques for detecting antibodies to influenza A and B viruses. *The Journal of hygiene* **91**:157–162.

Mancini, N. *et al.* (2011). A potential role for monoclonal antibodies in prophylactic and therapeutic treatment of influenza. *Antiviral Research*:1–12.

Mandelboim, O. *et al.* (2001). Recognition of haemagglutinins on virus-infected cells by NKp46 activates lysis by human NK cells. *Nature* **409**:1055–1060.

Marasco, W.A. and Sui, J. (2007). The growth and potential of human antiviral monoclonal antibody therapeutics. *Nature biotechnology* **25**:1421–1434.

Marcelin, G. *et al.* (2011). A contributing role for anti-neuraminidase antibodies on immunity to pandemic H1N1 2009 influenza A virus. *PloS one* **6**:e26335.

Marcelin, G., Sandbulte, M.R. and Webby, R.J. (2012). Contribution of antibody production against neuraminidase to the protection afforded by influenza vaccines. *Reviews in medical virology* **22**:267–279.

Margine, I., Hai, R., *et al.* (2013). H3N2 influenza virus infection induces broadly reactive hemagglutinin stalk antibodies in humans and mice. *Journal of virology* **87**:4728–4737.

Margine, I., Krammer, F., *et al.* (2013). Hemagglutinin Stalk-Based Universal Vaccine Constructs Protect Against Group 2 Influenza A Viruses. *Journal of virology*.

Markovic, I. *et al.* (2001). Synchronized activation and refolding of influenza hemagglutinin in multimeric fusion machines. *The Journal of cell biology* **155**:833–844.

Martin, K. and Helenius, A. (1991). Transport of incoming influenza virus nucleocapsids into the nucleus. *Journal of virology* **65**:232–244.

Martinez-Sobrido, L. *et al.* (2010). Hemagglutinin-Pseudotyped Green Fluorescent Protein-Expressing Influenza Viruses for the Detection of Influenza Virus Neutralizing Antibodies. *Journal of virology* **84**:2157–2163.

Massin, P. *et al.* (2010). Temperature sensitivity on growth and/or replication of H1N1, H1N2 and H3N2 influenza A viruses isolated from pigs and birds in mammalian cells. *Veterinary microbiology* **142**:232–241.

Mather, S. *et al.* (2013). Current progress with serological assays for exotic emerging/re-emerging viruses. *Future Virology* **8**:745–755.

Matrosovich, M., Stech, J. and Klenk, H.D. (2009). Influenza receptors, polymerase and host range. *Revue scientifique et technique (International Office of Epizootics)* **28**:203–217.

Matrosovich, M.N. *et al.* (1997). Avian influenza A viruses differ from human viruses by recognition of sialyloligosaccharides and gangliosides and by a higher conservation of the HA receptor-binding site. *Virology* **233**:224–234.

Matrosovich, M.N. *et al.* (1993). Probing of the receptor-binding sites of the H1 and H3 influenza A and influenza B virus hemagglutinins by synthetic and natural sialosides. *Virology* **196**:111–121.

Matrosovich, M.N., Klenk, H.-D. and Kawaoka, Y. (2006). Receptor Specificity, Host-Range, and Pathogenicity of Influenza Viruses. In: Kawaoka, Y. ed. *Influenza Virology: Current Topics*. Caister Academic Press, pp. 95–137.

Matrosovich, M.N., Matrosovich, T.Y., Gray, T., Roberts, N.A. and Klenk, H.D. (2004a). Human and avian influenza viruses target different cell types in cultures of human airway epithelium. *Proceedings of the National Academy of Sciences* **101**:4620–4624.

Matrosovich, M.N., Matrosovich, T.Y., Gray, T., Roberts, N.A. and Klenk, H.D. (2004b). Neuraminidase is important for the initiation of influenza virus infection in human airway epithelium. *Journal of virology* **78**:12665–12667.

McAuley, J.L. *et al.* (2007). Expression of the 1918 influenza A virus PB1-F2 enhances the pathogenesis of viral and secondary bacterial pneumonia. *Cell host \& microbe* **2**:240–249.

Meng, B., Marriott, A.C. and Dimmock, N.J. (2010). The receptor preference of influenza viruses. *Influenza and Other Respiratory Viruses* **4**:147–153.

Miller, M.S., Gardner, T.J., *et al.* (2013). Neutralizing Antibodies Against Previously Encountered Influenza Virus Strains Increase over Time: A Longitudinal Analysis. *Science translational medicine* **5**:198ra107–198ra107.

Miller, M.S., Tsibane, T., *et al.* (2013). 1976 and 2009 H1N1 influenza virus vaccines boost anti-hemagglutinin stalk antibodies in humans. *Journal of Infectious Diseases* **207**:98–105.

Mitnaul, L.J. *et al.* (2000). Balanced hemagglutinin and neuraminidase activities are critical for efficient replication of influenza A virus. *Journal of virology* **74**:6015–6020.

Molesti, E. *et al.* (2013). The production and development of H7 Influenza virus pseudotypes for the study of humoral responses against avian viruses. *Journal of molecular and genetic medicine : an international journal of biomedical research* **7**:315–320.

Molesti, E., Ferrara, F., *et al.* (2014). Discordant correlation between serological assays observed when measuring heterosubtypic responses against avian influenza H5 and H7 viruses in unexposed individuals. *BioMed research international* **2014**:231365.

Molesti, E., Wright, E., *et al.* (2014). Multiplex evaluation of influenza neutralizing antibodies with potential applicability to in-field serological studies. *Journal of immunology research* **2014**:457932.

Momose, F. *et al.* (2001). Cellular splicing factor RAF-2p48/NPI-5/BAT1/UAP56 interacts with the influenza virus nucleoprotein and enhances viral RNA synthesis. *Journal of virology* **75**:1899–1908.

Monto, A.S. (2008). Epidemiology of influenza. *Vaccine* **26**:D45–D48.

Monto, A.S. and Maassab, H.F. (1981). Ether treatment of type B influenza virus antigen for the hemagglutination inhibition test. *Journal of clinical microbiology* **13**:54–57.

Monto, A.S. *et al.* (2000). Clinical signs and symptoms predicting influenza infection. *Archives of Internal Medicine* **160**:3243–3247.

Montomoli, E. and Maria, T.C. (2014). Is influenza A/H10N8 a potential candidate for the next pandemic? *Pathogens and global health* **108**:213.

Morens, D.M. and Fauci, A.S. (2007). The 1918 influenza pandemic: insights for the 21st century. *The Journal of infectious diseases* **195**:1018–1028.

Moscona, A. (2005). Neuraminidase inhibitors for influenza. *The New England journal of medicine* **353**:1363–1373.

Moser, C. *et al.* (2007). Influenza virosomes as a combined vaccine carrier and adjuvant system for prophylactic and therapeutic immunizations. *Expert review of vaccines* **6**:711–721.

Mullarkey, C.E. *et al.* (2013). Improved adjuvanting of seasonal influenza vaccines: Preclinical studies of MVA-NP+M1 coadministration with inactivated influenza vaccine. *European journal of immunology* **43**:1940–1952.

Munster, V.J. *et al.* (2010). Insertion of a multibasic cleavage motif into the hemagglutinin of a low-pathogenic avian influenza H6N1 virus induces a highly pathogenic phenotype. *Journal of virology* **84**:7953–7960.

Murphy, B.R. *et al.* (1981). Hemagglutinin-specific enzyme-linked immunosorbent assay for antibodies to influenza A and B viruses. *Journal of clinical microbiology* **13**:554–560.

Nachbagauer, R. *et al.* (2014). Induction of Broadly Reactive Anti-Hemagglutinin Stalk Antibodies by an H5N1 Vaccine in Humans. *Journal of virology* **88**:13260–13268.

Nakada, S. *et al.* (1984). Influenza C virus hemagglutinin: comparison with influenza A and B virus hemagglutinins. *Journal of virology* **50**:118–124.

Nakai, K. (2000). Protein sorting signals and prediction of subcellular localization. In: *Sciencedirect.com*. Elsevier, pp. 277–344.

Narat, M. (2003). Production of antibodies in chickens. *Food Technology and Biotechnology* **41**:259–267.

Nayak, B. *et al.* (2010). Contributions of the Avian Influenza Virus HA, NA, and M2 Surface Proteins to the Induction of Neutralizing Antibodies and Protective Immunity. *Journal of virology* **84**:2408–2420.

Nayak, D.P. *et al.* (2009). Influenza virus morphogenesis and budding. *Virus research* **143**:147–161.

Nefkens, I. *et al.* (2007). Hemagglutinin pseudotyped lentiviral particles: Characterization of a new method for avian H5N1 influenza sero-diagnosis. *Journal of Clinical Virology* **39**:27–33.

Neumann, G. *et al.* (2005). An improved reverse genetics system for influenza A virus generation and its implications for vaccine production. *Proceedings of the National Academy of Sciences of the United States of America* **102**:16825–16829.

Neumann, G., Noda, T. and Kawaoka, Y. (2009). Emergence and pandemic potential of swine-origin H1N1 influenza virus. *Nature* **459**:931–939.

Ng, A.K., Wang, J.H. and Shaw, P.C. (2009). Structure and sequence analysis of influenza A virus nucleoprotein. *Science in China.Series C, Life sciences / Chinese Academy of Sciences* **52**:439–449.

Ni, Y. *et al.* (2005). Generation of a packaging cell line for prolonged large-scale production of high-titer HIV-1-based lentiviral vector. *The Journal of Gene Medicine* **7**:818–834.

Nicolson, C. *et al.* (2012). An additional oligosaccharide moiety in the HA of a pandemic influenza H1N1 candidate vaccine virus confers increased antigen yield in eggs. *Vaccine* **30**:745–751.

Nobusawa, E. *et al.* (1991). Comparison of complete amino acid sequences and receptor-binding properties among 13 serotypes of hemagglutinins of influenza A viruses. *Virology* **182**:475–485.

Noda, T. (2012). Native morphology of influenza virions. :1–5.

Noma, K. *et al.* (1998). Endogenous protease-dependent replication of human influenza viruses in two MDCK cell lines. *Archives of Virology* **143**:1893–1909.

Novel Swine-Origin Influenza A H1N1 Virus Investigation Team *et al.* (2009). Emergence of a novel swine-origin influenza A (H1N1) virus in humans. *The New England journal of medicine* **360**:2605–2615.

O'Neill, R.E. *et al.* (1995). Nuclear import of influenza virus RNA can be mediated by viral nucleoprotein and transport factors required for protein import. *The Journal of biological chemistry* **270**:22701–22704.

O'Neill, R.E., Talon, J. and Palese, P. (1998). The influenza virus NEP (NS2 protein) mediates the nuclear export of viral ribonucleoproteins. *The EMBO journal* **17**:288–296.

Oh, H.-L.J. *et al.* (2010). An antibody against a novel and conserved epitope in the hemagglutinin 1 subunit neutralizes numerous H5N1 influenza viruses. *Journal of virology* **84**:8275–8286.

Ohuchi, M. *et al.* (2006). Roles of neuraminidase in the initial stage of influenza virus infection. *Microbes and Infection* **8**:1287–1293.

Okumura, Y. *et al.* (2010). Novel Type II Transmembrane Serine Proteases, MSPL and TMPRSS13, Proteolytically Activate Membrane Fusion Activity of the Hemagglutinin of Highly Pathogenic Avian Influenza Viruses and Induce Their Multicycle Replication. *Journal of virology* **84**:5089–5096.

Okuno, Y. *et al.* (1993). A common neutralizing epitope conserved between the hemagglutinins of influenza A virus H1 and H2 strains. *Journal of virology* **67**:2552–2558.

Okuno, Y. *et al.* (1990). Rapid focus reduction neutralization test of influenza A and B viruses in microtiter system. *Journal of clinical microbiology* **28**:1308–1313.

Olsen, B. *et al.* (2006). Global patterns of influenza A virus in wild birds. *Science (New York, N.Y.)* **312**:384–388.

One Health Global Network *www.Onehealthglobal.Net* [Online]. Available at: http://www.onehealthglobal.net/ [Accessed: 24 March 2014].

Orlich, M., Gottwald, H. and Rott, R. (1994). Nonhomologous Recombination between the Hemagglutinin Gene and the Nucleoprotein Gene of an Influenza Virus. *Virology* **204**:462–465.

Ortega, J. *et al.* (2000). Ultrastructural and functional analyses of recombinant influenza virus ribonucleoproteins suggest dimerization of nucleoprotein during virus amplification. *Journal of virology* **74**:156–163.

Oshansky, C.M. *et al.* (2014). Seasonal influenza vaccination is the strongest correlate of cross-reactive antibody responses in migratory bird handlers. *mBio* **5**:e02107.

Osterhaus, A.D. *et al.* (2000). Influenza B virus in seals. *Science (New York, N.Y.)* **288**:1051–1053.

Ostrowski, L.E. *et al.* (2014). Restoring ciliary function to differentiated primary ciliary dyskinesia cells with a lentiviral vector. *Gene Therapy* **21**:253–261.

Owens, R.J. and Rose, J.K. (1993). Cytoplasmic domain requirement for incorporation of a foreign envelope protein into vesicular stomatitis virus. *Journal of virology* **67**:360–365.

Oxford, J.S., Yetts, R. and Schild, G.C. (1982). Quantitation and analysis of the specificity of post-immunization antibodies to influenza B viruses using single radial haemolysis. *The Journal of hygiene* **88**:325–333.

Pacchia, A.L. *et al.* (2001). An Inducible Packaging Cell System for Safe, Efficient Lentiviral Vector Production in the Absence of HIV-1 Accessory Proteins. *Virology* **282**:77–86.

Paddock, C.D. *et al.* (2012). Fatal Influenza B Infections: Time to Reexamine Influenza Research Priorities. *Journal of Infectious Diseases* **205**:870–872.

Palese, P. and Wang, T.T. (2011). Why Do Influenza Virus Subtypes Die Out? A Hypothesis. *mBio* **2**:e00150–11–e00150–11.

Palese, P. *et al.* (1974). Characterization of temperature sensitive influenza virus mutants defective in neuraminidase. *Virology* **61**:397–410.

Palladino, G. *et al.* (1995). Virus-neutralizing antibodies of immunoglobulin G (IgG) but not of IgM or IgA isotypes can cure influenza virus pneumonia in SCID mice. *Journal of virology* **69**:2075–2081.

Pantin-Jackwood, M.J. and Swayne, D.E. (2009). Pathogenesis and pathobiology of avian influenza virus infection in birds. *Revue scientifique et technique (International Office of Epizootics)* **28**:113–136.

Pappas, L. *et al.* (2014). Rapid development of broadly influenza neutralizing antibodies through redundant mutations. *Nature*:–.

Patel, M. *et al.* (2013). High efficiency gene transfer to airways of mice using influenza hemagglutinin pseudotyped lentiviral vectors. *The Journal of Gene Medicine* **15**:51–62.

Paterson, R.G., Russell, C.J. and Lamb, R.A. (2000). Fusion Protein of the Paramyxovirus SV5: Destabilizing and Stabilizing Mutants of Fusion Activation. *Virology* **270**:17–30.

Pavlovic, J., Haller, O. and Staeheli, P. (1992). Human and mouse Mx proteins inhibit different steps of the influenza virus multiplication cycle. *Journal of virology* **66**:2564–2569.

Peiris, J.S.M., Poon, L.L.M. and Guan, Y. (2012). Surveillance of Animal Influenza for Pandemic Preparedness. *Science* **335**:1173–1174.

Pekosz, A. and Lamb, R.A. (1999). Cell surface expression of biologically active influenza C virus HEF glycoprotein expressed from cDNA. *Journal of virology* **73**:8808–8812.

Pepin, S. *et al.* (2013). Safety and immunogenicity of a quadrivalent inactivated influenza vaccine in adults. *Vaccine* **31**:5572–5578.

Perera, R.A.P.M. *et al.* (2011). Seroconversion to pandemic (H1N1) 2009 virus and cross-reactive immunity to other swine influenza viruses. *Emerging infectious diseases* **17**:1897–1899.

Pica, N. and Palese, P. (2013). Toward a Universal Influenza Virus Vaccine: Prospects and Challenges. *Annual Review of Medicine* **64**:189–202.

Pica, N. *et al.* (2012). Hemagglutinin stalk antibodies elicited by the 2009 pandemic influenza virus as a mechanism for the extinction of seasonal H1N1 viruses. *Proceedings of the National Academy of Sciences* **109**:2573–2578.

Pielak, R.M. and Chou, J.J. (2010a). Flu channel drug resistance: a tale of two sites. *Protein & Cell* **1**:246–258.

Pielak, R.M. and Chou, J.J. (2010b). Influenza M2 proton channels. *Biochimica et biophysica acta*.

Pinto, L.H., Holsinger, L.J. and Lamb, R.A. (1992). Influenza virus M2 protein has ion channel activity. *Cell* **69**:517–528.

Pizzato, M. *et al.* (1999). Initial binding of murine leukemia virus particles to cells does not require specific Env-receptor interaction. *Journal of virology* **73**:8599–8611.

Plotkin, S.A. (2008). Vaccines: Correlates of Vaccine‐Induced Immunity. *Clinical Infectious Diseases* **47**:401–409.

Poch, O. *et al.* (1989). Identification of four conserved motifs among the RNA-dependent polymerase encoding elements. *The EMBO journal* **8**:3867–3874.

Poole, E. *et al.* (2004). Functional domains of the influenza A virus PB2 protein: identification of NP- and PB1-binding sites. *Virology* **321**:120–133.

Posada, D. (2008). jModelTest: Phylogenetic Model Averaging. *Molecular biology and evolution* **25**:1253–1256.

Posada, D. and Buckley, T.R. (2004). Model selection and model averaging in phylogenetics: advantages of akaike information criterion and bayesian approaches over likelihood ratio tests. *Systematic biology* **53**:793–808.

Postel, A. *et al.* (2011). Broad spectrum reactivity versus subtype specificity-trade-offs in serodiagnosis of influenza A virus infections by competitive ELISA. *Journal of virological methods* **173**:49–59.

Potter, C.W. and Oxford, J.S. (1979). Determinants of immunity to influenza infection in man. *British medical bulletin* **35**:69–75.

Price, J.V. *et al.* (2013). Characterization of influenza vaccine immunogenicity using influenza antigen microarrays. *PloS one* **8**:e64555.

Principi, N. *et al.* (2013). Influenza C virus–associated community-acquired pneumonia in children. *Influenza and Other Respiratory Viruses* **7**:999–1003.

Promega (2011). *Bright-Glo™ Luciferase Assay Systems*. Promega.

Pyhälä, R., Kleemola, M. and Visakorpi, R. (1985). The HI test modified by ether treatment in the sero-epidemiological surveillance of influenza B. *The Journal of hygiene* **94**:341–348.

QIAGEN (2012a). *HiSpeed® Plasmid Purification Handbook*. QIAGEN.

QIAGEN (2012b). *QIAprep® Miniprep Handbook*. QIAGEN.

QIAGEN (2012c). *QIAquick® Spin Handbook*. QIAGEN.

Qiu, D. *et al.* (1992). Western blot analysis of antibody responses to influenza virion proteins. *Immunology and cell biology* **70 (Pt 3)**:181–191.

Reading, P.C., Miller, J.L. and Anders, E.M. (2000). Involvement of the mannose receptor in infection of macrophages by influenza virus. *Journal of virology* **74**:5190–5197.

Reber, A. and Katz, J. (2013). Immunological assessment of influenza vaccines and immune correlates of protection. *Expert review of vaccines* **12**:519–536.

Reed, M.L. *et al.* (2009). Amino Acid Residues in the Fusion Peptide Pocket Regulate the pH of Activation of the H5N1 Influenza Virus Hemagglutinin Protein. *Journal of virology* **83**:3568–3580.

Reid, A.H., Taubenberger, J.K. and Fanning, T.G. (2004). Evidence of an absence: the genetic origins of the 1918 pandemic influenza virus. *Nature reviews.Microbiology* **2**:909–914.

Rein, J.L. *et al.* (2014). Death of woman with peripartum influenza B virus infection and necrotizing pneumonia. *Emerging infectious diseases* **20**:1258–1260.

Renegar, K.B. *et al.* (2004). Role of IgA versus IgG in the control of influenza viral infection in the murine respiratory tract. *The Journal of Immunology* **173**:1978–1986.

Richardson, J.C. and Akkina, R.K. (1991). NS2 protein of influenza virus is found in purified virus and phosphorylated in infected cells. *Archives of Virology* **116**:69–80.

Rimmelzwaan, G.F. and Sutter, G. (2009). Candidate influenza vaccines based on recombinant modified vaccinia virus Ankara. *Expert review of vaccines* **8**:447–454.

Rivera, K. *et al.* (1995). Probing the structure of influenza B hemagglutinin using site-directed mutagenesis. *Virology* **206**:787–795.

Robertson, J.S. *et al.* (2011). The development of vaccine viruses against pandemic A(H1N1) influenza. *Vaccine* **29**:1836–1843.

Robertson, J.S., Schubert, M. and Lazzarini, R.A. (1981). Polyadenylation sites for influenza virus mRNA. *Journal of virology* **38**:157–163.

Rodriguez-Boulan, E., Paskiet, K.T. and Sabatini, D.D. (1983). Assembly of enveloped viruses in Madin-Darby canine kidney cells: polarized budding from single attached cells and from clusters of cells in suspension. *The Journal of cell biology* **96**:866–874.

Rogers, G.N. *et al.* (1983). Single amino acid substitutions in influenza haemagglutinin change receptor binding specificity. *Nature* **304**:76–78.

Rose, M.A., Zielen, S. and Baumann, U. (2012). Mucosal immunity and nasal influenza vaccination. *Expert review of vaccines* **11**:595–607.

Rosenthal, P.B. *et al.* (1998). Structure of the haemagglutinin-esterase-fusion glycoprotein of influenza C virus. *Nature* **396**:92–96.

Rossman, J.S. and Lamb, R.A. (2011). Influenza virus assembly and budding. *Virology* **411**:229–236.

Rossman, J.S. *et al.* (2010). Influenza virus M2 ion channel protein is necessary for filamentous virion formation. *Journal of virology* **84**:5078–5088.

Rota, P.A. *et al.* (1990). Cocirculation of two distinct evolutionary lineages of influenza type B virus since 1983. *Virology* **175**:59–68.

Rowe, T. *et al.* (1999). Detection of antibody to avian influenza A (H5N1) virus in human serum by using a combination of serologic assays. *Journal of clinical microbiology* **37**:937–943.

Röhm, C. *et al.* (1996). Characterization of a novel influenza hemagglutinin, H15: criteria for determination of influenza A subtypes. *Virology* **217**:508–516.

Ruigrok, R.W., Calder, L.J. and Wharton, S.A. (1989). Electron microscopy of the influenza virus submembranal structure. *Virology* **173**:311–316.

Russell, C.A. *et al.* (2012). The Potential for Respiratory Droplet-Transmissible A/H5N1 Influenza Virus to Evolve in a Mammalian Host. *Science* **336**:1541–1547.

Russell, R.J. *et al.* (2006). The structure of H5N1 avian influenza neuraminidase suggests new opportunities for drug design. *Nature* **443**:45–49.

Russell, S.M., McCahon, D. and Beare, A.S. (1975). A single radial haemolysis technique for the measurement of influenza antibody. *The Journal of general virology* **27**:1–10.

Ryder, A.B. *et al.* (2014). A Viable Recombinant Rhabdovirus Lacking Its Glycoprotein Gene and Expressing Influenza Hemagglutinin and Neuraminidase Is a Potent Influenza Vaccine. *Journal of virology*.

Sadler, A.J. and Williams, B.R.G. (2008). Interferon-inducible antiviral effectors. *Nature reviews.Immunology* **8**:559–568.

Sakai, K. *et al.* (2014). The host protease TMPRSS2 plays a major role in in vivo replication of emerging H7N9 and seasonal influenza viruses. *Journal of virology* **88**:5608–5616.

Sakuma, T., Barry, M.A. and Ikeda, Y. (2012). Lentiviral vectors: basic to translational. *The Biochemical journal* **443**:603–618.

Salk, J.E. (1944). A simplified procedure for titrating hemagglutinating capacity of influenza virus and the corresponding antibody. *J Immunol*.

Sangster, M.Y. *et al.* (2013). B Cell Response and Hemagglutinin Stalk-Reactive Antibody Production in Different Age Cohorts following 2009 H1N1 Influenza Virus Vaccination. *Clinical and vaccine immunology : CVI* **20**:867–876.

Sant, A.J. *et al.* (2007). Immunodominance in CD4 T-cell responses: implications for immune responses to influenza virus and for vaccine design. *Expert review of vaccines* **6**:357–368.

Sauter, N.K. *et al.* (1992). Crystallographic detection of a second ligand binding site in influenza virus hemagglutinin. *Proceedings of the National Academy of Sciences of the United States of America* **89**:324–328.

Sawoo, O. *et al.* (2014). Cleavage of Hemagglutinin-Bearing Lentiviral Pseudotypes and Their Use in the Study of Influenza Virus Persistence Tripp, R. ed. *PloS one* **9**:e106192.

Schambach, A. *et al.* (2013). Biosafety Features of Lentiviral Vectors. *Human Gene Therapy* **24**:132–142.

Scheiffele, P., Roth, M.G. and Simons, K. (1997). Interaction of influenza virus haemagglutinin with sphingolipid-cholesterol membrane domains via its transmembrane domain. *The EMBO journal* **16**:5501–5508.

Schild, G.C., Pereira, M.S. and Chakraverty, P. (1975). Single-radial-hemolysis: a new method for the assay of antibody to influenza haemagglutinin. Applications for diagnosis and seroepidemiologic surveillance of influenza. *Bulletin of the World Health Organization* **52**:43–50.

Scholtissek, C. *et al.* (1978). On the origin of the human influenza virus subtypes H2N2 and H3N2. *Virology* **87**:13–20.

Schotsaert, M. *et al.* (2009). Universal M2 ectodomain-based influenza A vaccines: preclinical and clinical developments. *Expert review of vaccines* **8**:499–508.

Schrauwen, E.J.A. *et al.* (2011). Insertion of a multibasic cleavage site in the haemagglutinin of human influenza H3N2 virus does not increase pathogenicity in ferrets. *Journal of General Virology* **92**:1410–1415.

Schroeder, H.W. and Cavacini, L. (2010). Structure and function of immunoglobulins. *The Journal of allergy and clinical immunology* **125**:S41–52.

Scott, S. *et al.* (2012). The use of equine influenza pseudotypes for serological screening. *Journal of molecular and genetic medicine : an international journal of biomedical research* **6**:304–308.

Segal, M.S. *et al.* (1992). Disulfide bond formation during the folding of influenza virus hemagglutinin. *The Journal of cell biology* **118**:227–244.

Segura, M.M. *et al.* (2007). Production of lentiviral vectors by large-scale transient transfection of suspension cultures and affinity chromatography purification. *Biotechnology and Bioengineering* **98**:789–799.

Sekikawa, K. and Lai, C.J. (1983). Defects in functional expression of an influenza virus hemagglutinin lacking the signal peptide sequences. *Proceedings of the National Academy of Sciences of the United States of America* **80**:3563–3567.

Seladi-Schulman, J., Steel, J. and Lowen, A.C. (2013). Spherical influenza viruses have a fitness advantage in embryonated eggs, while filament-producing strains are selected in vivo. *Journal of virology* **87**:13343–13353.

Shahsavandi, S. *et al.* (2011). Specific subtyping of influenza A virus using a recombinant hemagglutinin protein expressed in baculovirus. *Molecular Biology Reports* **38**:3293–3298.

Shaw, M.W., Choppin, P.W. and Lamb, R.A. (1983). A previously unrecognized influenza B virus glycoprotein from a bicistronic mRNA that also encodes the viral neuraminidase. *Proceedings of the National Academy of Sciences of the United States of America* **80**:4879–4883.

Shelton, H. *et al.* (2013). Mutations in haemagglutinin that affect receptor binding and pH stability increase replication of a PR8 influenza virus with H5 HA in the upper respiratory tract of ferrets and may contribute to transmissibility. *Journal of General Virology* **94**:1220–1229.

Shelton, H. *et al.* (2011). Receptor binding profiles of avian influenza virus hemagglutinin subtypes on human cells as a predictor of pandemic potential. *Journal of virology* **85**:1875–1880.

Sheng, Z. *et al.* (2013). Genomic and evolutionary characterization of a novel influenza-C-like virus from swine. *Archives of Virology*.

Shibata, S. *et al.* (1993). Characterization of a temperature-sensitive influenza B virus mutant defective in neuraminidase. *Journal of virology* **67**:3264–3273.

Shinya, K. *et al.* (2006). Avian flu: Influenza virus receptors in the human airway. *Nature cell biology* **440**:435–436.

Shtyrya, Y.A., Mochalova, L.V. and Bovin, N.V. (2009). Influenza virus neuraminidase: structure and function. *Acta naturae* **1**:26–32.

Sieben, C. *et al.* (2012). Influenza virus binds its host cell using multiple dynamic interactions. *Proceedings of the National Academy of Sciences*.

Sieczkarski, S.B. and Whittaker, G.R. (2002). Influenza virus can enter and infect cells in the absence of clathrin-mediated endocytosis. *Journal of virology* **76**:10455–10464.

Sielaff, F. *et al.* (2011). Development of substrate analogue inhibitors for the human airway trypsin-like protease HAT. *Bioorganic & Medicinal Chemistry Letters* **21**:4860–4864.

Sinn, P.L., Sauter, S.L. and McCray, P.B. (2005). Gene therapy progress and prospects: development of improved lentiviral and retroviral vectors--design, biosafety, and production. *Gene Therapy* **12**:1089–1098.

Sivalingam, G.N. and Shepherd, A.J. (2012). An analysis of B-cell epitope discontinuity. *Molecular immunology* **51**:304–309.

Skehel, J.J. and Wiley, D.C. (2000). Receptor binding and membrane fusion in virus entry: the influenza hemagglutinin. *Annual Review of Biochemistry* **69**:531–569.

Skehel, J.J. *et al.* (1982). Changes in the conformation of influenza virus hemagglutinin at the pH optimum of virus-mediated membrane fusion. *Proceedings of the National Academy of Sciences of the United States of America* **79**:968–972.

Skowronski, D.M. *et al.* (2012). Cross-Lineage Influenza B and Heterologous Influenza A Antibody Responses in Vaccinated Mice: Immunologic Interactions and B/Yamagata Dominance. *PloS one* **7**:e38929.

Smith, D. (2003). Applications of bioinformatics and computational biology to influenza surveillance and vaccine strain selection. *Vaccine* **21**:1758–1761.

Smith, G.J.D. *et al.* (2009). Dating the emergence of pandemic influenza viruses. *Proceedings of the National Academy of Sciences* **106**:11709–11712.

Sommerfelt, M.A. (2011). T-cell-mediated and humoral approaches to universal influenza vaccines. *Expert review of vaccines* **10**:1359–1361.

Song, J.-M. *et al.* (2011). Vaccination inducing broad and improved cross protection against multiple subtypes of influenza A virus. *Proceedings of the National Academy of Sciences* **108**:757–761.

Squires, R.B. *et al.* (2012). Influenza research database: an integrated bioinformatics resource for influenza research and surveillance. *Influenza and Other Respiratory Viruses* **6**:404–416.

Stech, J. *et al.* (2011). Influenza B Virus With Modified Hemagglutinin Cleavage Site as a Novel Attenuated Live Vaccine. *Journal of Infectious Diseases* **204**:1483–1490.

Stech, O. *et al.* (2009). Acquisition of a Polybasic Hemagglutinin Cleavage Site by a Low-Pathogenic Avian Influenza Virus Is Not Sufficient for Immediate Transformation into a Highly Pathogenic Strain. *Journal of virology* **83**:5864–5868.

Steel, J. *et al.* (2010). Influenza Virus Vaccine Based on the Conserved Hemagglutinin Stalk Domain. *mBio* **1**:e00018–10–e00018–10.

Steinhauer, D.A. (1999). Role of hemagglutinin cleavage for the pathogenicity of influenza virus. *Virology* **258**:1–20.

Stephenson, I. *et al.* (2007). Comparison of neutralising antibody assays for detection of antibody to influenza A/H3N2 viruses: an international collaborative study. *Vaccine* **25**:4056–4063.

Stephenson, I. *et al.* (2009). Reproducibility of serologic assays for influenza virus A (H5N1). *Emerging infectious diseases* **15**:1252–1259.

Stephenson, I. *et al.* (2003). Sialic acid receptor specificity on erythrocytes affects detection of antibody to avian influenza haemagglutinin. *Journal of medical virology* **70**:391–398.

Stieneke-Gröber, A. *et al.* (1992). Influenza virus hemagglutinin with multibasic cleavage site is activated by furin, a subtilisin-like endoprotease. *The EMBO journal* **11**:2407–2414.

Strang, B.L. *et al.* (2004). Characterization of HIV-1 vectors with gammaretrovirus envelope glycoproteins produced from stable packaging cells. *Gene Therapy* **11**:591–598.

Stray, S.J., Cummings, R.D. and Air, G.M. (2000). Influenza virus infection of desialylated cells. *Glycobiology* **10**:649–658.

Subbarao, E.K. *et al.* (1992). Comparison of different approaches to measuring influenza A virus-specific hemagglutination inhibition antibodies in the presence of serum inhibitors. *Journal of clinical microbiology* **30**:996–999.

Subbarao, E.K., London, W. and Murphy, B.R. (1993). A single amino acid in the PB2 gene of influenza A virus is a determinant of host range. *Journal of virology* **67**:1761–1764.

Sugita, Y. *et al.* (2013). Configuration of viral ribonucleoprotein complexes within the influenza A virion. *Journal of virology* **87**:12879–12884.

Sui, J. *et al.* (2009). Structural and functional bases for broad-spectrum neutralization of avian and human influenza A viruses. *Nature Structural & Molecular Biology* **16**:265–273.

Sullivan, S.P. *et al.* (2010). Dissolving polymer microneedle patches for influenza vaccination. *Nature medicine* **16**:915–920.

Sun, Joseph C and Bevan, M.J. (2003). Defective CD8 T cell memory following acute infection without CD4 T cell help. *Science (New York, N.Y.)* **300**:339–342.

Sun, Xiangjie and Whittaker, G.R. (2003). Role for influenza virus envelope cholesterol in virus entry and infection. *Journal of virology* **77**:12543–12551.

Sun, Xiaoman *et al.* (2013). Bat-Derived Influenza Hemagglutinin H17 Does Not Bind Canonical Avian or Human Receptors and Most Likely Uses a Unique Entry Mechanism. *CellReports* **3**:769–778.

Svennevig, K., Prydz, K. and Kolset, S.O. (1995). Proteoglycans in polarized epithelial Madin-Darby canine kidney cells. *The Biochemical journal* **311 (Pt 3)**:881–888.

Swayne, D.E. (2000). Understanding the ecology and epidemiology of avian influenza viruses: implications for zoonotic potential. *Emerging diseases of animals. CC Brown and CA Bolin, eds. ASM Press, Washington, DC*:101–130.

Szécsi, J. *et al.* (2006). Targeted retroviral vectors displaying a cleavage site-engineered hemagglutinin (HA) through HA-protease interactions. *Molecular therapy : the journal of the American Society of Gene Therapy* **14**:735–744.

Takeda, K. and Akira, S. (2004). Microbial recognition by Toll-like receptors. *Journal of Dermatological Science* **34**:73–82.

Takeda, M. *et al.* (2003). Influenza virus hemagglutinin concentrates in lipid raft microdomains for efficient viral fusion. *Proceedings of the National Academy of Sciences of the United States of America* **100**:14610–14617.

Tamura, K. *et al.* (2011). MEGA5: molecular evolutionary genetics analysis using maximum likelihood, evolutionary distance, and maximum parsimony methods. *Molecular biology and evolution* **28**:2731–2739.

Tamura, S.-I. and Kurata, T. (2004). Defense mechanisms against influenza virus infection in the respiratory tract mucosa. *Japanese journal of infectious diseases* **57**:236–247.

Tan, G.S. *et al.* (2014). Characterization of a broadly neutralizing monoclonal antibody that targets the fusion domain of group 2 influenza a virus hemagglutinin. *Journal of virology* **88**:13580–13592.

Tan, Y.-C. *et al.* (2014). High-throughput sequencing of natively paired antibody chains provides evidence for original antigenic sin shaping the antibody response to influenza vaccination. *Clinical immunology (Orlando, Fla.)* **151**:55–65.

Tang, Y. *et al.* (2002). The gate of the influenza virus M2 proton channel is formed by a single tryptophan residue. *The Journal of biological chemistry* **277**:39880–39886.

Tarnow, C. *et al.* (2014). TMPRSS2 is a host factor that is essential for pneumotropism and pathogenicity of H7N9 influenza A virus in mice. *Journal of virology* **88**:4744–4751.

Taubenberger, J.K. and Morens, D.M. (2006). 1918 Influenza: the mother of all pandemics. *Emerging infectious diseases* **12**:15–22.

Taylor, S.C. and Posch, A. (2014). The Design of a Quantitative Western Blot Experiment. *BioMed research international* **2014**:1–8.

Tejeda, A.R. and Capua, I. (2013). Virus‐specific factors associated with zoonotic and pandemic potential. *Influenza and Other Respiratory …*.

Temperton, N.J. and Wright, E. (2009). Retroviral pseudotypes. *eLS*.

Temperton, N.J. *et al.* (2007). A sensitive retroviral pseudotype assay for influenza H5N1-neutralizing antibodies. *Influenza and Other Respiratory Viruses* **1**:105–112.

Tharakaraman, K. *et al.* (2013). Antigenically intact hemagglutinin in circulating avian and swine influenza viruses and potential for H3N2 pandemic. *Scientific reports* **3**.

The United States Pharmacopeial Convention (2010a). *<1032> Design and Development of Biological Assays*. *1032*:1–36.

The United States Pharmacopeial Convention (2010b). *<1033> Biological Assay Validation*. :1–25.

Thermo Fisher Scientific (2009). *Nanodrop 2000/2000c Spectrophotometer*. Thermo Fisher Scientific.

Thompson, C.I. *et al.* (2006). Infection of Human Airway Epithelium by Human and Avian Strains of Influenza A Virus. *Journal of virology* **80**:8060–8068.

Thompson, W.W. *et al.* (2003). Mortality Associated With Influenza and Respiratory Syncytial Virus in the United States. *JAMA* **289**:179–186.

Throsby, M. *et al.* (2008). Heterosubtypic Neutralizing Monoclonal Antibodies Cross-Protective against H5N1 and H1N1 Recovered from Human IgM+ Memory B Cells Unutmaz, D. ed. *PloS one* **3**:e3942.

Tinoco, J.C. *et al.* (2014). Immunogenicity, reactogenicity, and safety of inactivated quadrivalent influenza vaccine candidate versus inactivated trivalent influenza vaccine in healthy adults aged ≥18 years: a phase III, randomized trial. *Vaccine* **32**:1480–1487.

Toledo, J.R. *et al.* (2009). Polyethylenimine-based transfection method as a simple and effective way to produce recombinant lentiviral vectors. *Applied biochemistry and biotechnology* **157**:538–544.

Tong, S. *et al.* (2012). A distinct lineage of influenza A virus from bats. *Proceedings of the National Academy of Sciences* **109**:4269–4274.

Tong, S. *et al.* (2013). New World Bats Harbor Diverse Influenza A Viruses. *PLoS pathogens* **9**:e1003657.

Treanor, J.J. *et al.* (1990). Passively transferred monoclonal antibody to the M2 protein inhibits influenza A virus replication in mice. *Journal of virology* **64**:1375–1377.

Trebbien, R., Larsen, L.E. and Viuff, B.M. (2011). Distribution of sialic acid receptors and influenza A virus of avian and swine origin in experimentally infected pigs. *Virology Journal* **8**:434.

Tricco, A.C. *et al.* (2013). Comparing influenza vaccine efficacy against mismatched and matched strains: a systematic review and meta-analysis. *BMC medicine* **11**:153.

Tripathi, S., White, M.R. and Hartshorn, K.L. (2014). The amazing innate immune response to influenza A virus infection. *Innate Immunity* **21**:73–98.

Trombetta, C. *et al.* (2014). Overview of Serological Techniques for Influenza Vaccine Evaluation: Past, Present and Future. *Vaccines* **2**:707–734.

Tscherne, D.M., Manicassamy, B. and García-Sastre, A. (2010). An enzymatic virus-like particle assay for sensitive detection of virus entry. *Journal of virological methods* **163**:336–343.

Tse, L.V. *et al.* (2013). Plasmin-mediated activation of pandemic H1N1 influenza virus hemagglutinin is independent of the viral neuraminidase. *Journal of virology* **87**:5161–5169.

Tumová, B. and Schild, G.C. (1972). Antigenic relationships between type a influenza viruses of human, porcine, equine, and avian origin. *Bulletin of the World Health Organization* **47**:453–460.

Ulmer, J.B. *et al.* (1998). Protective CD4+ and CD8+ T cells against influenza virus induced by vaccination with nucleoprotein DNA. *Journal of virology* **72**:5648–5653.

Underwood, P.A. (1982). Mapping of antigenic changes in the haemagglutinin of Hong Kong influenza (H3N2) strains using a large panel of monoclonal antibodies. *The Journal of general virology* **62 (Pt 1)**:153–169.

Van Ranst, M. and Lemey, P. (2013). Genesis of avian-origin H7N9 influenza A viruses. *The Lancet*:1–2.

Vanderlinden, E. *et al.* (2010). Novel Inhibitors of Influenza Virus Fusion: Structure-Activity Relationship and Interaction with the Viral Hemagglutinin. *Journal of virology* **84**:4277–4288.

Varecková, E., Cox, N. and Klimov, A. (2002). Evaluation of the subtype specificity of monoclonal antibodies raised against H1 and H3 subtypes of human influenza A virus hemagglutinins. *Journal of clinical microbiology* **40**:2220–2223.

Varghese, J.N. *et al.* (1988). Structure of an escape mutant of glycoprotein N2 neuraminidase of influenza virus A/Tokyo/3/67 at 3 Å. *Journal of Molecular Biology* **200**:201–203.

Varki, A. (1992). Diversity in the sialic acids. *Glycobiology* **2**:25–40.

Varki, N.M. and Varki, A. (2007). Diversity in cell surface sialic acid presentations: implications for biology and disease. *Laboratory Investigation* **87**:851–857.

Vasin, A.V. *et al.* (2014). Molecular mechanisms enhancing the proteome of influenza A viruses: an overview of recently discovered proteins. *Virus research* **185**:53–63.

Veit, M. and Schmidt, M.F.G. (1993). Timing of palmitoylation of influenza virus hemagglutinin. *FEBS letters* **336**:243–247.

Veits, J. *et al.* (2012). Avian influenza virus hemagglutinins H2, H4, H8, and H14 support a highly pathogenic phenotype. *Proceedings of the National Academy of Sciences* **109**:2579–2584.

Vines, A. *et al.* (1998). The role of influenza A virus hemagglutinin residues 226 and 228 in receptor specificity and host range restriction. *Journal of virology* **72**:7626–7631.

Voelkel, C. *et al.* (2012). Pseudotype-Independent Nonspecific Uptake of Gammaretroviral and Lentiviral Particles in Human Cells. *Human Gene Therapy* **23**:274–286.

Vogel, F.R. *et al.* (2009). Emulsion-based adjuvants for influenza vaccines. *Expert review of vaccines* **8**:483–492.

Wagner, R., Matrosovich, M. and Klenk, H.-D. (2002). Functional balance between haemagglutinin and neuraminidase in influenza virus infections. *Reviews in medical virology* **12**:159–166.

Walker, J.A. *et al.* (1992). Location and character of the cellular enzyme that cleaves the hemagglutinin of a virulent avian influenza virus. *Virology* **190**:278–287.

Wang, C., Lamb, R.A. and Pinto, L.H. (1995). Activation of the M2 ion channel of influenza virus: a role for the transmembrane domain histidine residue. *Biophysical journal* **69**:1363–1371.

Wang, G. *et al.* (2014). H6 influenza viruses pose a potential threat to human health. *Journal of virology* **88**:3953–3964.

Wang, P., Palese, P. and O'Neill, R.E. (1997). The NPI-1/NPI-3 (karyopherin alpha) binding site on the influenza a virus nucleoprotein NP is a nonconventional nuclear localization signal. *Journal of virology* **71**:1850–1856.

Wang, Q. *et al.* (2007). Structural basis for receptor specificity of influenza B virus hemagglutinin. *Proceedings of the National Academy of Sciences of the United States of America* **104**:16874–16879.

Wang, T.T. and Palese, P. (2009). Universal epitopes of influenza virus hemagglutinins? *Nature Structural & Molecular Biology* **16**:233–234.

Wang, W. *et al.* (2011). Cross-Neutralizing Antibodies to Pandemic 2009 H1N1 and Recent Seasonal H1N1 Influenza A Strains Influenced by a Mutation in Hemagglutinin Subunit 2 Pekosz, A. ed. *PLoS pathogens* **7**:e1002081.

Wang, W. *et al.* (2008). Establishment of retroviral pseudotypes with influenza hemagglutinins from H1, H3, and H5 subtypes for sensitive and specific detection of neutralizing antibodies. *Journal of virological methods* **153**:111–119.

Wang, W., Castelán-Vega, J.A., *et al.* (2010). A mutation in the receptor binding site enhances infectivity of 2009 H1N1 influenza hemagglutinin pseudotypes without changing antigenicity. *Virology* **407**:374–380.

Wang, W., Xie, H., *et al.* (2010). Characterization of lentiviral pseudotypes with influenza H5N1 hemagglutinin and their performance in neutralization assays. *Journal of virological methods* **165**:305–310.

Wang, Y.-F. *et al.* (2012). Characterization of glycan binding specificities of influenza B viruses with correlation with hemagglutinin genotypes and clinical features. *Journal of medical virology* **84**:679–685.

Wasilewski, S. *et al.* (2012). Distribution of surface glycoproteins on influenza A virus determined by electron cryotomography. *Vaccine*:1–6.

Waterhouse, A.M. *et al.* (2009). Jalview Version 2--a multiple sequence alignment editor and analysis workbench. *Bioinformatics (Oxford, England)* **25**:1189–1191.

Weber, F. *et al.* (1998). A classical bipartite nuclear localization signal on Thogoto and influenza A virus nucleoproteins. *Virology* **250**:9–18.

Webster, R.G. *et al.* (1992). Evolution and ecology of influenza A viruses. *Microbiological reviews* **56**:152–179.

Wei, C.J. *et al.* (2010). Cross-neutralization of 1918 and 2009 influenza viruses: role of glycans in viral evolution and vaccine design. *Science translational medicine* **2**.

Weis, W. *et al.* (1988). Structure of the influenza virus haemagglutinin complexed with its receptor, sialic acid. *Nature* **333**:426–431.

Weksler, M.E. and Szabo, P. (2000). The Effect of Age on the B-Cell Repertoire. *Journal of Clinical Immunology* **20**:240–249.

Westgard, J.O. *et al.* (1977). Performance characteristics of rules for internal quality control: probabilities for false rejection and error detection. *Clinical chemistry* **23**:1857–1867.

White, J., Helenius, A. and Gething, M.J. (1982). Haemagglutinin of influenza virus expressed from a cloned gene promotes membrane fusion. *Nature* **300**:658–659.

Whittle, J.R.R. *et al.* (2011). Broadly neutralizing human antibody that recognizes the receptor-binding pocket of influenza virus hemagglutinin. *Proceedings of the National Academy of Sciences* **108**:14216–14221.

WHO Global Influenza Surveillance Network (2011). *Manual for the Laboratory Diagnosis and Virological Surveillance of Influenza*. World Health Organization.

WHO/OIE/FAO H5N1 Evolution Working Group (2008). Toward a unified nomenclature system for highly pathogenic avian influenza virus (H5N1). *Emerging infectious diseases* **14**:e1.

Wikramaratna, P.S. *et al.* (2013). The antigenic evolution of influenza: drift or thrift? *Philosophical Transactions of the Royal Society B: Biological Sciences* **368**:20120200.

Wiley, D.C., Wilson, I.A. and Skehel, J.J. (1981). Structural identification of the antibody-binding sites of Hong Kong influenza haemagglutinin and their involvement in antigenic variation. *Nature* **289**:373–378.

Wilson, I.A., Skehel, J.J. and Wiley, D.C. (1981). Structure of the haemagglutinin membrane glycoprotein of influenza virus at 3 A resolution. *Nature* **289**:366–373.

Wohlbold, T.J. and Krammer, F. (2014). In the shadow of hemagglutinin: a growing interest in influenza viral neuraminidase and its role as a vaccine antigen. *Viruses* **6**:2465–2494.

Wong, S.-S. and Webby, R.J. (2013). Traditional and new influenza vaccines. *Clinical microbiology reviews* **26**:476–492.

Wood, J.M. and Levandowski, R.A. (2003). The influenza vaccine licensing process. *Vaccine* **21**:1786–1788.

Wood, J.M. *et al.* (2001). A single radial haemolysis assay for antibody to H5 haemagglutinin. **1219**:761–766.

Wood, J.M. *et al.* (1994). Comparison of influenza serological techniques by international collaborative study. *Vaccine* **12**:167–174.

Wood, J.M. *et al.* (2012). Reproducibility of serology assays for pandemic influenza H1N1: collaborative study to evaluate a candidate WHO International Standard. *Vaccine* **30**:210–217.

Woodland, D.L., Hogan, R.J. and Zhong, W. (2001). Cellular immunity and memory to respiratory virus infections. *Immunologic research* **24**:53–67.

Organization (1980). A revision of the system of nomenclature for influenza viruses: a WHO memorandum. *Bulletin of the World Health Organization* **58**:585–591.

World Health Organization (2002). *WHO Manual on Animal Influenza Diagnosis and Surveillance.*

World Health Organization (2006). *Recommendations for the Preparation, Characterization and Establishment of International and Other Biological Reference Standards (Revised 2004)*. WHO Technical Report Series.

World Health Organization (2011). *Standardization of Terminology of the Pandemic a(H1N1)2009 Virus* [Online]. Available at: http://www.who.int/influenza/gisrs_laboratory/terminology_ah1n1pdm09/en/ [Accessed: 19 June 2014].

World Health Organization International Avian Influenza Investigative Team (2010). *Serological Diagnosis of Influenza by Microneutralization Assay*.

World Health Organization, Food and Agriculture Organization and World Organization for Animal Health (2014). *Standardization of Terminology for the Influenza Virus Variants Infecting Humans: Update* [Online]. Available at: http://www.who.int/influenza/gisrs_laboratory/terminology_variant/en/ [Accessed: 19 June 2014].

World Organization for Animal Health (2012). *Avian Influenza*.

World Organization for Animal Health *Manual of Diagnostic Tests and Vaccines For Terrestrial Animals 2014*.

Wrammert, J. *et al.* (2011). Broadly cross-reactive antibodies dominate the human B cell response against 2009 pandemic H1N1 influenza virus infection. *Journal of Experimental Medicine* **208**:181–193.

Wright, P.F. (1998). International standards for test methods and reference sera for diagnostic tests for antibody detection. *Revue scientifique et technique (International Office of Epizootics)* **17**:527–549.

Wright, P.F., Bryant, J.D. and Karzon, D.T. (1980). Comparison of influenza B/Hong Kong virus infections among infants, children, and young adults. *The Journal of infectious diseases* **141**:430–435.

Wu, Y. *et al.* (2014). Bat-derived influenza-like viruses H17N10 and H18N11. *Trends in microbiology* **22**:183–191.

Xu, G. *et al.* (1994). Specificity of sialyl-sugar chain mediated recognition by the hemagglutinin of human influenza B virus isolates. *Journal of biochemistry* **115**:202–207.

Xu, J. *et al.* (2012). Evolutionary History and Phylodynamics of Influenza A and B Neuraminidase (NA) Genes Inferred from Large-Scale Sequence Analyses. *PloS one* **7**:e38665.

Xu, R. *et al.* (2010). Structural basis of preexisting immunity to the 2009 H1N1 pandemic influenza virus. *Science* [Online] **328**:357–360. Available at: http://eutils.ncbi.nlm.nih.gov/entrez/eutils/elink.fcgi?dbfrom=pubmed&id=20339031&retmode=ref&cmd=prlinks.

Yamada, H. *et al.* (2004). Mitochondrial targeting sequence of the influenza A virus PB1-F2 protein and its function in mitochondria. *FEBS letters* **578**:331–336.

Yamamoto-Goshima, F. and Maeno, K. (1994). Approach to the involvement of influenza B neuraminidase in the cleavage of HA by host cell protease using low pH-induced cell fusion reaction. *Microbiology and immunology* **38**:819–822.

Yamano, S., Dai, J. and Moursi, A.M. (2010). Comparison of Transfection Efficiency of Nonviral Gene Transfer Reagents. *Molecular Biotechnology* **46**:287–300.

Yamashita, A. *et al.* (2010). Highly conserved sequences for human neutralization epitope on hemagglutinin of influenza A viruses H3N2, H1N1 and H5N1: Implication for human monoclonal antibody recognition. *Biochemical and biophysical research communications* **393**:614–618.

Yang, J. *et al.* (2014). Reliability of Pseudotyped Influenza Viral Particles in Neutralizing Antibody Detection. *PloS one* **9**:e113629.

Yasugi, M. *et al.* (2013). Human Monoclonal Antibodies Broadly Neutralizing against Influenza B Virus. *PLoS pathogens* **9**:e1003150.

Yoshimura, A. and Ohnishi, S. (1984). Uncoating of influenza virus in endosomes. *Journal of virology* **51**:497–504.

Yuan, J. *et al.* (2013). Origin and Molecular Characteristics of a Novel 2013 Avian Influenza A(H6N1) Virus Causing Human Infection in Taiwan. *Clinical Infectious Diseases*.

Yusuf, K., Soraisham, A.S. and Fonseca, K. (2007). Fatal influenza B virus pneumonia in a preterm neonate: case report and review of the literature. *Journal of perinatology : official journal of the California Perinatal Association* **27**:623–625.

Zamarin, D., Ortigoza, M.B. and Palese, P. (2006). Influenza A virus PB1-F2 protein contributes to viral pathogenesis in mice. *Journal of virology* **80**:7976–7983.

Zambon, M., Hayden, F.G. and Global Neuraminidase Inhibitor Susceptibility Network (2001). Position statement: global neuraminidase inhibitor susceptibility network. *Antiviral Research* **49**:147–156.

Zambon, M.C. (1999). Epidemiology and pathogenesis of influenza. *The Journal of antimicrobial chemotherapy* **44 Suppl B**:3–9.

Závada, J. and Rosenbergová, M. (1972). Phenotypic mixing of vesicular stomatitis virus with fowl plague virus. *Acta virologica* **16**:103–114.

Zebedee, S.L. and Lamb, R.A. (1988). Influenza A virus M2 protein: monoclonal antibody restriction of virus growth and detection of M2 in virions. *Journal of virology* **62**:2762–2772.

Zhang, B. *et al.* (2001). A highly efficient and consistent method for harvesting large volumes of high-titre lentiviral vectors. *Gene Therapy* **8**:1745–1751.

Zhang, F. *et al.* (2011). Infectivity of Pseudotyped Particles Pairing Hemagglutinin of Highly Pathogenic Avian Influenza a H5N1 Virus with Neuraminidases of The 2009 Pandemic H1N1 and a Seasonal H3N2. *Journal of Bioterrorism & Biodefense* **2**.

Zhang, K. *et al.* (2012). Dissection of Influenza A Virus M1 Protein: pH-Dependent Oligomerization of N-Terminal Domain and Dimerization of C-Terminal Domain. *PloS one* **7**:e37786.

Zhang, W., Jiang, Q. and Chen, Y. (2007). Evolution and variation of the H3 gene of influenza A virus and interaction among hosts. *Intervirology* **50**:287–295.

Zheng, B. *et al.* (2007). Rectification of age-associated deficiency in cytotoxic T cell response to influenza A virus by immunization with immune complexes. *The Journal of Immunology* **179**:6153–6159.

Zhirnov, O.P. *et al.* (2011). Aprotinin, a protease inhibitor, suppresses proteolytic activation of pandemic H1N1v influenza virus. *Antiviral chemistry \& chemotherapy* **21**:169–174.

Zhirnov, O.P., Golyando, P.B. and Ovcharenko, A.V. (1994). Replication of Influenza B virus in chicken embryos is suppressed by exogenous aprotinin. *Archives of Virology* **135**:209–216.

Zhirnov, O.P., Ovcharenko, A.V. and Bukrinskaya, A.G. (1984). Suppression of influenza virus replication in infected mice by protease inhibitors. *The Journal of general virology* **65 (Pt 1)**:191–196.

Zhou, J. *et al.* (2012). A Functional Variation in CD55 Increases the Severity of 2009 Pandemic H1N1 Influenza A Virus Infection. *Journal of Infectious Diseases* **206**:495–503.

Zhu, X. *et al.* (2012). Crystal structures of two subtype N10 neuraminidase-like proteins from bat influenza A viruses reveal a diverged putative active site. *Proceedings of the National Academy of Sciences* **109**:18903–18908.

Zhu, X. *et al.* (2013). Hemagglutinin homologue from H17N10 bat influenza virus exhibits divergent receptor-binding and pH-dependent fusion activities. *Proceedings of the National Academy of Sciences*.

Zimmer, S.M. and Burke, D.S. (2009). Historical perspective--Emergence of influenza A (H1N1) viruses. *The New England journal of medicine* **361**:279–285.

Zmora, P. and Pöhlmann, S. (2014). Microscopy as a useful tool to study the proteolytic activation of influenza viruses. In: Méndez-Vilas, A. ed. *Microscopy: Advances in Scientific Research and Education*. Formatex Research Center, pp. 725–731.

Zmora, P. *et al.* (2014). DESC1 and MSPL Activate Influenza A Viruses and Emerging Coronaviruses for Host Cell Entry. *Journal of virology* **88**:12087–12097.

Zufferey, R. *et al.* (1997). Multiply attenuated lentiviral vector achieves efficient gene delivery in vivo. *Nature biotechnology* **15**:871–875.

APPENDIX

A.1 Additional Figures and Tables for Chapter 3

INPUT
The symbol is used to identify the starting materials.

- HA gene (insert) source
- Vector

PROCESS
The symbol is used to identify the methodology as described in chapter 2.

- Transformation of competent *E. coli* cells (section 2.1.3)
- Determination of nucleic acid concentration (section 2.1.5)
- Polymerase chain reaction (section 2.1.8)
- DNA digestion using restriction endonucleases (section 2.1.9)
- DNA ligation (section 2.1.11)
- Colony PCR for recombinant clone screening (section 2.1.12)
- DNA gel electrophoresis (section 2.1.13)

PRE-DEFINED PROCESS
The symbol is used to identify a methodology performed following an external protocol (commercial kit) as described in chapter 2

- Isolation of plasmid DNA from bacterial culture (section 2.1.4)
- Sanger sequencing (section 2.1.7)
- Zero Blunt® TOPO® PCR Cloning Kit (section 2.1.10)
- PCR and digestion reaction purification (section 2.1.14)
- DNA fragment extraction from agarose gel (section 2.1.15)
- Site-direct mutagenesis of plasmid (section 2.1.16.1)

MULTIPLE PROCESS
The symbol is used to identify a prefixed path composed of a specified number of processes. The colours are the ones of the single processes

CONNECTORS
The symbols are used to connect different steps.
The solid black line identifies the flow followed.
The dashed grey line identifies the alternative flow. This line is used also in the symbol borders to identify alternative processes.

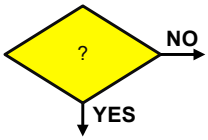

DECISION
The symbol is used to identify a decision point that can result in two different paths.

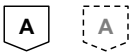

PAGE CONNECTORS
The symbol is used to create a cross-reference from a process on one page to a process on another page.

TERMINATOR
The symbol is used to indicate the end of a path.

- Positive results
- Negative results

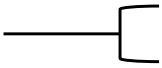

COMMENT
The symbol is used to identify comments, annotations and explanations.

Appendix Figure 1: Flow chart legend

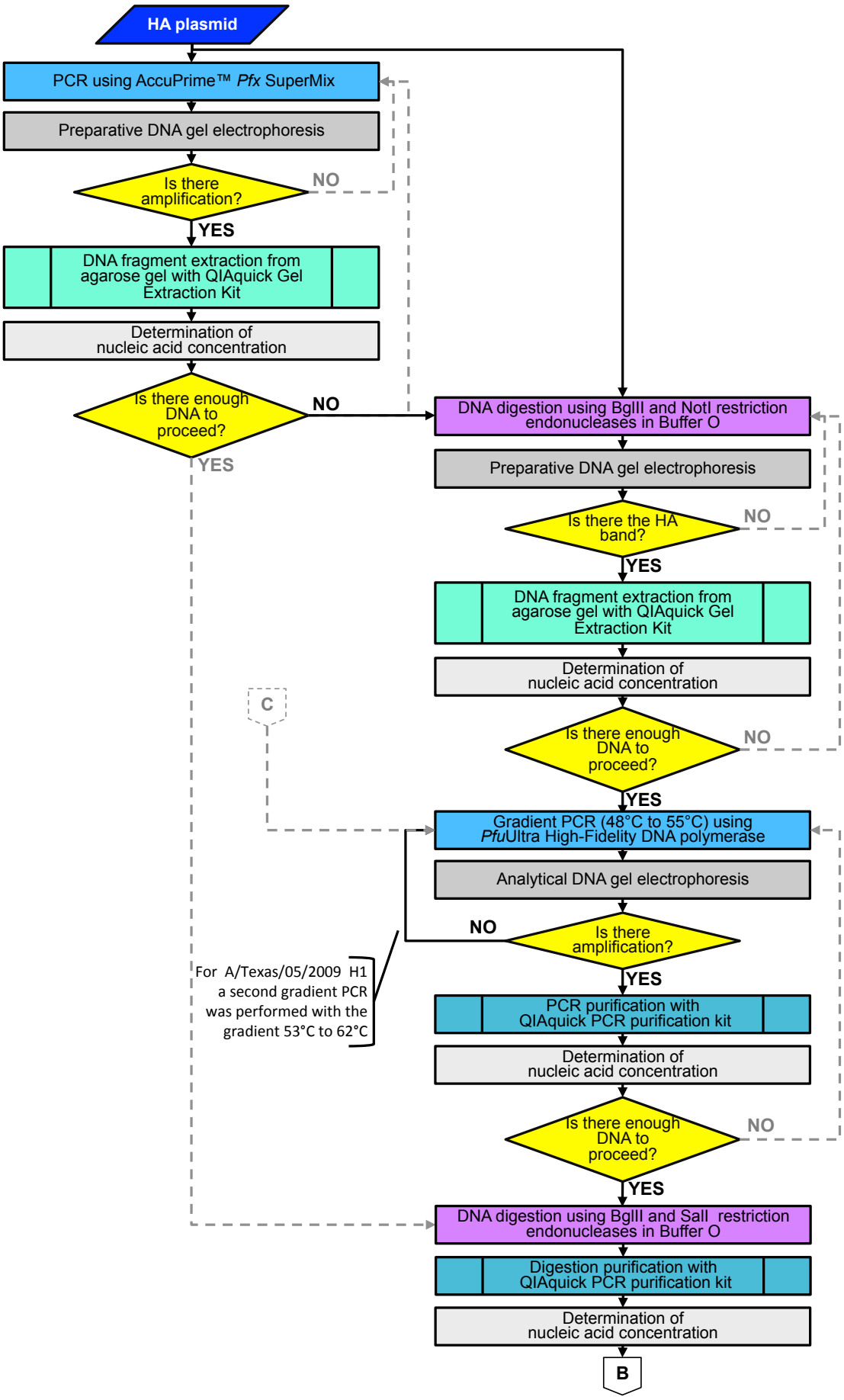
HA plasmid
PCR using AccuPrime™ Pfx SuperMix
Preparative DNA gel electrophoresis
Is there amplification?
NO
YES
DNA fragment extraction from agarose gel with QIAquick Gel Extraction Kit
Determination of nucleic acid concentration
Is there enough DNA to proceed?
NO
YES
DNA digestion using BglII and NotI restriction endonucleases in Buffer O
Preparative DNA gel electrophoresis
Is there the HA band?
NO
YES
DNA fragment extraction from agarose gel with QIAquick Gel Extraction Kit
Determination of nucleic acid concentration
C
Is there enough DNA to proceed?
NO
YES
Gradient PCR (48°C to 55°C) using PfuUltra High-Fidelity DNA polymerase
Analytical DNA gel electrophoresis
NO
Is there amplification?
YES
For A/Texas/05/2009 H1 a second gradient PCR was performed with the gradient 53°C to 62°C
PCR purification with QIAquick PCR purification kit
Determination of nucleic acid concentration
Is there enough DNA to proceed?
NO
YES
DNA digestion using BglII and SalI restriction endonucleases in Buffer O
Digestion purification with QIAquick PCR purification kit
Determination of nucleic acid concentration
B

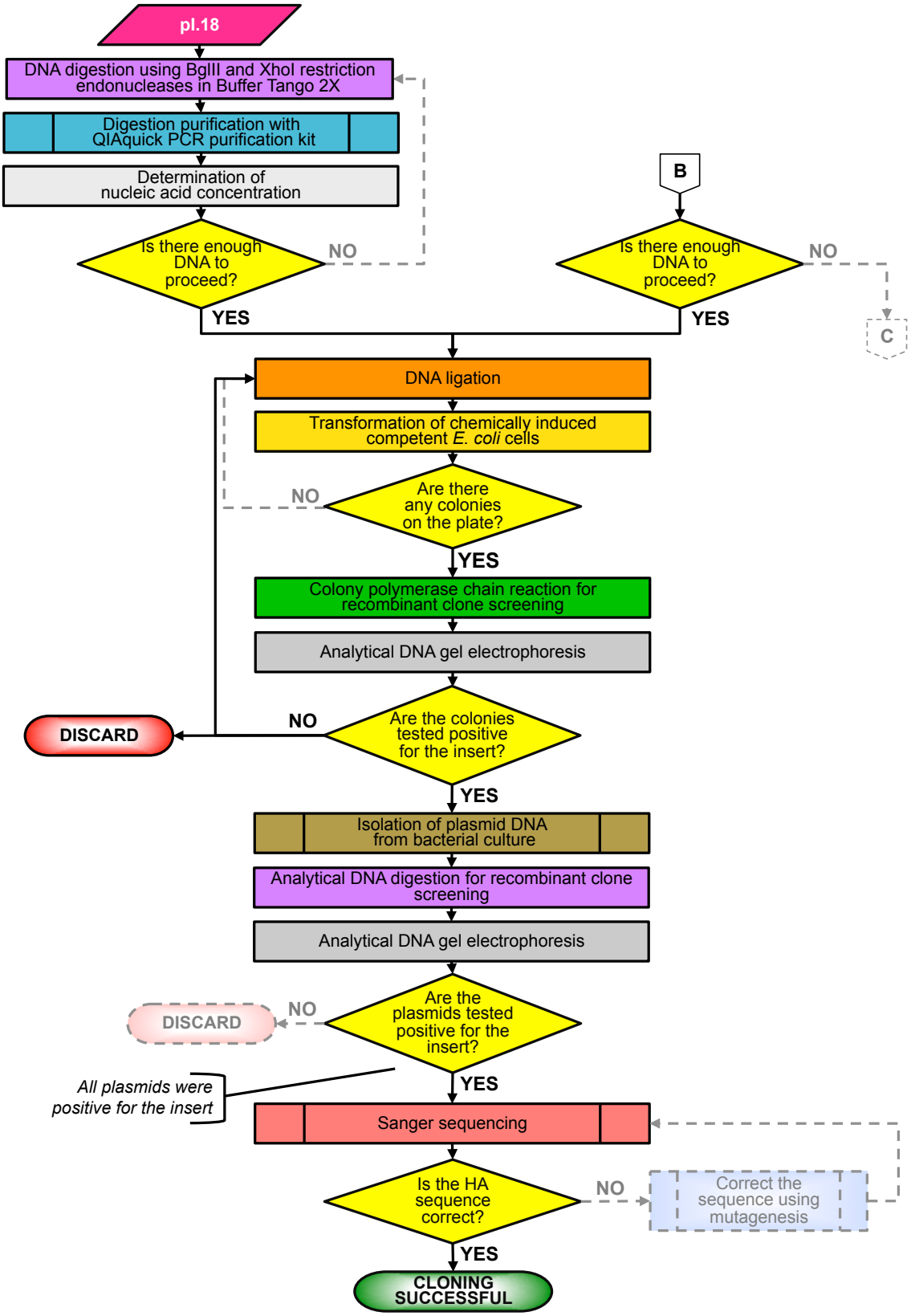

Appendix Figure 2: Flow chart outlining the cloning of A/Solomon Islands/3/2006 H1 and A/Texas/05/2009 H1 HAs into pI.18 expression vector

This subcloning strategy differs from the one reported in Figure 22 since to introduce the Kozak sequence, PCR was necessary. After failure of HA amplification through PCR using *Pfx* SuperMix, HA was amplified using gradient PCR on previously digested and purified HA. Other steps were followed as for HA cloning in Figure 23

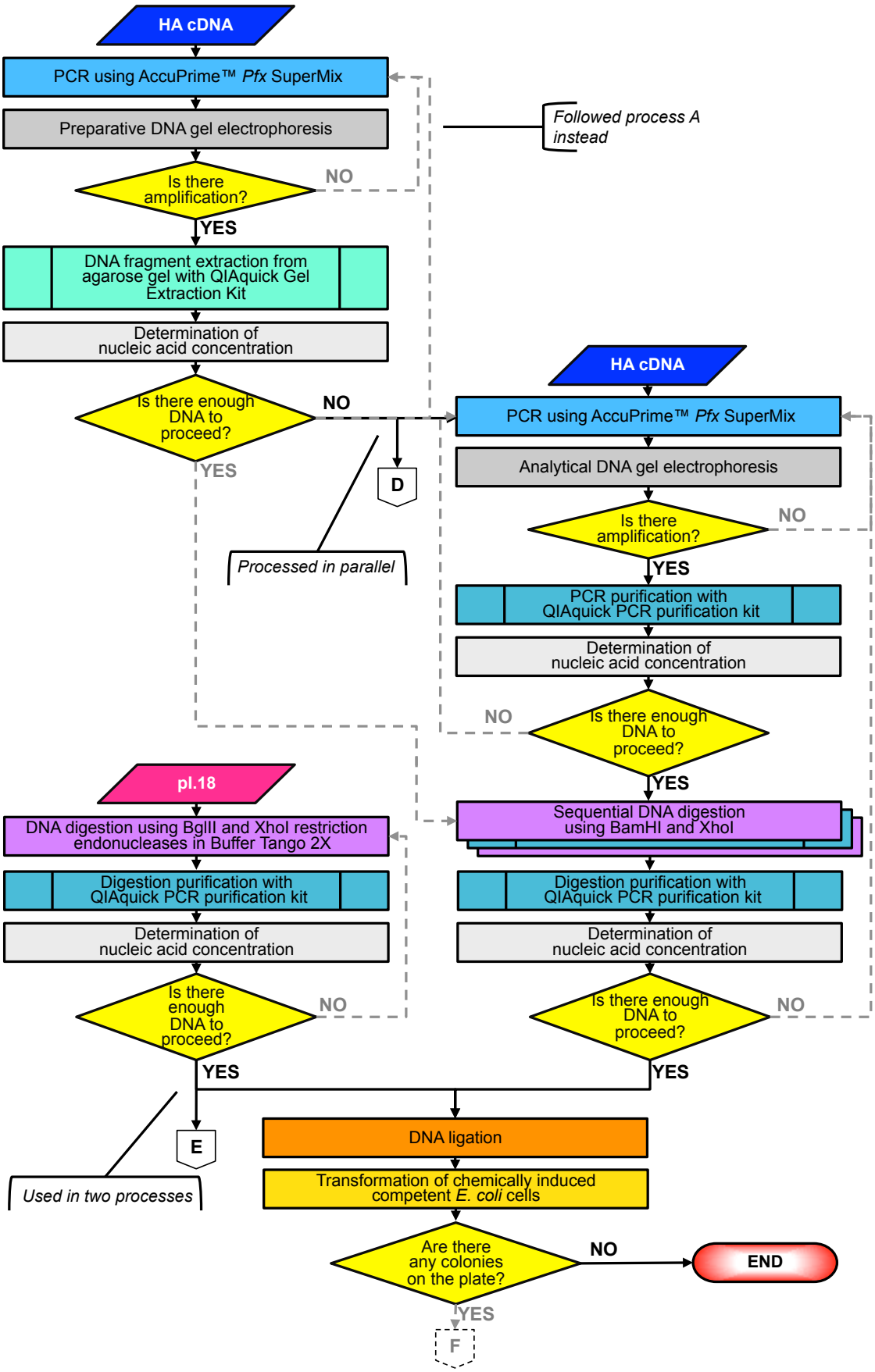
HA cDNA
PCR using AccuPrime™ Pfx SuperMix
Preparative DNA gel electrophoresis
Followed process A instead
Is there amplification?
NO
YES
DNA fragment extraction from agarose gel with QIAquick Gel Extraction Kit
Determination of nucleic acid concentration
Is there enough DNA to proceed?
NO
YES
D
Processed in parallel
HA cDNA
PCR using AccuPrime™ Pfx SuperMix
Analytical DNA gel electrophoresis
Is there amplification?
NO
YES
PCR purification with QIAquick PCR purification kit
Determination of nucleic acid concentration
NO
Is there enough DNA to proceed?
YES
pI.18
DNA digestion using BglII and XhoI restriction endonucleases in Buffer Tango 2X
Sequential DNA digestion using BamHI and XhoI
Digestion purification with QIAquick PCR purification kit
Digestion purification with QIAquick PCR purification kit
Determination of nucleic acid concentration
Determination of nucleic acid concentration
Is there enough DNA to proceed?
NO
Is there enough DNA to proceed?
NO
YES
YES
E
Used in two processes
DNA ligation
Transformation of chemically induced competent E. coli cells
Are there any colonies on the plate?
NO
END
YES
F

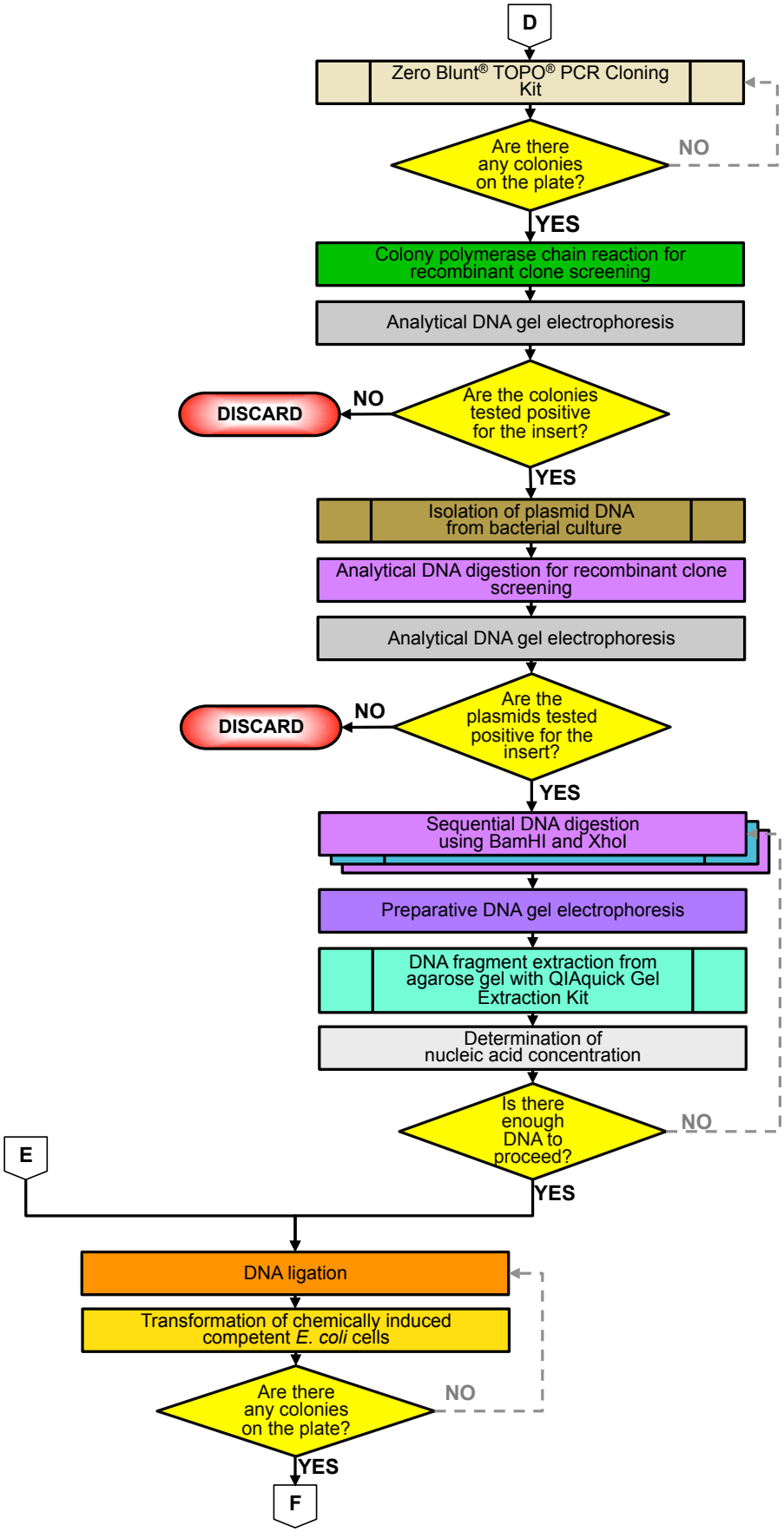
D
Zero Blunt® TOPO® PCR Cloning Kit
Are there any colonies on the plate?
NO
YES
Colony polymerase chain reaction for recombinant clone screening
Analytical DNA gel electrophoresis
Are the colonies tested positive for the insert?
NO
DISCARD
YES
Isolation of plasmid DNA from bacterial culture
Analytical DNA digestion for recombinant clone screening
Analytical DNA gel electrophoresis
Are the plasmids tested positive for the insert?
NO
DISCARD
YES
Sequential DNA digestion using BamHI and XhoI
Preparative DNA gel electrophoresis
DNA fragment extraction from agarose gel with QIAquick Gel Extraction Kit
Determination of nucleic acid concentration
Is there enough DNA to proceed?
NO
YES
E
DNA ligation
Transformation of chemically induced competent E. coli cells
Are there any colonies on the plate?
NO
YES
F

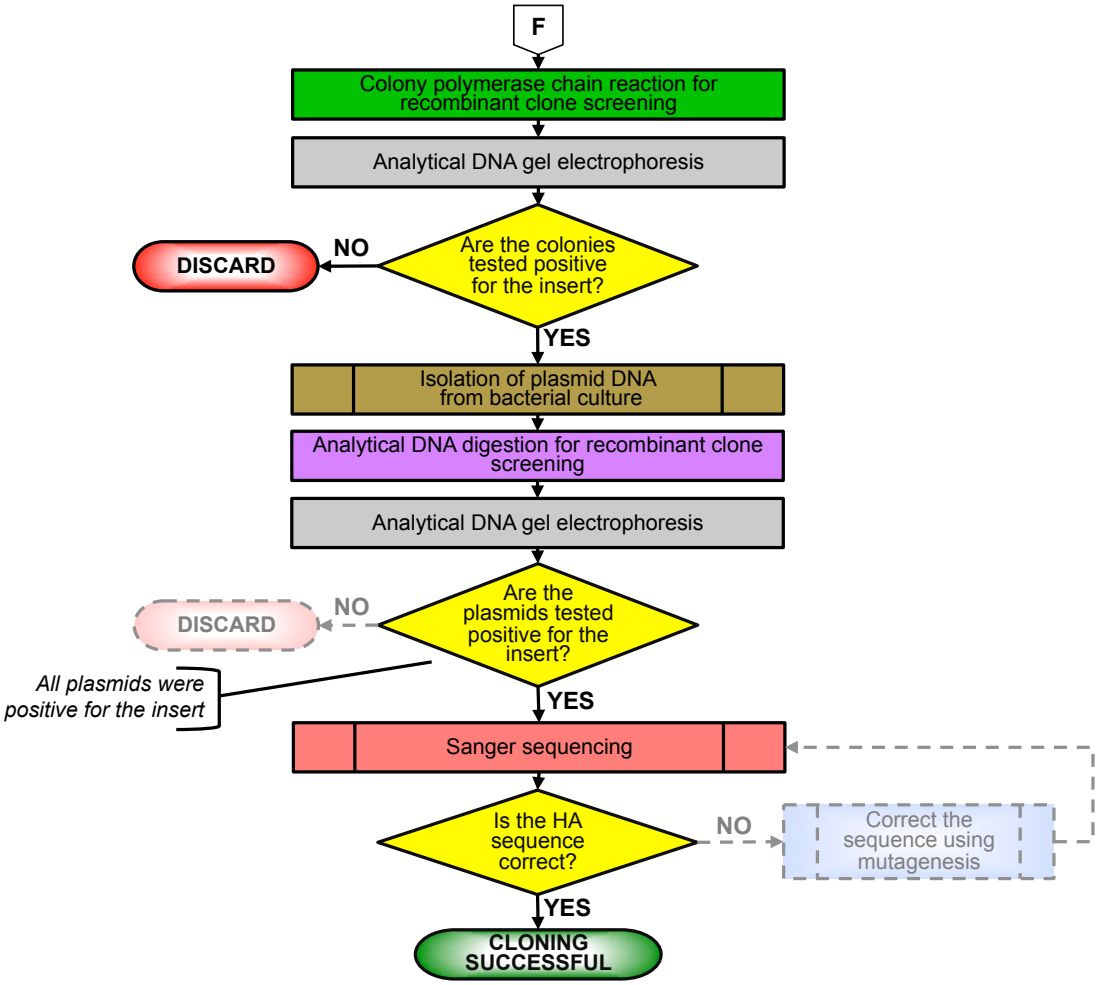

Appendix Figure 3: Flow chart outlining the cloning of A/Brisbane/59/2007 H1 HA into pI.18 expression vector

This subcloning strategy follows the concepts summarised in Figure 23. However, failure of efficient amplification and purification of HA gene have required cloning using a Zero Blunt® TOPO® PCR cloning kit. In parallel, traditional cloning was also performed without success. The plasmid resulting from the Zero Blunt® TOPO® PCR cloning was then used for a traditional sub cloning as shown in Figure 22.

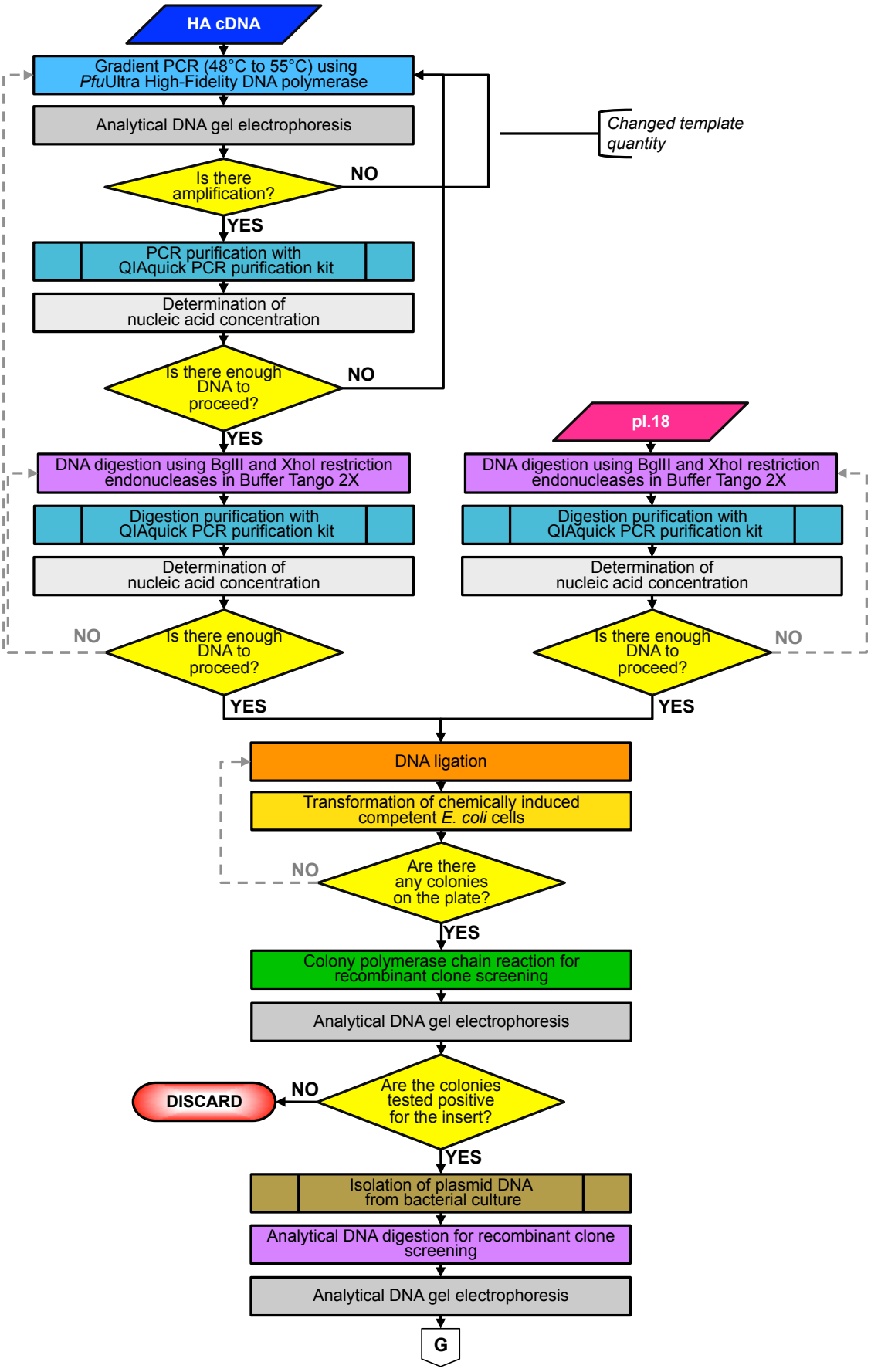
HA cDNA
Gradient PCR (48°C to 55°C) using PfuUltra High-Fidelity DNA polymerase
Analytical DNA gel electrophoresis
Changed template quantity
Is there amplification?
NO
YES
PCR purification with QIAquick PCR purification kit
Determination of nucleic acid concentration
Is there enough DNA to proceed?
NO
YES
pl.18
DNA digestion using BglII and XhoI restriction endonucleases in Buffer Tango 2X
Digestion purification with QIAquick PCR purification kit
Determination of nucleic acid concentration
Is there enough DNA to proceed?
NO
YES
DNA digestion using BglII and XhoI restriction endonucleases in Buffer Tango 2X
Digestion purification with QIAquick PCR purification kit
Determination of nucleic acid concentration
Is there enough DNA to proceed?
NO
YES
DNA ligation
Transformation of chemically induced competent E. coli cells
Are there any colonies on the plate?
NO
YES
Colony polymerase chain reaction for recombinant clone screening
Analytical DNA gel electrophoresis
Are the colonies tested positive for the insert?
DISCARD
NO
YES
Isolation of plasmid DNA from bacterial culture
Analytical DNA digestion for recombinant clone screening
Analytical DNA gel electrophoresis
G

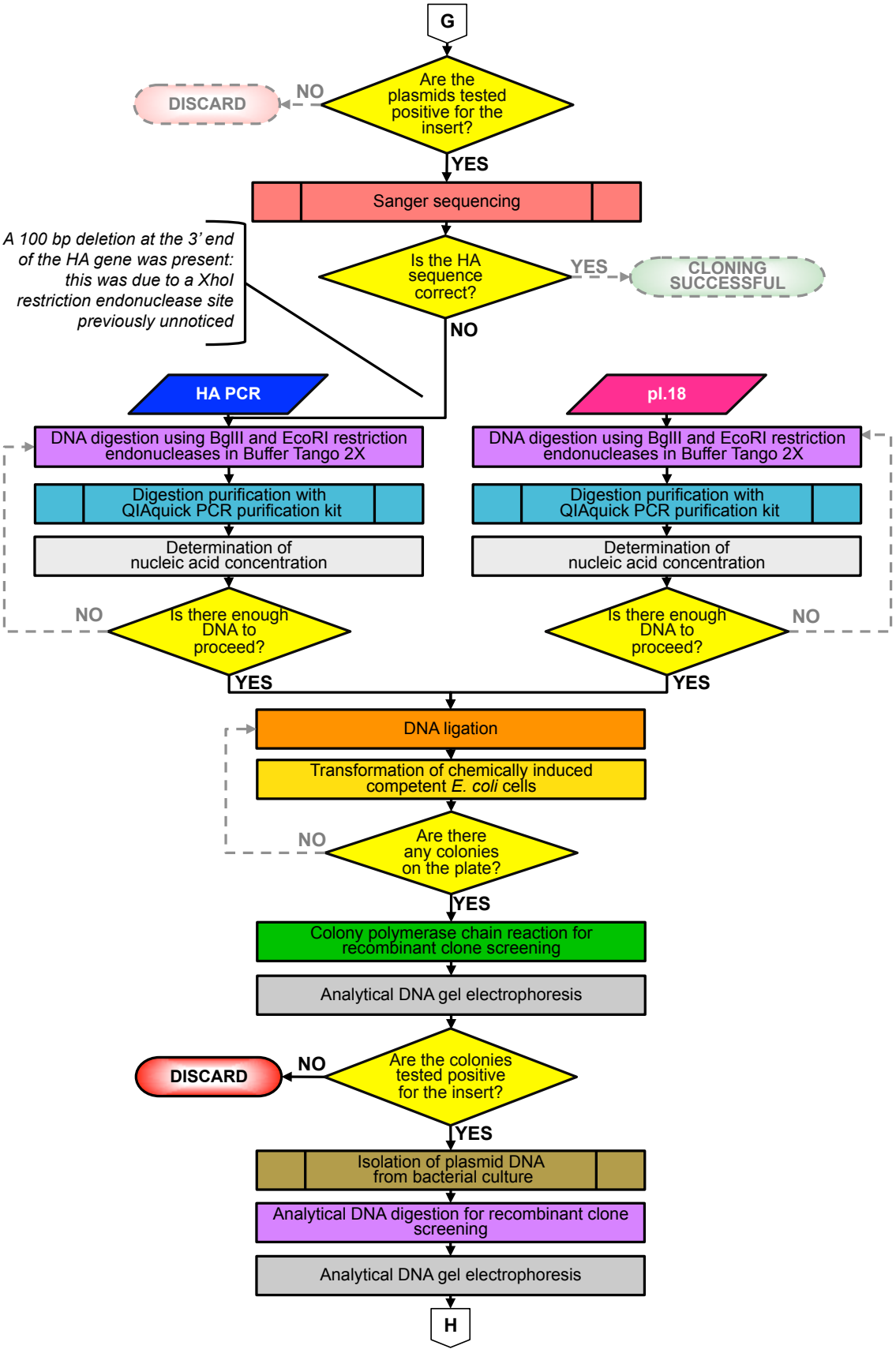
G
Are the plasmids tested positive for the insert?
NO
DISCARD
YES
Sanger sequencing
A 100 bp deletion at the 3' end of the HA gene was present: this was due to a XhoI restriction endonuclease site previously unnoticed
Is the HA sequence correct?
YES
CLONING SUCCESSFUL
NO
HA PCR
pI.18
DNA digestion using BglII and EcoRI restriction endonucleases in Buffer Tango 2X
DNA digestion using BglII and EcoRI restriction endonucleases in Buffer Tango 2X
Digestion purification with QIAquick PCR purification kit
Digestion purification with QIAquick PCR purification kit
Determination of nucleic acid concentration
Determination of nucleic acid concentration
NO
Is there enough DNA to proceed?
Is there enough DNA to proceed?
NO
YES
YES
DNA ligation
Transformation of chemically induced competent E. coli cells
NO
Are there any colonies on the plate?
YES
Colony polymerase chain reaction for recombinant clone screening
Analytical DNA gel electrophoresis
DISCARD
NO
Are the colonies tested positive for the insert?
YES
Isolation of plasmid DNA from bacterial culture
Analytical DNA digestion for recombinant clone screening
Analytical DNA gel electrophoresis
H

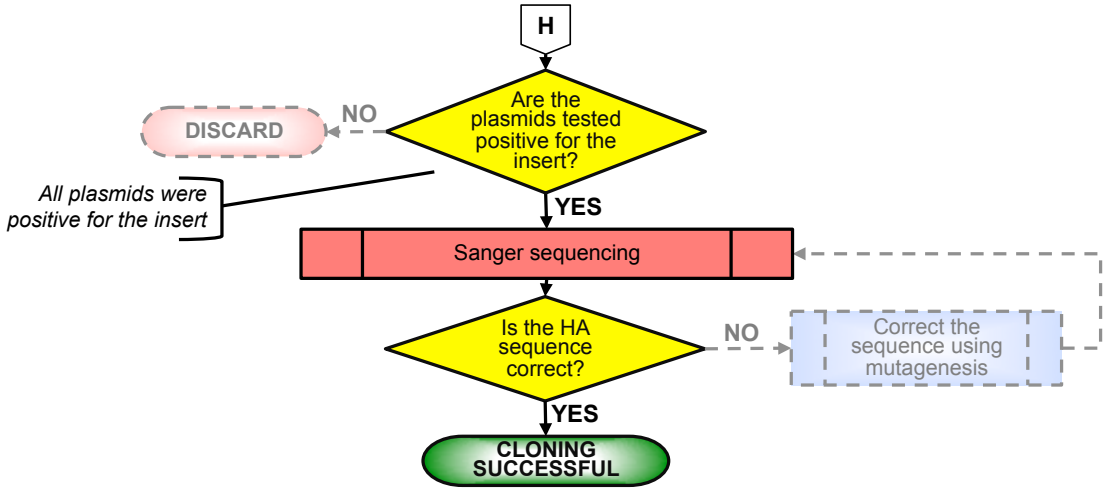

Appendix Figure 4: Flow chart outlining the cloning of A/duck/Italy/1447/2005 H1 HA into pI.18 expression vector

The strategy followed is similar to Figure 23. However for poor primer design (i.e. reverse primer with a restriction enzyme site already present in HA gene) reclining starting from PCR material was necessary using a sticky- and blunt-end (EcoRV) cloning strategy

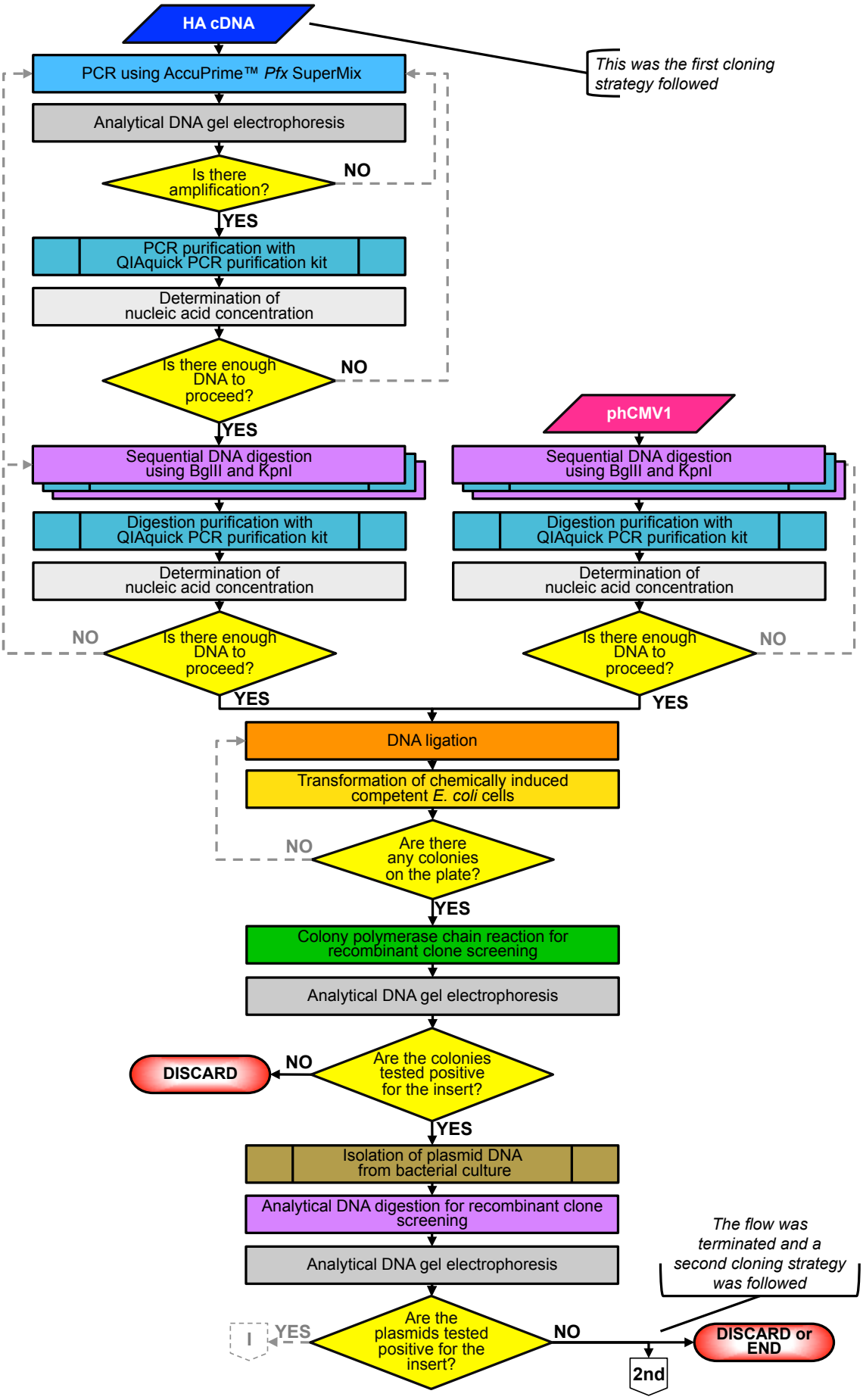
HA cDNA
This was the first cloning strategy followed
PCR using AccuPrime™ Pfx SuperMix
Analytical DNA gel electrophoresis
Is there amplification?
NO
YES
PCR purification with QIAquick PCR purification kit
Determination of nucleic acid concentration
Is there enough DNA to proceed?
NO
YES
phCMV1
Sequential DNA digestion using BglII and KpnI
Digestion purification with QIAquick PCR purification kit
Determination of nucleic acid concentration
Is there enough DNA to proceed?
NO
YES
Sequential DNA digestion using BglII and KpnI
Digestion purification with QIAquick PCR purification kit
Determination of nucleic acid concentration
Is there enough DNA to proceed?
NO
YES
DNA ligation
Transformation of chemically induced competent E. coli cells
Are there any colonies on the plate?
NO
YES
Colony polymerase chain reaction for recombinant clone screening
Analytical DNA gel electrophoresis
Are the colonies tested positive for the insert?
DISCARD
NO
YES
Isolation of plasmid DNA from bacterial culture
Analytical DNA digestion for recombinant clone screening
Analytical DNA gel electrophoresis
The flow was terminated and a second cloning strategy was followed
Are the plasmids tested positive for the insert?
I
YES
NO
DISCARD or END
2nd

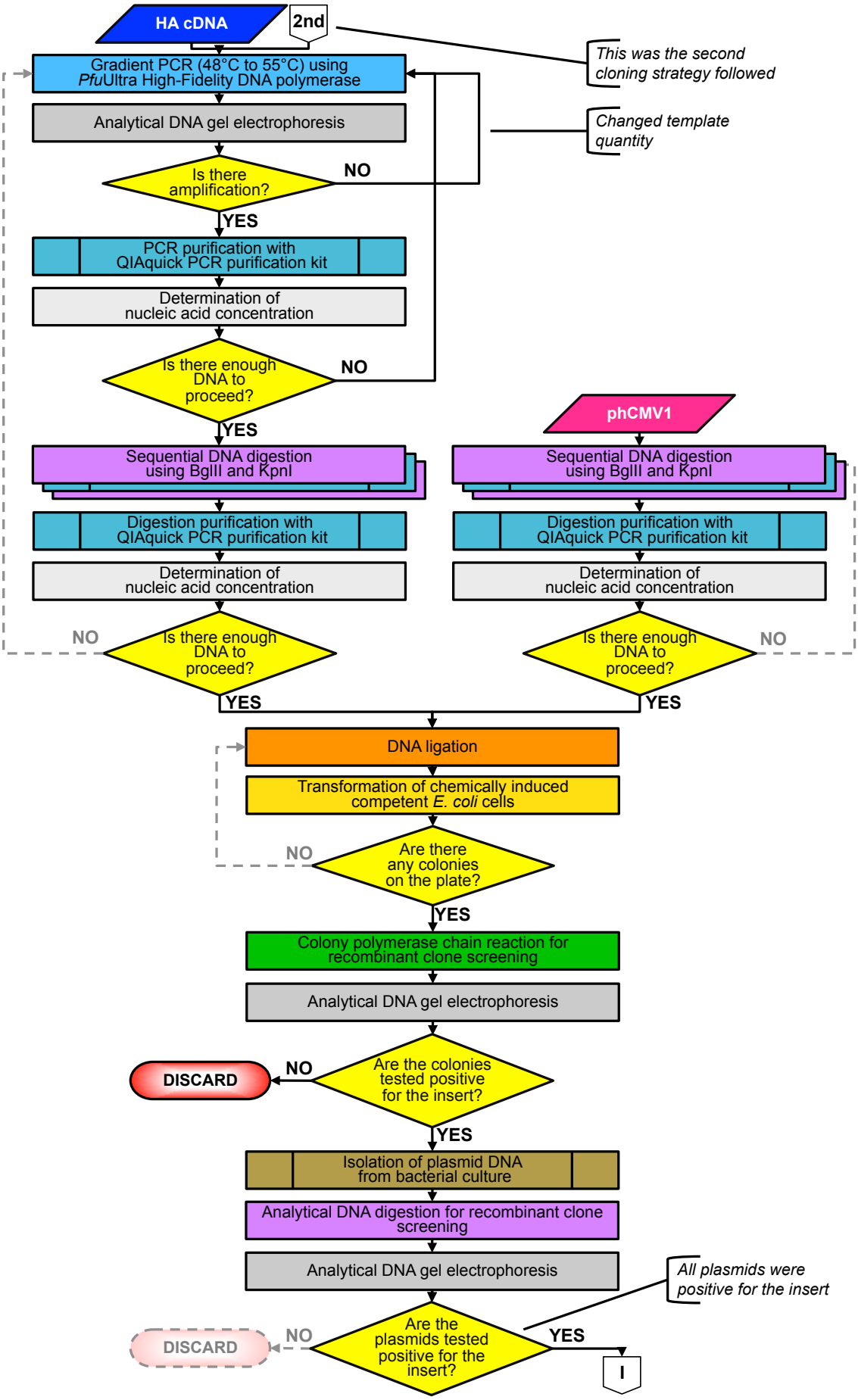
HA cDNA
2nd
This was the second cloning strategy followed
Gradient PCR (48°C to 55°C) using PfuUltra High-Fidelity DNA polymerase
Analytical DNA gel electrophoresis
Changed template quantity
Is there amplification?
NO
YES
PCR purification with QIAquick PCR purification kit
Determination of nucleic acid concentration
Is there enough DNA to proceed?
NO
YES
phCMV1
Sequential DNA digestion using BglII and KpnI
Digestion purification with QIAquick PCR purification kit
Determination of nucleic acid concentration
Is there enough DNA to proceed?
NO
YES
Sequential DNA digestion using BglII and KpnI
Digestion purification with QIAquick PCR purification kit
Determination of nucleic acid concentration
Is there enough DNA to proceed?
NO
YES
DNA ligation
Transformation of chemically induced competent E. coli cells
Are there any colonies on the plate?
NO
YES
Colony polymerase chain reaction for recombinant clone screening
Analytical DNA gel electrophoresis
Are the colonies tested positive for the insert?
DISCARD
NO
YES
Isolation of plasmid DNA from bacterial culture
Analytical DNA digestion for recombinant clone screening
Analytical DNA gel electrophoresis
All plasmids were positive for the insert
Are the plasmids tested positive for the insert?
DISCARD
NO
YES
I

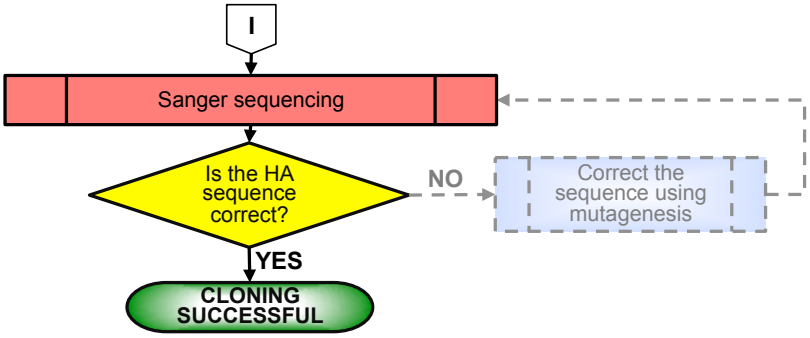

Appendix Figure 5: Flow chart outlining the cloning of A/duck/Germany/1215/1973 H2 HA into phCMV1 expression vector
After the failure of the first cloning of the HA after amplification with *Pfx* SuperMix, the HA gene was cloned following a procedure similar to the one outlined in Figure 23.

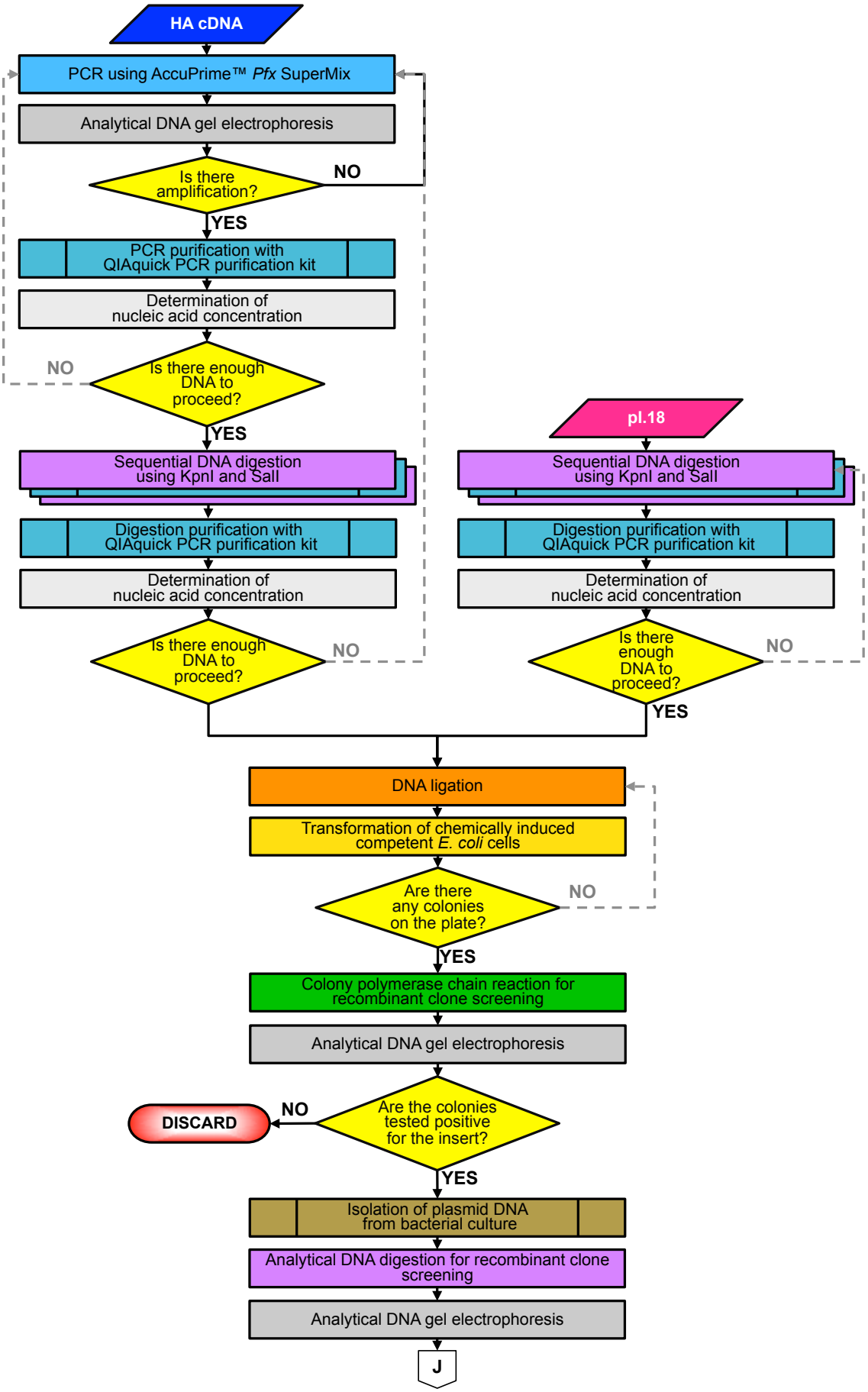
HA cDNA
PCR using AccuPrime™ Pfx SuperMix
Analytical DNA gel electrophoresis
Is there amplification?
NO
YES
PCR purification with QIAquick PCR purification kit
Determination of nucleic acid concentration
Is there enough DNA to proceed?
NO
YES
Sequential DNA digestion using KpnI and SalI
Digestion purification with QIAquick PCR purification kit
Determination of nucleic acid concentration
Is there enough DNA to proceed?
NO
pl.18
Sequential DNA digestion using KpnI and SalI
Digestion purification with QIAquick PCR purification kit
Determination of nucleic acid concentration
Is there enough DNA to proceed?
NO
YES
DNA ligation
Transformation of chemically induced competent E. coli cells
Are there any colonies on the plate?
NO
YES
Colony polymerase chain reaction for recombinant clone screening
Analytical DNA gel electrophoresis
Are the colonies tested positive for the insert?
NO
DISCARD
YES
Isolation of plasmid DNA from bacterial culture
Analytical DNA digestion for recombinant clone screening
Analytical DNA gel electrophoresis
J

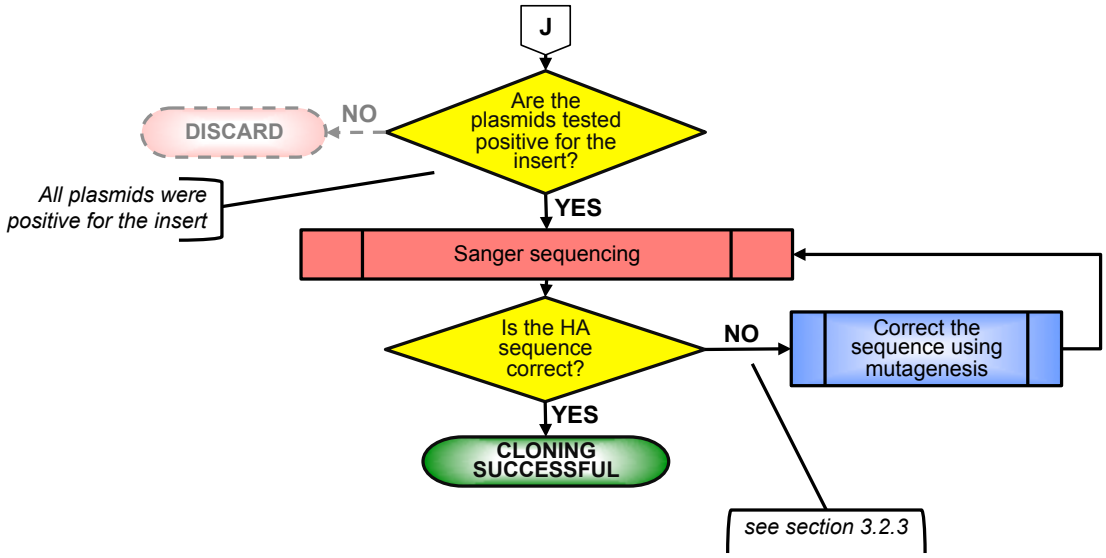

Appendix Figure 6: Flow chart outlining the cloning of A/California/7/2004 H3 HA into pI.18 expression vector

Cloning was successful after HA amplification using *Pfx* SuperMix and a procedure similar to Figure 23. However for a mutation present in the HA sequence, an additional corrective mutagenesis was required.

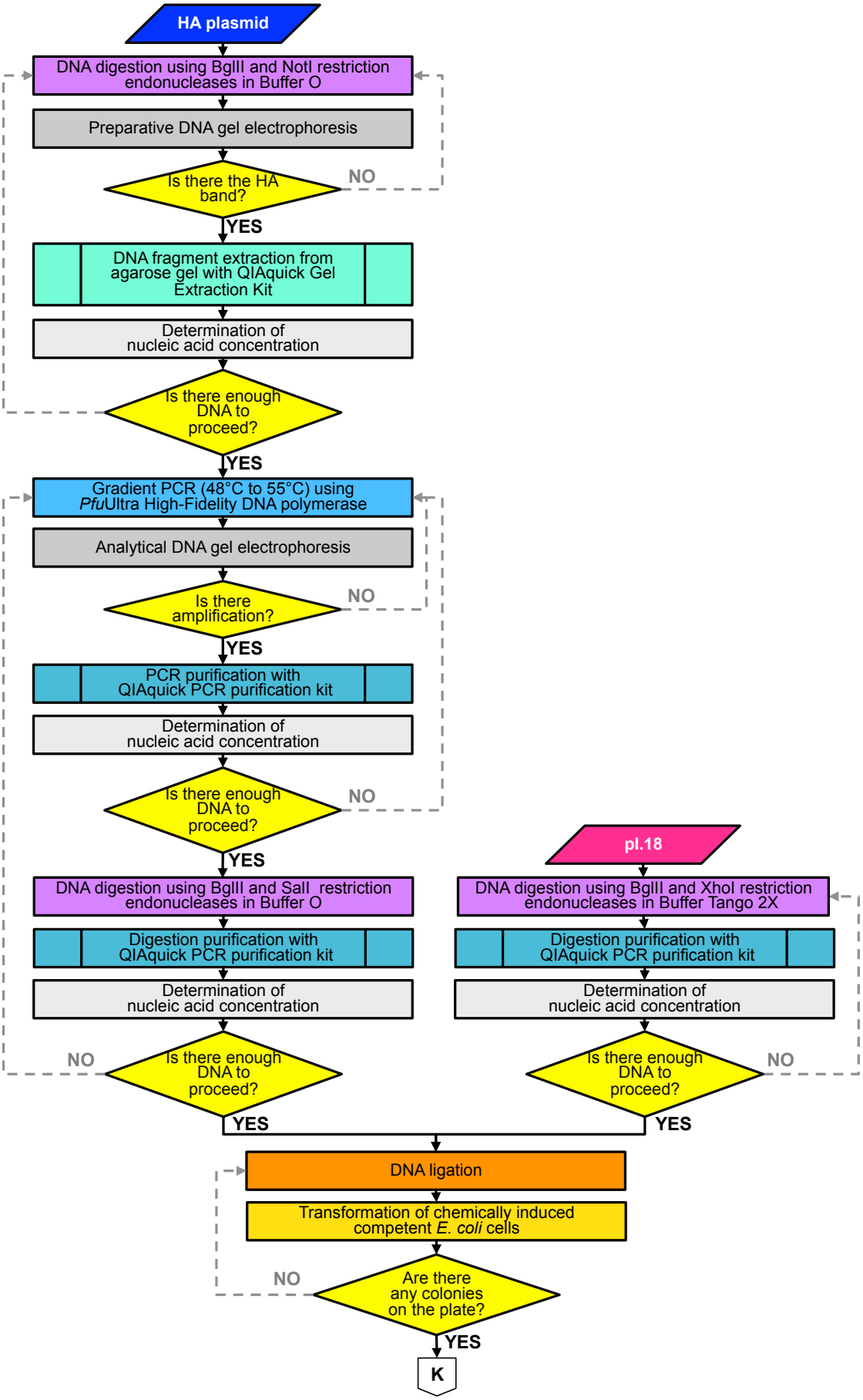
HA plasmid
DNA digestion using BglII and NotI restriction endonucleases in Buffer O
Preparative DNA gel electrophoresis
Is there the HA band?
NO
YES
DNA fragment extraction from agarose gel with QIAquick Gel Extraction Kit
Determination of nucleic acid concentration
Is there enough DNA to proceed?
YES
Gradient PCR (48°C to 55°C) using PfuUltra High-Fidelity DNA polymerase
Analytical DNA gel electrophoresis
Is there amplification?
NO
YES
PCR purification with QIAquick PCR purification kit
Determination of nucleic acid concentration
Is there enough DNA to proceed?
NO
YES
DNA digestion using BglII and SalI restriction endonucleases in Buffer O
Digestion purification with QIAquick PCR purification kit
Determination of nucleic acid concentration
Is there enough DNA to proceed?
NO
YES
pl.18
DNA digestion using BglII and XhoI restriction endonucleases in Buffer Tango 2X
Digestion purification with QIAquick PCR purification kit
Determination of nucleic acid concentration
Is there enough DNA to proceed?
NO
YES
DNA ligation
Transformation of chemically induced competent E. coli cells
Are there any colonies on the plate?
NO
YES
K

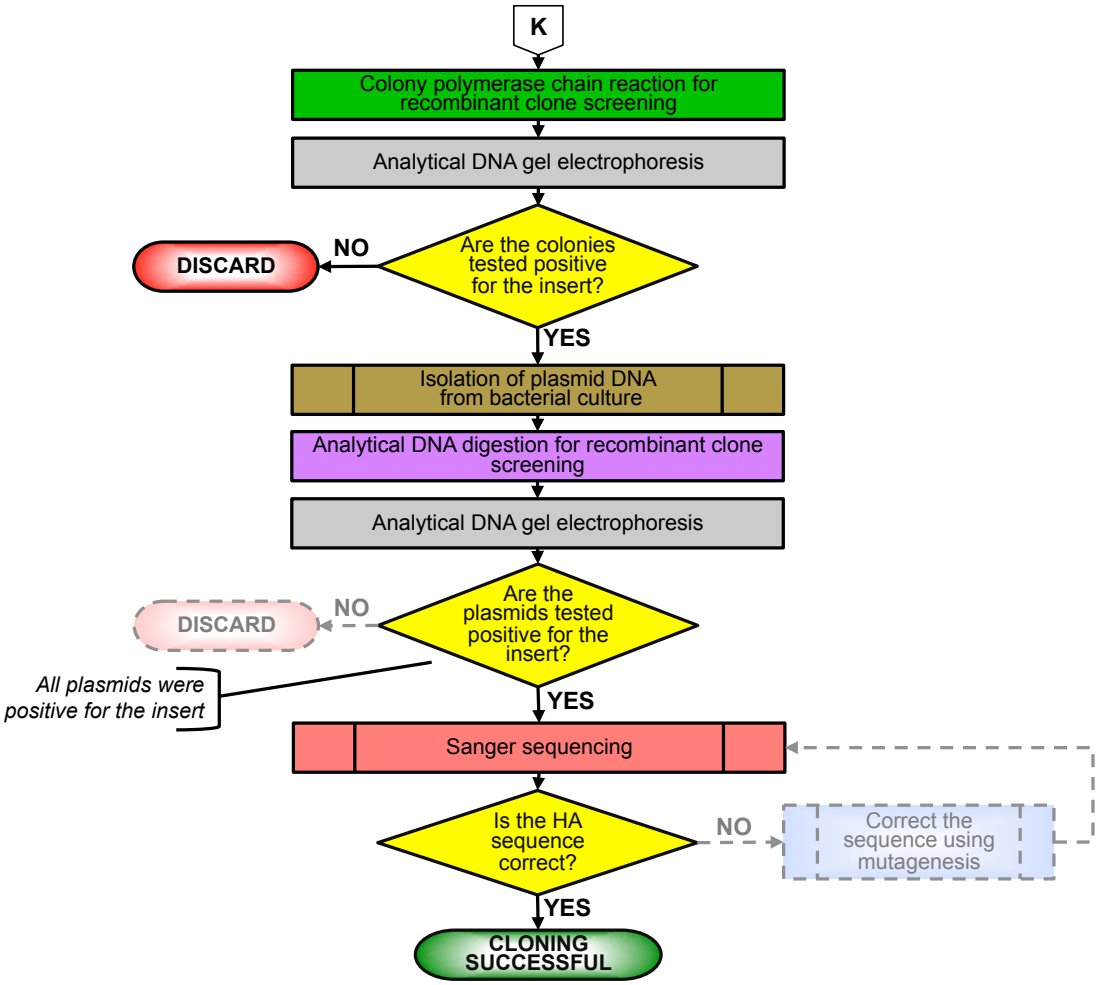

Appendix Figure 7: Flow chart outlining the cloning of A/Wisconsin/67/2005 H3 HA into pI.18 expression vector

HA gene from plasmid was digested and purified to be then used as starting material in a cloning procedure as reported in Figure 23.

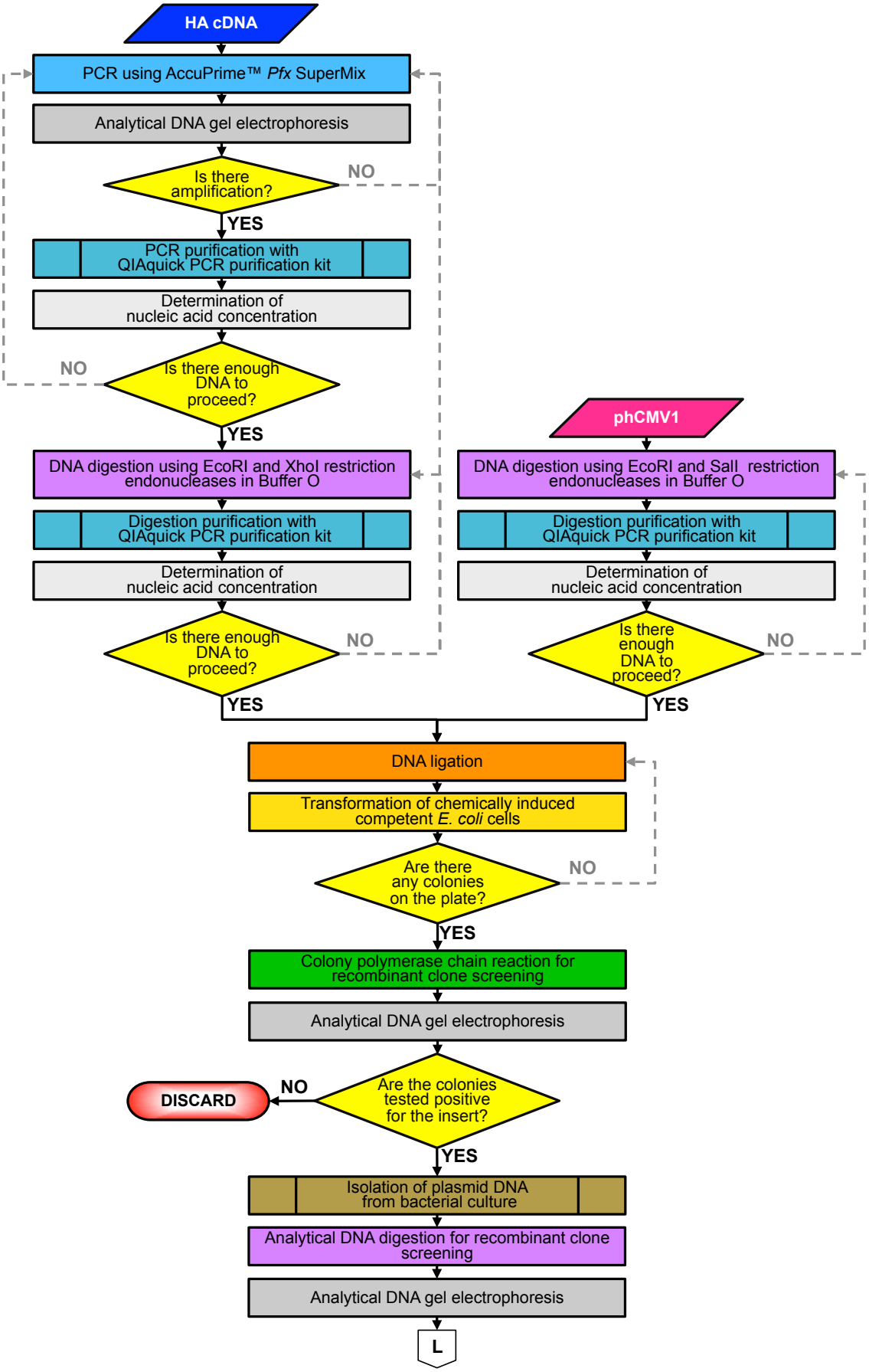
HA cDNA
PCR using AccuPrime™ Pfx SuperMix
Analytical DNA gel electrophoresis
Is there amplification?
NO
YES
PCR purification with QIAquick PCR purification kit
Determination of nucleic acid concentration
Is there enough DNA to proceed?
NO
YES
DNA digestion using EcoRI and XhoI restriction endonucleases in Buffer O
Digestion purification with QIAquick PCR purification kit
Determination of nucleic acid concentration
Is there enough DNA to proceed?
NO
YES
phCMV1
DNA digestion using EcoRI and SalI restriction endonucleases in Buffer O
Digestion purification with QIAquick PCR purification kit
Determination of nucleic acid concentration
Is there enough DNA to proceed?
NO
YES
DNA ligation
Transformation of chemically induced competent E. coli cells
Are there any colonies on the plate?
NO
YES
Colony polymerase chain reaction for recombinant clone screening
Analytical DNA gel electrophoresis
Are the colonies tested positive for the insert?
NO
DISCARD
YES
Isolation of plasmid DNA from bacterial culture
Analytical DNA digestion for recombinant clone screening
Analytical DNA gel electrophoresis
L

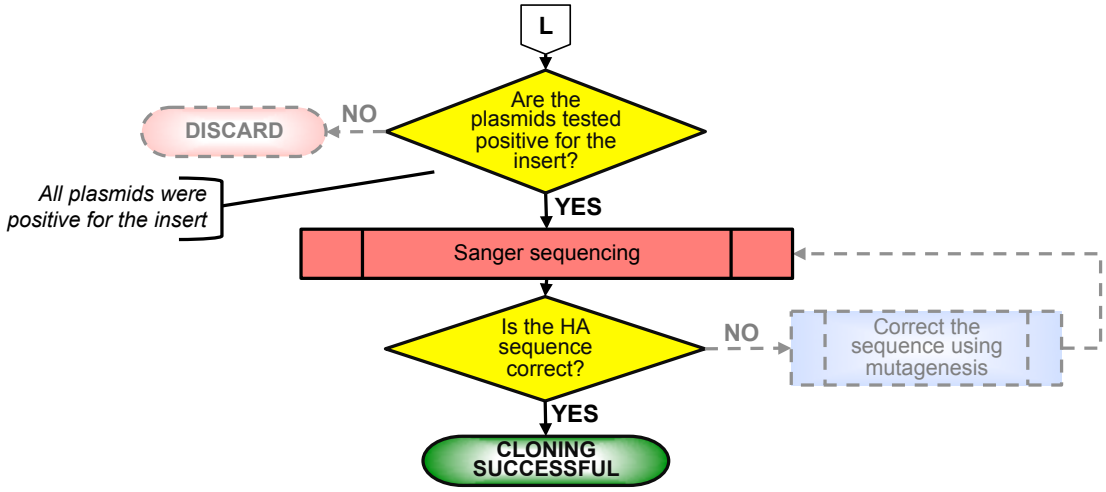

Appendix Figure 8: Flow chart outlining the cloning of A/turkey/Ontario/6118/1968 H8 HA into phCMV1 expression vector

Cloning was successful after HA amplification using *Pfx* SuperMix and procedure similar to Figure 23.

Appendix Table 1: Decision table for the production of influenza A pp

The protease-expressing plasmid quantities are for a 6-well transection. To perform the transfection in a 10 cm plate as described in section 2.3.2, it is necessary to double the quantities. The optimal quantity is highlighted in green. Titres of pp from optimization experiments are reported using the following code:

- indicates pp titres $<1\times10^{6}$ RLU/ml

+ indicates pp titres between 1×10^{6}-1×10^{7} RLU/ml;

++ indicates pp titres between 1×10^{7}-1×10^{8} RLU/ml;

+++ indicates pp titres between 1×10^{8}-1×10^{9} RLU/ml;

++++ indicates pp titres between 1×10^{9} and 1×10^{10} RLU/ml.

Conditions that were not tested are reported with a slash.

	HAT				TMPRSS2				TMPRSS4			
	500 ng	250 ng	125 ng	75 ng	500 ng	250 ng	125 ng	75 ng	500 ng	250 ng	125 ng	75 ng
A/South Carolina/1/1918 H1	/	++	++	/	/	-	-	/	/	+	++	/
A/Puerto Rico/8/1934 H1	/	++	++	/	/	+++	+++	/	/	+++	+++	/
A/New Caledonia/20/1999 H1	/	+++	+++	/	/	-	+	/	/	+++	+++	/
A/Solomon Islands/3/2006 H1	/	+	++	++	/	-	+	+	/	+	+++	++
A/Brisbane/59/2007 H1	/	++	+++	/	/	++	++	/	/	+++	+++	/
A/Texas/05/2009 H1*	+	+	+	/	-	-	-	/	-	+	+	/
A/duck/Italy/1447/2005 H1	+	+	++	/	-	-	-	/	-	++	++	/
A/Korea/426/1968 H2	/	++++	++++	/	/	++	++++	/	/	+++	++++	/
A/duck/Germany/1215/1973 H2	/	+	++	/	/	++	+	/	/	++	+	/
A/Udorn/307/1972 H3	/	++	++	/	/	+++	+++	/	/	+++	++	/
A/California/7/2004 H3	-	-	-	+	+	-	+	-	-	-	-	+
A/Wisconsin/67/2005 H3**	/	++	++	/	/	-	-	/	/	-	-	/
A/duck/Czechoslovakia/1956 H4	/	++	++	/	/	++++	+++	/	/	++	+++	/
A/Shanghai/2/2013 H7	/	+++	++	/	/	++	++	/	/	+++	+++	/
A/turkey/Ontario/6118/1968 H8	/	+++	+++	/	/	+	++	/	/	++++	++++	/
A/Hong Kong/1073/1999 H9	/	++	++	/	/	-	-	/	/	+++	+++	/
A/chicken/Germany/N49 H10	/	++	++	/	/	+++	+++	/	/	-	-	/
A/duck/Memphis/546/1974 H11	/	+++	++	/	/	++	++	/	/	+++	+++	/
A/duck/Alberta/60/1976 H12	/	+++	+++	/	/	-	+	/	/	++	+++	/
A/gull/Maryland/704/1977 H13	/	-	-	/	/	-	-	/	/	-	-	/
A/mallard/Astrakhan/263/1982 H14	/	++++	++	/	/	++	+++	/	/	++	+++	/
A/shearwater/West Australia/2576/1979 H15	/	++	+++	/	/	+++	++	/	/	+++	++++	/
A/black-headed gull/Sweden/2/1999 H16	/	++	+++	/	/	+	-	/	/	+	++	/
A/black-headed gull/Sweden/2/1999 H16 cleavage mutant	/	+++	-	/	/	+	-	/	/	-	+++	/

* Using 250 ng of HA encoding plasmid instead of 500 ng

**NA encoding plasmid is necessary to increase pseudotype titre

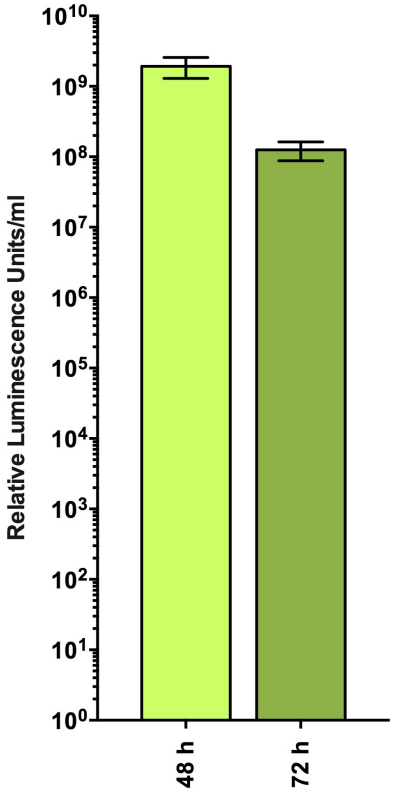

Appendix Figure 9: Comparison between 48 h and 72 h collections of A/duck/Czechoslovakia/1956 H4pp

H4pp was produced using the protocol described in section 2.3.1 and with the addition of 500 ng pCAGGS-TMPRSS2 to the transfection mix.

Appendix Figure 10: HAT (TMPRS11D) expression profile
A. Expression profile available *via* Expression Atlas database that shows the results of an expression experiment. Greater colour intensity means higher expression. **B.** Expression profile available *via* GeneHub-GEPIS database.

Experiment	Twenty seven tissues	Illumina Body Map	Mammalian tissues
adipose tissue			×
adrenal gland			×
animal ovary			×
appendix		×	×
bladder		×	×
bone marrow		×	×
brain	×		×
breast	×		×
cerebellum	×	×	
cerebral cortex		×	×
colon			×
duodenum		×	×
endometrium		×	×
esophagus		×	×
frontal lobe	×	×	
gall bladder		×	×
heart			
kidney			
leukocyte	×		×
liver			
lung			×
lymph node			×
pancreas		×	×
placenta		×	×
prefrontal cortex	×	×	
prostate			×
salivary gland		×	×
skeletal muscle	×		×
skin		×	×
small intestine		×	×
spleen		×	×
stomach		×	×
temporal lobe	×	×	
testis			
thyroid			×

A **B**

Appendix Figure 11: TMPRSS2 expression profile
A. Expression profile available *via* Expression Atlas database that shows the results of three different expression experiments. Greater colour intensity means higher expression. **B.** Expression profile available *via* GeneHub-GEPIS database.

Experiment	Twenty seven tissues	Illumina Body Map	Mammalian tissues
adipose tissue			×
adrenal gland			×
animal ovary			×
appendix		×	×
bladder		×	×
bone marrow		×	×
brain	×		×
breast	×		×
cerebellum	×	×	
cerebral cortex		×	×
colon			×
duodenum		×	×
endometrium		×	×
esophagus		×	×
frontal lobe	×	×	
gall bladder		×	×
heart			
kidney			
leukocyte	×		×
liver			
lung			×
lymph node			×
pancreas		×	×
placenta		×	×
prefrontal cortex	×	×	
prostate			×
salivary gland		×	×
skeletal muscle	×		×
skin		×	×
small intestine		×	×
spleen		×	×
stomach		×	×
temporal lobe	×	×	
testis			
thyroid			×

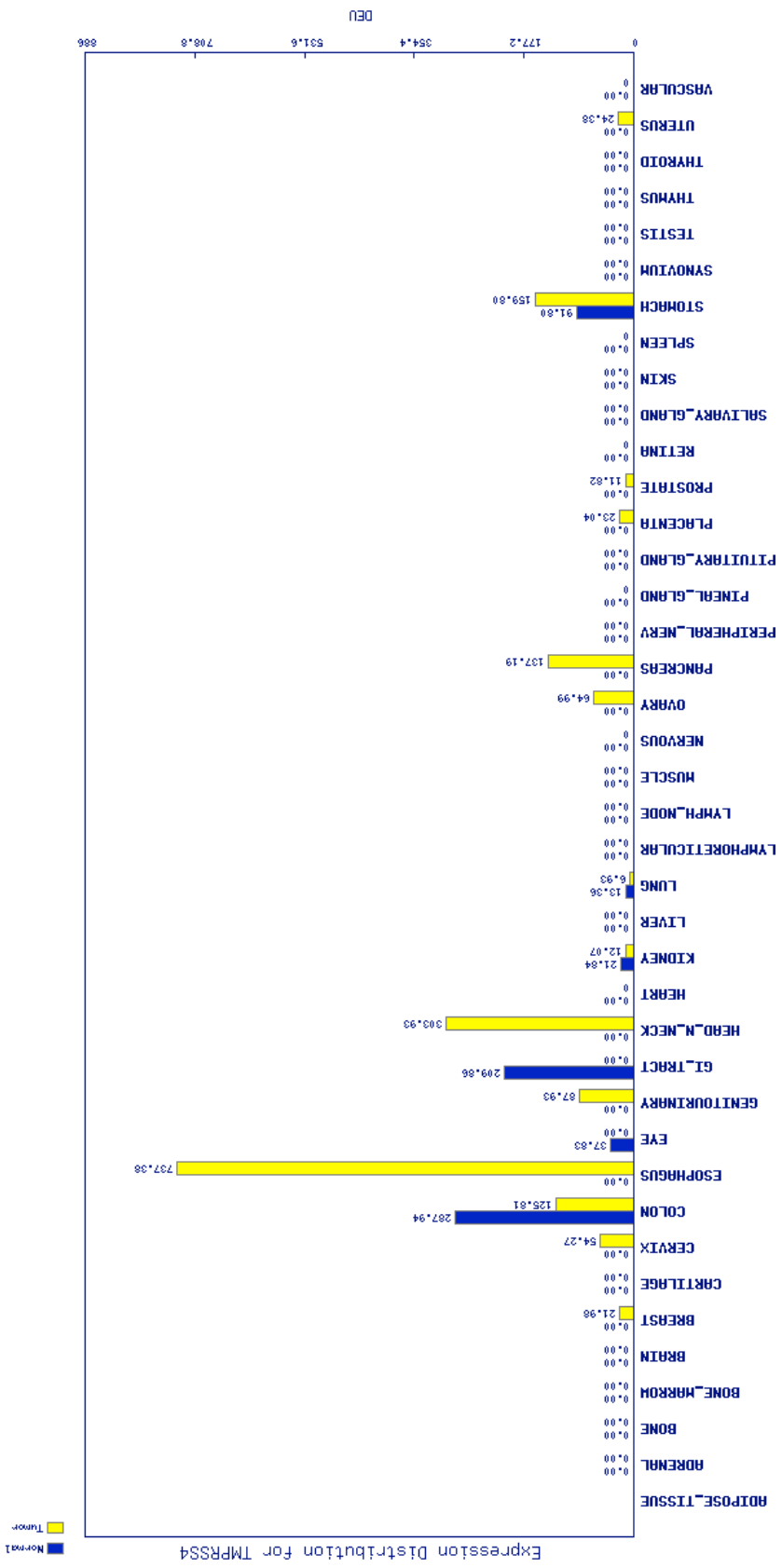

A B

Appendix Figure 12: TMPRSS4 expression profile

A. Expression profile available *via* Expression Atlas database that shows the results of three different expression experiments. Greater colour intensity means higher expression. **B.** Expression profile available *via* GeneHub-GEPIS database.

A.2 Chapter 4 R codes

A.2.1 Cross-reactivity map R code

```
#Load R packages
library(RColorBrewer)
library(gplots)

#Load cross-reactivity file (cross.csv)
refsera <-read.csv("cross.csv", sep=",")

#Transform the file in matrix
row.names (refsera) <-refsera$X
refsera<-refsera[,2:21]
refsera_matrix <-data.matrix(refsera)

#Create the personalized colour palette
my_palette <-colorRampPalette (c("white", "green4")) (n=17)

#Generate the map using heatmap.2 function and
#the personalized colour palette
refsera_heatmap <- heatmap.2 (refsera_matrix, Rowv=NULL,
     Colv=FALSE, dendrogram="none", col = my_palette, key=T,
     keysize=1, symkey=FALSE,density.info=c("none"), scale="none",
     margins=c(1,1), trace=c("none"),
     colsep=c(0,1,2,3,4,5,6,7,8,9,10,11,12,13,14,15,16,17,18,19,20
     ), rowsep=c(0,1,2,3,4,5,6,7,8,9,10,11,12,13,14,15),
     sepcolor="snow4", sepwidth=c(0.01,0.01), lmat=rbind( c(0, 4),
     c(0,1), c(2,3) ), lhei=c(1.5, 5, 0.5), lwid=c(0.1, 4))
```

A.2.2 Percentage identity map R code

```
#Load R packages
library(RColorBrewer)
library(gplots)

#Load csv the percentage identity file (ident.csv)
refsera_id <-read.csv("ident.csv", sep=",")

#Transform the file in matrix
row.names (refsera_id) <-refsera_id$X
refsera_id<-refsera_id[,2:21]
refsera_id_matrix <-data.matrix(refsera)

#Create the personalized colour palette
my_palette <-colorRampPalette (c("white", "green4")) (n=17)

#Generate the map using heatmap function and
#the personalized colour palette
#showing the percentage identity values
refsera_id_heatmap <- heatmap.2 (refsera_id_matrix, Rowv=NULL,
     Colv=FALSE, dendrogram="none", col = my_palette, key=T,
     keysize=1, symkey=FALSE,density.info=c("none"), scale="none",
     margins=c(1,1), trace=c("none"),
     colsep=c(0,1,2,3,4,5,6,7,8,9,10,11,12,13,14,15,16,17,18,19,20
     ), rowsep=c(0,1,2,3,4,5,6,7,8,9,10,11,12,13,14,15),
     sepcolor="snow4", sepwidth=c(0.01,0.01), lmat=rbind( c(0, 4),
     c(0,1), c(2,3) ), lhei=c(1.5, 5, 0.5), lwid=c(0.1, 4),
     cellnote=as.matrix(refsera_id),notecol="black")
```

A.3 Additional Figures and Tables for Chapter 5

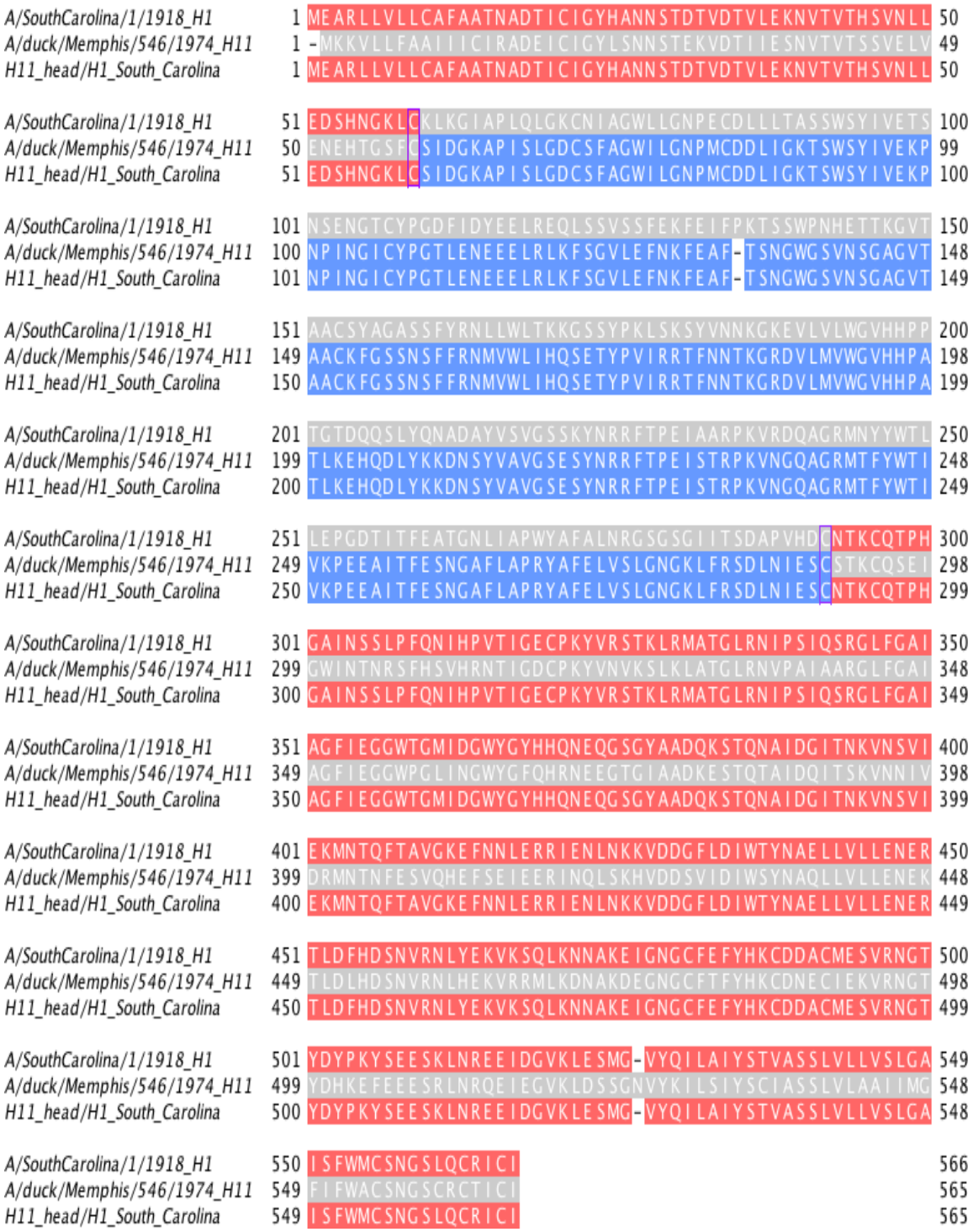

Appendix Figure 13: Alignment of A/South Carolina/1/1918 H1, A/duck/Memphis/546/1974 H1, and of the combined chimeric HA
The alignment shows the H1 stalk region in red and the H11 head region in blue.

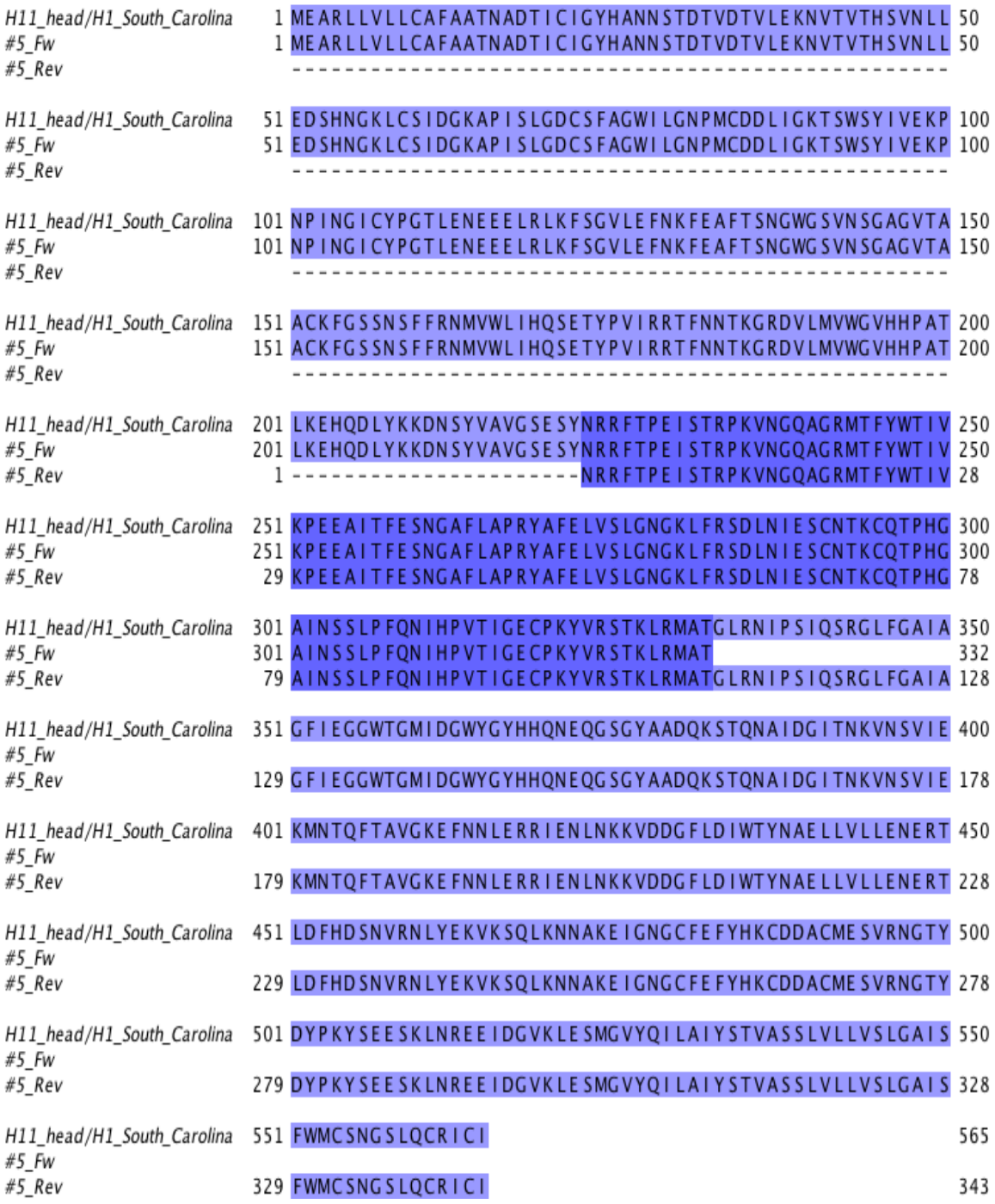

Appendix Figure 14: Alignment of the cloned chimeric HA Fw and Rev amino acid sequences with the assembled chimeric HA amino acid sequence

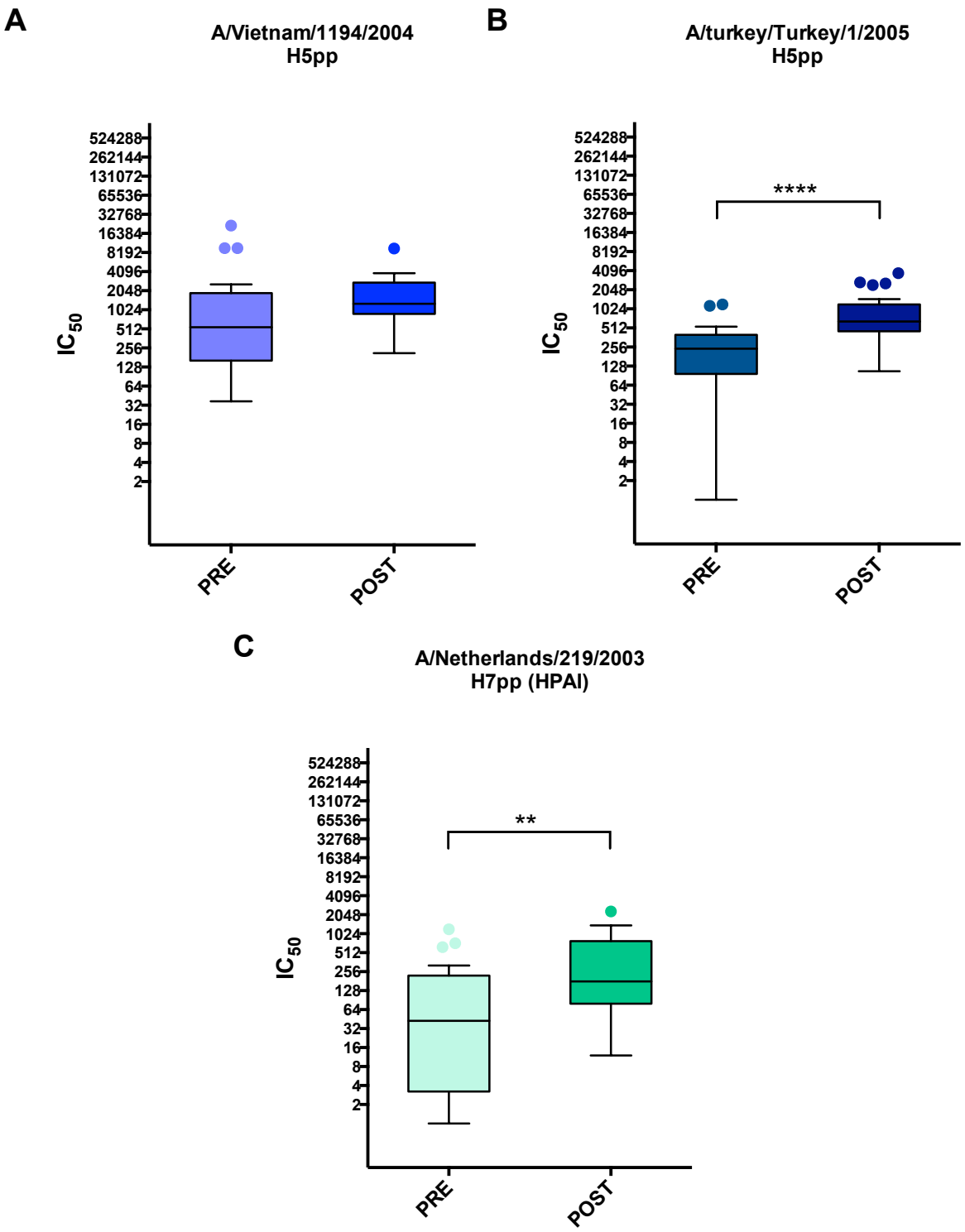

Appendix Figure 15: IC_{50} of sera tested with H5 and H7 pp-NT assay
Comparison between IC_{50} measured pre- and post-vaccination with A/Wisconsin/67/2005 (H3N2), A/Solomon Island/3/2006 (H1N1) and B/Malaysia/2506/2004. Data were generated by Dr. Eleonora Molesti (Universities of Greenwich and Kent, Medway, UK) and then re-analysed. **A.** Results against A/Vietnam/1194/2005 H5pp; **B.** Results against A/turkey/Turkey/1/2005 H5pp; **C.** Results against A/Netherlands/219/2003 H7pp.

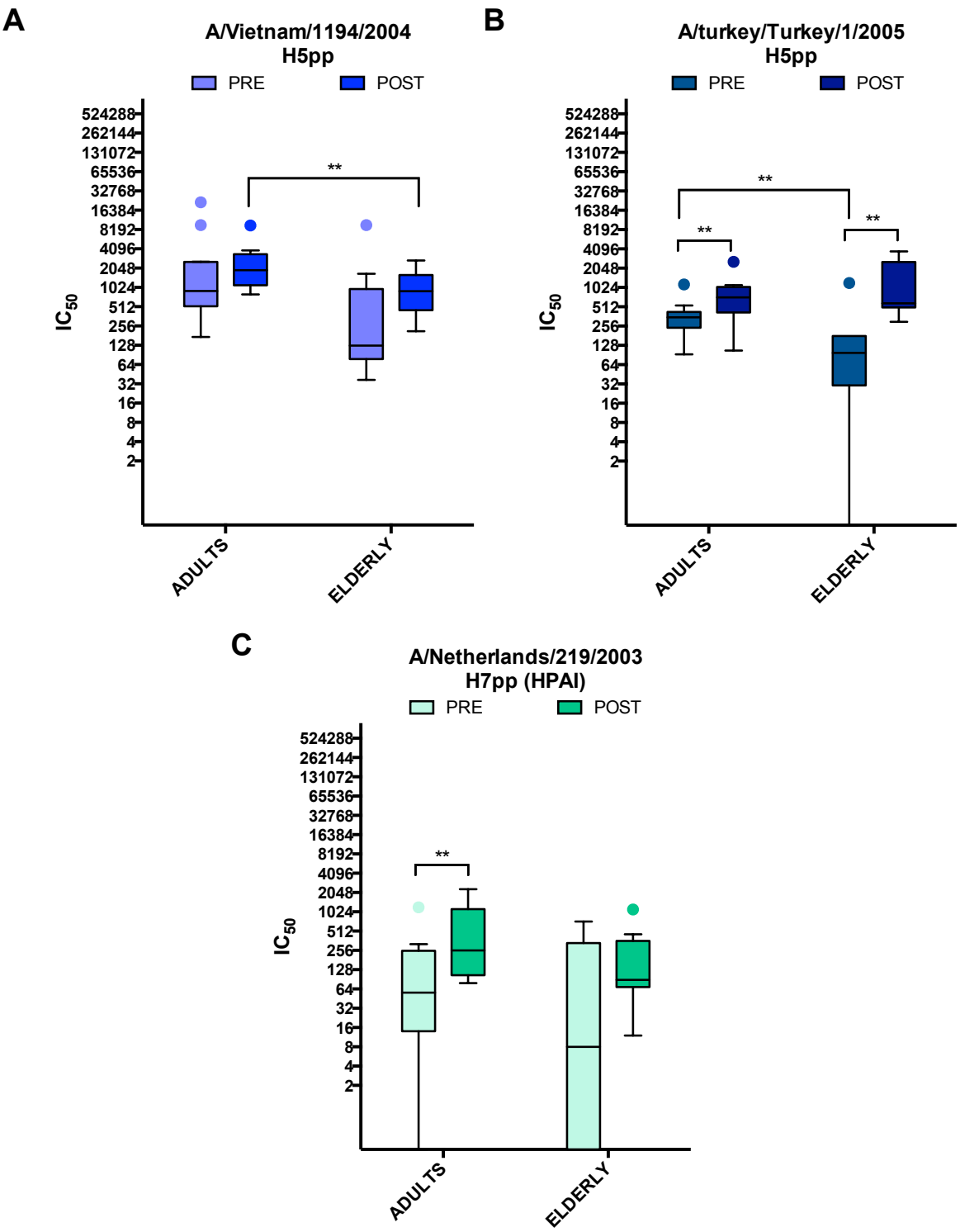

Appendix Figure 16: Age-stratified IC_{50} of sera tested with H5 and H7 pp-NT assay
Comparison between IC_{50} measured pre- and post-vaccination with A/Wisconsin/67/2005 (H3N2), A/Solomon Island/3/2006 (H1N1) and B/Malaysia/2506/2004. Data were generated by Dr. Eleonora Molesti Universities of Greenwich and Kent, Medway, UK) and then re-analysed. **A.** Results against A/Vietnam/1194/2005 H5pp; **B.** Results against A/turkey/Turkey/1/2005 H5pp; **C.** Results against A/Netherlands/219/2003 H7pp.

Appendix Table 2: Quartiles and medians of the IC_{50} distributions of the 2007-2008 study

		PRE	POST
A/Solomon Islands/3/2006 H1pp	1st Quartile	2129	41654
	Median	4811	65710
	3rd Quartile	15358	118267
A/Wisconsin/67/2005 H3 (A/Udorn/307/1972 N2) pp	1st Quartile	1311	3892
	Median	2465	5957
	3rd Quartile	11670	9257
A/New Caledonia/20/1999 H1pp	1st Quartile	6001	10981
	Median	8668	25822
	3rd Quartile	13432	87436
A/Korea/426/1968 H2pp	1st Quartile	2814	11142
	Median	4584	15683
	3rd Quartile	6529	25909
A/Udorn/307/1972 H3pp	1st Quartile	2549	5639
	Median	4925	6572
	3rd Quartile	7820	12063
A/duck/Czechoslovakia/1956 H4pp	1st Quartile	410	1170
	Median	746	1739
	3rd Quartile	1703	4541
A/Vietnam/1194/2005 H5pp	1st Quartile	161	884
	Median	544	1276
	3rd Quartile	1882	2747
A/turkey/Turkey/1/2005 H5pp	1st Quartile	96	455
	Median	242	649
	3rd Quartile	398	1201
A/Netherlands/219/2003 H7pp	1st Quartile	3	80
	Median	43	179
	3rd Quartile	222	781
A/Shanghai/2/2013 H7pp	1st Quartile	2692	3168
	Median	3575	4816
	3rd Quartile	4652	8275
A/chicken/Italy/1082/1999 H7pp	1st Quartile	139	180
	Median	619	343
	3rd Quartile	1235	651
A/Hong Kong/1073/1999 H9pp	1st Quartile	277	452
	Median	392	1131
	3rd Quartile	621	1669
A/chicken/Germany/N49 H10 pp	1st Quartile	941	2956
	Median	2975	6070
	3rd Quartile	4655	7533

A/duck/Alberta/60/1976 H12pp	**1st Quartile**	1	41
	Median	41	149
	3rd Quartile	87	255
A/mallard/Astrakhan/263/1982 H14pp	**1st Quartile**	238	0
	Median	352	84
	3rd Quartile	1400	1362
A/shearwater/West Australia/2576/1979 H15pp	**1st Quartile**	18	100
	Median	78	225
	3rd Quartile	193	892
A/South Carolina/1/1918 H1pp	**1st Quartile**	927	2584
	Median	1588	3558
	3rd Quartile	1997	5791
A/duck/Memphis/546/1974 H11pp	**1st Quartile**	0	0
	Median	1	21
	3rd Quartile	24	537
Chimeric H11 head/H1 stalk pp	**1st Quartile**	324	944
	Median	547	1609
	3rd Quartile	929	2782

Appendix Table 3: Quartiles and medians of the IC_{50} distributions of the 2007-2008 study after age- stratification

		ADULTS		ELDERLY	
		PRE	POST	PRE	POST
A/Solomon Islands/3/2006 H1pp	1st Quartile	1117	25414	3749	57939
	Median	2280	62831	14927	67767
	3rd Quartile	9441	123354	27536	123684
A/Wisconsin/67/2005 H3 (A/Udorn/307/1972 N2) pp	1st Quartile	1412	6150	645	13305
	Median	7775	19447	2207	82321
	3rd Quartile	17759	34291	6933	127519
A/New Caledonia/20/1999 H1pp	1st Quartile	4515	8638	2249	11508
	Median	5958	15146	3727	17605
	3rd Quartile	9458	24820	4276	29248
A/Korea/426/1968 H2pp	1st Quartile	5867	7399	2608	3678
	Median	6561	10527	3920	6691
	3rd Quartile	9724	29110	5331	9765
A/Udorn/307/1972 H3pp	1st Quartile	3129	5386	2197	5517
	Median	4891	6392	5230	6633
	3rd Quartile	5994	14075	8185	9966
A/duck/Czechoslovakia/1956 H4pp	1st Quartile	636	1316	313	1031
	Median	807	2352	417	1679
	3rd Quartile	2682	5406	1311	2870
A/Vietnam/1194/2004 H5pp	1st Quartile	520	1107	78	452
	Median	900	1907	127	892
	3rd Quartile	2552	3377	965	1602
A/turkey/Turkey/1/2005 H5pp	1st Quartile	242	418	30	501
	Median	350	716	97	581
	3rd Quartile	425	1040	179	2559
A/Netherlands/219/2003 H7pp	1st Quartile	14	105	0	69
	Median	56	256	8	89
	3rd Quartile	252	1128	332	360
A/Shanghai/2/2013 H7pp	1st Quartile	2888	4238	1753	2420
	Median	3505	6693	3718	3196
	3rd Quartile	4257	8502	4763	4730
A/chicken/Italy/1082/1999 H7pp	1st Quartile	114	447	199	533
	Median	770	1185	601	814
	3rd Quartile	1472	1632	855	1986
A/Hong Kong/1073/1999 H9pp	1st Quartile	2793	4463	581	1640
	Median	4546	6932	966	3604
	3rd Quartile	5145	7568	2297	8364
A/chicken/Germany/N49 H10 pp	1st Quartile	173	290	187	252
	Median	386	356	222	602
	3rd Quartile	779	519	358	759

A/duck/Alberta/60/1976 H12pp	**1st Quartile**	11	13	0	0
	Median	43	93	1	2
	3rd Quartile	107	1033	47	2572
A/mallard/Astrakhan/263/1982 H14pp	**1st Quartile**	29	120	15	94
	Median	89	539	40	155
	3rd Quartile	418	1075	119	777
A/shearwater/West Australia/2576/1979 H15pp	**1st Quartile**	84	252	20	197
	Median	160	449	134	307
	3rd Quartile	379	1676	214	995
A/South Carolina/1/1918 H1pp	**1st Quartile**	1006	2630	658	2409
	Median	1644	3472	1152	4350
	3rd Quartile	1913	5671	2357	6174
A/duck/Memphis/546/1974 H11pp	**1st Quartile**	0	5	0	0
	Median	1	19	0	22
	3rd Quartile	39	626	11	2508
Chimeric H11 head/H1 stalk pp	**1st Quartile**	471	1119	65	768
	Median	556	1848	319	1360
	3rd Quartile	1022	2537	771	4174

Appendix Table 4: Quartiles and medians of the IC_{50} distributions of the NCT00942071 clinical trial study

		day 0	day 21
A/New Caledonia/20/1999 H1pp	1st Quartile	3676	3135
	Median	4788	4736
	3rd Quartile	6236	6220
A/Korea/426/1968 H2pp	1st Quartile	7419	7704
	Median	9215	10871
	3rd Quartile	13430	14697
A/Udorn/307/1972 H3pp	1st Quartile	3473	7180
	Median	4938	9586
	3rd Quartile	9292	11544
A/Wisconsin/67/2005 H3 (A/Udorn/307/1972 N2) pp	1st Quartile	495	3345
	Median	998	5827
	3rd Quartile	1962	15729
A/duck/Czechoslovakia/1956 H4pp	1st Quartile	2121	1642
	Median	3023	2893
	3rd Quartile	3550	4184
A/Vietnam/1194/2004 H5pp	1st Quartile	279	694
	Median	618	1764
	3rd Quartile	1303	2392
A/turkey/Turkey/1/2005 H5pp	1st Quartile	364	797
	Median	901	1318
	3rd Quartile	1564	2327
A/Shanghai/2/2013 H7pp	1st Quartile	2338	3287
	Median	2964	4261
	3rd Quartile	4425	6285
A/Hong Kong/1073/1999 H9pp	1st Quartile	1422	6723
	Median	3023	8614
	3rd Quartile	6108	13346
A/chicken/Germany/N49 H10 pp	1st Quartile	122	190
	Median	294	315
	3rd Quartile	397	386
A/mallard/Astrakhan/263/1982 H14pp	1st Quartile	581	543
	Median	853	702
	3rd Quartile	1245	1476
A/shearwater/West Australia/2576/1979 H15pp	1st Quartile	312	341
	Median	497	759
	3rd Quartile	838	1220
A/South Carolina/1/1918 H1pp	1st Quartile	1045	1669
	Median	2736	3397
	3rd Quartile	4043	8896

A/duck/Memphis/546/1974 H11pp	**1st Quartile**	1	18
	Median	48	229
	3rd Quartile	364	1065
Chimeric H11 head/H1 stalk pp	**1st Quartile**	176	330
	Median	339	866
	3rd Quartile	647	2195

Appendix Table 5: Quartiles and medians of the IC_{50} distributions of the NCT00942071 clinical trial study after vaccine-regimen stratification

		TIV + placebo		TIV + MVA-NP+M1	
		day 0	day 21	day 0	day 21
A/New Caledonia/20/1999 H1pp	1st Quartile	4468	3375	3364	3135
	Median	5624	5871	3854	3750
	3rd Quartile	6763	7051	5404	5103
A/Korea/426/1968 H2pp	1st Quartile	7834	7842	6928	7388
	Median	11273	10620	8687	12659
	3rd Quartile	18309	14568	9529	14709
A/Udorn/307/1972 H3pp	1st Quartile	3923	7460	3258	6588
	Median	7239	11000	4575	9012
	3rd Quartile	10344	14284	6859	10981
A/Wisconsin/67/2005 H3 (A/Udorn/307/1972 N2) pp	1st Quartile	685	2563	323	3554
	Median	1186	4801	909	6442
	3rd Quartile	7220	12515	1616	18170
A/duck/Czechoslovakia/1956 H4pp	1st Quartile	1495	1282	2164	2025
	Median	2873	2029	3235	3362
	3rd Quartile	3545	3585	4149	5544
A/Vietnam/1194/2004 H5pp	1st Quartile	391	1063	151	600
	Median	677	1669	618	2074
	3rd Quartile	1552	4014	1303	2392
A/turkey/Turkey/1/2005 H5pp	1st Quartile	477	1053	304	616
	Median	849	1444	935	1318
	3rd Quartile	1983	2255	1564	2494
A/Shanghai/2/2013 H7pp	1st Quartile	2428	3599	2269	2703
	Median	3168	4307	2604	4261
	3rd Quartile	4720	6436	4467	6285
A/Hong Kong/1073/1999 H9pp	1st Quartile	1714	7461	1160	4819
	Median	4009	10901	2614	7989
	3rd Quartile	8119	17865	4917	11084
A/chicken/Germany/N49 H10 pp	1st Quartile	146	200	76	153
	Median	388	338	264	233
	3rd Quartile	421	384	384	396
A/mallard/Astrakhan/263/1982 H14pp	1st Quartile	548	534	697	531
	Median	733	693	945	1214
	3rd Quartile	1036	1013	1744	2224
A/shearwater/West Australia/2576/1979 H15pp	1st Quartile	227	105	312	580
	Median	447	394	586	856
	3rd Quartile	913	1092	732	2182
A/South Carolina/1/1918 H1pp	1st Quartile	991	1627	1665	1745
	Median	1981	3077	3170	3397
	3rd Quartile	4341	7282	3658	14916

A/duck/Memphis/546/1974 H11pp	**1st Quartile**	2	14	0	35
	Median	29	345	97	83
	3rd Quartile	784	4493	211	924
Chimeric H11 head/H1 stalk pp	**1st Quartile**	231	823	79	128
	Median	538	1744	256	486
	3rd Quartile	701	2249	383	2089

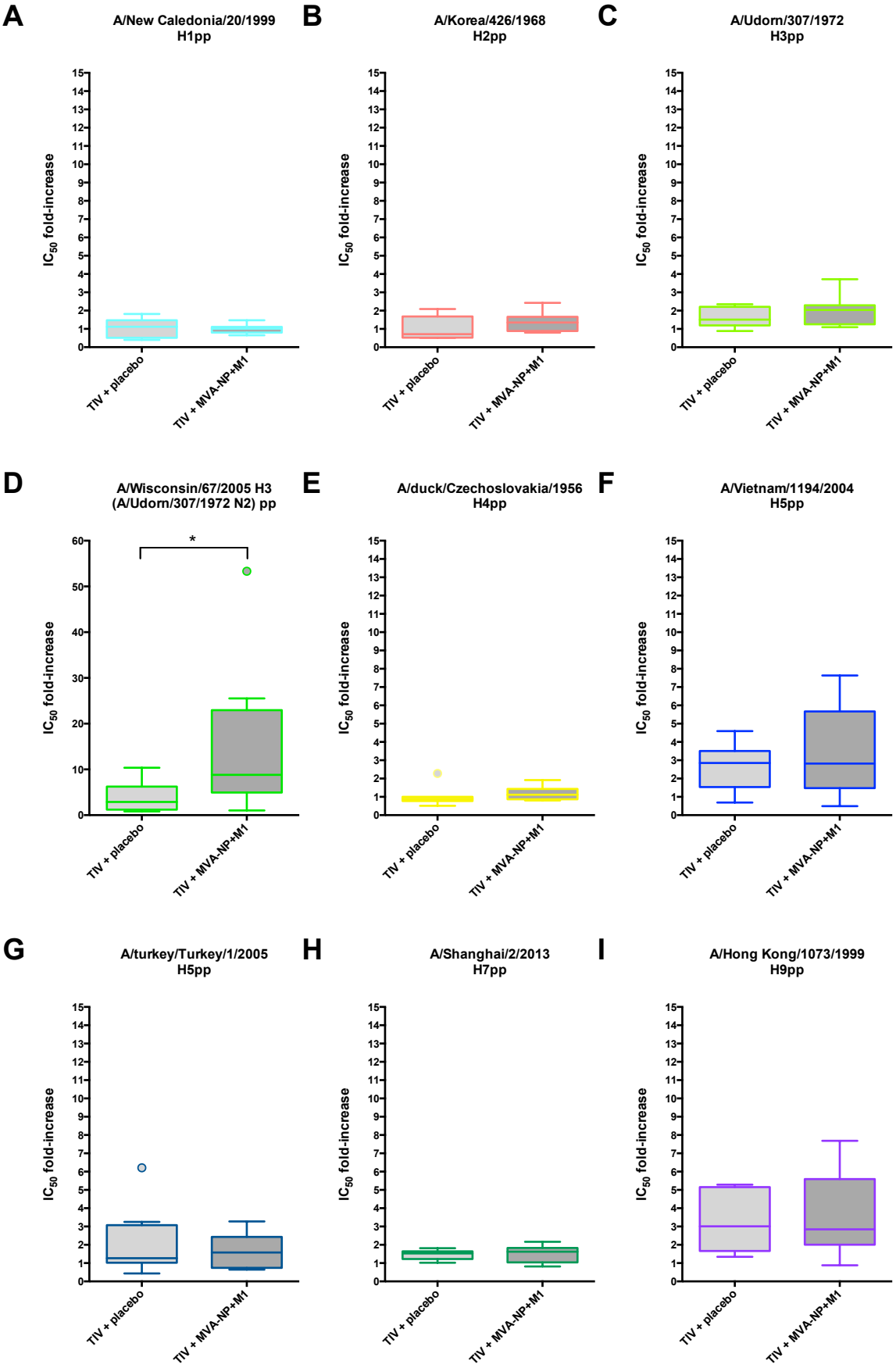
A
A/New Caledonia/20/1999
H1pp
B
A/Korea/426/1968
H2pp
C
A/Udorn/307/1972
H3pp
D
A/Wisconsin/67/2005 H3
(A/Udorn/307/1972 N2) pp
E
A/duck/Czechoslovakia/1956
H4pp
F
A/Vietnam/1194/2004
H5pp
G
A/turkey/Turkey/1/2005
H5pp
H
A/Shanghai/2/2013
H7pp
I
A/Hong Kong/1073/1999
H9pp
IC50 fold-increase
TIV + placebo
TIV + MVA-NP+M1
*

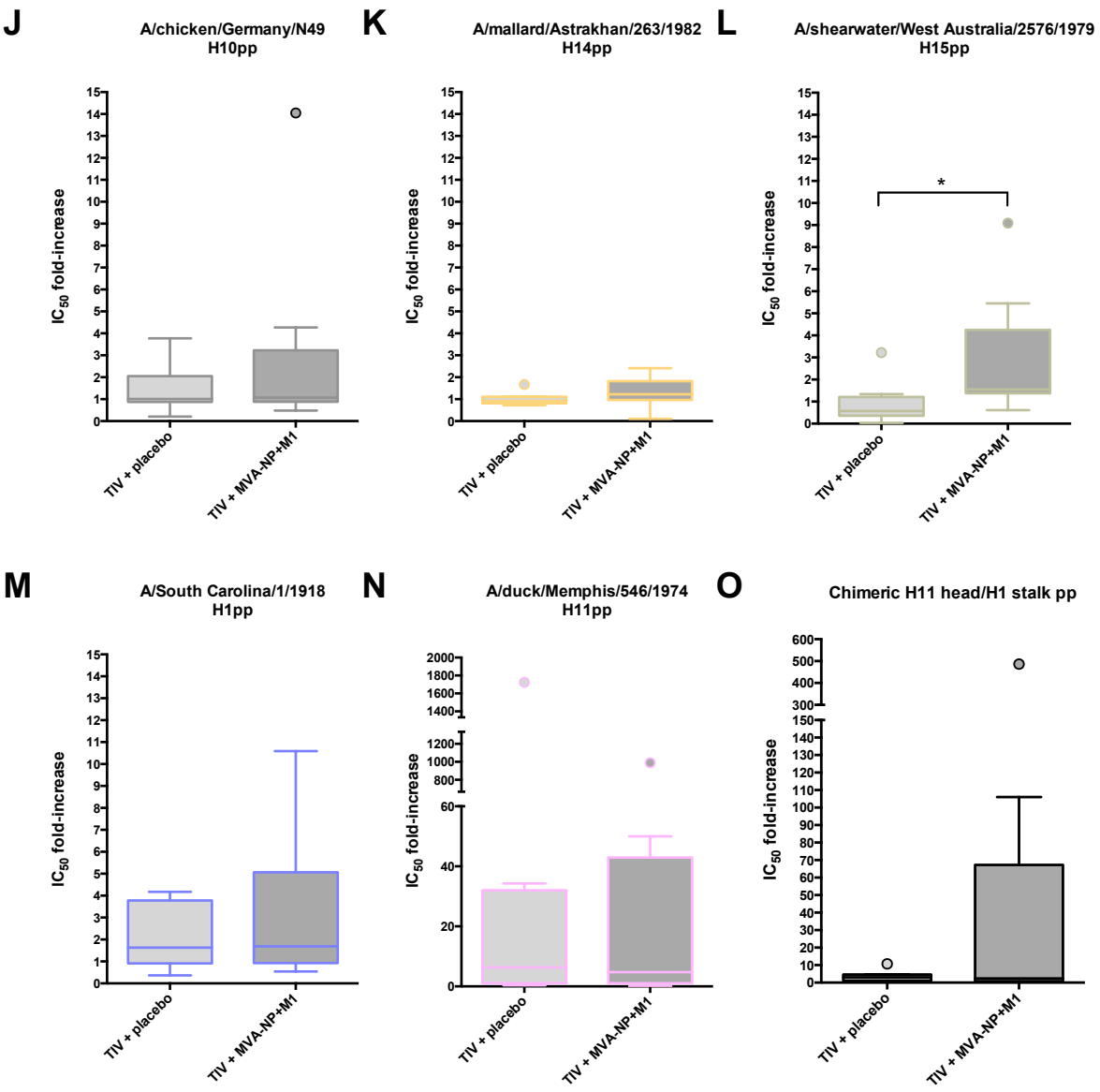

Appendix Figure 17: Fold-increase in the IC_{50} titres of the TIV + placebo and the TIV + MVA-NP+M1 groups

A. IC_{50} fold-increase against A/New Caledonia/20/1999 H1pp;
B. IC_{50} fold-increase against A/Korea/426/1968 H2pp;
C. IC_{50} fold-increase against A/Udorn/307/1972 H3pp;
D. IC_{50} fold-increase against A/Wisconsin/67/2005 (A/Udorn/307/1972 N2) H3pp;
E. IC_{50} fold-increase against A/duck/Czechoslovakia/1956 H4pp;
F. IC_{50} fold-increase against A/Vietnam/1194/2004 H5pp;
G. IC_{50} fold-increase against A/turkey/Turkey/1/2005 H5pp;
H. IC_{50} fold-increase against A/Shanghai/2/2013 H7pp;
I. IC_{50} fold-increase against A/Hong Kong/1073/1999 H9pp;
J. IC_{50} fold-increase against A/chicken/Germany/N49 H10pp;
K. IC_{50} fold-increase against A/mallard/Astrakhan/263/1982 H14pp;
L. IC_{50} fold-increase against A/shearwater/West Australia/2576/1979 H15pp;
M. IC_{50} fold-increase against A/South Carolina/1/1918 H1pp;
N. IC_{50} fold-increase against A/duck/Memphis/546/1974 H11pp;
O. IC_{50} fold-increase against chimeric HA pp.

A.4 Additional Figures and Tables for Chapter 6

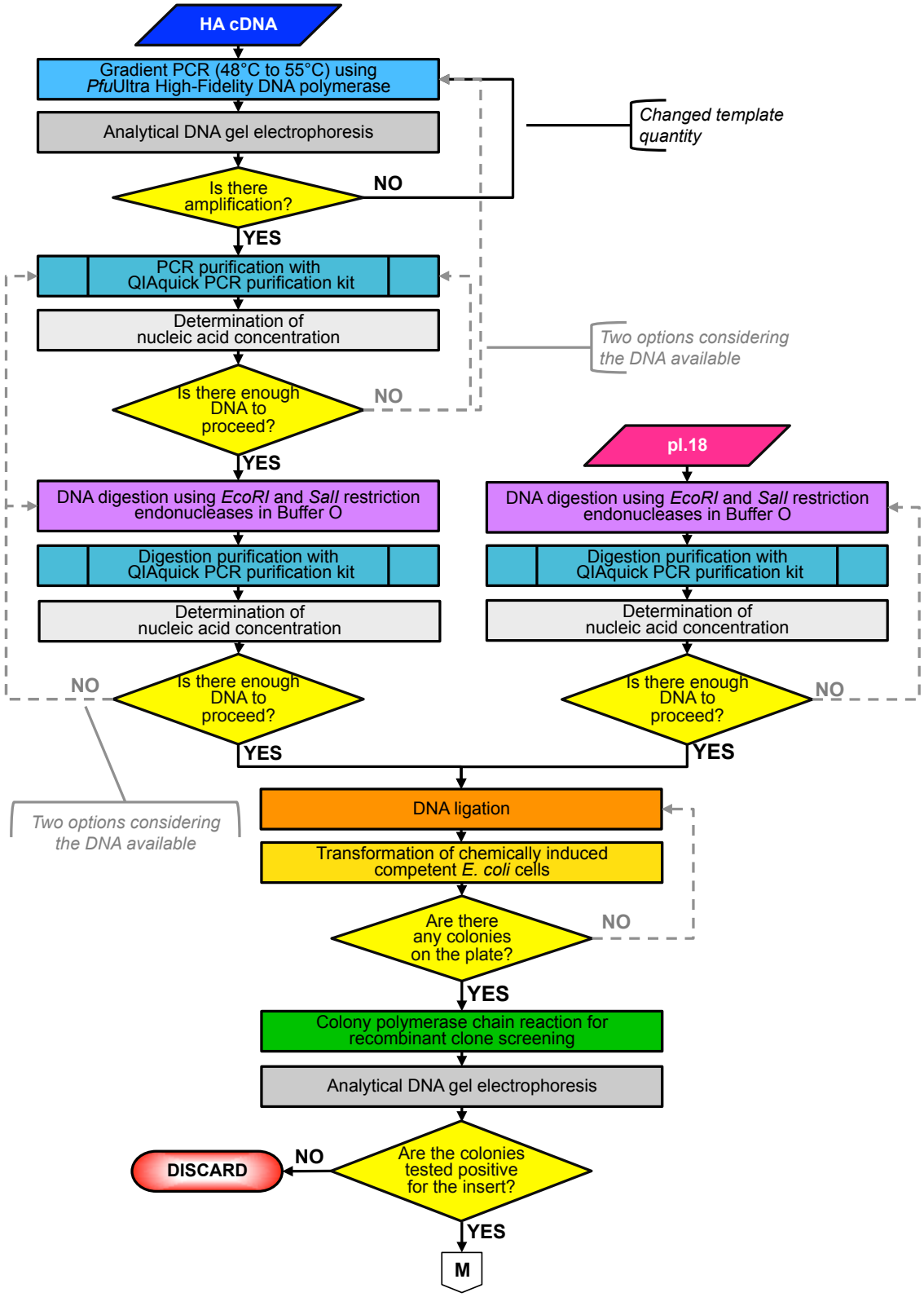

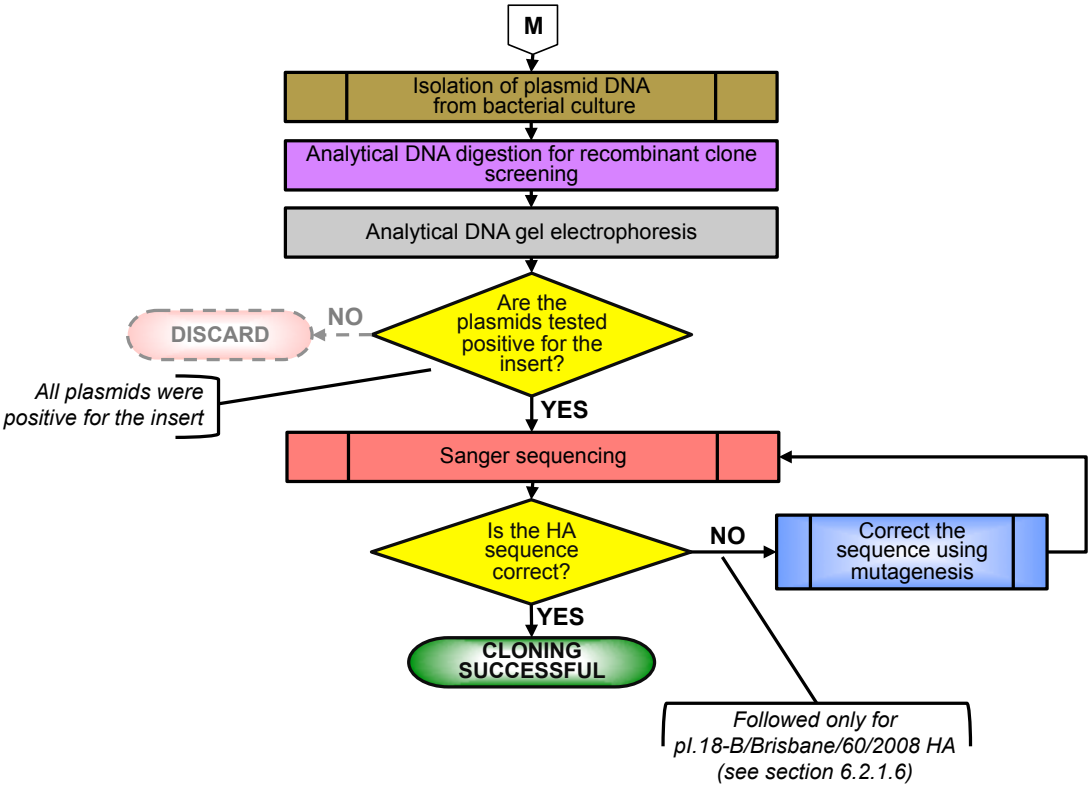

Appendix Figure 18: Flow chart outlining the cloning of B/Brisbane/60/2008 and B/Bangladesh/3333/2007 HAs into pI.18 expression vector

All details are reported in Chapter 6. Cloning procedure was similar to the one reported in Figure 23, without requirement of DNA ligation repeat. However mutagenesis was required to correct the B/Brisbane/60/2008 HA sequence.

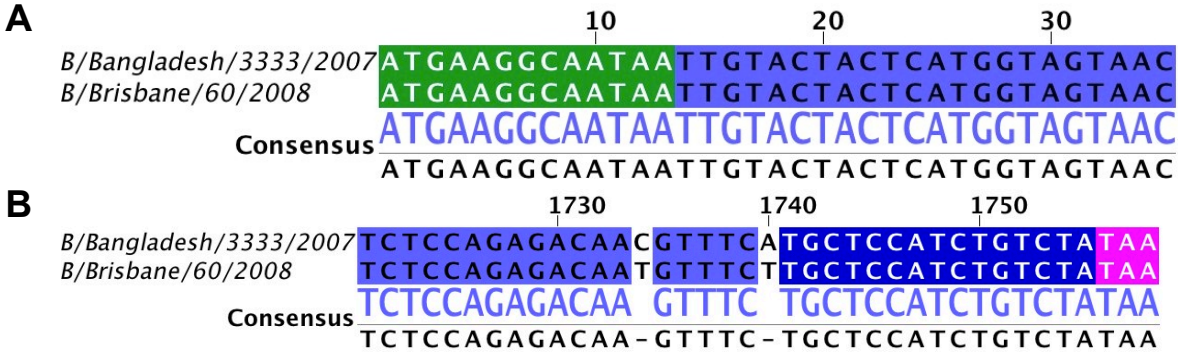

Appendix Figure 19: Alignment of the B/Bangladesh/3333/2007 and B/Brisbane/60/200 HA sequences

The regions of the 5' and 3' end encoding sequences used to design the primer have 100% nucleotide identity. **A.** 5' end encoding region in which the sequence used to design the primer is highlighted in green; **B.** 3' end encoding region in which the sequence used to design the primer is highlighted in blue and the stop codon in pink.

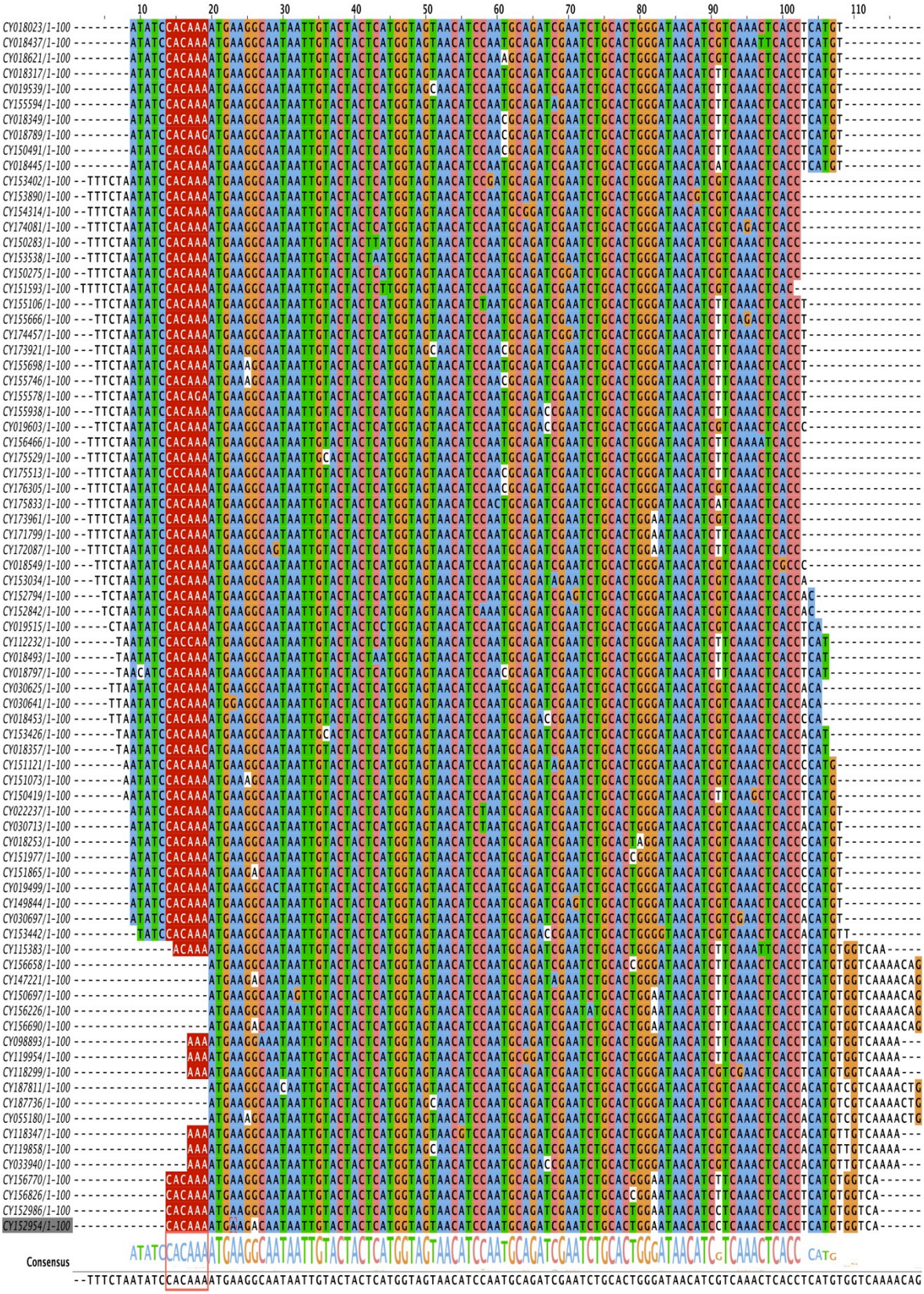

Appendix Figure 20: Alignment of the first 100 nucleotides of the circulating influenza B segment 4 (HA)

In the figure only the non-redundant sequences are shown. Consensus sequence is also reported. The putative Influenza B Kozak sequence CACAAA is highlighted in red.

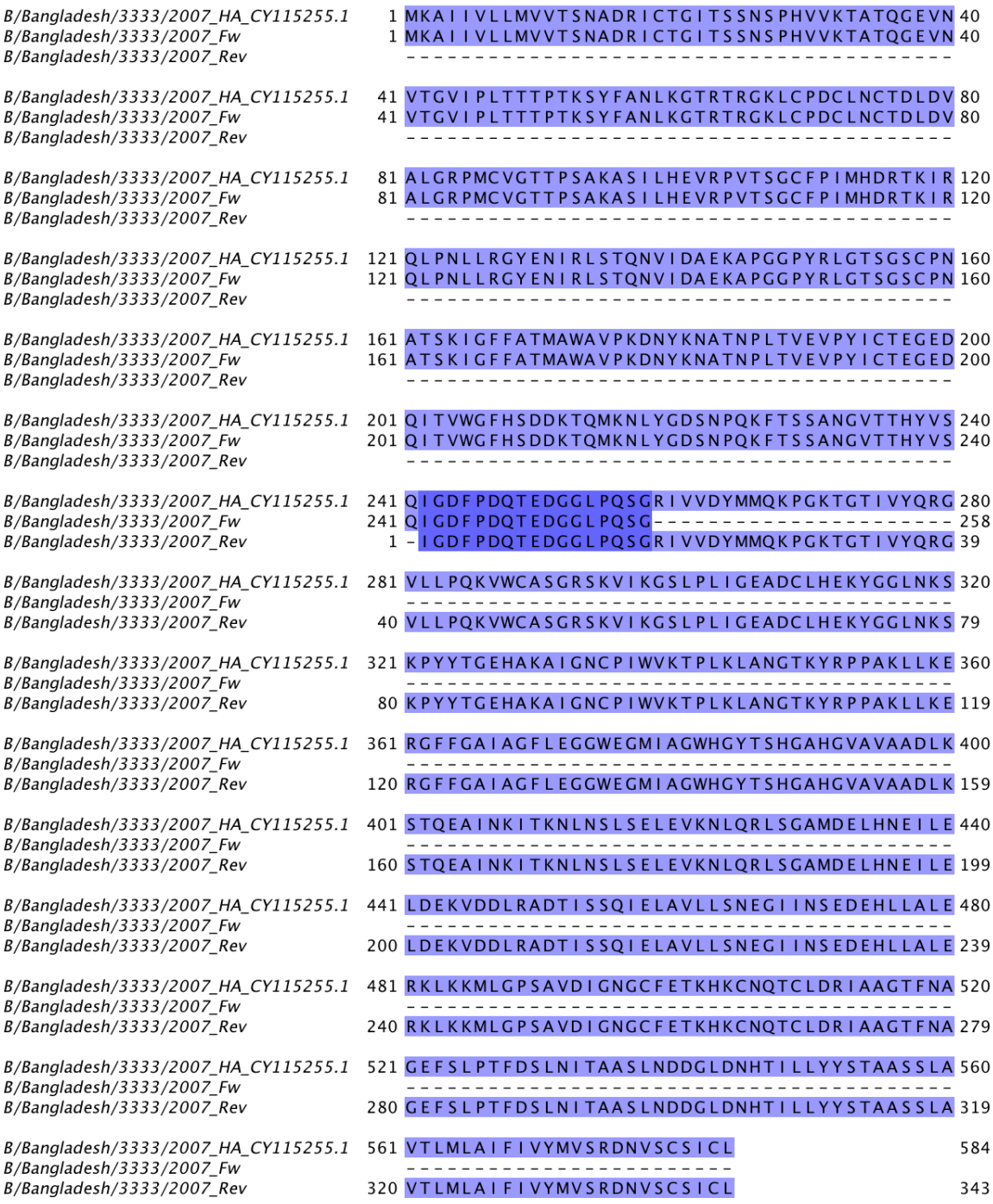

Appendix Figure 21: Alignment of the cloned B/Bangladesh/3333/2007 HA Fw and Rev sequences with the database amino acid sequence

Appendix Table 6: Decision table for the production of influenza B pp

The protease-expressing plasmid quantities are for a 6-well transection. To perform the transfection in a 10 cm plate as described in section 2.3.2, it is necessary to double the quantities. The optimal quantity is highlighted in green. Titres of pp from optimization experiments are reported using the following code:

- indicates pp titres $<1\times10^6$ RLU/ml
+ indicates pp titres between 1×10^6-1×10^7 RLU/ml;
++ indicates pp titres between 1×10^7-1×10^8 RLU/ml;
+++ indicates pp titres between 1×10^8-1×10^9 RLU/ml;
++++ indicates pp titres between 1×10^9 and 1×10^{10} RLU/ml.
Conditions that were not tested are reported with a slash.

	HAT			TMPRSS2			TMPRSS4		
	500 ng	250 ng	125 ng	500 ng	250 ng	125 ng	500 ng	250 ng	125 ng
B/Bangladesh/3333/2007	++++	++++	++++	++	+++	+++	++++	++++	++++
B/Hong Kong/8/1973	/	++++	++++	/	++	+++	/	+++	+++
B/Victoria/2/1987	/	+++	++++	/	+	+++	/	+++	++++
B/Yamagata/16/1988	/	+++	++++	/	+	+++	/	++++	++++
B/Florida/4/2006	/	++++	++++	/	++	+++	/	+++	++++
B/Brisbane/60/2008	/	++	++	/	-	-	/	++	+++

Appendix Table 7: Quartiles and medians of the IC_{50} distributions reported in Figure 85

	B/Brisbane/60/2008 pp		B/Hong Kong/8/1973 pp		B/Florida/4/2006 pp	
	day 0	day 21	day 0	day 21	day 0	day 21
1st Quartile	5179	9487	1721	4614	413.6	1782
Median	11103	12886	2722	7448	1250	3308
3rd Quartile	31627	26065	4508	9815	2212	4557

Appendix Table 8: Quartiles and medians of the IC_{50} distributions reported in Figure 86

		TIV + placebo		TIV + MVA-NP+M1	
		day 0	day 21	day 0	day 21
B/Brisbane/60/2008 pp	1st Quartile	9503	9996	3122	9421
	Median	21198	14226	5228	12886
	3rd Quartile	27902	42864	35366	26054
B/Hong Kong/8/1973 pp	1st Quartile	2979	6795	1399	4326
	Median	4236	8657	2024	5083
	3rd Quartile	8053	10837	2676	8973
B/Florida/4/2006 pp	1st Quartile	1425	2683	391	1011
	Median	2047	3904	606	2638
	3rd Quartile	4253	5200	1278	3743

A.5 Preliminary Experiments

Appendix Table 9: Evaluation of pseudotype particles using Nanosight LM10

	A/Udorn/307/1972 H3pp	Δ envelope pp
Mode (nm)	130	126
Mean (nm)	162.46	150.94
Standard Deviation(nm)	61.23	50.33
Equivalent particle concentration (particles/ml)	7.16×10^{8}	3.52×10^{8}

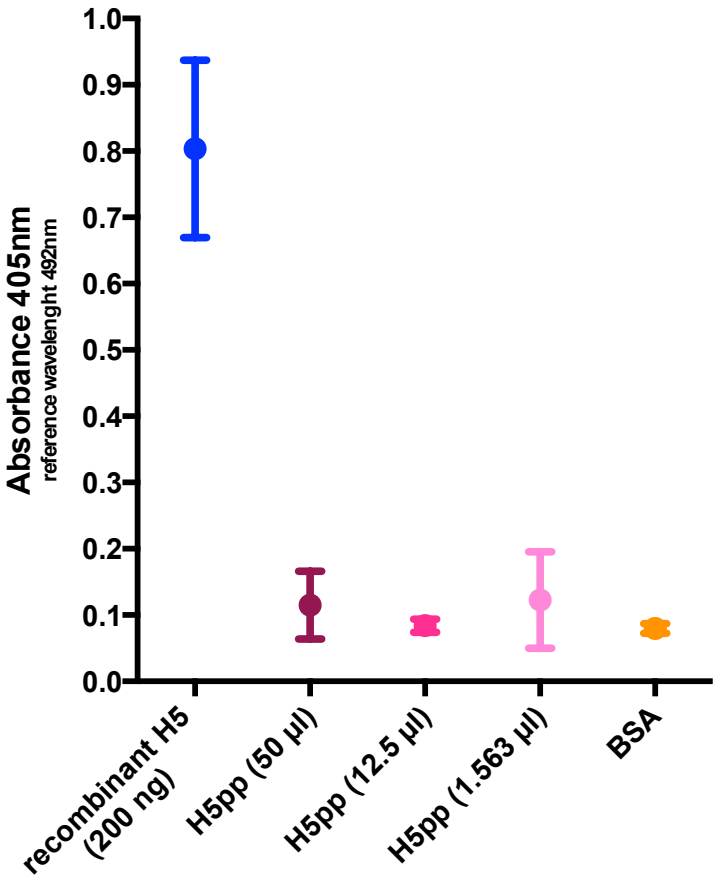

Appendix Figure 22: HApp do not coat ELISA plates
Different amount of A/Vietnam/1203/2004 H5pp, 200 ng of recombinant A/Vietnam/1203/2004 H5 (recombinant H5), and 500 ng of BSA (Sigma-Aldrich, cat.no.) were coated on an ELISA plate, and subsequently detected using anti-A/turkey/Turkey/1/2005 H5N1 (APHA) diluted at 1:500 in PBS (Sigma-Aldrich, cat.no. D8537) and rabbit anti-chicken IgY (whole molecule)−Peroxidase antibody (Sigma-Aldrich, cat.no. A9046) diluted at 1:4000 in PBS.

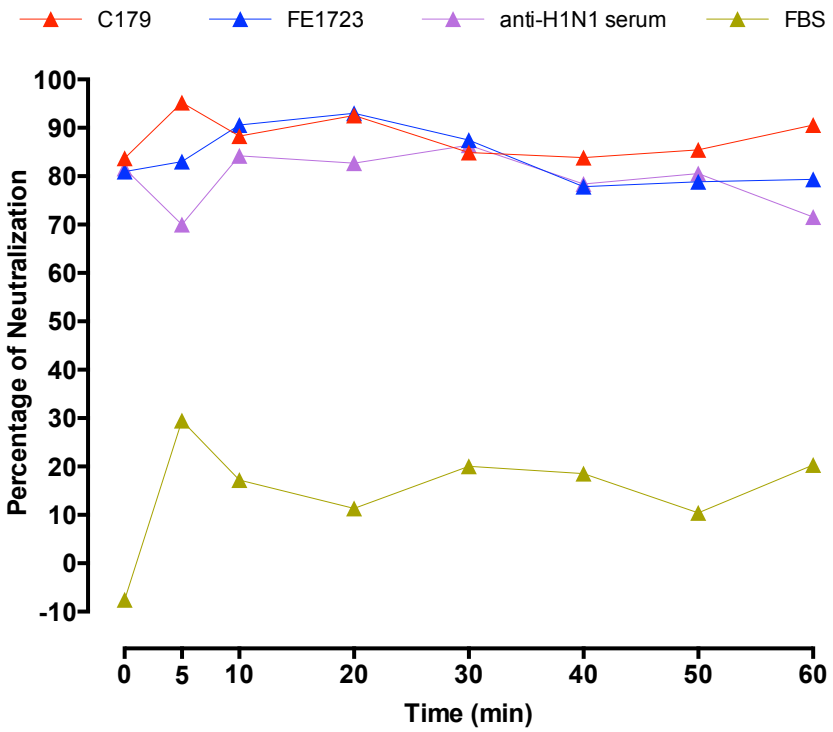

Appendix Figure 23: Pp post-attachment neutralization assay performed at RT
HEK293T/17 cells and A/South Carolina/1/1918 H1pp were incubated together and then 4 different antibody preparations (at a concentration corresponding to their IC_{90}) were added to the cell-pp mix at different time-points.
C179 was used since it is a stalk directed antibody and can neutralize influenza virus after virus post-attachment to cells. FE1723 was kindly provided by Dr. Davide Corti (Institute for Research in Biomedicine, Bellinzona, Switzerland), and neutralized H1pp *via* binding of the HA head region and does not neutralize influenza virus post-attachment. The anti-A/duck/Italy 1447/2005 (H1N1) serum was also used. FBS was used as neutralization negative control.

A.6 List of publications

Ferrara, F., Molesti, E., Böttcher-Friebertshäuser, E., Cattoli, G., Corti, D., Scott, S. D. and Temperton, N. J. (2013) The human Transmembrane Protease Serine 2 is necessary for the production of Group 2 influenza A virus pseudotypes, *Journal of molecular and genetic medicine : an international journal of biomedical research*, 7, pp. 309–314.

Ahmed, M. S., Jacques, L. C., Mahallawi, W., **Ferrara, F**., Temperton, N., Upile, N., Vaughan, C., Sharma, R., Beer, H., Hoschler, K., McNamara, P. S. and Zhang, Q. (2015) Cross-reactive immunity against influenza viruses in children and adults following 2009 pandemic H1N1 infection, *Antiviral Research*, 114, pp. 106–112.

Benfield, C., Smith, S. E., Wright, E., Wash, R. S., **Ferrara, F.**, Temperton, N. J. and Kellam, P. (2015) Bat and pig Interferon-Induced Transmembrane Protein 3 restrict cell entry by influenza virus and lyssaviruses, *Journal of General Virology*.

Lacek, K., Urbanowicz, R. A., Troise, F., De Lorenzo, C., Severino, V., Di Maro, A., Tarr, A. W., **Ferrara, F.**, Ploss, A., Temperton, N., Ball, J. K., Nicosia, A., Cortese, R. and Pessi, A. (2014) Dramatic Potentiation of the Antiviral Activity of HIV Antibodies by Cholesterol Conjugation, *Journal of Biological Chemistry*.

Mahallawi, W. H., Kasbekar, A. V., McCormick, M. S., Hoschler, K., Temperton, N., Leong, S. C., Beer, H., **Ferrara, F.**, McNamara, P. S. and Zhang, Q. (2013) Infection with 2009 H1N1 influenza virus primes for immunological memory in human nose-associated lymphoid tissue, offering cross-reactive immunity to H1N1 and avian H5N1 viruses, *Journal of virology*, 87(10), pp. 5331–5339.

Mallajosyula, V. V. A., Citron, M., **Ferrara, F.**, Lu, X., Callahan, C., Heidecker, G. J., Sarma, S. P., Flynn, J. A., Temperton, N. J., Liang, X. and Varadarajan, R. (2014) Influenza hemagglutinin stem-fragment immunogen elicits broadly neutralizing antibodies and confers heterologous protection, *Proceedings of the National Academy of Sciences*, 111(25), pp. E2514–23.

Molesti, E., Cattoli, G., **Ferrara, F.**, Böttcher-Friebertshäuser, E., Terregino, C. and Temperton, N. (2013) The production and development of H7 Influenza virus pseudotypes for the study of humoral responses against avian viruses, *Journal of molecular and genetic medicine : an international journal of biomedical research*, 7, pp. 315–320.

Molesti, E., **Ferrara, F.**, Lapini, G., Montomoli, E. and Temperton, N. (2014) Discordant correlation between serological assays observed when measuring heterosubtypic responses against avian influenza H5 and H7 viruses in unexposed individuals, *BioMed research international*, 2014, p. 231365.

Scott, S., Molesti, E., Temperton, N., **Ferrara, F.**, Böttcher-Friebertshäuser, E. and Daly, J. (2012) The use of equine influenza pseudotypes for serological screening, *Journal of molecular and genetic medicine : an international journal of biomedical research*, 6, pp. 304–308.

Smith, S. E., Gibson, M. S., Wash, R. S., **Ferrara, F.**, Wright, E., Temperton, N., Kellam, P. and Fife, M. (2013) Chicken Interferon-Inducible Transmembrane Protein 3 Restricts Influenza Viruses and Lyssaviruses In Vitro, *Journal of virology*, 87(23), pp. 12957–12966.